SECRET

MARTIN MARIETTA ENERGY SYSTEMS LIBRARIES
3 4456 0360854 9

ORNL 963
Reactors-Research
and Power

Vol. I

31 A

CENTRAL RESEARCH LIBRARY
DOCUMENT COLLECTION

DECLASSIFIED
Classification Changed To:
By Authority Of: GDC 10/3/62
By: [illegible] 7/23/63

AEC RESEARCH AND DEVELOPMENT REPORT

[redacted]

TID 1108

LABORATORY RECORDS

MATERIALS TESTING REACTOR PROJECT HANDBOOK

J.H. BUCK
C.F. LEYSE

CE
D
LIB
DO NOT TRANSFER T
If you wish someone else to see this docu
send in name with document and the library will
arrange a loan.

OAK RIDGE NATIONAL LABORATORY
OPERATED BY
CARBIDE AND CARBON CHEMICALS COMPANY
A DIVISION OF UNION CARBIDE AND CARBON CORPORATION
UCC
POST OFFICE BOX P
OAK RIDGE, TENNESSEE

SECRET

[redacted]

ORNL-963

This docu[redacted] of 584 pages. [redacted] Series A.

Contract No. W-7405, eng 26

31A

MATERIALS TESTING REACTOR PROJECT HANDBOOK

Prepared Jointly by Argonne National Laboratory
and
Oak Ridge National Laboratory

John H. Buck ..... Editor
Carl F. Leyse ..... Associate Editor

Prepared at the request of the MTR Steering Committee

Date Issued

MAY 7 1951

MARTIN MARIETTA ENERGY SYSTEMS LIBRARIES
3 4456 0360854 9

OAK RIDGE NATIONAL LABORATORY
operated by
CARBIDE AND CARBON CHEMICAL COMPANY
A Division of Union Carbide and Carbon Corporation
Post Office Box P
Oak Ridge, Tennessee

R[redacted]
Th[redacted] contents in
defin[redacted] penalties under

INTERNAL DISTRIBUTION

1. G. T. Felbeck
2. C. E. Center
3. C. E. Larson
4. A. M. Weinberg
5. J. H. Frye
6. J. A. Swartout
7. F. C. VonderLage
8. A. H. Snell
9. E. H. Taylor
10. F. L. Steahly
11. K. Z. Morgan
12. M. E. Ramsey
13. J. A. Cox
14. C. Cagle
15. F. M. Tench
16. M. M. Mann
17. J. H. Buck
18. R. M. Jones
19. W. H. Jordan
20. W. M. Breazeale
21. J. A. Lane
22. C. E. Winters
23. R. C. Briant
24-26. W. M. Hawkins
27. D. S. Billington
28. E. O. Wollan
29. E. J. Murphy
30. Physics Library
31-32. Chemistry Library
33. Biology Library
34. Health Physics Library
35. Metallurgy Library
36-37. Training School Library
38-64. Central Files

EXTERNAL DISTRIBUTION

65-93. Argonne National Laboratory
94-101. Atomic Energy Commission, Washington
102. Battelle Memorial Institute
103-106. Brookhaven National Laboratory
107. Bureau of Ships
108-113. Carbide and Carbon Chemicals Company (Y-12 Area)
114. Chicago Patent Group
115. Chief of Naval Research
116-119. duPont Company
120. H. K. Ferguson Company
121-124. General Electric Company, Richland
125. Hanford Operations Office
126-129. Idaho Operations Office
130. Iowa State College
131-134. Knolls Atomic Power Laboratory
135-137. Los Alamos
138. Massachusetts Institute of Technology (Kaufmann)
139. National Advisory Committee for Aeronautics
140-141. New York Operations Office
142. North American Aviation, Inc.
143. Patent Branch, Washington
144-145. Phillips Petroleum Company, Bartlesville, Oklahoma (R. L. Doan)
146-163. Phillips Petroleum Company, Oak Ridge (W. Crawford)
164. Savannah River Operations Office
165-166. University of California Radiation Laboratory
167-170. Westinghouse Electric Corporation
171-173. Wright-Patterson Air Force Base
174-188. Technical Information Service, Oak Ridge

ACKNOWLEDGMENT

The MTR Project Handbook has been made possible only through the co-operation of every member of the MTR groups at Argonne National Laboratory and Oak Ridge National Laboratory. Some have written the initial draft for entire chapters, some for sections of chapters, and many have spent much time and effort in gathering and collating data. All this work was essential to the completion of the Handbook, and the editors sincerely hope that the report fulfills the expectations of the Committee and every other member of the Project.

TABLE OF CONTENTS

Chap. 1 INTRODUCTION — GENERAL DESCRIPTION AND HISTORY OF THE MTR 1.1

1.1 General Description of the Reactor, Its Location, and Facilities 1.1

1.1.1 Brief general description of the Materials Testing Reactor 1.1
1.1.2 Location 1.2
1.1.3 Availability of utilities and supplies 1.2
1.1.4 AEC central facilities 1.2
1.1.5 MTR facilities 1.4
1.1.6 Climate 1.5
1.1.7 Geology 1.6

1.2 History of the MTR 1.6

1.2.1 Need for reactor 1.6
1.2.2 Design and administrative history 1.7

1.3 Reference Reports 1.18

1.4 Reference Drawings 1.18

Chap. 2 ENGINEERING DESCRIPTION OF THE REACTOR 2.1

2.1 Reactor Enclosure Tank 2.1

2.1.1 Tank sections A and E 2.2
2.1.2 Tank section B 2.2
2.1.3 Tank sections C and D 2.3
2.1.4 Top and bottom plugs 2.4

2.2 The Active Lattice and Supporting Structure 2.4

2.3 The Control Rods 2.9

2.3.1 Shim-safety control rods 2.9
2.3.2 Regulating rods 2.13
2.3.3 Miscellaneous equipment connected with control rods 2.15

2.4 Reflector 2.19

2.4.1 Beryllium 2.19
2.4.2 Graphite 2.23

2.5 Thermal Shield 2.32

2.5.1 The steel plate structure 2.32
2.5.2 Neutron curtain in the MTR 2.35
2.5.3 The neutron window 2.35

2.6 The Biological Shield 2.36

2.7 Cooling 2.36

2.7.1 Water cooling 2.36
2.7.2 Air cooling 2.38

2.8 Monitoring Equipment 2.40

2.8.1 Monitor tubes 2.40
2.8.2 Thermocouples 2.42

2.9 Handling Tools 2.42
2.9.1 Design summary 2.44

2.10 Reference Reports 2.46

2.11 Reference Drawings 2.47

Chap. 3 EXPERIMENTAL FACILITIES 3.1

3.1 Horizontal and Down Beam Experimental Holes 3.1

3.1.1 Introduction 3.1
3.1.2 Beam hole liners and components 3.4
3.1.3 Beam hole dummy plugs 3.12
3.1.4 Horizontal through hole facility 3.14
3.1.5 Other horizontal experimental and instrument holes 3.17
3.1.6 Services 3.18
3.1.7 Coffins 3.18

3.2 Vertical Experimental and Instrument Holes 3.22

3.2.1 Instrument holes 3.23
3.2.2 Experimental holes 3.24

3.3 Thermal Column 3.25

3.3.1 General description 3.25
3.3.2 Thermal column experimental facilities 3.28

3.4 Shielding Facility 3.29

3.5 Pneumatic Rabbits 3.30

3.6 Hydraulic Rabbits 3.31

3.7 Reference Reports 3.32

3.8 Reference Drawings 3.33

Chap. 4 PHYSICS OF THE MATERIALS TESTING REACTOR 4.1

4.1 Review of Requirements 4.1

4.2 Flux Calculations 4.2

4.3 Reactivity Losses 4.10

4.3.1 Xe^{135} and Sm^{149} poisoning 4.14

4.3.2 Depletion of U^{235} and other fission product poisoning 4.18

4.3.3 Temperature coefficient 4.18

4.3.4 Thorium blanket 4.20

4.3.5 Other reactivity losses 4.20

4.3.6 Total reactivity of reactor 4.20

4.4 Dynamics of the Reactor 4.23

4.5 Heat Production, Transfer, and Removal 4.24

4.5.1 Calculations of heat inside active lattice 4.25

4.5.2 Calculations of heat in beryllium and in foreign materials near active lattice 4.26

4.5.3 Heating and cooling of the graphite reflector 4.28

4.5.4 Heating and cooling of the thermal shield 4.29

4.5.5 Cooling requirements at reduced power levels and after shutdown 4.29

4.6 Shielding Summary 4.36

4.6.1 Fundamental concepts 4.37

4.6.2 Concrete shield design 4.47

4.6.3 Supplementary shielding problems 4.60

4.7 Reference Reports 4.86

Chap. 5 CONTROL SYSTEM 5.1

5.1 Introduction 5.1

5.1.1 Review of requirements 5.1
5.1.2 General features of the MTR control system 5.2

5.2 Measuring Instruments 5.4

5.2.1 Reactor instruments 5.4
5.2.2 Rod position and motion indicators 5.15
5.2.3 Auxiliary facilities instruments 5.17

5.3 Rod Motion Controls 5.20

5.3.1 Safety rod clutches 5.20
5.3.2 Motor drive of shim rods 5.22
5.3.3 Motor drive of regulating rods 5.24
5.3.4 Control system during maintenance shutdown 5.28

5.4 Control Console 5.30

5.5 Control System and Operator 5.34

5.5.1 Automatic rod insertion 5.34
5.5.2 Operator initiative and the procedure panel 5.35

5.6 Reactor Operation 5.42

5.6.1 Start-up operation 5.42
5.6.2 Shutdown 5.43
5.6.3 Manipulation of operating level 5.43
5.6.4 Operation in face of difficulty 5.44

5.7 General Summary 5.46

5.7.1 Basic principles 5.46
5.7.2 Responsibility of operator 5.50

5.8 Control and Instrument Centers 5.51

5.8.1 Reactor control and instrument center 5.51
5.8.2 Process-water control and instrument center 5.54

5.9 Glossary of Terms and Symbols 5.54

5.10 Reference Reports 5.57

5.11 Reference Drawings 5.58

Chap. 6 CANAL AND CANAL HANDLING FACILITIES 6.1

6.1 Canal 6.1

6.1.1 General description 6.1
6.1.2 Canal purge system 6.4
6.1.3 Canal flushing 6.5
6.1.4 Heating and ventilation of canal tunnel 6.5
6.1.5 Canal lighting 6.5
6.1.6 Canal crane 6.5

6.2 Unloading Mechanism 6.6

6.2.1 General description 6.6
6.2.2 Operation sequence 6.8
6.2.3 Control system 6.8

6.3 Canal Storage 6.11

6.3.1 Beryllium assemblies 6.11
6.3.2 Standard fuel assemblies 6.11
6.3.3 Shim-safety rods 6.11
6.3.4 Regulating rods 6.12

6.4 Assembly Disposal 6.12

6.4.1 Sawing machine 6.12
6.4.2 Chip collector 6.12
6.4.3 Transfer to decay storage 6.14
6.4.4 Transfer coffin 6.14

6.5 Reference Reports 6.15

6.6 Reference Drawings 6.16

Chap. 7 PROCESS-WATER SYSTEM 7.1

7.1 Introduction 7.1

7.2 The System in General 7.1

7.2.1 General description of the system 7.1
7.2.2 Stand-by and emergency features 7.4
7.2.3 Instrumentation and flow balance 7.5
7.2.4 Water-cooled experimental plugs and rabbits 7.7
7.2.5 Process water building 7.7

7.3 Major Components of the System 7.8

7.3.1 Sump tank 7.8
7.3.2 Process pumps 7.8
7.3.3 Working reservoir 7.11
7.3.4 Valve pit 7.12
7.3.5 Seal tank and pump 7.12
7.3.6 Flash evaporators 7.12
7.3.7 Piping 7.14

7.4 Bases for Design 7.15

7.4.1 Flow quantity and heat transfer 7.15
7.4.2 Degasification 7.16
7.4.3 Water quality and materials of construction 7.18
7.4.4 Induced activity 7.21
7.4.5 Shielding 7.23
7.4.6 Cooling after shutdown 7.23

7.5 Reference Reports 7.29

7.6 Reference Drawings 7.31

Chap. 8 REACTOR COOLING-AIR AND CONTAMINATED-AIR SYSTEMS 8.1

8.1 Reactor Cooling-air System 8.1

8.1.1 Introduction 8.1
8.1.2 Air flow data 8.1
8.1.3 Inlet air filters 8.5
8.1.4 System within reactor structure 8.7
8.1.5 Exit ducts 8.9
8.1.6 Blowers, fans, and auxiliaries 8.9
8.1.7 Instrumentation and control 8.11
8.1.8 Shielding 8.12

8.2 Contaminated-air System 8.14

8.2.1 Introduction 8.14
8.2.2 Air flow data 8.14
8.2.3 System from hoods to scrubber 8.14
8.2.4 Scrubber 8.14

8.2.5 Exit duct from scrubber 8.16
8.2.6 Exhaust fans and auxiliaries 8.16
8.2.7 Instrumentation and control 8.16
8.2.8 Shielding 8.17

8.3 Blower and Fan House 8.18

8.3.1 Introduction 8.18
8.3.2 Air ducts and plenum chamber 8.18
8.3.3 Blower and fan cells 8.20
8.3.4 Miscellaneous 8.20

8.4 Stack 8.21

8.4.1 Introduction 8.21
8.4.2 Activity of stack gases 8.21
8.4.3 Stack height 8.22
8.4.4 Stack diameter 8.23
8.4.5 General construction 8.23

8.5 Reference Reports 8.24

8.6 Reference Drawings 8.25

Chap. 9 SITE AND BUILDINGS 9.1

9.1 Site Plan 9.1

9.2 Reactor Building 9.5

9.2.1 General building details 9.7
9.2.2 First floor 9.8
9.2.3 Second and third floors 9.13
9.2.4 Basement 9.14

9.3 Reactor Building Wing 9.16

9.3.1 General building details 9.16
9.3.2 First floor 9.17
9.3.3 Basement 9.21
9.3.4 Future additions 9.23

9.4 Service Buildings and Areas 9.23

9.4.1 Service building, Area 14 9.23
9.4.2 Limited-area control house, Area 20 9.23
9.4.3 Exclusion-area control house, Area 21 9.24
9.4.4 Canteen, Area 16 9.24
9.4.5 Plug storage, Area 11 9.24
9.4.6 Reactor service building 9.24
9.4.7 Other buildings and areas 9.25

9.5 Reference Reports 9.26

9.6 Reference Drawings 9.27

Chap. 10 SUPPORTING FACILITIES AND AUXILIARIES 10.1

10.1 Steam Plant 10.1

10.2 Electrical Systems 10.1

10.2.1 Introduction 10.1
10.2.2 Sources of electrical power 10.2
10.2.3 Distribution systems 10.4
10.2.4 Load power factor 10.7
10.2.5 Electrical grounding 10.7

10.3 Water 10.8

10.3.1 Introduction 10.8
10.3.2 Water requirements 10.8
10.3.3 Water analysis 10.10
10.3.4 Demineralization system 10.12
10.3.5 Softeners 10.13
10.3.6 Acid-neutralization system for cooling-tower make-up water 10.14
10.3.7 Design and operating data summary 10.14
10.3.8 Instrumentation, laboratory, and housing 10.15

10.4 Effluent Control 10.15

10.4.1 Introduction 10.15
10.4.2 Retention basin 10.16
10.4.3 Effluent pond 10.18
10.4.4 Nonprocess active effluents 10.18

10.5 Cooling Towers 10.20

10.5.1 General description 10.20

10.5.2 Heat load 10.20

10.5.3 Operation and description of cooling towers and basins 10.21

10.5.4 Pumping station 10.22

10.5.5 Instrumentation 10.22

10.5.6 Emergency operation 10.23

10.5.7 Design data 10.23

10.6 Process Radiation Instrumentation and Area Monitoring 10.24

10.6.1 Process radiation instrumentation 10.24

10.6.2 Area monitoring 10.26

10.7 Reference Reports 10.28

10.8 Reference Drawings 10.29

Appendix 1 CRITICALITY STUDIES ON ENRICHED URANIUM—HEAVY WATER SYSTEMS A1.1

A1.1 Experimental Arrangement A1.1

A1.2 Critical Mass Experiments A1.3

A1.3 Reference Report A1.11

Appendix 2 WORK ON CRITICAL EXPERIMENTS, JULY 1946 TO DECEMBER 1948 A2.1

A2.1 Critical Experiments with Al + H_2O Moderator and Heavy Water, Light Water, and Beryllium Reflectors A2.1

A2.1.1 Experimental facilities A2.1

A2.1.2 Pile geometry and design A2.3

A2.1.3 Results and discussion A2.5

A2.2 Further Critical Experiments on Enriched Reactors with Al + H_2O Moderator and Solid Beryllium Reflector A2.11

A2.2.1 Experimental facilities A2.11

A2.2.2 Experimental results A2.13

A2.3 Reference Reports A2.20

Appendix 3 CRITICAL EXPERIMENTS ON SIMULATED MTR STRUCTURE A3.1

A3.1 The Excess Reactivity of U-Al-H_2O Reactors, with Be Reflector, as a Function of Geometry and Reflector Composition A3.1

A3.2 Effects of the Experimental Holes Through the Reflector A3.5

A3.3 Neutron Distributions A3.10

A3.4 Gamma Heat Production in the Reflector A3.11

A3.5 Control Rod Experiments A3.18

A3.6 Reference Reports A3.20

Appendix 4 MOCK-UP A4.1

A4.1 Description of Facility A4.1

A4.2 Mechanical Experiments A4.6

A4.2.1 Stress-strain measurements A4.6
A4.2.2 Control system A4.7

A4.3 Hydraulic Experiments A4.16

A4.3.1 Flow in reflector outside the fuel lattice A4.17
A4.3.2 Flow and pressure drops inside fuel lattice A4.23

A4.4 Handling Tools A4.29

A4.5 Nuclear Experiments A4.29

A4.5.1 Critical mass determination A4.29
A4.5.2 Regulating-rod calibration A4.32
A4.5.3 Temperature coefficient A4.36
A4.5.4 Effect of an empty experimental beam hole A4.37
A4.5.5 Effect of water flow A4.37
A4.5.6 Performance of control and safety circuits A4.37
A4.5.7 Measurement of neutron fluxes A4.38
A4.5.8 Heat production in graphite, thermal shield, and concrete A4.51
A4.5.9 Attenuation of gamma rays inside reactor tank A4.57

A4.6 Reference Reports A4.69

Appendix 5 BERYLLIUM A5.1

A5.1 Chemical and Mechanical Tests A5.1

A5.2 Manufacture and Specifications of MTR Beryllium A5.2

A5.3 Danger Coefficient and Total Danger Sum (TDS) as Applied to Beryllium A5.5

A5.4 Reference Reports A5.6

Appendix 6 FUEL ELEMENTS A6.1

A6.1 Development A6.1

A6.2 Construction of Plates A6.3

A6.3 Fabrication of the Fuel Elements A6.5

A6.4 Reference Reports A6.8

A6.5 Reference Drawings A6.9

Appendix 7 PROPERTIES OF SHIELDING MATERIALS A7.1

Appendix 8 SHIELDING CALCULATION AIDS A8.1

Appendix 9 PNEUMATIC RABBITS A9.1

A9.1 General Description of Proposed Re-entry Shuttle System A9.1

A9.2 Proposed Equipment and Facilities for Re-entry Shuttle System A9.1

A9.2.1 Rabbit tube A9.4

A9.2.2 Electric air-controlled gate valve A9.4

A9.2.3 Shuttle transfer A9.5

A9.2.4 Laboratory Selector A9.5

A9.2.5 Shock absorber A9.5

A9.2.6 Delivery stations and delivery-station shock absorbers A9.8

A9.2.7 Pneumatic driving system A9.8

A9.2.8 Vacuum system A9.9

A9.3 Operation of Re-entry Shuttle System A9.9

A9.3.1 Pressure drop A9.11

A9.3.2 Anticipated operating curves A9.11

A9.3.3 Shuttle material A9.13
A9.3.4 Cooling of the shuttle A9.13
A9.3.5 Shielding A9.14
A9.3.6 Use of air vs. CO_2 for propellant A9.14

A9.4 Reference Reports A9.14

A9.5 Reference Drawings A9.14

Appendix 10 HYDRAULIC RABBITS A10.1

[redacted]

LIST OF TABLES

Table 2.3.A	Cadmium-Uranium Shim Rods	2.10
Table 2.3.B	Regulating Rod	2.13
Table 2.7.A	Summary of Results of Calculations and Experiments Leading to Design of Water-flow System	2.37
Table 2.8.A	Locations of Thermocouples	2.43
Table 3.A	Summary of Experimental Facilities	3.2
Table 4.2.A	Fluxes in Light Water and Heavy Water Reactors	4.3
Table 4.3.A.	Partial Temperature Coefficients at 20°C, Al-H_2O Neutron Temperature	4.19
Table 4.3.B	Minimum Reactivity Losses Which Must Be Allowed for in Reactor	4.20
Table 4.5.A	Reduction Factors After Shutdown	4.33
Table 4.5.B	Cumulative Heat After Shutdown	4.34
Table 4.5.C	Fall-off of Heat Rates and Water Rates	4.35
Table 4.6.A	Total Cross-sections of Portland and Barytes Concretes at 5 Mev	4.41
Table 4.6.B	Total Cross-sections of Ordinary and Barytes Concretes in 1- to 2-Mev Range	4.42
Table 4.6.C	Required Biological Shield Thickness	4.57
Table 4.6.D	Elements with High γ-Ray Activities	4.83
Table 4.6.E	Induced Activity of Commercial Materials	4.85
Table 5.2.A	Reactor Radiation Instruments	5.5
Table 5.2.B	Relation of Lower Level to Instruments	5.7
Table 5.5.A	Causes of Automatic Rod Insertion	5.36
Table 7.4.A	Activity of MTR Process Water	7.24
Table 7.4.B	Minimum Process-water Flow After Shutdown	7.27
Table 7.4.C	Process-water Temperature After Shutdown	7.27

[redacted]

Table 8.1.A	Approximate Pressure Drops in Reactor Air System	8.3
Table 8.1.B	Activity of Reactor-cooling Air	8.13
Table 8.1.C	Shielding Requirements for the Reactor Air System	8.13
Table 8.2.A	Shielding Requirements for the Contaminated-air System	8.18
Table 8.4.A	Production of A^{41} in the MTR	8.22
Table 10.3.A	Total Water Requirements	10.10
Table 10.3.B	Raw-water Analysis	10.11
Table 10.3.C	Demineralized-water Analysis	10.12
Table 10.3.D	Water System Design and Operating Data	10.14
Table 10.4.A	Water Flows to Retention Basin	10.17
Table 10.6.A	Area Radiation Monitoring Instruments	10.27
Table A1.A	Amounts of U^{235} Required for Criticality in Various D_2O Systems	A1.8
Table A1.B	Collected Dimensions and Constants of the Experiments	A1.10
Table A2.A	Critical Masses in Kilograms of U^{235}	A2.9
Table A2.B	Relations Between Thermal Flux at Certain Locations in the Reactor and That at Center of Core	A2.19
Table A3.A	Critical Mass and Poison Content (Excess k) of U-Al-H_2O Reactors with Be Reflector	A3.4
Table A3.B	Effect of Experimental Holes in the High-flux Reactor Critical Assemblies	A3.7
Table A3.C	Summary of Total Effect of Experimental Holes	A3.8
Table A4.A	Water Velocities in Various Reflector Channels	A4.20
Table A4.B	Flow Rates for Various Reflector Holes	A4.21
Table A4.C	Flow Rates at Pressure Tap 41	A4.22
Table A4.D	Flow Rates in Reflector	A4.22
Table A4.E	Pressure Drops and Flow Rates Through Tank Section D	A4.27

Table A4.F	Experimental Values for Temperature Coefficient	A4.36
Table A4.G	Neutron Flux in Mid-plane (First Series)	A4.40
Table A4.H	Neutron Flux in Mid-plane (Second Series)	A4.48
Table A4.I	Horizontal Traverse	A4.49
Table A4.J	Traverses Behind Hole 17 on Surface of Graphite	A4.50
Table A4.K	Heat Production in Mid-plane, Graphite Reflector	A4.64
Table A4.L	Measured Heat Production in Top and Bottom Planes of Graphite Reflector	A4.65
Table A6.A	Fuel Assembly Plates	A6.2
Table A7.A	Properties of Shielding Materials	A7.1
Table A7.B	Summary of Some Declassified Nuclear Data	A7.7

[redacted]

[redacted]

LIST OF FIGURES

Fig. 2.2.A	Cross Section of Fuel Assembly	2.6
Fig. 2.2.B	Fuel Assembly Unit No. 136	2.7
Fig. 2.3.A	Shim-Safety Rod with Fuel	2.11
Fig. 2.3.B	Shim-Safety Rod with Beryllium	2.12
Fig. 2.3.C	Regulating Rod	2.14
Fig. 2.4.A	Beryllium Below Centerline of Reactor	2.20
Fig. 2.4.B	Top View of Beryllium	2.21
Fig. 2.4.C	Beryllium A-Piece	2.22
Fig. 2.4.D	Beryllium Assembly	2.24
Fig. 2.4.E	Beryllium Assembly	2.25
Fig. 2.4.F	Partial Beryllium Assembly	2.26
Fig. 2.4.G	Beryllium Showing HB and DB Holes	2.27
Fig. 2.4.H	Permanent Graphite	2.29
Fig. 2.4.I	Graphite Assembly and Numbering System	2.30
Fig. 2.4.J	Part of Graphite West Wall	2.31
Fig. 2.5.A	Top Thermal Shield Design	2.34
Fig. 2.7.A	Hole Pattern for the Graphite Reflector	2.39
Fig. 2.8.A	Reactor Tank Monitor Tube Assembly	2.41
Fig. 2.A	MTR North-South Vertical Section	2.48
Fig. 2.B	MTR East-West Vertical Section	2.49
Fig. 2.C	MTR Horizontal Section	2.50
Fig. 2.D	Pictorial Cross Section, Reactor Tank	2.51
Fig. 2.E	MTR General Assembly	2.52
Fig. 2.F	MTR Top Plug Assembly	2.53
Fig. 3.1.A	Typical Beam Hole Liner and Components	3.5
Fig. 3.1.B	Typical Beam Hole Water-cooled Dummy Plug	3.6
Fig. 3.1.C	Typical Beam Hole Air-cooled Dummy Plug	3.7

Fig. 3.1.D	Horizontal Through Hole Facility	3.8
Fig. 3.1.E	Universal Coffin	3.20
Fig. 3.3.A	Thermal Column — Cutaway View Without Graphite Filter or Surrounding Concrete	3.26
Fig. 3.3.B	Graphite Assembly for Thermal Column	3.27
Fig. 3.A	View of North Face of Reactor	3.34
Fig. 3.B	View of East Face of Reactor	3.35
Fig. 3.C	View of South Face of Reactor	3.36
Fig. 3.D	View of West Face of Reactor	3.37
Fig. 3.E	View of Top of Reactor	3.38
Fig. 3.F	Location of Experimental Facilities on Reactor Top	3.39
Fig. 3.G	Reactor Building First Floor Plan	3.40
Fig. 4.2.A	Neutron Flux Distributions and Adjoint Functions	4.4
Fig. 4.2.B	Neutron Flux Distributions and Adjoint Functions	4.5
Fig. 4.2.C	Neutron Flux Distributions and Adjoint Functions	4.6
Fig. 4.2.D	Longitudinal Flux Distributions	4.7
Fig. 4.2.E	Distribution Measured from Center of 40 cm Dimensions	4.8
Fig. 4.2.F	Thin Slab (11 × 60 × 70 cm) Core	4.9
Fig. 4.2.G	Neutron Distribution, 40 × 30 × 60 Slab Pile With and Without Thorium Breeding Sheet Present	4.11
Fig. 4.3.A	Reactivity Loss, $-\delta k/k$, Due to Xe^{135}, Sm^{149}, 25 Depletion, and Build-up of Low-cross-section Fission Products as Function of Time of Operation	4.15
Fig. 4.3.B	Reactivity Loss, $-\delta k/k$, Due to Xe^{135}, Sm^{149}, 25 Depletion, and Build-up of Low-cross-section Fission Products as Function of Time of Operation up to 36 hr	4.16
Fig. 4.3.C	Extra Reactivity Change After Shutdown	4.17
Fig. 4.3.D	$\delta k/k$ Which Must Be Taken Up by Control Rods or Poisons to Keep Pile Critical vs. Mass of 25 in Pile	4.22
Fig. 4.5.A	Average Heat Distribution in Reflector Around Slab Pile	4.27
Fig. 4.5.B	Heat Production in Reflector for Slab or Square Loading	4.30

Fig. 4.5.C	Cooling Requirements as Function of Power	4.31
Fig. 4.6.A	Photon Flux as Function of Energy for Dose Rate = 0.01 rep/8 hr	4.38
Fig. 4.6.B	Fast-neutron Flux for One-tenth Tolerance Dose	4.39
Fig. 4.6.C	Indium Foil Activation Against Depth in Pile Shield	4.44
Fig. 4.6.D	Pictorial Representation of Required Shield Thicknesses	4.54
Fig. 4.6.E	Geometric Factor Illustration	4.56
Fig. 4.6.F	Thickness Required for Given Attenuation with Relaxation Lengths of 8.2 and 10 cm	4.59
Fig. 4.6.G	Map of Neutron and Gamma Rays in Corner Regions of Concrete at Mid-plane	4.61
Fig. 4.6.H	Comparison of Overall Barytes Concrete Thickness with Design Requirements	4.62
Fig. 4.6.I	Comparison of Overall Barytes Concrete Thickness with Design Requirements	4.63
Fig. 4.6.J	Cross Section of a Duct Through the Shield	4.79
Fig. 5.1.A	Control System Block Diagram	5.3
Fig. 5.2.A	Materials Testing Reactor Instrumentation Block Diagram	5.6
Fig. 5.2.B	Neutron-sensitive 3-in. P.C.P. Ionization Chamber	5.9
Fig. 5.2.C	Compensated Ionization Chamber	5.11
Fig. 5.2.D	Fission Chamber Assembly	5.12
Fig. 5.2.E	Shim Rod Limit Switches	5.16
Fig. 5.2.F	Regulating-rod Limit Switches	5.18
Fig. 5.3.A	Sigma Amplifier and Safety Preamp Circuits	5.21
Fig. 5.3.B	Magnet Amplifier Circuit	5.23
Fig. 5.3.C	Servo Input Signal	5.25
Fig. 5.3.D	Servo Amplifier and Servo Preamp Circuit	5.27
Fig. 5.4.A	Control Console Layout	5.31
Fig. 5.5.A	Block Diagram Including Procedure Panel	5.47
Fig. 5.8.A	Reactor Control Room and Instrument Panel Layout	5.53
Fig. 5.8.B	Process Water Building Control and Instrument Panel Layout	5.55

[redacted]

[redacted]

Fig. 6.1.A	Reactor Building — Basement Plan	6.2
Fig. 6.2.A	Unloading Mechanism	6.7
Fig. 6.2.B	Unloading Mechanism Control System	6.10
Fig. 6.4.A	Sawing Mechanism	6.13
Fig. 7.2.A	Schematic Diagram of MTR Process Water System	7.2
Fig. 7.2.B	Process Water Building Floor Plans	7.9
Fig. 7.2.C	Process Water Building Sections	7.10
Fig. 7.4.A	Process Water Pipe Shielding	7.25
Fig. 8.1.A	Reactor-air System Schematic Flow Diagram	8.2
Fig. 8.1.B	MTR Air System	8.8
Fig. 8.2.A	Contaminated-air System Schematic Flow Diagram	8.15
Fig. 8.3.A	Blower and Fan House Layout	8.19
Fig. 9.1.A	MTR Site — Artist's Sketch	9.2
Fig. 9.1.B	Site Plan	9.3
Fig. 9.2.A	Reactor Building and Wing — Artist's Sketch	9.6
Fig. 9.2.B	Reactor Building — First Floor Plan	9.9
Fig. 9.2.C	Reactor Building — Second and Third Floors	9.10
Fig. 9.2.D	Reactor Building — Basement Plan	9.11
Fig. 9.3.A	Reactor Building Wing — First Floor	9.18
Fig. 9.3.B	Reactor Building Wing — Basement	9.22
Fig. 10.2.A	Electrical Underground Distribution and Site Lighting	10.5
Fig. 10.3.A	MTR Water System	10.9

[redacted]

Fig. A1.A	Tank and Fuel Arrangement	A1.2
Fig. A1.B	Tube Sheet Lattice Arrangement	A1.4
Fig. A1.C	Radial Neutron Distribution in 2.58 g/l Assembly	A1.5
Fig. A1.D	Longitudinal Neutron Distribution in 2.58 g/l Assembly	A1.6
Fig. A2.A	Section Through Assembly and Control Rooms	A2.2
Fig. A2.B	Assembly for D_2O Reflector	A2.4
Fig. A2.C	Assembly for Beryllium Reflector	A2.6
Fig. A2.D	Reactor Assembly Beryllium Reflector	A2.7
Fig. A2.E	Radial Neutron Distributions — Beryllium Reflector	A2.8
Fig. A2.F	Vertical Distribution — Beryllium Experiment	A2.10
Fig. A2.G	Reactor Assembly	A2.12
Fig. A2.H	Approach to Criticality, Bare Pile, Al/H_2O Volume Ratio 0.65	A2.14
Fig. A2.I	Approach to Critical, Slab Pile, Lattice 65-Be-2	A2.16
Fig. A2.J	Square Be Pile, Lattice 65-Be-1, Lateral Neutron Distribution	A2.17
Fig. A2.K	Square Be Pile, Lattice 65-Be-1, Neutron Distributions Along Diagonal	A2.18
Fig. A3.A	Reactor Assembly	A3.3
Fig. A3.B	Critical Assemblies, Location of Holes in Reflector	A3.6
Fig. A3.C	Effect of Absorber, 10 × 10 × 10 cm, 0.020-in. Cd Box	A3.9
Fig. A3.D	Lattice 65-Be-3 (2.94 kg) Lateral Traverse	A3.12
Fig. A3.E	4-kg Slab Pile (71 × 22.5 × 66 cm), 2% H_2O in Be; Neutron Distributions (Along Axis of 6-in. Hole at Edge of Reactor)	A3.13
Fig. A3.F	4-kg Slab Pile (71 × 22.5 × 66 cm), Seven 6-in. Holes in Reflector, Lateral Neutron Distributions (Along Axis of Center Hole)	A3.14
Fig. A3.G	4-kg Slab Pile (71 × 22.5 × 66 cm), Seven 6-in. Holes in Reflector, Lateral Neutron Distributions (Along Axis of Edge Hole)	A3.15
Fig. A3.H	4-kg Slab Pile (71 × 22.5 × 66 cm), Seven 6-in. Holes in Reflector, Longitudinal Neutron Distributions (Along Axis of End Hole)	A3.16

[redacted]

[redacted]

Fig. A3.I	Traverse Taken Between Two Deep Holes at Mid-height of Pile	A3.17
Fig. A3.J	Gamma Heat Production in Reflector of 3-kg Pile (71 × 17 × 66 cm)	A3.19
Fig. A4.A	Diagram of Pile Tank	A4.2
Fig. A4.B	MTR Mock-Up Assembly for Low-power Experiments	A4.4
Fig. A4.C	Layout of Holes for Flux Measurements Outside of Reactor Tank	A4.5
Fig. A4.D	Rate of Fall — Safety Rod	A4.10
Fig. A4.E	Deceleration of Safety Rod	A4.11
Fig. A4.F	Westinghouse-built MTR Magnet No. 1, Load vs. Release Current	A4.13
Fig. A4.G	Typical Magnet Release Tests	A4.14
Fig. A4.H	Location of Pressure Taps Above Thimbles	A4.18
Fig. A4.I	Location of Pressure Taps Below Thimbles	A4.19
Fig. A4.J	Cross Section of MTR	A4.24
Fig. A4.K	Velocity-Pressure Drop Curve for Fuel Assemblies	A4.25
Fig. A4.L	Calibration of Cadmium Shim-Safety Rod	A4.28
Fig. A4.M	Tank Cover for Use in Assembly	A4.30
Fig. A4.N	Upper Grid Assembly Handling Tool	A4.31
Fig. A4.O	Reactor Tank Showing Arrangement of Lattice and Beryllium Reflector	A4.33
Fig. A4.P	Calibration of Regulating Rod	A4.34
Fig. A4.Q	Sensitivity of Regulating Rod	A4.35
Fig. A4.R	Thermal-neutron Flux in Mid-plane of Active Lattice	A4.41
Fig. A4.S	Thermal-neutron Flux in Top Plane of Active Lattice	A4.42
Fig. A4.T	Vertical Traverse in Hole 45	A4.43
Fig. A4.U	Vertical Traverse in Hole 19	A4.44
Fig. A4.V	Vertical Traverse in Hole 34	A4.45
Fig. A4.W	Neutron Attenuation in Water Above Reactor Lattice	A4.47
Fig. A4.X	Arrangement of Paraffin and Steel Thermal Shield Showing Foil Exposure Slots	A4.52

[redacted]

Fig. A4.Y	Neutron Attenuation in Paraffin Behind Thermal Shield	A4.53
Fig. A4.Z	Horizontal Traverse Between Paraffin and Steel	A4.54
Fig. A4.AA	Vertical Traverse Between Paraffin and Steel	A4.55
Fig. A4.BB	10 cm^3 Graphite Ionization Chamber Used in MTR Mock-Up Heat Production Measurements	A4.56
Fig. A4.CC	Heat Production in Hole 19	A4.58
Fig. A4.DD	Heat Production in Hole 34	A4.59
Fig. A4.EE	Heat Production in Hole 26	A4.60
Fig. A4.FF	Heat Production in Hole 45	A4.61
Fig. A4.GG	Heat Production in Barytes Concrete Block	A4.62
Fig. A4.HH	Vertical Gamma Attenuation in Water — MTR Mock-Up	A4.63
Fig. A4.II	Horizontal Gamma Traverses in Water Above Lattice in MTR Mock-Up	A4.67
Fig. A4.JJ	Chamber Elevations for Horizontal Gamma Traverses and Relative Locations of Graphite, Air, and Concrete in MTR Mock-Up	A4.68
Fig. A6.A	Fuel Rod Production	A6.4
Fig. A7.A	Mass Absorption Coefficients vs. Energy	A7.2
Fig. A7.B	Mass Absorption Coefficients vs. Energy	A7.3
Fig. A7.C	Mass Absorption Coefficients vs. Energy	A7.4
Fig. A7.D	Mass Absorption Coefficients vs. Energy	A7.5
Fig. A7.E	Energy Dependence of Gamma-ray Linear Absorption Coefficients	A7.6
Fig. A8.A	Shielding Formulas	A8.3
Fig. A8.B	Graph — Functions for Shielding Calculation	A8.4
Fig. A8.C	Graph — Functions for Shielding Calculation	A8.5
Fig. A8.D	Graph — Functions for Shielding Calculation	A8.6
Fig. A8.E	Graph — Functions for Shielding Calculation	A8.7
Fig. A8.F	Self-absorption Distance Z of Disk or Cylinder as a Function of Radius C	A8.8

[redacted]

[redacted]

Fig. A9.A	Pneumatic Shuttle Layout	A9.2
Fig. A9.B	Schematic Layout — Pneumatic Shuttle System	A9.3
Fig. A9.C	Shuttle Transfer Layout — Pneumatic Shuttle	A9.6
Fig. A9.D	Single Contact Shock Absorber Pneumatic Shuttles	A9.7
Fig. A9.E	Anticipated Operating Curves	A9.12
Fig. A10.A	Vertical Hydraulic Rabbit Piping Arrangement	A10.2

[redacted]

PREFACE

This Handbook for the Materials Testing Reactor has been put together at the request of the MTR Steering Committee.* It was the feeling of the Committee that the principal purposes for the report should be (1) to give a semidetailed description of the reactor, and (2) to explain, in so far as possible, the reasons for the design. In order to carry out these purposes the Handbook has been divided into a series of chapters and appendixes as follows:

Chapter 1 presents a general description of the reactor and its auxiliaries and an account of the administrative history of the project.

Chapter 2 gives a description of the reactor as it is now being built. While this chapter inevitably gives some of the reasons for the present design, the main background and experiments leading to the MTR are described in Appendixes 1 through 6.

Chapter 3 describes the experimental facilities provided in the reactor. Some facilities that have been proposed and will probably be built later are described in Appendixes 9 and 10.

The various aspects of the physics of the reactor are described in Chapter 4, which leads up to the control of the reactor discussed in Chapter 5. Some general nuclear data are given in Appendixes 7 and 8.

Chapters 6 through 10 are devoted to a description of the necessary auxiliary units to the reactor proper and the reasons for their design.

Extensive bibliographies and lists of reference drawings are given at the end of each chapter so that the reader, if he wishes, may find further details in original reports and memoranda. In addition, it is planned that the Project File, which has been maintained by the Chairman of the Steering Committee, will be transferred to the operating company at the MTR site. This file includes all reports, memoranda, and correspondence dealing with the Project.

*S. McLain, Chairman; M. M. Mann, ORNL, and J. R. Huffman, ANL, members; W. H. Zinn, ANL, and A. M. Weinberg, ORNL, Ex-officio members.

[redacted]

Chapter 1

INTRODUCTION — GENERAL DESCRIPTION AND HISTORY OF THE MTR

1.1 GENERAL DESCRIPTION OF THE REACTOR, ITS LOCATION, AND FACILITIES

1.1.1 Brief General Description of the Materials Testing Reactor. The Materials Testing Reactor as currently (Jan. 1, 1951) being constructed at the Reactor Testing Station (RTS), Arco, Idaho is a high-flux heterogeneous enriched-fuel reactor. The active part of the reactor consists of closely packed vertical-plate assemblies, the individual plates being made of aluminum-clad uranium-aluminum alloy. The plates are spaced to allow water flow between them, the water thus serving as both coolant and moderator.

Immediately surrounding the small enriched lattice is a primary reflector of beryllium metal which is also water cooled. This whole assembly of active lattice and beryllium reflector is mounted in a tank system through which the water flows and which contains the control rods and their bearings. Outside the tank system are a secondary reflector of graphite, a thermal shield, and a biological shield, the whole forming an approximate cube of about 34 ft to a side.

As the name implies, the reactor has been designed primarily to allow the testing of various materials in high-intensity radiation. To accomplish this purpose about one hundred experimental holes have been provided, some going through each of the four walls and top and bottom of the reactor.

Six horizontal beam holes, a through facility, and some rabbit holes allow experiments to be performed within 2 in. of the active lattice. In addition, where the highest possible fast flux is required, spare control rod holes and unused spaces in the active lattice can be utilized if desired.

Six down-beam holes, available from balconies on the north and south faces of the reactor, go to the wall of the tank and "see" the lattice through 2-in. holes in the beryllium. The remainder of the holes, mostly available from the top of the reactor, penetrate into various parts of the graphite zone.

The east wall of the reactor has access to a thermal column which is provided with nine horizontal and two vertical access holes. Depending upon future demands, space is available through the west wall for a shielding facility or another thermal column.

The entire reactor structure is housed in a steel and concrete building approximately 130 ft square with a laboratory building adjoining. Other buildings at the site house water demineralizing and cooling facilities, air pumping and filtering equipment, steam, sewage disposal plants, etc.

The evolution of this reactor from its initial concept to the present design is described in Section 1.2.2.

1.1.2 Location.* The MTR site is located in block 14 of a plot formerly known as the U.S. Naval Proving Ground. This plot, now renamed the Reactor Testing Station, is located in the Snake River Valley plain of southeastern Idaho. The Idaho Office of AEC has established its Central Facilities at the former naval test firing station located approximately 2 miles north of U.S. Route 20. The MTR site is about 4 miles north and slightly west of Central Facilities. Pocatello, the largest town in the area and most likely local supply source, is approximately 70 road miles from the MTR site. The other towns of size in this area are Blackfoot (43 road miles from the site) and Idaho Falls (50 road miles from the site). The total population of this section of Idaho numbers about 68,000.

1.1.3 Availability of Utilities and Supplies. The Reactor Testing Station is linked to the three towns previously mentioned by U.S. Routes 20 and 191. These are both considered all-weather highways. There is also a new road direct from Idaho Falls to the Testing Station. The AEC Central Facilities area is already served by a Union Pacific branch line. A spur line runs to the reactor site. Approximately forty-one motor freight and passenger carriers are certified to operate in this area.

1.1.4 AEC Central Facilities. For the benefit of the MTR and other reactor projects on this station, the AEC has set up Central Facilities on the location formerly occupied by the naval firing station. The items included in this group of facilities are those which are of benefit to all projects on the site. The intent is that Central Facilities can give better and more economical service than if similar smaller facilities were set up at each reactor project site.

It is currently (Jan. 1, 1951) planned that Central Facilities will serve the functions and provide the facilities listed below.

Craft shops. These include carpenter, pipe, sheet metal, electrical, and automotive shops. The shops will be equipped with machines and staffed to do all types of maintenance work and limited alterations.

* Sections 1.1.2 through 1.1.7 contributed by ANL.

Machine shop. A large machine shop is planned to take care of all maintenance, machining, equipment rework, and the bulk of original machine work necessary for the projects on the Reactor Testing Station.

Electronic and instrument shop. This shop is planned to service health physics instruments, radio equipment, alarm system, intercommunication system, etc. This includes all equipment directly under the jurisdiction of the AEC. Servicing of reactor, process, and experimental instruments will be handled by the operating contractor of each particular reactor project.

Stores and supplies. Central Facilities will furnish janitorial and office supplies; standard spare parts such as small motors and pumps; fabrication materials such as lumber, steel, and nonferrous metals; and operating supplies such as fuel oil, gas cylinders, acids, and caustic.

Communications. This will include a central switchboard exchange for long distance calls, teletype service, and mail service from Idaho Falls to the various projects.

Transportation. This will include a motor pool of light and heavy vehicles. Some of the light vehicles will be permanently assigned to projects. All equipment will be maintained at the Central Facilities garage.

Refuse disposal. This will include disposal of radioactive solid and liquid wastes as well as garbage and waste paper.

Road maintenance. This will include all road repairs and snow removal.

Health service. This will include a dispensary and laboratory. A doctor will be in charge full time and will have sufficient equipment for periodic physical examinations.

Health physics. It is currently planned that all project health physics functions will be handled by Central Facilities.

Fire protection. A central fire department is to be provided. To augment this, each site will have one pumper truck with one full-time fireman per shift.

Meteorology. The U. S. Weather Bureau will handle this function.

Photographic and reproduction service.

Security. A central guard and security system exists from which guards will be assigned to each reactor site. Screening and clearing of visitors is carried out at Central Headquarters.

1.1.5 MTR Facilities. Following is a short summary of MTR facilities, all of which are more fully discussed in later sections of this handbook.

Roads and parking lot. A two-lane blacktop road runs from AEC Central Facilities to the MTR site. A parking lot is located outside the west perimeter fence directly adjacent to the main entrance gate. Two-lane blacktop roads provide access to all areas within the site that require vehicle services. A 10-ft-wide patrol road is provided along the inside of the perimeter fence.

Yard facilities. All process piping, sewer lines, fire lines, and electrical distribution lines are located underground. The only exception is the circuit for the perimeter fence lighting system. Fire hydrants and hose houses are placed at strategic locations throughout the site. An electric substation that transforms power from 138 kv to 2400 volts is located on the site.

Safety and security. A security building is located near the main entrance gate. This building will provide guard quarters, a first aid station, space for telephone and radio communications equipment, and quarters for firemen and a fire truck. Additional security is to be provided by means of two personnel control houses; one will be located at the main site entrance and one at the entrance to the exclusion area.

Canteen. A small canteen is provided on the site. Cafeteria type service is provided, with foods that are prepared at Central Facilities.

Steam plant. This building houses three 16,500-lb/hr oil-fired steam generators. The steam enters a 135-psi steam distribution system for site-wide use. This building also contains an emergency Diesel electric generator and the plant and instrument air compressors.

Water supplies and treatment. Two deep wells are located on the site; each one is capable of delivering the normal site demands. Water passes through reservoir tanks and is pumped from there to the Demineralizer Building. Here one portion is demineralized, another chlorinated, and a third softened and chlorinated. The reactor uses demineralized water in a recirculating cooling system. An overhead working reservoir in this loop provides the flow

of water to the reactor. The reactor water is cooled in a flash evaporator system located in the Process Water Building. Cooling water for the evaporators is reused after it is circulated through a cooling tower. The fire loop and canal utilize raw water. The water in general use throughout the site is blended, partially softened, well water. The water used in the cooling-tower system is acid-neutralized well water.

Reactor Building. This building houses the reactor and its control room auxiliaries. It is designed for the use of experimenters. A large amount of open floor space is available on both the ground and basement levels. A 30-ton crane is available for handling shielded coffins, etc. A canal containing 18 ft of water is located at the basement level and extends outside the building. This canal contains the equipment necessary for handling the spent fuel elements from the reactor.

Reactor Building wing. This building is largely a laboratory and shop facility. It has, in addition to the laboratories designed for low-level work, a machine shop, an instrument shop, a staff shop, a small glass shop, men's and women's locker rooms, stores, shipping and receiving rooms, and a counting room. A basement located under the entire first floor contains a battery room, fireproof storage vault, and heating and ventilating equipment for both the Reactor Building and wing building.

Water disposal. Sewage is treated in a sewage-treatment plant located outside the east perimeter fence. Any waters suspected of being radioactive are monitored; if found to be highly active, they are retained in underground tankage. Waters that are only slightly radioactive are discharged to a retention basin which provides both a decay period and dilution. Both the retention basin and the sewage-disposal plant discharge their effluent to a leaching bed located directly east of the southest corner of the perimeter fence.

Hot gas disposal. The reactor-cooling air is discharged to the atmosphere from a 250-ft stack located on the site. Contaminated air from the laboratories is treated for removal of acidic vapors and then discharged into the atmosphere via the same stack.

1.1.6 Climate. The area is semiarid with an average yearly precipitation of about 10.4 in. Precipitation varies from 15 to 20 in. in wet years

to 5 to 10 in. in dry years. Floods are unlikely, as the maximum precipitations ever recorded were 2.6 in. in one month, 2/3 in. in 24 hr, and ½ in. in 1 hr. Snow has fallen in all months except August, but practically none has occurred from June through September. The average yearly snowfall is 35 in. The maximum snowfall in one month was 26 in., and the maximum depth of snow on the ground at one time was 19 in.

At Pocatello the average relative humidity ranges from 53 to 79% in the morning (8:00 A.M.), 26 to 71% at noon, and 24 to 72% in the late afternoon. The higher average relative humidities occur in winter and in the early morning.

Because of the slightly higher elevation of the site area as compared with Pocatello, its situation in the lee of prevailing westerlies, and its distance from the moisture supply represented by the Snake River and its irrigation system, the average wet-bulb temperature at the site is somewhat lower than that of Pocatello, which has a July wet-bulb temperature of approximately 55°.

1.1.7 Geology. The terrain of this area is flat except for the billowy character of the lava and the rather numerous craters and cinder buttes. The relief of the terrain is not more than 5 to 10 ft; the altitude is about 4930 ft above sea level. On both sides of the lava plains, running southwest-northeast, are mountain chains.

1.2 HISTORY OF THE MTR

1.2.1 Need for Reactor. The reactor described in this report is the result of an evolutionary process in the design of a machine conceived for the express purpose of facilitating the conception and design of future reactors for military and peace-time applications. It is of paramount importance that a facility exist which is capable of furnishing quickly a great number of physical, chemical, biological, and engineering data at thermal- and fast-neutron fluxes greater than 10^{14} and high γ-ray intensities, on the basis of which future reactors can be designed within controllable and permissible limits of uncertainty in operating characteristics. The Materials Testing Reactor (MTR) has been designed and will operate for this prime purpose. In addition, there are incorporated features which provide for the following

experimental lines of investigation:

1. Production of sizeable amounts of the fissionable isotope U^{233} for the next stage in the study and utilization of a potentially more plentiful material than U^{235}.

2. Production of sizeable amounts of high-specific-activity radioisotopes which are not recoverable directly from fission products.

3. The acquisition of scientific and engineering experience in design, construction, and operation of an enriched reactor at elevated power levels (30,000 kw) and neutron fluxes ($> 10^{14}$), which is possible for the first time in the MTR.

The preliminary designs for a high-flux enriched reactor, which would produce the U^{233} isotope through conversion of thorium, were begun in 1944 as a consequence of the fear that Pu^{240} would constitute a serious contaminant in the plutonium product from Hanford reactors. It was soon decided that the simplest large-scale converter would be a plate reactor, water moderated and heavy water reflected, with a thorium blanket on the outside. Aside from the reflector, which was subsequently changed to beryllium, the present MTR design largely follows the original design philosophy for the U^{233} production unit with such additional design features as to meet the needs listed above.

1.2.2 Design and Administrative History. Late in 1944 the Chemistry Division at Clinton Laboratories proposed the construction of a 50-kw homogeneous uranium–heavy water reactor whose main use would be to produce easily extractable fission products. Work on a 50-kw homogeneous reactor continued until 1945, when it was decided that the power of the reactor should be raised sufficiently to demonstrate the feasibility of a thermal energy breeder. The power output of such a breeder with a three-year doubling time (of fissionable material produced to fissionable material consumed) is about 10,000 kw.* This was set as the early goal for a homogeneous reactor. The thermal-neutron flux in such a reactor was calculated to be about 2×10^{14} neutrons/cm^2-sec. The reactor was conceived as a prototype homogeneous reactor and thermal breeder; in addition, it would be an experimental tool with a flux greater that that of the Canadian reactor (NRX).

*Doubling time formula is given approximately by $T = 10^6/(P/M)G$, where P = power in kilowatts, M = critical mass in kilograms, G = breeding gain, and T is measured in days.

Considerable advance was made by the theoretical group in the following problems:

1. The dimensioning of control and safety systems.
2. Stability during operation.
3. Temperature, density, and concentration coefficients of the reactor.
4. The effect of a thimble (side hole) on reactivity.
5. Utilization of the leakage neutrons in a thorium rod assembly.

Additional problems arose which led to difficulties in conception of control and technology of a homogeneous reactor. Principally, there was the instability of a homogeneous reactor which contains bubbles of gas arising from the disintegration of solvent molecules and the generation of fission products. While the reduction of power to a 50-kw level would have eliminated the problem of bubbling instability, this would have defeated the purposes of such an enriched reactor, i.e., high-thermal and fast-neutron fluxes and all the advantages which follow from them. Accordingly, the alternative was to go ahead with another type of reactor which would produce similar flux conditions, and use it to study the problems of the homogeneous reactor by small-scale experiments at high flux. A heavy water—moderated and heavy water—cooled enriched *heterogeneous* reactor was first designed.

The critical experiments which were performed as a prelude to the heterogeneous reactor design were carried out in the spring and summer of 1946; they are summarized in Appendixes 1, 2, and 3. These experiments were designed to obtain empirical information on features such as:

1. The critical size of enriched reactors as a function of concentration of fissionable isotope U^{235}.
2. The effectiveness of the heavy water reflector.
3. The temperature coefficient of reactor reactivity.
4. The effectiveness of control rods.
5. The effect of holes such as thimbles in the active region and experimental recesses leading through the reflector.
6. The neutron flux distributions throughout the reactor.
7. The effect of poison (absorber of neutrons).
8. The measurement of the utilization of thermal neutrons in a ring of thorium rods in the heavy water reflector around the active part of the reactor.

The initial set of critical experiments described in Appendix 1 provided invaluable information for future experiments of the same type which would have to be performed prior to or along with designs for major reactors of the enriched class. The essentially primitive features of the experiment consisted in the reactor being hand-loaded and manually controlled. In later critical experiments, which were undertaken when the design of the MTR began to crystallize into permanent form, an excellent opportunity became available to develop and test servo mechanisms for pile operation, particularly, the control of reactors capable of fast periods arising from the considerably increased excess reactivity required of an enriched reactor of the MTR type.

On the basis of theoretical calculations by the Physics Division, the Technical Division of Clinton Laboratories submitted a design proposal in May, 1946 for a high-flux thermal reactor of heterogeneous core, light water—cooled and heavy water—moderated and —reflected, with a ring of thorium rods for U^{233} production. The use of light water as a coolant was believed preferable to the use of heavy water because light water increased the operation flexibility of the machine. A brief description of this proposal is given.

The nuclear fuel, U^{235}, was to be contained in "sandwiches" consisting of a central sheet of aluminum-uranium alloy, clad on both sides with aluminum to confine the fission products and prevent corrosion of fuel elements. These thin sandwiches were to be coiled into spirals having some clearance (water passage) between successive turns of the spiral, and the spirals would be placed in and secured to aluminum tubes of about 2 in. diameter. About thirty such tubes would make a triangular lattice of about 6-in. spacing. The spirals of fuel were to be removed when the isotope enrichment of U^{235} fell to about nine-tenths of the original value. Such "spent" spirals of fuel were to be processed for U^{235} and fission products, and the U^{235}, after the addition of new U^{235}, would be returned for incorporation into a new fuel plate spiral and another cycle through the reactor. The tubes were to be considerably longer than the uranium-bearing spiral which they contained, and they would pass vertically through a cylindrical aluminum tank with their upper ends protruding for connection to the cooling-water supply.

The cooling water would be discharged from the lower end after passing through the spiral passages of the fuel plates. The aluminum tank was to be about 61½ in. high by 69 in. in diameter and filled almost to the top with

heavy water to act as moderator and reflector. Piercing the tank vertically outside the uranium lattice would be a circle of tubes similar to the fuel tubes to contain thorium for production of U^{233} by capture of leakage neutrons. The fuel required was estimated at 3 kg of U^{235}, and, at a maximum total power of 30,000 kw, the consumption of the fissionable isotope U^{235} would be about 30 g per day. The thermal-neutron flux would be about 2×10^{14}, and the fast or virgin flux would be about 1.5×10^{13}.

Upon critical examination of the above design, it was pointed out by Prof. Eugene Wigner that an important gain in fast flux could be obtained by using light water for both coolant and moderator. This change would result in a smaller reactor, and because fast (virgin) flux is proportional to power per unit volume, a 30,000-kw reactor of the proposed type could produce a fast flux of approximately 1×10^{14} and a thermal flux about equal (2×10^{14}) to that of the previous design. This could be accomplished by fabricating the uranium-aluminum alloy into flat aluminum-clad fuel plates, and then putting the plates close together. In this way a fuel unit would assume the shape of a long rectangular pipe with the parallel fuel plates brazed into two opposite sides. A rectangular fuel unit has considerable structural advantages in assembly of a core, allowing for close arrangement and hence smaller volume. In addition, a further volume decrease is gained with light water moderation.

Actually, in the previous design with heavy water moderation and reflection, the reflector merely provided space for experiments that could be realized otherwise. In August, 1946 it was therefore decided to eliminate heavy water altogether, decrease the core volume by arranging flat fuel plates with close spacing in a rectangular array to be light water—cooled and —moderated, and to make the reflector out of beryllium. The decision with respect to beryllium was made possible by the rapidly improving situation in 1946 in the metallurgical techniques of handling and fabricating this metal on a production basis of tons rather than pounds.

Beryllium is more effective than heavy water as a reflector; it has good corrosion resistance, it can withstand radiation damage more effectively than graphite, and, like heavy water, it supplies additional neutrons by virtue of the γ-ray neutron (γ,n) reaction in which neutrons are emitted by beryllium under the γ-ray irradiation. [The (γ,n) threshold in beryllium is approximately 1.7 Mev.]

Simultaneously, the Technical Division commenced redesign of the basic reactor and its auxiliaries.[1,2] The design and fabrication of the multiplate fuel assembly and of the beryllium reflector assembly were two of the most difficult problems which arose.

Thus, by the summer of 1946, the design for the experimental high-flux reactor had evolved from an initially homogeneous-fluid reactor to an all-metallic rigid machine aside from the cooling fluid (ordinary water).

The use of light water moderation and cooling with beryllium reflection initiated an intensive theoretical analysis, on the part of the Theoretical Group of the Physics Division at Clinton Laboratories, of the expected characteristics of such an enriched reactor. At the same time, the program of critical experiments was expanded considerably in scope and facilities to provide experimental information and check on theory both as to basic principles and detailed conclusions. The experiments are described in Appendix 2.

While the critical experiments were going on, the AEC assigned the Kellex Corporation to work on the high-flux reactor early in 1947 as design contractor. Monsanto Chemical Company, the contractor for operation of Clinton Laboratories, was to be the construction manager. Design work continued throughout 1947 under this contractural arrangement so that by the fall of 1947 the design was very well advanced.

Between November, 1947 and January, 1948 certain administrative decisions were made which changed plans for construction of the MTR or High Flux Reactor at Clinton Laboratories. The Kellex Corporation was withdrawn as design contractor in November, 1947. On December 27, 1947 the AEC announced a decision to centralize reactor development at Argonne National Laboratory (ANL). This included responsibility for the High Flux Reactor. It was also announced that Monsanto Chemical Company would terminate its direction of Clinton Laboratories and that the Carbide and Carbon Chemicals Division of the Union Carbide and Carbon Corporation would assume direction early in 1948. The name of the laboratory was officially changed to Oak Ridge National Laboratory (ORNL).

Work on the High Flux Reactor continued at ORNL during early 1948, and also at ANL toward the latter part of 1948. Further critical experiments for the verification of design choices and the design and construction of the High Flux Reactor mock-up were carried on at ORNL. The critical experiments

were directed toward the study of the characteristics of small enriched reactors which simulated the structure of the proposed High Flux Reactor. These experiments were performed to confirm several of the results derived from theoretical considerations (MonP-272) and also to obtain empirical knowledge of certain features of the High Flux Reactor which were not readily calculable because of complications of geometry or composition.

The site of the reactor was at the time left in some doubt. Although a site near Chicago was considered, the opinion of the Reactor Safeguard Committee was that a reactor of this power level ought not to be placed near a large city. Since at this time the Idaho Reactor Proving Grounds was in the process of being established, it was decided to locate the MTR at this site.

It was recognized further by the AEC that the problems of radiation effects in materials of construction were among those foremost in the field of reactor development. Shortly after a meeting presided over by George Weil at ANL in October, 1948, at which the projected radiation-damage experimental needs were reviewed, it was decided to proceed with completion of design and construction of the High Flux Reactor. In recognition of one of its prime purposes, the machine, which for a short time had been called the Reactor Development Reactor, was renamed the Materials Testing Reactor (MTR).

Thus in November, 1948 a directive was issued to ANL to proceed with the project. It was further directed that ANL and ORNL form a working partnership for this project in order that advantage might be taken of the facilities and experience at ORNL peculiar to this reactor.

In accordance with the directive, the managements of the two laboratories organized a Steering Committee for the project. The Committee consisted of the following people: Dr. Stuart McLain, Chairman; Dr. J. R. Huffman, ANL, to supervise project work at ANL; Dr. M. M. Mann, ORNL, to supervise project work at ORNL. Dr. W. H. Zinn and Dr. A. M. Weinberg, acted as ex-officio members and to guide the Committee to solutions of many difficult problems.

The Committee was authorized[1] by ANL and ORNL to discharge the following responsibilities:

1. To organize the efforts of ANL and ORNL in completing the design of the MTR, its immediate associated facilities, including the building and site plans, and carrying out all development work and tests necessary.

2. To negotiate a contract or contracts for the engineering design and construction of the reactor and its facilities as described above.

3. To transmit information and specifications to the contractor or contractors.

4. To approve all final drawings and materials and construction specifications submitted by the contractor or contractors.

5. To negotiate for the procurement of special materials obtained through the AEC or its agencies and to approve the specifications for these materials.

6. To inspect the construction of the reactor and its facilities and suggest and approve any necessary changes in collaboration with the design contractors.

7. To supervise the writing of the design and operating manuals.

8. To supervise the initial tests and operation of the reactor and authorize any necessary changes.

9. To test and accept the final plant from the contractor or contractors in respect to its functional and operational adequacy.

At the time the Steering Committee was organized no AEC operations office had been formed for the Reactor Testing Station and a site hadnot been selected. The Committee was therefore the only group in existence which was qualified to prosecute and/or procure pertinent information for the AEC relative to the items listed above. Subsequently the Idaho Operations Office (IDO) assumed responsibility for either all or portions of items 2, 3, 6, and 8.

Meanwhile, the Committee apportioned the technical work of the project between ANL and ORNL in the following manner: ORNL was assigned responsibility for the reactor structure, including the reactor proper, the beryllium reflector, the reactor tanks, the graphite reflector, the thermal shield, the concrete shield, and major items contained therein. ANL was assigned the reactor cooling-water and cooling-air systems, some experimental facilities within the reactor, the reactor building, and all supporting facilities and buildings on the MTR site.

In order to minimize difficulties of overlapping responsibility, specific assignments in merging areas were made as follows:[4]

1. Experimental hole plugs (except the 3- by 3-in. vertical facility) and coffins would be designed by ANL. The experimental hole liners would be designed by ORNL.

2. The experimental shielding facility would be designed by ORNL.

3. ORNL would design channels for the pneumatic rabbits. ANL would carry out the experimental work and design of propulsion equipment. On the hydraulic rabbits, ORNL would design the channels, propulsion equipment, and the conduits to the small canal. ANL would design handling equipment beyond this point.

4. The nominal diameter of the experimental holes given on DRP-64 would be used for the inside diameter of the liner.

5. Spectrometer and slurry experiment facilities in the reactor structure would be designed by ORNL.

6. ANL would design the hot-materials-handling equipment in the basement.

7. Reactor control instruments would be designed by ORNL. The control instruments for the water, steam, and air systems would be designed by ANL.

8. Electrical layout for power, conduits, cables, etc. outside the reactor structure would be designed by ANL. ORNL would specify special power requirements for reactor control.

9. The discharge chute to the canal would be designed by ORNL. All handling equipment in the canal would be ANL's responsibility.

Subsequently, upon request by ANL, ORNL assumed responsibility under item 1 for all plugs except for those facilities containing radiation doors (all HB and DB holes). Furthermore, since the HB and DB plugs essentially determine the liner requirements, it was decided that ANL would specify the liners as well as the plugs for these holes.

The stage was then set for the design contractor, and the Committee expended considerable time and effort during the late winter and spring of 1949 in gathering information relative to a large number of engineering concerns and their capacities and abilities. This information was transmitted to the AEC with recommendations. In the late spring of 1949 the IDO was organized, and IDO assumed the task of contract negotiation.

The Chemical Plants Division of the Blaw-Knox Construction Company was selected as architect-engineer for the MTR in July, 1949, and early in August, 1949 the Committee initiated formal contact and transmission of information to this concern so that engineering design could begin.

The fall of 1949 was spent in the usual opening stages of generalized project planning, preparation of preliminary flow diagrams, and elucidation of special phases of the work for the benefit of the design contractor. Blaw-Knox sent a number of its people to Oak Ridge for periods of a few days to several months to work with ORNL personnel, particularly those in the reactor-control and mechanical-design groups. Blaw-Knox personnel also paid frequent visits to ANL to establish the fundamental design data for ANL's sections of the project.

During this period, the hydraulic and mechanical experiments on the full-scale model (mock-up) of the reactors* at Oak Ridge were drawing to a close, and preparations were underway for a series of critical experiments in this facility.

It appeared proper then to consider the question of detailed design of the reactor proper. ORNL had prepared detailed drawings for and had negotiated and supervised the construction of the mock-up reactor. Furthermore, the details of the reactor tanks and components were essentially "frozen" and subject to changes attendant only to experimental findings from the mock-up experiments or to improvements in materials.

Upon consideration of these facts by the parties concerned (Steering Committee, IDO, ORNL, and Blaw-Knox), it was suggested that ORNL assume the responsibility for design and procurement of the reactor tank sections B, C, and D, the internal components,** and the top and bottom plugs. Tank sections A and E, being fixed permanently in the concrete structure, were considered as part of that structure and consequently remained with Blaw-Knox for detailed engineering.

IDO then issued a formal request to Oak Ridge Operations (ORO) in February, 1950 that ORNL be authorized to carry out this work, and approval was granted early in March, 1950.

Special problems of design and procurement arose next in the field of reactor control instruments. It was first decided that pilot models of these instruments and associated circuitry would be supplied by ORNL. However, early in 1950, in the interest of saving time, ORNL agreed to supply the full complement of special reactor-control instruments and associated circuits (see Controls, Chap. 5).

*See description of mock-up and its purposes in Appendix 4.
**See detailed description of reactor in Chap. 2.

In early 1949 the situation with regard to beryllium technology and procurement had reached a stage such that the Steering Committee felt it advisable to solicit the services of an experienced and ranking metallurgist to coordinate the necessary experimental development and procurement program, and to ensure that the MTR receive acceptable material on schedule. Although beryllium metallurgy had undergone marked progress during the later stages of the war and the years following, a dependable supply of high-grade metal was not yet completely assured, and the techniques of fabrication of complex shapes had not been demonstrated on a production scale.

The Committee was fortunate in obtaining the services of Prof. J. L. Gregg of Cornell University as consultant to ORNL and Metallurgical Coordinator for the MTR; it was due primarily to the efforts of Prof. Gregg that the Committee was able to decide in the early summer of 1949 that hot-pressed (sintered) beryllium could be used for the MTR reflector. The choice of hot-pressed as opposed to extruded material allowed a major simplification of reflector components with attendant reduction of fabrication problems (see Chap. 2).

Another problem of special material also confronted the Steering Committee during 1949, namely, that of graphite for the secondary reflector and thermal column. Techniques of graphite purification had improved considerably in the few years following the war, and ANL was assigned the task of gathering pertinent data and specifications for the various grades of graphite available. Their study resulted in the decision of the Committee to use GBF graphite for the thermal column and that portion of the permanent graphite in front of the thermal column because of its very low induced activity and relatively large diffusion length, these properties being of distinct advantage to experimenters using thermal columns.

It was mentioned above that critical experiments had been planned for the mock-up in Oak Ridge. Preparations for these experiments occupied the fall of 1949, and in January, 1950 this full-scale model of the MTR was brought to criticality. During the spring, summer, and early fall of 1950 this reactor was operated hundreds of times at power levels of a few hundred watts, and many measurements of vital importance to the MTR were made. As an example, it was on the basis of these measurements that the final design details of the graphite and thermal shield were evolved and the overall design of these items was finally approved.

In February, 1950 the Fluor Corporation, Ltd. of Los Angeles, California was appointed by IDO as construction contractor for the MTR, and the first formal contact between IDO, Fluor, Blaw-Knox, and the Steering Committee was made in March, 1950. Up to July 20, 1950 the Steering Committee approved all design and construction drawings before issuance, but after this date, in order to expedite construction, a major portion of this control authority was relinquished.[5] From July 20, 1950 the Steering Committee acted as consultants to IDO, Blaw-Knox, and Fluor, except that the responsibility for the conceptual design process and functional layouts remained with the Committee.

Ground was finally broken for the MTR in May, 1950. As of Jan. 1, 1951 the Reactor Building steel structure was completed and the side walls were being erected. Concrete had been poured for the sub-pile room ceiling, and preparations were being made to set tank section E. Completion of all construction is scheduled for Oct. 1, 1951.

1.3 REFERENCE REPORTS

(1) Leverett, M. C. and Huffman, J. R., *Process Design Information 1000 Project - General and 1100 Area*, MonN-262, March 4, 1947.

(2) Huffman, J. R., *et al.*, *Feasibility Report on Clinton High Flux Pile*, MonT-433, December 1, 1947.

(3) McLain, S., *Minutes of First Steering Committee Meeting*, ORNL CF-48-12-83, December 2, 1948.

(4) McLain, S., *Minutes of Fourteenth Steering Committee Meeting*, ANL-SM-26, June 1, 1949.

(5) Jones, W. W., *Blaw-Knox Conference Notes No. 75*, July 7, 1950.

(6) Winkleblack, R. K., *Site Survey Study*, ANL-SM-20, April 12, 1949.

(7) Smith, Hinchman, and Grylls, Inc., *Survey Report - Fort Peck, Montana; Pocatello, Idaho Sites*, March 26, 1949.

(8) Leyse, C. F., *Meteorological Conditions at the Reactor Test Site*, ANL-EKF-54, May 10, 1950.

1.4 REFERENCE DRAWING

(Blaw-Knox Construction Company Drawing)

DWG. NO.	TITLE
BKC-3150-801-50	Yard, Key Plan

Chapter 2

ENGINEERING DESCRIPTION OF THE REACTOR

In this chapter of the handbook an attempt will be made to describe the structure and function of all the parts of the reactor enclosed within and including the biological shield. Since this is not a construction manual, details not required to explain the functions of any part will be omitted. Such details can be obtained from the reference drawings and reports listed at the end of this chapter.

The general design of the reactor is shown in Figs. 2.A, B, C, and D,* which are a north-south vertical section, an east-west vertical section, a horizontal section, and a pictorial cross-section, respectively. Overall dimensions are given in Fig. 2.A, but is should be noted that in all construction drawings the horizontal centerline of the reactor (i.e., the centerline of experimental holes HB-2 and HB-5 of Fig. 2.A) is arbitrarily taken as elevation 100 ft. On this basis the first floor is at elevation 96 ft 6 in. and the top of the reactor is at elevation 120 ft 6 in.

It will be seen from these general drawings that the reactor is divided into four main sections:

1. The tank system containing the active lattice and beryllium reflector, both of which are water cooled.
2. The graphite reflector, consisting of a replaceable pebble zone and a permanent block graphite zone, both air cooled.
3. The thermal shield which forms a heavy iron box around the reactor, except where the tank sections extend through it.
4. The biological shield.

The various experimental facilities and the canal will be discussed in Chaps. 3 and 6, respectively.

2.1 REACTOR ENCLOSURE TANK

Tank Sections A, B, C, D, and E

The general tank system, approximately 30 ft tall, is shown in Figs. 2.A and B while the details of the construction, gasketing, etc. are shown in

*For convenience in reading, Figs. 2.A through 2.F are placed at the end of the chapter.

Fig. 2.E. The tanks provide the means of funneling water through the active lattice and beryllium and provide supports for the active lattice, the reflector, and the control rod bearings. They are bolted together and by the use of aluminum gaskets are made into a watertight system. The design of the gaskets and torque required on the flange bolts have been tested at ORNL in a full-size mock-up test.*

2.1.1 Tank Sections A and E. Both of these tank sections[1] are made of stainless steel and are to be permanently embedded in the concrete of the biological shield. However, they are initially supported independently of the concrete on a structural steel frame.[2] The bottom of this frame is shown under tank section E in Fig. 2.B and the vertical members are shown just outside the thermal shield in Fig. 2.C. Both tank sections are to be welded to this frame before the concrete is poured.

Tank section E is required in the structure both to act as a water exit under the active lattice and to provide space for the control rod extensions. For ease of construction and smooth water flow, it is made the same diameter as tank section D.

Tank section A serves two purposes: (1) as an entrance for the cooling water stream, and (2) as a container for the radiation shield (water) used during shutdown operations. During shutdown approximately 17 ft of water will be required as a cover for the active lattice. Tank section A is built with water inlets and overflow lines near the top to fulfill this requirement. It will also be noted that tank section A is large enough in diameter to permit tank sections B, C, and D to be put in or lifted out through it. This provides for mounting the lighter tank sections B, C, and D after tank sections A and E have been finally set, and, in case of damage, permits replacement of these tanks.

The proper operation of the control rods depends upon the alignment of the tank sections, and it is essential that the top flange of tank section E be set accurately horizontal and that tank section A and all the beam holes in the concrete be aligned accurately to this flange.

2.1.2 Tank Section B. Tank section B is a bellows type expansion joint made up of two convolutions of thin stainless steel welded to stainless steel

**MTR Flange Mock-Up Test*, ORNL memo, to be issued.

flanges for attachment to tank sections A and C. This permits free thermal expansion and contraction of the tank sections without applying excessive stress to the structural setup. Removal of this section permits filling of the pebble zone.

2.1.3 Tank Sections C and D. These tank sections are essentially one in function but are split for ease in manufacturing. The split between C and D is so dimensioned that the support castings for the active lattice can be mounted conveniently. These sections are hollow aluminum cylinders of 1 in. wall thickness and 54¼ in. I.D. The diameter was determined by the active lattice and beryllium reflector requirements. The wall thickness was determined by the strength required to sustain the water pressure and the weight of the support castings, but it is made as thin as possible, consistent with these requirements, so that the neutron absorption will not be too great. In general the tank has a 1-in.-thick wall except for a 1-ft band around the center where the wall is 1¼ in. thick.

Tank section D is pierced by several holes to provide experimental facilities close to the active lattice. Most of these, for the six HB thimbles, are at the centerline of the lattice and pierce the thick section of the tank wall. These six thimbles are extruded aluminum tubes of 6 in. I.D. and 5/16 in. wall, sealed at the end adjacent to the lattice by a 7/8-in.-thick aluminum plate set parallel to the lattice face. They are welded into the tank wall in position to receive the ends of the HB liners. As described in Section 2.4.1, the beryllium reflector is machined to fit around these thimbles with sufficient clearance for proper flow of cooling water (see also Section 2.7.1).

In addition to the thimble holes, tank section D is pierced by the aluminum bar containing the HR-1 and HR-2 pneumatic rabbit holes and by the HT-1 facility. The aluminum bar containing the rabbit holes is shown in Figs. 2.D and 2.4.A. It reaches to the bottom of the reflector merely to simplify the beryllium machining and stacking. The rabbit holes themselves pass just under the extension of HG-9 and within 1 in. of the east face of the active lattice.

The HT-1 facility through the tank is a square aluminum tube with approximately 4¾ in. inside dimensions and ½-in.-thick walls. It runs just under the beam holes close to the west face of the active lattice, as shown in Fig. 2.D.

Alongside the lattice the inner wall is extended down to the bottom of the reflector to facilitate the packing of the beryllium. Both the bar containing HR-1 and HR-2 and HT-1 tube are welded into tank section D, keeping this a watertight unit.

In order to give support to the inner ends of the DB, HR-3, HR-4, HG-5, HG-6, and HG-9 liners, sockets are welded onto tank section D at appropriate places. Some of these are shown in Fig. 2.D.

2.1.4 Top and Bottom Plugs. The top and bottom plugs complete the watertight shell around the active lattice and form part of the support system for the control rods.

The bottom plug, shown in Fig. 2.E , is a hollow stainless steel shell filled with lead shot to complete the shielding requirements under the reactor. Its total weight is approximately 6 tons, and, while it can be removed, only the direst necessity would justify such a step. Through the bottom plug pass the discharge chute, hydraulic rabbit tubes, and the monitor tubes (see later sections for description of these). This plug also supports the shim-rod lower shock absorbers (see Section 2.3.3).

The top plug (see Fig. 2.F) serves not only as the upper tank closure but also as the primary support for the control rods and their drive mechanisms. Like the bottom plug, it is a hollow stainless steel shell partially filled with lead shot to fulfill shielding requirements. On this plug is mounted a platform which supports the control motors, limit switches, etc. for the control rods. Underneath the top plug on four supports hangs the spider which holds the bearings for the 12 control rods (see Section 2.2).

Since the top plug must be taken off in order to replace fuel elements or control rods, it is designed to be easily lifted by the overhead crane and lowered to a "dry dock" on the first floor.

2.2 THE ACTIVE LATTICE AND SUPPORTING STRUCTURE

The fuel for the reactor will be 95.3% enriched uranium alloyed with aluminum and made up into aluminum-clad plates 0.060 in. thick.* Because of

*A brief description of the development and manufacturing process of the fuel plates and assemblies is given in Appendix 6.

the picture-frame type of construction used, no uranium is exposed to the cooling water. Eighteen of these plates, each approximately 2.8 in. wide and 24-5/8 in. long, will be made into a single fuel assembly. The plates, with a 0.118-in. space between them, are brazed into aluminum side plates, and the assembly is then equipped with aluminum end boxes. A cross-section of the assembly is shown in Fig. 2.2.A, and a picture of a completed fuel piece is shown in Fig. 2.2.B.

Referring to Fig. 2.2.B, the bottom end of the fuel assembly is seen near the lower right-hand side of the picture. Both end boxes are, of course, open to allow water to pass freely through the assembly from top to bottom.

Each of the fuel assemblies contains approximately 140 g of U^{235}, and it is expected that the MTR will contain about 23 of these units when in full operation. The arrangement of these units into a lattice and their supporting structure can best be seen by referring to Figs. 2.D and E.

Referring to Fig. 2.D., it will be seen that the end boxes of the fuel assembly fit into the upper and lower assembly grids. The spring section of the upper end box (see Fig. 2.2.B) allows each assembly to be held firmly and still allows for expansion and tolerance limitations. The eight square holes in the upper assembly grid are for the shim-safety rods which extend all the way through the reactor.

The actual assembly of all these parts is best seen in Figs. 2.D and E. The lower support casting, which is bolted to tank section D, supports the lower assembly grid and the lower bearing grid. The upper support casting, which rests on an extension from the upper flange of tank section D, supports a removable assembly of the upper assembly grid, the grid spacer, and the upper bearing grid. This assembly can be locked in place or lifted as a unit by the upper locking mechanism.

A further set of control-rod guide bearings, mounted in the spider, is fastened to the top plug by four long support tubes. When the top plug is lowered, the four corners of the spider fit over pins on the spider support ring, which then holds the spider in the correct position. In order to allow for machining tolerances and slight errors in lowering the top plug, the spider is actually hung on the support rods by rather light springs. In this way, while the bearings and spider are attached to the top plug, they are

DWG. #10388

[redacted]

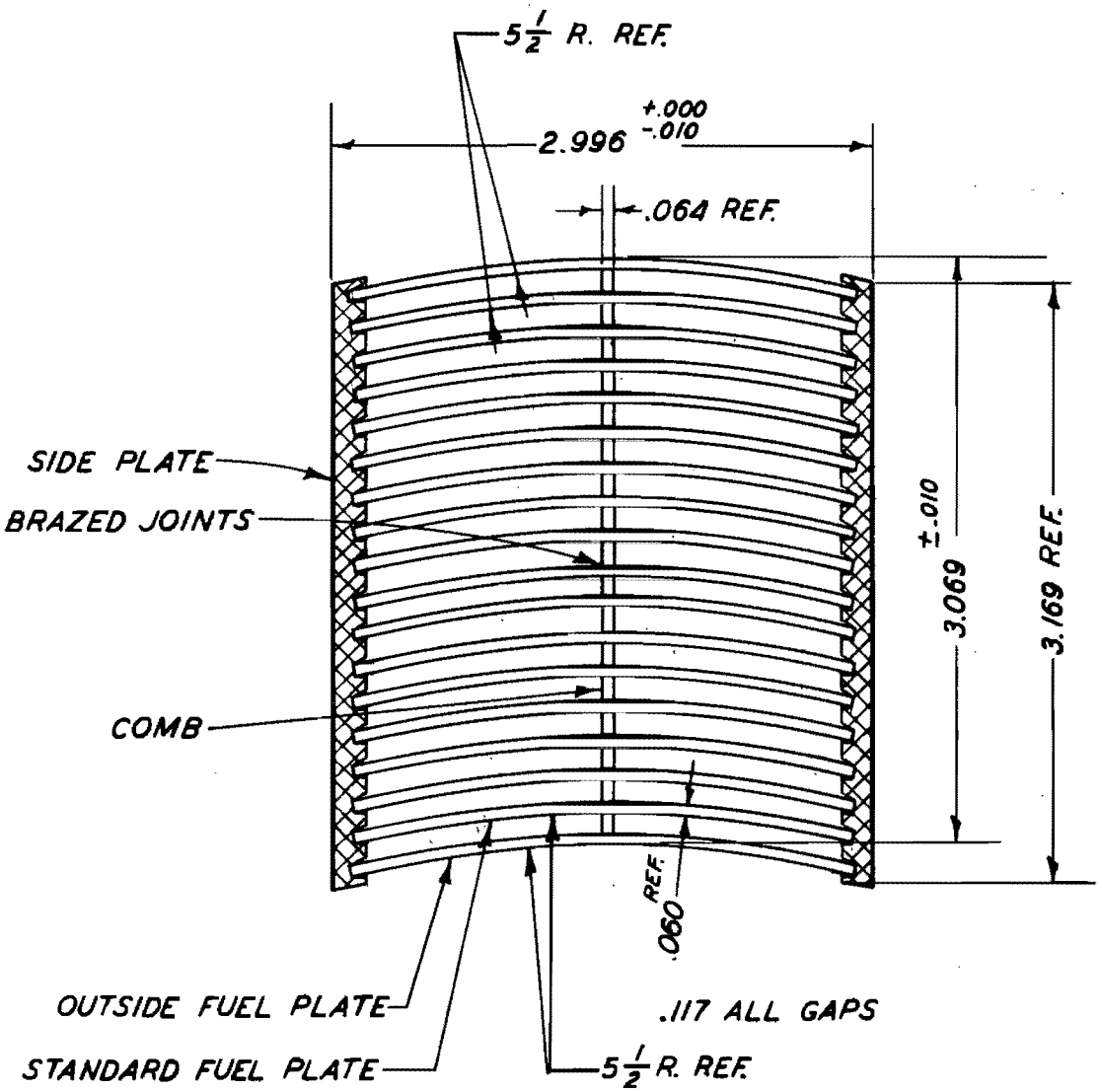

FIG. 2.2.A

M.T.R.

CROSS SECTION OF FUEL ASSEMBLY

OAK RIDGE NATIONAL LABORATORY

FIG. 2.2.B

FUEL ASSEMBLY UNIT NO. 136

Y-1805

aligned by the rigid spider support ring which is bolted to the top flange of tank section B.

In initial assembly, since the control rods must operate freely, it is essential that the lower shock absorbers mounted on the bottom plug and all bearings in the various grids line up accurately. The lower shock absorbers are adjustable as a group and the final doweling of the support grids and top plug will not be made until the system is assembled. It is now planned to assemble and fit tank section D, the upper and lower support castings, and the internal parts of this tank section at ORNL before shipment to Arco. Final adjustment of the shock absorbers and the doweling of the top plug will then be done in Idaho.

Once the system is aligned, fuel is loaded by means of special handling tools in the following manner: With the top plug off, the upper grid assembly is lifted from the upper support casting and placed on a special support rack mounted on the spider support ring. The shim-safety rods are then placed in position, being supported by the lower grids and the shock absorbers. Finally, the fuel assemblies are lowered into the lower assembly grid one at a time (with due regard to criticality, of course). When enough fuel is loaded, empty spaces in the lattice are filled with beryllium pieces ("L" pieces) of the same shape and size as the fuel elements. When this operation is completed, the upper grid assembly is lowered over the top end boxes and clamped down, the control rods at the same time extending through the upper bearing grid. The top plug, now holding the upper halves of the control rods extending through the spider, is then lowered and bolted down.

Present plans call for a narrow slab loading, nine assemblies long by three wide. The assembly grids allow 45 places (including shim-safety rods) with the long side of the grids oriented in the east-west line. The lattice is to be initially loaded on the north side, thus putting one row of four shim-safety rods in the central line of fuel assemblies. In keeping with this plan, it will be noted that HG-9 is placed off-center as far as the structure is concerned but will "look" at the center of the loaded lattice. In this arrangement, experimental holes HB-1, 2, and 3 and DB-1, 2, and 3 will receive a higher fast flux than the holes on the opposite side which "see" the lattice through two additional rows of beryllium.

Unloading of the reactor is accomplished by essentially the reverse of the above procedure for loading, but, if the reactor has been operated for some time, the fuel elements will be too hot to lift out through the top. In this case they must be lowered through the discharge chute into the canal. An outline of the procedure is as follows: With the shim rods and regulator rods disconnected and resting in their lowest position, the top plug is unbolted, lifted, and carried by the crane to the "dry dock." The upper grid assembly is then lifted from its support casting and placed on the support rack on the spider ring. Before any fuel elements are lifted, the beryllium pieces D-1 and D-2 (see Fig. 2.4.A) are lifted and placed to one side of tank section D. Then the discharge chute plug is lifted, leaving the discharge chute clear to the receiver cylinder in the canal. A fuel assembly or control rod may then be raised clear of the active lattice, moved sideways to the discharge chute, and lowered to the receiver cylinder in the canal. Removal from the receiver into the canal is fully described in Chap. 4.

2.3 THE CONTROL RODS

The MTR control rods are of two main classes, the shim-safety rods and the regulating rods. All of them are designed to lower the reactivity of the reactor when they are inserted, and when fully in, i.e., resting in their shock absorbers, they will overcome an excess reactivity of greater than 40%. It will be shown in Chap. 6 that it is necessary to have approximately 19% excess reactivity built into the reactor; hence the control rods provide an adequate margin of safety.

2.3.1 Shim-safety Control Rods. The shim-safety control rods, as their name implies, serve the purpose of providing both regulation and safety control. It has already been noted that there are places for eight shim-safety rods running through the active lattice. At present it is planned to use two types of rods. Four of them will be constructed to bring fuel sections, each containing 14 fuel plates, into the lattice as they are raised and will be used in the four positions in the middle of the fuel slab. The remaining four will have beryllium in the lower section since they are in the beryllium section of the lattice grid. All eight have cadmium sheet in the upper section, and this section will reside in the lattice when the rods rest in the lower shock absorbers.

The two types of shim-safety rods are shown in Figs. 2.3.A and B. As experience is gained with the reactor, the fuel or beryllium sections of four or five of the rods may be replaced with thorium for production of U^{233}.

The rods as shown extend from the shock absorbers up through the upper bearing grid. They are raised from this position by means of an electromagnet on the bottom of the lifting shaft, which extends through the top plug to the motor drive mechanism. This magnetic clutch provides the "scram" or safety feature of the rods. Its operation will be described fully in Chap. 5. It will be noted that the armature section at the top of the safety rods contains a spring which acts like a universal joint so as to aid proper seating of the magnet onto the top of the rod.

Under normal operation the shim-safety rods are driven by means of the magnetic clutch and vertical lifting shaft by reversible three-phase induction motors and worm drives (see Fig. 2.F). The motors are remotely controlled by reversing contactors, suitably interlocked and having the usual complement of upper and lower limit switches. The advantage of the induction motor is that no accident can make it run in excess of synchronous speed; therefore, the danger of over-speed withdrawal of the shim-safety rods is eliminated. No brake is required since the worm and screw drive is self-locking.

Pertinent data on the shim-safety rods are summarized in Table 2.3.A.

TABLE 2.3.A

Cadmium-Uranium Shim Rod

Weight of rod	110 lb
Weight of magnetic clutch	~ 40 lb
Weight of drive shaft	35 lb
Total weight of rod, shaft, and clutch	185 lb
Water pressure load on rod, assuming approximately 40 lb/in.^{2}	290 lb
Drive motor power	1/6 hp
Drive motor speed	1725 rpm
Water flow area (upper section)	5.06 sq in. (32.6 sq cm)
Water flow area (uranium section)	4.2 sq in. (26.1 sq cm)
Water flow area (lower section)	5.06 sq in. (32.6 sq cm)
Water flow area (cadmium section)	5.04 sq in. (32.4 sq cm)

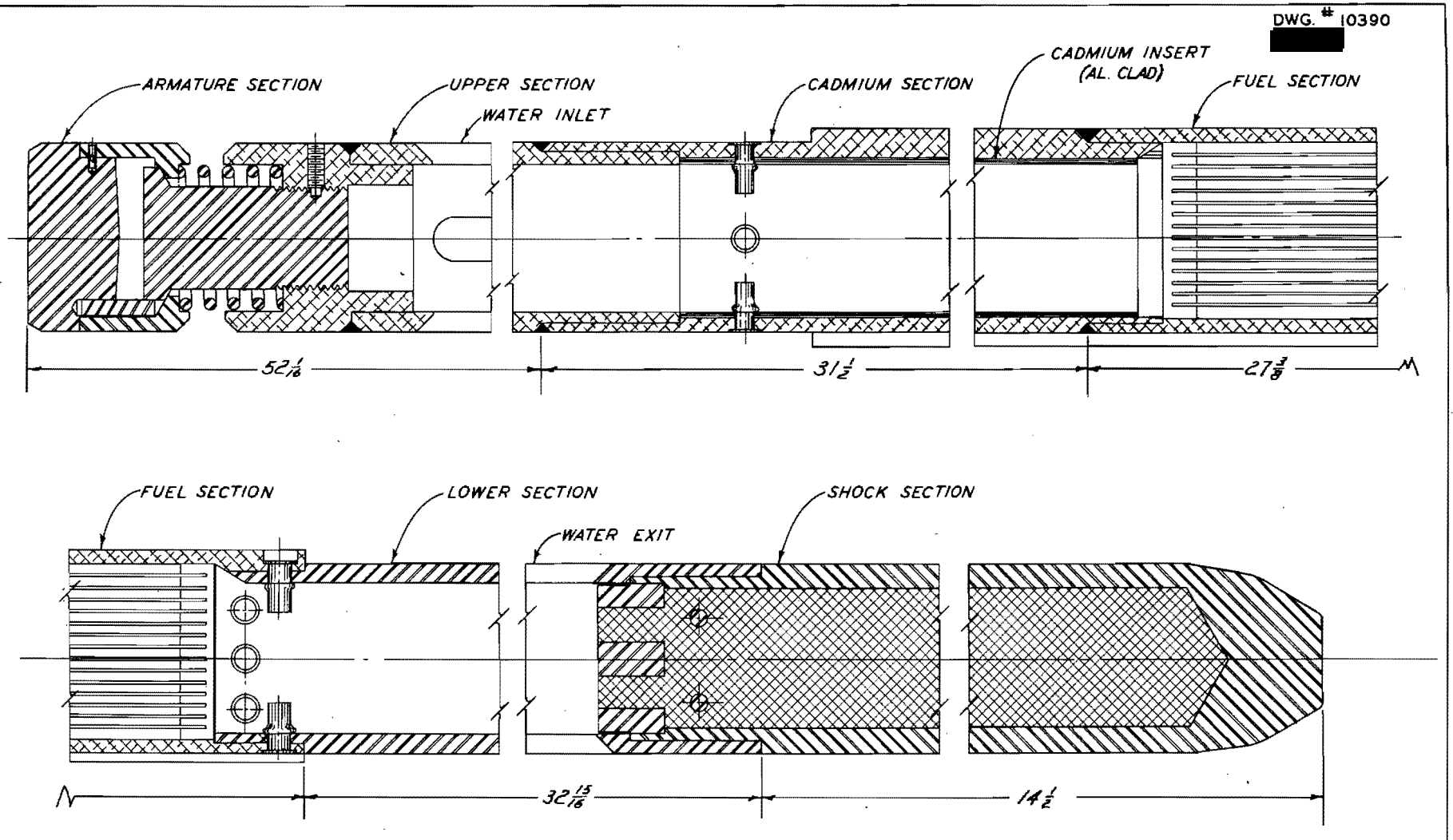

FIG. 2.3.A
M.T.R
SHIM-SAFETY ROD WITH FUEL

OAK RIDGE NATIONAL LABORATORY

DWG. # 10389 [redacted]

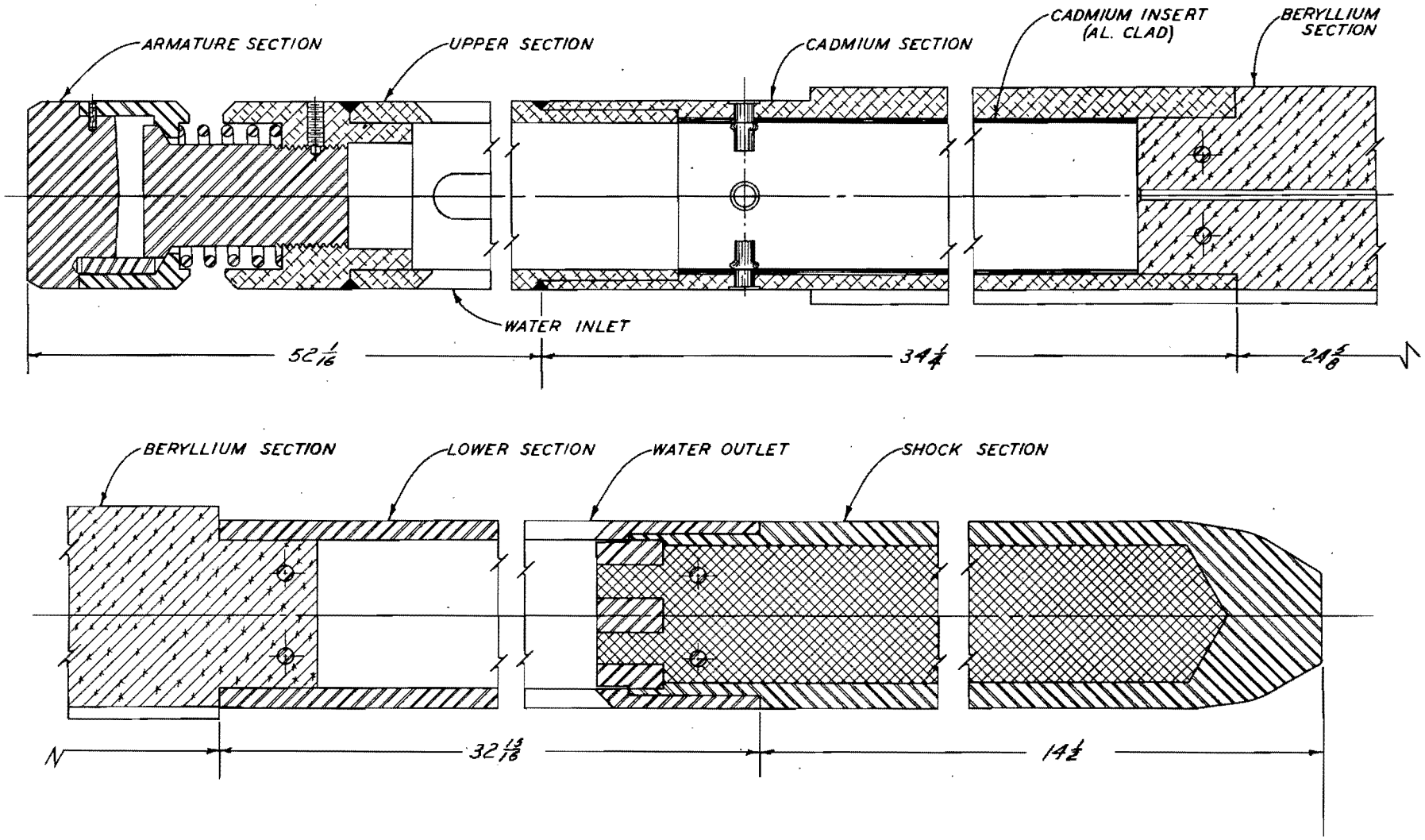

FIG. 2.3.B
M.T.R
SHIM SAFETY ROD WITH BERYLLIUM

OAK RIDGE NATIONAL LABORATORY

2.3.2 Regulating Rods. The regulating rods are designed to provide continuous control of the reactor. While four locations are provided for these rods in the beryllium reflector (see Fig. 2.4.A), normally only one will be used for control with one more as a stand-by. The remaining two locations can then be used for hydraulic rabbit tubes.

As shown in Fig. 2.3.C, each rod is 1½ in. in diameter and consists of an upper aluminum section, a middle section containing cadmium sandwiched in aluminum tubing, and a lower aluminum section. Guide bearings are provided in the upper and lower support castings. The regulating rod itself is connected by a quick-release mechanism to the regulating-rod support shaft, which is guided by bearings in the spider and the top plug platform.

When connected to its support shaft, each regulating rod is driven by a low-inertia electric motor through a pinion and rack integral with the shaft. The motor will be driven by an amplidyne as described in Chap. 5.

When disconnected the regulating rod rests on the top of the upper bearing grid. In this position the lower tip of the regulating rod and the lower tip of the cadmium section are 60 and 12 in., respectively, below the center of the pile lattice. Table 2.3.B summarizes the pertinent data for the regulating rods.

TABLE 2.3.B

Regulating Rod

Composition	Cadmium-aluminum
Weight of regulating rod	10.5 lb
Weight of drive rod	36.0 lb
Weight of water in drive rod	9.0 lb
Total weight of combined rods	55.5 lb
Buoyant force of regulating rod	8.1 lb
Buoyant force of drive rod	9.8 lb
Total buoyant force	17.9 lb
Resistance force of rod through pile section (friction)	~ 7.4 lb
Acceleration	~ 1.3 g
$\Delta k/k$ per rod	~ 0.005
Drive motor rated power	1 hp

DWG. # 10391 [redacted]

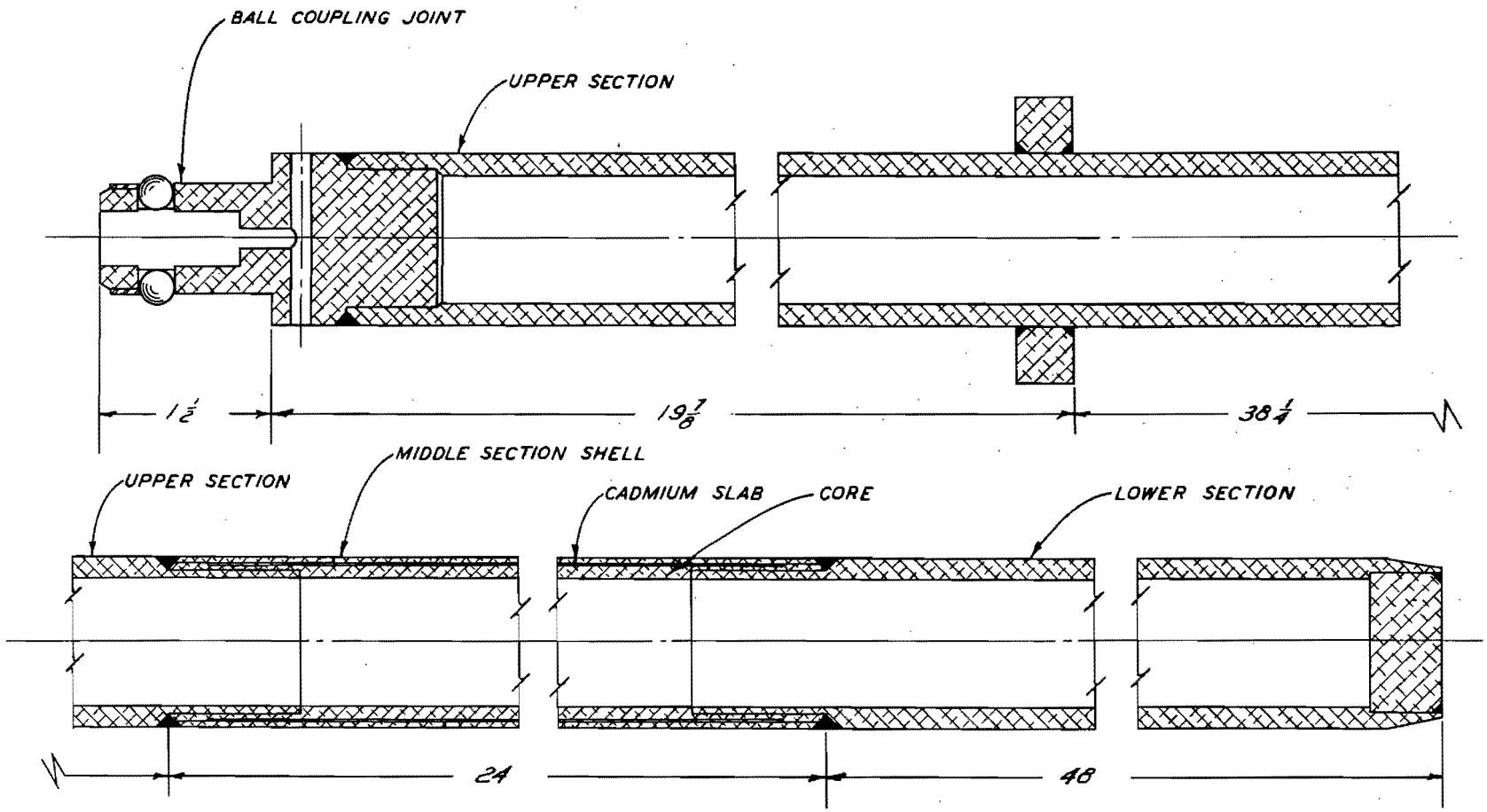

FIG. 2.3.C
M.T.R.
REGULATING ROD

OAK RIDGE NATIONAL LABORATORY

2.3.3 Miscellaneous Equipment Connected with Control Rods. *Drive Shafts.* The drive or support shafts for the control rods primarily provide a connecting link between the rods and their driving mechanism. The drive shafts are made up in three sections. The top section of stainless steel carries the rack or acme thread to fit the driving mechanism. The two lower sections are of aluminum, the middle piece being filled with lead shot to reduce gamma radiation; the bottom section carries the electromagnet in the case of the shim rods and the quick-release mechanism in the case of the regulating rods.

Upper and Lower Rack Housing and Cover, Regulating Rod. The upper rack housing, fabricated from cast iron, is fastened to the upper surface of the top plug platform (see Fig. 2.F). It functions as part of the guide and bearing for the regulating-rod drive rack, houses the rack pinion, and locates the regulating-rod speed reducer and position indicator. The rack housing cover is bolted to the housing and completes the regulating-rod guide and bearing. Microswitch brackets are fastened to the rack housing cover, five of which are located on one side of the vertical centerline and two on the other side. One of the latter, the long bracket, accommodates two microswitches, which are adjustable with respect to each other. These microswitches are used in the interlock system which controls the relative motions and positions of the regulator and shim rods. This system is fully discussed in Chap. 5.

The lower rack housing, attached to the undersurface of the top plug platform, functions as a seal for the regulating-rod drive shaft and as a means of support for the lower shock absorber.

Upper and Lower Shock Absorbers, Regulating Rod. The upper shock absorber is bolted to the upper surface of the upper rack housing and cover. It performs the function of dissipating the energy in the motor when the amplidyne armature circuit fails to stop the servo motor on the regulating-rod upstroke. It also serves as the upper end housing for the regulating-rod drive. The shock absorber is capable of resisting a force greater than 1300 lb occurring when the rod moves upward with a velocity of 4 ft/sec.

The upper end of the drive rack engages a plunger and moves it against an oil cushion, forcing the oil through an annulus between a flange on the plunger and the tapered wall of the housing. The oil is retained in the chamber formed between the housing and the guide by means of "O" ring seals.

A spring returns the plunger to its normal position. A threaded plug is provided in the top of the shock absorber to permit access to the rod locking device.

The lower shock absorber is fastened to the lower rack housing and is similar in principle to the upper shock absorber. It performs the function of dissipating the energy in the servo motor when the rod is driven to its lowest position.

Drive-rod Top Plug Seal. The top plug seal for both the regulating and shim drive rods is designed to prevent water leakage where the drive rods pass through the top plug. A packing nut, when tightened against its seat in the seal housing, holds chevron leather packings against the wall of the seal housing and the drive rod. As an added precaution against the leakage of contaminated water from the reactor, a purging system is incorporated into the design. This is accomplished by introducing a supply of fresh water under the seal at a pressure slightly greater than the water in the reactor tank. The water flows through the annulus between the regulating-rod drive and its bearings into the reactor tank.

Position Indicators. The regulating- and shim-rod position indicators have been designed to indicate the exact position of the rods at any time. Rod positions may be read by means of direct-reading dial indicators at the platform of the top plug and by means of remote selsyn-driven (dial) indicators at the console in the control room.

The regulating-rod primary indicators at the top plug platform consist of a double-disk dial operated by means of suitable gearing. The outer disk shows the position of the rod in inches while the inner disk indicates to hundredths of an inch. One complete revolution of the outer disk provides indication for 30 in. of travel of the rod, while the inner disk makes one revolution for each inch of travel of the rod.

The secondary position indicator at the console consists of a dial pointer which moves 240° for 12 in. of travel of the regulating rod. This provides 20° of rotation of the pointer for each inch of rod travel.

The shim-rod primary indicators at the top plug platform consist of standard counters with five digits driven through suitable reduction gearing attached to a flexible shaft, which in turn is driven directly from the

shim-safety rod drive motor. These indicators will show the position of the rod to thousandths of an inch.

The shim-rod secondary position indicator at the console consists of a dial pointer which rotates 9° for each inch of rod travel; thus for a total travel of the rod of 31 in., the dial will rotate 279°.

The secondary indicator in both cases is operated by means of a receiver selsyn. The regulating-rod-driver selsyns are located at the regulating-rod driver, while those for the shim rods are located under the top plug platform. All are driven by means of suitable gearing, and in all cases either the primary or secondary indicators may be removed for servicing without affecting the other.

Speed Reducer and Motor Coupling, Shim-safety Rod. The speed reducer consists essentially of a helical gear and pinion supported by ball bearings, mounted in a housing which bolts to the upper rack housing. The position indicator operates from a bevel gear fastened to the helical gear shaft. Gears and bearings are lubricated by immersion in oil. An oil seal, pressed into the pinion bearing cap, prevents oil leakage around the pinion shaft.

The motor coupling functions as the connection between the speed-reducer shaft and the motor shaft. It consists of a splined collet which fits the spline shaft of the motor and is taper-pinned to the speed-reducer drive shaft. The taper pin acts as a shear pin in case an excessive load is placed upon the shim rod. The collet is threaded and tapered for an adjustable nut. When the nut is tightened, it clamps the collet to the splined motor shaft, thus eliminating any lost motion between motor and speed-reducer shaft.

Magnetic Clutch. This clutch is essentially a horseshoe or bipolar electromagnet. The pole cores and yokes are made of laminated S.A.E. 1010 steel, 1/16-in. laminations insulated with baked-on bakelite varnish 0.002 in. thick. The energizing coils have 3500 turns of No. 25 Formex-coated copper wire, wound on forms of Fosterite Vacuum Impregnate.

The clutch housing is grounded and forms one side of a circuit which indicates when the magnetic clutch is supporting the shim-safety rod. The casing consists of a watertight can of type 304 stainless steel, with welded seams, gasketed at the top with polyethylene. The bottom is flanged and tapped for a diaphragm sealing flange. Nonmagnetic shim material consists of a single sheet of stainless steel 0.008 in. thick and a sheet of mica 0.002 in. thick.

The oil filling used for this clutch is perfluorodimethylcyclohexane. Pressure build-up due to gassing of the oil is avoided by a vent to atmosphere through the cable channel.

On the basis of previous test data, the holding force of this clutch should be a minimum of 500 lb at 100 mamp current, and it should release a 600-lb load held at 140 mamp current in 15 msec or less.

All component parts have been tested separately, and two complete magnets have been assembled and are now undergoing tests in the mock-up.

Bearings. Each shim-safety rod is guided by two bearings consisting of four spring plates, in each of which there are mounted three stainless steel—encased graphite rollers. These plates are mounted in a steel cage and are located in the upper and lower guide grids. The center of the upper bearing is located 3 ft 10-5/8 in. from the centerline of the reactor and is supported by the upper grid support. The centerline for the lower bearing is located 4 ft ¾ in. below the centerline of the reactor and is supported from the lower grid support.

Bottom Absorber, Shim-safety Rod. The bottom shock absorbers for the shim-safety rods are located on a plate mounted on the bottom plug. They consist merely of dash-pots into which plungers mounted on the bottom of the shim rods fit. Since they are on the bottom plug, they are always filled with water, which acts as the damping fluid.

These shock absorbers also contain a mechanism[3] which indicates whether or not the rods are seated in the shock absorber and are therefore fully in the reactor. This is accomplished by introducing a high-pressure demineralized-water line through the bottom plug into each shock absorber. The pressure in this line will be maintained above that normally at the bottom of tank section E, so that when the shock absorber is not seated water flows up into the tank. When the rod is seated, however, the flow is decreased and appropriate signals from the pressure meters inform the reactor operator of the situation.

2.4 REFLECTOR

2.4.1 Beryllium. It has been indicated in Chap. 1 that as far as is known beryllium is the best reflector from a nuclear point of view, its use having been questionable only because of supply difficulties and lack of data on its chemical and mechanical properties. The initial tests on beryllium and the selection of the type of production used are discussed in Appendix 5. The following section describes the final form of the MTR beryllium reflector.

The beryllium section of the MTR reflector is all contained inside tank section D (see Fig. 2.4.A), occupying the space between the active lattice and the tank wall. This beryllium has a finished weight of about 5750 lb and a volume of nearly 50 cu ft. The total height of the reflector is 39-3/8 in. (approximately 100 cm); the layout and shape of the pieces are shown in Figs. 2.4.A and B. These diagrams are cross-sections below and above the beam holes, and they show that the majority of the pieces are continuous throughout the 100 cm length.

Following is a brief description of the various pieces shown in Figs. 2.4.A and B: The key pieces are those numbered E-1 through E-4, which contain large holes throughout their length for passage of the regulating rods. These pieces are mounted and held rigidly in position by the regulating-rod bearing mount in the lower grid (see Fig. 2.D). The A pieces (A-1 through A-43) are fitted with "end boxes" which fit tightly into the holes in the lower support grid (see Fig. 2.E). Tolerances are such as to allow an average spacing of 0.020 in. between pieces. The remainder of the pieces are large heavy blocks machined to fit into their respective places and are not rigidly held. The water film between surfaces prevents surface abrasion, and appropriate holes are provided for the passage of cooling water. For example, each A piece has an axial hole 3/16 in. in diameter and a semicircular groove down each face 1/8 in. in diameter (see Fig. 2.4.C). It should be noted that the axial 3/16-in. hole was necessitated not by the volume of cooling water required but by the surface necessary for heat transfer and by the surface stress set up by heat differentials in the beryllium.

The large pieces N-1, N-2, N-3, N-4, F-1, and F-2 are semicircular on the bottom to fit over, but not touch, the HB thimbles. These pieces actually rest on the lower beryllium pieces N-5, etc., which are grooved on top to fit

DWG. # 10385 [redacted]

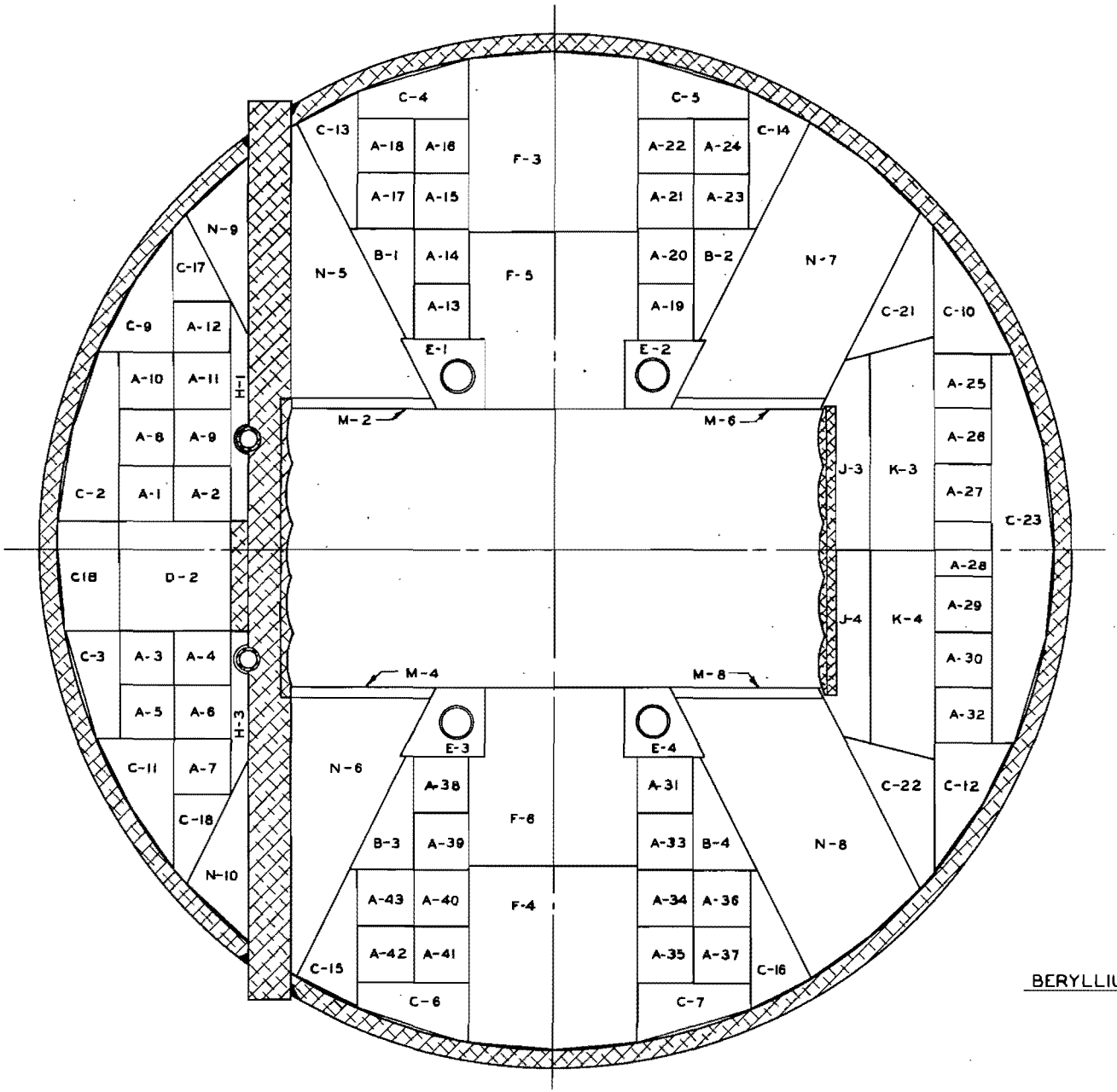

FIG. 2.4.A

M.T.R

BERYLLIUM BELOW ℄ OF REACTOR

OAK RIDGE NATIONAL LABORATORY

DWG. # 10386
[redacted]

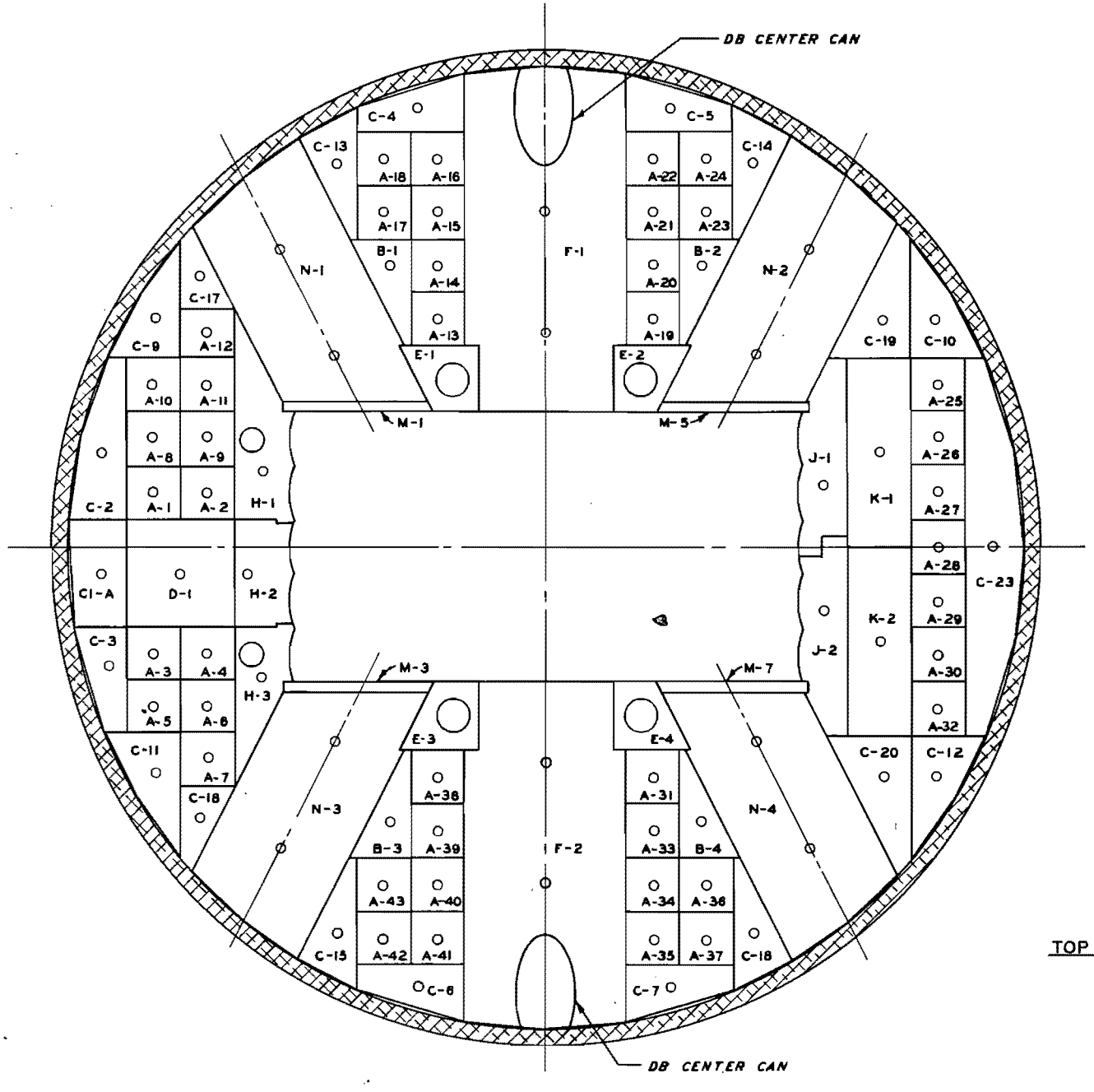

FIG. 2.4.B
M.T.R.
TOP VIEW OF BERYLLIUM

OAK RIDGE NATIONAL LABORATORY

DWG. #10384

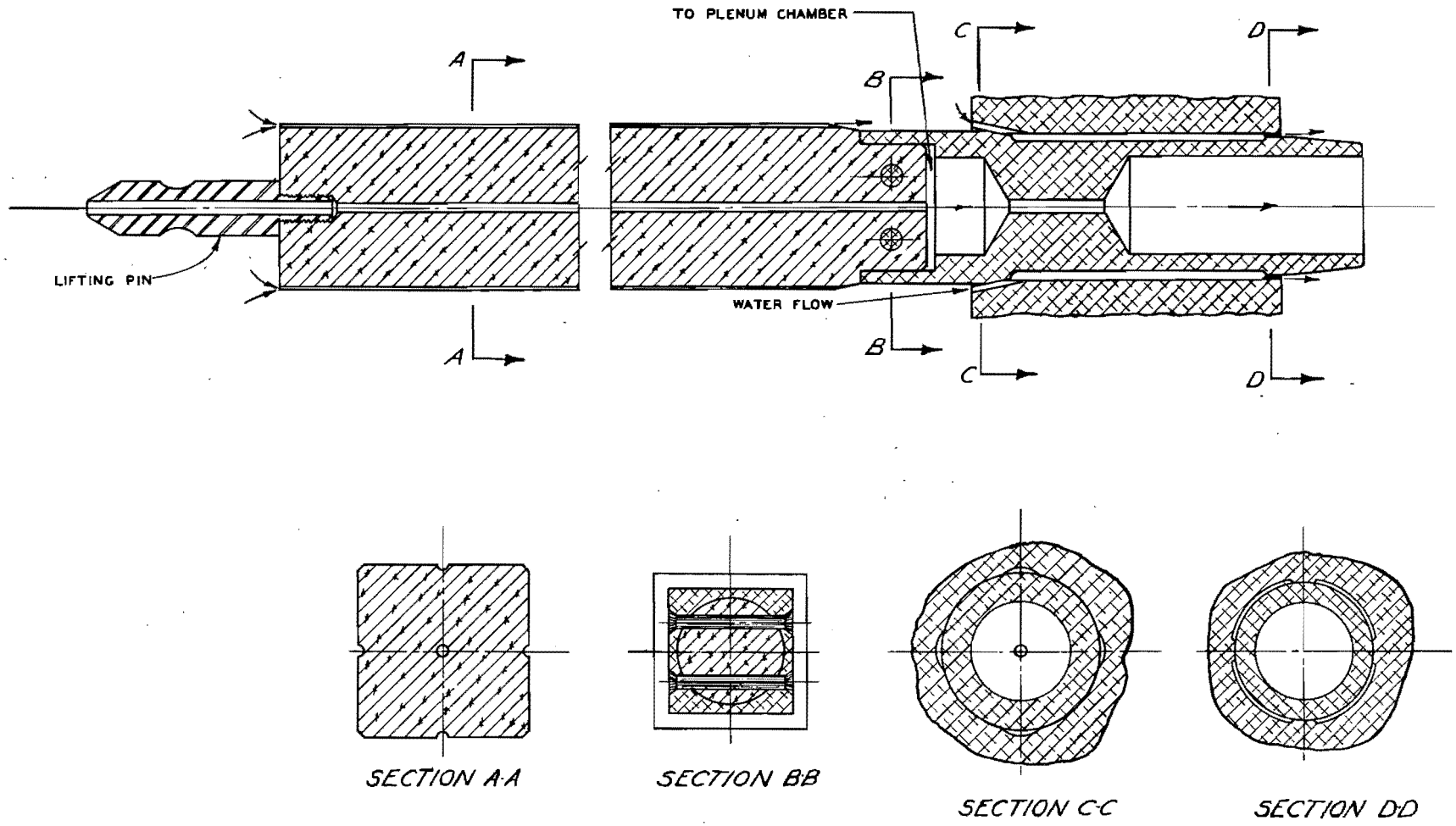

FIG. 2.4.C
M.T.R.
BERYLLIUM A - PIECE

OAK RIDGE NATIONAL LABORATORY

under the respective thimbles. Plates M-1 through M-8 are fastened to the N pieces to provide a narrow tight-fitting collar around the inner end of the thimbles. This prevents water leakage from the reflector into the lattice (see Section 2.7.1). The packing is somewhat complicated by the aluminum bar which contains the holes for the horizontal pneumatic rabbits (see Section 3.5.1). This bar is shown between N-5 and N-9 and between N-6 and N-10 in Fig. 2.4.A.

While the beryllium pieces C-1-A and C-1-B, as well as D-1 and D-2, are shown as separate pieces, they are mechanically joined by a sealed, empty aluminum can which effectively eliminates the reflector from hole HG-9. D-1 and D-2 form the plug for the discharge chute and are lifted out as one piece when it is necessary to use the chute. Piece A-31 is drilled out to provide space for the permanent antimony source (see Chap. 4).

Figures 2.4.D through G are photographs of the MTR beryllium assembled at the Y-12 shops prior to final fitting. Figure 2.4.D shows the complete assembly except for one E piece. Figure 2.4.E shows the same assembly with some of the pieces raised to show the water-cooling grooves. Figures 2.4.F and G show some of the larger blocks and the holes for the HB thimbles. The wooden beam passing through the left side of the reflector, as shown in these pictures, represents the HT-1 liner (see Chap. 3).

No final figure has yet been made available for the total cost of the MTR beryllium, but the present estimate, including raw material, processing, and machining, amounts to $1,000,000 to $1,300,000.

2.4.2 Graphite. Part of the purpose of the MTR is to provide as large a neutron flux as possible over as great a volume as possible. To accomplish this it was decided to include a secondary reflector of graphite[4] outside the main reactor tanks.

The main problem faced in the design of the graphite reflector was to take care of the graphite expansion due to both radiation (Wigner disease) and/or temperature. To overcome this difficulty the graphite reflector is composed of two zones: a pebble zone which is adjacent to the reactor tank and extends for a minimum of 40 cm from the tank wall to form a square; and a permanent graphite zone 12 ft overall north and south, 14 ft overall east and west, and 9 ft 4 in. high (see Figs. 2.A and C).

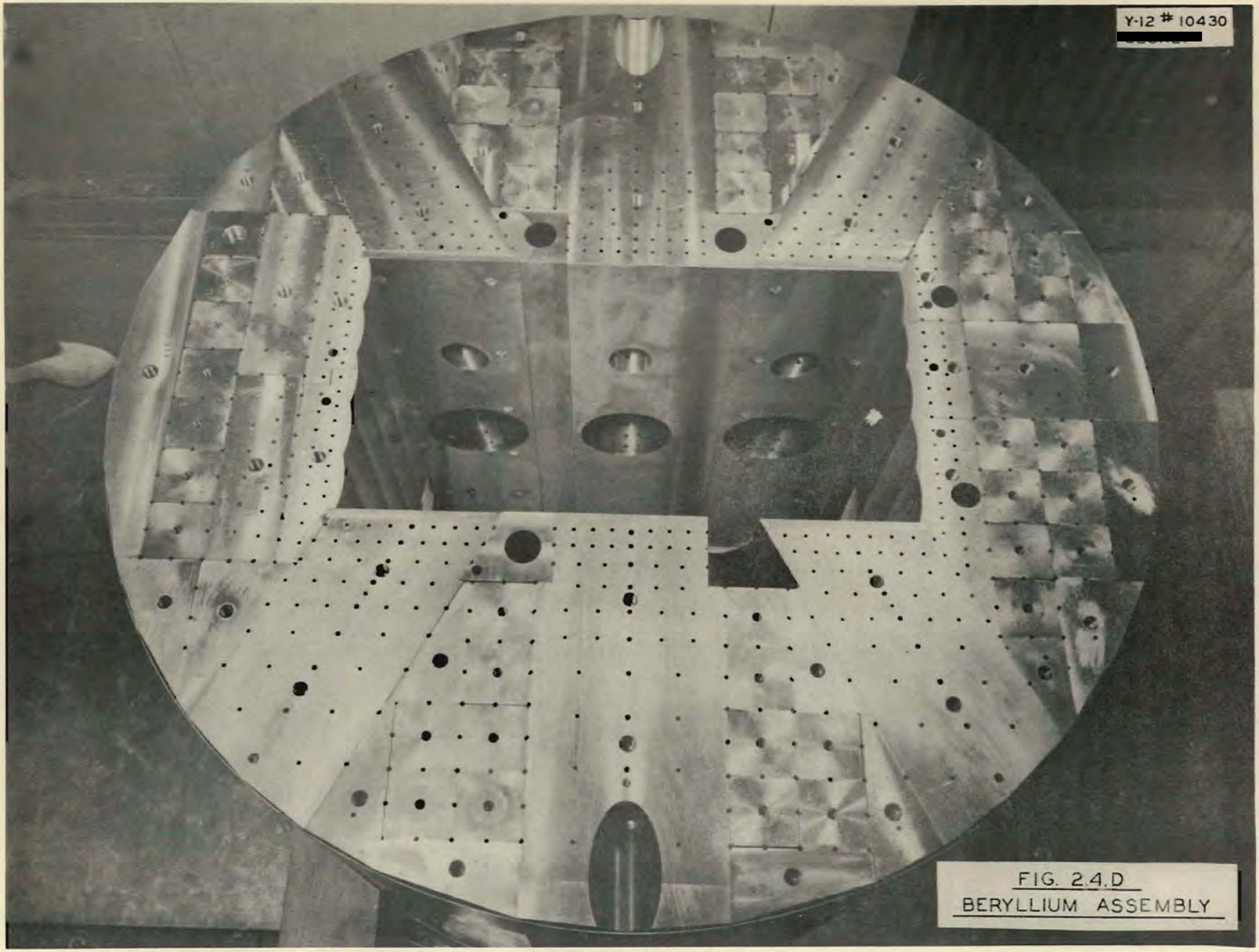

FIG. 2.4.D
BERYLLIUM ASSEMBLY

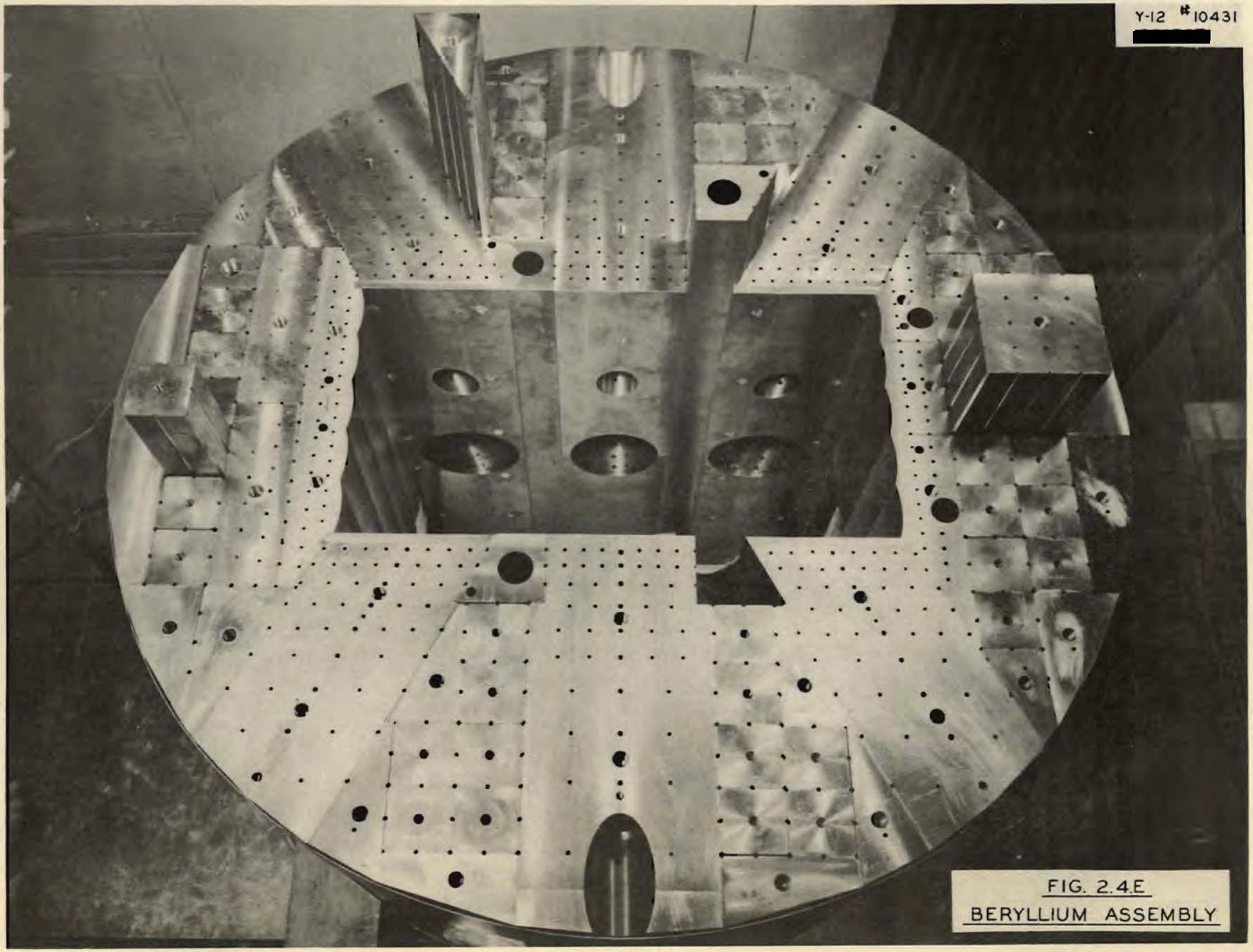

FIG. 2.4.E
BERYLLIUM ASSEMBLY

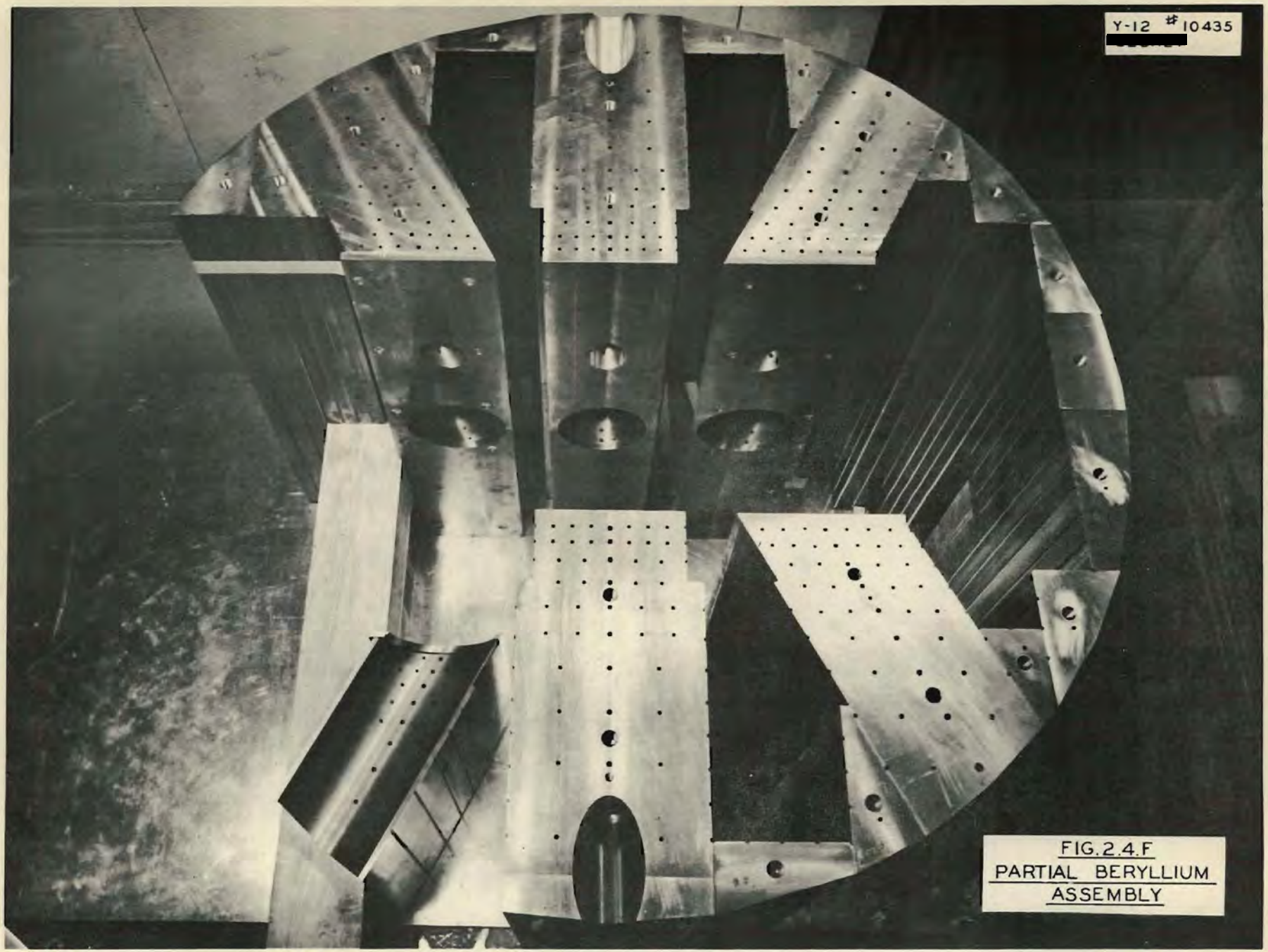

FIG. 2.4.F
PARTIAL BERYLLIUM
ASSEMBLY

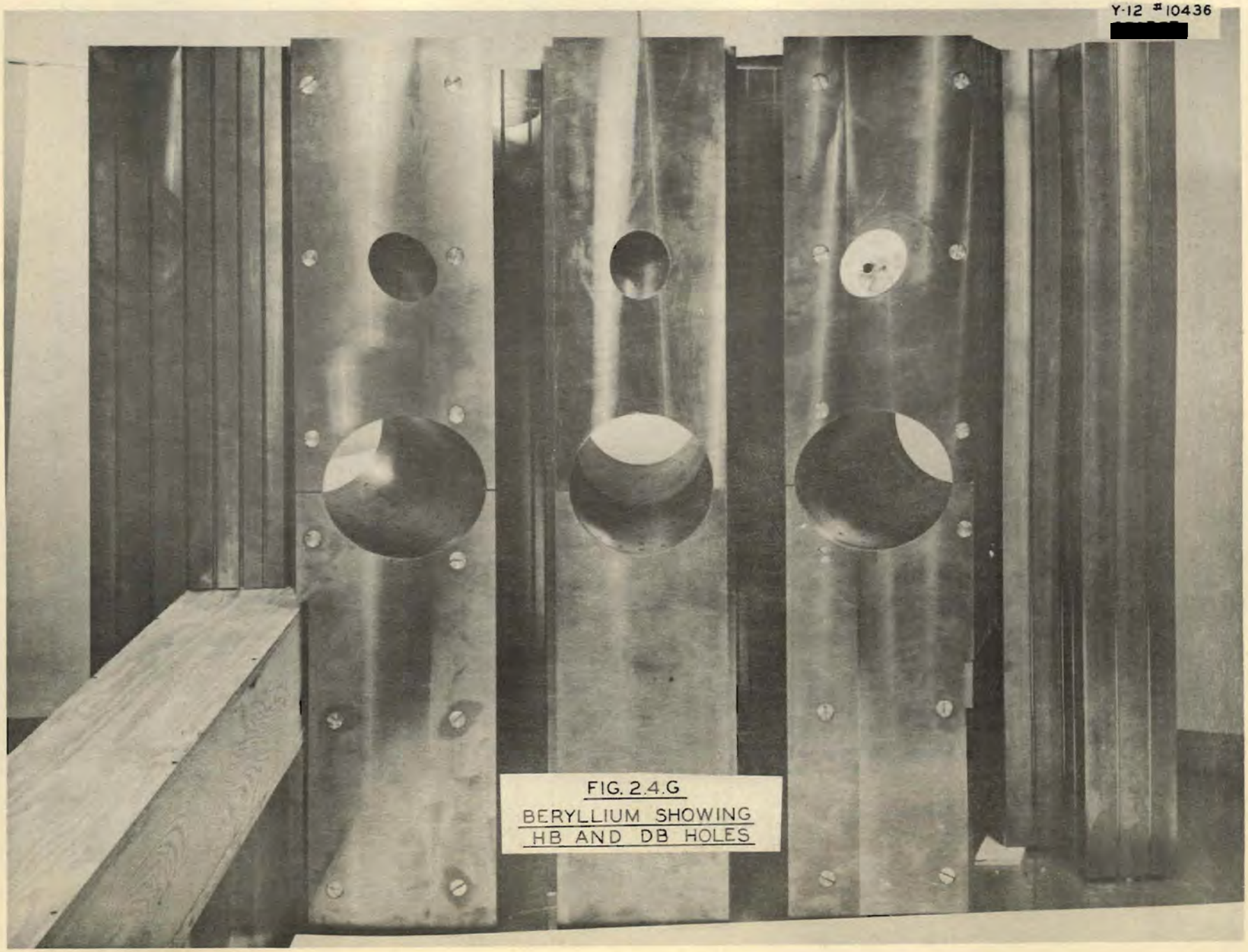

FIG. 2.4.G
BERYLLIUM SHOWING
HB AND DB HOLES

The pebble zone is a volume 7 ft 4 in. square by 9 ft high surrounding the reactor tank and filled by some 700,000 1-in.-diameter AGOT graphite pebbles. The pebbles rest on a base plate mounted on the lower thermal shield plate and are free to expand upward. In this way any expansion due to radiation effects or temperature increase will merely raise the level of the balls without exerting undue stress on the tank wall or the permanent graphite.

Two discharge chutes in the pebble support plate can be opened into a discharge bin, thus allowing for removal of the pebbles at any time. This easy removal of the pebbles carries out the MTR feature which provides for removable B, C, and D tank sections (see Section 2.3.1). Furthermore, since the pebbles are in the highest flux region of the graphite reflector, any radiation damage will affect them first and they can be replaced.

The permanent graphite is composed largely of 4- by 4-in. graphite bars stacked to a height of 9 ft 4 in. with the bottom located 4 ft below the centerline of the active section (i.e., at elevation 96 ft; see Section 2.3.1). The system of stacking the graphite is shown in Figs. 2.4.H and I. The first of these figures shows the overall relationship of all four walls at one level while the second figure illustrates the stacking and numbering system. It will be noted that every other row has a 4- by 6-in. block at each end to allow for the staggering of the rows.

The stacking was, of course, complicated by the experimental holes penetrating the permanent graphite. These larger holes were cut into the walls by clamping a group of bars together and drilling through the assembly. Each wall array is made integral by a system of 1- by 1-in. keys, and the entire assembly is keyed at its inner face to the supporting rails. This means that any expansion will be outward, tending to compress the ½ in. of soft asbestos which fills the gap between the permanent graphite and the thermal shield. As of January 1, 1951 the graphite machining was about 30% completed at the Y-12 shops. Each wall will be erected and checked there before shipment to Idaho. Figure 2.4.J is a picture of the lower part of the west wall being erected at Y-12.

Each wall of the permanent graphite is mounted on rails running parallel to its length. The rails are supported by jack screws which are fastened to the lower plate of the bottom thermal shield and pass through clearance holes in the inner plate of the lower thermal shield (see Fig. 2.A). The support rails must be accurately leveled in order that the graphite will stack properly and be in correct location for the beam holes.

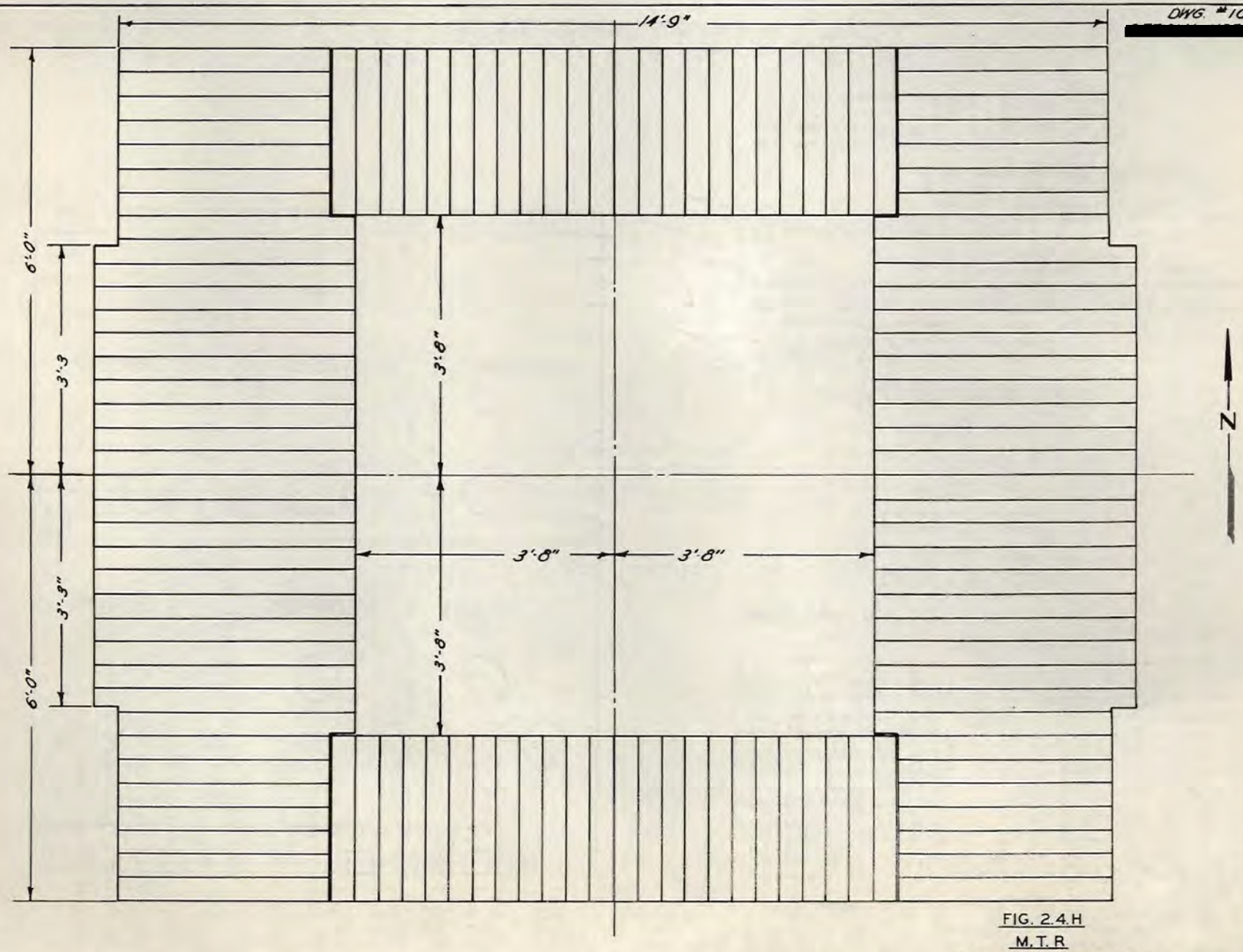

FIG. 2.4.H
M.T.R
PERMANENT GRAPHITE
OAK RIDGE NATIONAL LABORATORY

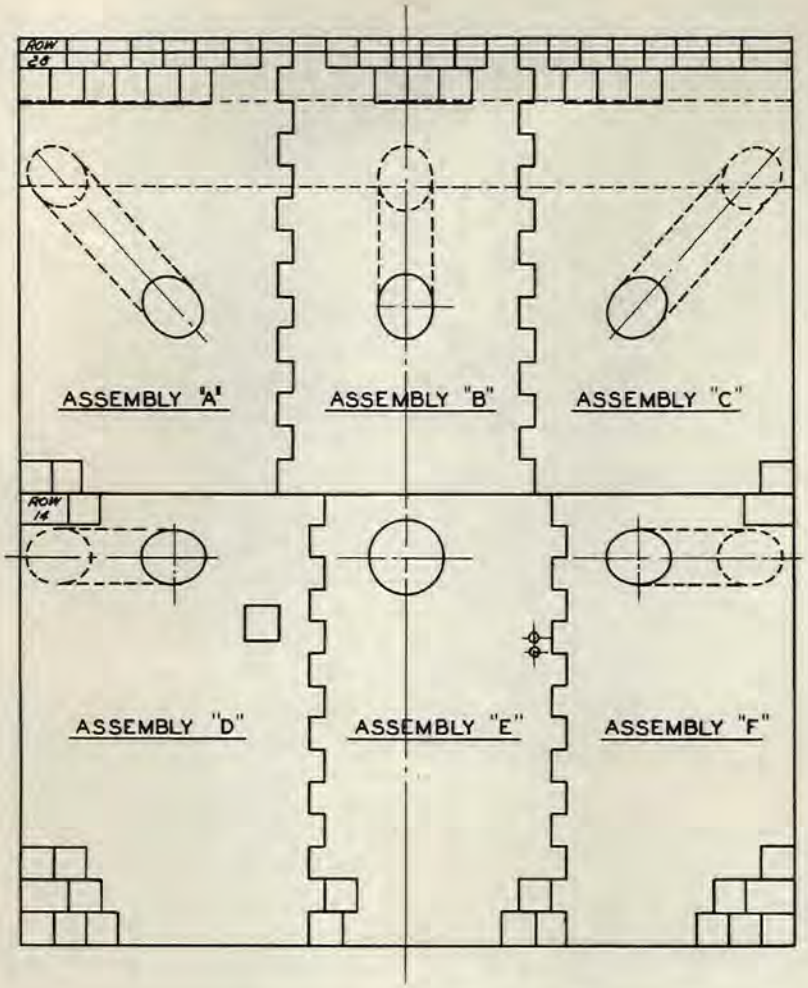

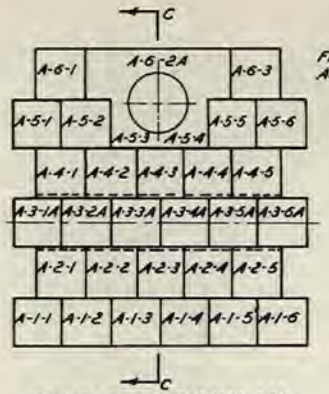

SAMPLE ASSEMBLY "A"

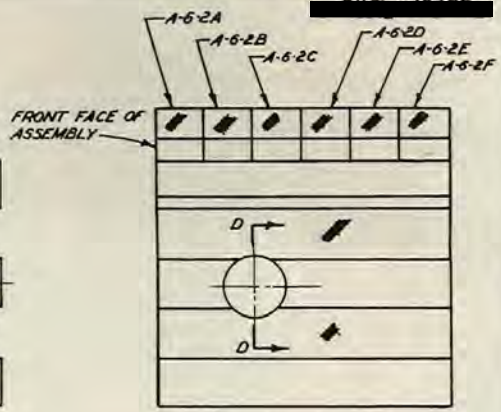

SECTION C-C

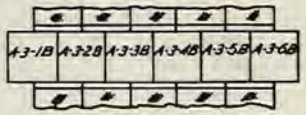

SECTION D-D

KEY TO MATCH-MARKING SYSTEM

All individual blocks are to be match-marked as shown in Sample Assembly "A" and described below:

1st Symbol (Letter) - Assembly in which block appears.

2nd Symbol (Number) - Row in the Assembly in which block appears.

3rd Symbol (Number) - Position of the block in the row; Numbers starting from left side of the Assembly. Viewed from center of Reactor.

4th Symbol (Letter) - Position of the block from front face of Assembly. Letters starting from front face of Assembly. (See Sections C-C and D-D) This Symbol is used only where one block does not extend the full depth of the Assembly.

West Wall Assembly	A, B, C, D, E, F
East Wall Assembly	G, H, J, K, L, M
South Wall Assembly	N, P, Q, R, S, T
North Wall Assembly	U, V, W, X, Y, Z

FIG. 2.4.I

GRAPHITE ASSEMBLY & NUMBERING SYSTEM

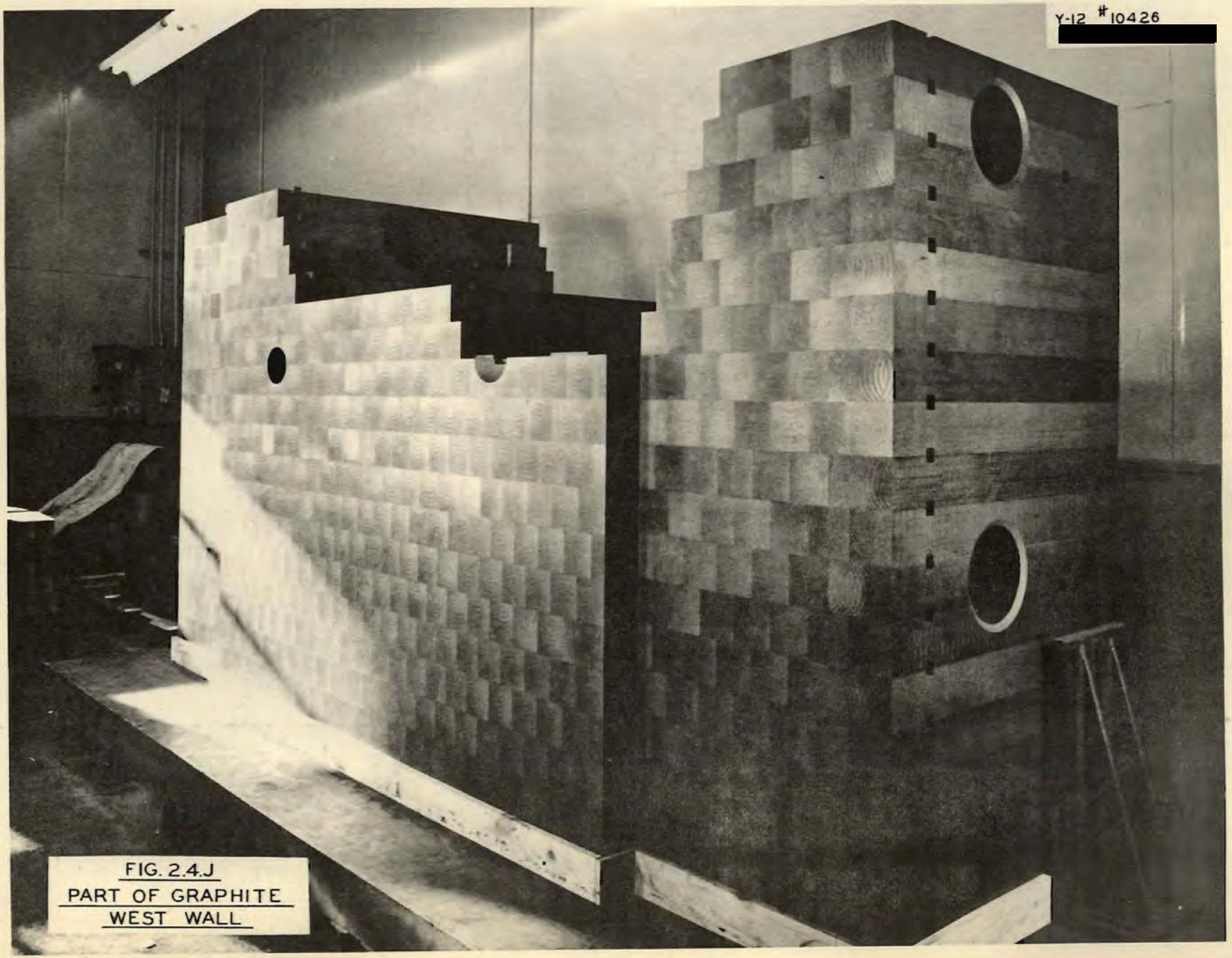

FIG. 2.4.J
PART OF GRAPHITE
WEST WALL

A great deal of work was done before a final choice was made of the kind of graphite to be used in the reflector. High-purity graphite is, of course, desirable because of lower induced activity and lower neutron absorption. Experimental work[5] showed that the induced activity of the best available type of graphite (GBF and AGOT) was largely due to the 49-day iron which was present in concentrations of 1 ppm in GBF and 10 ppm in AGOT. While AGOT had a somewhat higher induced activity and absorption than GBF, its cost was only two-thirds of that of the GBF. As a balance between usefulness and economy it was decided to make the thermal column[6] and its extension through the permanent graphite out of GBF, the remainder of the permanent graphite being AGOT. The only exception to this was the need for a few 4- by 6-in. blocks in stacking, and these were obtainable only in AGHT graphite. The final graphite reflector and thermal column will consist of the following:[7]

APPROXIMATE FINISHED WEIGHT (tons)

Pebbles, AGOT		19
Permanent zone,	AGOT	48
	AGHT	1.5
	GBF	25

The graphite reflector, owing to the heat absorbed in it, must be cooled. This is done by drawing large quantities of air through holes in the permanent graphite and through the interstices between the balls in the pebble zone. This cooling system is fully described in Section 2.7.2.

2.5 THERMAL SHIELD

2.5.1 The Steel Plate Structure. The thermal shield[8] of the Materials Testing Reactor is that part of the reactor structure between the solid graphite zone and the concrete biological shield. It has been established that a 50°F temperature drop across the concrete biological shield[9] is the temperature differential which can be tolerated without danger of failure within the concrete structure due to induced thermal stresses. The MTR thermal shield is a large steel structure which reduces the neutron and gamma flux to such an extent that a comparatively low heat generation due to radiation occurs in the concrete.

The thermal shield, consisting of 4-in.-thick steel plates, may be visualized in so far as orientation with respect to the rest of the reactor is concerned by referring to Figs. 2.B and C, which are vertical and horizontal sections through the reactor, respectively.

The approximate overall size is as follows: 16 ft in the north-south direction, 14 ft in the east-west direction, and 12 ft 6 in. in height. The thermal shield, whose heat generation rate is approximately 95 kw, is cooled by an induced-draft air system which also serves as the graphite cooling system (see Section 2.7.2). The primary supporting structure is composed of four vertical "WF" columns with the load transmitted to these columns at the four corners of the bottom plate.[2]

The bottom plate of the lower thermal shield, while resting directly on the steel supporting structure, is in direct contact with the barytes concrete below it. This helps to cool the concrete by direct thermal contact. The upper plate of the lower thermal shield is in two parts. An inner ring 14 in. wide is welded directly to tank section E (see Fig. 2.E) in order to provide maximum cooling for this section.[8] The outer section is supported from the lower plate and is air cooled only.

The solid graphite is supported from the lower plate of the bottom thermal shield plate (as described in Section 2.4.2). The two plates of the upper thermal shield are independently supported from the concrete above them, and, with the exception of one point, which is a metal expansion joint—air seal, the top plates do not touch the side plates of the thermal shield. Figure 2.5.A shows the top plate arrangement. The eight side plates all rest on the lower plate of the bottom thermal shield and are essentially independent units. The four inner plates, and similarly the four outer plates, are loosely connected at the top corners by dumbbell-shaped pins which fit in oversize slots in the tops of adjacent plates.

Two important experimental facilities, the thermal column and the shielding facility (see Sections 3.1 and 3.2), require that a section approximately 6 by 6 ft be removed from the east and west thermal-shield side plates. Two components are added to the thermal-shield design by these facilities: (1) the neutron window, and (2) the neutron-absorbing curtain. The locations of these components may be visualized by referring to Figs. 2.B and C. When the 6- by 6-ft hole is cut in the thermal shield, it becomes necessary to replace

DWG. #10564

[redacted]

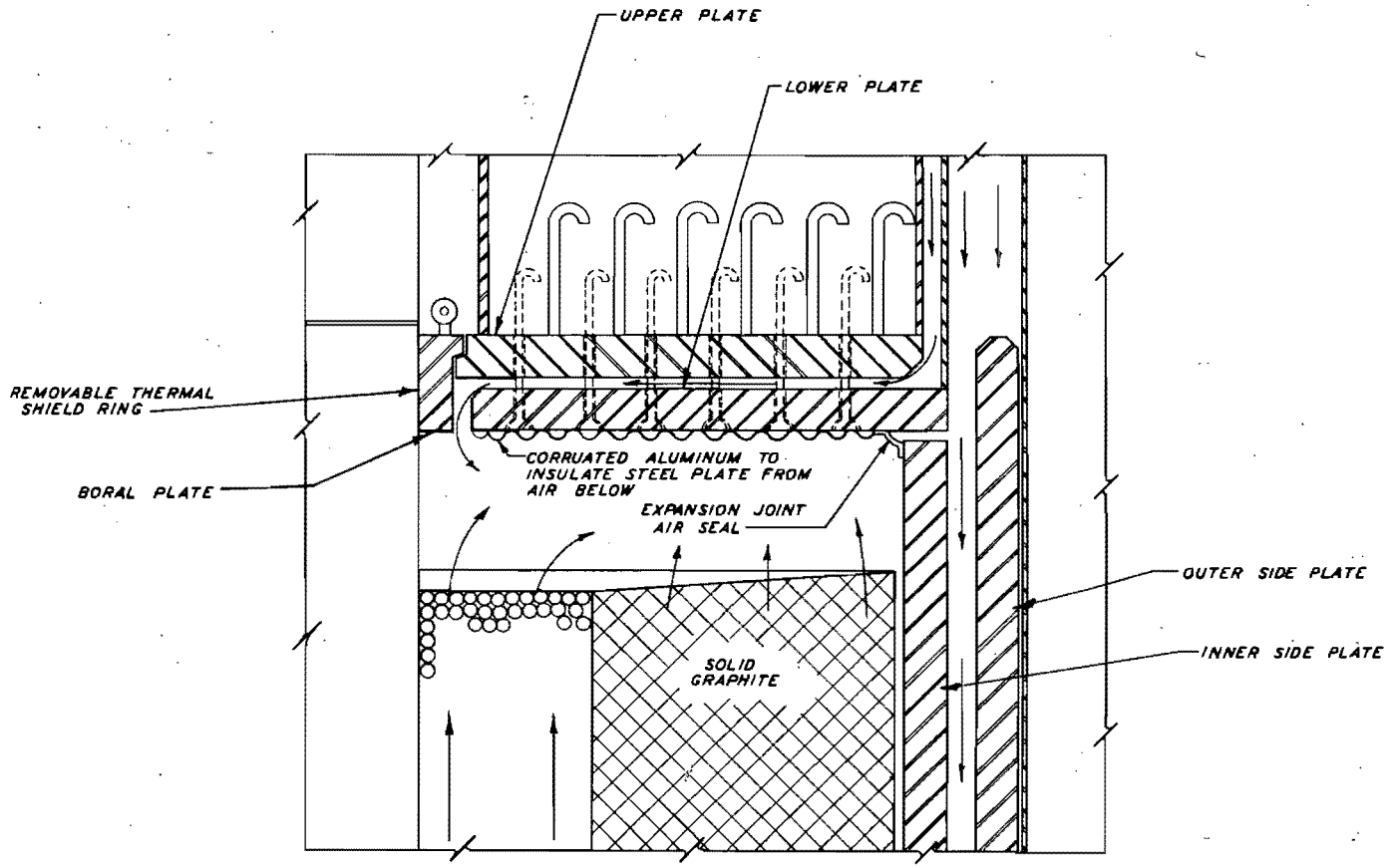

FIG. 2.5.A

TOP THERMAL SHIELD DESIGN

the steel removed on the thermal column side by a material that will absorb gamma radiation impinging on the inner side of the thermal shield and yet allow passage of thermal neutrons into the thermal column. The lead replacing the steel in this region is called the "neutron window." The "neutron-absorbing curtain" is a simply constructed remotely operated neutron shutter, which permits turning "on" and "off" the thermal-neutron streams to the thermal column and the experimental shielding facility.

2.5.2 Neutron Curtain in the MTR. A 6 ft 6 in. square sheet of ¼-in.-thick boral mounted in an aluminum frame will serve as the neutron curtain. This curtain will be used during operation, if desired, to cover the face of the thermal column and reduce the number of thermal neutrons entering the column. It will have rollers at its four corners that will travel in vertical guides mounted in the 3-in. space between the two 4-in. thermal shield plates.

A 2-in. by 7-ft vertical slot in the biological shield from the bottom of the thermal shield to the sub-pile room ceiling will house the curtain when it is not in use. To shield against radiation streaming, the lower portion of this slot will be filled with 2-ft-deep removable barytes concrete blocks supported from the sub-pile room ceiling by 6-in.-square steel bars which serve as additional shielding.

A lifting mechanism mounted on the top of the reactor structure raises or lowers the curtain as desired. After removing the concrete and steel shielding at the bottom of the curtain slot, the curtain can be lowered into the canal and a new curtain installed if necessary.

Provisions have also been made for installation of a curtain on the west side of the thermal shield at the face of the shielding facility; however, no curtain or lifting mechanism will be furnished initially.

2.5.3 The Neutron Window. The neutron window is a 3-in. sheet of lead placed between the permanent graphite and the thermal column to absorb gamma radiation but permit easy neutron passage. The lead sheet is mounted in a steel frame and placed in the approximately 6- by 6-ft hole in the outer thermal shield.

2.6 THE BIOLOGICAL SHIELD

The biological shield (see Fig. 2.A) around the reactor is designed to reduce by absorption the high neutron and gamma fluxes escaping through the reflector. The shield is designed to reduce these radiations to a safe level for personnel and to a level at which sensitive instruments can be operated outside the shield. This design limit and the basis for the design are summarized in Section 4.6.

The shield is penetrated by about one hundred holes of various sizes. Embedded in the concrete and welded to the steel plates which act as inner and outer form plates for the concrete are all the permanent liners for the experimental holes. One of the major problems in the construction of the reactor will be the alignment of these liners. As indicated in Section 2.1.1, the top of tank section E is the only reference point available, and accuracy is essential if the HB and DB inner liners are to fit into their respective locations in the tank section D wall.

The MTR shield is being built of barytes concrete in which the gravel part of the mix is approximately 93% $BaSO_4$. It was at first thought that only certain critical sections of the shield would be made of barytes, but, owing to difficulty of mixed pours, it was decided that a more satisfactory shield would be obtained if barytes was used throughout. In order to simplify the construction procedure and obtain a uniformly dense concrete, it is now planned to use the "Prepack" method for setting all the biological shield.

2.7 COOLING

2.7.1 Water Cooling. The theoretical and experimental bases for the cooling-water requirements are outlined in Chap. 4, where it is pointed out that the primary cooling requirement is a high speed (30 ft/sec) flow of the water through the fuel assemblies. Such a rate of flow allows good heat transfer from the metal (small film drop) but does not produce sufficient turbulence to distort the fuel plates.[10] The external water system described in Chap. 7 is designed to produce sufficient pressure (40 lb/in.^{2}) to cause a flow of 30 ft/sec through the fuel elements. Since this pressure forces approximately 20,000 gal/min through the lattice and beryllium, the temperature rise at 30,000-kw operation is only about 11°F.

Since the water flow in the beryllium and in the lattice are essentially in parallel, the water pressure across the reflector is also 40 lb/in.^{2},[11] and to obtain sufficient heat transfer area in the beryllium the cooling holes had to be fairly large (3/8 in. diameter). This, of course, allowed too much water to pass through the reflector, and a plenum chamber (see Fig. 2.E) is used under the beryllium to take some of the pressure drop and thus reduce the water flow. This means that the water while in the beryllium tends to flow inward from the beryllium to the lattice. To prevent this disturbance in the water flow, the inner beryllium pieces are overlapped and closely fitted. A tight beryllium collar is fitted around the inner end of each of the HB thimbles and DB aluminum cans. In addition, the lower support casting has a ½-in. ledge around the edges of the center opening to prevent water from running under the beryllium into the lattice volume.

The calculations and experiments leading up to the above design of water flow system in the active lattice and reflector have been previously reported[11] and are given in Appendix 4. Table 2.7.A summarizes the results.

TABLE 2.7.A

LOCATION	PRESSURE DROP (psi)	FLOW (gpm)
Upper support casting	3	13,140
Upper assembly grid		2,600
Top and sides	9	1,920
Bottom	12	680
Fuel assemblies (23)	37	11,190
Beryllium assemblies (14)	37	31
Interstices		2,600
Beryllium reflector	30	2,920
Lower grid support	10	2,920
Lower assembly grid	10	2,600
Shim rods		
Cadmium	40	3,380
Thorium	40	2,900
Overall pressure drop	40	
Total flow		
With cadmium shim rods		20,120
With thorium shim rods		19,640

It is planned to make a final check on the water flow through the lattice and the reflector in the MTR before it is finally put into operation. Any flow discrepancies then found in the actual equipment can be corrected by enlarging or blocking water exit holes in the lower grid assembly.

2.7.2 Air Cooling. The thermal shield and the graphite are cooled by air drawn through them from the Reactor Building. The amount of heat that must be removed is indicated in Chap. 4; the external air system to provide proper air flow is described in Chap. 8.

The air enters at the top edges of the thermal shield through a system of 22 ducts which distributes it evenly to all four sides of the shield.[12] It is drawn out from the space above the graphite through two large holes in opposite corners of the upper thermal shields.

The major part of the air flows between the side plates of the thermal shield and then into the space between the bottom thermal shields. Holes in the upper plate of the bottom thermal shield distribute the air into the pebble zone and into the cooling holes of the permanent graphite. A small amount of this air goes outside the outer side plates of the thermal shield to help cool the concrete. By means of baffles in the inlet ducts some of the air is drawn between the two plates of the upper thermal shield and then through holes in the lower plate into the space above the graphite.

Since about 60% of the heat production in the graphite is in the pebble zone, the system has been designed to distribute the air in approximately this ratio between the pebble zone and the permanent graphite. In the pebble zone the air flows in the interstices between the pebbles, while in the graphite zone cooling is accomplished by allowing air to flow in the system of cooling holes illustrated in Fig. 2.7.A.

Since graphite begins to oxidize (0.0005 to 0.0009% per day) at about 570°F, this temperature was considered to be the maximum allowable for 45,000-kw operation. With this limit it was found[13] that the required cooling in the pebble zone could be obtained by an air flow of 840 lb/min, which requires a pressure drop of 26 in. of water. This gives an average exit air temperature of 205°F from the pebble zone if the air is heated 15°F in the thermal shield to 90°F. To this air is added the 684 lb/min flow through the permanent graphite and experimental facilities and the 174 lb/min to cool the top

[redacted]

DWG. 8605

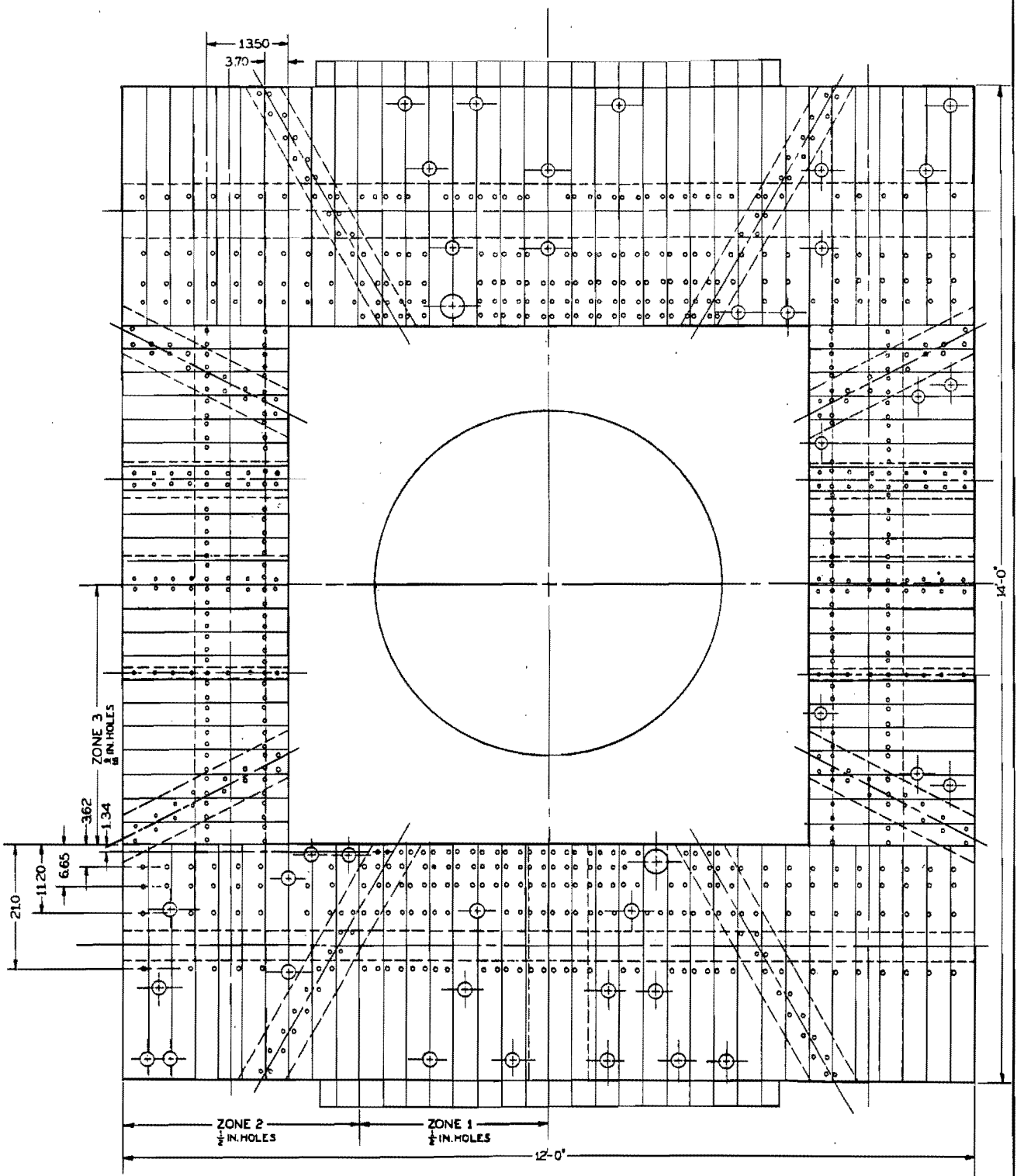

FIG. 2.7.A

HOLE PATTERN FOR THE GRAPHITE REFLECTOR

thermal shield. Thus the total air flow is approximately 1700 lb/min. For 75°F inlet air, the exit air temperatures are 150 and 185°F for reactor operation at 30,000 and 45,000 kw, respectively.

In addition to the graphite cooling, it is necessary to provide enough air to properly cool the liners of the experimental facility holes, i.e., the HB, DB, HG-9, and HT-1 holes and the vertical graphite holes in the pebble bed. Cooling in these liners is considered adequate if no local temperature exceeds 500°F.

The HG-9 liner is the most critical of these holes with regard to cooling. The aluminum liner for this facility is perforated top and bottom to match the graphite cooling holes in the plug.

It is calculated that the HB and DB liners will be sufficiently cooled by the normal air-cooling pattern and conduction along the liners, but some supplementary air is drawn between the liners and plugs from outside the reactor. This air flows into the pebble zone through perforations in the liners.

2.8 MONITORING EQUIPMENT

In order to obtain as much information as possible concerning the reactor and to supply some of the data required by the control system, monitor tubes and thermocouples will be built into the reactor structure. Their functions in the control system are discussed in Chap. 5 (Section 5.2.1); their physical structures and locations are described briefly below.

2.8.1 Monitor Tubes. The monitor tube system is designed to measure flow, temperature, and activity of the cooling water leaving the reactor lattice. To do this, 37 monitor tubes are inserted through and supported by the bottom plug. They extend up through the length of tank section E into the end boxes of the fuel elements. In general, of course, less than 37 fuel elements will be used, but the reactor lattice has space for this number plus eight shim rods (a 9 by 5 lattice array).

The structure of a monitor tube is shown in Fig. 2.8.A. It consists of a housing which acts as a support and enclosure for four small tubes. Three of these tubes are open at the end, two being used as pitot total and static

NOT CLASSIFIED

DDP-128

ITEM	DWG.	MATERIAL	DESCRIPTION	QTY.
1	DDP-121	304 S.S.	Pitot Tip	1
2	DDP-122	304 S.S.	Extension Tube	1
3	DDP-123	304 S.S.	Reducing Bushing	1
4	DDP-124	304 S.S.	Spacer	1
5	DDP-125	304 S.S.	Housing	1
6	DDP-126	304 S.S.	Distributor Body	1
7		Lead	Chemical Lead ASTM B29-40T	as needed
8		304 S.S.	1/4" O.D. 24ga. Tubing	as needed

ASSY USED ON

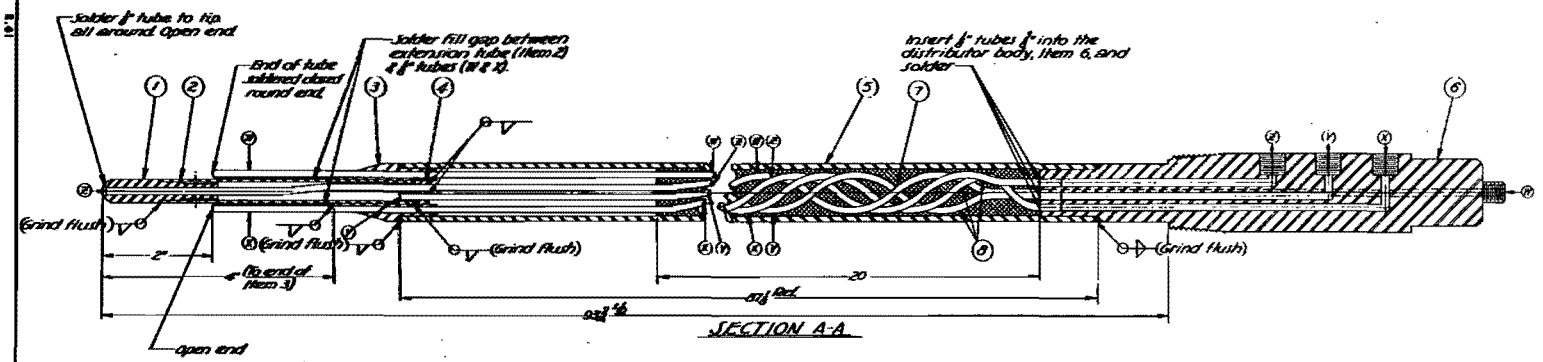

NOTES:

1. Each 1/4" tube must spiral thru at least 270° in housing.
2. Silver solder (Hard)

LEGEND:

(W) – Thermocouple Sheath.
(X) – Activity Sample Line
(Y) – Pitot Static Pressure Line
(Z) – Pitot Total Pressure Line

APPROVED FOR CONSTRUCTION

NOT CLASSIFIED

TOLERANCE UNLESS OTHERWISE SPECIFIED FRACTIONS ± 1/64 DECIMALS ± .005
BREAK ALL SHARP EDGES UNLESS OTHERWISE SPECIFIED.
FINISH MARKS ASA STANDARD
DO NOT SCALE THIS DRAWING

APPD.	DATE
[illegible]	8-31-50
O.J.M.	8-31-50
[illegible]	8-31-50
NMM	8-31-50

OAK RIDGE NATIONAL LABORATORY
TECHNICAL DIV. — P.O. BOX P. — OAK RIDGE, TENN.

MTR 105 BLDG.

REACTOR TANK MONITOR TUBE ASSEMBLY

DRAWN BY C.W. Dier — DATE 8-16-50 — SCALE 1"=1"
CHECKED BY [illegible] — DATE 8-22-50 — DRAWING NO. DDP-128 — REV.

REV. NO.	REVISION	APPD.	DATE

FIG. 2.8.A

pressure lines and one as a means of obtaining water samples directly from the fuel elements. The fourth tube has a thermocouple inserted so as to be in contact with its closed end.

It will be noted in the drawing that the four tubes are spiraled down through 20 in. of lead to provide adequate shielding. The whole monitor tube is held in the bottom plug by the threaded section of the distributor body so that if necessary any or all of the monitor tubes can be removed or replaced.

2.8.2 Thermocouples. In order to obtain some information on the temperatures of the thermal and biological shields, thermocouples will be embedded at 47 points throughout the reactor structure. The locations of these 47 points are given in Table 2.8.A.[14] As a factor of safety, two thermocouples will be attached to the steel or embedded in the concrete at these points. It should be noted that the locations given in Table 2.8.A are recommended best points, but construction difficulties may cause a shift in some of these locations. As-built drawings should be consulted for final placement data. It is currently planned to bring out the thermocouple leads in small conduits to junction boxes on the north and east faces of the reactor structure.

In addition to the above thermocouples, it is now planned to place two or more similar couples in the concrete near the HB and HT-1 liners. This will enable the operator to check on the concrete temperature when high-temperature experiments are being run in any of these holes.

2.9 HANDLING TOOLS

In the preceding sections of this chapter it has been tacitly assumed that some means will be available for handling various sections of the reactor through 20 ft of water. With the aid of experience gained on the mock-up, tools have been designed[15] and are being built to handle fuel assemblies, removable reflector pieces, regulating rods, shim rods, upper assembly grid, upper support casting, and spider support ring. In addition, a working platform to cover the top of the tank when open, underwater lights, a viewing tube, and reflector storage racks are also being built. Other tools which may be needed at a later date have been designed but are not at present being built. A brief summary of these tools with the reference drawings is given below.

TABLE 2.8.A

POINT IDENTIFICATION NO.*	ELEVATION	NORTH OF E-W CENTERLINE	SOUTH OF E-W CENTERLINE	EAST OF N-S CENTERLINE	WEST OF N-S CENTERLINE
1	100 ft 0 in.	6 ft 0½ in.		0 ft 10 in.	
2	100 0	6 7½		0 11	
3	100 0	7 9		1 1	
4	100 0	7 0½		1 10	
5	100 0	7 9		2 0	
6	100 0	8 6		2 2	
7	100 0	9 9		2 4	
8	100 0	11 0		2 6	
9	100 0	6 0½		6 11	
10	100 0	6 7½		7 6	
11	100 0	8 3		8 3	
12	100 0	6 6		8 9	
13	100 0	8 6		9 9	
14	100 0	3 5		7 0½	
15	100 0	3 4		8 0½	
16	100 0	3 6		8 9	
17	100 0	3 8		9 6	
18	100 0	3 10		11 0	
19	100 0	4 0		14 0	
20	100 0	0 8		7 10	
21	100 0		6 ft 0½ in.	0 10	
22	100 0	3 5½			8 ft 9 in.
23	106 5	0 0		3 9	
24	107 2	0 0		3 9	
25	107 11	0 0		3 9	
26	96 4	0 0		7 7½	
27	96 2	0 0		8 6	
28	94 8	0 0		3 10	
29	93 11	0 0		4 0	
30	93 2	0 0		4 2	
31	91 8	0 0		4 4	
32	91 0	0 0		4 6	
33	93 2	2 8		4 2	
34	107 11	2 9		3 9	
35	106 5	3 9		0 0	
36	107 2	3 9		0 0	
37	107 11	3 9		0 0	
38	110 6	8 6		0 0	
39	106 5	5 10		0 0	
40	106 2	6 0½		0 0	
41	95 5	6 4½		0 0	
42	95 6	4 0		0 0	
43	94 8	3 6		0 0	
44	94 8	4 0		0 0	
45	94 8	6 11½		0 0	
46	94 1	3 9		0 0	
47	93 3	3 9		0 0	

*Two thermocouples will be located at each point.

2.9.1 Design Summary. *(a) Compound Coupling "T" Handle, DRP-452.* To facilitate operation of tools with a compound shaft, a standard quick-disconnect coupling has been designed. A short handle with this standard coupling attached to one of the tool bodies will be used for pickup of the respective reactor component. One of four handles of various lengths will be used for lowering the part down the discharge chute. A lifting ring is welded on top of the handles as an adapter for the small hoist hook.

(b) Shim-rod Tool, DRP-440. Hooks, actuated by a toggle mechanism, engage the water slots on the shim rod when removal is desired. Compound "T" Handles Nos. 1 and 3 are to be used with this tool.

(c) Regulating-rod Tool, DRP-458. A ball-socket joint using the balls on the end of the regulating rod will be used to remove the rod. Compound "T" Handles Nos. 1 and 4 are to be used with this tool.

(d) Reflector-removal Tool, DRP-497. A ball-socket joint adapting the bullet-nosed pin on the end of removable reflector pieces will be used to lift these pieces. Two tools will be built since, if storage on the side of the tank is desired, a short body tool will be necessary, but, if discharge of the reflector piece is desired, a long body tool will be used. The lead plug in the discharge chute will be lifted with the short body tool.

Compound "T" Handles Nos. 1 and 2 will be used for putting "A" and "D" pieces in the storage racks, while Nos. 1 and 5 will be used for putting the lead plug in a storage rack or discharge "A" pieces.

(e) Fuel-removal Tool, DRP-461. Retractable pins inserted radially into the snouts on the ends of fuel assemblies and "L" type reflector pieces will be used to lift these reactor components. Compound "T" Handles Nos. 1 and 5 will be used with this tool.

(f) Top Working Platform, DRP-439. A 7-ft-diameter 1-ft-high cylinder will support a circular table that can be rotated manually and will serve as a working platform. A 2-ft-wide 5-ft-long slot in the table will permit vertical access to the reflector and fuel elements. The platform, which weighs approximately ¼ ton, will be equipped with lifting slings which attach to the upper assembly grid tool, which in normal operation will be the first and last tool used.

(g) Spider Support Lifting Sling, DRP-470. A collapsible sling fabricated from three ½-in. rods with turnbuckles for adjustment will be used for lifting the spider support ring.

(h) Upper Support Casting Wrench Assembly, DRP-490. A wrench which has an inner rod that screws into the bolt head will be used for removing the upper support casting bolts.

(i) Viewing Tube Assembly, DRP-549. A tube with a plastic sight glass is to be mounted on the working platform. The lower end of this tube will extend below the water in the tank, thus allowing better vision.

(j) Upper Assembly Grid Tool, DRP-489. A tool with hooks on the end will catch the toggle mechanism and lift the upper assembly grids. The assembly grids will be temporarily stored on platforms oriented as shown on DRP-558 on the spider support ring.

(k) Upper Support Casting Tool, DRP-492. This tool hooks horizontal pins on the casting main support arms.

(l) Underwater-light Wiring Diagram, DRP-530. A variable autotransformer and a 110-watt 20-volt center-tap transformer will supply four underwater lights with power.

(m) Underwater-light Assembly. A watertight steel housing with a transparent plastic lens will encase the sealed-beam lights to prevent accidental breakage.

(n) "A" Piece Rack, DRP-526; Discharge Tube Plug Rack, DRP-528; "D" Piece Rack, DRP-529. Racks will be bolted to the spider support ring for storage of reflector pieces. Orientation of the racks is shown in DRP-558.

(o) Regulating-rod Bearing and "E" Piece Tool, DRP-476.* A tool with spreading pawls will be used to pick up the regulating-rod bearings and the "E" pieces. It is intended that one tool be used for all bearings. Since there is a 6-ft difference in elevation of the bearings, the tool is a compromise as to overall length. Compound "T" Handles Nos. 1 and 5 will be used with this tool.

(p) Lower Assembly Grid Tool, DRP-546.* Like the regulating-rod bearing tool, this tool has spreading pawls for lifting. This tool is used with compound "T" Handle No. 1.

*Will be built at a later date.

(q) Lower Guide Grid Wrench, DRP-539.* A wrench which has an inner rod that screws into the bolt head will be used to remove the lower guide grid bolts.

(r) Shock-absorber Plate Wrench, DRP-536.* This tool is similar to the wrench above.

(s) Torque Wrench Extension for Sockets, DRP-491.* This tool is used to adapt a torque wrench to the bolts 10 to 30 ft away.

(t) Shock-absorber Support-plate Tool, DRP-464.* This tool consists of four hooks on an extension rod which will engage eye bolts on the plate for lifting.

(u) Lower Guide Grid Tool, DRP-493.* This tool is similar to the shock-absorber support plate tool.

(v) Tapped Segment Ring Lifting Tool, DRP-460.* This tool is used for lifting various segment rings on the reactor tank.

*Will be built at a later date.

2.10 REFERENCE REPORTS

(1) Gill, J. P., *MTR Report, Tank Sections A and E,* ORNL CF-49-11-217, November 22, 1949.

(2) Gall, W. R., *MTR Report on Reactor Structural Steel,* ORNL CF-49-11-273, November 29, 1949.

(3) Engberg, R. E., *Shim-safety Rod Lower Shock Absorber Position Indicator System, MTR Design Report, Controls,* ORNL CF-51-3-68, March 30, 1951.

(4) Zapp, F. C., *MTR Report on Graphite Reflector,* ORNL CF-49-10-88, October 6, 1949; *Addendum No. 1 on Graphite Report,* ORNL CF-49-11-176, November 17, 1949; *Addendum No. 2 on Graphite Report,* ORNL CF-50-2-143, February 20, 1950; *Addendum No. 3 on Graphite Report,* ORNL CF-50-3-171, March 31, 1950.

(5) Lane, J. A., *Induced Activity in Graphite,* ORNL CF-49-10-183, October 18, 1949.

(6) Lane, J. A., *Thermal Column Graphite,* ORNL CF-50-1-20, January 5, 1950.

(7) Zapp, F. C., *Graphite for the Materials Testing Reactor,* ORNL CF-50-1-30, January 10, 1950.

(8) Sholl, W. E., *Thermal Shield for the MTR*, ORNL CF-50-1-125, January 25, 1950.

(9) McWherter, J. R., *Thermal Stress in Concrete Shield, MTR Project*, ORNL CF-49-9-69, September 8, 1949.

(10) Briggs, R. B., *Technical Division Section II, Report for Period July 15 - September 15, 1947*, ORNL CF-47-9-560, September 15, 1947.

(11) Kasper, S., *Water Flow in the MTR*, ORNL CF-50-6-102, June 15, 1950.

(12) Gall, W. R., *MTR Report on Internal Air System*, ORNL CF-49-11-208, November 21, 1949.

(13) Briggs, R. B., *Cooling of the Graphite Reflector for the MTR*, ORNL CF-50-3-102, March 20, 1950; *Cooling of the Graphite Reflector for the MTR*, ORNL CF-50-1-45, January 10, 1950.

(14) McWherter, J. R., *Permanent Thermocouples in the MTR Structure*, ORNL CF-50-7-142, July 27, 1950.

(15) McWherter, J. R., *MTR Reactor Tank Handling Tool Design*, ORNL CF-51-1-19, January 4, 1951.

2.11 REFERENCE DRAWINGS

DWG. NO.	TITLE
BKC-3150-565-1	Neutron Curtain System, General Arrangement - Reactor Structure
BKC-3150-565-2	Neutron Curtain System, Sections and Details - Reactor Structure
ORNL TD-1339	Controls Assembly
ORNL TD-1399	General Assembly
ORNL DRP-392	Bottom Plug Vertical Rabbit Assembly
BKC-3150-502-1 through 8 and 10	Thermal Shield
BKC-3150-502-9 and 13 through 18	Air Ducts
BKC-3150-502-19 and 20	Pebble Bins
BKC-3150-503-1 through 10	Thermal Shield
BKC-3150-504-1 through 34	Graphite

DWG. #10197 [redacted]

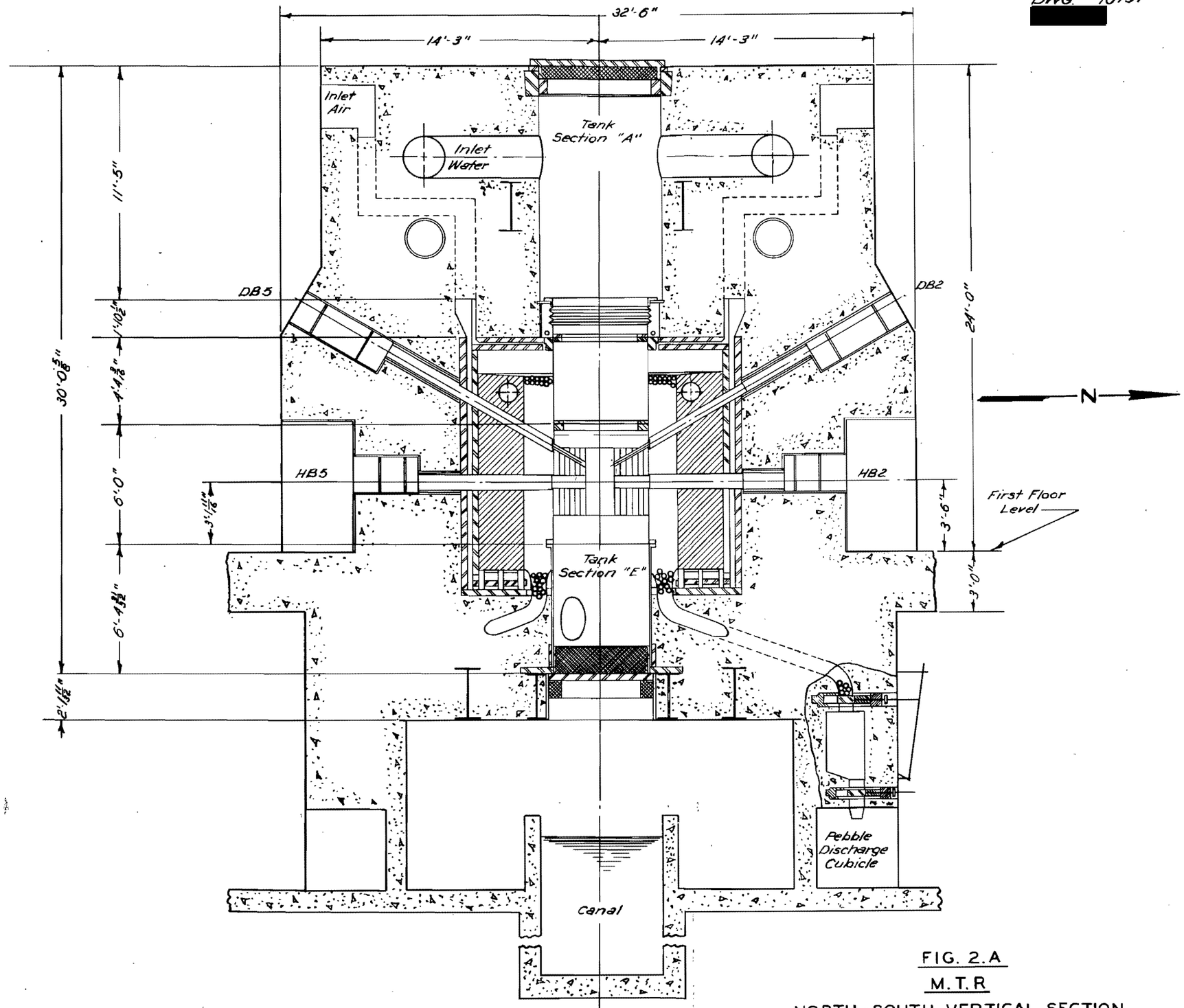

FIG. 2.A

M.T.R

NORTH-SOUTH VERTICAL SECTION

OAK RIDGE NATIONAL LABORATORY

DWG. # 10198 [redacted]

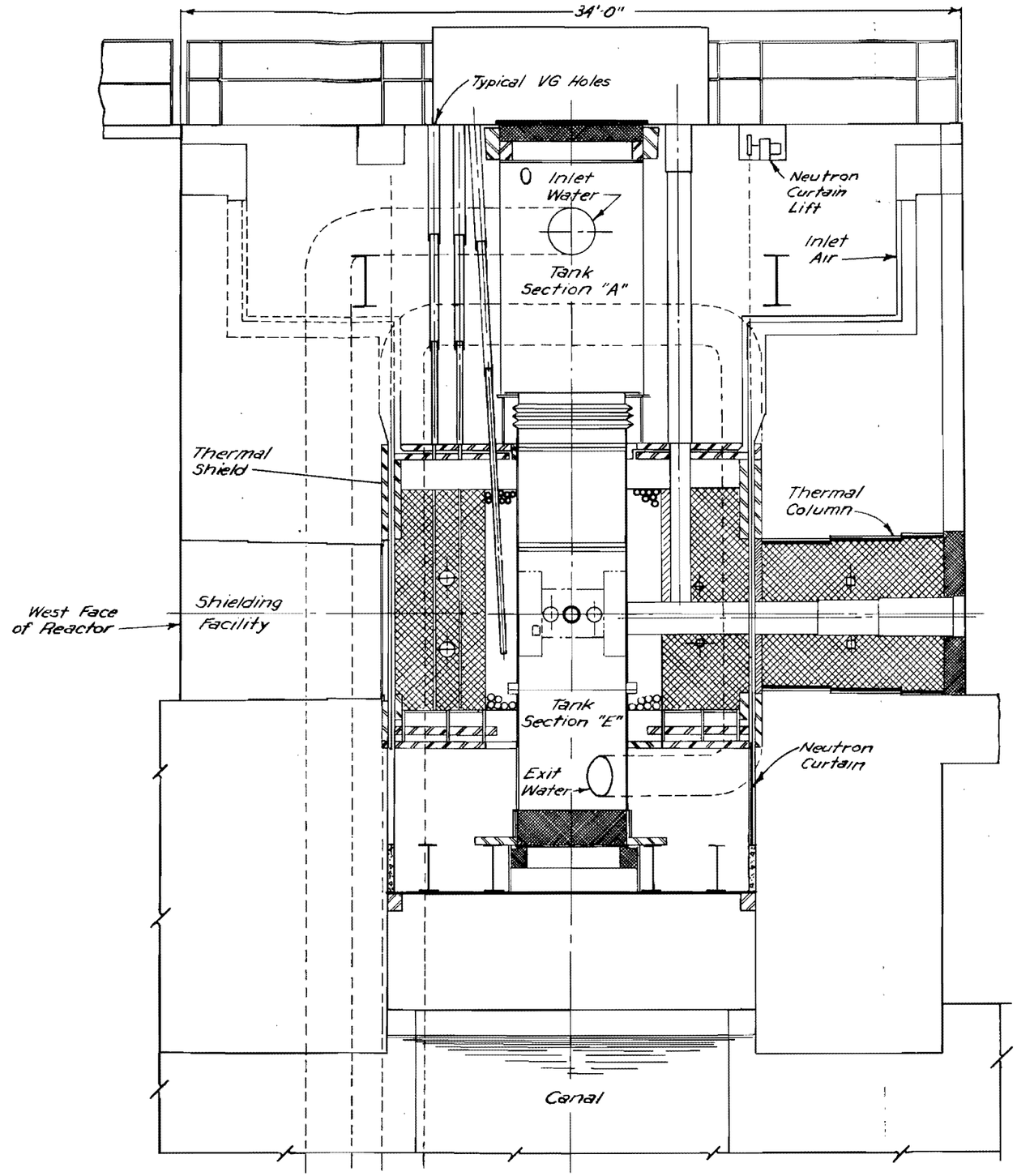

FIG. 2.B

M.T.R.

EAST-WEST VERTICAL SECTION

OAK RIDGE NATIONAL LABORATORY

DWG. #10199 [redacted]

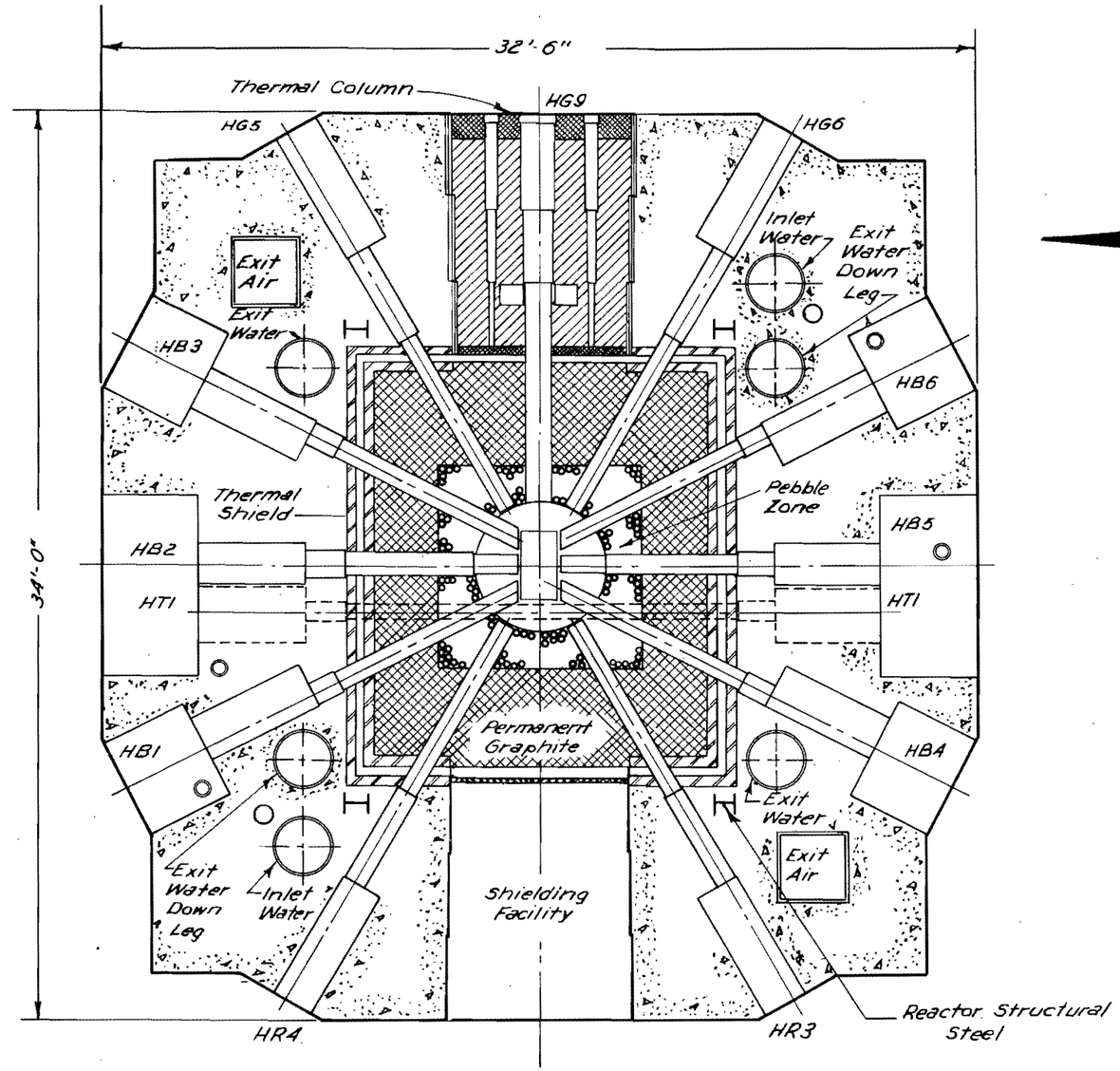

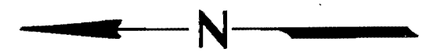

FIG. 2.C
M.T.R
HORIZONTAL SECTION

OAK RIDGE NATIONAL LABORATORY

DWG. NO. 10394 [redacted]

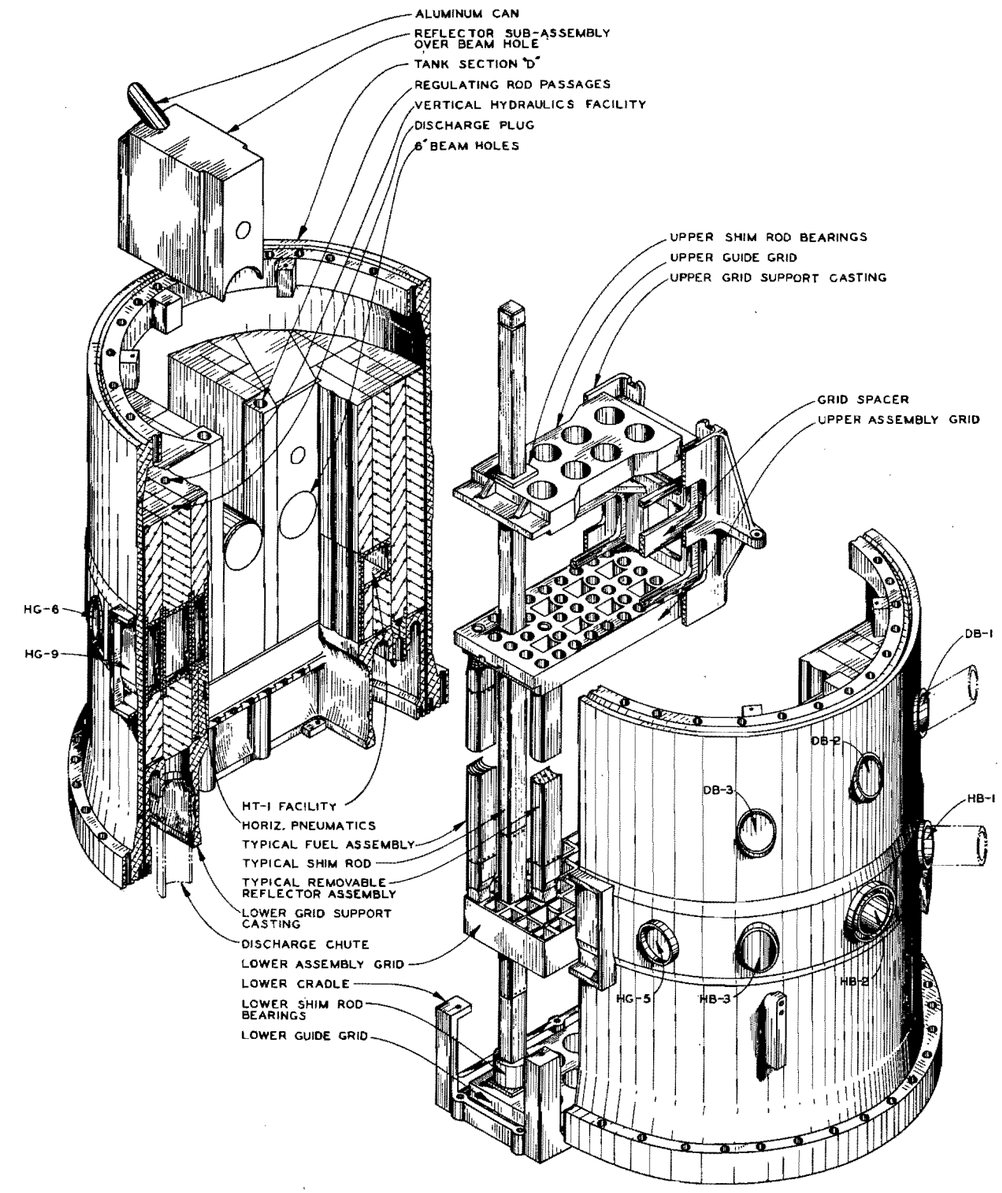

FIG.-2.D

PICTORIAL CROSS SECTION

REACTOR TANK

OAK RIDGE NATIONAL LABORATORY

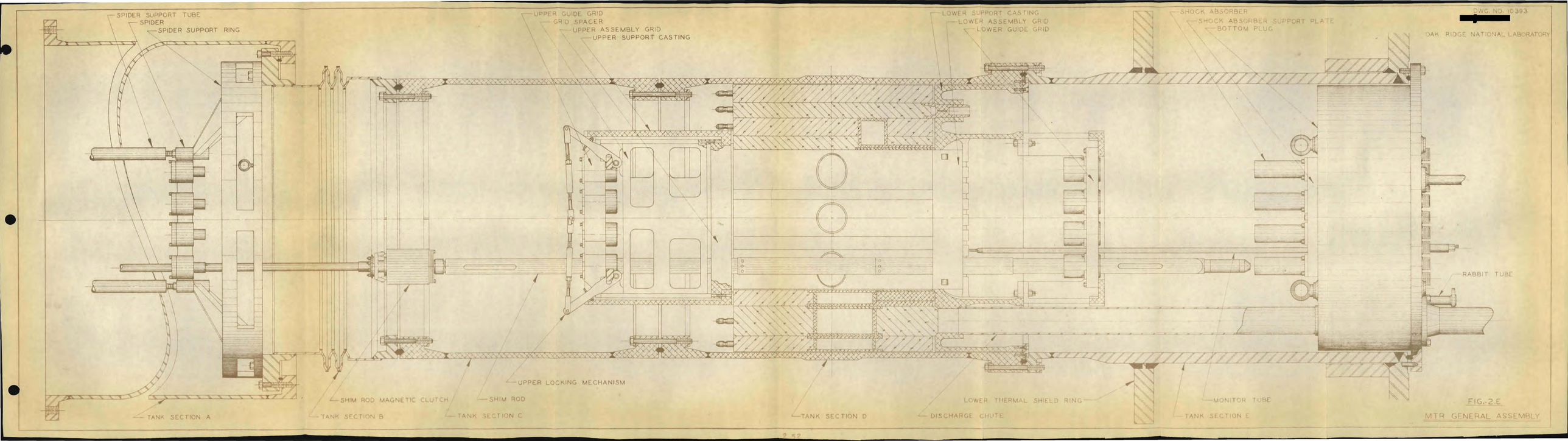

FIG. 2.E

MTR GENERAL ASSEMBLY

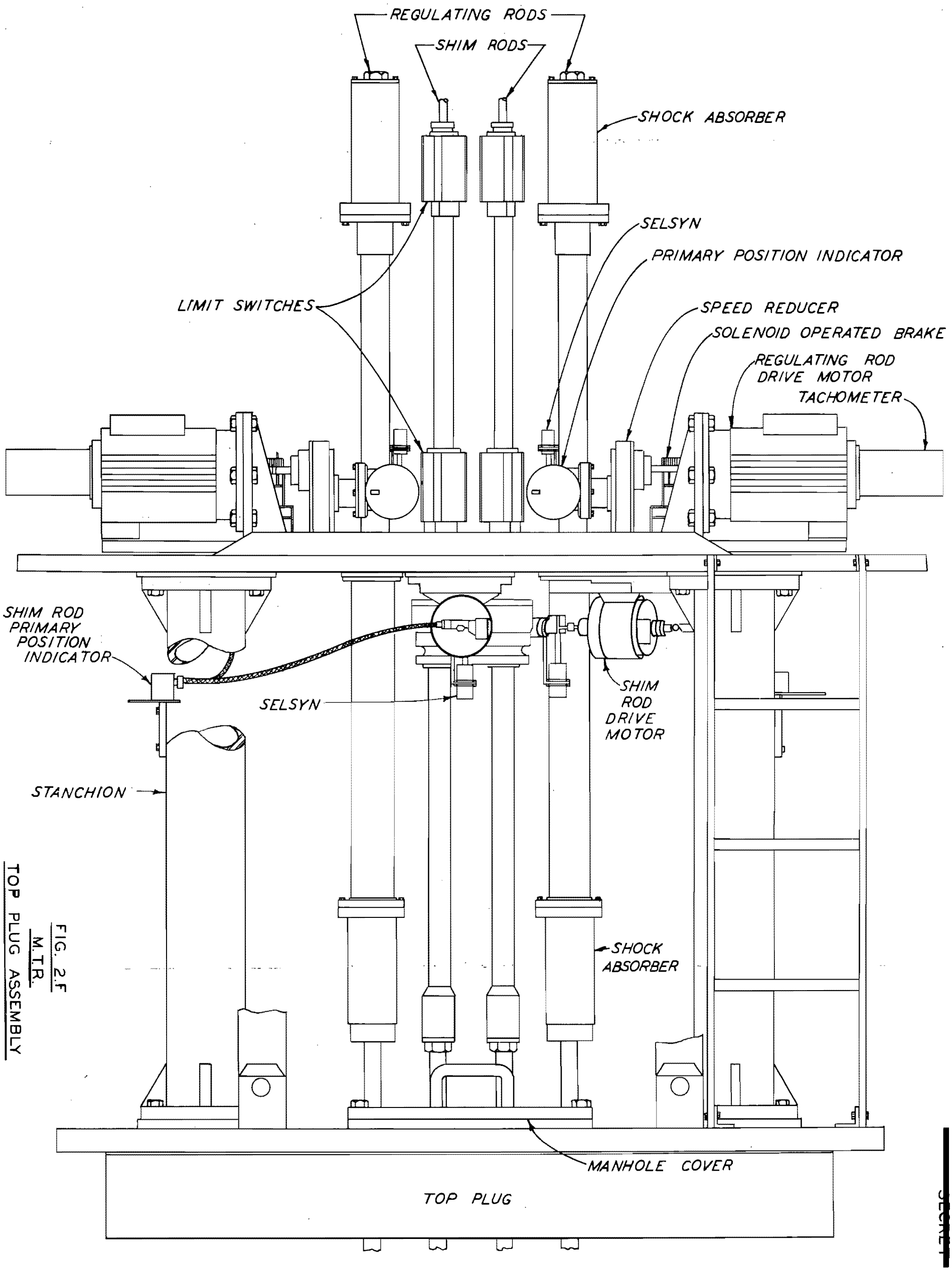

FIG. 2.F
M.T.R.
TOP PLUG ASSEMBLY

DWG. # 10392
SECRET

OAK RIDGE NATIONAL LABORATORY

Chapter 3

EXPERIMENTAL FACILITIES

In order to fulfill the purpose of the MTR the experimental facilities provided have been designed to be as varied and as flexible as possible. The locations of the various facilities are shown in Figs. 3.A through 3.F,* and the relationship of the side holes to the Reactor Building is shown in Fig. 3.G. The location of the holes relative to the active lattice has been shown in Figs. 2.A through 2.D.

The experimental facilities and the estimated fluxes obtainable at 30-megawatt operation are listed in Table 3.A. It must be emphasized that the fluxes given are only estimates based on the best data available before actual operation of the MTR. It is hoped that a supplement to this report will be issued after actual measurements have been made in the reactor.

3.1 HORIZONTAL AND DOWN BEAM EXPERIMENTAL HOLES**

3.1.1 Introduction. There are 17 large experimental holes that lead from the reactor faces either to the reactor tank wall or to the active lattice. These holes are treated separately from the vertical graphite holes (see Section 3.4) because their sizes and locations require special design attenuation and handling techniques. They are characterized by the presence in each of a special radiation door, the sole purpose of which is to minimize danger to personnel in the Reactor Building during plug-handling operations. Since these holes provide the largest volumes of high flux in the reactor, they are the most dangerous and their use will probably be correspondingly difficult and complicated. They are as follows:

(1) Six Horizontal Beam Holes, HB-1 Through HB-6. These holes extend horizontally from the reactor face to the active lattice. Holes HB-2 and HB-5 are 8 in. in diameter to the reactor tank wall and 6 in. in diameter from the reactor tank wall to the active lattice. Holes HB-1, 3, 4, and 6 are 6 in. in diameter throughout.

(2) Six Down Beam Holes, DB-1 Through DB-6. These are 6-in.-diameter inclined holes which extend from the upper north and south faces to the reactor tank. They are located directly above the horizontal beam holes. Inside the tank wall they are essentially extended to the lattice by 2-in.-I.D. sealed empty aluminum cans in the beryllium reflector.

*For convenience in reading, Figs. 3.A through 3.G are placed at the end of this chapter.

**Section 3.1, except 3.1.5, ANL contribution.

TABLE 3.A

Summary of Experimental Facilities

TYPE OF HOLE	FACILITY DESIGNATION	SIZE	APPROACH	ESTIMATED FLUX, MAX. (neutrons/cm^2-sec)	
				THERMAL	FAST*
Beam	HB-1, 2, 3	6-in. I.D. in Be	Horizontal to core edge**	5×10^{14}	7×10^{13}
Beam	HB-4, 5, 6	6-in. I.D. in Be	Horizontal to Be in active section	2.8×10^{14}	2×10^{11}
Beam	DB-1, 2, 3, 4, 5, 6	6-in. I.D.	Inclined down to tank; 2-in.-I.D. can channel to core	4×10^{13}	5×10^{10} (DB2 only)
Beam	HG-5, 6	6-in. I.D.	Horizontal to tank wall	8×10^{13}	
Beam	HG-9	10 by 16 in.	Horizontal to tank wall; 5- by 12-in. fast-neutron channel to core	8×10^{13}	4×10^{12}
Access	VG-9	10 by 10 in.	Vertical from top access to HG-9	3×10^{13}	
Thermal column	T-2	6 by 6 ft	Horizontal to Pb window	1×10^{12}	
Thermal	T-2—H-1, 2	4 by 4 in.	East-west horizontal across T-2	2×10^{10}	
Thermal	T-2—H-3, 4, 5, 6, 7, 8	4 by 4 in.	Horizontal within and parallel to T-2	6×10^{11}	
Thermal	T-2—V-1, 2	12 by 12 in.	Vertical from top of reactor to T-2	2×10^{11}	
Through	HT-1	4-7/8 by 4-7/8 in.	Horizontal through reactor tank	1.8×10^{14}	3×10^{13}
Through	HI-2, 3	10¾-in. I.D.	East-west horizontal through graphite	10^{13}	
Through	HG-1, 2	8-in. I.D.	North-south horizontal through graphite	10^{13}	
Through	HG-3, 4	4-in. I.D.	North-south horizontal through graphite	10^{13}	
Through	VT-2	2¾ by 2¾ in.	Vertical through shim rod hole	2.5×10^{14}	1×10^{14}
Through	VG-2, 4	4-in. I.D.	Vertical through graphite	3×10^{13}	
Pneumatic rabbit	HR-1, 2	1-in. I.D.	Horizontal through reactor tank	1.6×10^{14}	4×10^{13}
Pneumatic rabbit	HR-3, 4	4-in. I.D.	Horizontal to reactor tank	8×10^{13}	
Hydraulic rabbit	VH-3, 4	1¼-in. I.D.	Vertical from top in spare regulating rod holes	2.5×10^{14}	10^{13}
Hydraulic rabbit	VH-1, 2	1-in. I.D.	Vertical from basement in Be	2.4×10^{14}	

*Neutrons having energies greater than 1 Mev.

**One can be for ¼ mile beam, and one for neutron spectrometer if desired.

TABLE 3.A (Cont'd)

TYPE OF HOLE	FACILITY DESIGNATION	SIZE	APPROACH	ESTIMATED FLUX, MAX. (neutrons/cm^2-sec)	
				THERMAL	FAST*
Vertical	VG-1, 3, 5, 6	4-in. I.D.	Slant from top into pebble zone	3×10^{13}	
Vertical	VG-7, 10-14, 16-20	2½-in. I.D.	Slant from top into pebble zone	5×10^{13}	
Vertical	VG-23-26, 29-41, 43, 45-55, 57-62	2-in. I.D.	Vertical from top into permanent graphite	10^{13} to 10^{12}	
Vertical	VC-1-9, 11-13	2-in. I.D.	Vertical from top into concrete		
Fast flux	About 40 Be assemblies; removable reflector pieces	3 by 3 in.	Vertical from top tank***	5×10^{14}	7×10^{13}
Fast flux	About 15 Be assemblies; removable core pieces	3 by 3 in.	Vertical from top tank***	5×10^{14}	7×10^{13}
Gamma	GT-1, 2	6-in. I.D.	Vertical from top γ-ray thimbles in water	500 r/hr	
Shielding	Facility		Horizontal from west	10^{12}	
Instrument	VN-1, 2, 3, 4, 5, 6	2½-in. I.D.	Slant from top	5×10^{13}	
Instrument	VG-8, 15	2-in. I.D.	Slant from top	5×10^{13}	
Instrument	VG-27, 28, 42, 44, 56	2-in. I.D.	Vertical from top	10^{13} to 10^{12}	

***Charged or discharged only when reactor is shut down and top plug is removed.

Note: These estimated neutron-flux values are based on beryllium or graphite (according to material penetrated) in the experimental holes. Actually, experimental apparatus and samples will cause local "sinks" and reduce the flux attainable for a particular experiment.

(3) Two Horizontal Graphite Holes, HG-5 and HG-6. These are 6-in.-diameter horizontal holes which extend to the reactor tank.

(4) Two Horizontal Rabbit Holes, HR-3 and HR-4. These are 4-in.-diameter horizontal holes which extend to the reactor tank. (The 1-in. holes HR-1 and HR-2 are discussed in Section 3.5.)

(5) One Horizontal Through Hole, HT-1. This is a hole 4-11/16 in. square which extends from one reactor face to the opposite face. It goes through the reactor tank and lies adjacent to one side of the active lattice.

In formulating the design of these holes, considerable thought was given to the future needs of the experimenters who will use these facilities. Other factors that had a strong influence on the experimental hole design are radiation hazards, material selection, cooling requirements, and the configuration of the reactor itself.

Several design proposals were prepared and the relative merits of each were consolidated into the design illustrated in Fig. 3.1.A. The hole liner and its components as shown are essentially the same for all the beam holes listed above. Designs of the dummy plugs used in the different holes are shown in Figs. 3.1.B, C, and D.

3.1.2 Beam Hole Liners and Components. The prime objective in design of the hole liner and its components was flexibility. It was necessary therefore to consider the adaptability of holes to experimental plugs of varying design and the maintenance, repair, or replacement of the hole components, including the removable sections of the liners. The configuration and sizes of the hole liners in the biological shield are dictated primarily by the location and size of the radiation doors. The outer shields, the radiation doors and drive mechanisms, the tapered portion of the liners, and the graphite zone liners have been made removable with the hope that radiation levels will permit realization of additional flexibility.

Graphite Zone Liner. The graphite zone liner is the portion of the experimental hole liner which extends from the thermal shield to the reactor tank. It is a ¼-in.-thick aluminum tube secured at one end to the removable steel liner and supported at the other end by a pilot ring on the reactor tank. The liner is removable and is not permanently secured to the reactor tank because this tank is designed as a removable component.

NOT CLASSIFIED
Dwg. # 10751

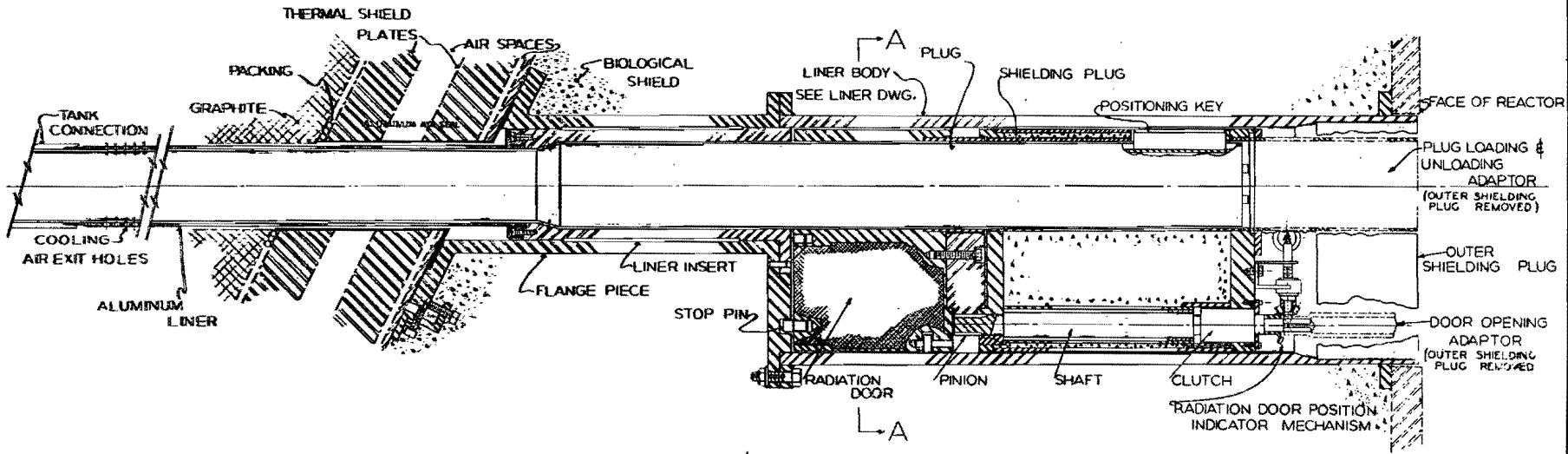

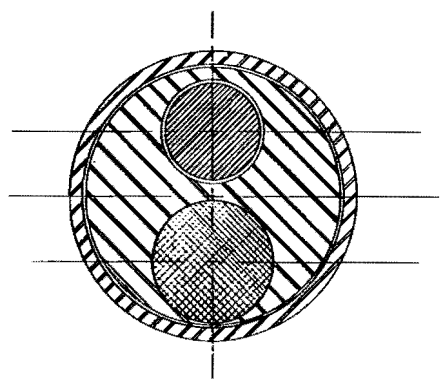

SECTION AA

TOLERANCES	ARGONNE NATIONAL LABORATORY		TYPICAL BEAM HOLE LINER AND COMPONENTS
	This drawing is the property of the Argonne National Laboratory		
	SCALE NONE		FIG. 3.1.A

NOT CLASSIFIED
Dwg. #10752

NOTE:
ALL DIMENSIONS SHOWN ARE TYPICAL
OF WATER-COOLED PLUGS

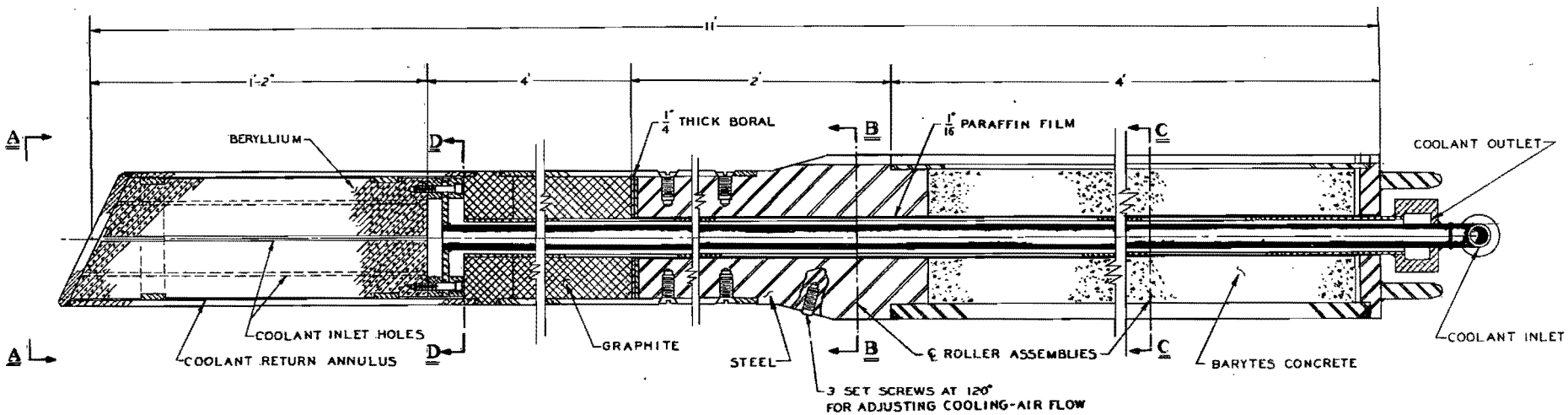

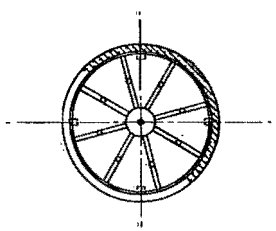

SECTION A
(SHOWN WITHOUT END PLATE)

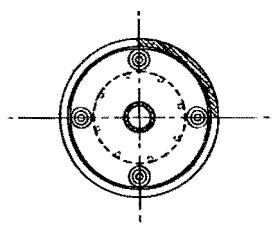

SECTION D

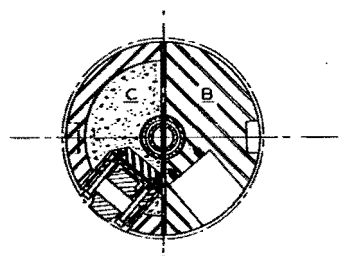

SECTION B & C

ARGONNE NATIONAL LABORATORY
This drawing is the property of the Argonne National Laboratory

TYPICAL BEAM HOLE
WATER-COOLED DUMMY PLUG

FIG. 3.1.B

NOT CLASSIFIED

Dwg. #10750

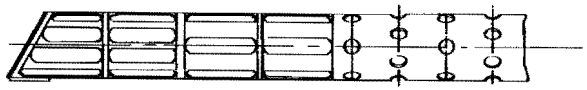

ARRANGEMENT OF TIP COOLING OPENINGS

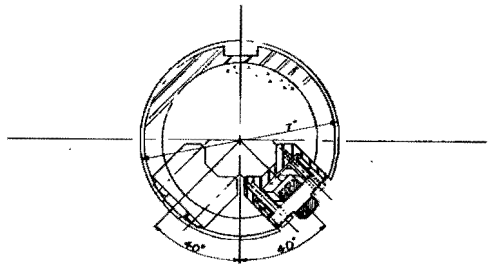

SECTION A - ROLLER ASSEMBLIES

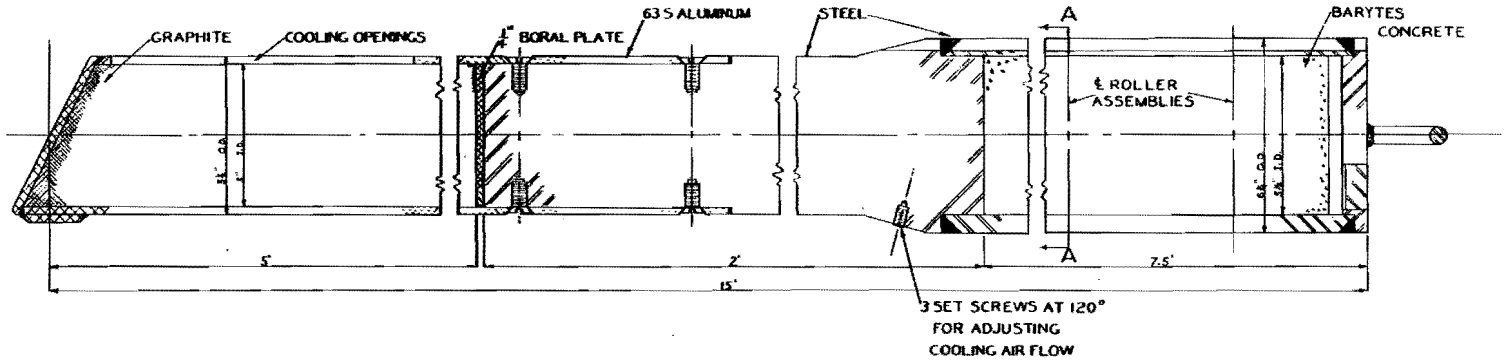

NOTE DIMENSIONS ARE TYPICAL OF ALL AIR COOLED PLUGS

TOLERANCES: FRACTIONAL TOL. ± 1/16, DECIMAL TOL. ± .005, ANGLE ± 1/2°; UNLESS OTHERWISE NOTED	ARGONNE NATIONAL LABORATORY — This drawing is the property of the Argonne National Laboratory	SYM. / CHANGE / DATE / BY	
DRAWN C.C. 1-10-51; HOLTEN; LEAST	SCALE NONE	PART TYPICAL BEAM HOLE; ASSEMBLY AIR COOLED DUMMY PLUG	
		SHEET 1 OF 1; DWG. NO. FIG. 3.1.C	

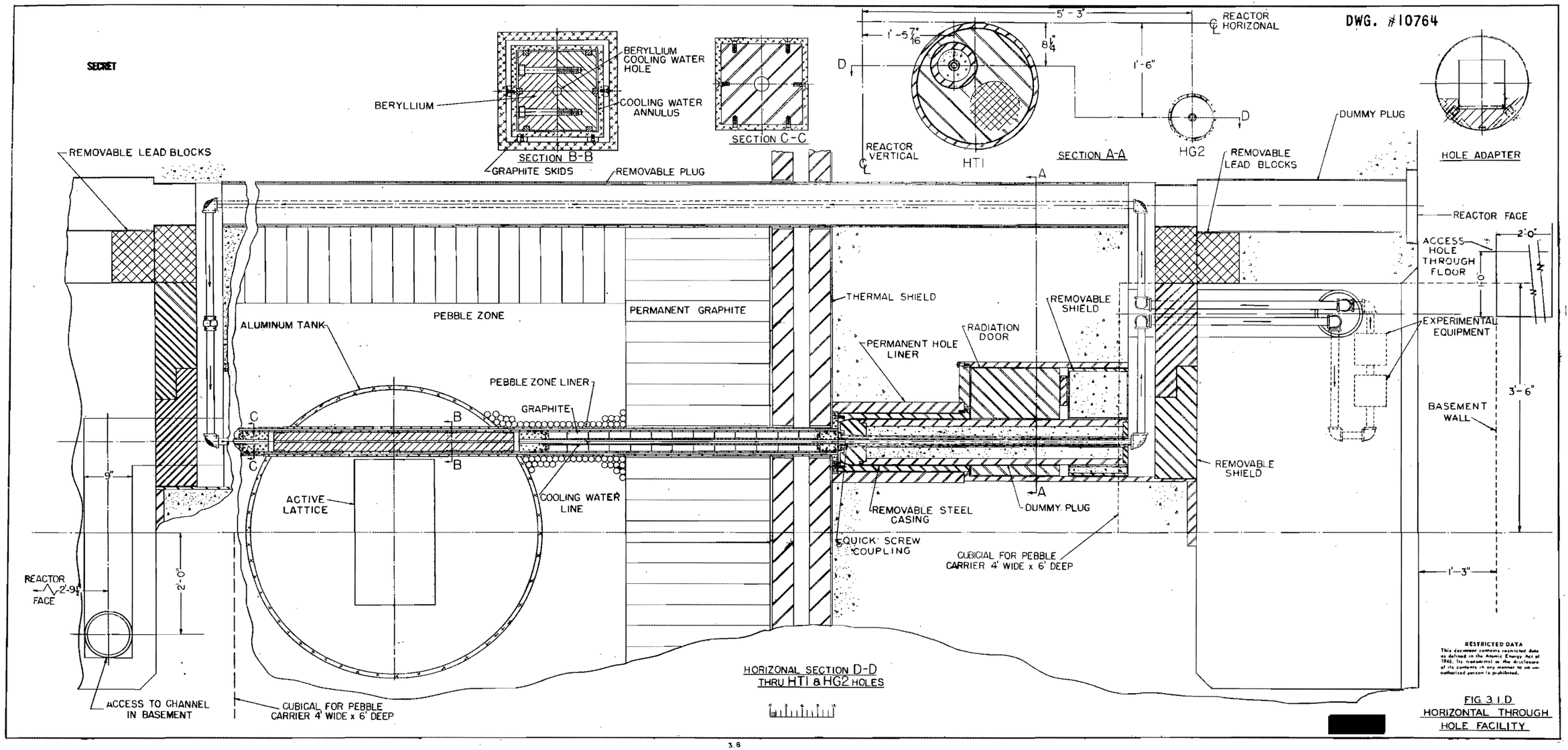

FIG. 3.1.D
HORIZONTAL THROUGH HOLE FACILITY

The liner is constructed of aluminum because of its relatively low long-lived induced activity.[1] Aluminum also has a relatively low neutron absorption cross-section, which is desirable for reactor component materials in the region of the reactor tank. In this regard a compromise had to be made in the selection of 52S alloy in preference to 2S, 3S, 61S, or 63S owing to the former's substantial advantage in high-temperature physical properties.

Cooling of the liner is accomplished primarily by the air that cools the graphite reflector. In the pebble zone the liner is exposed directly to the air flow, while in the permanent graphite zone numerous vertical cooling holes in the graphite provide for air circulation through an annulus between the liner and the graphite. Secondary cooling is provided by air drawn in from the reactor face through an annulus between the plug and the liner and exhausted into the pebble zone by means of a suitable hole pattern in the liner near the reactor tank. The mechanical design and selection of alloy were based on a maximum temperature of 570°F. A thermocouple provided on each HB liner at a point near the reactor tank permits the checking of the maximum liner temperature. This is particularly important when a high-temperature experiment is conducted in the experimental hole. The thermocouple leads are carried out the beam hole to the reactor face. Instruments for reading the thermocouples are not provided as permanent fixtures.

Sufficient endwise clearance, 3/8 in., between the end of the liner and the tank wall is provided to allow for thermal expansion; 1/32 in. is allowed for radial expansion of the tube within the pilot ring.

Removable Steel Liner. The removable steel liner extends from the thermal shield to the radiation door.

Experimentation and calculation have shown that to prevent neutron streaming through the annulus formed by the dummy plug and the hole liner, two steps in the annulus are required.[2] One of these is as close to the thermal shield as practical and the second is near the outer face of the concrete shield. The tapered portion of the hole forms the first step, and the removable steel shield at the outer face forms the second step.

This liner section is removable primarily because to it is secured the graphite zone liner, which must be removable. Secondarily, it is desired that this liner be removable since it may be found desirable to change the configuration of the hole in order to serve special experimental requirements.

It is anticipated that the induced activity of the steel liner will be low enough to permit handling with standard safety measures. Also, owing to the dry air conditions prevailing at the site, ordinary carbon steel is used with no attempt at corrosion prevention other than the application of a light film of oil. The oils recommended for this purpose, selected because of their good resistance to radiation damage, are Dow Corning Silicone Fluids Nos. 701, 702, 703, and 710 and Carbide and Carbon Chemicals Corporation Ucon Lubricants 50-HB-280-X, DLB-265-BX, 75-H-480, LB-300-X. Paints and platings were rejected due to the probability of flaking. The same holds true in respect to all other beam hole components in which steel is exposed only to air.

Permanent Steel Liner. The permanent steel liner provides a housing for the removable steel liner, the radiation door, the removable concrete shield, and the removable steel shield (see Fig. 3.1.A). For the 6-in. beam holes it consists of two carbon steel cylinders. One is approximately 22 in. in diameter, and the other is about 11 in. in diameter. The 11-in.-diameter cylinder is eccentrically secured to an end plate on the large cylinder; it houses the removable steel liner. The large cylinder houses the radiation door, the removable concrete shield, and the removable steel shield.

The permanent steel liners of the HB holes are provided with annular air spaces to serve as heat dams. Also wrapped around the outer surface of the liners and embedded in the biological shield concrete are cooling-water coils. The heat dams and cooling coils prevent overheating of the concrete when these experimental holes are used for high-temperature experiments. To provide for the determination of concrete temperatures, thermocouples are embedded in the concrete near the cooling coils.

Radiation Door. A lead door within the reactor structure is provided to attenuate radiation from the experimental hole when the plug is removed.[2] The thickness of the door has been calculated to reduce γ-ray activity to tolerance during reactor shutdown. Opening and closing of the door are accomplished from the reactor face.

After considerable investigation of door types, the radiation door shown in Fig. 3.1.A was adopted. It is a round billet of steel with two eccentrically located holes; one hole forms a portion of the beam hole while the other is filled with lead and provides a radiation shield. The door is free to

rotate inside the large steel liner by means of several rollers located in recesses in its surface. A gear sector bolted to the door and driven by a pinion and shaft provides the drive. The drive shaft extends to the reactor face, thereby permitting remote operation by an electric motor mounted on the coffin or manual operation from the reactor face.

Owing to the eccentric positions of the lead-filled hole and the open hole, considerable force is needed to hold the radiation door in certain positions. A special anti-kickback clutch is provided to make it impossible for the door to move unless driven or allowed to turn by rotation of the external drive shaft. The design is "fail safe" in case the drive becomes disengaged. When the beam hole components are removed, care must be taken that the radiation door is in a "free down" position so that the end-position locating pin will not be sheared when the removable shield is withdrawn. Associated with the radiation door is its position indicator. This is mounted on the face of the reactor over the cubicle to indicate the actual door position.

Removable Concrete Shield. To fill the void space in the large steel liner outside the radiation door, a steel-encased concrete cylinder is provided for necessary shielding. Eccentrically located in the concrete billet is a steel-encased cylindrical hole of approximately 10 in. I.D. which forms a portion of the experimental hole. Removal of this shield permits access to the radiation door.

Removable Steel Shield. Between the removable concrete shield and the removable steel shield is a void 5 in. wide which is used for cooling-water pipe connections. Behind this space is a round steel billet mounted flush with the reactor face, which provides a convenient shield for the plug cooling-water connections. This billet is of necessity readily removable. Based on calculations of cooling-water activity, this steel is required to be approximately 8 in. thick.[2]

In addition to providing a shield for the cooling-water lines, this steel billet forms the second step to prevent neutron streaming through the plug annulus and as a step to prevent neutron and γ-ray streaming down the annulus surrounding the radiation door and the concrete shield.

Beam Hole Adapter. This adapter consists of a steel tube with a flanged end that is bolted to the removable concrete shield before plug insertion or withdrawal. Its purpose is to guide and support the dummy plug, during insertion or removal, through a 13-in. gap which exists when the steel shield plate is removed.

3.1.3 Beam Hole Dummy Plugs. When the experimental holes are not being used they are filled by dummy plugs. The conceptual design shown in Fig. 3.1.B is typical of the plugs for HB-1 through HB-6 and HT-1. Dummy plugs for the other facilities are similar except for the absence of beryllium tips and provisions for water cooling. Figure 3.1.C illustrates the air-cooled plugs for the latter holes.

The water-cooled plugs are constructed in three detachable sections. The sections are: (1) the beryllium tips, (2) the graphite section, and (3) the concrete and steel section. With this type of construction it is possible that an experimental plug may conform to the dummy plug as far as the graphite and concrete sections are concerned. If more experimental space is required, it may conform only to the concrete section.

In choosing plug materials, an effort has been made to duplicate in so far as possible the materials in the reactor sections surrounding the experimental holes. The result of this procedure is that neutron fluxes in the reflector regions, beryllium, and graphite, are maintained at practical maxima. Materials for the plug casing have been chosen for minimum neutron absorption and induced activity, consistent with structural requirements. Outside the thermal shield materials have been determined by shielding and structural considerations.

To compensate for such factors as plug deflection, plug fabrication tolerances, and reactor component erection tolerances, an annular clearance of ¼ in. is allowed in the beryllium and graphite sections of the plug and experimental hole. From the thermal shield to the reactor face, the maximum annular clearance is 1/8 in. A closer fit can be tolerated here because the plug is well guided in this section by the plug rollers, and, because of the heavy construction of this section of the plug, there is little deflection.

Plug Cooling. Owing to the high heat generation in the beryllium tips of the horizontal beam hole plugs (HB-1 to HB-6), water cooling is provided. The

arrangement is illustrated in Fig. 3.1.B. Cooling water is directed through the plug by means of two concentric pipes. The inner pipe serves as the supply line, and the outer pipe serves as the return. The supply line directs the water to a manifold, which in turn divides the flow through several longitudinal holes in the beryllium section. At the far end of the beryllium, the water fans out through radial slots and into the annulus formed between the beryllium and its aluminum can. The water is returned through this annulus to the return line manifold, then into the return line, and back into the process-water stream. The thermal stress in the beryllium was the controlling factor in the determination of cooling-water distribution and rate of flow.[3]

The graphite sections of the water-cooled plugs are cooled with the same pipes that direct the cooling water to the beryllium tips. The graphite is fitted snugly over the pipes to assure good thermal contact. This is the primary reason that the concentric pipe design was adopted, since it is difficult to assure a snug graphite fit over two separate pipes.

The aluminum shell encasing the graphite is cooled by air flowing along the annulus. Air is drawn in at the reactor face and passes along the shield and beam hole plug annuli, is metered by the fit at the tapered section at the thermal shield, flows along the annulus between the plug casing and graphite zone liner, and passes out into the pebble zone through holes in the liner near the tank wall. The amount of air is determined by the requirement that the temperature of the aluminum shell of the plug shall not exceed 500°F since beyond this temperature the 63S alloy used suffers rapid loss of strength. Higher strength alloys such as 24S, 52S, and 75S were not used owing to the high induced activity they would acquire. Cooling of the shell by conduction of heat through the graphite to the water-cooling pipes is probably impractical because of differential expansion.

The water pipes are securely attached to the beryllium section and are allowed to "float" in the steel and concrete sections. Also, because of thermal expansion the graphite must slide a little over the outer tube, and it is therefore not clamped tightly to this tube. Calculations indicate that dangerous amounts of radiation will not "stream" down the cooling pipes even when they are empty of water. If, however, experience indicates that some shielding is necessary, a twisted stainless steel strip may be used in the center tube and a flat strip formed in a helix may be used in the annulus.

The plugs penetrating only to the reactor tank wall are cooled by air drawn along the annulus from the reactor face and into the main reactor air stream through holes in the graphite zone liner. The amount of cooling air that flows through the annulus is regulated by means of spacers located on the plug taper. The thickness of these spacers determines the clearance between the plug and the liner at the taper and consequently sets the pressure drop as well as the resulting air flow through the annulus. Here again the design is based on a maximum aluminum and graphite temperature of 500°F. Again, the casing expands more than the graphite; therefore the casing is perforated with holes which permit the cooling air to contact the graphite and thereby provide direct air cooling.

Dust Control. As a standard health precaution, an air velocity of 150 ft/min into the reactor through the plug annulus will be maintained during plug removal. A similar velocity will be maintained during normal operation to minimize passage of dust into the reactor room. In all cases the air-cooling requirements of the plugs exceed Health Physics requirements during operation. To provide sufficient velocity during plug removal the holes through the pebble zone liner into the pebble zone have been made large enough to provide the necessary air flow with only the shutdown fan operating.[4]

3.1.4 Horizontal Through Hole Facility. The horizontal through hole is a 4-11/16 in. square hole that extends from one reactor face to the opposite face. It goes through the reactor tank adjacent to one side of the active lattice. The general philosophy in providing the through hole has been to make available for experimentation a facility with high flux, ample space, and a single-pass cooling system. Experimenters have expressed a strong desire for such a facility, i.e., one with which they can irradiate future reactor fuel elements under simulated operating conditions.

The hole liners and components are generally the same for this facility as for the beam holes previously discussed, the only difference being that there is a complete liner for each end of the hole, each with a radiation door and other related liner components. The plug, however, presented more difficult problems than the plugs discussed in the foregoing section. For this reason a separate discussion on the plug for the through hole is warranted.

As a basis for design, the following premises were established:

1. The cooling system for the beryllium shall be a single-pass system, i.e., the water enters at one side of the reactor and leaves at the other side.

2. There shall be no blind water connections which will have to be made up after insertion within the reactor structure, and the complete cooling circuit for the plug shall be arranged to allow testing for leaks prior to insertion in the experimental hole. This dictates that one section of the plug shall contain a complete cooling-water line, which will extend from one side of the reactor to the other.

3. A coolant return loop and a means for hookup to the experimental plug and associated equipment shall be provided. This would then complete the desired single-pass cooling system.

4. A space in the Reactor Building shall be made accessible for setting up experimental equipment. This is desirable because the external equipment needed for the testing of the reactor fuel elements is quite extensive, and in some cases may have to be heavily shielded.

The design of the facility is shown in Fig. 3.1.D. It will be noted that the plug consists of three separate sections. The square section contains the beryllium, the graphite, and the complete cooling-water pipe, while the other two sections are merely round dummy plugs that fit over the extended water pipes of the square plug. These dummy plugs are identical in shape and construction to the concrete sections of the 8-in. horizontal beam hole plugs. The water pipes can be disconnected at the thermal shield by means of specially designed screwed connections so that they may be removed with the round dummy plugs.

To cool the beryllium section, one end of the extended water pipe is connected to the supply-water line; the other end is connected to the drain line. In an attempt to forecast future demands of this facility, a coolant return loop is provided. The 8-in. horizontal graphite hole, HG-2, has been chosen to serve as the coolant return loop. It is ideal because it runs parallel to the through hole, HT-1, and also passes completely through the reactor.

In Fig. 3.1.D is also shown a coolant pipe located in the center of a graphite plug inside the HG-2 hole. This plug is rather long, but upon removal it can be cut into two or three sections, thereby permitting the use of standard coffins for handling.

The two coolant lines are joined at one end of the reactor by means of a simple crossover pipe; at the other end of the reactor, a vertical conduit leading down to a slurry cubicle in the basement is indicated. The intention here is to connect coolant lines to the end of each plug, direct them through the conduit, and complete the circuit in the reactor basement. All piping, except that emerging into the basement, is thus completely shielded, and no bulky temporary shielding walls will be needed in the main floor cubicles. The primary reason for providing additional experimental setup space in the basement is that the equipment required for a recirculatory system is probably extensive, i.e., the setup may include pumps, heat exchangers, heaters, pressurizing equipment, control panels, associated piping and valving, etc.

A consensus indicates that some experiments may require a coolant loop that is in a low flux zone. For this type of experiment the use of this HG-2 hole as a coolant loop would not be desirable since the flux in the center of this facility is approximately 10^{10} neutrons/cm^2-sec. Also, passages to the basement large enough to accommodate heavily insulated pipes subject to linear expansions of about 6 in. are required for high-temperature tests.

To satisfy both these conditions, space for an alternate cooling loop is provided in an inactive reactor zone together with large slots through the main floor. A 12-in. hole running from side to side of the reactor structure below the first floor and parallel to the HT-1 hole provides space for the alternate loop. Access to this hole is accomplished by means of 12- by 24-in. holes through the floor in front of the HT-1 cubicles. In the basement the desired piping may be directed along the ceiling directly under the first floor and thence to the 12-in. hole. This setup gives the desired low flux condition and allows an experimenter to install his own piping, insulation, etc., to suit his requirements of temperature and thermal expansion.

In regard to insertion and withdrawal, the round portion of the experimental hole has an adapter or tray which enables the square plug to pass

smoothly through the larger round section of the hole. After the square plug is in position, the adapter is removed to clear the hole for the insertion of the round dummy plugs. Small graphite skids are fastened to the square plug to assure proper clearances and also permit smooth insertion. The round dummy plugs are fitted with rollers identical to those used for the 8-in. horizontal beam hole plugs. 24S aluminum is selected for the sheath over the beryllium and graphite. Owing to the over-shadowing high activity induced in the beryllium, there is little to be gained from the use of 63S aluminum in this location.

Cooling provisions for the beryllium, graphite, and aluminum are similar to those used in the HB holes.

3.1.5 Other Horizontal Experimental and Instrument Holes. In addition to the main experimental holes described in the previous sections, there are six more horizontal through holes. Four of these, HG-1 through HG-4, are for experimental use; the other two, HI-2 and HI-3, are for reactor control instruments.

Experimental Holes. The locations of holes HG-1 through HG-4 can be seen in Figs. 3.A and C. HG-1 and HG-2 go through the full length of the east graphite wall while HG-3 and HG-4 penetrate the west wall. The first two holes are 8 in. in diameter, the latter two 4 in. in diameter through the graphite.

For start-up, plugs will be supplied only for the ends of these holes and the section through the graphite will be left empty. The plugs supplied will be barytes concrete through the biological shield tipped with a 10¼-in. aluminum casting through the thermal shield. The inner face of the aluminum section will be covered with a ¼-in. boral plate to reduce the neutron flux into the plug. A 1-in.-I.D. steel pipe is spiraled through each plug so that electrical or plumbing connections can be made to experimental equipment in the holes.

As indicated in Section 3.1.4, hole HG-2 may possibly be used as a return path for liquids or slurries used in HT-1 hole experiments.

Instrument Holes. Access to HI-2 and HI-3 is obtained through the east and west faces of the reactor structure. These holes are to be used for the

compensated ion chambers (see Chap. 5) for the log *N* and galvanometer circuits of the reactor control system. Both holes have a minimum diameter of 10¾ in. and are plugged only through the biological and thermal shields. The plugs used are barytes concrete tipped with a 30-in.-long aluminum casting. A 4-in.-diameter hole runs through the center of the plug to within 4 in. of the inner end. This allows the tip of the ion chamber to be inserted to the inner side of the thermal shield. An adjustment on the ion chamber insertion rod enables the chamber to be moved back as much as 18 in. from the inner position.

3.1.6 Services. All the experimental beam holes are provided with standard service facilities. These services are divided into two categories, internal services and external services.

The internal services, so-called because they are located within the biological shield, are primarily concerned with providing the cooling fluid for the experimental and dummy plugs, and are all connected to a common header to permit plug flushing and also ready change-over to another plug coolant. They include the following: (1) process-water supply, (2) process-water return, (3) demineralized-water supply, (4) spare liquid line, (5) warm drain to sump, and (6) compressed air.

The external services are located in trenches around the reactor face and are primarily concerned with servicing experimental equipment exterior to the experimental plugs. They include the following: (1) demineralized-water supply, (2) auxiliary blended cooling water, (3) compressed air, (4) hot gas exhaust, (5) steam, (6) 120-volt a-c supply, (7) 120-volt a-c supply for regulation, (8) 240-volt a-c supply, (9) two 2-in. spare conduits, (10) one 4-in. spare conduit, and (11) intercom or telephone.

3.1.7 Coffins. Whenever the occasion arises to insert or retract a plug, a heavy lead-shielded coffin is accurately aligned at the chosen experimental facility. After proper alignment, the plug is withdrawn from or inserted into the beam hole. The coffin requirements for the MTR experimental holes can be satisfied by three coffins, each coffin to take care of one of the following three groups of holes:

1. Main Beam Holes HB-1, 2, 3, 4, 5, and 6, HG-5 and 6, HR-3 and 4, and the Through Hole HT-1. A coffin for these facilities, designated as a "Universal Coffin," is provided for reactor operation;

it is shown in Fig. 3.1.E. It is rather heavy owing to the 10 in. of lead necessary for shielding the beryllium parts of most of the plugs of this group. The gross weight as shown, with the HT-1 hole adapter attached, is 41,000 lb. An electric tractor with a special lift type trailer towing attachment is provided to move the coffin. To facilitate its operation the concrete roadway from the reactor face to the plug storage facility is made level and is adequately reinforced at its expansion joints to safely support this heavy load. A pull rod is furnished for manually moving the plugs out of or into their holes in the reactor or plug-storage facility. Lead plugs are furnished for shielding the open ends during the HT-1 loading or unloading operation. A roll-over device for converting from HT hole to HB hole operation is also provided.

2. All VN Holes, DB Holes, and All VG Holes Other than VG-9. A proposal for a coffin for this group has been made,[12] but the final design has been postponed pending the experience to be gained in the operation of the Universal Coffin of Group 1. The proposed coffin differs from the Universal mainly in being smaller and lighter and having a motorized winch for retracting or inserting plugs. Also, a special crane sling is utilized to align the coffin at the vertical and inclined beam holes. About 6 in. of lead shielding is adequate to handle all the dummy plugs for these holes, but provision should be made for adding layers of lead for "hot" experimental plugs.

3. HG-9, VG-9, and HI-2 and 3. The coffin for this group will be rather large in any case. For removal of dummy plugs it should have lead shielding about 6 in. thick, but for a major HG-9 experiment much more shielding will be necessary. The design of a coffin for this group has been postponed pending the operational experience to be gained with the Universal Coffin of Group 1.

Universal Coffin Design and Operation. The Universal Coffin as used for the HB holes is made up of three sections having a total length of approximately 18 ft. The first section is approximately 33 in. in diameter and is about 4 ft 5 in. long. It has the coffin mounting flange and a radiation door at one end. The middle section, shaped like a frustum of a cone tapering from approximately 33 to 20 in. in diameter, is about 6 ft long. The third section is simply a steel tube with flanges at each end, and on it are mounted all the driving mechanisms for operating the radiation door in the beam hole liner. A trunnion together with jacks and traverse bases permits exact alignment of the coffin after approximate placement of the dolly.

DWG. # 10766 [redacted]

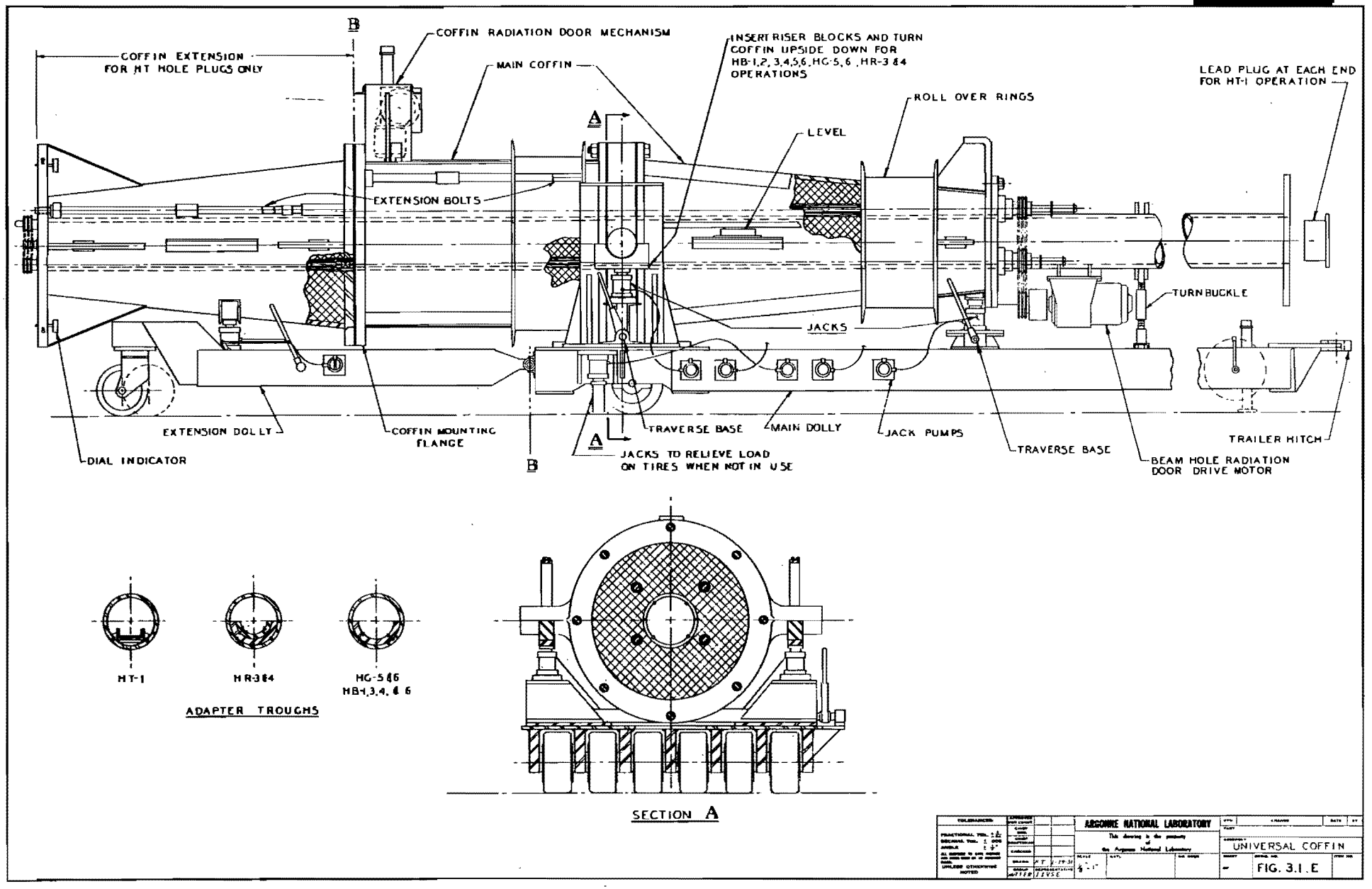

The radiation door in the coffin is lead and is approximately 10 in. thick. The mechanism for opening and closing this door consists of an electric motor—driven worm gear which drives an acme screw shaft to open or close the door. The door is accurately located when open as it forms a part of the pathway on which the HB-2, HB-5, and HT-1 plugs roll.

The dolly is used for aligning the coffin at the horizontal beam holes and plug-storage facility, and also for horizontal transportation. It is a rigid frame of welded construction supported by six heavy-duty rubber-covered wheels mounted on a common axis. To simplify maneuvering of the coffin during transportation and alignment, the dolly is operated like a two-wheeled trailer and is moved by an electric tractor. The tractor is fitted with a special trailer hook which can be hydraulically (or electrically) operated to raise or lower the front end of the dolly.

For properly aligning the coffin with the horizontal experimental beam holes in the reactor or the holes in plug storage, manually operated traverse mechanisms for lateral movement of the coffin are provided at both ends of the dolly. Vertical alignments are provided for by three manually operated hydraulic jacks. Differential movement of the two jacks at the heavy end will provide rotational adjustment to fit the bullet type dowels on the reactor face and plug-storage face. A machinist's level at the side of the coffin gives the approximate level position for the first stage of attachment. When the coffin is slid onto the dowels and is within ¼ in. of the cubicle face, four dial indicators on the coffin flange begin to indicate actual squareness with the cubicle face. The cubicle face will be erected square with the centerline of the beam hole within very close tolerances; hence it is the proper guide for coffin alignment. After the jacks and traverse bases have been readjusted to bring the dial indicators to a common reading, the bolts are inserted and tightened in order to clamp the coffin securely to the cubicle face.

Removal or insertion of the plug is performed manually by means of a long rod. When the plug is in the coffin, radiation doors in both the beam hole and coffin must be closed before the coffin is pulled away.

To insert the plug in the plug-storage facility a similar procedure is followed except that because of large clearances attaching bolts are not needed.

HT-1 Hole Operation. Special procedure is necessary for operation with the HT-1 hole. The coffin is removed from the dolly by the crane and rolled over 180° on a special fixture. It is then lowered on the dolly with the trunnion riser blocks removed. When the coffin and dolly extensions are bolted on, the coffin is ready for use.

After the water-cooling pipes of the HT-1 plug are disconnected at the thermal shield, the round plug that extends from the cubicle face to the thermal shield is removed at each end and the radiation doors are closed. These plugs are then placed in plug storage. A special tray for handling the square HT-1 plug is placed in the coffin before returning it to the reactor. After the coffin is bolted in place, the beam hole radiation door is opened and the tray is slid into the beam hole up to the thermal shield. The plug is pulled out onto the tray, which can be kept from sliding out by a push rod, and the tray and plug are then pulled into the coffin. An annular shielding plug is used at the outer end of the coffin to reduce radiation from the end of the plug. After the radiation door in the beam hole is closed, the coffin is unbolted and pulled ahead about 1 ft so that a radiation plug may be inserted in the end. The coffin is then transported to plug storage and the plug is slid off its tray into one of the square plug-storage holes.

3.2 VERTICAL EXPERIMENTAL AND INSTRUMENT HOLES

The MTR has 71 experimental and instrument holes accessible from the top of the reactor. The general layout of the top surface of the reactor with essential dimensions indicated is shown in Fig. 3.E. Details of the hole locations and the numbers assigned to them are given in Fig. 3.F. It is only fair to warn the reader that holes VG-21 and VG-22 are nonexistent — they were lost in the shuffle.

It will be noted in Fig. 3.F that some of the holes go into the pebble zone and others into the permanent graphite, while two extend through the reactor structure and are accessible from the basement of the Reactor Building. The way in which the holes into the pebble zone slant in toward the reactor tank is shown in Fig. 2.B. All the facilities entering the pebble zone have complete liners, steel through the concrete, then fluted aluminum tubes in the graphite. Cooling inside the liner is provided by air which leaks around the

plugs and into the pebble zone through holes in the bottom of the liner tube.

All the vertical holes into the permanent graphite have liners in the concrete but not in the graphite. In order to maintain proper air flow in the permanent graphite, these experimental holes must always be plugged during operation by concrete plugs through the biological shield and by full-length graphite plugs in the graphite region.

In general the graphite plugs will be tailor-made to suit particular experiments, but it is expected that the barytes plugs used for start-up will be adequate for most experimental setups. These barytes plugs are all provided with stainless steel tubes spiraled through them so that electrical leads, etc. can be brought out from the experimental equipment. These tubes are 1 in. in diameter for the pebble zone holes, VG-9, T2-V1, and T2-V2, and ½ in. in diameter for the permanent graphite holes. In all cases the graphite plugs are suspended from the barytes plugs by a rod and clevis arrangement.

3.2.1 Instrument Holes. The holes presently reserved for instruments required in the operation of the reactor are VN-1 through VN-6, VG-8, 15, 27, 28, 42, 44, and 56, and GM-1 and 2.

Holes VN-1 through VN-6 are sloping holes with their lower ends 2 ft 8 in. from the vertical centerline of the reactor at elevation 100 ft 5 in. (i.e., just above the horizontal centerline of the reactor). The hole liners are 3-in.-I.D. aluminum tubing in the pebble zone. The ion chambers for the safety and log *N* circuits are suspended in these holes by rods from the barytes plugs which fill the top 6 ft of the holes. In each hole the ion chamber position is set roughly by the length of the supporting rod, but this position may be adjusted ±6 in. by a threaded shaft which extends through the top plug.

VG-8 and VG-15 are pebble zone holes reaching to elevation 98 ft 4 in. which are to be used for fission chambers. Since the fission chambers will be most useful near the centerline of the reactor during start-up, but above the thermal shield during high-power operation, winches are provided above VG-8 and VG-15 to raise and lower the chambers. Total motion of approximately 12 ft is provided by this means.

The instrument holes, VG-27, 28, 42, 44, and 56 are vertical holes extending to elevation 96 ft 0 in. in the permanent graphite. They will contain

neutron thermometers suspended in graphite plugs.

The remaining instrument holes, GM-1 and GM-2, are thimbles projecting into the exit water lines. They provide space for the γ-ray ion chambers which monitor the N^{16} activity in the exit water.

3.2.2 Experimental Holes. Holes VG-1, 3, 5, and 6 are pebble zone holes with 4-in.-I.D. fluted aluminum liners extending to elevation 96 ft 2-5/8 in. At the bottom the centerline of these holes is approximately 2 ft 8 in. from the vertical centerline of the reactor. For start-up they are equipped with barytes plugs from which are suspended 3¾-in.-diameter GBF graphite plugs.

Holes VG-7, 9, 10, and 16 through 20 are also pebble zone holes but with 2½-in.-I.D. liners extending to elevation 98 ft 4 in. At this elevation the centerline of the liners is 2 ft 10 in. from the vertical centerline of the reactor. The graphite plugs provided for start-up are 2¼ in. in diameter.

VG-23 through 62, except VG-27, 28, 42, 44, and 56, are vertical permanent graphite holes at various distances from the reactor (see Figs. 3.E and F) extending to elevation 96 ft. There is no liner in the graphite zone, but for start-up 1¾-in. graphite plugs are suspended in the 2-in. holes in the graphite.

VG-2 and 4 are through holes accessible from the top of the pile and from the sub-pile room. Barytes plugs are provided through both top and bottom biological shields, and a rod and clevis arrangement allows the graphite plug to be fastened to the top plug. The bottom plug is inserted from the sub-pile room and bolted to the sub-pile room ceiling. Through the graphite the holes are each 4 in. in diameter, requiring a 3¾-in. GBF plug.

VG-9 is a large (10 by 10 in.) square hole penetrating the permanent graphite to elevation 100 ft 6 in. directly above HG-9. The centerline of the hole is 4 ft 5 in. from the vertical centerline of the reactor. The graphite section of the plug is GBF, 9¾ by 9¾ in.

T-2—V-1 and T-2—V-2 are thermal column holes, 12½ by 12½ in., through the top of the thermal column liner. Each of the GBF graphite plugs is suspended by a ½-in. steel rod from the barytes plug. This rod goes through the graphite plug and is welded to ¼-in. steel plate at the bottom of the plug, which is at the same level as the steel liner of the thermal column.

The other two experimental holes provided in the reactor are intended for γ-ray experiments. These holes, GT-1 and GT-2, are stainless steel thimbles, 6 in. in I.D., projecting into the exit water lines where the N^{16} activity will be high.

In addition to the above experimental holes, twelve 2-in.-I.D. holes are provided in the concrete. These holes, designated VC-1 through 9 and VC-11 through 13, penetrate the south wall of the biological shield to elevation 92 ft. Their location is indicated in Fig. 3.E around the south instrument cubicle (to the right of GM-1) and between the cubicle and the outer edge of the reactor top. It is expected that these holes will be useful for thermocouples or for shielding measurements.

3.3 THERMAL COLUMN

3.3.1 General Description. The purpose of the thermal column is to provide a readily accessible field of thermalized neutrons for experimentation.[13] In order to create such a field of thermal neutrons the permanent graphite (see Section 2.4.2) is extended to the outer edge of the biological shield through a 6-ft-square hole in the thermal shield and the concrete. Graphite is used because it is a good moderator with low absorptivity and hence can create an almost pure field of thermal neutrons at high intensity over a large volume.

Figure 3.3.A is a cut-away view of the thermal column with the graphite removed. The graphite stacking is shown in Fig. 3.3.B. In Fig. 3.3.A, the steel liner adjacent to the concrete serves to absorb radiation from the thermal column in a manner analogous to the thermal shield around the reactor proper. The cadmium sheet next to the steel absorbs impinging slow neutrons so that the steel liner will exhibit a minimum of induced radioactivity after pile shutdown.

Since not all the neutrons are thermal, some (a flux of about 10^3 to 10^4 neutrons/cm^2-sec) will reach the steel. This is sufficient, after extended operation, to induce biologically dangerous activity in the steel so that persons entering the empty column during reactor shutdown must be protected. For this reason the 2-in. lead liner is provided over the neutron-absorbing sheet.

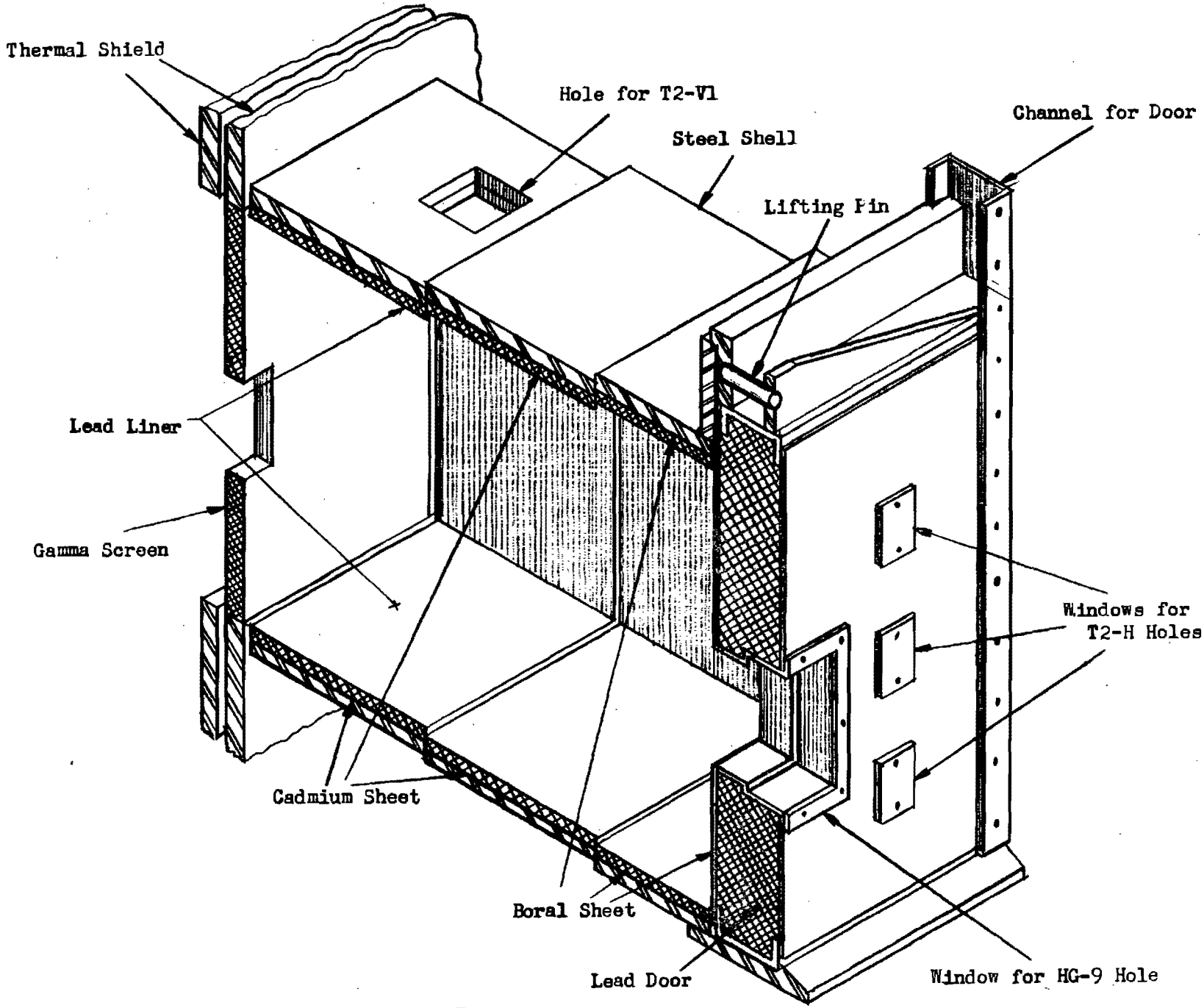

FIGURE 3.3.A
THERMAL COLUMN- CUTAWAY VIEW WITHOUT GRAPHITE FILLER OR SURROUNDING CONCRETE

[redacted]

Dwg. #8352

Dwg. #8353

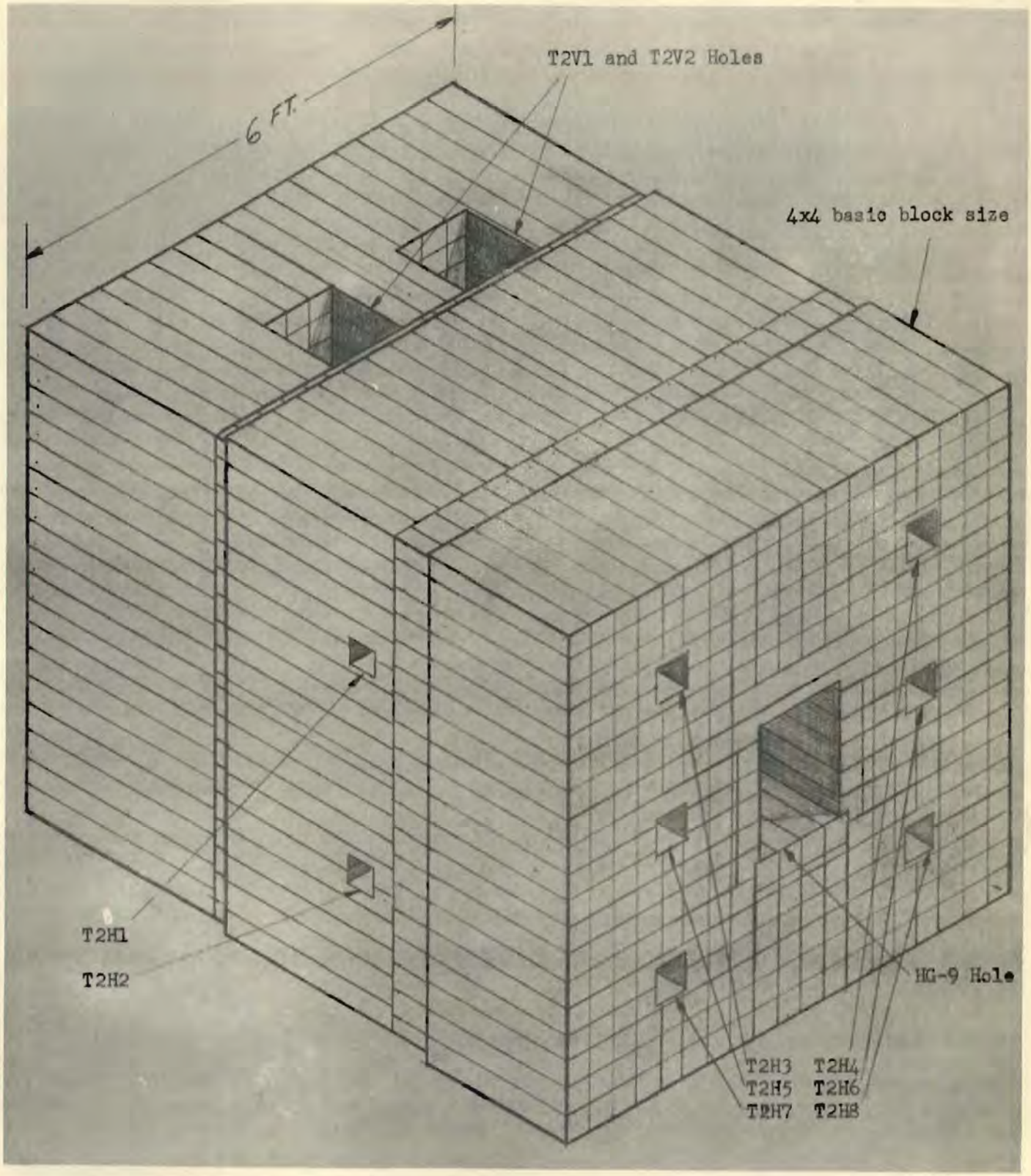

FIGURE 3.3.B
GRAPHITE ASSEMBLY FOR THERMAL COLUMN

Because of its relative cheapness and availability, cadmium sheet is used wherever possible for the neutron-absorbing liner. However, since cadmium emits a highly energetic γ ray upon absorbing a neutron, its use is restricted to those places where adequate shielding from these hard γ's is present. In the outermost section of the liner (see Fig. 3.3.A) and on the inner face of the lead door, boral[14] (boron carbide—aluminum sheet), which gives off a much weaker γ, is used.

To prevent streaming of fast neutrons from the reactor, the liner as well as the graphite filler makes at least two sidesteps between the outer face of the graphite reflector and the lead door. Scattering steps are also provided for biological shielding in the apertures and around the edges of the lead door. As indicated in Section 2.4.2, GBF graphite is used since it is the purest commercially obtainable.

The lead door indicated in Fig. 3.3.A is designed to reduce the radiation from the thermal column to the same level as that through the concrete biological shield. It can be raised with the overhead crane and held in an elevated position by lever-actuated pawls.

3.3.2 Thermal Column Experimental Facilities. The thermal-column experimental facilities include one large horizontal hole and 10 small holes, as follows:

Horizontal Holes:

HG-9	9 × 15 in.	To D tank
T-2—H-3 through T-2—H-8	4 × 4 in.	To γ-ray screen
T-2—H-1 and T-2—H-2	4 × 4 in.	90° column accessible on north or south face of reactor

Vertical Holes:

T-2—V-1 and T-2—V-2	12 × 12 in.	Accessible at top of reactor

In some respects the HG-9 hole should not be considered as part of the thermal column since it provides access to the fast-neutron flux directly from the active lattice through sealed empty cans in the beryllium. However, with

appropriate plug arrangements the fast flux can be utilized by one experiment and still not disturb the thermal column.

The holes normal to the direction of the thermal column are expected to be extremely useful in providing very pure fields of thermal neutrons although at somewhat reduced intensity.

3.4 SHIELDING FACILITY

The proposed shielding facility for the MTR has become a victim of delay and economy. During the early design stages of the MTR it was recognized that the problems associated with the shielding of nuclear reactors were among the most serious in the industry. It was felt therefore that to be a completely versatile test reactor the MTR should include a facility for shielding experimentation, and the 6- by 6-ft hole on the west side, which was formerly a second thermal column, was redesigned for this purpose. However, the shielding problem became so urgent that a Bulk Shielding Facility was designed and built at ORNL. When the MTR costs were reviewed in the spring of 1950, it was decided that since the Bulk Shielding Facility would be in operation long before the MTR, considerable money could be saved by eliminating the shielding facility for the reactor.

As a result of the above decision, the MTR biological shield now contains a 6- by 6-ft hole which will be filled, for the present, with closely packed barytes blocks. However, in the hope that eventually this facility may be used for a thermal column or other experiments, the following steps have been taken to permit removal of the concrete blocks without danger of overexposure to radiation:

1. The 6- by 6-ft hole will have a well-anchored steel liner. During construction this liner will be provided with tapped holes so that at some future time lead plates can be fastened to it as each layer of concrete blocks is removed.

2. The inner end of the hole is covered by a quickly removable boral sheet.

3. Means are provided for raising a 2-in. lead door up between the thermal shield plates to cover the hole.

In this way it is hoped that the concrete blocks can be removed and graphite or other material stacked in during reactor shutdown. In addition, a deep water shield tank is set into the floor immediately in front of the shielding facility hole.

The preliminary design of the shielding facility as planned in November, 1949 is fully described in ORNL CF-49-12-30.[15]

3.5 PNEUMATIC RABBITS

The pneumatic rabbits provide the Materials Testing Reactor with facilities to irradiate small samples of material in the high-neutron fields of the reactor. The horizontal holes that constitute the pneumatic rabbit facilities are HR-1, 2, 3, and 4. However, any beam hole can be adapted to provide additional shuttle facilities. Holes HR-3 and 4 are of 4 in. I.D. and extend inward only to the reactor tank. Holes HR-1 and 2, which are 1-in. in diameter, extend completely through the reactor and pass within 1 in. of the active lattice (see Fig. 2.D).

The only parts of these facilities which actually exist in the construction are the holes and liners and the vacuum exhaust lines within the reactor. It is intended that the HR-1 hole always be used for "through shuttles," i.e., shuttles that pass directly through the reactor. The equipment for this hole and the HR-3 and 4 holes will bedesigned and set up by the experimenters, and it is therefore not discussed further.

The HR-2 hole is intended primarily for "re-entry shuttles," i.e., shuttles that are stopped at the active lattice for a given interval and then propelled out the same side through which they entered. The additional equipment for this system is not included in the present construction, but a design proposed[16] by ANL is discussed in Appendix 9. The proposed re-entry shuttle equipment provides for the introduction of the shuttles into the system in the basement and provides a means of propelling them to the inner end of the rabbit tube. After a predetermined irradiation period in the reactor, they can be expelled either to the laboratories in the Reactor Building wing or to an unloading station in the basement. The major components of the system, all fully described in Appendix 9, are a loading terminal, shock absorber, transfer unit, laboratory selector, and unloading terminals.

3.6 HYDRAULIC RABBITS

The hydraulic rabbit system for the MTR consists of two 1-in.-I.D. vertical tubes running through the bottom plug into the east end of the beryllium reflector (see Figs. 2.D and 2.4.A and B) and a 1.31-in.-I.D. tube through each of the regulating rod holes not in use.

Only the tubes inside the reactor and through the bottom plug are being provided in present construction. However, a tentative design for the entire system proposed by ORNL is outlined in Appendix 10.

3.7 REFERENCE REPORTS

(1) Persiani, P. J., *Calculation of Induced Gamma Activity in Commerical Materials*, ANL-EKF-7, October 11, 1949.

(2) Krisberg, N. L., *Calculations on Plug Design*, ANL-EKF-21, September 23, 1949.

(3) Lennox, D. H., *Beryllium Cooling in Experimental Hole Plugs*, ANL-EKF-1, May 2, 1949.

(4) Leyse, C. F., *MTR Shutdown Air Requirements*, ANL-EKF-30, January 10, 1950.

(5) Krisberg, N. L., *Open Beam Hole Area Permitted, etc.*, ANL-EKF-22, December 7, 1949.

(6) Lennox, D. H., *Cooling of Down Beam Hole Plugs*, ANL-EKF-6, September 20, 1949.

(7) Sullivan, T. E. and Schultz, A. B., *Experimental Holes, Plugs, and Related Facilities*, ANL-ABS-6, June 16, 1949.

(8) Sullivan, T. E., *Experimental Facility Proposals*, ANL-ABS-7, July 27, 1949.

(9) Sullivan, T. E., *Requirements and Basis of Design - Experimental Hole Plugs*, ANL-ABS-9, October 5, 1949.

(10) Sullivan, T. E., *Proposal - Horizontal Through Hole Plug*, ANL-ABS-12, November 25, 1949.

(11) Sullivan, T. E., *Addendum to Requirements and Basis of Design Experimental Hole Plugs Report*, ANL-ABS-17, March 27, 1950.

(12) Paleczny, M. P., *Coffins and Coffin Handling - MTR Design Report 21* (ANL).

(13) Thomas, T. H., *Materials Testing Reactor Report on Thermal Column*, ORNL CF-50-2-28, February 6, 1950.

(14) McKinney, V. L. and Rockwell, T., *Boral, a New Thermal Shield*, ORNL-242, September 6, 1949.

(15) Sholl, W. E., *MTR Design Report on Experimental Shielding Facility*, ORNL CF-49-12-30, December 8, 1949.

(16) Nicoll, D. and Lennox, D. H., *Design Report No. 44 - Pneumatic Shuttle*, ANL-ABS-16, March 27, 1950.

(17) Scott, D., *Pneumatic Rabbits in the X-Pile*, ORNL CF-47-11-35, October 31, 1947.

(18) Scott, D., *Status of the Pneumatic Rabbit Design in the High Flux Pile*, ORNL CF-48-6-134, June 9, 1948.

3.8 REFERENCE DRAWINGS

DWG. NO.	TITLE
BKC-3150-92-9A	Service Facilities for Experimental Plugs
BKC-3150-522-1	HB-1, 3, 4, and 6 - Liner
BKC-3150-522-2	HB-1, 3, 4, and 6 - Plug
BKC-3150-522-3	HB-1, 3, 4, and 6 - Radiation Door
BKC-3150-522-4	HB-1, 3, 4, and 6 - Shielding Plug
BKC-3150-522-5	HB-1 to 6, DB-1, HT-1, HR-3 and 4, HG-5 and 6 - Outer Shield Plug
BKC-3150-524-1	Typical Assembly of Liner, Plug, Radiation Door, and Shielding Plug
BKC-3150-544-1	HG-1 to 4 - Liner Assembly
BKC-3150-544-2	HG-1 to 4 - Plugs
BKC-3150-519-1	HI-2 and 3 - Mechanical Design
BKC-3150-519-2	HI-2 and 3 - Plugs
BKC-3150-564-2	Plug Coffin
BKC-3150-564-10	Coffin Radiation Door Drive
BKC-3150-554-2	VN-1 to 6 - Details
BKC-3150-551-1	VG-1, 3, 5, 6, 7, 10, 11, 12, 13, 14, 16 through 20 - Liner and Plug
BKC-3150-557-1	VG-23 through 62 except 27, 28, 42, 44, and 56 - Liner and Plug
BKC-3150-557-4	VG-27, 28, 42, 44, and 56 - Neutron Thermometer Equipment
BKC-3150-550-1	GT-1 and 2 - Gamma Thimble Plug
BKC-3150-562-1	VC-1 through 13 except VC-10 - Liner and Plug
BKC-3150-515-1 through 9	T-2 Thermal Column
BKC-3150-516-1	T-2—V-1 Thermal Column Liner
BKC-3150-516-2	T-2—V-1 Thermal Column Plug
BKC-3150-558-1	T-2—H-1 to T-2—H-8 Graphite Plugs - Reactor Structure
BKC-3150-514-1	Shielding Facility Arrangement
BKC-3150-538-1 through 10	HR-1 and 2 - Rabbit Tubes
BKC-3150-540-1 through 5	HR-3 and 4 - Rabbit Tubes

DWG # 10204 [redacted]

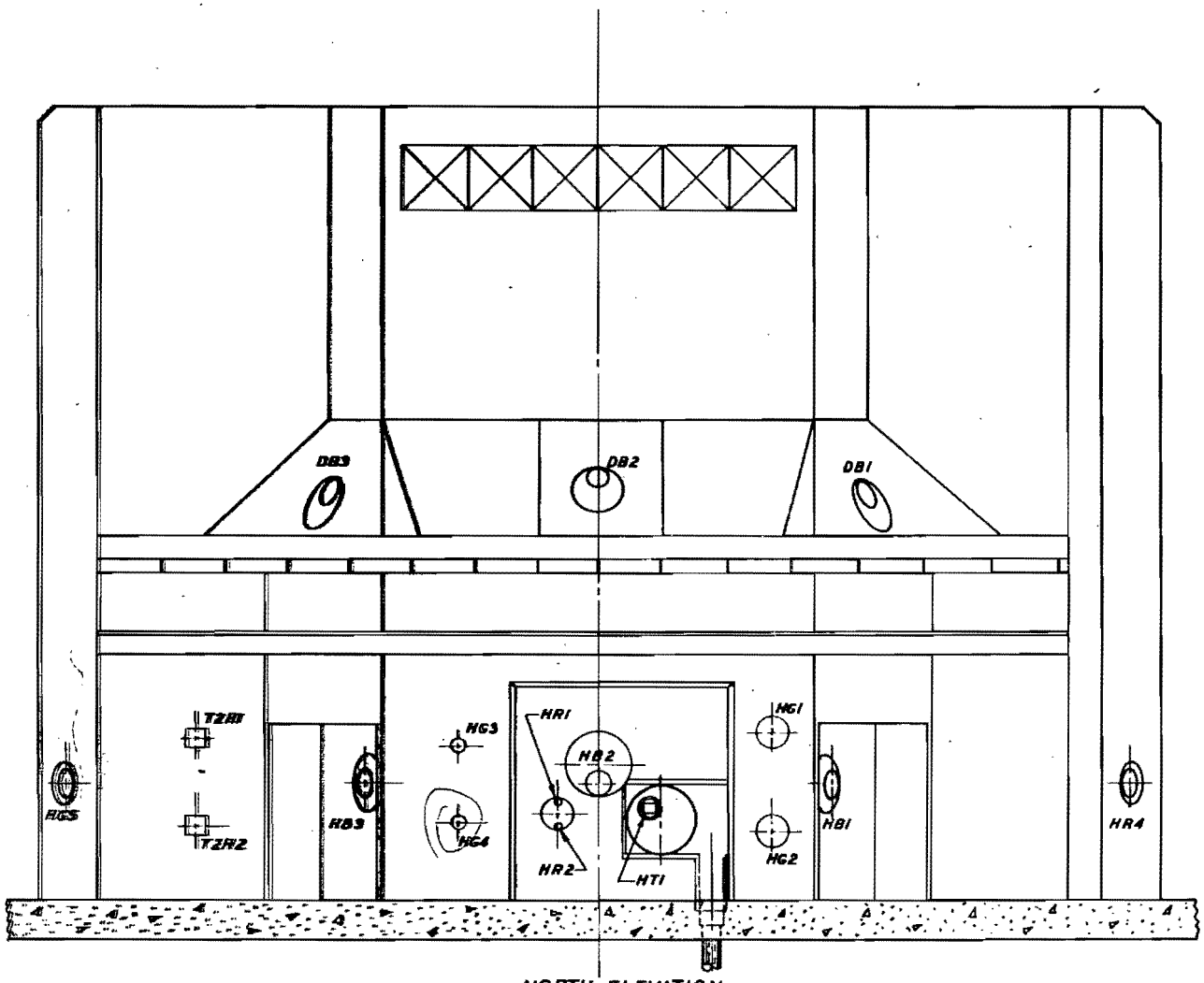

NORTH ELEVATION

FIG. 3-A

MTR

VIEW OF NORTH FACE OF REACTOR

DWG. #10202 [redacted]

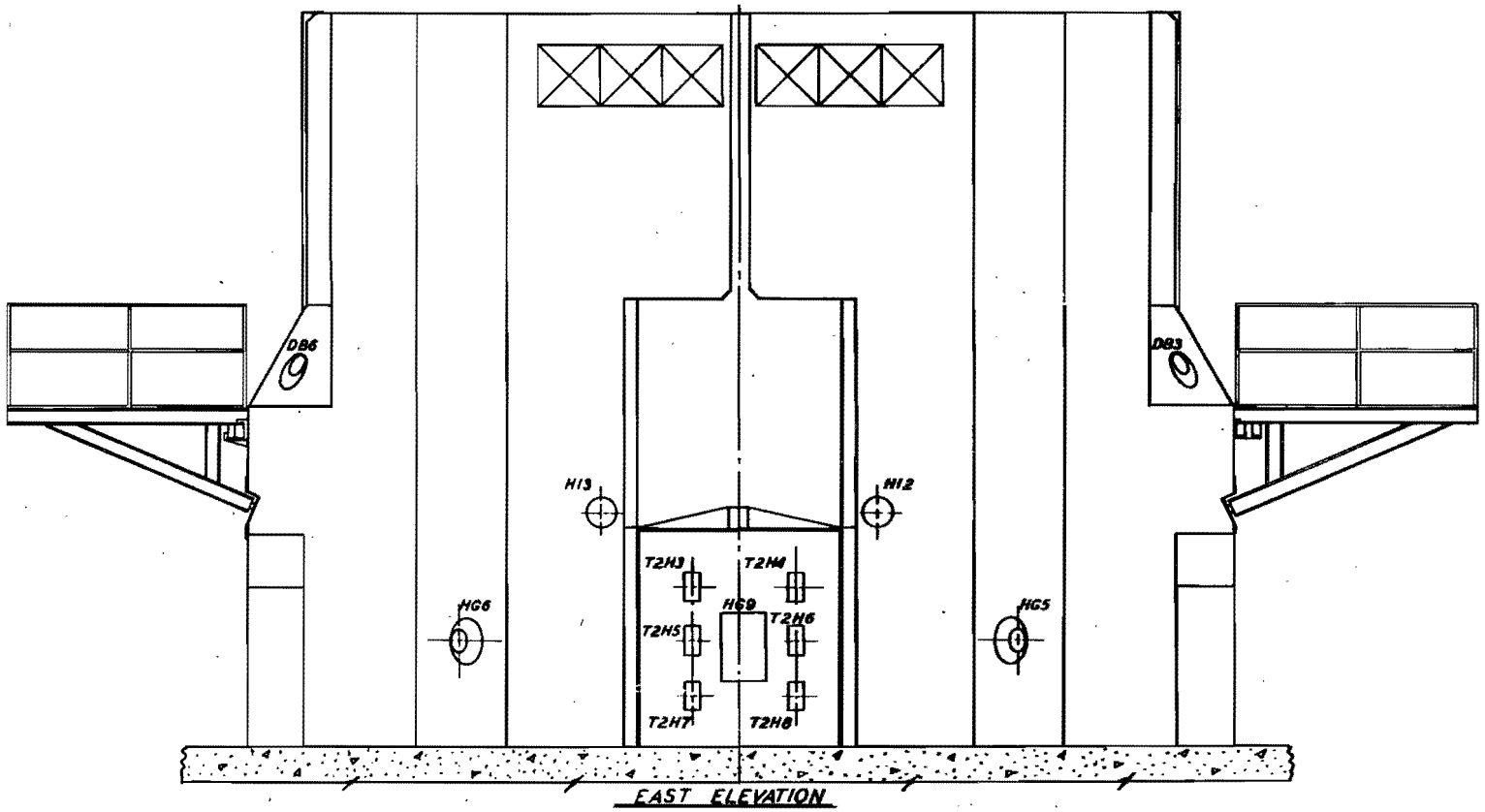

FIG. 3.B

MTR

VIEW OF EAST FACE OF REACTOR

DWG. #10203 [redacted]

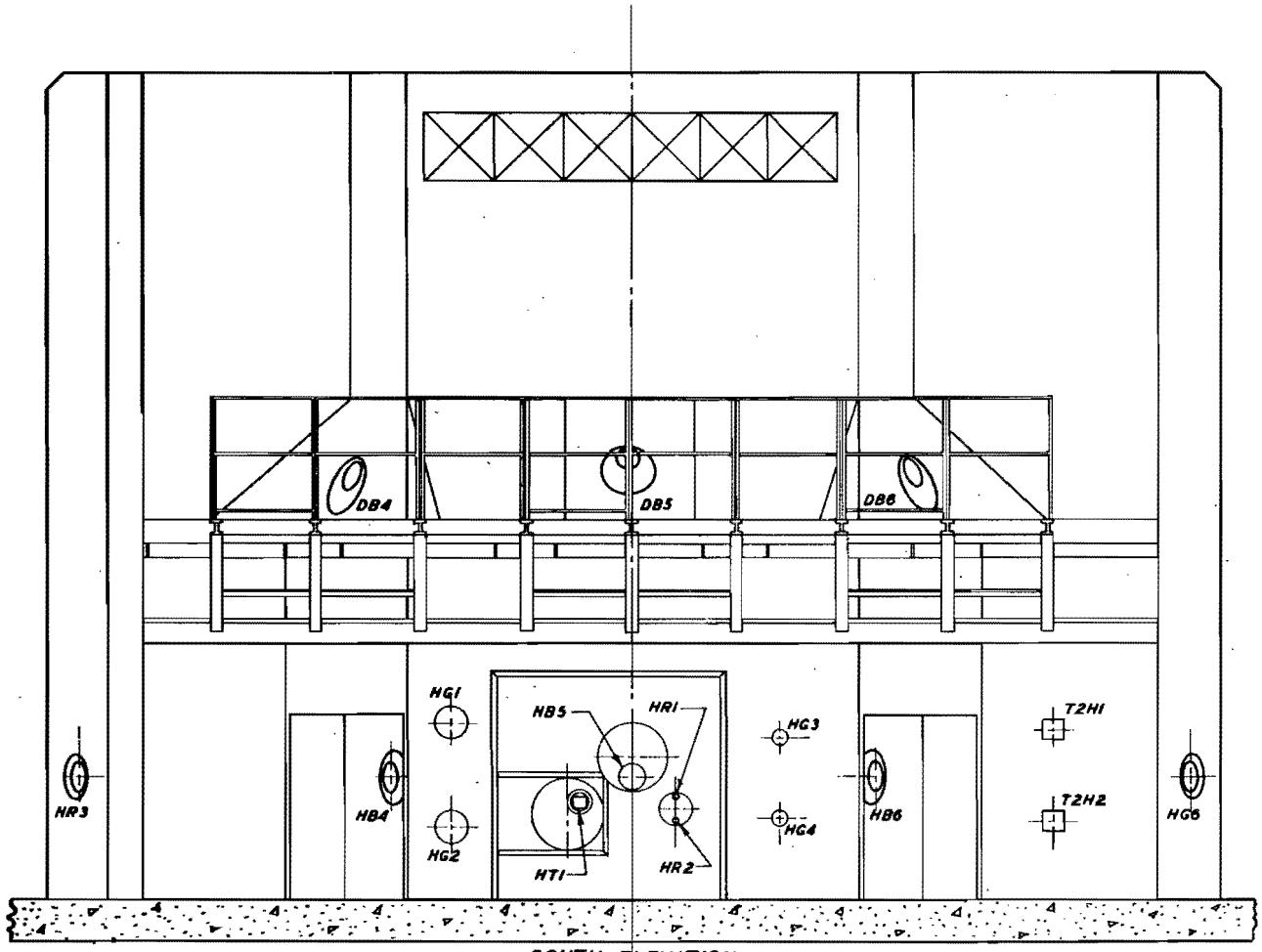

SOUTH ELEVATION

FIG. 3. C

MTR

VIEW OF SOUTH FACE OF REACTOR

DWG. #10-201 [redacted]

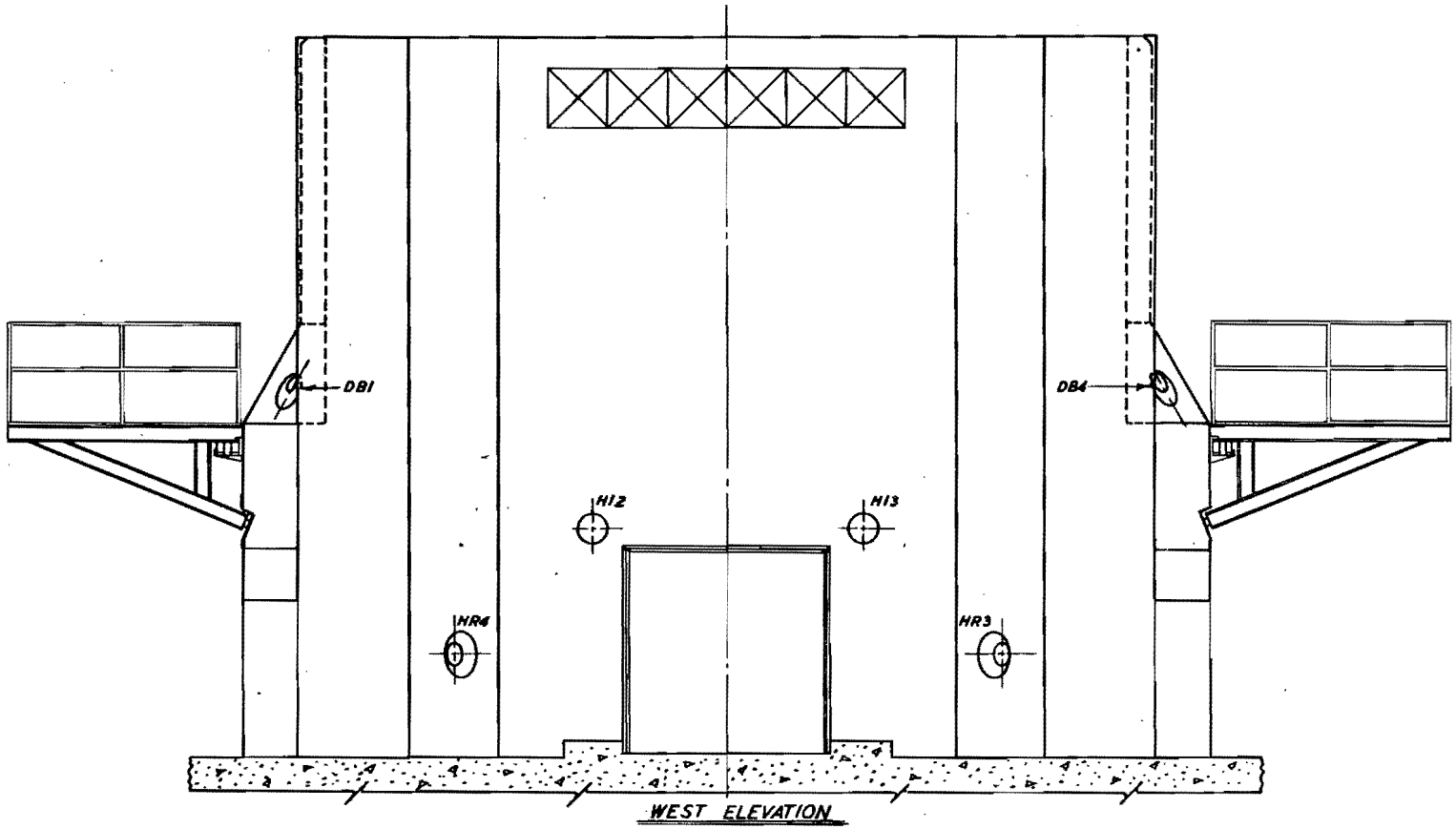

FIG. 3.D
MTR
VIEW OF WEST FACE OF REACTOR

DWG. # 10517 [redacted]

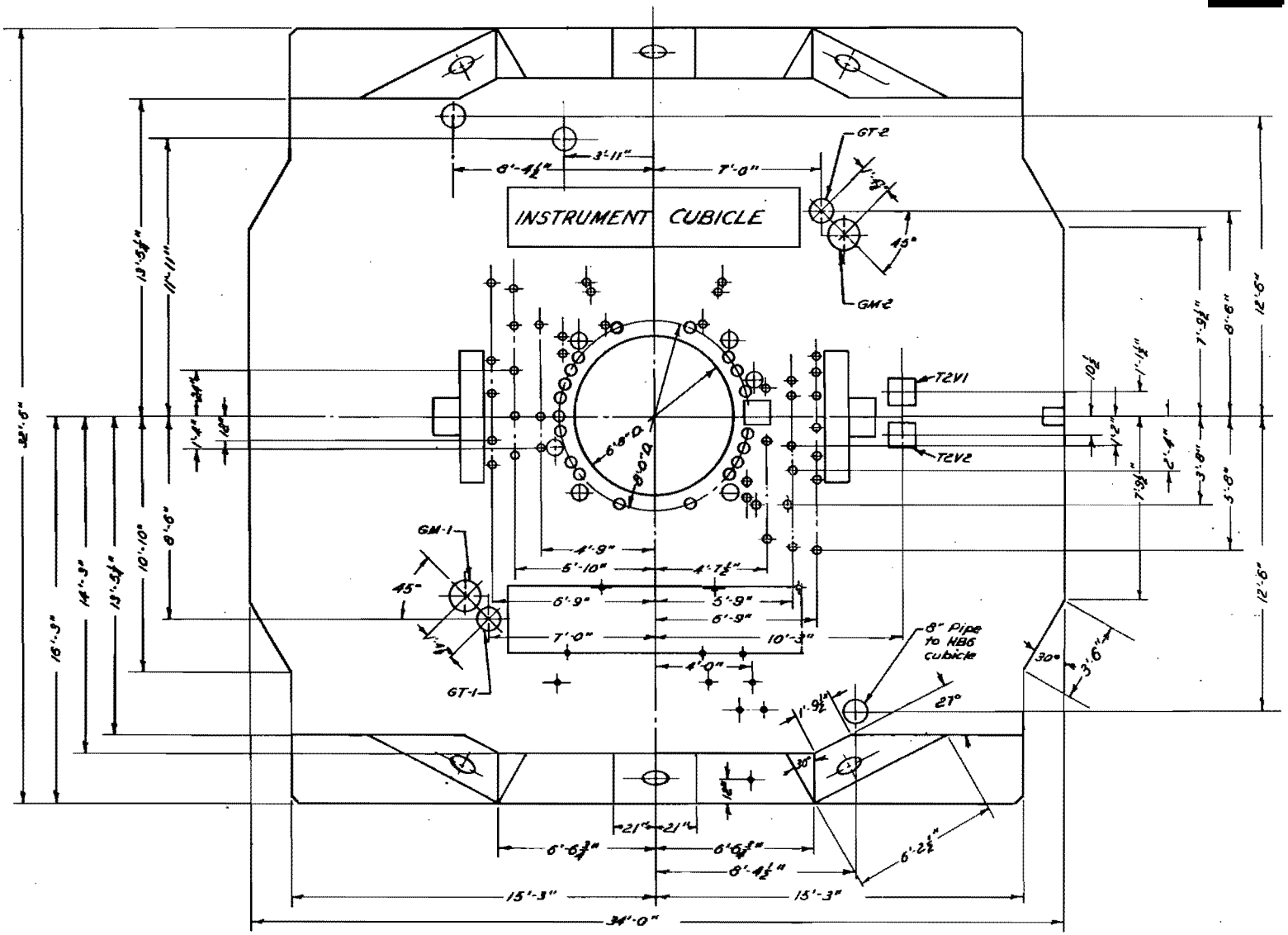

FIG. 3.E.
MTR
VIEW OF TOP OF REACTOR

OAK RIDGE NATIONAL LABORATORY

DWG. # 10518 [redacted]

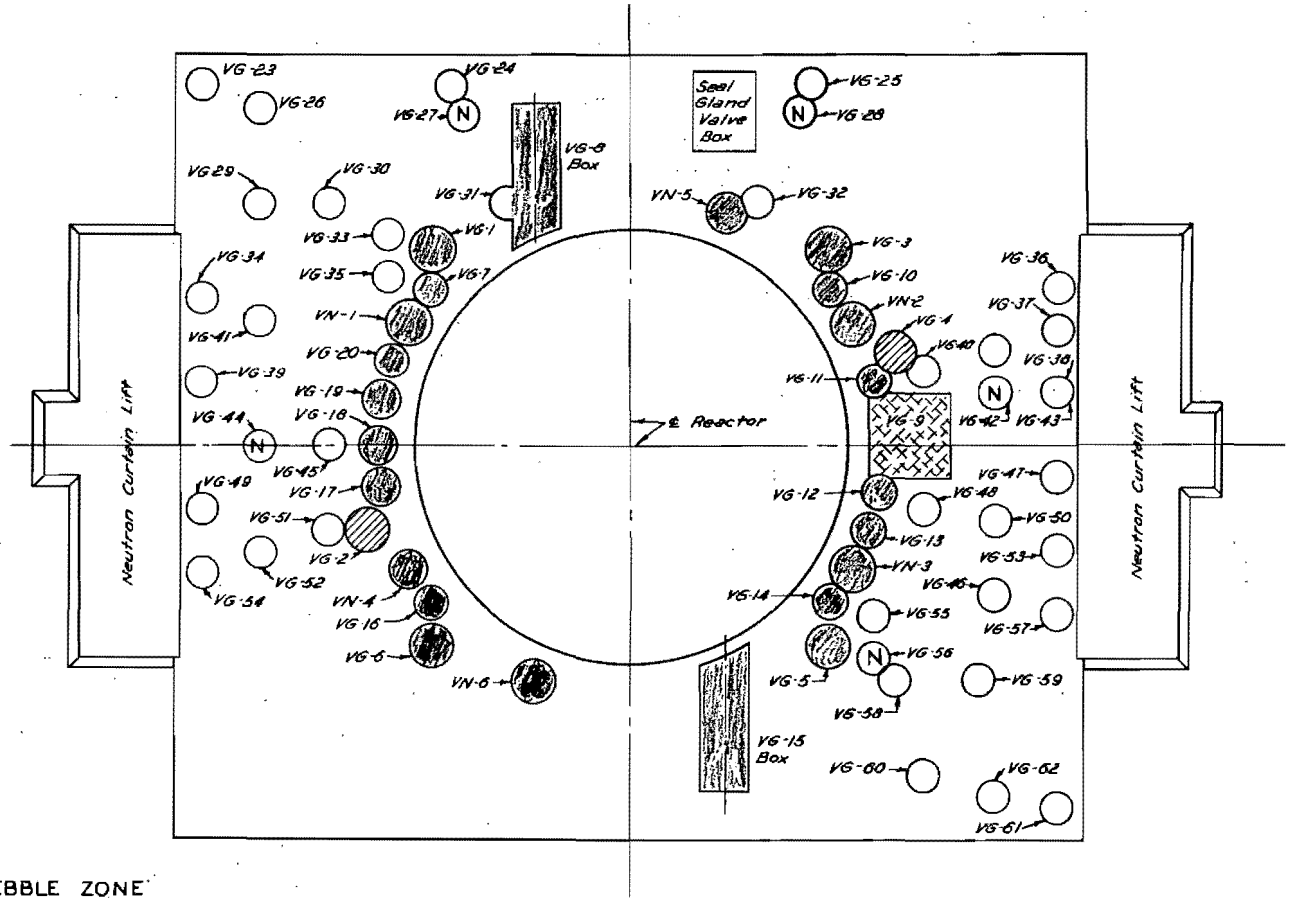

IN PEBBLE ZONE

THRU HOLES

TO HG-9 HOLE

N ----- NEUTRON THERMOMETER HOLE

FIG. 3.F

MTR

LOCATION OF EXP. FACILITIES ON REACTOR TOP

OAK RIDGE NATIONAL LABORATORY

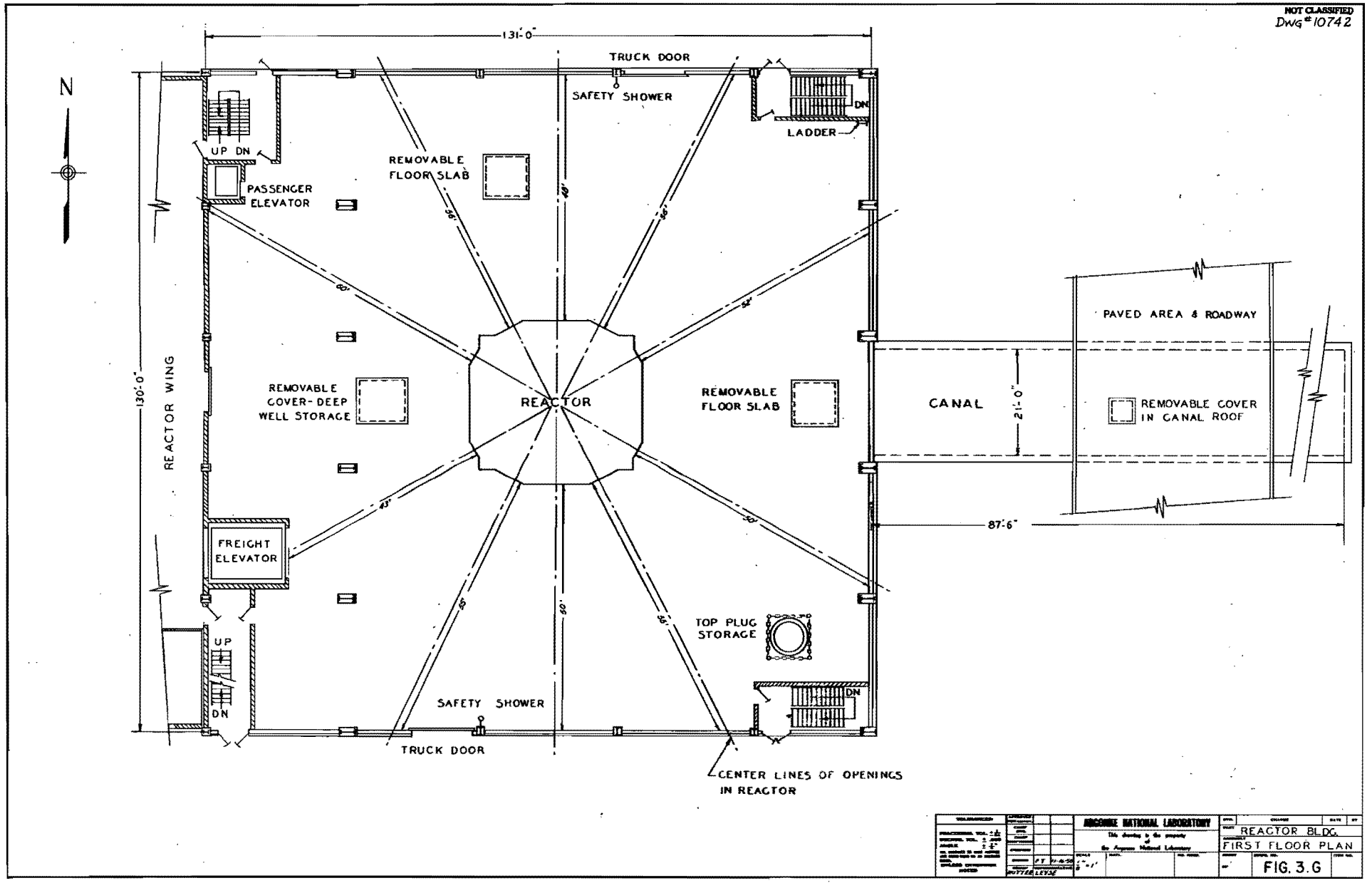
NOT CLASSIFIED
DWG # 10742
N
131'-0"
TRUCK DOOR
SAFETY SHOWER
DN
LADDER
UP DN
PASSENGER ELEVATOR
REMOVABLE FLOOR SLAB
130'-0"
REACTOR WING
REMOVABLE COVER-DEEP WELL STORAGE
REACTOR
REMOVABLE FLOOR SLAB
PAVED AREA & ROADWAY
CANAL
21'-0"
REMOVABLE COVER IN CANAL ROOF
87'-6"
FREIGHT ELEVATOR
TOP PLUG STORAGE
UP
DN
SAFETY SHOWER
TRUCK DOOR
CENTER LINES OF OPENINGS IN REACTOR
ARGONNE NATIONAL LABORATORY
REACTOR BLDG.
FIRST FLOOR PLAN
FIG. 3.6

Chapter 4

PHYSICS OF THE MATERIALS TESTING REACTOR

4.1 REVIEW OF REQUIREMENTS

The general aims of the Materials Testing Reactor are:

1. Attainment of a very high fast-neutron and thermal-neutron flux for general experimental and testing purposes.

2. Production, in sizeable quantities, of U^{233}, C^{14}, and other isotopes of interest in R.W.

3. Attainment of a flexible reactor in which the disposition of fissionable material may be readily altered in conformity with experimental needs.

4. Production of epithermal neutrons of the highest possible energy in order to test the behavior of reactor materials under high-intensity radiation (fast neutrons and γ rays).

5. Attainment of a reactor of such simplicity in design, servicing, and operation that it can serve as a prototype for research centers in which the AEC may deem a nuclear reactor desirable in the future.

In order for the reactor to satisfy these requirements, careful consideration had to be given to the minimum quantity of fissionable material which would be necessary at the flux level desired, the amount of foreign matter to be inserted, the need to reactivate the reactor within a few hours or less after shutdown and overcome fission product poisoning, temperature effect, and depletion of fissionable material, to name the most important.

This chapter will review briefly some of the theoretical considerations that were worked on in parallel with the critical experiments described in Appendixes 1, 2, and 3. Sections 4.2, 4.3, and 4.4 cover essentially the same material as MonP-272. Section 4.5 discusses heat production and removal. Section 4.6, on Shielding, is given in considerable detail because it covers the particular shielding problems of the present MTR and illustrates the assumptions and methods used in such calculations. It is to be hoped that

enough data will be taken from the MTR to check the validity of these calculations.

4.2 FLUX CALCULATIONS

One of the most important reasons for using a small-volume light water—moderated core instead of the large-volume heavy water—moderated core described in MonP-108 and in Appendix 1 is that the virgin neutron flux (fission neutrons which have suffered no collisions) and the γ-ray flux are much higher. The virgin flux, ϕ_0, is related to the number of fission neutrons produced per cubic centimeter, Q,* and to the inelastic macroscopic cross-section for virgin neutrons Σ_{in} by the relation

$$\phi = Q/\Sigma_{in}$$

The above equation is correct if the reactor dimensions are large compared to the mean free path, Σ_{in}^{-1}, of virgin neutrons.

In the present reactor Q is given by $\eta\Sigma_{U^{235}}\phi_s$ where ϕ_s is the average slow flux, 2×10^{14} cm^{-2} sec^{-1}, and $\Sigma_{U^{235}} = 0.059$ cm^{-1}, corresponding to 35.7 g of U^{235} per liter of reactor. The mean free path of virgin neutrons in the core of light water plus aluminum, with $V_{Al}/V_{H_2O} = 0.75$, is about 5 cm; thus

$$\phi_0 \approx 1.2 \times 10^{14} \text{ cm}^{-2} \text{ sec}^{-1}$$

The old proposed heavy water—moderated reactor had a core volume almost ten times greater than the present one, while the total power output, 3×10^4 kw, and virgin-neutron mean free path was the same. Its average virgin flux was thus smaller by a factor of 10. A comparison of the slow, resonance, and fast flux in these light water and heavy water reactors is given in Table 4.2.A.

A second desirable characteristic of the small-core light water—moderated reactor is that the thermal-neutron flux distribution is essentially flat in the core and for a short distance into the beryllium reflector is equal to or greater than the average core flux. The holdup of thermal neutrons in the

*The quantity Q is therefore proportional to the power per unit volume of the reactor.

TABLE 4.2.A

Fluxes in Light Water and Heavy Water Reactors

	LIGHT WATER	HEAVY WATER
Power (kw)	30×10^3	30×10^3
Power/volume (kw/liter)	357	37
Maximum virgin nv	$\sim 1.2 \times 10^{14}$	$\sim 0.15 \times 10^{14}$
Maximum epithermal nv	$\sim 6 \times 10^{14}$	$\sim 5 \times 10^{14}$
Maximum slow nv	$\sim 2 \times 10^{14}$	$\sim 2 \times 10^{14}$

reflector is due to the smaller rate of absorption in the beryllium as compared to the high k core.

The magnitude of the rise in the reflector depends on the size and shape of the reactor. In Figs. 4.2.A, B, and C the radial flux distributions as calculated for three cylindrical reactors with different k values are shown. In the largest reactor (lowest $k = 1.373$) the thermal flux rise in the reflector is least pronounced. The larger the reactor, the lower the rate of thermalization, which is proportional to ϕ_f, becomes in the reflector. This results in a decreased ϕ_s in the reflector. For a thin-slab reactor (Fig. 4.2.F) the rise of ϕ_s in the reflector is most pronounced because of the relatively high rate of thermalization in the beryllium near the core. The change from a circular to a rectangular horizontal cross-section reactor hardly affects the neutron flux distributions (compare Figs. 4.2.A and E).

Longitudinally the thermal flux in the $k = 1.373$ cylindrical reactor (Fig. 4.2.D) drops only by a factor of 2 before again rising in the top (or bottom) water plus aluminum reflector. The actual longitudinal distribution will be even flatter than that calculated because the side beryllium reflectors are longer than the reactor proper, and therefore extend into the top and bottom reflector region.

The thermal-neutron distribution in the reactor and its reflector will be modified by the presence of control rods, the thorium-breeding blanket, if

[redacted]

Dwg. No. 10894

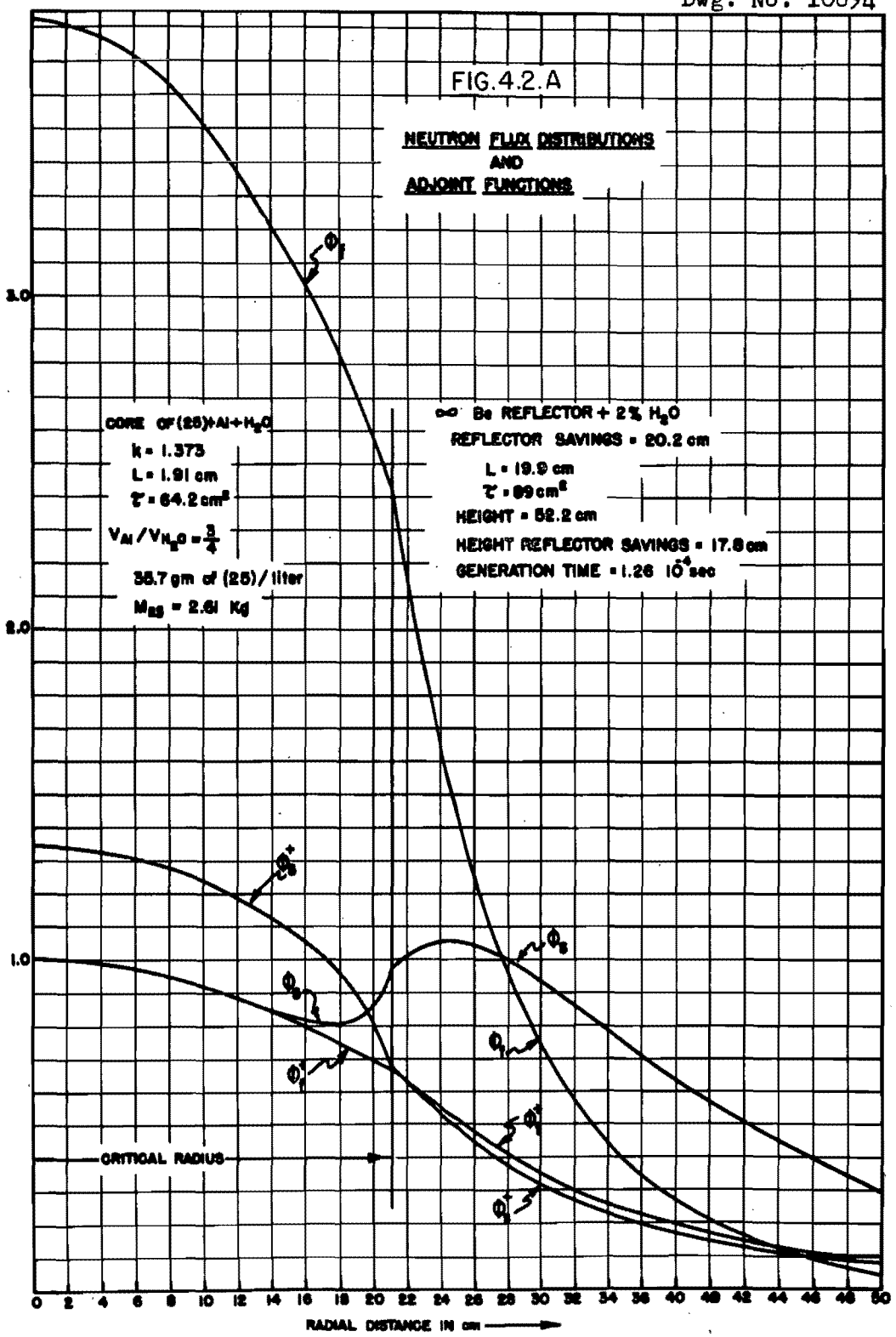

[redacted]

DWG. NO. 10895 [redacted]

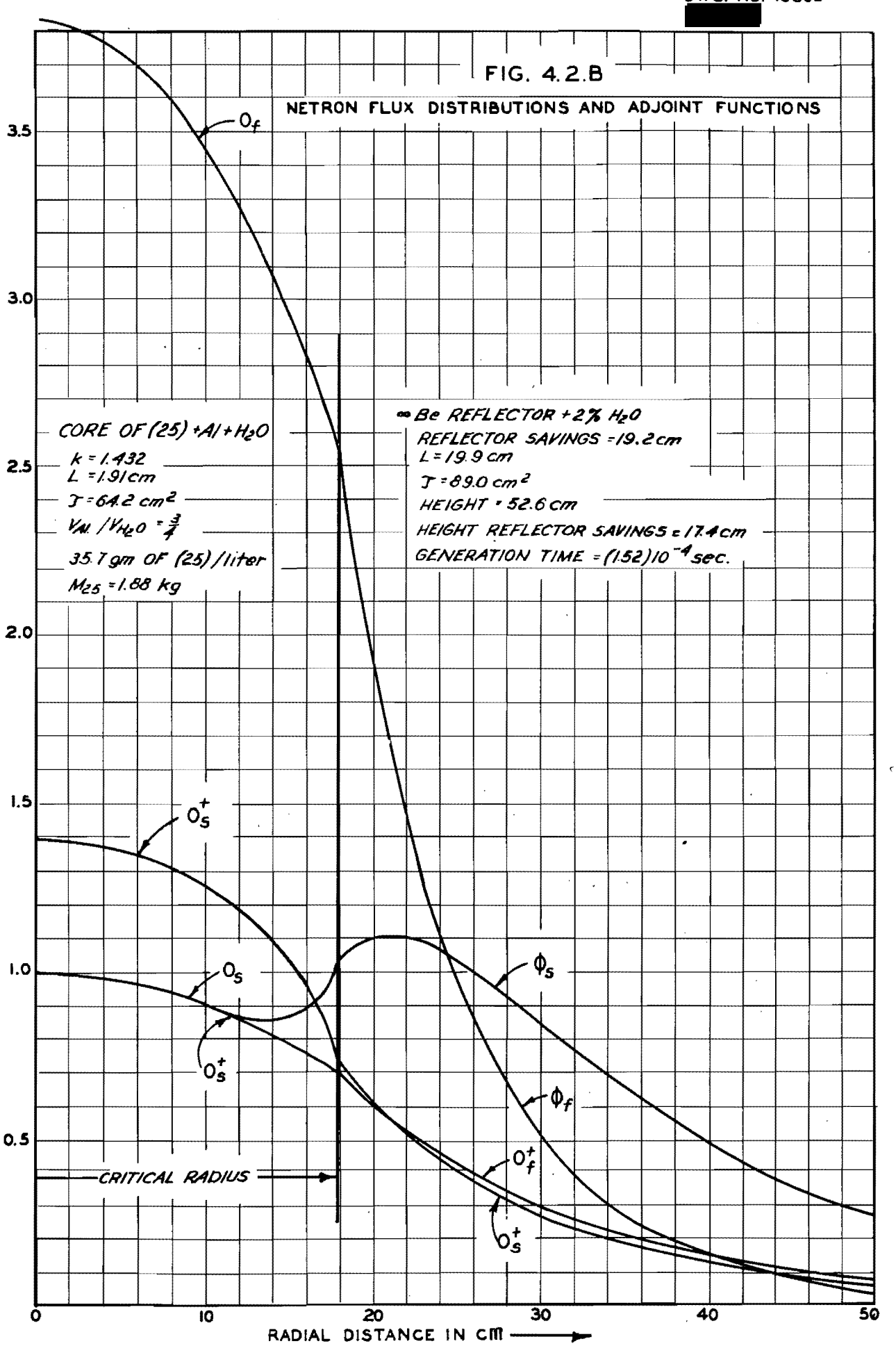

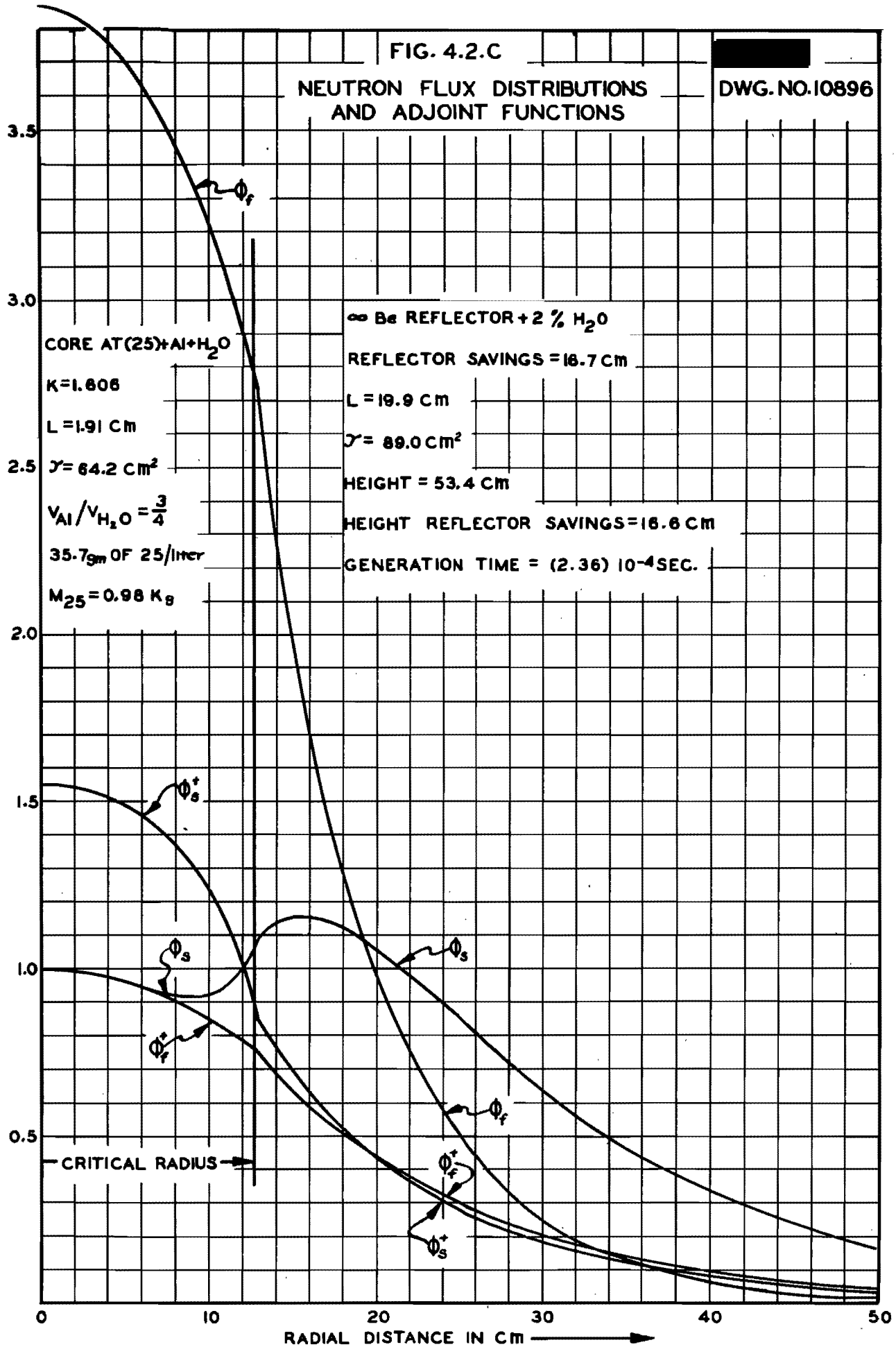
FIG. 4.2.C
NEUTRON FLUX DISTRIBUTIONS AND ADJOINT FUNCTIONS
[redacted]
DWG. NO. 10896
∞ Be REFLECTOR + 2 % H_2O
REFLECTOR SAVINGS = 16.7 Cm
L = 19.9 Cm
γ = 89.0 Cm²
HEIGHT = 53.4 Cm
HEIGHT REFLECTOR SAVINGS = 16.6 Cm
GENERATION TIME = (2.36) 10^{-4} SEC.
CORE AT(25)+Al+H_2O
K=1.606
L = 1.91 Cm
γ = 64.2 Cm²
$V_{Al}/V_{H_2O} = \frac{3}{4}$
35.7gm OF 25/liter
M_{25} = 0.98 Kg
ϕ_f
ϕ_s^+
ϕ_s
ϕ_f^+
CRITICAL RADIUS
3.5
3.0
2.5
2.0
1.5
1.0
0.5
0
10
20
30
40
50
RADIAL DISTANCE IN Cm

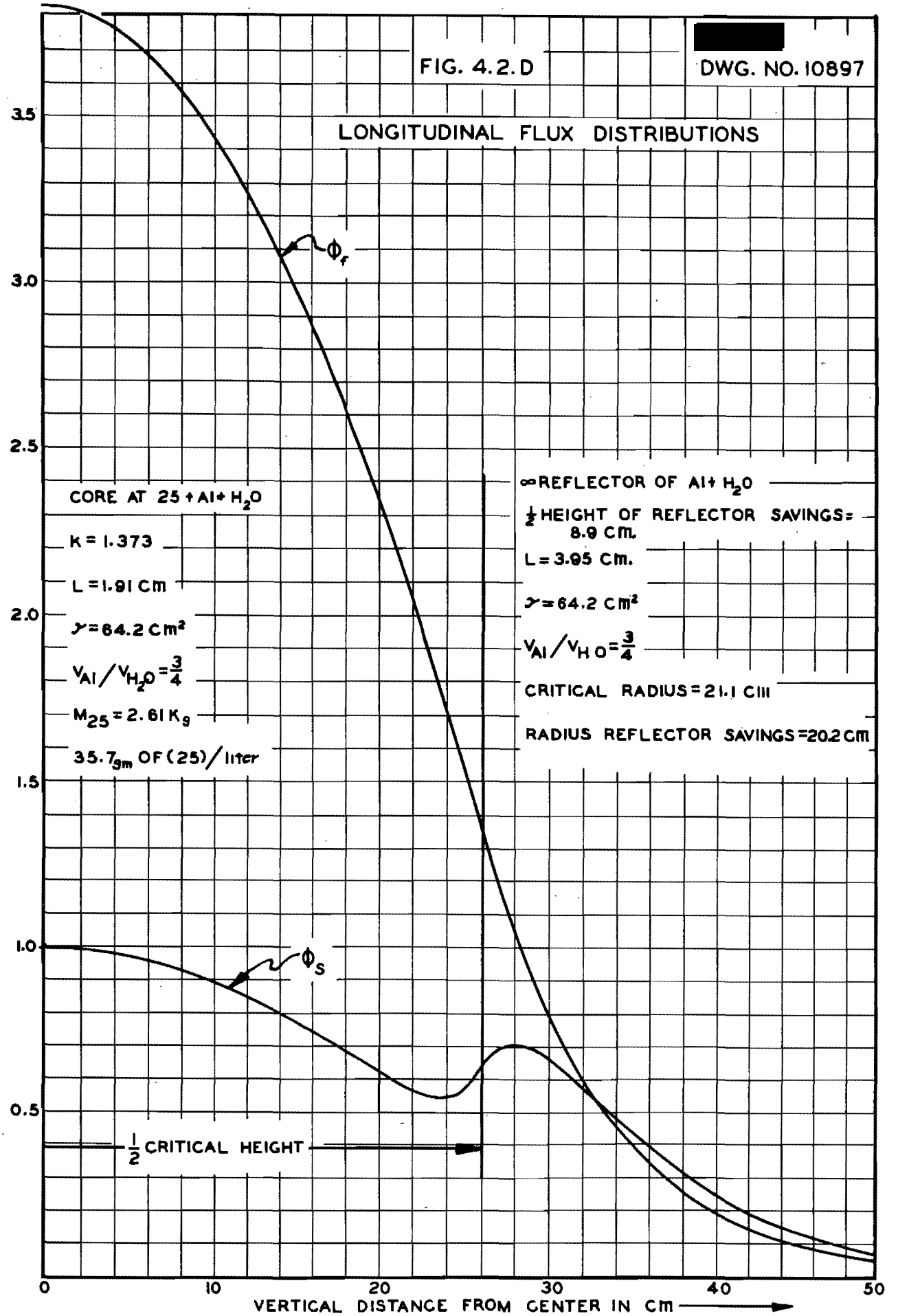
FIG. 4.2.D
[redacted]
DWG. NO. 10897
LONGITUDINAL FLUX DISTRIBUTIONS
ϕ_f
ϕ_s
CORE AT 25 + Al + H_2O
K = 1.373
L = 1.91 Cm
γ = 64.2 Cm²
$V_{Al}/V_{H_2O} = \frac{3}{4}$
M_{25} = 2.61 Kg
35.7 gm OF (25)/liter
∞ REFLECTOR OF Al + H_2O
½ HEIGHT OF REFLECTOR SAVINGS = 8.9 Cm.
L = 3.95 Cm.
γ = 64.2 Cm²
$V_{Al}/V_{H_2O} = \frac{3}{4}$
CRITICAL RADIUS = 21.1 Cm
RADIUS REFLECTOR SAVINGS = 20.2 Cm
½ CRITICAL HEIGHT
3.5
3.0
2.5
2.0
1.5
1.0
0.5
0
10
20
30
40
50
VERTICAL DISTANCE FROM CENTER IN Cm

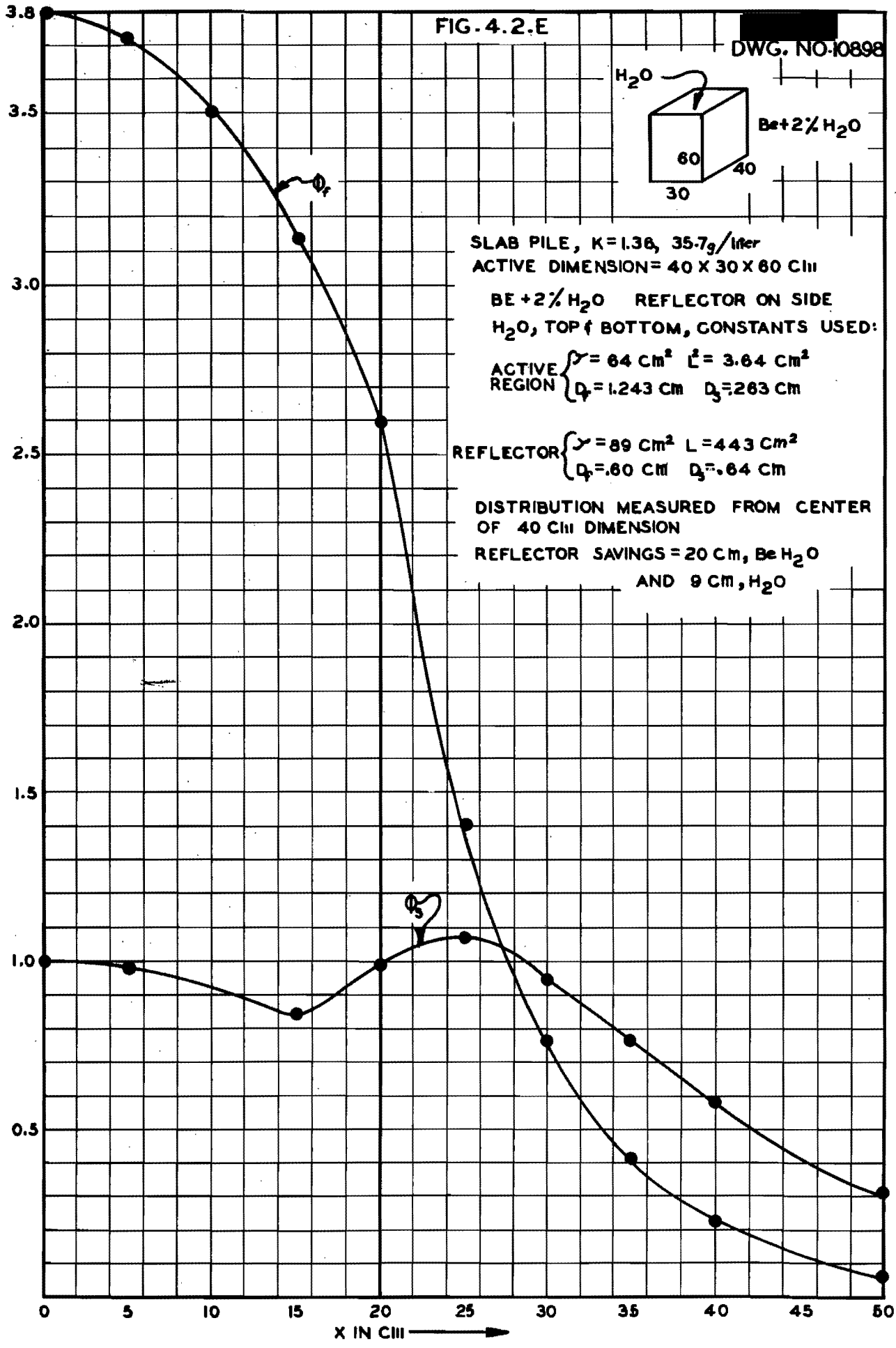
FIG. 4.2.E
[redacted]
DWG. NO-10898
H_2O
Be+2% H_2O
60
40
30
SLAB PILE, K=1.36, 35.7g/liter
ACTIVE DIMENSION = 40 X 30 X 60 Cm
BE + 2% H_2O REFLECTOR ON SIDE
H_2O, TOP & BOTTOM, CONSTANTS USED:
ACTIVE REGION γ = 64 Cm² L^2 = 3.64 Cm²
D_f = 1.243 Cm D_s = .263 Cm
REFLECTOR γ = 89 Cm² L = 4.43 Cm²
D_f = .60 Cm D_s = .64 Cm
DISTRIBUTION MEASURED FROM CENTER OF 40 Cm DIMENSION
REFLECTOR SAVINGS = 20 Cm, Be H_2O
AND 9 Cm, H_2O
Φ_f
Φ_s
3.8
3.5
3.0
2.5
2.0
1.5
1.0
0.5
0
5
10
15
20
25
30
35
40
45
50
X IN Cm

[redacted]

FIG. 4.2.F

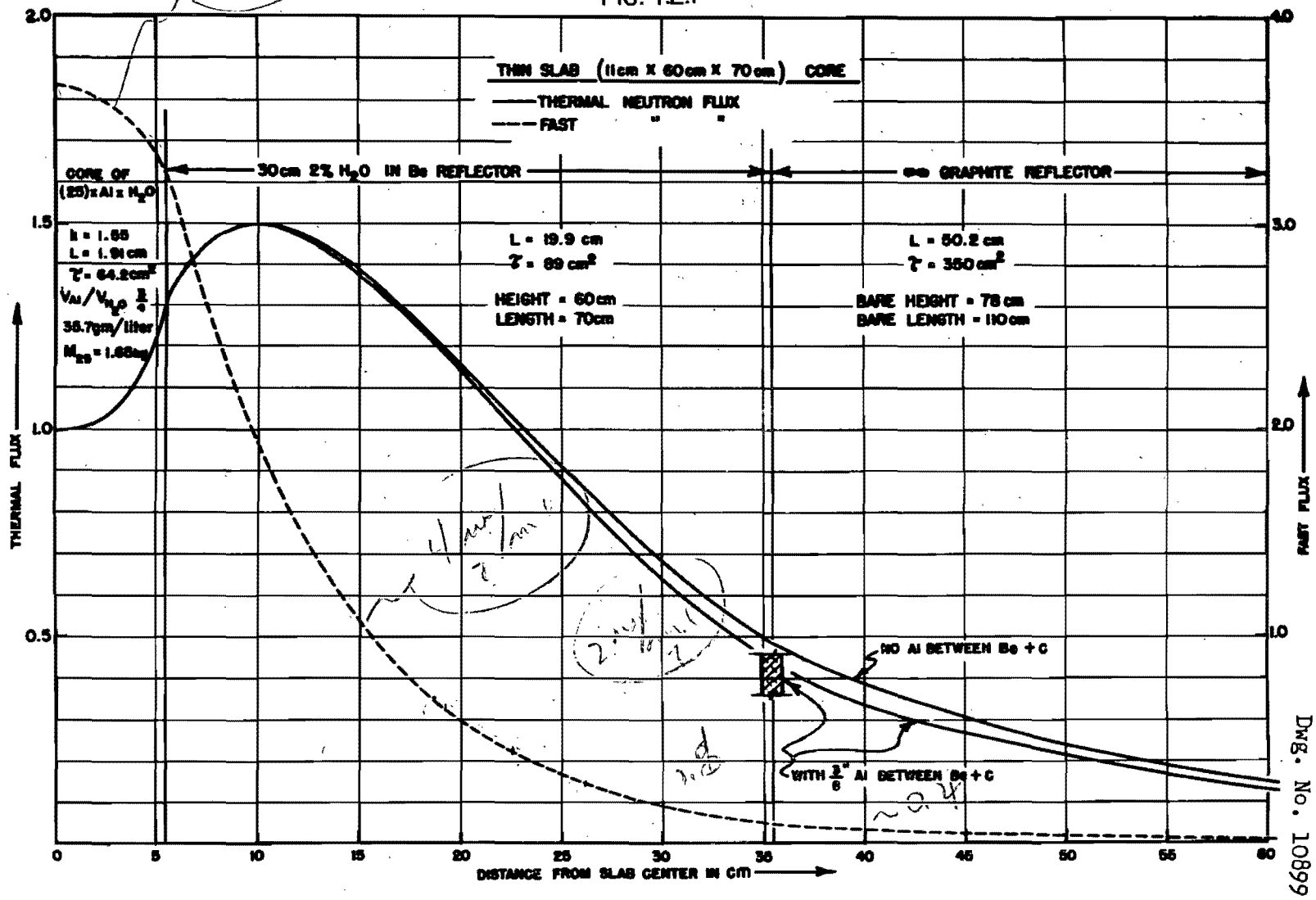

Dwg. No. 10899

4.9

used, and the aluminum tank wall. When cadmium control rods are near the center of the core, the flux in the reflector is relatively greater than the average core thermal flux because the cadmium rods cause a central depression of the neutron flux. A high ratio of reflector to average core neutron flux makes for maximum experimental usefulness with minimum expenditure of fuel.

The thermal flux in the useful experimental region is lowered considerably when a thorium blanket surrounds the reactor. Figure 4.2.G shows the magnitude of this depression produced by a sheet of thorium 1.26 cm thick placed at 20 cm from both sides of the rectangular cross-section core. Its effect on k is slight; $\Delta k/k = -0.4\%$.

The presence of the aluminum tank wall between the beryllium and graphite lowers the thermal flux slightly. At its position nearest to the core (30 cm) when the core is the thinnest possible slab (thus highest flux at the aluminum-graphite boundary), the aluminum depresses the thermal flux by only 14% as shown in Fig. 4.2.F. This figure may be used to estimate the flux at various positions in the reflector when thorium is not present. If the thermal flux is normalized to 2×10^{14} at the edge of the reactor, then the flux will rise to about 2.3×10^{14} in the beryllium 5 cm from the reactor surface. At the beryllium-graphite interface the slow neutron flux is about 6×10^{13}, and at the thermal shield it is about 3×10^{11}. These figures are, of course, very rough.

The calculations of the flux distributions were made according to a simple two-group diffusion theory. Experiments described in Appendix 2 indicate that these calculations predict a smaller slow-neutron rise in the reflector than is actually observed.

4.3 REACTIVITY LOSSES

For various reasons, e.g., Xe^{135} poisoning, depletion of U^{235}, etc., the reactivity of the reactor is lower during high-power operation than during zero-power operation. The reactor therefore must be built considerably larger than is necessary to be critical in the cold, clean state. Before summarizing the reactivity losses which are entailed by Xe^{135} + Sm^{149}, depletion of U^{235}, and temperature rise, the conventions for expressing reactivity loss will be reviewed briefly.

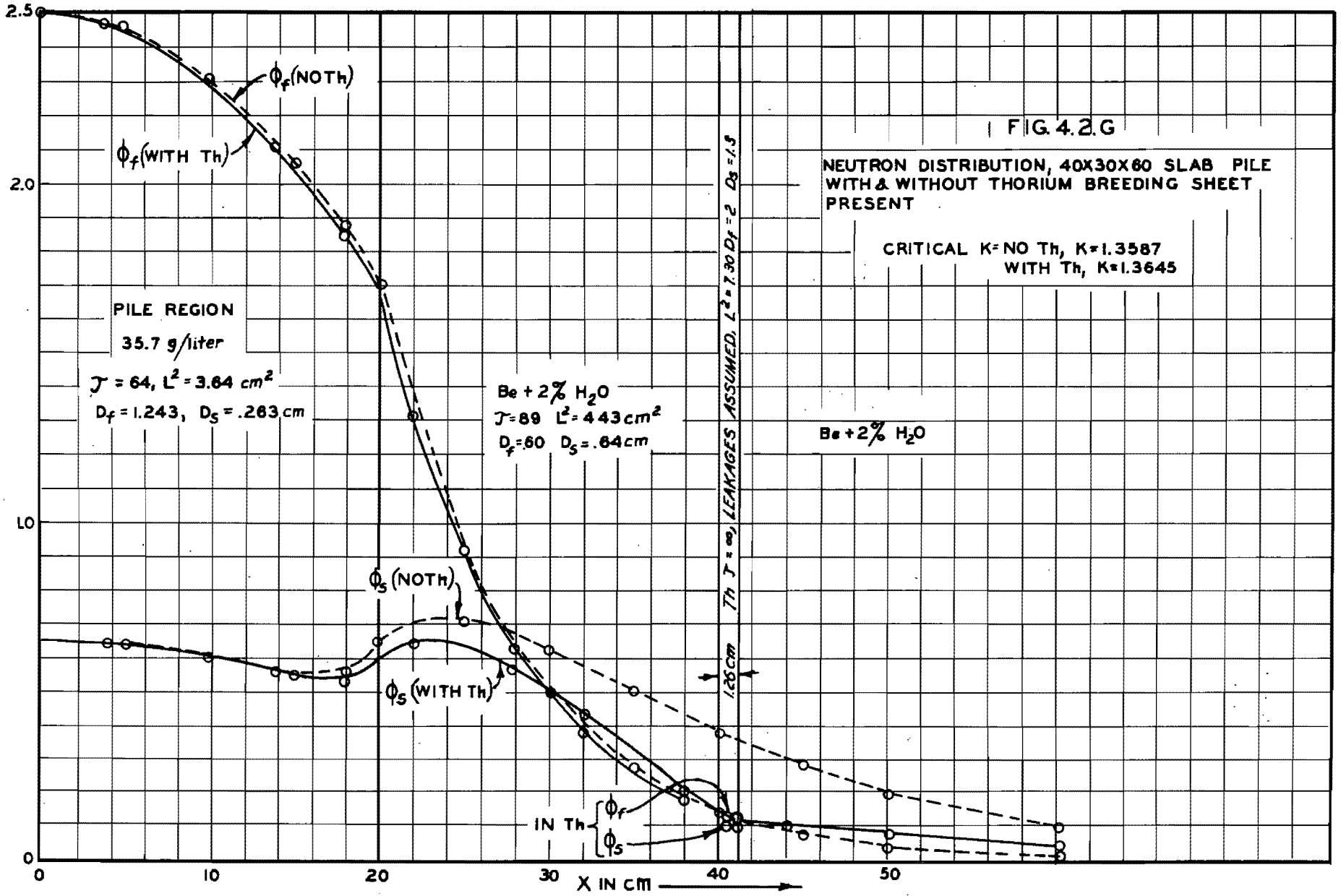

DWG. NO. 10900

[redacted]

If a poison is placed in or removed from a reactor which is just critical, the neutron density will decay or rise with a period T. This period is directly proportional to the change in reactivity, which we denote by

$$\Delta k_{eff}/k_{eff}$$

by the usual in-hour formula

$$\frac{\Delta k_{eff}}{k_{eff}} = \frac{l}{kT} + \sum_i \frac{\beta_i \tau_i}{\tau_i + T} \tag{1}$$

where l is the generation time, and β_i and τ_i are the abundance and the mean life of the ith delayed neutron group. The k in this formula is always the value of k *after* the change in poison has been made.

It is possible to calculate the reactivity change $\Delta k_{eff}/k_{eff}$, and therefore the period T, in terms of the absorption cross-section of the poison and its position in the reactor. More generally, if any perturbation is imposed on the reactor, e.g., if the density of the moderator is changed, then the reactivity will change in a manner which is calculable in terms of the magnitude of the perturbation and its position in the reactor.

The critical equation in two-group reactor theory is

$$k = (1 + \tau B^2)(1 + L^2 B^2)$$

where τ = age of fission neutrons.

L = diffusion length.

B^2 = "buckling" or "Laplacian" of the reactor.

When

$$\frac{k}{(1 + \tau B^2)(1 + L^2 B^2)} = 1$$

the system is chain reacting and in a steady state, and k_{eff} is defined as

$$k_{eff} = \frac{k}{(1 + \tau B^2)(1 + L^2 B^2)} .$$

In the MTR core $\tau \approx 64\ \text{cm}^2$, $L^2 \approx 3.5$ cm, and $B^2 \approx 10^{-2}\ \text{cm}^{-2}$.

If an absorber is uniformly distributed in the core, it will affect k primarily but, to a much lesser extent, it will also affect L^2. The latter effect can be neglected when $L^2 << \tau$ and we may then write

$$\frac{\Delta k_{eff}}{k_{eff}} = \frac{\Delta k}{k}$$

It will be recalled that

$$k = p\epsilon\eta f$$

when

η = number of neutrons produced for each thermal neutron absorbed in uranium. = 2.1

ϵ = fast multiplication factor = $\frac{\text{number of fast neutrons from all fissions}}{\text{number of neutrons from thermal fissions}}$

p = resonance escape probability = fraction of neutrons escaping resonance capture and thus becoming thermal neutrons.

f = thermal utilization factor = fraction of all thermal neutrons produced which is absorbed in fuel material.

However, in a small enriched reactor such as the MTR, both p and ϵ are sufficiently close to unity that, to a very good approximation,

$$k = \eta f = \eta \frac{\Sigma_{U^{235}}}{\Sigma_{reactor}}$$

where $\Sigma_{U^{235}} = N\sigma_{U^{235}}$.

$$\Sigma_{reactor} = N\sigma_{U^{235}} + N\sigma_{H_2O} + N\sigma_{Al} + N\sigma_{poison}$$

It is then possible to write, when an absorber is placed in the core,

$$\frac{\Delta k}{k} = \frac{\Delta\Sigma}{\Sigma_{reactor}}$$

In this expression k and $\Sigma_{reactor}$ always pertain to the situation *after* a change has been made.

The effect of a local change in the reactor is a fairly sensitive function of position. Experiments described in Appendix 3 have shown that an absorber is about twice as effective in the center of the core as at the edge, and the importance of an absorber diminishes rapidly as its distance from the core increases. This, of course, means that experiments can be done in the reflector, where the thermal flux is very high, without producing a major change in reactivity.

For detailed treatment of the equations and effects discussed above, the reader is referred to Glasstone and Edlund, *Elements of Nuclear Reactor Theory*.[65]

The major perturbations which occur in the reactor are Xe^{135} + Sm^{149} poisoning, U^{235} depletion, and temperature rise. The reactivity loss, $\Delta k/k$, for each of these has been calculated and is discussed below.

4.3.1 Xe^{135} and Sm^{149} Poisoning. When the reactor operates at a uniform flux of 2×10^{14}, i.e., at 10,000 kw per kilogram of U^{235}, the steady state reactivity loss due to Xe^{135} is $\Delta k/k = 3.9\%$ and that due to Sm^{149} is $\Delta k/k = 1.0\%$, making a total steady state loss of 4.9%. The manner in which these losses are reached after start-up is indicated in Figs. 4.3.A and B.

After shutdown the Xe^{135} produced by I^{135} decay builds up and goes through a maximum at 11 hr; at this time the additional reactivity loss due to Xe^{135} growth = 40.6%. The total extra Xe^{135} loss is somewhat less than this because any Xe^{135} which is already present at shutdown simply decays without going through a maximum. The time course of the Xe^{135} which grows from I^{135} is shown in Fig. 4.3.C (curve labeled $I^{135} \longrightarrow Xe^{135} \longrightarrow Cs^{135}$), and the time course of the Xe^{135} which decays directly is given in the curve labeled $Xe^{135} \longrightarrow Cs^{135}$.

The Sm^{149} is a daughter of Il^{149}; its concentration therefore increases after shutdown. The extra loss due to it would, at very long times after shutdown, eventually reach $\Delta k/k = 3.3\%$.

The overall time behavior of the extra reactivity loss is also given in Fig. 4.3.C. It is seen that in order to override the Xe^{135} + Sm^{149} loss at

[redacted]

FIG.4.3.A

REACTIVITY LOSS $\frac{-\delta K}{K}$, DUE TO Xe^{135}, Sm^{149}, 25 DEPLETION AND BUILD UP OF LOW CROSS-SECTION FISSION PRODUCTS AS FUNCTION OF TIME OF OPERATION

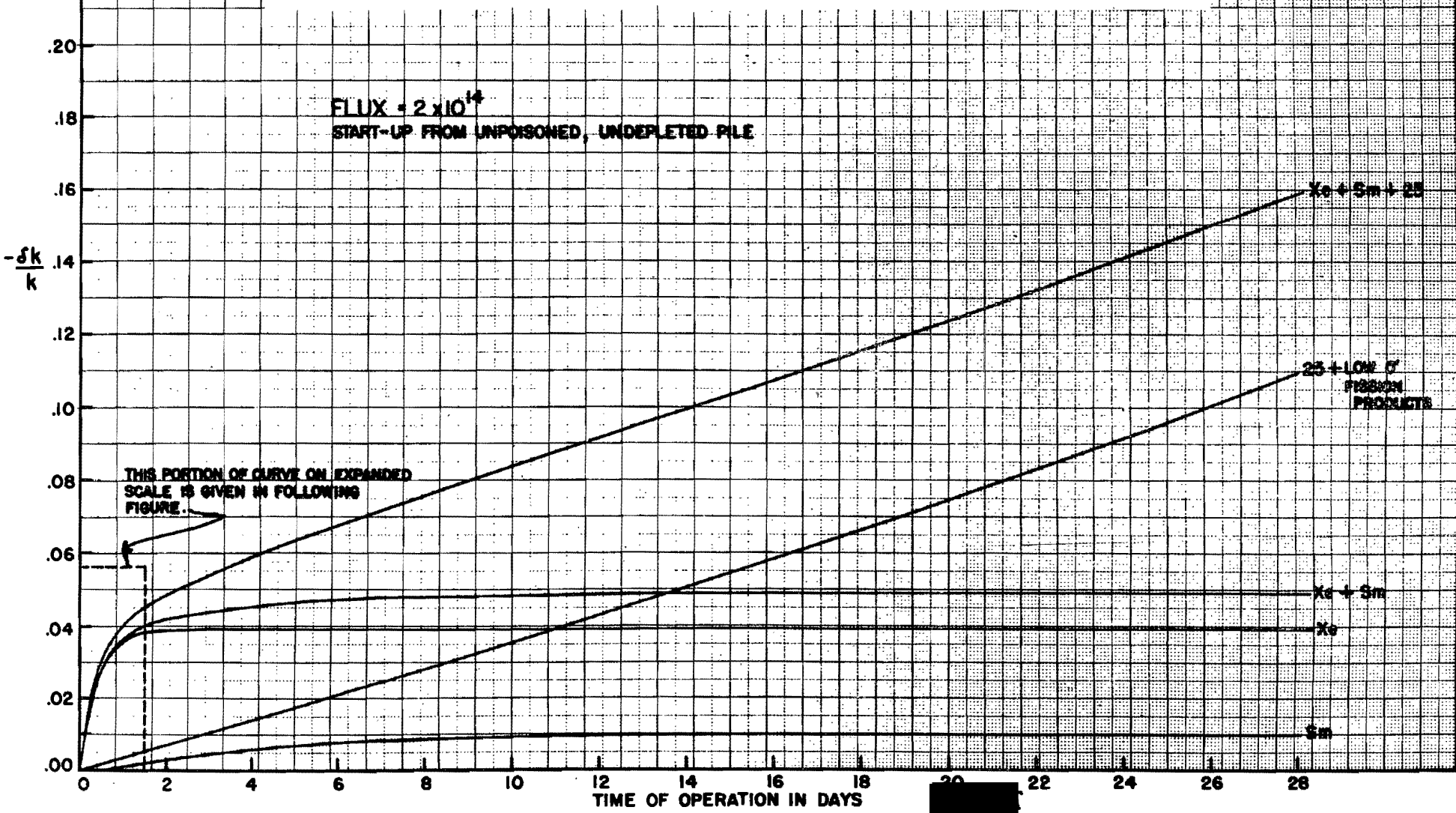

[redacted]

Dwg. No. 10902

[redacted]

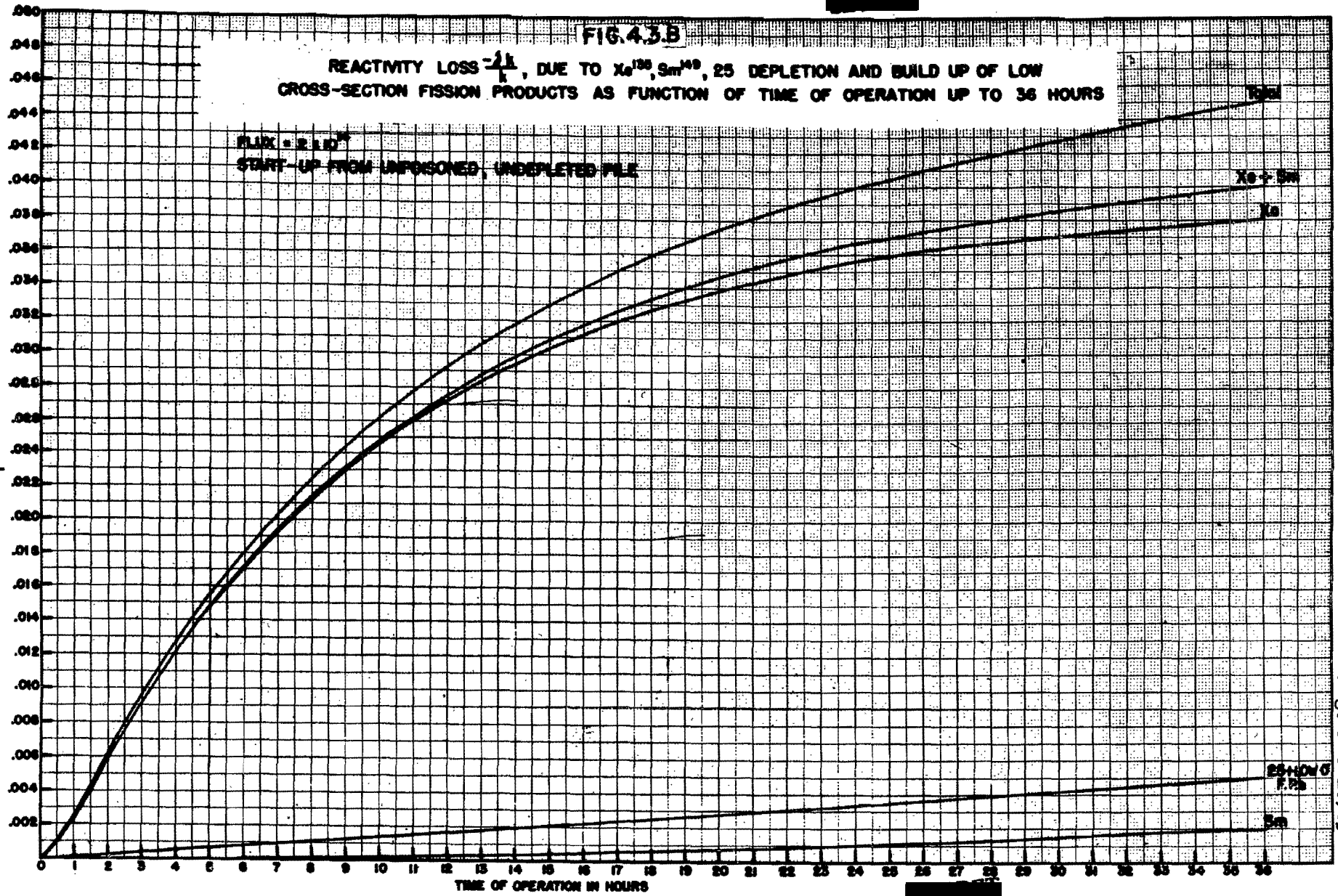

[redacted]

Dwg. No. 10903

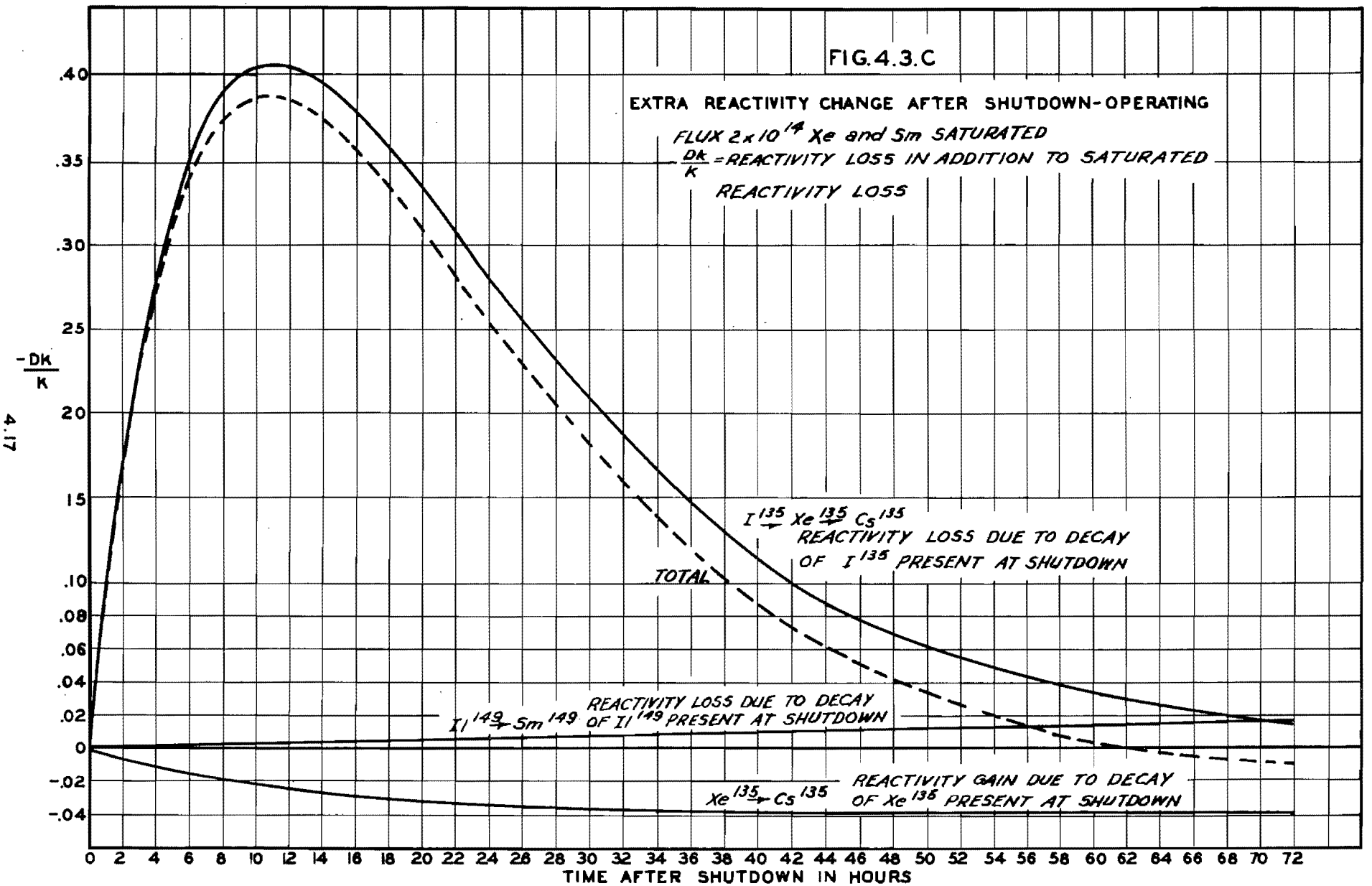
FIG. 4.3.C
EXTRA REACTIVITY CHANGE AFTER SHUTDOWN-OPERATING
FLUX 2x10^14 Xe and Sm SATURATED
Dk/K = REACTIVITY LOSS IN ADDITION TO SATURATED REACTIVITY LOSS
I^135 → Xe^135 → Cs^135
REACTIVITY LOSS DUE TO DECAY OF I^135 PRESENT AT SHUTDOWN
TOTAL
REACTIVITY LOSS DUE TO DECAY OF I1^149 PRESENT AT SHUTDOWN
I1^149 → Sm^149
REACTIVITY GAIN DUE TO DECAY OF Xe^135 PRESENT AT SHUTDOWN
Xe^135 → Cs^135
-Dk/K
.40
.35
.30
25
20
15
.10
.08
.06
.04
.02
0
-.02
-.04
0 2 4 6 8 10 12 14 16 18 20 22 24 26 28 30 32 34 36 38 40 42 44 46 48 50 52 54 56 58 60 62 64 66 68 70 72
TIME AFTER SHUTDOWN IN HOURS

DWG. NO. 10904

all times, an excess k equal to the sum of the net extra loss, 38.8%, plus the equilibrium loss, 4.9%, or $\Delta k/k$ = 43.7% is needed.

It was not regarded as a practical necessity that so much reactivity be built unto the reactor that it could override the Xe^{135} at all times after shutdown.* However, there should be sufficient extra reactivity so that every accidental scram does not keep the reactor shut down for several days. It was felt that if the reactor can override ½ hr of accumulated Xe^{135} + Sm^{149}, it will ordinarily have sufficient operational flexibility. To achieve this it is necessary, according to Fig. 4.3.C, to build into the reactor an excess reactivity of 9.6% (4.7% for reactivity loss in 30 min after shutdown plus 4.9% equilibrium loss). With this available $\Delta k/k$ the machine can be started up within the first half hour after a scram, or after two days if not started during the "grace" period.

It should be clear from this discussion that much more care is needed to shut down and start up this reactor than is needed for the graphite reactors.

4.3.2 Depletion of U^{235} and Other Fission Product Poisoning. It is estimated that there will be a loss of 0.35% per day in $\Delta k/k$ attributable to the depletion of U^{235} and accumulation of low-cross-section fission products (σ_a is assumed to be 50 barns per fission) if the reactor runs at 10,000 kw per kilogram. A running cycle of about ten days was used for the computation, which means that about 3.5% in $\Delta k/k$ must be available to override the depletion loss. The depletion and low-cross-section fission product loss is plotted as a function of time in Figs. 4.3.A and B (curves labeled "25"). The total loss due to depletion, low-cross-section fission products, and Xe^{135} + Sm^{149} is also given in these figures.

4.3.3 Temperature Coefficient. As the temperature of the reactor rises, the reactivity falls. The reactivity temperature coefficient, defined as the change in $\Delta k/k$ per degree centigrade temperature rise in the reactor, is the sum of three partial coefficients. These partial coefficients arise from

1. Expansion of the fuel-bearing aluminum plates,
2. Expansion of water between fuel plates,
3. Change in microscopic cross-sections with temperature.

*Operational requirements of the STR, designed subsequently to the MTR, have dictated that sufficient reactivity be incorporated to override Xe^{135} at all times.

Effects 1 and 2 are functions of the bulk temperature of the plates and H_2O, respectively. Effect 3 is a function only of the neutron temperature. To determine the neutron temperature from the H_2O temperature is not easy; it is supposed that the two are equal.

In Table 4.3.A are tabulated the partial temperature coefficients at 20°C calculated for three cylindrical reactors of 12.78, 17.85, and 21.12 cm active radii, respectively. All are approximately 53 cm high and V_{Al}/V_{H_2O} = 0.75. The usual adjoint perturbation theory was used for the calculation.

TABLE 4.3.A

Partial Temperature Coefficients at 20°C, Al-H_2O Neutron Temperature

Reactor	r = 12.78 k = 1.606	r = 17.85 k = 1.432	r = 21.12 k = 1.373
Coefficient (1) in $\Delta k/k$/°C	-1.6×10^{-5}	-1.4×10^{-5}	-1.3×10^{-5}
Coefficient (2)	-3.8×10^{-5}	-3.0×10^{-5}	-2.8×10^{-5}
Coefficient (3)	-15.7×10^{-5}	-10.5×10^{-5}	-8.9×10^{-5}
Total coefficient	-21×10^{-5}	-15×10^{-5}	-13×10^{-5}

During summer operation at 10 kw/per gram of U^{235} the water will enter the reactor at about 100°F (39°C) and leave it at 115°F (47.3°C). The maximum aluminum temperature will be about 50°C higher than the average water temperature. The lowest reactor temperature will occur during winter shutdown; at this time water and aluminum will be at about 10°C. Thus the yearly temperature range of the water (and the neutrons) is about 35°C, and the temperature range of the aluminum is about 70°C. The maximum reactivity loss in the k = 1.606 reactor due to temperature rise is therefore: 0.11% in $\Delta k/k$ due to aluminum temperature rise and 0.68% in $\Delta k/k$ due to water and neutron temperature rise, making a total of 0.79%. For the k = 1.373 reactor the figure would be 0.5%. The temperature loss computed here is total loss from winter shutdown to summer operating conditions. The loss in reactivity from summer

shutdown to summer operating is very much less than 0.78%; it is only about 0.2%, which is the amount of $\Delta k/k$ that must be held by the regulating rods. The larger variation between summer and winter operation and shutdown can be taken care of by the shim rods.

4.3.4 Thorium Blanket. The calculated critical masses are for a reactor with an infinite Be + H_2O reflector on the side. Actually there may be a thorium blanket about 15 cm away from the surface of the 22- by 70-cm rectangle which reduces the reactivity by about 0.7% in $\Delta k/k$. This is rather an overestimate of the thorium effectiveness because for most reactor loadings the distance from the reactor interface to the thorium blanket will probably be more than 15 cm.

4.3.5 Other Reactivity Losses. Experimental setups around and in the reactor lattice will further reduce the reactivity of the machine. An additional 5% in $\Delta k/k$ was arbitrarily assigned to handle this. It is estimated that this margin in $\Delta k/k$ represents an absorber of total cross-section 330 cm^2 placed uniformly in a 2-kg reactor.* It may be pointed out that in the present ORNL reactor, the total poison cross-section which will take up the excess available for experiments, i.e., about 0.5%, is 4000 cm^2 if spread uniformly or 500 cm^2 if concentrated at the center.

4.3.6 Total Reactivity of Reactor. The overall minimum excess reactivity built into the reactor is summarized in Table 4.3.B.

TABLE 4.3.B

Minimum Reactivity Losses Which Must Be Allowed for in Reactor

SOURCE OF LOSS	$\Delta k/k$ (%)
Xe^{135} + Sm^{149}	9.6
Depletion + low-cross-section fission products	3.5
Temperature	0.8
Others	5.0
Total	18.9

*The critical experiments discussed in Appendix 3 indicate that $\Delta k/k$ for experiments and apparatus will be less than that assigned here.

From the curve of critical mass versus k in Fig. 4.3.D it may be estimated that about 2.6 kg is needed to ensure an excess $\Delta k/k$ of 18.9%.

Because of the thorium blanket (which reduces the reactivity by about 0.7% in $\Delta k/k$, depending on the disposition of the active lattices) and because of the holes in the reflector, the amount of U^{235} needed to give an excess reactivity of 18.9% is a little larger than 2.6 kg for a reactor built with an Al/H_2O volume ratio of 0.70.

The exact critical mass is not crucially important since the reactor is designed so that as much as 6 kg of U^{235} can be loaded by replacing all the removable beryllium. With this loading the excess reactivity is $\Delta k/k$ = 29%. It would, of course, be undesirable to use this large loading regularly since this would mean, for fixed total power, a reduction in flux. If the critical mass calculations are correct, then the average slow flux attainable in the machine will in fact be 2×10^{14} at 30 megawatts; if the critical masses turn out to be higher than calculated, then the flux at 30 megawatts will be reduced in proportion.

[redacted]

Dwg. No. 10901

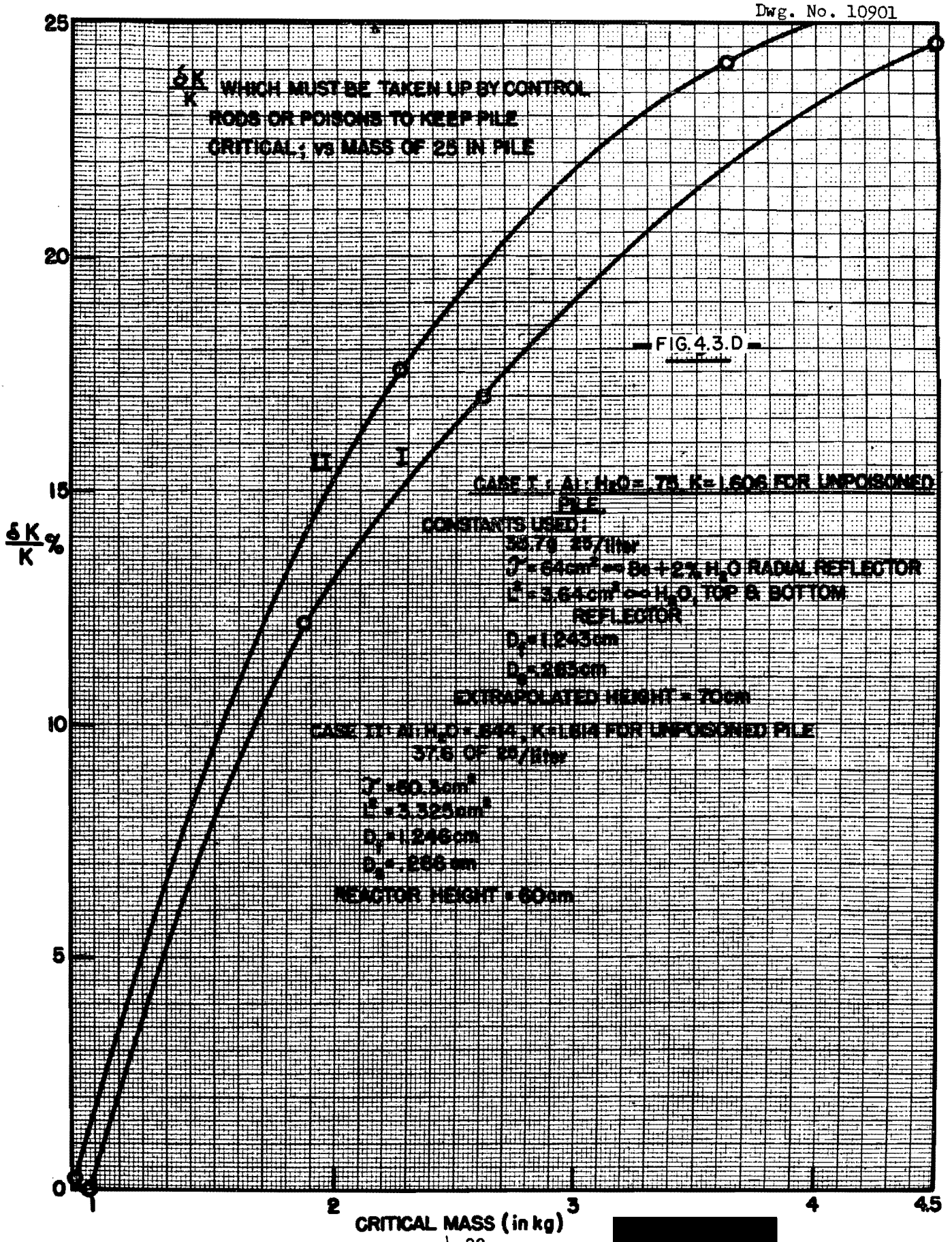

[redacted]

4.4 DYNAMICS OF THE REACTOR

A proper analysis of the time-dependent behavior of a reactor operating on thermal neutrons must take into account the important effects on its criticality, reactivity, and stability which arise from such factors as fission products of high thermal-neutron capture cross-section, depletion, temperature, average neutron lifetime in the reactor, flux level, and reactor period. As has been seen in the requirements placed on the reactor, considerable excess reactivity must be built into the active core before start-up. The control rods must keep the reactivity below the critical value before and during start-up.

Two start-ups must be considered separately, first for the case for the clean, cold reactor, and second for the case when the reactor has been shut down from a high level and must be started up again quickly. When an enriched reactor starts from a cold, clean state to a power level of 3×10^7 watts, as in the MTR, the range to be covered by control instruments is from $10^{-18} \times$ full power to unity $\times$ full power (in terms of total number of fissions per second, 3×10^7 watts requires about 10^{18} fissions/sec).

In order to bring the lower part of this range into the operating region of convenient instruments a neutron source (e.g., Po-Be) is always inserted in the reactor to produce about 10^7 neutrons/sec. With such a source in place in a cold, clean reactor, start-up time of half an hour has been selected as sufficiently slow for safety and not objectionably long for convenience. The rods therefore are withdrawn at an average rate of 0.01% $\Delta k/k$ per second, which is accomplished by withdrawing at the rate of 0.1% per second for ½ sec, followed by a waiting period of 4½ sec. This "intermittent" speed is equivalent to introducing step changes in reactivity at regular intervals, and the increasing transient periods become an indication of the approach to criticality.

If it is assumed that a "start-up accident"* occurs in which rods are withdrawn continuously at a rate equivalent to $\Delta k/k \approx 0.1\%$ per second, the neutron level will rise only a factor of 100 in several minutes. However, at the end of this time the reactor will be supercritical, on a rising period of approximately 10 sec, and in a few more seconds will have a period of approximately 1 sec. Under these conditions the reactor will have passed prompt

*See Chap. 5.

critical long before the level is reached at which the safety instruments are set to operate. If all controls have failed, the minimum period expected, pessimistically estimated at about 1/30 sec, must be countered by safeties capable of 30-msec response. In this event the power would momentarily rise to about three times "normal" overload power or about four times operating power. It has been demonstrated in the MTR Mock-Up that rods will actually begin to drop in about 0.015 sec.

In restarting the reactor after a short shutdown, the time available is limited by xenon growth; hence the rods must be withdrawn as quickly as possible. However, the considerations of the preceding paragraph indicate that the maximum tolerable rod withdrawal is 0.1% $\Delta k/k$ per second. This, then, has been fixed as the "high" rate of rod withdrawal and permits complete withdrawal of all rods in about 6 min.

When the MTR is normally at full load, the excess reactivity may amount to 20% in k. All the controls will take up about 40% in k at most, so that a dead, cold reactor has a k of about 0.8. This imposes great caution in start-up, and the control arrangement as described in Chap. 5 makes it impossible to start the reactor or operate it without a source of sufficient strength.

The provision of a source has been conveniently brought about by utilizing an arrangement of antimony plus beryllium. ${}_{51}Sb^{124}$ is a γ-ray emitter
1.73 ? of ~~0.03~~ Mev with a 60-day half-life; it is conveniently made from natural ${}_{51}Sb^{123}$ by neutron absorption. Such a source is therefore kept active in a going reactor. It has the advantages of cheapness and sufficiently long half-life to maintain high activity for several days after shutdown.

4.5 HEAT PRODUCTION, TRANSFER, AND REMOVAL

As has been previously indicated, the fuel assemblies and the beryllium reflector are water cooled. In the reflector the water acts primarily as a coolant, but in the active lattice it acts as both coolant and moderator. This means that the quantity of water (moderator) in the active lattice at any time must be determined by nuclear considerations, but the speed with which it passes through the lattice is determined by heat transfer requirements.

The high flux requirements of the MTR require a reactor with the smallest possible critical mass. This is accomplished by building the reactor with the optimum U^{235}/H ratio,[1,2] which in this case means choosing the appropriate U^{235}/H_2O ratio. With these nuclear requirements in mind, the amount of uranium per fuel plate was determined by the optimum amount of uranium in uranium-aluminum alloy, and the thickness of each plate was determined by the practicability of the picture frame construction and required rigidity of the plate structure (see Appendix 6). The U^{235}/H ratio was then fixed by the spacing between the plates.

The above considerations led to the present design of the MTR fuel assemblies with spacing of 0.117 in. between plates. Heat transfer calculations[3] then showed that satisfactory heat transfer could be obtained with a water velocity of approximately 30 ft/sec through these spaces. Once this figure was established, further calculations[4] and experiments (see Appendix 4) established the pressure differentials required and the resultant quantity of water through the reactor. By this means the necessary pressure drop across the fuel assemblies was found to be about 40 psi, which, because of parallel flow, is also the pressure drop across the beryllium reflector. It should be noted that this pressure produces a flow of approximately 20,000 gpm through the reactor and beryllium, resulting in a water temperature rise of only about 11°F for 30,000-kw operation.

The original calculations for heat production are reported in MonP-272. Since that time these figures have been experimentally checked in critical experiments (see Appendix 3) and in the Mock-Up (see Appendix 4). For convenience the initial results given in MonP-272 are restated in Sections 4.5.1 and 4.5.2, while the later figures based on experiment are given in Appendixes 3 and 4. A check on all these figures will, of course, be made in the early days of operation of the MTR.

4.5.1 Calculations of Heat Inside Active Lattice. The assembly plates will contain a concentration of U^{235} of about 20.4 mg/cm^2. At a power output of 10 kw per gram, which corresponds to a slow flux of about 2×10^{14}, the heat taken out of each side of an assembly plate is about 24 cal/cm^2/sec. With a flow velocity of 30 ft/sec in the reactor core and a plate separation of 0.117 in., the heat transfer coefficient, with no scale formation, should be about 0.9 cal/cm^2/sec/°C, or 6300 Btu/hr/ft^2/°F. The film temperature drop is therefore 27°C.

1.8x6,300x27 = 306,000 Btu/hr/ft

These are average figures. Along the mid-plane of the core, the flux is about 1.3 times the longitudinal average; at the core-reflector interface this can be increased by as much as another factor of 1.2 when the loading is in the form of a very thin slab. Finally, in the neighborhood immediately surrounding a thorium shim rod there is a further local heating of about 20%, which arises because of the rather large dead layer of H_2O-Al (13 mm) between active assembly and thorium. The hottest spot in the reactor may therefore have a power output which is $1.3 \times 1.2 \times 1.2 = 1.87$ times the average. Thus the maximum film drop could be as high as 50°C even without any scale formation. If the average power output is 10 kw per gram,* the reactor is loaded as a thin slab, and a thorium shim rod happens to be close to the core-reflector interface.

4.5.2 Calculations of Heat in Beryllium and in Foreign Materials Near Active Lattice. Outside the core, heat is produced primarily from absorption of γ rays. Some of these come from the reactor itself, and some arise from neutron capture in beryllium, in thorium, and in graphite.

The calculation of the heat distribution in the reflector was based on the neutron distribution for the very thin slab reactor without any thorium (Fig. 4.2.F) since in this case the heat load in the reflector is heaviest. The results are given in Fig. 4.5.A. To simplify the computation of the γ-ray absorption, the core and reflector were assumed to be infinite slabs; this leads to an overestimate of the heat load since the neutron flux was assumed to be uniform over the whole core and equal to 2×10^{14}.

The added heat flux per experimental hole is about $0.03A^2/R^2$ kw,** where A is the cross-sectional area of the hole, and R is the distance from the core surface to the face of the hole opposite the core surface, provided A is much smaller than R^2. For the 6-in. hole, $R \approx 40$ cm, the total heat flux is about 0.6 kw or 3.5 watts/cm^2. The pile γ-ray heat flux at 40 cm in the absence of a hole is 3.5 watts/cm^2; hence, the hole increases the load due to the γ-ray heat by a factor of 2, or the total heat flux increases from 4.6 watts/cm^2 (see Fig. 4.5.A) to $4.6 + 3.5 = 8.1$ watts/cm^2.

The greatest heat load outside the core occurs in the mid-plane of the beryllium reflector at the interface between beryllium and core. This maximum

*The specific power (average) for the reactor is 300 kw/liter.

**0.03 is the approximate average γ-ray heat flux at surface of lattice.

DWG. NO. 10905 [redacted]

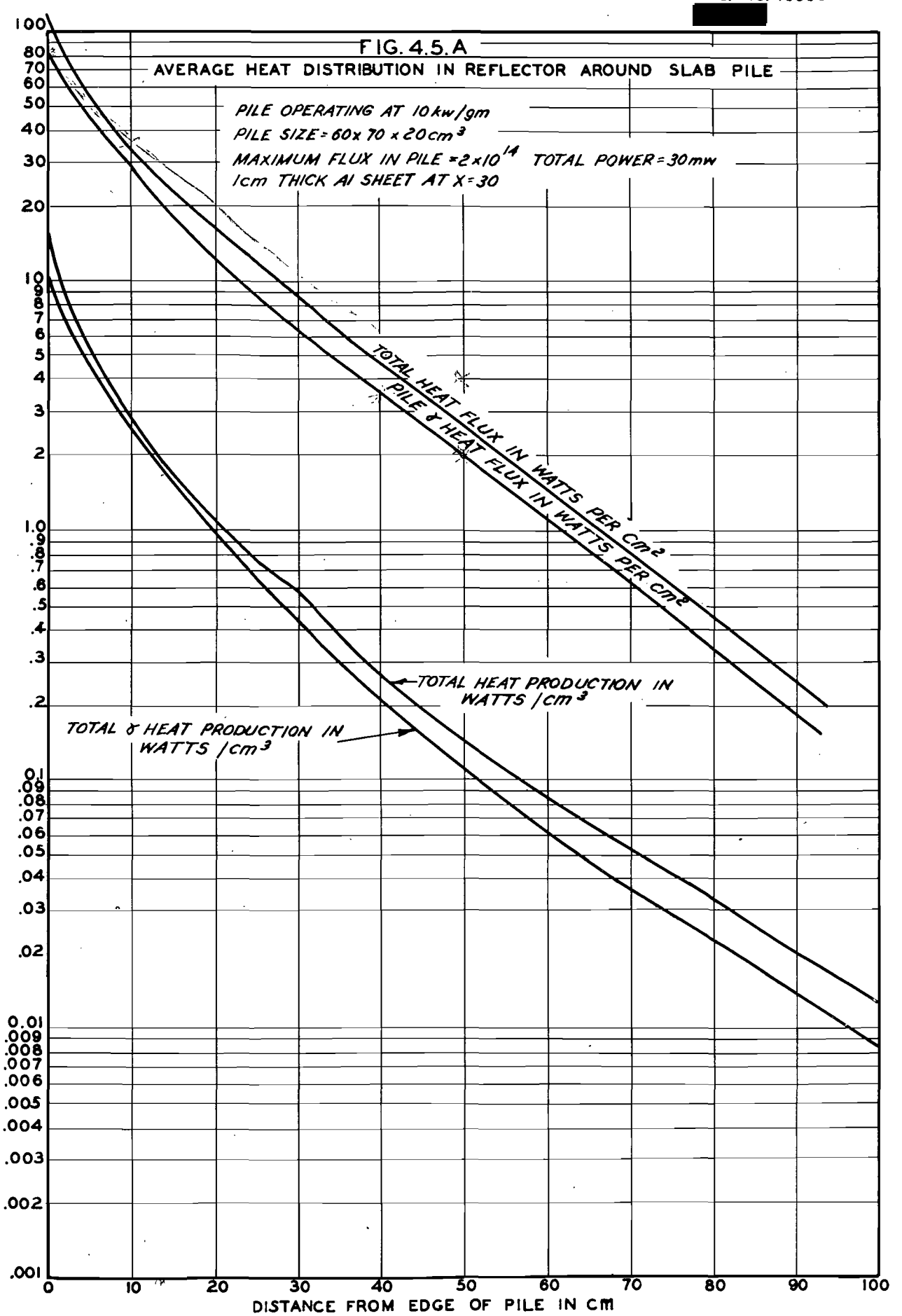

might be as much as 16 watts/cm^3 or 3.84 cal/cc/sec. If the beryllium is shaped like a slab, cooled on both front and back faces, the temperature rise in the center is

$$\Delta T = \frac{qx^2}{2k} = 4.8x^2$$

where q is the heat production (= 3.84 cal/cc/sec), x is the half-thickness of the slab, k is the thermal conductivity and is equal to 0.4 cal/deg/cm/sec. A temperature rise of 75°C, which is probably safe, allows the slabs to be 8 cm thick.

Foreign materials, such as control rods or experiments which are placed in the center of the core, will be heated even more strongly than the beryllium. The γ-ray heat production at the center of the reactor is about 5.85 cal/cc/sec; this is essentially the γ-ray heat absorbed in the reactor. Since the reactor has an average density of about 1.7 g/cc, an estimate of the heat production in a foreign body placed at the center of the reactor will be about 5.85/1.7 = 3.4 cal/g/sec. Thus in beryllium, density 1.85 g/cc, the heat load is 6.3 cal/cc/sec, while in thorium, density 11 g/cc, the heat load due to reactor γ's alone is 38 cal/cc/sec.

In addition to the reactor γ's, the U^{233} fission in the thorium creates a heat load which is not negligible. It is unwise to run the U^{233} concentration in the thorium beyond 0.1% because at this time about one-tenth of the captures in thorium lead to fission. The additional heat load in the thorium due to U^{233} fissions is about 22 cal/cc/sec. The total load in the thorium rods may therefore be as high as 60 cal/cc/sec.

4.5.3 Heating and Cooling of the Graphite Reflector. This subject is covered fully in a report[5] on the cooling of the graphite reflector. Heat production in the graphite is based on the curves given in MonP-272 and the data obtained in critical experiments (Appendixes 2 and 3) and is normalized for a slab reactor of the following characteristics:

Power (kw)	30,000
U^{235} in reactor (kg)	3.5 (23 assemblies + half of 4 shim rods)
Mev/fission	187
Fissions/sec	9.9×10^{17}
Average nv (thermal)	2.0×10^{14}
Specific power (kw/liter)	300

The results of these calculations are shown in Fig. 4.5.B. In this figure the curves are discontinuous owing to the pebble zone which is indicated between points *AA* and *CC* for slab and square loading, respectively.

The total heat to be removed from the pebble bed was estimated by dividing the bed into several zones and calculating the heat production from the curves in Fig. 4.5.B. By this method it was found that the total heat produced in the pebble bed is about 420 kw with the reactor operating at 45,000 kw.

The total heat to be removed from the permanent graphite was found by a method similar to that used in the pebble zone and amounts to about 330 kw with the reactor operating at 45,000 kw.

4.5.4 Heating and Cooling of the Thermal Shield. Heat production in the thermal shield has been calculated,[6,7] and these calculations show a total heat production of 47.5 kw in the thermal shield for operation at 30,000 kw. These figures were obtained by estimating the neutron fluxes and multiplying these fluxes by 60×10^{-14}, the heat production for a flux of 1 neutron/cm^2-sec at the surface of the steel. This figure assumes that reactor and reflector γ rays produce an amount of heat equal to that produced by capture γ rays in the steel.

The temperature produced in the steel by this heat production is highest in the bottom thermal shield and in the east side wall with slab loading. With the present design of the shield (see Section 2.5.1) and air flow of 25,000 cfm it is estimated that the maximum steel temperature in the bottom shield will not exceed the air temperature by more than 150°F at 60,000-kw operation. Furthermore, the maximum temperature of the steel next to the concrete will be less than 70°F above the air temperature.

Temperatures in the east side wall are high because of proximity to the active lattice (slab loading on east side). Present design calls for insulation between the graphite and the steel in the side walls to reduce heat conduction from the graphite into the steel.

4.5.5 Cooling Requirements at Reduced Power Levels and After Shutdown. The cooling requirements at reduced power levels have been calculated;[8] the results are plotted in Fig. 4.5.C.

[redacted]

Dwg. #8599

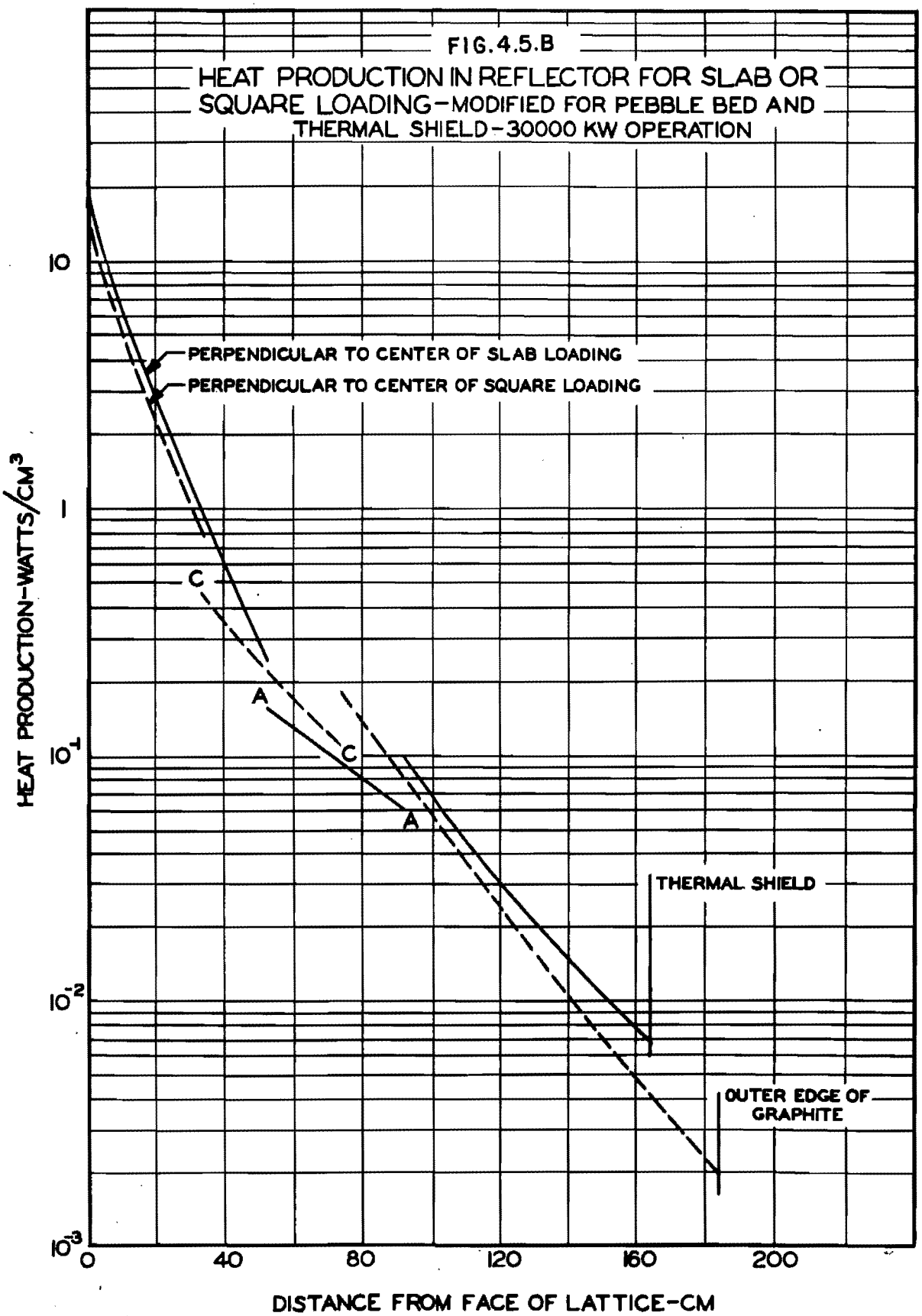

[redacted]

Drawing # 8733

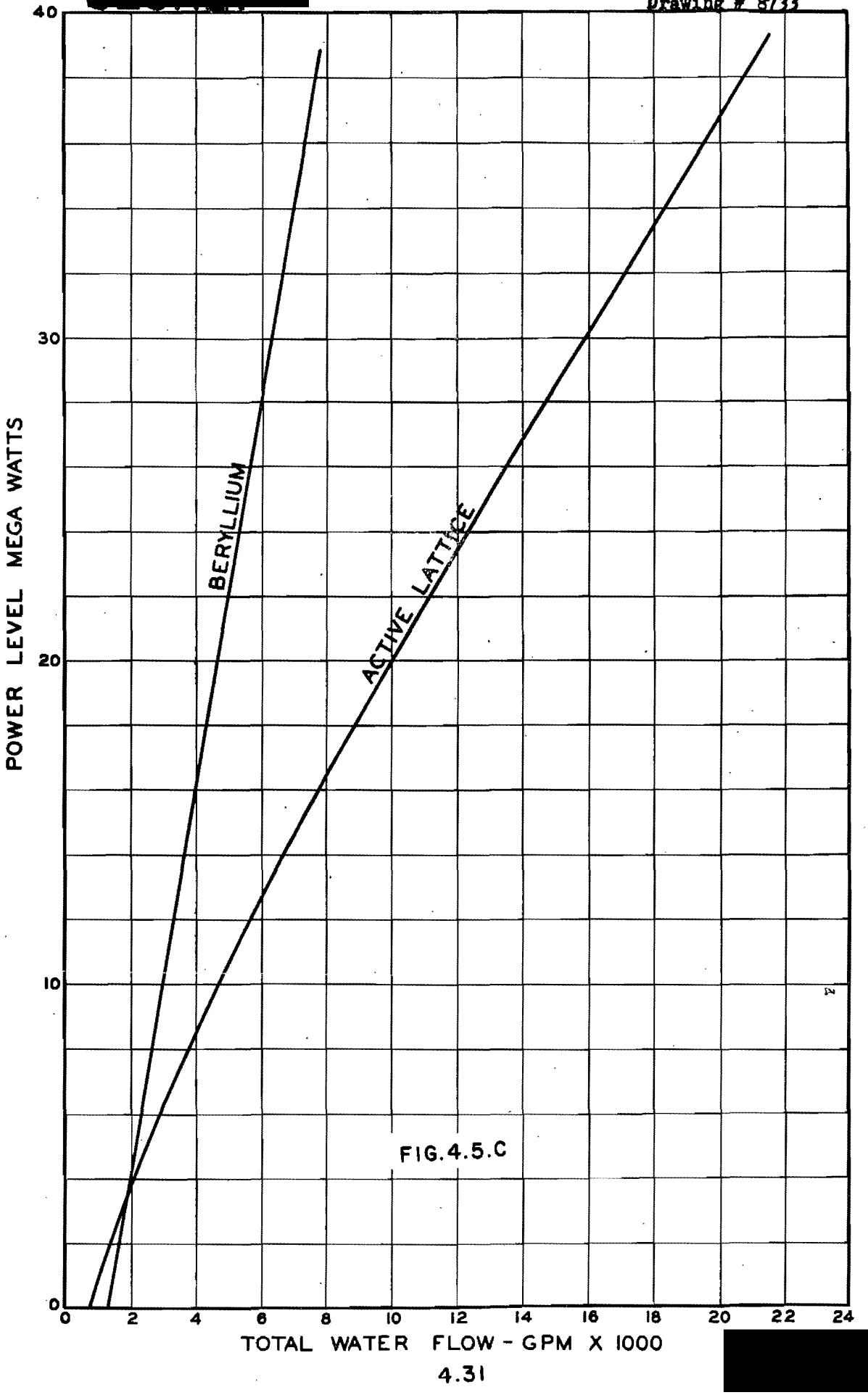

FIG. 4.5.C

[redacted]

The problem of cooling after shutdown has been extensively studied, and a full report has been written.[9] After shutdown the power level is given by the formula developed by Way and Wigner:[10,11]

$$P = BF\ [t^{-0.2} - (t + T)^{-0.2}] \qquad \text{Mev/sec}$$

where

F = fissions/sec-kw

t = seconds after shutdown

T = seconds of pile operation

During operation the power level is given by

$$P = 187F \qquad \text{Mev/sec}$$

so that the reduction factor is $A[t^{-0.2} - (t + T)^{-0.2}]$. Experimental and extrapolated values of the reduction factors given in Table 4.5.A show that A varies between 0.80 and 0.90 over a range of 360 sec to 4 days for a 20-day irradiation period.

Using the equation for decay given above, the heat generated in the tank after shutdown, assuming no losses from the tank, is given by:

$$H = \int_0^t 30{,}000(0.08)\ [t^{-0.2} - (t + T)^{-0.2}]\ dt$$

$$= 3{,}000\ [t^{0.8} - (t + T)^{0.8} + (T)^{0.8}] \qquad \text{kw-sec}$$

Using a 20-day irradiation, then, for t values up to a few hours,

$$H = 3{,}000\ t^{0.8}\ \text{kw-sec} \quad = 2.42\ t^{0.8}\ \text{cal/cm}^2\text{/sec}$$

which gives the values listed in Table 4.5.B.

TABLE 4.5.A

Reduction Factors After Shutdown

COOLING TIME	$t^{-0.2}-(t+T)^{-0.2}$	10-DAY OPERATION			20-DAY OPERATION			40-DAY OPERATION		
		(kw/g)	F	A	(kw/g)	F	A	(kw/g)	F	A
6 min	0.252	2.00	2×10^{-2}	0.0795	1	2×10^{-2}	0.0795	0.52	2.08×10^{-2}	0.0825
12	0.213	1.65	1.65×10^{-2}	0.0775	0.86	1.72×10^{-2}	0.0806	0.445	1.78×10^{-2}	0.0835
18	0.191	1.49	1.49×10^{-2}	0.0780	0.78	1.56×10^{-2}	0.0815	0.405	1.62×10^{-2}	0.0848
24	0.177	1.38	1.38×10^{-2}	0.078	0.73	1.46×10^{-2}	0.0824	0.378	1.51×10^{-2}	0.0853
30	0.167	1.32	1.32×10^{-2}	0.079	0.70	1.38×10^{-2}	0.0826	0.360	1.44×10^{-2}	0.0863
36	0.159	1.25	1.25×10^{-2}	0.0786	0.67	1.32×10^{-2}	0.0830	0.345	1.38×10^{-2}	0.0868
42	0.153	1.20	1.20×10^{-2}	0.0785	0.64	1.28×10^{-2}	0.0835	0.340	1.36×10^{-2}	0.0889
48	0.147	1.16	1.16×10^{-2}	0.0789	0.62	1.24×10^{-2}	0.0842	0.330	1.32×10^{-2}	0.0898
54	0.142	1.12	1.12×10^{-2}	0.0789	0.60	1.24×10^{-2}	0.0845	0.315	1.26×10^{-2}	0.0888
1 hr	0.138	1.09	1.09×10^{-2}	0.0790	0.58	1.16×10^{-2}	0.0840	0.305	1.22×10^{-2}	0.0885
2	0.113	0.89	8.9×10^{-3}	0.0787	0.48	9.6×10^{-3}	0.0850	0.260	1.04×10^{-2}	0.092
5	0.085	0.67	6.7×10^{-3}	0.0788	0.37	7.4×10^{-3}	0.0871	0.200	8×10^{-3}	0.0941
10	0.066	0.52	5.2×10^{-3}	0.0782	0.29	5.8×10^{-3}	0.0879	0.163	6.5×10^{-3}	0.0985
1 day	0.046	0.36	3.6×10^{-3}	0.0783	0.21	4.2×10^{-3}	0.0913	0.122	4.88×10^{-3}	0.106
2	0.0345	0.255	2.5×10^{-3}	0.0738	0.155	3.1×10^{-3}	0.0898	0.092	3.68×10^{-3}	
4	0.0232	0.164	1.64×10^{-3}	0.0707	0.105	2.1×10^{-3}	0.0905	0.066	2.6×10^{-3}	
10	0.0126	0.075	7.5×10^{-4}	0.0555	0.054	1.08×10^{-3}	0.0855	0.035	1.42×10^{-3}	
20	0.0075	0.035	3.5×10^{-4}	0.0466	0.0270	5.4×10^{-4}	0.072	0.019	7.6×10^{-4}	
50	0.0032	0.0097	9.7×10^{-5}	0.0303	0.0083	1.66×10^{-4}	0.052	0.0065	2.6×10^{-4}	
100	0.0012	0.00305	3.05×10^{-5}	0.0254	0.0027	5.4×10^{-5}	0.045	0.00235	9.4×10^{-5}	

TABLE 4.5.B

Cumulative Heat After Shutdown

t	$t^{0.8}$	(kw-sec)	(Btu)	(cal)
1 sec	1	3,000	2,840	715,000
2	1.74	5,220	4,950	1,248,000
5	3.62	10,900	10,340	2,600,000
10	6.3	18,900	17,900	4,510,000
30	15.2	45,600	43,300	10,920,000
60	26.5	79,500	75,400	19×10^6
5 min	96	288,000	273,000	68.7×10^6
10	106	498,000	473,000	119.2×10^6
30	400	1,200,000	1,140,000	287×10^6
1 hr	700	2,100,000	1,990,000	501×10^6
2	1,220	3,670,000	3,480,000	876×10^6

Using the equations on page 4.32 the fall-off of the heat rates and the corresponding water requirements are given in Table 4.5.C.

It will be noted that the water flow drop-off must be governed by the beryllium requirements since the heat source in the beryllium does not decrease as rapidly as in the lattice.

TABLE 4.5.C

Fall-off of Heat Rates and Water Rates

TIME	REACTOR LATTICE				BERYLLIUM		REACTOR LATTICE, Be CONTROLLING	
	(kw)	(cal/cm^2-sec)	(gpm)	(ft/sec)	(kw)	(gpm)	(gpm)	(ft/sec)
0 sec	1,950	1.525	850	1.95	350	518	3,570	8.2
1	1,840	1.43			330			
5	1,300	1.01			234			
10	1,120	0.87	488	1.12	201	298	2,050	4.7
30	877	0.68			158			
1 min	715	0.55			128			
2	606	0.47			109			
6	490	0.38			88			
12	416	0.32			74			
30	326	0.25			58			
1 hr	269	0.21	118	0.27	48	72	498	1.13
2	220	0.17			39			
10	129	0.10	56	0.09	23	34	236	0.54
1 day	90	0.07			16			
2	67	0.05			12			
4	45	0.03	20	0.05	8	12	82	0.19

4.6 SHIELDING SUMMARY

The first approach to the design of the biological shield of the Materials Testing Reactor was the comparison of the neutron and γ-ray fluxes incident on the graphite reflector of this reactor with similar fluxes in the Clinton and Hanford reactors.[12] Since experience at Oak Ridge and Hanford had demonstrated the adequacy of the shields on existing reactors, these were used to establish the required thickness of the MTR shield. On this basis, the original design consisted of an 8-in. iron thermal shield surrounded by 9 ft of ordinary concrete. This was estimated to give a γ-ray attenuation of a factor of about 10^{10} and a neutron attenuation of about 10^{12}. In addition, the equivalent shielding above the active lattice was set at 17½ ft of water plus 21 in. of iron.

In order to compensate for voids in the concrete shield due to air ducts, water lines, service facilities, and experimental holes, it was originally proposed to substitute iron slabs or heavy aggregate concrete for the ordinary concrete where necessary. As the detailed design of the shield progressed, however, the required amount of supplementary shielding increased to the point where the design became extremely complicated. For this reason it was decided to use barytes ore, which is substantially heavier than the aggregate used in ordinary concrete, as the aggregate for the entire concrete portion of the shield in order to provide adequate shielding without additional iron slabs and at the same time maintain the given external dimensions of the pile structure. Although the use of barytes aggregate concrete with a density of 3.5 g/cc results in a considerable over-design of certain portions of the shield, the flexibility and simplicity of a homogeneous structure was considered preferable to the complicated design involving iron slabs, iron aggregate, and ordinary concrete.

The fundamental conceptual design of the thermal and biological shield having been established, a comprehensive survey of the adequacy of this shield was carried out using layouts of the specific arrangement of the experimental holes and service facilities as made by the MTR design group. Both theoretical and empirical considerations of shielding were used to estimate neutron and γ-ray intensities throughout the shield. In general, the proposed design was found to be satisfactory except in a few places such as in

the vicinity of the exit water lines. These few places in the shield that were found to be slightly inadequate with the barytes aggregate concrete are protected with additional iron.

The following discussion is divided into three parts. The first part reviews fundamental principles of shielding theory and establishes the basis for the calculations. The second part summarizes the calculations and results pertaining to the main concrete structure, and the final part discusses numerous supplementary shielding problems associated with the design of the reactor structure.

4.6.1 Fundamental Concepts. *Design Tolerances.* In the first discussions of the reactor shield the designers assumed that when γ-ray radiation predominated, the radiation intensity should be 0.01 r per 8 hr. Later the neutron tolerances were established as one-tenth the values suggested by the September, 1949 Chalk River Conference. The permissible neutron dose measured in reps* is less than the γ-ray tolerance in roentgens because of the greater damage ascribed to neutrons. (Complete coverage of this subject is given in Evans'[13] report to the National Research Council.)

For use in calculations it is desirable to express these limiting intensities as fluxes. The flux values chosen are:

6- to 10-Mev neutrons	5 neutrons/cm^2-sec, equivalent to 0.1 mrep/hr
6-Mev γ rays	100 photons/cm^2-sec, equivalent to 1.2 mr/hr

These represent the allowed radiation leakage where one of the components is completely dominant. When both neutrons and γ rays are present, it is necessary to consider the combined effects.

The conservative nature of the choices for the limiting tolerable fluxes is revealed by Figs. 4.6.A and B, which indicate that the choices correspond to very high-energy radiation. Neutrons and γ rays in this energy range comprise only a small fraction of the total radiation to be attenuated.

Attenuation of Penetrating Radiation. The barytes concrete prescribed as the main structural material for the MTR biological shield is described in a report[14] concerned principally with the composition of the concrete together with its structural and handling characteristics.

*rep = roentgen equivalent, physical.

1 rep = 93 ergs/gm absorbed in tissue
$E_{absorbed} = 1.6 \times 10^6 \, \mu(E) \, \phi(E)$ ergs/sec
$\mu(E)$ = Tissue Absorption Cross-Section Fig. A.7.B. - A.7.D.
$\phi(E)$ = γ-Ray Energy Flux ~ Mev/cm²/sec

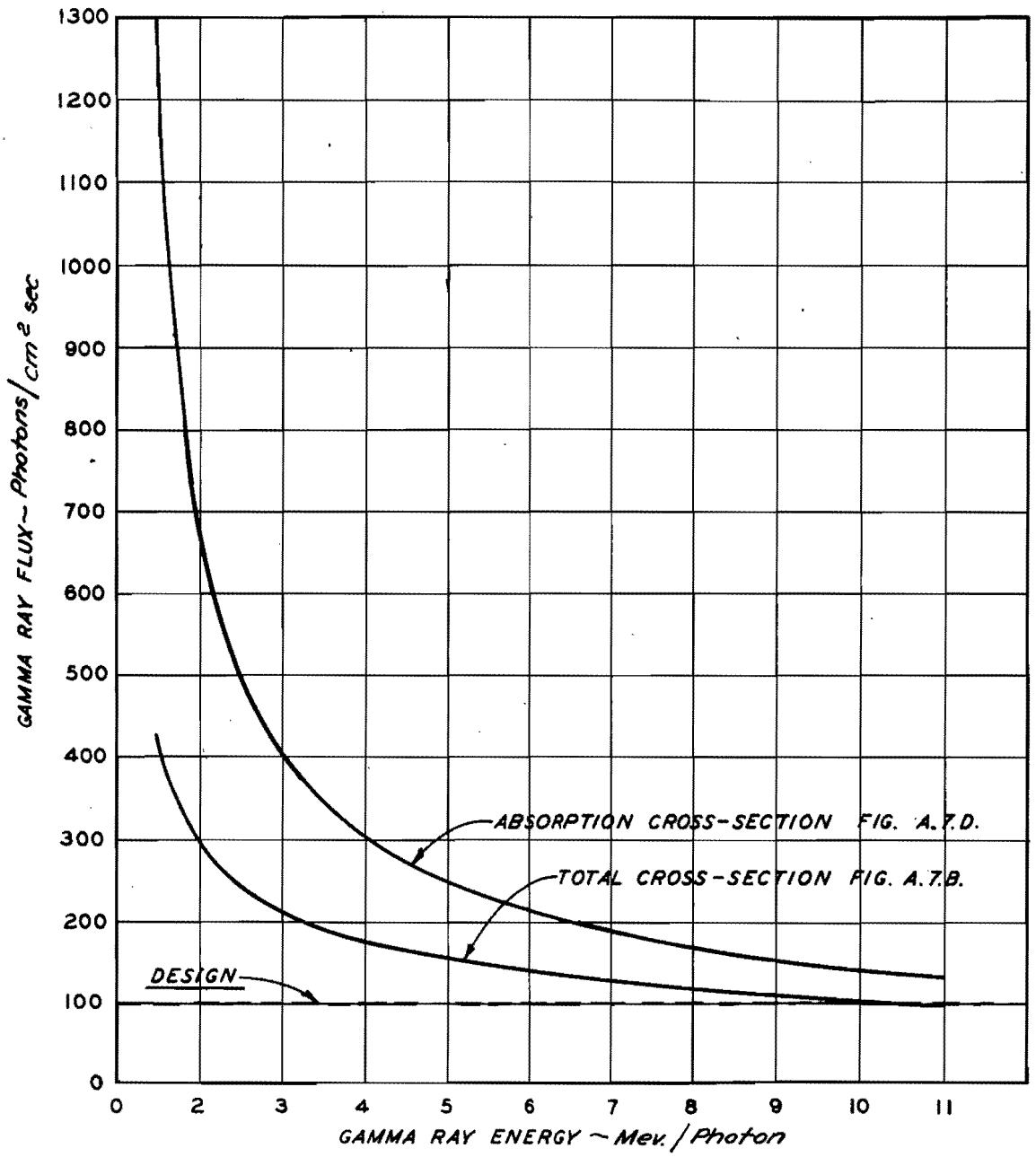

FIG 4.6.A.

PHOTON FLUX AS FUNCTION OF ENERGY
FOR DOSE RATE = 0.01 rep/8hr

DWG. #10520
NOT CLASSIFIED

BASIC:
TOLERANCE = 0.3 rep FOR 40 HR WEEK
NEUTRON RELATIVE BIOLOGICAL EFFECTIVENESS = 10
DOSE CALCULATED BY BURNETT AS PER AEGD-2173
WITH 1 REP = 95 ERGS PER GRAM TISSUE

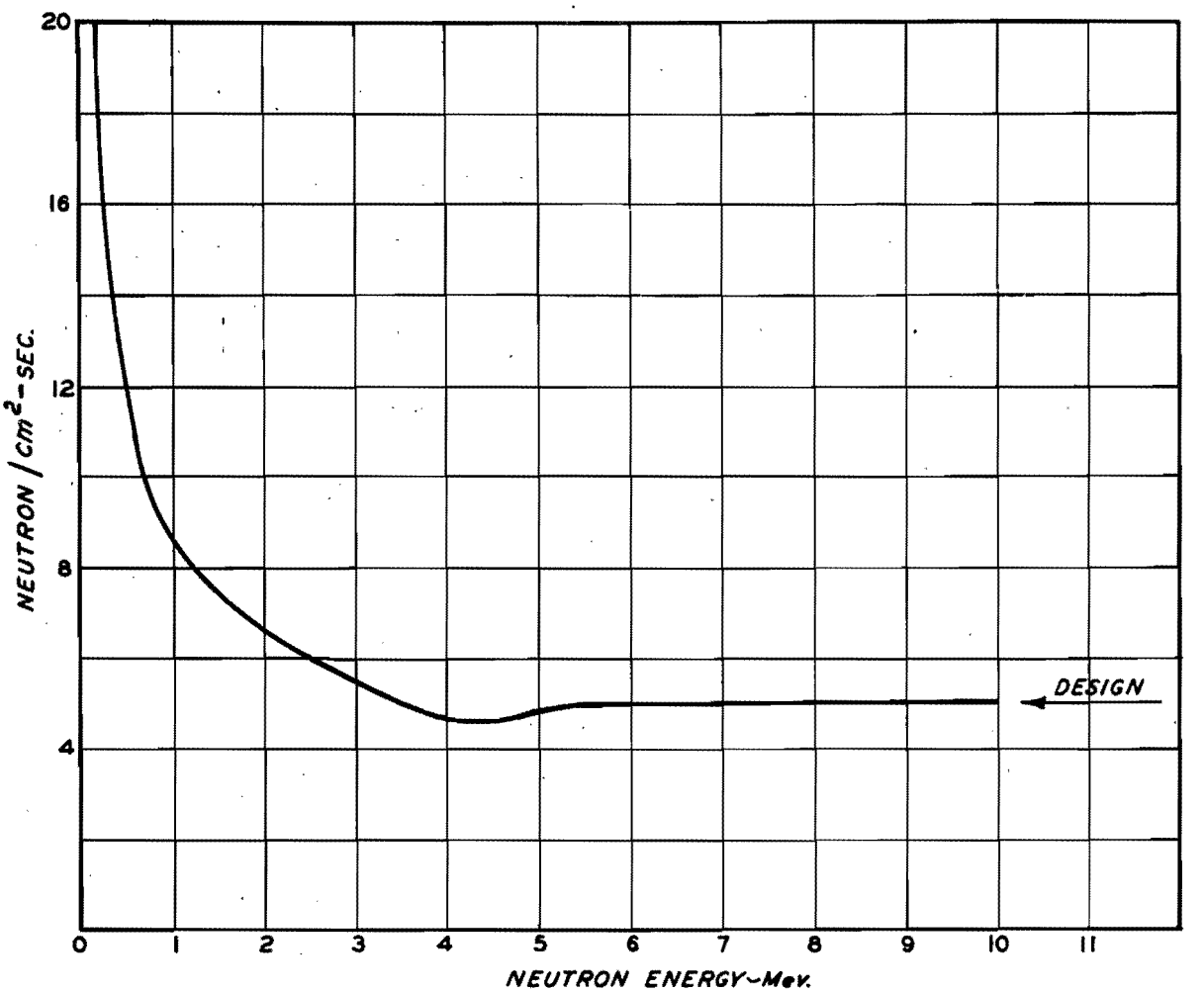

FIG. 4.6.B.
FAST NEUTRON FLUX FOR ONE-TENTH TOLERANCE DOSE

While some properties of barytes concrete have been determined experimentally, its radiation attenuation characteristics have not been investigated extensively. γ-ray attenuation experiments[15,16] using a 6-curie radiocobalt source give results which indicate that the γ-ray attenuation as compared with ordinary concrete varies as the ratio of the densities. The only neutron attenuation data available consist of some measurements in the shield of the British "GLEEP" reactor, which employs a barytes concrete biological shield following a 6-in. iron thermal shield. The available data are discussed in the section on neutron characteristics of barytes concrete.

In the absence of more experimental results it was necessary to estimate the attenuation characteristics of barytes concrete. The procedure used for estimating the neutron relaxation length amounts to an extrapolation of the observations on neutron attenuation in ordinary concrete.

1. Neutron Attenuation. (*a*) Estimate of Neutron Relaxation Length in Barytes Concrete. From experience it is found that a fairly reliable estimate of the neutron relaxation length for a material may be obtained by comparing its total macroscopic cross-section with that of a similar material, e.g., concrete of somewhat similar composition, whose asymptotic relaxation length is known. The Σ_t at an energy of 2 to 8 Mev for the "known" material is taken to be the reciprocal of the observed relaxation length. In order to make these quantities equivalent, it is necessary to assign suitable values of σ_t to one or more dominant constituents of the system. The Σ_t values so determined are then used to compute the Σ_t of the "unknown" material and its relaxation length is taken to be Σ_t^{-1}.

In this instance, inspection of Table 4.6.A reveals that oxygen is atomically predominant in both barytes and ordinary concrete. Therefore adjustment of σ_t for oxygen is indicated. The calculations have been carried out for 5 Mev (Table 4.6.A) and for 1 to 2 Mev (Table 4.6.B), with the former being considered more meaningful. Much of Table 4.6.B has been extracted from a previous report.[17]

The composition of the barytes concrete may be taken as:

Portland cement	517 lb/cu yd
Aggregate	5060
Water	316

TABLE 4.6.A

Total Cross-sections of Portland and Barytes Concretes at 5 Mev

ELEMENT	PORTLAND CONCRETE			BARYTES CONCRETE			
		CURED		AS MIXED		CURED	
	σ_t (barns)	M (milligram-atoms per cc)	$M\sigma_t$ [(barns) x (mg-atoms)/cc]	M (milligram-atoms per cc)	$M\sigma_t$ [(barns) x (mg-atoms)/cc]	M (milligram-atoms per cc)	$M\sigma_t$ [(barns) x (mg-atoms)/cc]
Fe	2.8	0.13	0.36	0.11	0.31	0.11	0.31
H	1.5	4.8	7.2	20.6	31.9	5.17	7.75
O	1.3*	71.8	93.5	71.2	92.6	63.5	82.5
Mg	2.0	0.2	0.4	0.2	0.4	0.2	0.4
Ca	2.0	14.5	29.0	3.4	8.85	3.4	8.85
Si	2.3	1.56	3.6	4.1	9.44	4.1	9.44
Al	2.4	0.44	1.5	0.4	0.96	0.4	0.96
S	2.5	0.06	0.15	12.0	30.0	12.0	30.0
C	1.2	10.8	13.0				
Ba	5.0**			11.9	59.6	11.9	59.6
	Totals		148.7		234.0		199.8
		Σ_t	(0.1487 x 0.602) = 0.0895 cm^{-1}		0.141 cm^{-1}		0.120 cm^{-1}
		Σ_t^{-1}	11.1 cm		7.1 cm		8.2 cm

*Chosen to make Σ_t^{-1} for ordinary concrete be approximately 11 cm. The oxygen cross-section has a minimum at around 5 Mev extending to about this value (ORNL-417).

**No experimental values available. Estimates from formulas in ORNL-433 give σ_t around 5.3 barns at 5 Mev.

TABLE 4.6.B

Total Cross-sections of Ordinary and Barytes Concretes in 1- to 2-Mev Range

ELEMENT	PORTLAND CONCRETE			BARYTES CONCRETE			
		CURED		AS MIXED		CURED	
	σ_t (barns)	M (milligram-atoms per cc)	$M\sigma_t$ [(barns) x (mg-atoms)/cc]	M (milligram-atoms per cc)	$M\sigma_t$ [(barns) x (mg-atoms)/cc]	M (milligram-atoms per cc)	$M\sigma_t$ [(barns) x (mg-atoms)/cc]
Fe	2.8	0.13	0.36	0.11	0.31	0.11	0.31
H	2.5	4.76	11.9	20.6	51.5	5.17	12.9
O	1.2*	71.8	86.2	71.2	85.4	63.5	76.4
Mg	2.2	0.2	0.44	0.2	0.44	0.2	0.44
Ca	2.0	14.5	29.0	3.4	6.8	3.4	6.8
Si	2.8	1.56	4.37	4.1	11.5	4.1	11.5
Al	2.5	0.44	1.1	0.40	1.0	0.40	1.0
S	2.5	0.06	0.15	12.0	30.0	12.0	30.0
C	1.6	10.8	17.3				
Ba	5.0**			11.9	59.5	11.9	59.5
	Total		150.8		246.5		198.9
	Σ_t		$(150.8 \times 10^{-3})(0.602) = 0.0908\ cm^{-1}$		$0.148\ cm^{-1}$		$0.210\ cm^{-1}$
	Σ_t^{-1}		11 cm		6.8 cm		8.3 cm

*This value of σ_t, chosen to make Σ_t^{-1} = 11 cm for ordinary concrete, happens to coincide with a minimum in the oxygen cross-section at about 1.4 Mev (ORNL-417).

**The assignment of σ_t = 5 barns for Ba is a conservative (i.e., low) estimate, more in line with reliable experimental work on other elements. The only known experimental values for Ba are from 6 to 7 barns at energies of 2 to 3 Mev (cited in ORNL-433). The formulas of ORNL-433 give estimates of σ_t = 6.4 barns and 5.8 barns at 1 and 2 Mev, respectively.

where the aggregate is assumed to be 94% $BaSO_4$ and 6% SiO_2 by weight (SiO_2 is the mineral most commonly associated with $BaSO_4$ in barytes ore). A "cured" cement contains the same amounts of cement and aggregate but has the water reduced to 78 lb/cu yd, which is the amount required to hydrate the cement. The Σ_t^{-1} values of 7.1 and 8.2 cm, respectively, given in Table 4.6.A, indicate the range in which the observed relaxation lengths may be expected to fall. It is of interest to note that the maximum Σ_t^{-1} at 1 to 2 Mev (Table 4.6.B) is 8.3 cm.

The measurements of neutron attenuation in barytes concrete mentioned previously were originally transmitted in a letter from the U.K. Scientific Mission to the U.S. Atomic Energy Commission.[18] The barytes concrete for the biological shield of GLEEP was of a slightly different "recipe" from the ORNL mix but yielded a material of density 3.5 g/cc. The experimental results as transmitted are presented in Fig. 4.6.C. It is of interest to note that the curves *A* and *B* for neutron measurements in barytes concrete exhibit relaxation lengths of 7.2 and 8.1 cm, respectively.

In view of the calculation which was outlined, a neutron relaxation length of 8.2 cm was used in the analysis of the shield performance.

(*b*) The Effect of Iron on Fast Neutrons. The introduction of a layer of iron into a neutron shield principally results in the attenuation of neutrons above 1 Mev by inelastic scattering to lower energies. As a result of this process, the neutron spectrum is shifted toward lower energy, and the neutrons emerging from the iron can be rapidly attenuated by water, concrete, or some other good shielding material for low-energy neutrons.

These effects are illustrated in the sketch on p. 4.46 which is based on some ORNL experiments.[19] Fission neutrons enter the iron from the left. The observed relaxation length of about 9 cm in the iron is probably due to slowing down and absorption of neutrons in the low-energy part of the spectrum. The neutrons which emerge from the iron are predominantly grouped near the "window" in the iron cross-section which occurs around 1 Mev.

[redacted]

Drawing # 9647

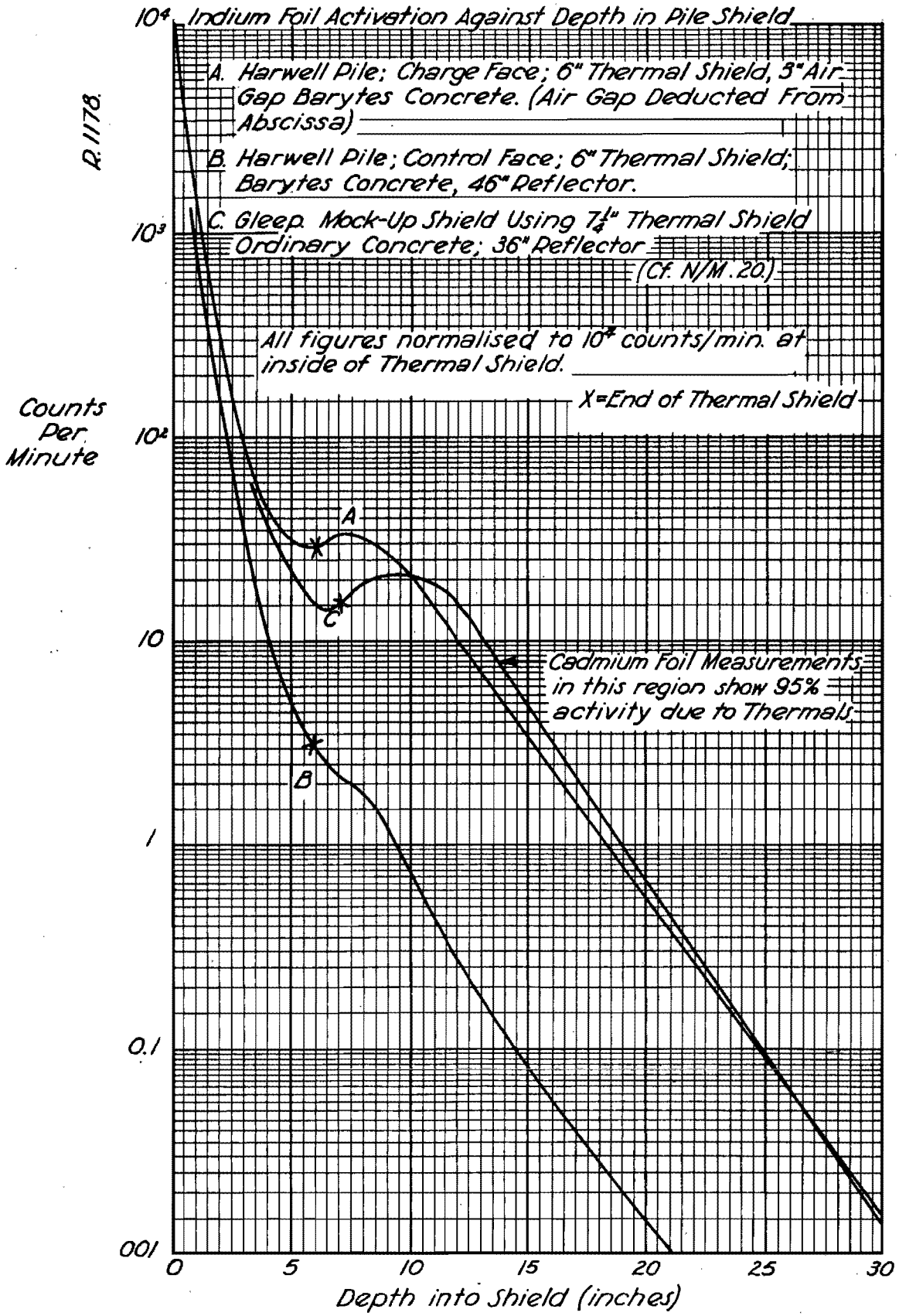

FIG. 4.6.C.

[redacted]

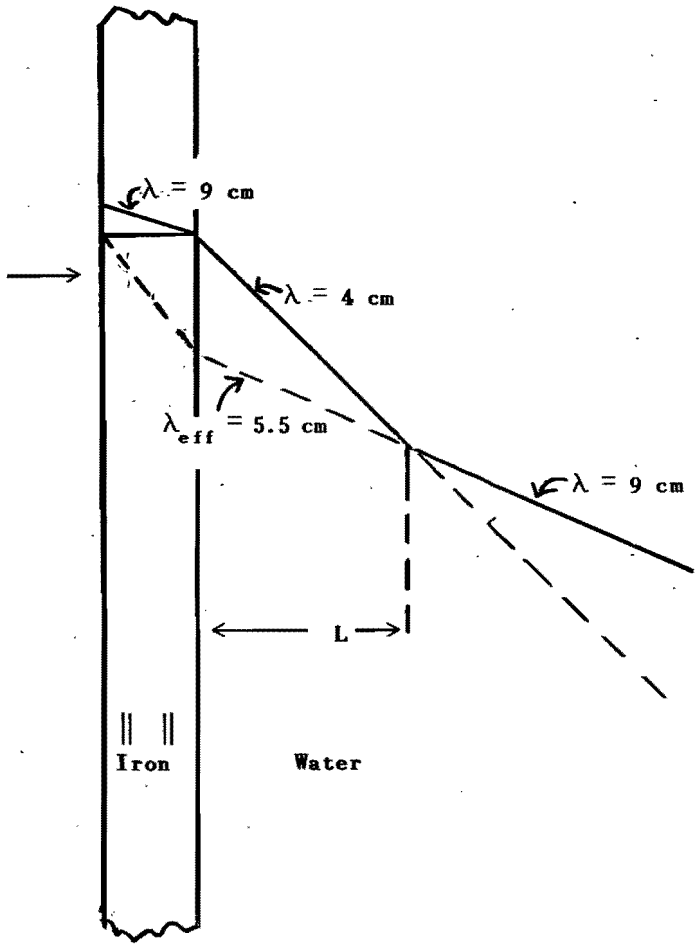

The observed 4-cm relaxation length reflects the rapid attenuation of these neutrons. Finally, the 9-cm attenuation length in H_2O, characteristic of the most penetrating part of the incident spectrum, is observed. The distance L at which this occurs increases with the thickness of the iron layer. In these experiments, it appears to be about 70 cm for iron 7 to 10 in. thick. In barytes concrete L will be roughly the same.

2. Gamma-Ray Attenuation and Absorption. The attenuation of gamma radiation follows an approximately exponential law,

$$\phi_E \approx \phi_0 B e^{-b} \tag{1}$$

where B is the so-called "build-up factor"* and b is the thickness of the shield measured in relaxation lengths. ϕ_E is the energy flux of radiation measured conveniently as Mev/cm^2-sec. The exact form of the equation depends on the geometry of the particular problem.

(*a*) Absorption Coefficients. To calculate b in Eq. (1), we write

$$b = \mu_1 r_1 + \mu_2 r_2 + \mu_3 r_3 + \ldots \tag{1a}$$

*The "build-up" factor pertains to the amount of radiation which penetrates a shield as compared with the amount predicted on the basis of simple exponential attenuation. For γ rays this exponential attenuation employs total cross-sections (see Appendix 7) which includes scattering in addition to energy absorption. The γ radiation emerging from a thick shield contains a scattered component many times greater than the component which penetrates the shield directly. The factor describing this excess for a given system is the B value.

where r_1, r_2, r_3 are the various thicknesses, in centimeters, of shield material measured along a line from the gamma source to the observer. μ_1, μ_2, μ_3 are the γ-ray absorption coefficients, in cm^{-1}, of the various shield materials. The values of μ for various elements are given in Figs. A7 and B.

The γ rays to be attenuated by a reactor shield are almost entirely of energy 8 Mev or lower. Very frequently the exact energy of the radiation is not known. For example, suppose that it is desired to attenuate 8-Mev γ's with water followed by lead. A large fraction of the γ rays is reduced in energy by scattering in the water. After the radiation penetrates the water, most of the γ rays may have energies in the range of 3 to 4 Mev, which corresponds to the minimum in the absorption coefficient of lead. Experience has shown that it is not unduly pessimistic in most cases to assume the minimum value of the absorption coefficient for all calculations.

(*b*) Build-up Factor. The values of B are determined usually by theoretical considerations of scattering of γ-ray radiation in the shield. Unfortunately there are uncertainties in the theoretical treatments and no consistent equations or values of B are available at present. It is important to note, however, that the exponential e^{-b} is the dominating factor in the attenuation equation. For example, for a 20-in. lead shield and 3-Mev γ rays, $e^{-b} \approx 10^{-10}$. Under these conditions $B \approx 10$, so that $\phi_E \approx \phi_0 10^{-9}$. If 10^{-10} attenuation is required, it is necessary only to increase the shield thickness to 22 in. In view of the slow variation of ϕ_E with the value of B, the designer should survey the various theoretical values of B and select one which appears to result in a safe shield design. A very simple approximation which is always conservative is to assume $B = b$; i.e., the value of the build-up is numerically equal to the number of relaxation lengths. This approximation was employed in the design of the concrete shield.

(*c*) γ-Ray Characteristics of Barytes Concrete. Although the γ-ray attenuation properties of barytes concrete have not been the subject of extensive experimentation, it is expected that the extrapolation of the data for ordinary concrete may be done with confidence. The usual design value for the asymptotic γ-ray relaxation length in ordinary concrete is 15 cm.[20] The barytes concrete prescribed for the shield has a density of 3.5 g/cc. The relaxation length used in the shield analysis has been extrapolated from the accepted value for ordinary concrete simply by postulating that the relaxation length varies inversely as the mass density. On this basis, the design relaxation length for γ rays in barytes concrete is 10 cm.

4.6.2 Concrete Shield Design. The general configuration of the biological shield was laid out on the basis of above cited (Fig. 4.6.1) tolerance limits. However, it was necessary to analyze the resulting shield to be sure that the leakage radiation had been reduced to at least design tolerance. In this analysis it was first attempted to determine whether or not the specified overall thickness of shielding was adequate. Secondly, a number of specific locations in the structure were studied where it was apparent that the shield effectiveness had been impaired by the detail design requirements. This section is concerned with the problem of the overall shield analysis.

Attenuation of Radiations. 1. Primary γ-Ray Attenuation. In checking a shield it is necessary to treat separately the γ rays and the neutrons which are incident on the inner face of the concrete. The disposition of the γ-ray problem was accomplished in the following manner:

The heat production in the thermal shield due to (1) the absorption of capture γ rays formed in the iron and in the graphite, and (2) the absorption of γ rays from the core has been reported in detail.[21,22] These reports give a value of 6.7×10^{-16} watts/cc produced at the outer face of the iron per unit thermal neutron flux at the inner face. It is estimated that less than half of this is due to γ rays from the core.

Since $\mu = 0.235\ \text{cm}^{-1}$ for 8-Mev γ rays in iron (the minimum value according to ORNL-421), the γ-ray flux at the outer face of the thermal shield is

$$\phi_E(0) = \frac{\text{nv} \times 6.7 \times 10^{-16}}{1.6 \times 10^{-13}} \times \frac{1}{0.235} \qquad (2)$$

or

$$\phi_E(0) = 0.018\ \text{nv} \qquad \text{Mev/cm}^2\text{-sec}$$

This states that at any point on the outside of the thermal shield the γ-ray energy flux is just 0.018 times the neutron flux at the corresponding point on the inside face of the thermal shield. An examination of the calculations shows that the variation of the neutron flux in the immediate vicinity of the point of interest has a negligible effect on the value of the γ-ray flux.

Assuming that the emergent γ rays have energies between 3 and 8 Mev, the upper limit for the emergent γ-ray flux is

$$\phi(0) = 0.006 \text{ nv} \qquad \gamma \text{ rays/cm}^2\text{-sec} \tag{2a}$$

A face of the iron thermal shield may be considered to be a slab surface with a uniform volume source of γ rays of strength Q_v γ rays/cc-sec. The resultant γ-ray energy flux in the concrete is described by the expression[23]

$$\phi_E = B\frac{Q_v E}{2\mu_s}\left[F_1(b_1) - F_1(b_3)\right] \qquad \text{Mev/cm}^2\text{-sec} \tag{3}$$

where

b_1 = concrete thickness in relaxation lengths.

$b_3 = b_1$ + thickness of iron in relaxation lengths.

The iron is sufficiently thick that the second F_1 term is negligible. At the steel concrete interface $b_1 = 0$, $F_1(0) = 1$, $B = 1$, and

$$\phi_E(0) = \frac{Q_v E}{2\mu_s} \qquad \text{Mev/cm}^2\text{-sec}$$

Hence (dropping the subscript on b_1),

$$\phi_E = B\phi_E(0)F_1(b) \qquad \text{Mev/cm}^2\text{-sec}$$

When the number of relaxation lengths measured through the shield is large,

$$F_1(b) \approx \frac{e^{-b}}{b}$$

Furthermore, as noted previously, we assume that $B \approx b$.

Thus, in general, for a thick shield,

$$\phi_E \approx \phi_E(0)\ e^{-b} \qquad \text{Mev/cm}^2\text{-sec} \tag{4}$$

or

$$\phi \approx \phi(0)\ e^{-b} \qquad \gamma \text{ rays/cm}^2\text{-sec} \tag{4a}$$

The application of the foregoing methods to the detailed analysis of the shield is a straightforward matter if conservative values for the incident neutron and γ-ray fluxes can be chosen. For γ rays the analysis was based on thermal neutron flux maps.[21,22] The shield was checked at a large number of points by the method described. For convenience, a table of representative attenuations is included at the end of this section. It is to be noted that the calculated fluxes are overestimates as compared with the experiments performed on the Mock-Up.[24]

Previously it was shown [Eq. (2a)] that

$$\phi(0) = 0.006 \text{ nv}$$

Hence, the value of the γ-ray energy flux at the outside surface of the concrete is

$$\phi = 0.006 \text{ nv } e^{-b} \qquad \gamma \text{ rays/cm}^2\text{-sec} \tag{5}$$

This formula provided the basis for checking the shield. The procedure is as follows: On a layout drawing, e.g., Fig. 4.6.J (p. 4.79), a straight line is constructed from some point on the outer surface of the thermal shield to the outer surface of the concrete. The emergent γ-ray flux, ϕ, is calculated by setting nv equal to the thermal-neutron flux at the graphite-iron interface directly inside the point where the line touches the thermal shield; b is taken to be the path length in relaxation lengths through the concrete — and whatever other material may be traversed — to the outer surface [Eq. (1a)].

2. Neutron Attenuation. Although the neutron attenuation problem is much more difficult to solve than the corresponding γ-ray problem, it is possible to adopt a "recipe" which will yield conservative results. The neutrons which enter the concrete are born in the reactor core with energies corresponding to the familiar fission spectrum. In the process of leaking out of the core and successively penetrating the beryllium and graphite reflectors, the spectrum changes to one in which most of the neutrons are grouped near thermal energies with the remainder in some kind of "tail" which extends to very high energies. The effect of the iron thermal shield on these high-energy neutrons has been described previously. Because of the large capture cross-section, the thermal neutrons which diffuse through the iron are attenuated rapidly in the concrete. However, the degraded but only slightly attenuated fast neutrons must be slowed down and captured in the concrete. Furthermore, the secondary γ rays from these neutron captures must be reduced to tolerance by the shield.

In the recipe adopted for treatment of the fast-neutron attenuation, it is assumed that all fast neutrons entering the concrete are captured after penetrating the concrete by a distance equal to the "age displacement." The secondary γ rays so formed are then postulated to all flow outward with the estimated 10 cm relaxation length. The required shielding is calculated on the basis that these γ rays and the neutrons are to be attenuated to tolerance. It can be shown that this is a more conservative procedure than that of considering an exponentially distributed source of capture γ rays from the absorption of the neutrons in the shield.[20]

The "age displacement" is readily derived, and previous literature[31] gives the result

$$\phi_{th}(Z) \approx \exp \frac{-(Z-\frac{\tau}{\lambda})}{\lambda} \qquad (6)$$

Thus the thermal neutrons are also distributed exponentially. However, they have been "displaced" to a larger value of Z by the distance τ/λ, and this is called the "age displacement."

It is reported* that τ for ordinary concrete is about 350 cm^2 and this value has been employed for barytes concrete. Using λ = 11 cm, the age displacement is τ/λ = 31.8 cm. For barytes concrete this displacement was rounded off to 1 ft for use in the calculation of required shield thickness.

No clear-cut method for estimating the neutron current leaving the thermal shield was established analytically. Therefore, the final analysis of the concrete with respect to neutron effects was held in abeyance until certain experimental data were available from the Mock-Up. These data are principally measurements of thermal-neutron flux and of the cadmium ratios at various points in the reactor.

In addition, there was a special experiment designed to establish empirically the total neutron leakage through 8 in. of steel. In this experiment steel bricks were placed in a stack 8 in. thick and 4 ft square. This stack was erected next to the outside surface of the graphite. The steel in turn was backed by a 21-in.-thick stack of paraffin also 4 ft square in the transverse dimensions. Bare and cadmium-covered indium foils placed in the paraffin were activated by the neutrons which penetrated the steel. Complete details of the experiments and the interpretation of the reduced data have been reported elsewhere.[25,26]

This single measurement of the neutron current leaving the thermal shield has been the basis for estimating the current leaving all parts of the shield. The additional data employed in extrapolating the results of this experiment were the thermal fluxes and cadmium ratios at the outer surface of the graphite.

The reasoning employed is as follows:

1. It is observed that the presence of the iron changes the thermal flux at the outer surface of the graphite by not more than 20%. For shielding calculations, the flux may be considered to be unaffected by the presence of the iron.

2. The cadmium ratios on the outer surface of the graphite are very insensitive to changes in distance from the core. This is interpreted to indicate that the spectrum at all positions on the outside of the graphite is nearly at equilibrium.

3. With these data it seems reasonable to postulate that (*a*) the observed thermal flux at the surface of the graphite is proportional to the total flux there, and (*b*) the cadmium ratios at this location are proportional to the fraction of fast neutrons (of the iron-penetrating variety) in the spectrum.

*Private communication from H. P. Sleeper.

In this system the current penetrating the iron is proportional to the fast-neutron flux at the iron-graphite interface. For a slowly varying spectrum, ϕ_f is nearly proportional to the total flux, ϕ_t. To correct for the variations in the spectrum, ϕ_f/ϕ_t is considered to vary inversely as the observed cadmium ratios ρ_{Cd}. Thus the leakage current J_l varies as follows:

$$J_l \approx \phi_f \approx \frac{\phi_{tot}}{\rho_{Cd}} \approx \frac{\phi_{th}}{\rho_{Cd}}$$

Thus the formula used for estimating the neutron leakage current out of the thermal shield is

$$(J_l)_i = J_l \left[\frac{\rho_{Cd}}{\phi_{th}}\right]_{exp} \left[\frac{\phi_{th}}{\rho_{Cd}}\right]$$

where

ϕ_{th} = thermal flux at inner surface of steel, nv/cm^2-sec.

ρ_{Cd} = ratio of activation of bare and cadmium-covered foils.

J_l = leakage current, neutrons/cm^2-sec, experimentally measured.

Subscript "exp" refers to experiment.

Subscript i refers to point under consideration.

Substituting the experimental values,[25] this equation becomes

$$(J_l)_i = 65 \times \frac{1700}{7.9 \times 10^6} \left[\frac{\phi_{th}}{\rho_{Cd}}\right]_i$$

$$(J_l)_i = 1.3 \times 10^{-2} \left[\frac{\phi_{th}}{\rho_{Cd}}\right]_i \qquad (7)$$

Variation of Required Concrete Thickness. The required thickness of the concrete varies from point to point of the thermal shield for two reasons. First, the shielding required opposite the edges and corners of the thermal

shield is reduced by a geometric factor below that required opposite the center of a face of the thermal shield. Secondly, the γ-ray flux leaving the edges and corners of the thermal shield is lower than that leaving a face because of the reduction of the thermal-neutron flux at the inner face of the thermal shield at these locations. The manner in which the minimum design thickness varies is shown in Fig. 4.6.D. The thickness required opposite the center of a face was calculated and this was established as the required thickness opposite the entire face. The minimum shielding required opposite a vertical edge is shown in the figure as a quarter cylinder whose radius equals the thickness required opposite the center of the edge. The shield required opposite a top corner is shown as an octant of a sphere. At points showing a sharp discontinuity in the required shield thickness the greater thickness was used in design.

In order to determine the geometric factor, consider the accompanying sketch, Fig. 4.6.E. This shows a thickness t of concrete and a set of annular rings drawn on the surface of the thermal shield. The thermal shield may be assumed to be a surface source which emits radiation having a cosine distribution. The γ-ray flux at point P, which is a distance a from the surface element of area $r\ d\theta\ dr$ emitting $\phi(0)$ γ's/cm^2-sec with a cosine distribution is given by

$$\phi = \int_{\phi=0}^{\pi} \int_{r=0}^{\infty} B\ \frac{\phi(0)\ \cos\theta}{\pi a^2}\ e^{-\mu a}\ r \int dr \int d\phi \qquad \gamma \text{ rays/cm}^2\text{-sec}$$

where it is assumed that the face of the thermal shield is infinite in extent. Upon integration this yields

$$\phi = 2B\ \phi(0)\ F_1(b)$$

where $b = \mu t$ and $F_1(b) = b \int_b^{\infty} \frac{e^{-y}\ dy}{y^2}$ (see Appendix 7).

DWG # 10526 [redacted]

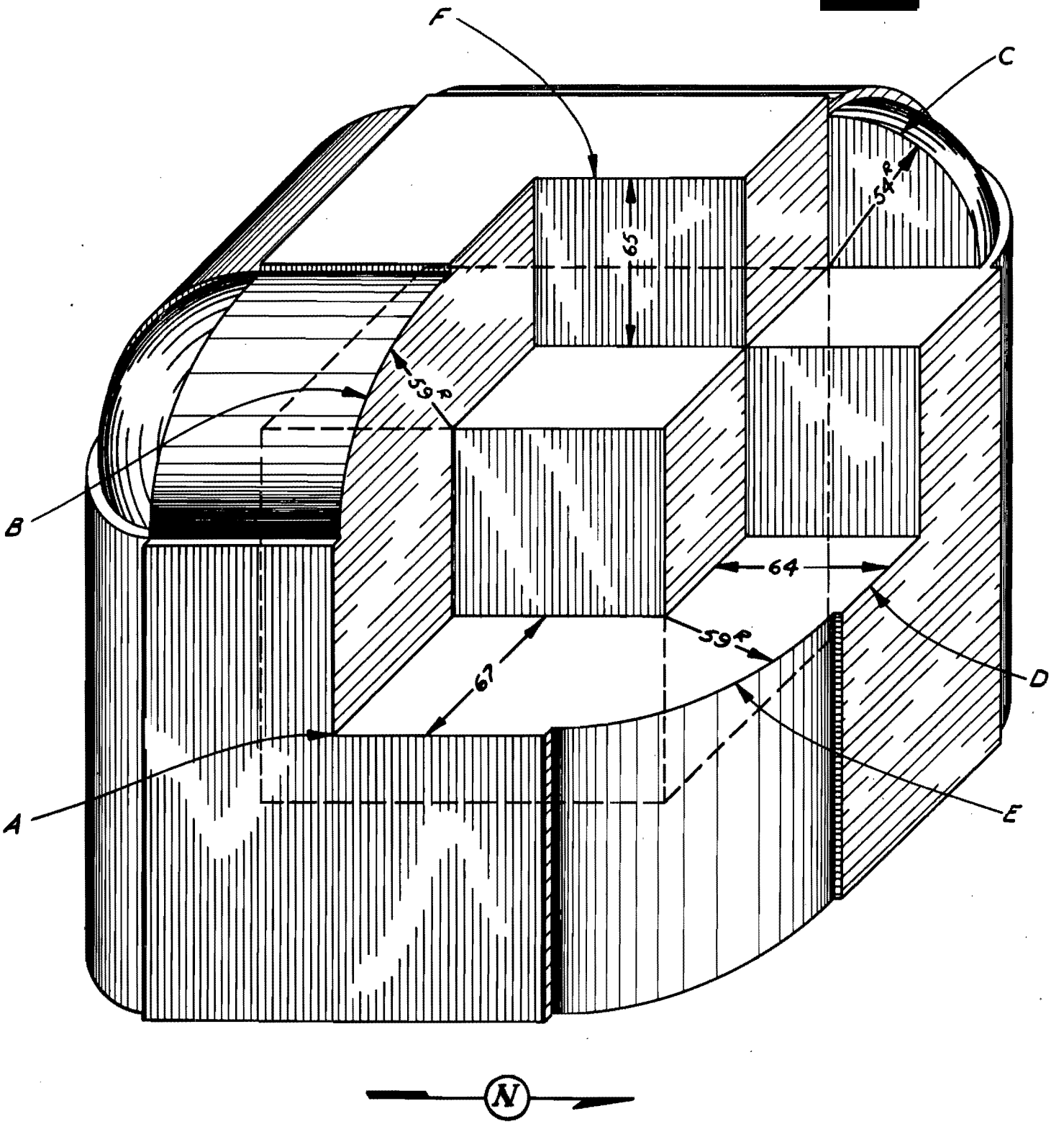

FIG-4.6 D

PICTORIAL REPRESENTATION OF REQUIRED SHIELD THICKNESSES

This is just twice the value given previously using the assumption that the thermal shield is an infinite slab source instead of an infinite plane source with a cosine distribution. The calculations are considered sufficiently conservative that the factor of 2 is neglected. Thus after using approximations for B and $F_1(b)$ as shown previously, the γ flux at P is, as given in Eq. (4a),

$$\phi = \phi(0)\ e^{-b} \qquad \gamma \text{ rays/cm}^2\text{-sec}$$

Actually the thermal shield is not infinite in extent. However, it should be observed in Fig. 4.6.E that as the radius r increases, the path length a through the concrete increases and consequently the contribution of radiation from the outlying surface elements decreases. Graphical integrations have shown that with the concrete thicknesses to be used, the only significant amount of radiation arriving at a point P on the surface of the concrete originates in a circle of radius $r = 4$ ft on the surface of the thermal shield. Therefore a negligible error is introduced by the assumption of an infinite surface for the thermal shield.

Calculation of Shield Thicknesses. The foregoing design procedures and tolerances have been used to tabulate the required thickness of barytes concrete in various regions of the shield. Table 4.6.C presents the results of thickness calculations together with an explanation. As an example, the attenuation opposite the center of the vertical edges, E, is discussed in detail.

According to the argument earlier in this section and with reference to Fig. 4.6.D, the geometrical factor is ½. Preliminary calculations[28] led to an estimate of a thermal flux of 5×10^{10} neutrons/cm^2-sec at the graphite-steel interface. Although this figure was supported by early experiments on the MTR Mock-Up, a flux of 10^{11} was employed in design as a conservative figure. Equation (2a) gives for the primary γ-ray flux emerging from the thermal shield,

$$\phi(0) = 0.006\ nv_{th} = 6 \times 10^8 \qquad \gamma \text{ rays/cm}^2\text{-sec}$$

DWG. #10525
NOT CLASSIFIED

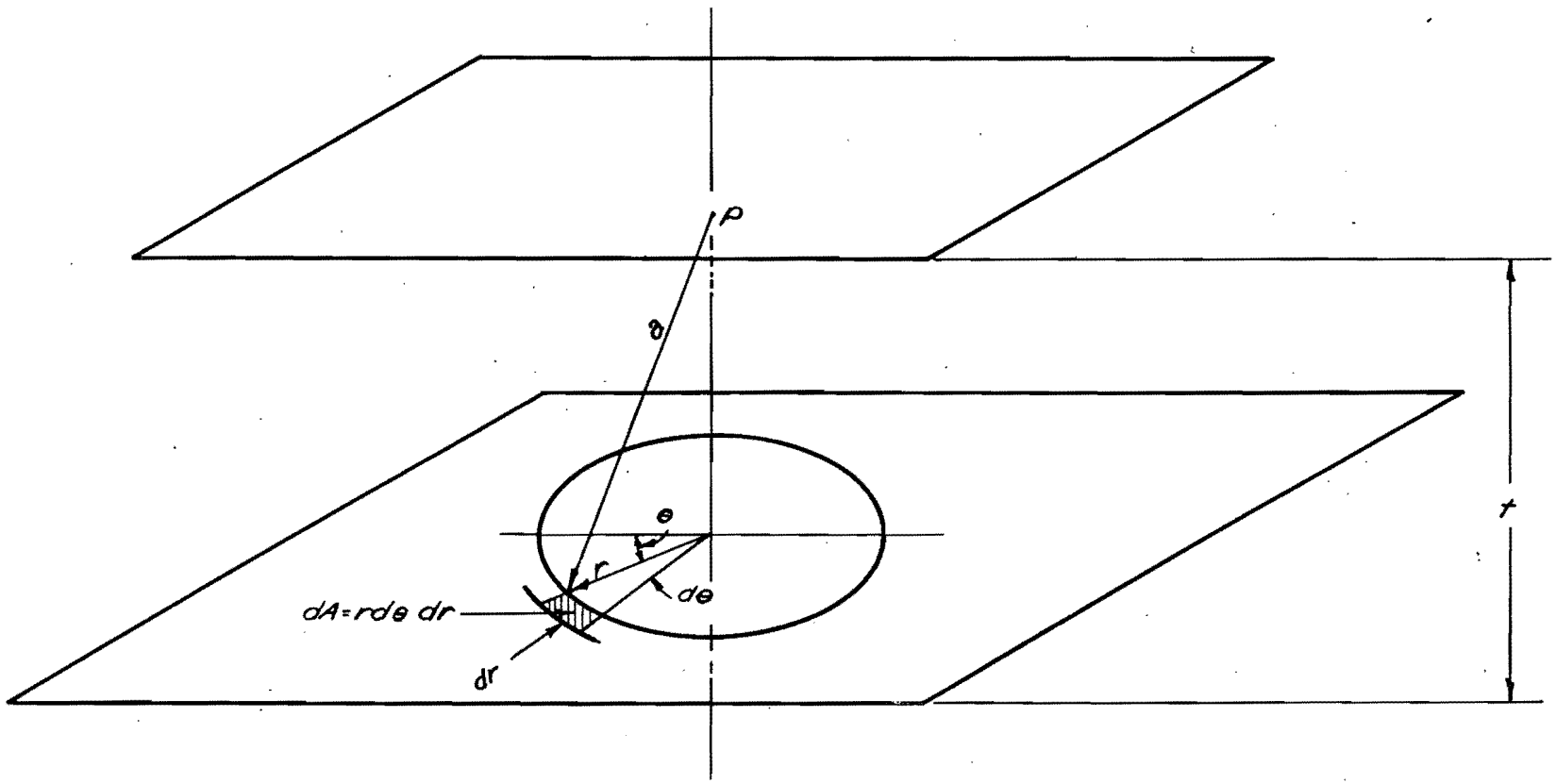

FIG. 4.6.E.

GEOMETRIC FACTOR ILLUSTRATION

TABLE 4.6.C

Required Biological Shield Thickness

Position	Geometrical Factor	nv_{th} Calculated (n/cm^2-sec)	nv_{th} Experimental (n/cm^2-sec)	nv_{th} Design (n/cm^2-sec)	γ-Ray Flux Emerging from Thermal Shield (γ rays/cm^2-sec)	Cd Ratio for Design	Neutron Leakage Current Emerging from Thermal Shield (n/cm^2-sec)	Shield Thickness Beyond 1 in. to Attenuate Concrete Capture γ Rays (in.)	Total Shield Thickness to Attenuate Capture Concrete γ Rays (in.)	Total Shield Thickness Required to Attenuate γ Rays Emerging from Thermal Shield (in.)	Total Shield Thickness Required to Attenuate Neutron Leakage Current (in.)
(1)	(2)	(3)	(4)	(5)	(6)	(7)	(8)	(9)	(10)	(11)	(12)
A. Center of N-S vertical faces	1	4×10^{11}	3×10^{11}	4×10^{11}	2.4×10^{9}	900	5.8×10^{6}	44	56	67.2	45
B. Center of top horizontal edges	½	0.5×10^{11}	0.5×10^{11}	1×10^{11}	0.6×10^{9}	1000	1.3×10^{6}	37.2	49.2	59	40.5
C. Top corners	¼	0.25×10^{11}	0.1×10^{11}	0.5×10^{11}	0.3×10^{9}	1000	0.65×10^{6}	35	47	54	38
D. Center E-W vertical faces	1	2×10^{11}	2.5×10^{11}	2×10^{11}	1.2×10^{9}	1000	2.6×10^{6}	40.5	52.5	64	42.5
E. Vertical edges at center plane	½	0.5×10^{11}	0.5×10^{11}	1×10^{11}	0.6×10^{9}	1000	1.3×10^{6}	37.2	49.2	59	40.5
F. Top face	1	2.5×10^{11}	0.7×10^{11}	2×10^{11}	1.2×10^{9}	1000	2.6×10^{6}	40.5	52.5	65	42.5
G. Bottom face	1	6×10^{11}	2×10^{11}	3×10^{11}	1.8×10^{9}	300	3.9×10^{6}	41.5	53.5	66	43.5

(1) Letters A-G refer to Fig. 4.6.G.

(2) See page 4.53.

(3) See references 27 and 28.

(4) Deduced from preliminary results of MTR Mock-Up operation.[30]

(5) Conservative value chosen for design calculations.

(6) Calculated from Eq. (2a) in text.

(7) Uncertainties in reported Cd ratios due to low saturated activities from Mock-Up experiments led to adoption of 1000 as maximum value for ρ_{Cd}.

(8) Calculated from Eq. (7) in text.

(9) Attenuation to 100 γ rays/cm^2-sec after converting neutrons in column 8 to γ rays.

(10) Values in column 9 plus 12 in.; evaluated with the aid of Fig. 4.6.H.

(11) Attenuations of values in column 6 to 100 γ rays/cm^2-sec; evaluated with the aid of Fig. 4.6.H.

(12) Attenuation of values in column 8 to 5 n/cm^2-sec; evaluated with the aid of Fig. 4.6.H.

The calculation of the neutron current depends on the choice of the cadmium ratio as discussed earlier in this section. Although examination of the Mock-Up experimental results indicates values ranging from 1200 to 2000 at this distance from the core, a value of 1000 is used for design in an effort again to be conservative. From Eq. (7),

$$J_l = 0.013 \frac{nv_{th}}{\rho_{Cd}} = 1.3 \times 10^6$$

The attenuations required can now be calculated. For the primary γ rays, the attenuation factor is

$$\frac{100}{\frac{1}{2} \times 6 \times 10^8} = 3.3 \times 10^{-7}$$

where 100 γ rays/cm^2-sec is the tolerance dosage. This factor, by Fig. 4.6.F, calls for about 59 in. of material equivalent to barytes concrete (λ = 10 cm). The conversion of neutrons to capture γ rays at the 1-ft displacement distance into the concrete requires attenuation by a factor of

$$\frac{100}{1.3 \times 10^6} = 7.7 \times 10^{-5}$$

which is equivalent to approximately 37 in. of barytes concrete. Adding 12 in. to this gives a total thickness of 49 in. of barytes concrete required outside the thermal shield to attenuate these γ rays. Finally, the neutron attenuation proper can be checked. This requires a reduction factor of

$$\frac{5}{1.3 \times 10^6} = 3.85 \times 10^{-6}$$

where 5 neutrons/cm^2-sec is the tolerance dosage. This corresponds to 40.5 in. of barytes concrete.

According to these calculations, the attenuation requirements of the γ rays are completely dominant. This conclusion is most readily visualized by

DWG. #10418
NOT CLASSIFIED

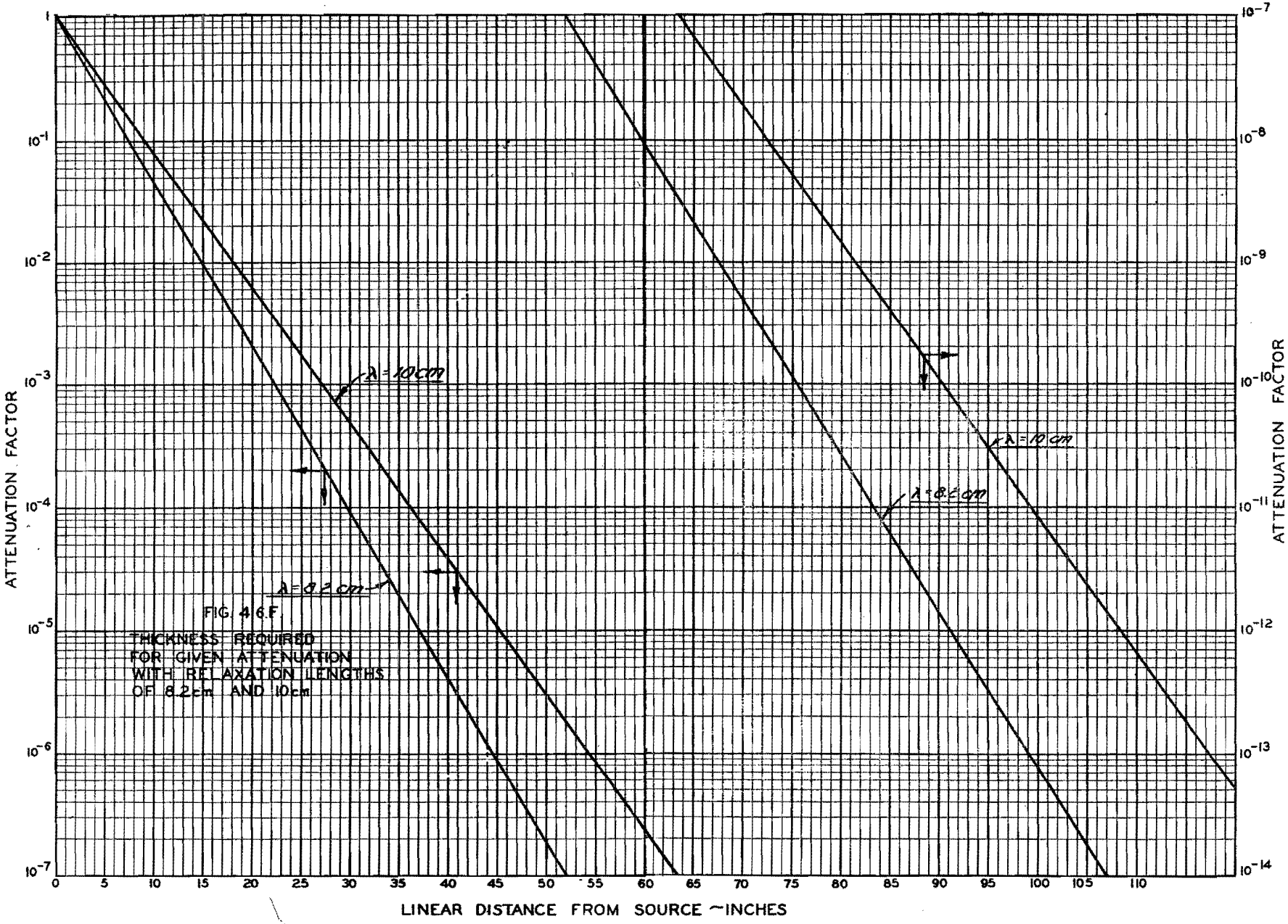

FIG. 4.6.F
THICKNESS REQUIRED
FOR GIVEN ATTENUATION
WITH RELAXATION LENGTHS
OF 8.2cm AND 10cm

reference to a graph such as Fig. 4.6.G. The thermal neutrons at the graphite-steel interface are clearly reduced to a negligible amount by absorption in the steel. The neutrons which penetrate the steel, and their concomitant secondary γ rays, are also negligible in comparison with the primary γ rays leaving the thermal shield. The concrete thicknesses shown are for the most unfavorable locations in the corner regions (Figs. 4.6.H and I). Although the concrete alone is not quite sufficient to reduce these γ rays to tolerance in one instance, the iron walls of the exit air duct are more than sufficient to complete the required attenuation. From Figs. 4.6.G and H the design thickness may be compared with the actual thickness of the concrete; some representative relatively weak locations in the shield are indicated.

4.6.3 Supplementary Shielding Problems. In addition to the most important problem of determining the adequacy of the concrete portion of the biological shield, there are a number of other shielding problems relative to the design of the MTR and associated facilities. These are listed as follows:

1. Shielding requirements of top and bottom plugs.
2. Shielding of inlet and exit water lines.
3. Thermal column shielding.
4. Radiation leakage through ducts in reactor structure.
5. Design of experimental hole plugs.
6. Shielding of external facilities.
7. Shielding requirements for handling active plugs, beryllium, and fuel assemblies.

Details of calculations and design considerations have been issued in various memoranda. These are reviewed below for the purpose of presenting a coherent picture of the shielding requirements of the MTR.

Shielding Requirements of the Top and Bottom Plugs.[34-40] 1. Top Plug Requirements. The shielding of radiation above the active lattice is accomplished by the water in the reactor tank plus the top plug. The depth of water in the reactor tank is adjusted to provide adequate protection after shutdown of the reactor and after the top plug has been removed. Thus the proper design of this portion of the shield depends on the radiation after shutdown as well as during operation of the reactor. The original design established the requirements to be 17½ ft of water plus a 21-in. iron plug. Actually, however, the plug was made hollow with provision for filling it up

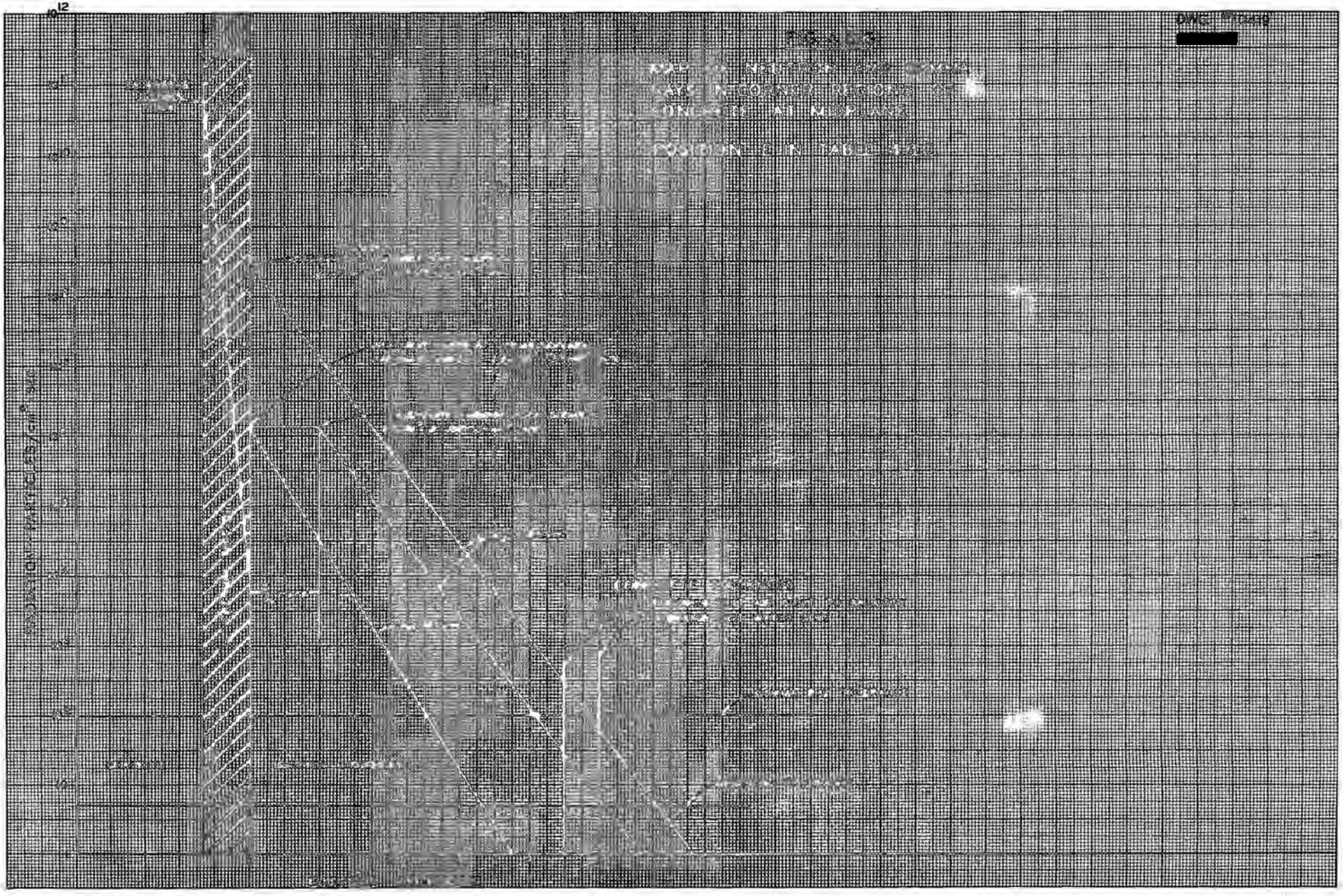
DWG. #10419
FIG. 4.63
MAP OF NEUTRON FLUX
AT INCORNER REGIONS OF
ONE-TIE AT MIDPLANE
POSITION 8 IN TABLE 4.6
10^{12}
NEUTRON FLUX, NEUTRONS/cm² sec

DWG. # 10421 [redacted]

LINE	IRON	WATER	BARYTES CONCRETE	TOTAL EQUIV CONCRETE	REQUIRED CONCRETE THICKNESS TABLE III
	IN.	IN.	IN.	IN.	IN.
1.	2	22	71	85	67
2	12	22	33	70	67
3	11	–	45	71	59
4	2	–	66	71	67

REFERENCE DRAWING

BK 3150-502-1

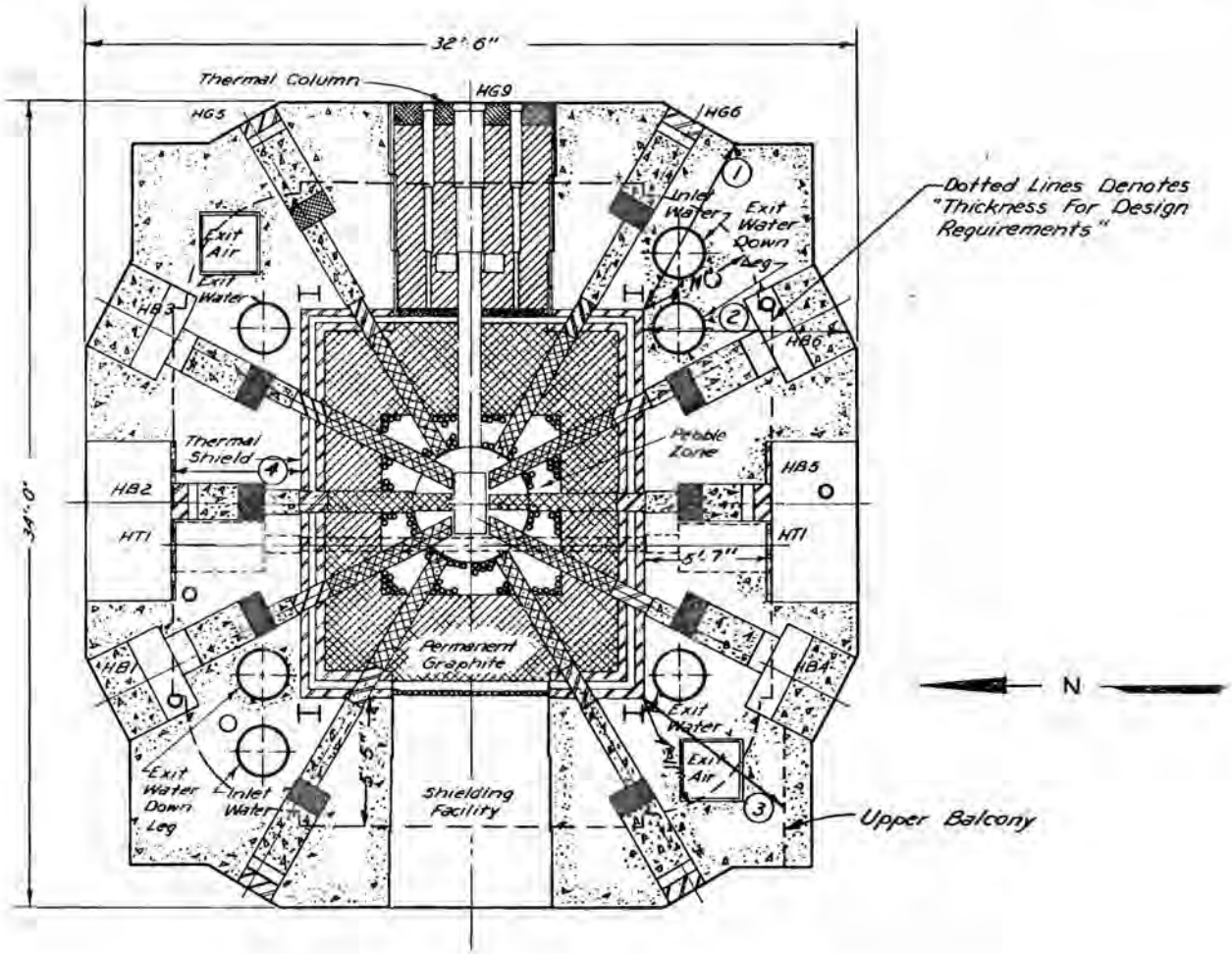

FIG. 4.6.H.

COMPARISON OF OVERALL BARYTES CONCRETE THICKNESS WITH DESIGN REQUIREMENTS

DWG. # 10420 [redacted]

LINE	THICKNESS				REQUIRED CONCRETE THICKNESS TABLE III
	IRON	WATER	BARYTES	TOTAL EQUIV. CONCRETE	
	IN.	IN.	IN.	IN.	IN.
1	1.5	-	77	80	54
2	2	-	95	100	54
3	10	22	50	82	66
4	55	20	9	84	66

REFERENCE DRAWINGG
BK 3150 502-4

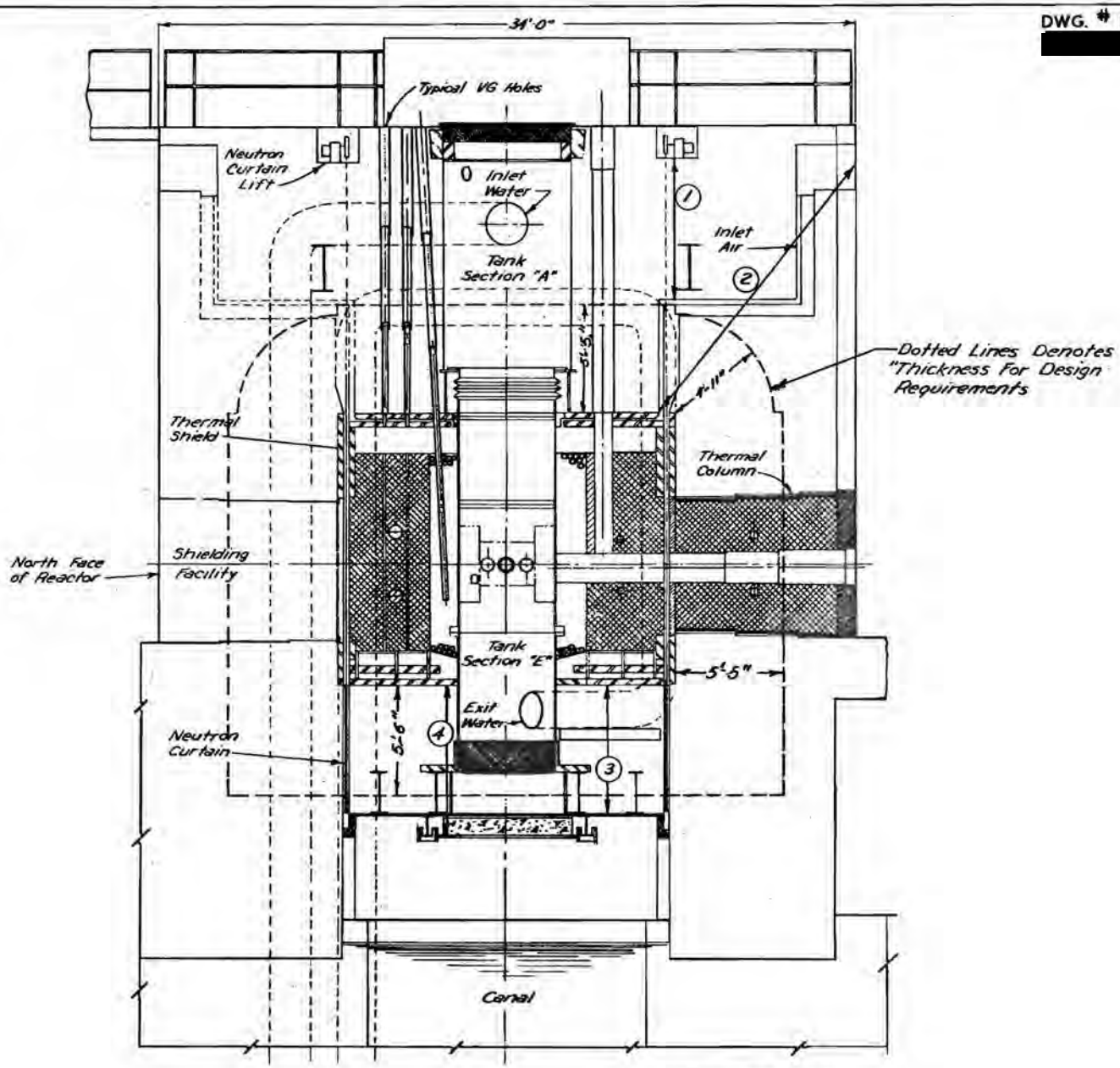

FIG. 4.6I

COMPARISON OF OVERALL BARYTES CONCRETE THICKNESS WITH DESIGN REQUIREMENTS

to 8 in. with lead or lead shot. Thus the design and construction of the top plug could proceed independently of the exact shielding requirements, which would be determined by actual measurements in the Mock-Up at a later date. These measurements were carried out and reported in ORNL CF-50-8-85.[32] The data extrapolated to conditions of operation of the MTR indicate that without the top plug the γ-ray intensity will be about 200 mr/hr at 30 mw power. This means that 7 in. of lead shot plus the 3 in. of steel in the plug are required to reduce the γ-ray intensity to 1.2 mr/hr at 60 mw power. The following paragraphs summarize the calculations used as a basis for the design of the top plug and a comparison of calculated values with data from the Mock-Up.

(*a*) Gamma Production in the Active Lattice. It is assumed that on the average, a 72- by 24- by 60-cm portion of the core will contain active fuel elements. With such a loading, there will be about 3.5 kg of U^{235} in the core and at 30 mw the average neutron flux will be 2×10^{14}. The γ-ray source in the active section is given as follows:

SOURCE	REACTOR CROSS SECTION, $N\sigma$ (cm^2)	γ RAYS PER CAPTURE	
U fission	4900	5	1-Mev fission γ's
		2	2.5-Mev fission product γ's
U capture	800	1	6-Mev γ
H_2O capture	1320	1	2-Mev γ
Al capture	588	1	8-Mev γ
Th capture	610	1	6-Mev γ

The source strength is given by the product of the neutron flux, cross-section, and γ-ray energy per capture divided by the core volume. Combining γ-rays of similar energies gives the following source spectrum:

GAMMA SOURCE (Mev)	Q_v (Mev/cc-sec)	(watts/cc-sec)	μ_s (cm^{-1})
1	47.5×10^{12}	7.6	0.099
2.5	52.6×10^{12}	8.4	0.072
6	16.3×10^{12}	2.6	0.044
8	9.0×10^{12}	1.44	0.039

At large distances from the reactor centerline, the radiation intensity may be calculated by simple conventional formulas. Thus for each of the γ-ray sources, the intensity is given by

$$I = 1.9 \times 10^{-3} \frac{Q_v A}{4\pi \mu_s a^2} e^{-\mu a/1.2}$$

where

I = intensity, mr/hr.

1.9×10^{-3} = conversion factor, Mev to mr/hr.

Q_v = source strength, Mev/cc-sec.

A = area of top of active section, cm^2.

μ_s = absorption coefficient of core, cm^{-1}.

a = distance above active lattice = 565 cm.

μ = absorption coefficient of water, cm^{-1}.

1.2 = factor for forward scattering.

Therefore,

$$I = 8.2 \times 10^{-7} \frac{Q_v}{\mu_s} e^{-565(\mu/1.2)}$$

Using this equation and values of Q_v shown in the previous table, the resultant γ-ray intensities I at the top plug are given in the following table:

GAMMA SOURCE (Mev)	$\mu/1.2$ (cm^{-1})	$565\mu/1.2$	$e^{-\mu a/1.2}$	I (mr/hr)
1	0.058	32.8	10^{-14}	
2.5	0.033	18.7	10^{-8}	
6	0.023	13.0	2.2×10^{-5}	670
8	0.020	11.3	1.2×10^{-5}	2300
Total intensity without top plug				3000

This theoretical value is a factor of 15 above the values measured in the Mock-Up. The difference is presumably due to the fact that the assumed energy of the capture γ rays is too high. Recent capture γ-ray spectral data[33] verify this and show that the average energy of aluminum capture γ rays is in the range 5 to 7 Mev rather than 8 Mev.

(*b*) Mock-Up Data. Vertical measurements were made through approximately 11 ft of water, starting at a point 4 ft above the horizontal centerline of the reactor. Three horizontal traverses were made at various depths. The low intensity of Mock-Up operation (i.e., 270 watts) did not permit measurement of the attenuation of the full depth of water. However, since the attenuation was exponential over a factor of 1000, it was felt that an extrapolation of an additional factor of 100 could be made with reasonable certainty. This value, multiplied by 10^5 to allow for the difference in power level between the Mock-Up and the MTR, indicates that a γ-ray flux of approximately 200 ± 100 mr/hr would be transmitted through the water. To reduce this to 1/10 tolerance (1.2 mr/hr) at 60 mw power requires an attenuation factor of 300 by the lead and iron in the top plug. This is equivalent to 5.7 relaxation lengths. Since the top plug contains 2½ in. of steel or 1.5 relaxation lengths, an additional 3½ in. of lead or 6 in. of lead shot is required for the top plug.

(*c*) Radiation Intensity After Shutdown. The total γ-ray activity following infinite operation of a reactor is, according to estimates by K. Way,[10] given by

$$(Q_0E) = 6.3\ ft^{-0.2} \qquad \text{Mev/sec}$$

where

f = fissions/sec in source.

t = time after shutdown.

The hard γ-ray activity (about 3 Mev) after shutdown, however, depends on the yield and decay of specific fission product chains. These have been measured by the photoneutron threshold reaction in heavy water. The average lifetime and yield of the γ rays of energies higher than this value are:

t (mean)	A_γ (yield/fission)	ENERGY (Mev)
76 hr	0.0015	~3
6.3 hr	0.0042	~3
2.4 hr	0.045	2.6
39 min	0.038	2.6
11 min	0.046	3
3.4 min	0.132	2.6
59 sec	1.58	2.25
3.6 sec	0.675	3.4

Using the same method as in the calculation of the radiation intensity during operation of the reactor, but considering only the hard fission product γ rays listed above, the γ-ray intensity at the top of the reactor well may be calculated as a function of the time after shutdown. In this case the source term at 30 mw power is given by

$$30{,}000 \times 3.1 \times 10^{13} = 9.3 \times 10^{17} \text{ fissions/sec}$$

$$Q_v = \frac{(9.3 \times 10^{17})(A_\gamma E)_t}{24 \times 72 \times 60} \qquad \text{Mev/cc-sec}$$

and

$$Q_v = 9 \times 10^{12}(A_\gamma E)_t$$

The radiation intensity at the surface of the water after shutdown is

$$I = 6 \times 10^6 (A_\gamma E)_t \frac{e^{-530(0.035)}}{\mu_s}$$

Assuming average energy of hard γ-rays to be 2.75 Mev,

$$I = 1.4(A_\gamma E)_t \qquad \text{mr/hr}$$

Values of $(A_\gamma E)_t$, Q_v, and the γ-ray intensity at various times after shutdown are shown in the following table:

TIME AFTER SHUTDOWN	$(A_\gamma E)_t$ (Mev/fission)	Q_v (Mev/cc-sec)	I (mr/hr)
10 sec	4.37	39.5×10^{12}	6.2
10 min	0.32	2.9×10^{12}	0.5
1 hr	0.11	1.0×10^{12}	0.15
1 day	0.003	0.027×10^{12}	0.04

This indicates that the water gives adequate protection following an elapsed time greater than 10 min after shutdown of the reactor.

2. Shielding Requirements of the Bottom Plug. The original design of the reactor tank closure beneath the active lattice consisted of numerous layers of steel and water. In view of the large number of water monitoring tubes penetrating this section, the construction of such a plug was difficult. The present design consists of a steel cylinder filled with lead. The water monitoring tubes which penetrate this plug and which during operation carry active water are shielded by a sliding concrete door beneath the bottom plug.

Personnel in the sub-pile room are thus shielded from the γ rays leaving the active lattice by both the lead plug and the concrete door. The required thickness of the lead portion of this shield is calculated as follows: Data from the Mock-Up on the radiation escaping upward through the water may be used to estimate the intensities below the active lattice since reactor components are approximately the same above and below the centerline. The bottom plug starts at a point 245 cm below the active lattice. At this level, the γ intensity during operation at 30 mw power will be 4×10^7 mr/hr. Since previous calculations as well as the slope of the curve of Mock-Up data indicate that the energy of the hard γ-ray components (i.e., capture γ-rays from Al, Fe, Be, etc.) is about 5 Mev or lower, the following absorption coefficients based on this energy may be used for estimating the required amounts of lead and barytes concrete:

ABSORBER	μ (cm^{-1})
H_2O	0.03
Fe	0.235
Pb	0.46
Pb shot (D = 6.8)	0.28
Barytes concrete	0.10

At 12.5 ft from the active lattice (minimum distance of approach), the γ-ray intensities will be

$$I = \frac{(4 \times 10^7)(245)^2}{(385)^2} e^{-b} \qquad \text{mr/hr}$$

where

$$b = \mu_{Fe} X_{Fe} + \mu_{Pb} X_{Pb} + \mu \text{ concrete X concrete}$$

The proposed design consists of 17 in. of lead shot and 3 in. of iron in the bottom plug plus 9 in. of barytes concrete and 1 in. of iron in the door beneath the bottom plug.

Thus

$$b = 4(0.6) + 17(0.71) + 9(0.25) = 16.7$$

$$e^{-b} = 5.4 \times 10^{-8}$$

and

$$I = 0.9 \text{ mr/hr in the sub-pile room}$$

The bottom plug and concrete door give adequate protection from pile radiation.

3. Leakage Around Top and Bottom Plugs. Leakage around the sides of the top and bottom plugs is prevented by supplementary shielding rings at the edges of the plugs. The required thicknesses of these rings were established by measuring, on appropriate drawings, the actual thicknesses of water, steel,

concrete, etc. along many different paths and adding shielding where necessary to give the same total attenuation as on the reactor vertical centerline. In all cases conservative data were used to establish the required total attenuation, which resulted in some overdesign at these locations. Specific details of calculations are summarized in MTR Shield Survey Reports.[30,31]

4. Thickness of Door Under Bottom Plug. In addition to shielding the water monitor tubes, the door under the bottom plug must protect personnel from neutrons escaping the steel thermal shield. Calculations verifying the adequacy of the door for neutron protection are reviewed as follows:

Neutron source: 3×10^9 fast neutrons/cm^2-sec incident on inner face of 8-in. steel thermal shield.

Neutron tolerance: 100 neutrons/cm^2-sec, corresponding to 10 mr/hr.

The neutron attenuation by the 9½-in. of steel, whose effective relaxation length is 4.9 cm, is

$$e^{-23/4.9} = 10^{-2}$$

The neutron attenuation by the biological shield (2 ft 9 in. barytes concrete), whose relaxation length for neutrons is 8.2 cm, is

$$e^{-10.3} = 3.5 \times 10^{-5}$$

The neutron attenuation in the door (9 in. barytes concrete) is

$$e^{-2.8} = 6.2 \times 10^{-2}$$

The total neutron attenuation is 2.2×10^{-8}, i.e., the neutron intensity below the door will be about 70 neutrons/cm^2-sec, which is below tolerance.

Shielding of Inlet and Exit Water Lines. 1. Shielding of Exit Water Lines.[34-38] The activity of the water leaving the reactor is due mainly to the N^{16} activity formed from the reaction $O^{16}(n,p)N^{16}$. This is a fast-neutron reaction having a threshold at about 9.5 Mev and a cross-section of about 1 barn. Since a small fraction (about 1/50,000) of the fission neutrons have energies above 9.5 Mev, the *effective* cross-section per fission neutron is about 0.014 mb or 1.4×10^{-29} cm^2. The activity of the water leaving the reactor is given by

$$A = nv\,\sigma_f(1 - e^{-\lambda T})e^{-\lambda t}$$

where

nv = fast flux in lattice = 10^{14} neutrons/cm^2-sec at 30 mw.

σ_f = cross-section for N^{16} production = 0.014 mb or 4.68×10^{-7} cm^2 per cubic centimeter of water.

λ = N^{16} decay constant = 0.092 sec^{-1}.

T = exposure time in lattice = 1/15 sec.

t = decay time after leaving lattice.

A = activity, disintegrations/cc-sec.

Thus

$$A = 2.88 \times 10^5\, e^{-\lambda t} \text{ dis/cc-sec.}$$

Since the average energy of the N^{16} γ ray is 6.5 Mev, the water activity is $1.85 \times 10^6\, e^{-\lambda t}$ Mev/cc-sec.

The required shielding of the exit water lines varies with the distance from the active core owing to the relatively rapid decay of N^{16}. Referring to drawing DRP-69, which shows the layout of air ducts and water lines within the reactor structure, the activity at critical locations along the exit water lines may be calculated from the flow rate and corresponding decay times. The water activity at strategic points is summarized as follows, based on a flow rate of 20,000 gpm:

LOCATION	DECAY TIME (sec)	WATER ACTIVITY FROM N^{16} (Mev/cc-sec)
A. Leaving reactor tank	2.3	1.5×10^6
B. Vertical rise at reactor centerline	4.1	1.28×10^6
C. Center of top of loop	6.6	1.0×10^6
D. Leaving reactor structure	15	4.6×10^5
E. Leaving Reactor Building	26	1.7×10^5
F. Entering seal tank	63	5.5×10^3

The required shielding may be calculated by the method outlined in the Project Handbook CL-697, VF 5, for a cylindrical source. The intensity at the surface of a shield b cm thick is

$$I = \frac{QR^2}{2(b + z)} F(B)$$

where

I = γ-ray intensity, Mev/sec.

Q = source strength, Mev/cc-sec.

R = radius of pipe, 30.5 cm.

$B = \nu z + \mu b$ (ν = absorption coefficient of water and μ = absorption coefficient of shield).

z = effective position of line source equivalent to distributed source (CL-697, VF 5, Fig. 5).

$F(B)$ = distribution function (CL-697, VF 5, Fig. 2).

At point A the shield consists of 5 ft of barytes concrete plus some iron. The γ-ray intensity at the ceiling of the sub-pile room due to N^{16} is calculated from the following data:

$Q = 1.5 \times 10^6$ Mev/cc-sec.

z = 18 cm (from CL-697, VF 5).

$\nu = 0.026$ cm^{-1}.

b = 153 cm.

$\mu = 0.09$ cm^{-1}.

$F(B) = 2.5 \times 10^{-7}$.

$$I = \frac{(1.5 \times 10^6)(30.5)^2}{2(171)} (2.5 \times 10^{-7}) = 1 \text{ Mev/sec} = 2 \times 10^{-3} \text{ mr/hr}$$

Thus the contribution of the water activity to the intensity in the sub-pile room is negligible.

2. Shielding of Water Inlet Lines.[39-44] The residual activity of the process water after decay of N^{16} is due to the neutron activation of dissolved minerals and aluminum recoil activity. The significant reactions are listed as follows:

REACTION	MECHANISM	$t_{1/2}$	CROSS-SECTION	RECOIL RANGE IN Al (cm)
$Na^{23}(n,\gamma)Na^{24}$	Neutron absorption	14.8 hr	0.5 b	
$O^{18}(n,\gamma)O^{19}$	Neutron absorption	29.4 sec	0.44 μb	
$Al^{27}(n,\gamma)Al^{28}$	Slow recoil	2.3 min	0.21 b	1.2×10^{-6}
$Al^{27}(n,\gamma)Al^{28}$	Fast recoil	2.3 min	0.4 mb	2.4×10^{-4}
$Al^{27}(n,p)Mg^{27}$	Fast recoil	10.2 min	2.8 mb	2.4×10^{-4}
$Al^{27}(n,\alpha)Na^{24}$	Fast recoil	14.8 hr	0.6 mb	2.4×10^{-4}
$Mn^{55}(n,\gamma)Mn^{56}$	Slow recoil	2.6 hr	13.0 b	1×10^{-5}

The activity of the process water excluding N^{16} activity is calculated for the following system conditions:

Flow rate	=	20,000 gpm
Purge rate	=	50 gpm
System holdup	=	348,000 gal
Cycle time	=	17.4 min or about 1000 sec
Activation time	=	1/15 sec
Slow flux	=	2×10^{14} neutrons/cm^2-sec
Fast flux	=	1×10^{14} neutrons/cm^2-sec
Area of exposed Al	=	10^6 sq cm
Water composition		
Ca		1 ppm
Mg		0.5 ppm
Cl		1 ppm
Al		0.05 ppm
Fe		0.05 ppm
Na		5 ppm
K		1 ppm
F		0.1 ppm
N		0.02 ppm

The activity due to the absorption of neutrons by dissolved minerals after recycle equilibrium is reached is

$$A = \frac{\lambda K}{(1 - Be^{-\lambda T})}$$

where

A = activity, dis/cc-sec.

λ = decay constant, sec^{-1}.

K = isotope reduction per cycle.

B = concentration factor = 20000/20050 $\approx$ 1.

T = cycle time.

K = $nv\Sigma at$ (for half-lives >> t).

Σ_a = cross-section of mineral per cubic centimeter of water.

The aluminum recoil activity is

$$A = \frac{nv\ \sigma_a(0.602)\ (\text{range})\ (\text{area})\ D\lambda}{4\omega F(1 - Be^{-\lambda T})}$$

where

σ_a = cross-section, barns.

Range = recoil range, cm.

Area = 10^6 cm^2.

D = density of aluminum.

F = cycle flow rate, cc/sec.

ω = atomic weight of recoil nucleus.

Principal activities in the water entering the reactor are:

	(dis/cc-sec)	E (Mev)	(Mev/cc-sec)
Na^{24}	1160	2.2	2550
Mg^{27}	488	1.48	725
Mn^{56}	145	2.13	310
Al^{28}	26	1.80	50
Total			3635

The activity due to accidental exposure of core material, resulting from loss of Al cladding from a fuel plate, is calculated as follows: The fractional escape of fission recoils from the surface of a slab source is $1/4\alpha$, where α is the ratio of the mass thickness of the slab to the range of the fission fragments, or $5.6 \times 10^{-3}/1.05 \times 10^{-4} = 54$. Thus the fraction $1/4(54) = 1/216$ will escape from an exposed surface. At 30 mw there are 10^{18} fissions/sec or 6.7×10^{12} fissions/cc-sec. The number of fission fragments escaping per square centimeter is therefore 3×10^{10}. Since the flow rate per plate is 28 gpm, the activity in the water is 1.75×10^{7} fissions/cc-sec.

Although the activity of the fission fragments which escape into the water is due to the fission products, these decay relatively rapidly. According to K. Way,[10] the disintegration energy is $0.3t^{-0.8}$ Mev/sec (fission). After 1000 seconds, it will be 1.2×10^{-3} Mev/sec (fission), or the total activity per square centimeter of fuel plate exposed is 2.1×10^{4} Mev/cc-sec. Since there are 18 plates per fuel assembly and 25 fuel assemblies, the activity per square centimeter exposed in the reactor core will be 47 Mev/cc-sec. For activity to be detectable, at least 10 sq cm of U-Al alloy must be exposed.

The shielding of the inlet water lines required due to the residual fission product and recoil activity may be calculated by conventional methods outlined previously. For the above conditions about 1 ft of barytes aggregate concrete is required for the inlet lines.

Thermal Column Shielding.[45-48] This large hole through the biological shield, though filled with graphite, produces a difficult γ-ray shielding problem. For this reason the thermal column sides must be lined with cadmium, steel, and lead plates, and the face must be provided with a removable γ

shield. This removable shield is in the form of a sliding lead door, 10 in. thick, which may be raised for access to the column.

1. Neutron Flux Calculations. The original calculations of the thermal-neutron flux in the thermal-column graphite were carried out in 1947.[45] These data were later corrected for changes in the design of the graphite reflector by multiplying by a factor of 3. This normalizes values to a figure of 3×10^{12} neutrons/cm^2-sec at the inside of the thermal column which is in agreement with calculated neutron-flux distribution curves[24] and data from the Mock-Up previously cited.

2. Required Thickness of Sliding Lead Door. A maximum value of the radiation intensity penetrating the graphite in the thermal column may be obtained by considering the column to consist of a number of slab sources with the contribution of each concentrated at its surface. Each neutron absorbed in the graphite gives rise to a 6-Mev γ ray. Assuming each slab to be 25 cm thick, a slab x cm from the outside of the thermal column gives rise to

$$I = \frac{I_0}{2} F_0(\mu x + \nu a) \qquad \gamma\text{'s/cm}^2\text{-sec}$$

where

$$I_0 = N\sigma_a \; t \; S(x) = 25 \; (4 \times 10^{-4}) \; S(x) = 10^{-2} \; \gamma\text{'s/cm}^2\text{-sec.}$$

$S(x)$ = thermal flux at x.

μ = absolute coefficient of graphite = 0.03 cm^{-1}.

ν = absolute coefficient of lead = 0.44 cm^{-1}.

a = thickness of lead door

$$F_0(b) = \int_b^\infty \frac{e^{-y}}{y} \, dy \qquad \text{(from CL-697, VF)}$$

Contributions from each section of the thermal column with a 10-in. lead door are summarized as follows:

DISTANCE FROM DOOR, x (cm)	$S(x)$ (n/cm^2-sec)	$\mu x + \nu a$	$F_0(\mu x + \nu a)$	I (γ/cm^2-sec)
0	0	11.25	1.14×10^{-6}	0
25	1.9×10^{9}	12.0	5×10^{-7}	5.0
50	7.5×10^{9}	12.75	2×10^{-7}	7.5
75	1.7×10^{10}	13.50	1×10^{-7}	8.5
100	3.6×10^{10}	14.25	4.5×10^{-8}	8.0
125	7.2×10^{10}	15.0	2×10^{-8}	7.2
150	1.4×10^{11}	15.75	8×10^{-9}	5.6
175	2.5×10^{11}	16.52	4×10^{-9}	5.0
200	4.5×10^{11}	17.25	1.8×10^{-9}	4.0
225	8.4×10^{11}	18.0	9×10^{-10}	3.8
250	1.5×10^{12}	18.75	4×10^{-10}	3.0
275	3.0×10^{12}	19.5	2×10^{-10}	3.0
				60.6

This is equivalent to 480 Mev/cm^2-sec or about 1 mr/hr, which is below 1/10 tolerance.

Radiation Leakage Through Ducts in Reactor Structure.[49-52] The numerous holes penetrating the biological shield complicate the problem of designing a satisfactory shield. The total intensity outside the shield is increased in the vicinity of holes by radiation penetrating the section of the shield which is effectively thinner. Additional radiation may be received by scattering from the walls of the opening. Experiments which have been performed with shields penetrated by curved or staggered ducts indicate that the direct penetration through the thin part of the shield is usually more effective than scattering in increasing the γ intensity in the vicinity of the opening. This is especially true for ducts with multiple bends. To determine the adequacy of the biological shield in the vicinity of an opening, the following procedure may be used:

By inspection of a layout of the shield structure, a danger point is selected and a line along the path of minimum attenuation determined. This line is generally in a direction from the outer to the inner mouth of the duct. The intensity contribution of the surface element at the source of the minimum path is calculated, as well as the contribution of all neighboring surface elements which can be "seen" through the effectively thinner portion of the shield. These neighboring contributions usually fall off very rapidly as elements further from the minimum line are considered.

The intensity contribution of each surface element is calculated by assuming it to be a point source. Figure 4.6.J represents a cross-section of a duct through the shield. For each surface element ΔA, the contribution at P is

$$I = \frac{I_0 \; e^{-b}}{R^2}$$

where

$I_0 = \phi_A \; E(\Delta A) \cos \theta / \pi.$

$\phi = \gamma/\text{cm}^2\text{-sec}$ at source.

$E = \gamma$-ray energy.

$b = \mu r_1 + \mu r_2 + \ldots$

r_1, r_2 = actual sections of shield penetrated.

μ = absolute coefficient of shield.

R = distance from source to point $P = t \sec \theta$

For simple geometries, the variation of b from element to element can be approximated by a simple mathematical expression and the total intensity found by integration. Otherwise the easiest approach is to measure the actual thickness of shield material traversed along a straight line from each source element and add algebraically the separate intensity contributions. The total intensity should be multiplied by a B factor to allow for the forward scattering in the shield. This is usually about a factor of 10 for thick shields.

The contribution of radiation scattered along the duct from the walls of the duct may be estimated by the same method as determining the scattering by mass elements within the shield itself. Essentially the method consists of breaking the scatterer (i.e., the duct wall) into a number of mass elements ΔM and assuming each to be a point of secondary radiation. The energy of the secondary γ rays is a function of the energy of the primary and the angles of incidence and reflection. The secondary intensity is the sum of all the point sources considered. A detailed analysis of the calculation of scattered radiation is given in ORNL-710.[4]

DWG. #10801
NOT CLASSIFIED

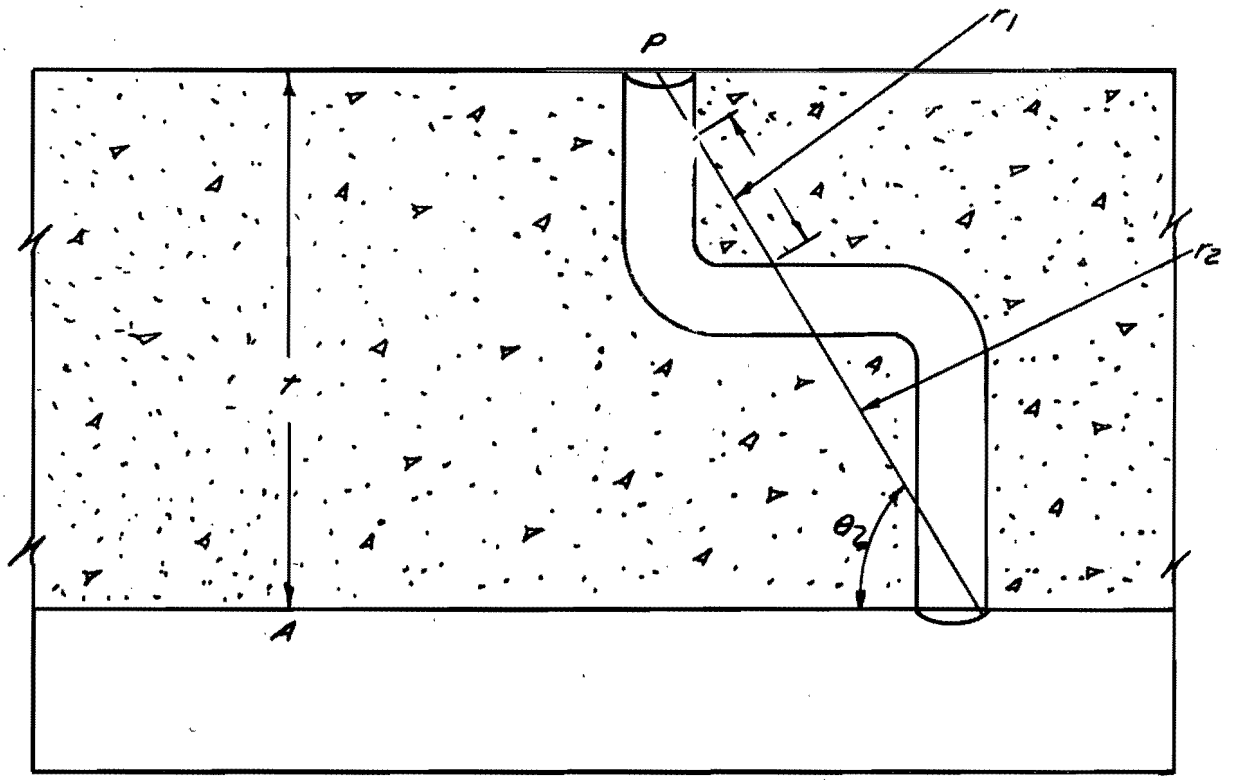

FIG. 4.6.J

Design of Experimental Hole Plugs.[53-57] In general, the problem of designing plugs adequate to prevent escape of radiation from experimental holes during operation of the reactor may be simplified by duplicating in the plug the various portions of the shield through which it passes. Precaution must be taken to stop radiation leakage through the annulus between the beam hole liner and the plug by providing a number of steps. These should be kept to a minimum, however, since each step increases the diameter of the plug which must be shielded after removal from the reactor. The amount of radiation leaking through the annulus may be estimated by the same method as for voids in the shield, which has been described previously. The major contribution is the radiation penetrating the effectively thinner portions of the plug, rather than that from scattering around the step. The leakage through the annulus around the beam hole plug depends therefore on the width of the annulus and size of the step in the plug rather than on the number of steps. Measurements of the radiation through a narrow staggered channel by Gamertsfelder (in a report by Stone[57]) may be used to verify this. For the MTR main beam holes, a ½-in. step with a 1/8-in. annulus gives adequate protection.

1. Shielding Requirements After Removal of Plug. In order to protect personnel after the plug has been removed and after shutdown of the reactor, each beam hole is equipped with a lead radiation door 12 in. thick. The radiation intensity at the outside of the beam hole with the lead door closed is estimated as follows: It has been shown previously that 10 min after shutdown the reactor core emits 2.9×10^{12} Mev/cc-sec of hard γ-ray radiation. Since at relatively large distances from the reactor the core acts like a point source, the intensity at the end of an open beam hole is given by

$$I = \frac{1.9 \times 10^{-3}\, Q_v A}{4\pi\mu_s a^2}\, e^{-\mu x} \qquad \text{mr/hr}$$

where

Q_v = energy emitted per unit volume of core.
A = area of beam hole = 180 cm^2.
μ_s = absolute coefficient of core = 0.07 cm^{-1}.
a = length of beam hole = 475 cm.
μ = absolute coefficient of lead = 0.46 cm^{-1}.
x = thickness of radiation door = 12 in.

Thus

$$I = \frac{(1.9 \times 10^{-3})(2.9 \times 10^{12})180}{4\pi(0.07)(475)^2} e^{-14} = 5 \times 10^6(0.9 \times 10^{-6}) = 4.5 \text{ mr/hr}$$

Although this intensity is one-half tolerance, the decay of fission products reduces the value to one-tenth tolerance at 1 hr after shutdown.

In addition to affording protection after shutdown, the lead shielding door can be used in conjunction with a relatively simple neutron shielding plug during operation of the reactor to provide additional flexibility to the experimental facilities.

Shielding Requirements of External Facilities.[58,59] 1. External Water System. The activity of the water in the external system due to the neutron absorption of dissolved minerals reaches an equilibrium level which depends on the time of activation in the core, the amount of purge, and the recycle time. Based on the operating conditions listed below, the average activity of the water in the external system will be about 3700 γ rays/cc-sec. These have an average energy of 2 Mev.

2. Operating Conditions. The following operating conditions were used:

Power level	30 mw
Flow rate	20,000 gpm
Purge	50 gpm
Cycle time	1000 sec
Average decay time	500 sec
Water activity	7400 Mev/cc-sec

The shielding of the working reservoir and associated pipes is accomplished by first installing a fence 15 ft from the pipes, and then shielding the pipes to a height of 20 ft with 10- or 12-in. concrete blocks and shielding a portion of the reservoir itself with 2 in. of iron. Considering that only two of the 24-in. pipes will be filled with water at any one time, the γ-ray intensity adjacent to the concrete blocks will be 10 mr/hr and outside the fence 1 mr/hr. On the reservoir platform with the water shielded by 2½ in. of iron, the γ-ray intensity will be about 5 mr/hr.

3. External Air System. The activity of the pile-cooling air is due mainly to A^{41} with minor contributions from N^{16} and O^{19}. The physical and nuclear properties of these gases are listed below.

ELEMENT	REACTION	ABUNDANCE IN AIR (%)	σ_a	$t_{1/2}$	E_γ (Mev)
Nitrogen	$N^{15}(n,\gamma)N^{16}$	0.30	0.02 mb	7.4 sec	6.5
Oxygen	$O^{18}(n,\gamma)O^{19}$	0.04	0.2 mb	29.4 sec	1.6
Argon	$A^{40}(n,\gamma)A^{41}$	0.94	0.62 b	110 min	1.3

At 150°F and 25.5 in. Hg, 1 cu ft of air contains 3.1×10^{21} atoms of N^{15}, 4.2×10^{20} atoms of O^{18} and 4.9×10^{21} atoms of A^{40}. At 60 mw the average thermal-neutron flux in the air within the reactor is 4×10^{12} neutrons/cm^2-sec and the total volume of air in the reactor is about 850 cu ft. At 30,000 cfm the exposure time of the air in the reactor is about 2 sec. The number of atoms of A^{41} formed per second per cubic foot is

$$(4 \times 10^{12})\ (4.9 \times 10^{21})\ (0.62 \times 10^{-24}) = 1.2 \times 10^{10}$$

and the disintegration energy per cubic foot will be

$$(1.2 \times 10^{10})\ (2)\ (1.3)\frac{0.693}{6600} = 3.3 \times 10^{6} \text{ Mev/cu ft-sec}$$

The disintegration energy due to O^{19} is

$$(4 \times 10^{12})\ (4.2 \times 10^{20})\ (0.2 \times 10^{-27})\ (2)\ (1.6)\frac{0.693}{29.4} = 2.6 \times 10^{4} \text{ Mev/cu ft-sec}$$

The disintegration energy due to N^{16} is calculated similarly to be 3×10^{5} Mev/cu ft-sec. The shielding required to reduce the γ intensities to desired tolerances is summarized in Chap. 8, Table 8.1.C.

Shielding Requirements for Handling Activated Equipment and Materials.[56,60-64] The handling of equipment and materials which have been subjected to neutron irradiation constitutes one of the most important shielding considerations in the operation of a nuclear reactor. Each item presents a special problem and must be handled as such. The following paragraphs present general background for calculation of induced activities. For more detailed information on special problems, the listed references should be consulted.

1. Activities of Important Elements. The following table summarizes the elements which give rise to relatively high-energy γ-ray activity. Calculations are based on a flux of 10^{14} neutrons/cm^2-sec and irradiation to saturation (i.e., irradiation times long compared to half-life). For shorter irradiation times values should be multiplied by $(1 - e^{-\lambda T})$, where T is the irradiation time and λ the decay constant.

TABLE 4.6.D
Elements with High γ-Ray Activities

ELEMENT	ACTIVE ISOTOPE	HALF-LIFE	(curies/g)	γ-RAY ENERGY (Mev)
Sodium	$_{11}Na^{23}$	14.8 hr	32	1.38, 2.76
Magnesium	$_{12}Mg^{26}$	10.2 min	0.6	0.84 (100%), 1.01 (20%)
Aluminum	$_{13}Al^{27}$	2.4 min	13	1.80
Titanium	$_{22}Ti^{50}$	72 days	0.071	1.0
Vanadium	$_{23}V^{51}$	3.8 min	140	1.5
Chromium	$_{24}Cr^{50}$	26.5 days	15	0.32
Manganese	$_{25}Mn^{56}$	2.59 hr	390	0.82 (100%), 1.77 (30%)
Iron	$_{26}Fe^{58}$	46 days	0.029	1.10 (50%), 1.30 (50%), 2.06 (20%)
Cobalt	$_{27}Co^{59}$	5.3 years	610	1.16, 1.32
		10.7 min	18	1.5 (10%)
Copper	$_{29}Cu^{63}$	12.8 hr	59	1.35 (2.5%)
		5 min	14	1.30
Zinc	$_{30}Zn^{64}$	250 days	6	1.14 (45%)
	$_{30}Zn^{68}$	13.8 hr	0.4	0.44

The induced activities of some important reactor materials have been measured in the Oak Ridge reactor. Data are summarized in Table 4.6.D for irradiations at a thermal flux of 10^{12} neutrons/cm^2-sec. At higher flux levels, the values may be increased proportionally as long as the ratio $nv\sigma/\lambda$ is small,

where

nv = thermal flux, neutrons/cm^2-sec.

σ = absorption cross-section of activated atom, cm^2/atom.

λ = decay constant of active atom, sec^{-1}.

When the cross-section of the active atom is greater than 1000 barns and the half-life greater than 50 days, the saturation activities are reduced by fluxes of the order of 10^{14} neutrons/cm^2-sec. Under ordinary conditions, however, the saturation activity is relatively unaffected.

TABLE 4.6.E

Induced Activity of Commercial Materials

MATERIAL	TIME IN REACTOR (hr)	LEAD ABSOLUTE COEFFICIENT (cm^{-1})	ACTIVITY[1] (photons/sec-g) AT 10^{12} FLUX			
			4 to 5 hr decay	10 hr decay	100 hr decay	1000 hr decay
GBF graphite	4400	0.62	1.5×10^4	1.2×10^4	9.0×10^2	$< 2 \times 10^2$
CS graphite	4400	0.62	4.2×10^4	3.6×10^4	1.5×10^4	1.1×10^4
C-18 graphite	15000	0.58	5.5×10^5	5.2×10^5	3.2×10^5	2.6×10^5
Beryllium	12000	0.58	6.9×10^6	3.8×10^6	1.5×10^6	1.1×10^6
2S aluminum	15000	0.57		1.4×10^7	5.9×10^5	3.4×10^5
Stainless steel						
Type 304	1000	0.59	3.2×10^8	1.05×10^8	5.0×10^7	2.8×10^7
Type 310	1000	0.57	9.7×10^8	2.7×10^8	6.2×10^7	3.9×10^7
Type 316	1000	0.61	9.7×10^8	2.7×10^8	4.9×10^7	2.9×10^7
Type 347	1000	0.56	8.5×10^8	2.3×10^8	5.4×10^7	3.3×10^7
Type 405	1000	0.57	2.8×10^7	9.5×10^7	3.5×10^7	1.8×10^7
Type 430	1000	0.62	2.6×10^8	8.0×10^7	3.6×10^7	1.8×10^7
Type 445	1000	0.58	4.5×10^8	1.35×10^8	4.8×10^7	2.2×10^7
Carpenter 20	1000	0.52	6.0×10^8	2.6×10^8	7.2×10^7	4.1×10^7
Concrete						
Brookhaven[2]	700	0.49	4.0×10^8	9.0×10^7	5.0×10^6	3.0×10^6
Ordinary[3]	700	0.55	9.1×10^7	5.3×10^7	1.8×10^6	4.7×10^5
Barytes[4]	700	0.51	4.3×10^7	1.9×10^7	8.3×10^6	2.0×10^6

(1) The ionization chamber was calibrated with Co^{60} of 1.2 Mev average photon energy.

(2) The Brookhaven cement contained 58.2% limonite, 29.1% portland cement, 12.7% H_2O.

(3) The ordinary concrete contained 56% rock, 25.5% sand, 10.4% portland cement, 8.1% H_2O.

(4) The barytes concrete contained 46% barytes coarse, 40% barytes fine, 9.6% portland cement, 4.4% H_2O.

4.7 REFERENCE REPORTS

(1) Greuling, E., *Theory of Water Tamped Water Boiler*, LA-399, September 27, 1945.

(2) Beck, D. K., Callihan, D., and Murray, R. L., *Critical Mass Studies, Part II*, K-126, January 23, 1948.

(3) *Technical Division Section II Monthly Reports*, 1947 and 1948.

(4) Kasper, S., *Water Flow in the MTR*, ORNL CF-50-6-102, June 15, 1947.

(5) Briggs, R. B., *Cooling of Graphite Reflector for MTR*, ORNL CF-50-3-102, March 20, 1950; *Temperature in Bottom Thermal Shield Proposed for MTR*, ORNL CF-50-1-45, January 10, 1950.

(6) Briggs, R. B., *Heat Production in Bottom Thermal Shield of MTR*, ORNL CF-49-12-1, December 1, 1949.

(7) Briggs, R. B., *Neutron Fluxes and Heat Production in Top and Side Thermal Shields of MTR*, ORNL CF-50-1-18, January 6, 1950; *Effect of Conduction of Heat from Graphite Reflector Upon Temperature in East Side Thermal Shield of MTR*, ORNL CF-50-7-125, July 24, 1950.

(8) Lane, J. A., *Cooling Requirements at Reduced Power Levels*, ORNL CF-50-4-17, April 3, 1950.

(9) Huffman, J. R., *Cooling After Shutdown*, ORNL CF-48-6-155, June 7, 1948.

(10) Way, K., and Wigner, E. P., *The Rate of Decay of Fission Products*, MonP-303, May 19, 1947; "The Rate of Decay of Fission Products," *Phys. Rev.* **73**, 1318 (June 1, 1948).

(11) Way, K., *Fission Product Poisoning, Lecture 16, Clinton Laboratories Training Program*, M-3690, April 14, 1947.

(12) Weinberg, A. M., *Estimate of the Shielding Requirements for the High Flux Pile*, ORNL CF-46-11-66, November 1, 1946.

(13) Evans, R. D., "Radioactivity Units and Standards," *Nucleonics*, Vol. 1, No. 2, pp. 32-43, October 1947.

(14) Tirpak, E. G., *Report on the Use of Barytes Aggregates in Concrete for Shielding Purposes*, ORNL-667, April 13, 1950.

(15) Burnett, T. H. J., *High Density Concrete Shielding Test*, ORNL CF-49-12-75, December 19, 1949.

(16) Burnett, T. H. J., *Subsequent Tests - MTR Shield Efficiency*, ORNL CF-50-8-183, March 29, 1950.

(17) Podgor, S., *Neutron Relaxation Length in Barytes Concrete*, ORNL CF-50-4-54, April 13, 1950.

(18) Lansing, N. F., *Letter and Attachment re Barytes Cement by M. Greenhill to C. E. Knesel*, ORNL CF-50-9-54, September 15, 1950.

(19) Blizard, E. P., and Clifford, C. E., *Measurements of Iron and Borated Water Shield in the Lid Tank - Experiment 10,* ORNL CF-50-12-47, December 14, 1950.

(20) Blizard, E. P., *Reactor Shielding with an Iron Aggregate Concrete, Comparison with Ordinary Concrete,* ORNL-209, March 16, 1949.

(21) Briggs, R. B., *Heat Production in the Bottom Thermal Shield of the Materials Testing Reactor,* ORNL-CF-49-12-1, December 1, 1949.

(22) Briggs, R. B., *Neutron Fluxes and Heat Production in the Top and Side Thermal Shields of the MTR,* ORNL CF-50-1-18, January 6, 1950.

(23) Rockwell, T., and Kitzes, A. S., *Theoretical and Practical Aspects of Shielding,* ORNL-710, pp. 272-292, September 29, 1950.

(24) Briggs, R. B., *Comparison of Design Neutron Fluxes and Heat Production in the Graphite Reflector and Thermal Shield of the Materials Testing Reactor with Values Measured in the MTR Mock-Up,* ORNL CF-50-7-86, July 20, 1950.

(25) Beall, S. E., *Reactor Physics Experiments in the MTR Mock-Up,* ORNL-972 (to be issued).

(26) Lansing, N. F., *Approximate Analysis by E. P. Blizard of Experiment to Measure Neutron Penetration of the Thermal Shield,* ORNL CF-51-2-31, February 2, 1951.

(27) Lane, J. A., *Top Plug Shielding Calculations,* ORNL CF-48-8-305, August, 18, 1948.

(28) Lane, J. A., *Shielding Requirements for the Top and Bottom Plugs,* ORNL CF-50-7-7, July 17, 1950.

(29) Lansing, N. F., *Thickness of Door Under Bottom Plug,* ORNL CF-50-6-25, June 2, 1950.

(30) Thornton, G., *MTR Shield Survey Report No. 2,* ORNL CF-49-10-184, October 19, 1949.

(31) Thornton, G., *MTR Shield Survey Report No. 3,* ORNL CF-49-12-18, December 5, 1949.

(32) Clifford, C. E., and Mauney, T. H., *Gamma Attenuation Measurements Through Water in the MTR Mock-Up,* ORNL CF-50-8-85, November 3, 1950.

(33) Hamermesh, B., *Neutron Capture Gamma Ray Spectra,* ANL-4447, May 1, 1950.

(34) Smith, N. M., *Shielding of the External Water Pipes in the High Pressure Water Pile,* ORNL CF-48-3-264, March 4, 1948.

(35) Smith, N. M., *Is Shielding of Sub-Pile Room from Pile Water Activity Adequate?* ORNL CF-49-1-238, January 18, 1949.

(36) Noderer, L. C., *Shielding of Water Inlet Pipes,* ORNL CF-49-6-200, June 10, 1949.

(37) Lane, J. A., *Calculation of Pile Coolant Activities,* ORNL CF-49-7-240, July 26, 1949.

(38) Lane, J. A., *Water Monitoring Shielding,* ORNL CF-50-3-86, March 17, 1950.

(39) Farmer, W. S., *Activities in Process Water,* ORNL CF-47-4-115, April 7, 1947.

(40) Lane, J. A., *Calculation of Pile Coolant Activities,* ORNL CF-49-7-240, July 26, 1949.

(41) Noderer, L. C., *Shielding of Water Inlet Pipes,* ORNL CF-49-6-200, June 10, 1949.

(42) Lennox, D. H., *Process Water Activity,* ANL-EKF-44, March 8, 1950.

(43) Lane, J. A., *Activity of Process Water from Exposure of Core Material,* ORNL CF-49-10-186, October 21, 1949.

(44) Persiani, P. J., *Activity of the Process Water Effluent,* ANL-EKF-56, July 13, 1950.

(45) Noderer, L. C., and Coveyou, R., *Thermal Column Neutron Flux,* ORNL CF-47-9-305, September 3, 1947.

(46) Lansing, N. F., *Thermal Neutron Flux Calculations,* ORNL CF-49-11-167, November 16, 1949.

(47) Lane, J. A., *Thermal Column Shielding Requirements,* ORNL CF-50-6-20, June 3, 1950.

(48) Thomas, T. H., *MTR Report on Thermal Column,* ORNL CF-50-2-28, June 16, 1950.

(49) Smith, N. M. and Whitcombe, D., *Is Leakage of Radiation Out of Air Intake Labyrinth Excessive?* ORNL CF-49-4-86, April 7, 1949.

(50) Lane, J. A., *Neutrons Streaming Through Pebble Discharge Chute,* ORNL CF-50-1-157, January 30, 1950.

(51) Lane, J. A., *Shielding Neutron Curtain Slot,* ORNL CF-50-7-14, July 6, 1950.

(52) Rockwell, T., and Kitzes, A. S., *Theoretical and Practical Aspects of Shielding,* ORNL-710, September 29, 1950.

(53) Persiani, P. J., *Shielding of Horizontal Beam Hole Plug,* ANL-EKF-8, October 12, 1949.

(54) Krisberg, N. L., *Calculations on Plug Design,* ANL-EKF-21, September 23, 1949.

(55) Lane, J. A., *Required Thickness of Vertical Graphite Hole Plugs,* ORNL CF-50-4-16, April 3, 1950.

(56) Persiani, P. J., *Shielding of Plugs During Transfer into Coffins*, ANL-EKF-9, October 13, 1949.

(57) Stone, R. S., *Health, Radiation, and Protection*, CH-630, May 7, 1943.

(58) Krisberg, N. L., *Memo on Shielding Requirements of the Reservoir and Associated Pipes*, ANL-EKF-23, December 1, 1949; Krisberg, N. L., *Shielding Calculations for the Working Reservoir and Associated Pipes*, ANL-EKF-24, December 7, 1949.

(59) Leyse, C. F., *Shielding of External Reactor Air System*, ANL-EKF-32, January 26, 1950.

(60) Persiani, P. J., *Shielding of Removable Beryllium Assemblies*, ANL-EKF-10, October 14, 1949.

(61) Lennox, D., *Fuel Assembly Coffin*, ANL-EKF-38, February 9, 1950.

(62) Persiani, P. J., *Calculation of Induced Activities in Commercial Materials*, ANL-EKF-7, October 11, 1949.

(63) Zora, V., *Water Shield Requirements for the MTR Canal*, Blaw-Knox Report No. A-333-3-S, April 21, 1950.

(64) Wilson, I. L., *Some Data on Pile Irradiations*, CRE-414, March, 1949.

(65) Glasstone, S., and Edlund, M. C., *The Elements of Nuclear Reactor Theory*, Parts II and III, TID 385 and 386, November, 1950.

Chapter 5

CONTROL SYSTEM

5.1 INTRODUCTION

The preceding three chapters of the Handbook have described the reactor, its use, and the physics of its design. In this chapter the reactor control system and some of the philosophy behind it will be discussed. Like that of the rest of the MTR, the development of the controls has gone on over the last five years; therefore no separate historical development is attempted.

The main portion of the chapter is devoted to a description of the control instruments and system as they now exist in the MTR. While this description inevitably contains some of the history and philosophy of the controls, a separate section is included at the end to discuss some of the reasons for using the present control system.

5.1.1 Review of Requirements. It has been shown in Chap. 4 that the k of the MTR is very much larger than that of the early uranium-graphite reactors and that considerable excess reactivity will be used in order to handle losses due to fuel depletion, experiments, fission product poisons, etc. Any control system designed for such a reactor not only must be able to maintain the machine at any given power but, when necessary, must also be able to overcome quickly all the excess reactivity.

The speed with which the controls must act depends upon the maximum rate at which the reactor can rise in power. Suppose that in a clean, cold reactor some mishap allows the rods to be withdrawn at their maximum rate; as an example, assume this rate to be equivalent to a $\Delta k/k \approx 0.1\%$ per second. In the first few minutes the neutron level will rise only by a factor of ~100, but at the end of this time the reactor will be supercritical and on a rising period of approximately 10 sec. In a few more seconds the period will be approximately 1 sec. It has been calculated[1] that the minimum period expected before the power goes above normal operation level will be about 1/30 sec. Such a period must be countered by safeties capable of a 30-msec response. Even with this speed of response the power would momentarily rise to about three times "normal" overload power or to about four times operating power.

From the above paragraph it is obvious that the control rods must not be withdrawn too rapidly, but another condition is imposed in restarting the reactor after a short shutdown. In this case the time available is limited by xenon growth (see Chap. 4); hence the rods must be withdrawn as quickly as possible. In order to fulfill both these conditions, the control system has been designed to limit the "high" rate of rod withdrawal to an equivalent $\Delta k/k$ of 0.1% per second.

The above paragraphs briefly review the main dynamic requirements of the control system. The control system described in the following sections is designed to fulfill these requirements and provide a means of maintaining the reactor at any given power level.

5.1.2 General Features of the MTR Control System. A block diagram, showing the essential elements of the reactor control system, is given in Fig. 5.1.A. In this diagram the light lines indicate flow primarily of information, signal, or effect; the heavy lines indicate flow primarily of energy. It is understood that this diagram shows only the major relationships among the control system elements.

The reactor is shown to be subject to effects of the control rods, auxiliary facilities, and certain disturbances. The reactor in turn affects certain instruments which produce information to be transmitted to the operator and to the control system. The operator and the control system also receive information from selsyns and other indicators of rod position or rod motion. On the basis of the information received, taken together with the operator's actions or instructions, the control system transmits to the motors or magnets (also called "clutches") appropriate control signals. The motors or magnets then cause corresponding rod motions, which in turn affect the reactor. Thus the main control loop is a closed path, indicated in the diagram by light lines.

The heavy lines indicate the flow of energy from an external source to the control system to operate amplifiers, relays, etc., and to motors, magnets, and the auxiliary facilities to operate pumps, fans, etc. These are the principal power demands relevant to the control system. To isolate the control system from fluctuations and interruptions of external power an energy conversion and storage unit is provided. The status of this unit is reported by certain instruments to the operator, who can exert a limited degree of

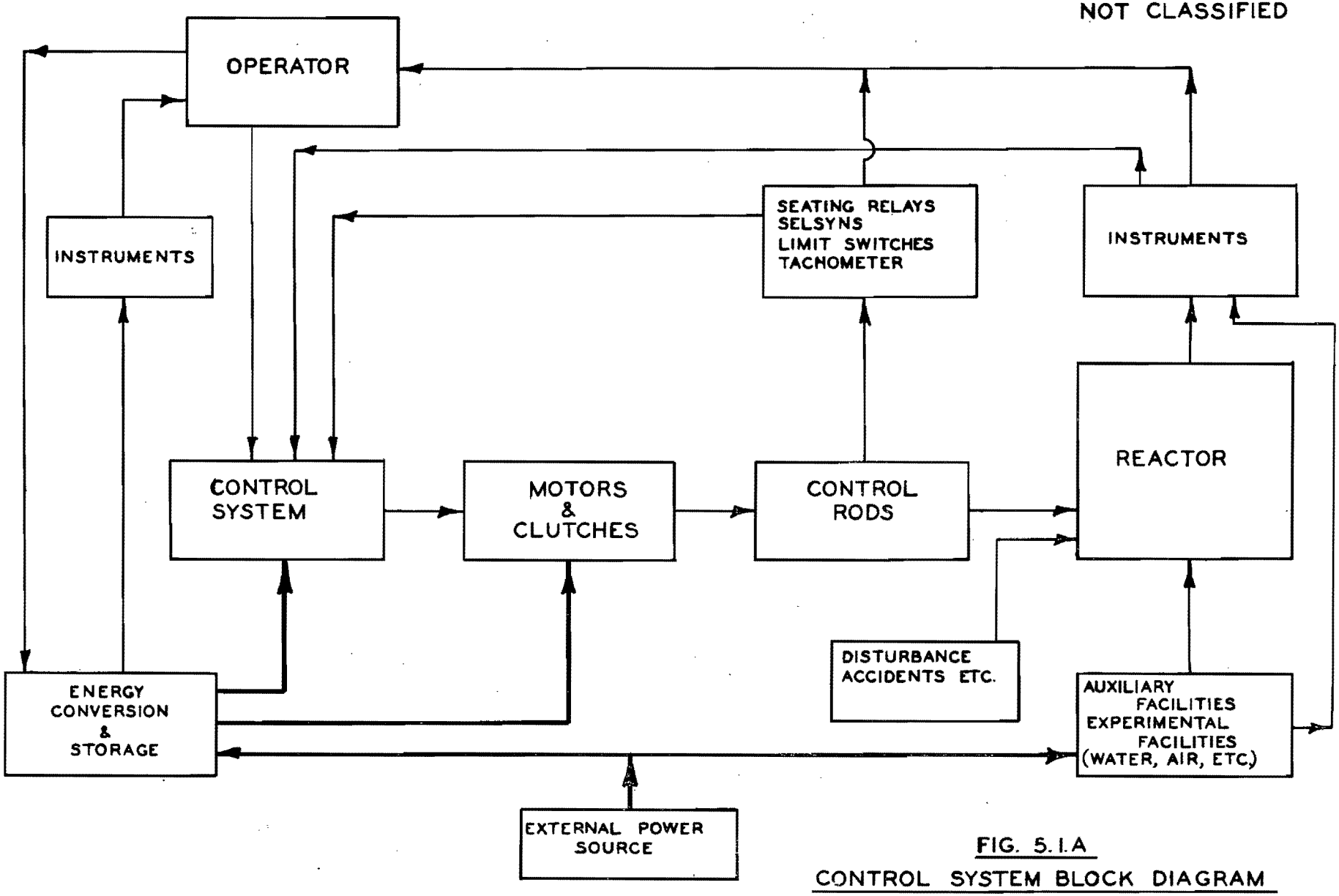

FIG. 5.1.A
CONTROL SYSTEM BLOCK DIAGRAM

control on it. Full discussions of the power distribution system and of the auxiliary facilities are given elsewhere (Chaps. 3, 6, 7, 8, and 10), but they are included here to the extent that they are interrelated with the control problem.

5.2 MEASURING INSTRUMENTS

There are three groups of instruments furnishing information to the operator and to the control system: (1) the reactor instruments measuring neutron flux or power level, (2) the rod position and motion indicators, and (3) the instruments for the auxiliary facilities and energy conversion and storage. These groups will be discussed in the order mentioned. The way in which the instrument signals are presented to the operator, recorded, or used in the control system will be discussed in later sections.

5.2.1 Reactor Instruments. It is necessary to draw a rather arbitrary line separating reactor instruments from instruments on the auxiliary facilities, particularly the cooling water. Reactor instruments will be understood to include radiation instruments measuring neutron level in the reactor and radioactivity in the water, temperature instruments measuring distribution of exit water temperature across the active lattice and temperatures in the thermal and biological shields, and pitot tubes measuring distribution of water flow across the bottom (exit) of the active lattice. (See Fig. 5.2.A).

The reactor radiation instruments are listed in Table 5.2.A. It will be noticed that with one exception these instruments are located in the reactor. The one exception, the water monitor chambers, can reasonably be included with the reactor instruments since they monitor water samples from the 37 sampling tubes distributed across the bottom of the active lattice.

The parallel circular plate (PCP) and compensated ionization chambers and the fission chamber are of ORNL design and manufacture. The air wall and water monitor chambers are made by General Electric Company, and the boron thermopiles are made by Nuclear Instrument and Chemical Corporation.

When the MTR was proposed in 1946, the best available ionization chamber had a useful range of about 10^4. The development of the compensated ionization chamber with useful range of better than 10^6 was the first step. Early

TABLE 5.2.A

Reactor Radiation Instruments

NAME OF INSTRUMENT	REFERENCE ITEM NO.	USE	REACTOR LOCATION
Parallel circular plate ionization chamber	650-1A, 2A, 3A	Safety	VN-1, 2, 3
	652-1A, 2A	Servo signal	VN-5, 6
Compensated ionization chamber	650-4A, 5A	Log *N* and period signal	HI-2, 3
	654-2A	Galvanometer signal	HI-2
Fission chamber, travel 12 ft	654-3A	Counting rate signal	VG-8
Air wall ionization chamber (G.E. No. 9737334G1)	650-11C, 11D	Water flow N^{16} monitoring	GM-1, 2
Water monitor ionization chamber (G.E. No. 9737814)	653-5A, 6A	Water sample monitoring	Monitoring room
Boron thermopiles		Neutron flux in graphite	VG-27, 28, 42, 44, 56

attempts to develop a $d(\log N)$ meter of the vibrating condenser type were unsuccessful and a log N and period meter based on the logarithmic characteristic of the diode proved to be highly satisfactory. This instrument, with a useful range of approximately 10^6, matching the compensated ionization chamber, has become extremely important to the control system.

In an early attempt to cover still lower neutron intensities, the modulated ionization chamber was proposed. This device utilized the periodic motion of an absorber placed before the ionization chamber which resulted in a modulated signal proportional to neutrons only. This was abandoned in favor of the fission chamber and counting rate meter which, by repositioning the fission chamber, is capable of covering a range of 10^{11}. Since this device has a long integrating time, it was felt that the resultant time delays would make it an unsatisfactory instrument for automatic control, and it is therefore used as an adjunct to manual control.

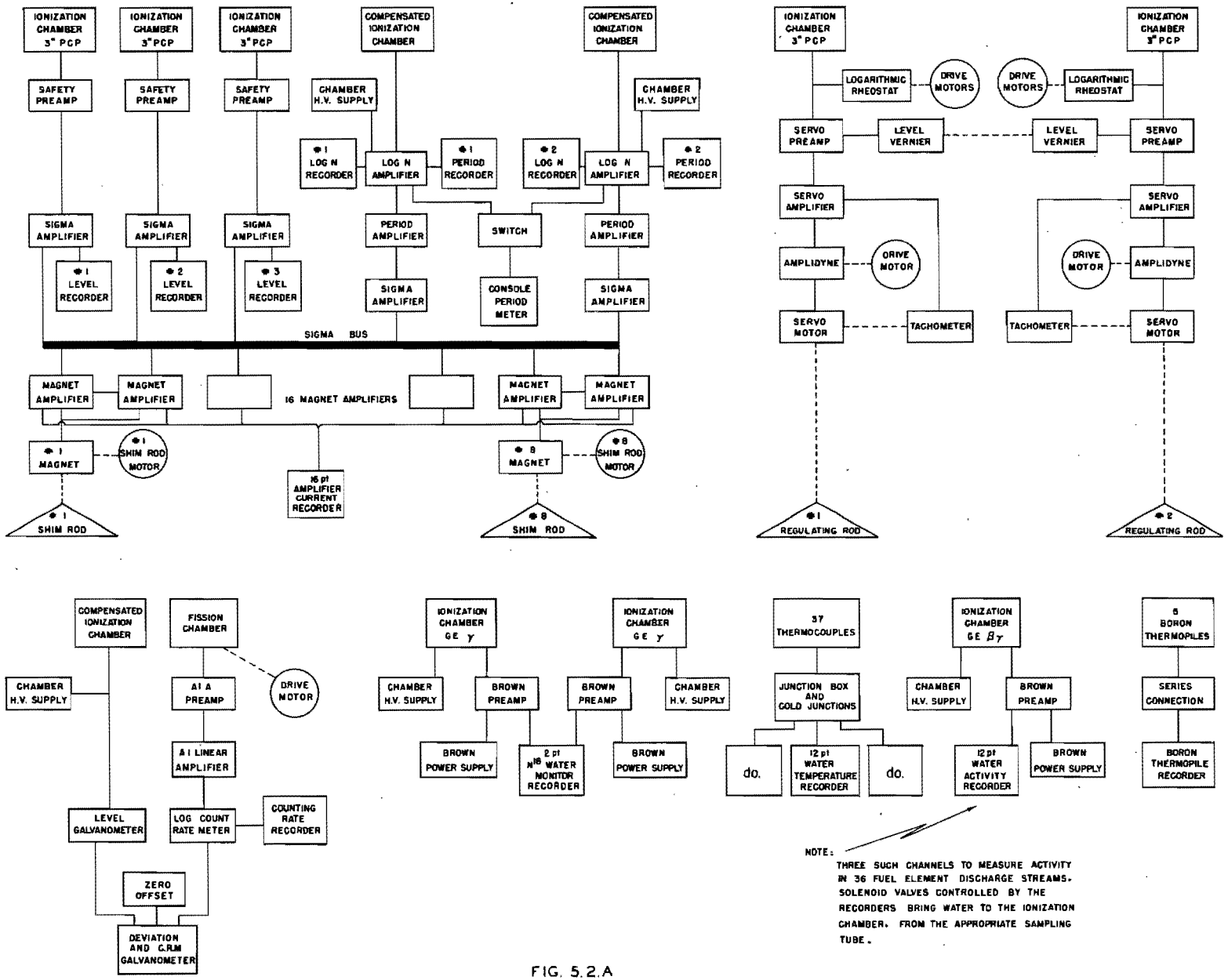

FIG. 5.2.A

MATERIALS TESTING REACTOR INSTRUMENTATION BLOCK DIAGRAM

The importance of having proper instruments for control purposes is made evident by consideration of Table 5.2.B, which shows the relation of power (or neutron) level considered in four definite ranges to the choice of instrument and control action. These ranges, as suggested by H. W. Newson[1] or as applied to the MTR, serve as convenient divisions of the entire range of reactor operation. At the lowest level is the *source range* which lies below

TABLE 5.2.B

Relation of Lower Level to Instruments[1]

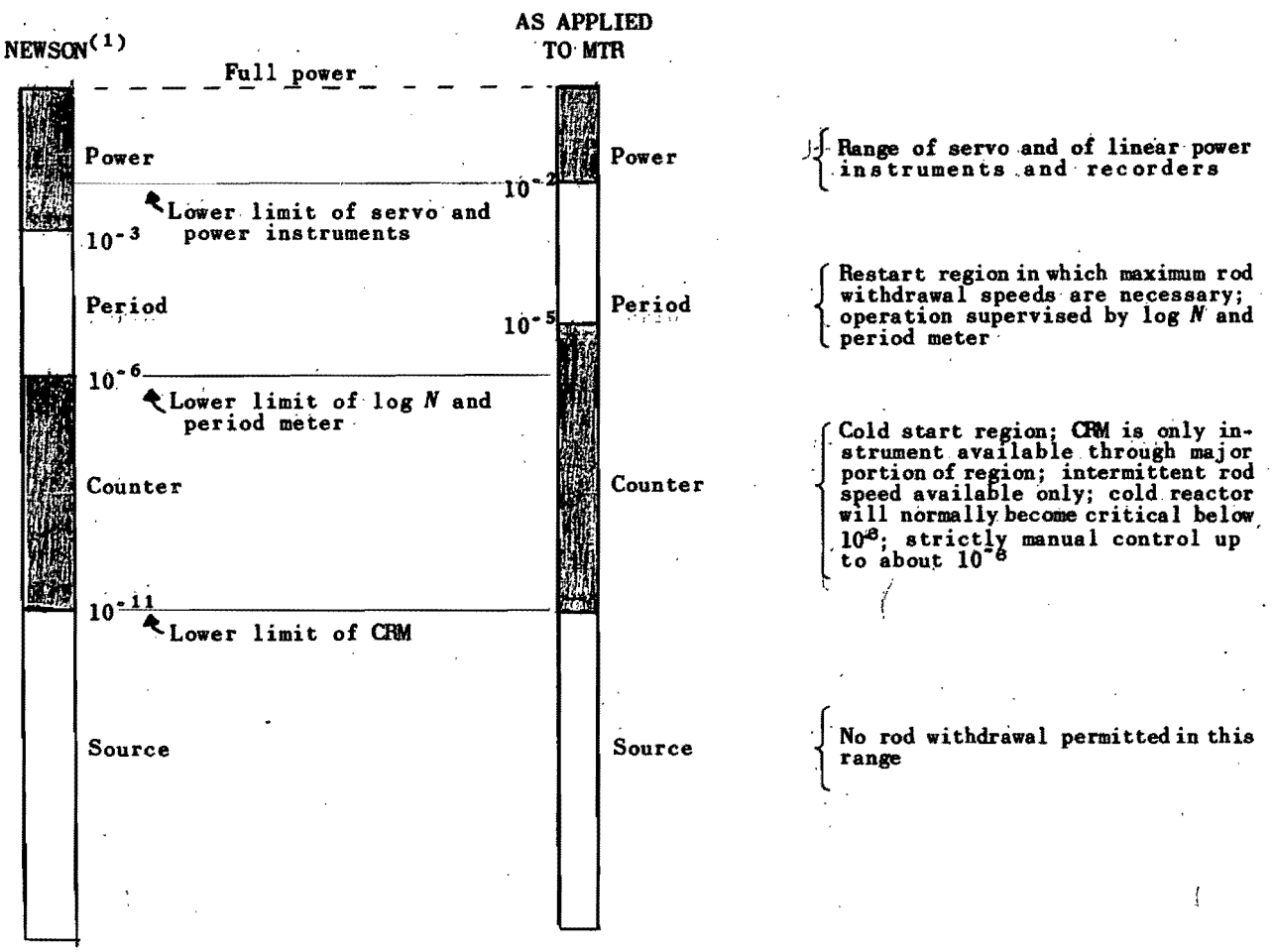

the range of the counting rate meter and in which rod withdrawal should be prohibited. Until the level is raised above 10^{-11} of full power by a suitable source (cf. Chap. 4), the Δk of the reactor should be kept negative; i.e., rods should not be withdrawn. Next comes the *counter range,* in which the fission chamber and counting rate meter combination is the source of a reliable signal. For the MTR only intermittent rod withdrawal is permitted in this range. The lower limit of the period meter makes the transition to the *period range.* By the time this range is reached, the cold, clean reactor will have become critical and the level will be rising on a stable period. Finally comes the *power range,* over which an appreciable fraction of full power may be measured.

PCP Chambers. The PCP chambers are designed, constructed, and located in the reactor so as to give high-speed response to changes in neutron flux coming from the core of the reactor. The construction is shown in Fig. 5.2.B. The active section consists of a set of graphite disks, each of which is coated on both sides with B^{10}. Alpha particles are emitted by the $B^{10}(n,\alpha)Li^7$ reaction when neutrons bombard these disks. These alpha particles cause the ionization which the chamber measures. Thickness of boron coating (0.3 mg/cm^2) on the graphite disks is chosen so as to give maximum ionization current (about 50 μamp at their operating flux of 10^{10} neutrons/cm^2-sec).

The chamber is made of materials (magnesium shell, graphite electrodes, quartz insulators) that do not become highly radioactive under neutron bombardment. Furthermore, the long body of graphite ending in a boron plastic plate at the base shields the connectors and cables from the high neutron flux. This makes handling and servicing of the chamber after it has been in the reactor permissible without elaborate shielding. The chambers cannot be located as near the reactor tank as would be desirable because of the high neutron flux. The next best thing seemed to be to locate the chambers in holes, looking directly toward the tank, with collimating boral sleeves ahead of the chamber to enhance their inherent directional sensitivity to flux directly from the tank. With this arrangement the major delay is the time, estimated at 5 to 10 msec, for neutrons to get from the core through the tank and into the graphite. Thus it is possible to provide a safety signal well within the 30-msec limit set by consideration of reactor kinetics. (A report on the PCP chamber is in progress.)

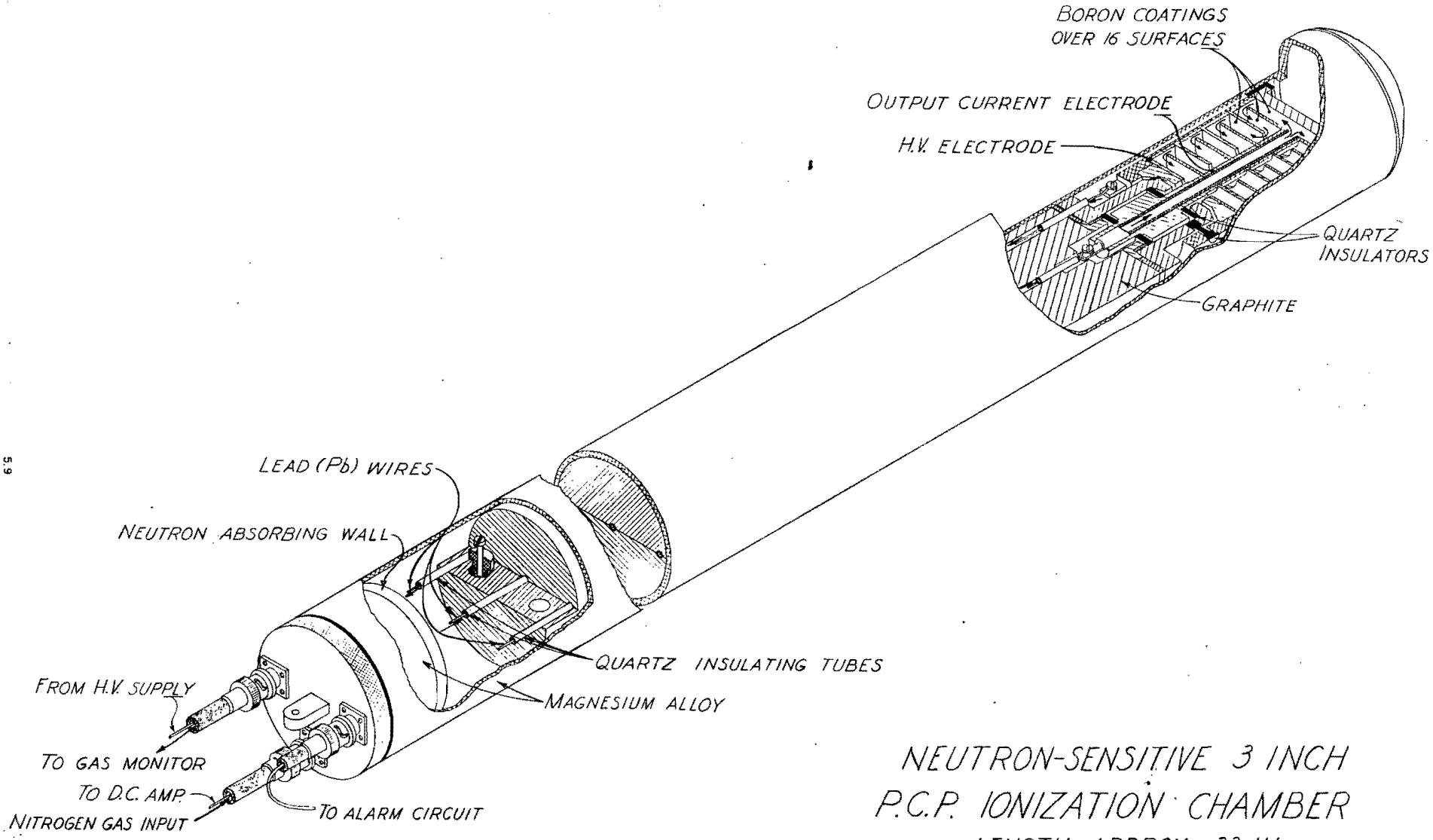

NEUTRON-SENSITIVE 3 INCH
P.C.P. IONIZATION CHAMBER
LENGTH- APPROX. 33 IN.

Q-975-7

NOT CLASSIFIED

FIG. 5.2.B

Compensated Ion Chamber. The compensated ionization chamber is designed to give reliable measurement of neutron flux over a large range, particularly in the presence of relatively intense gamma radiation. The construction, shown in Fig. 5.2.C, features two separate chamber volumes. The inner volume is contained between a movable cup electrode and a fixed inner electrode shell; the outer volume is between this inner shell and an outer electrode shell. The two volumes being approximately equal, the effects of gamma radiation on the two should also be equal. In addition, the outer volume is made sensitive to neutrons by B^{10} coatings applied to the electrode surfaces. Then if the cup electrode is at negative potential and the outer shell electrode at positive potential with respect to the inner shell, the net current carried by the inner shell will be a measure of neutrons alone. Close balancing of the two volumes for zero gamma signal is carried out by moving the cup electrode, thus varying the inner volume. As in the PCP's, the sensitive end of the chamber is made of low-activity materials (pure graphite electrodes, quartz insulators, lead wires, and magnesium shell) and the main body of the chamber is made long to provide shielding of the chamber base from neutrons. The preamplifier circuit used with PCP chambers is shown later in Fig. 5.3.A.

The compensated chamber is to be operated from 100-μamp current at full operating level (N_F) down to 10^{-4} μamp at the bottom of its range. The flux at the chamber when the reactor is at N_F is presumably somewhat over 10^{10}.

Fission Chamber. The fission chamber is designed to give neutron measurements at low flux levels. The construction, shown in Fig. 5.2.D, is quite simple. A brass shell carries a nickel liner with a coating of U^{235} on its inside surface. A central anode rod of graphite, ¼ in. in diameter, is supported on a coaxial connector. Neutrons absorbed in the U^{235} produce fission fragments which ionize the gas in the chamber. The voltage pulse thus created by each fission is amplified and counted. These fission pulses are large, and by proper biasing of the amplifier can be counted separately from the lesser currents due to alpha or gamma radiation; i.e., neutron flux can be accurately measured even in the presence of intense gamma radiation. With the anode at +270 volts, the fission pulse height is some 50 μv across the 450 $\mu\mu$f of cable capacitance. The chamber efficiency is one pulse in a flux of 100 neutrons/cm^2-sec. By using argon gas a short, sharp pulse may be obtained. However, the chamber performance is then very sensitive to gas

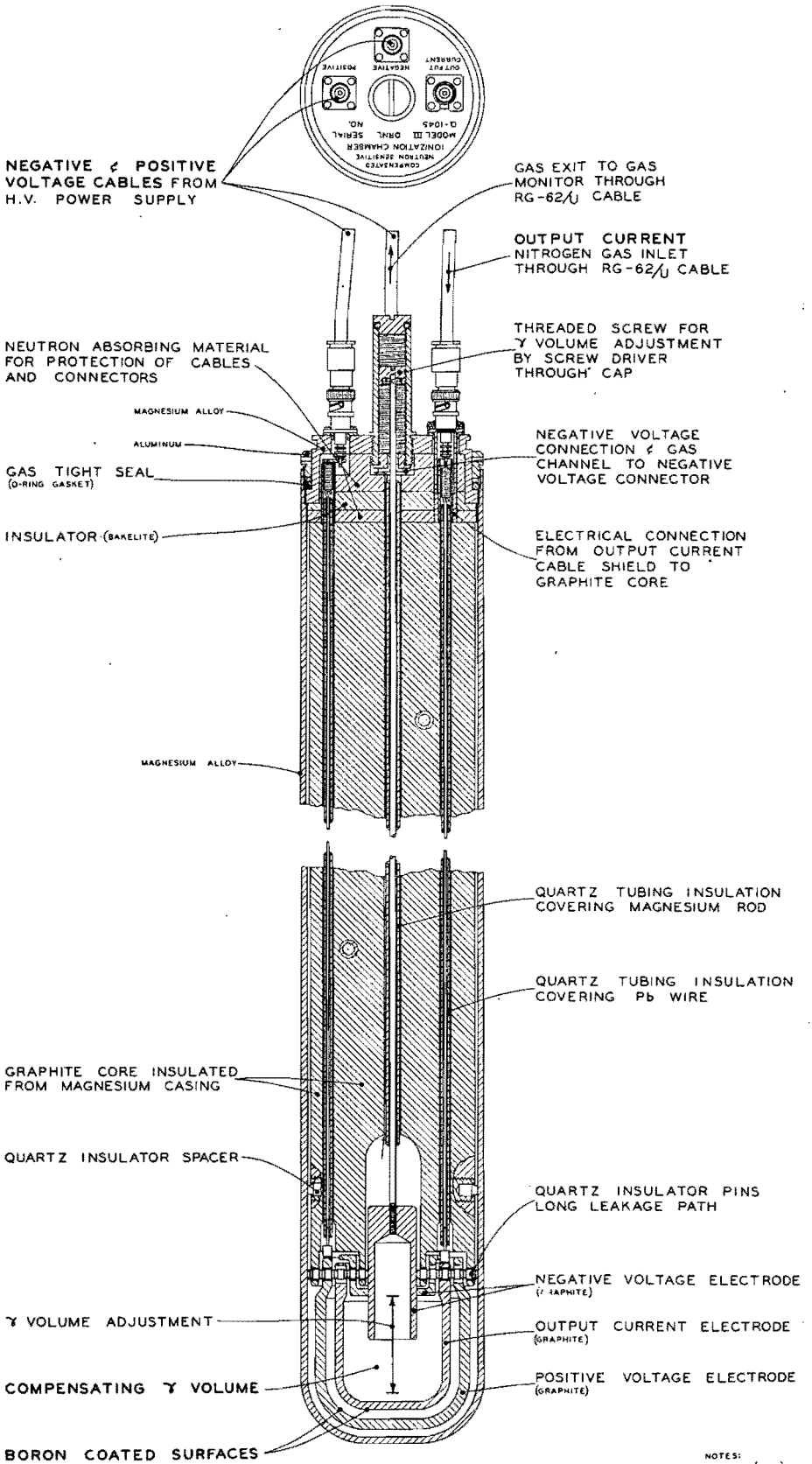

NOTES:
ARROWS (——) INDICATE NORMAL PATH OF GAS FLOW.
OUTSIDE DIAMETER OF CHAMBER 3-3/4"
APPROXIMATE LENGTH OF CHAMBER 36"

FIG. 5.2.C

COMPENSATED IONIZATION CHAMBER NEUTRON SENSITIVE

ORNL Q-1045

Q-1045-10

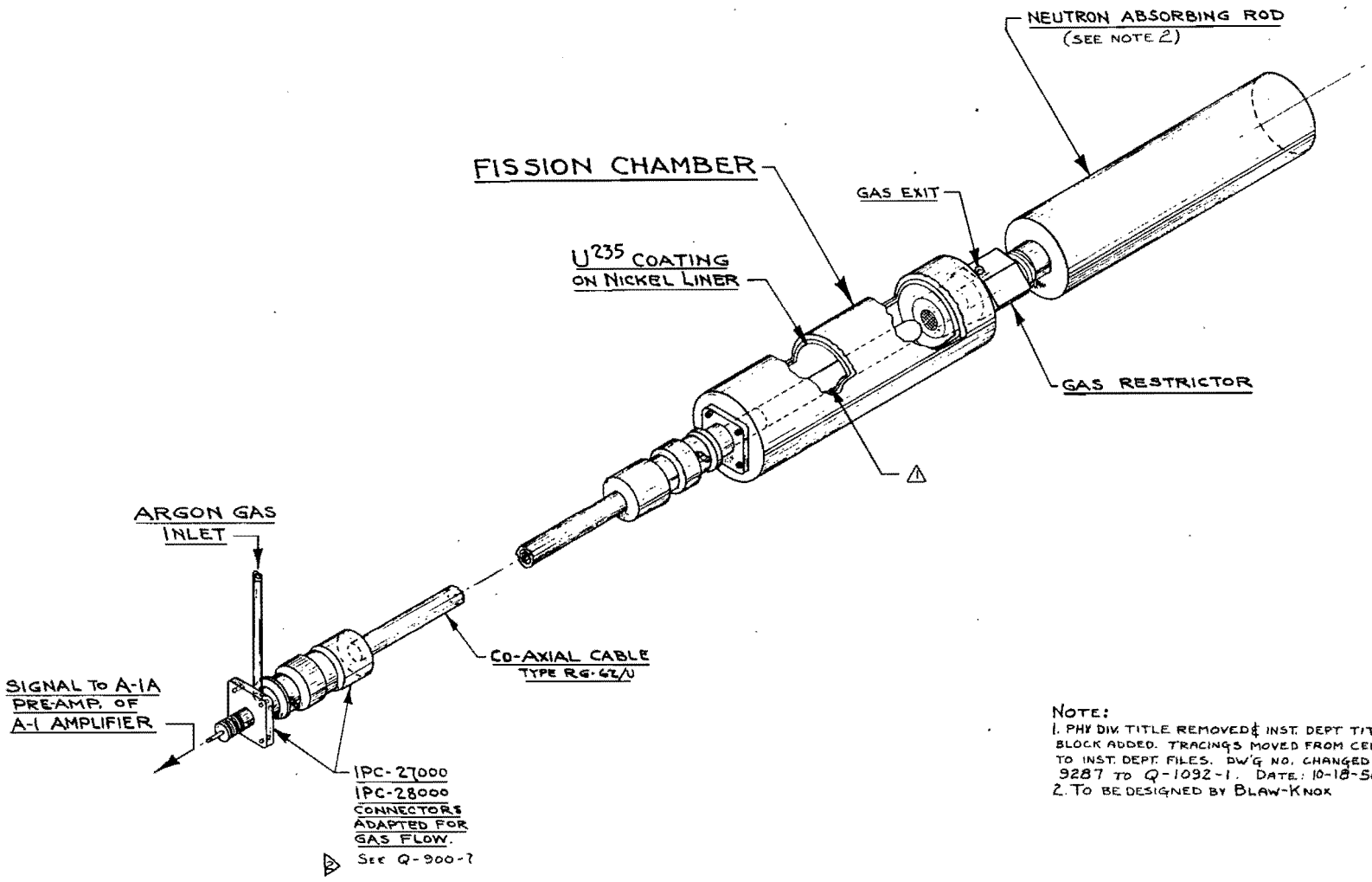

NOTE:
1. PHY DIV. TITLE REMOVED & INST. DEPT. TITLE BLOCK ADDED. TRACINGS MOVED FROM CENT. FILES TO INST. DEPT. FILES. DW'G NO. CHANGED FROM 9287 TO Q-1092-1. DATE: 10-18-50
2. TO BE DESIGNED BY BLAW-KNOX

DESIGNED BY ORNL PHYSICS DIVISION

REVISIONS			
DATE	CODE	CHANGE	CHK.
10-18-50	1	ELECTRODE CHANGED	
10-19-50	2	SEE Q-900-7, PL 2 ADDED	

UNITS OF MEASUREMENT UNLESS OTHERWISE SPECIFIED
FRACTIONS ±
DECIMALS ±
ANGLES ±

FIRST USED
DESIGNED J.C. GUNDLACH
DRAWN BY E. ANDREWS
STARTED
FINISHED MAY 1950
CHECKED
APPROVED

OAK RIDGE NATIONAL LABORATORY
INSTRUMENT DEPARTMENT

FISSION CHAMBER ASSEMBLY

SCALE NONE | Q-1092-1 | C

NOT CLASSIFIED
PER

FIG. 5.2.D

BLAW-KNOX Co. No 654-3a

impurities and to supply voltage; to minimize these difficulties the argon is deliberately mixed with about 5% carbon dioxide. Under these conditions, pulses are distinguishable up to a limiting rate of nearly a million per second. The lower pulse rate limit is set by background, which, aside from electrical pick-up noise, is the negligible (1 count per hour) spontaneous fission occurring in U^{238}. The counting-rate meter used with the fission chamber, however, has a useful range from 1 to 10^4 counts per second, and this is therefore the working counting range of the complete instrument.

To increase the neutron flux range of the instrument provision is made for moving the chamber over a maximum distance of 12 ft, from outside the thermal shield to a point well inside it. This travel corresponds to an estimated neutron flux variation of 10^7. At the innermost position the minimum flux to be expected (say from a source at start-up of a clean reactor) would be about 10^3, corresponding to 10 counts per second. The maximum flux (reactor at N_F) at the inner position would be 10^{13}, and at the outer position about 10^6, corresponding to 10^4 counts per second, the upper limit of the rate meter. In view of this range the fission chamber will be used at three established positions in its instrument hole, motion from one to the other giving a neutron flux range multiplication of about 3×10^3, which is comfortably within the counting rate range of 10^4. Means of moving the chamber are semiautomatic and are tied in with the control circuitry to be discussed later. The exact locations of the three operating positions must be considered a part of installation-calibration procedure. Also entering into the calibration is the neutron absorbing rod shown in Fig. 5.2.D. Besides plugging the hole in which the fission chamber moves, this rod furnishes, in choice of dimensions and materials, further means of achieving desired chamber sensitivities in the three locations.

The three types of ionization chambers discussed thus far (PCP, compensated, and fission chambers) have in common the property of being open chambers with continuously flowing gas. The nitrogen used in the PCP and compensated chambers is fed in through the signal cables and returned through power supply cables, being monitored (for flow rate) on the end of the return cable. The mixture of argon and carbon dioxide used in the fission chamber is fed in through the only cable going to this instrument and then is vented as indicated in Fig. 5.2.D. The decision to use continuously purged gas in these chambers was based largely on the expectation of less trouble in assembly, operation, and maintenance of the instruments. A somewhat incidental advantage is that the gas flow keeps the signal cables free of moisture.

Air-wall Ionization Chamber. The air-wall ionization chamber (G.E. No. 9737334G1) is used to measure the energetic 7-sec gamma activity of N^{16} formed in the $O^{16}(n,p)N^{16}$ process by neutron bombardment of the cooling water. The chambers are located in thimbles in the outlet flow. This signal should constitute a good overall measure of the average reactor core flux. The chamber is 5 in. in diameter by 19 in. long, with cylindrical electrodes. The name "air-wall" signifies that it is made of materials having nearly the same atomic number as air, and hence giving similar scattering. Sensitivity is 5×10^{-12} amp in a gamma ray intensity of 12.5 mr/hr.

Water Monitor Chambers. The water monitor chambers (G.E. No. 9737814) are used in the monitoring room to measure beta and gamma activity in the water drawn through the 37 sampling tubes from the exit face of the active lattice. Thus the distribution of radioactivity in the water flow through the lattice can be observed. Water from each of the 37 tubes is examined every 2 min by an automatic cycling device. The water is held up long enough for the N^{16} activity to become small, so the observed activity is either that induced by the flux in the demineralized cooling water or else it is evidence of a fission break (rupture of fuel element) in the core. Sensitivity of this chamber is 3×10^{-13} amp for 12.5 mr/hr.

Boron Thermopiles. The boron thermopiles are used for an additional check on neutron flux level. They are located in the graphite (VG-27, 28, 42, 44, 56; see Fig. 3.F) all at the same horizontal level. These instruments consist of a large number of thermocouple junctions in series, with alternate junctions coated with boron. The coated junctions become warm owing to absorption of neutrons, thus yielding a net voltage which is a measure of neutron flux. The instrument case is about ½ in. in diameter by 6 in. long. The approximate sensitivity is 6 mv in a flux of 10^{12}. Internal resistance is of the order of 3 to 4 ohms. By proper mounting and thermal insulation of the thermocouples the instruments may be made quite insensitive to ambient temperature (say, 40 μv/°C). For transient conditions the time constant is about 1 sec.

Other Instruments. In addition to the foregoing reactor instruments, all of which measure radiation, there are various temperature and water flow measurements to be mentioned. Each of the 37 sampling tubes is actually part of a triple-function assembly: sampling tube, pitot tube for flow measurement, and thermocouple for water temperature measurement. Knowledge of distribution of water flow velocity and temperature is of obvious value. There

are also numerous thermometric devices used for observing temperatures in other parts of the reactor. Most important of these, from the control standpoint, is the pair of thermocouples in the inlet and outlet water lines, measuring the temperature rise which is then multiplied by total water flow to give power absorbed from the reactor. A venturi flow meter feeds signal to a flow recorder, and the thermocouples feed a differential temperature recorder. Impedances in these recorders are connected in a bridge circuit in such a way that the bridge output is proportional to the product of the two signals. The detector for this bridge is thus the power level recorder.

In the thermal and biological shields there are about fifty positions for thermocouples (see Chap. 2). The signals from these instruments, however, tie into the control of the reactor only through the one annunciator channel reserved for them.

5.2.2 Rod Position and Motion Indicators. Instantaneous positions of all control rods are reported to the operator by selsyns. The generators (transmitters), mounted on the rod drive shafts, are Ford Instrument Company "Telesyn," type 3HG. The motors (receivers), mounted on the control room console, are the same brand, type IF. In addition, the positions of the rods with respect to certain fixed positions are detected by means of lever-operated microswitches. These limit-switch signals go to the control system and to the operator. The shim-safety rods operate two limit switches (see Fig. 5.2.E). The upper switch operates when the rod is withdrawn about 30 in. from the fully inserted position. (The exact location of this limit position is to be adjusted in the field so as to take account of two factors: the actual maximum withdrawal mechanically possible, and the need for keeping some sensitivity of safety rod action.) The lower limit switch is a "back-up" switch whose action would usually be forestalled by action of the other shim rod switches, the clutch (magnet) switch and the seat switch. If the rod is engaged in its holder so the clutch switch is closed, the seat switch would operate to stop the motors when the rod is fully inserted. If the rod has been released (e.g., by safety action) and is resting on the bottom, then the clutch switch would operate to stop the motors as the holder comes into place. Thus the lower limit switch would act only if the rod were not in the reactor or if the clutch or seat switches failed.

The seat switches are mercoid pressure switches which operate on the water pressure change caused by seating of the rod and subsequent reduction of

DWG. # 10546
NOT CLASSIFIED

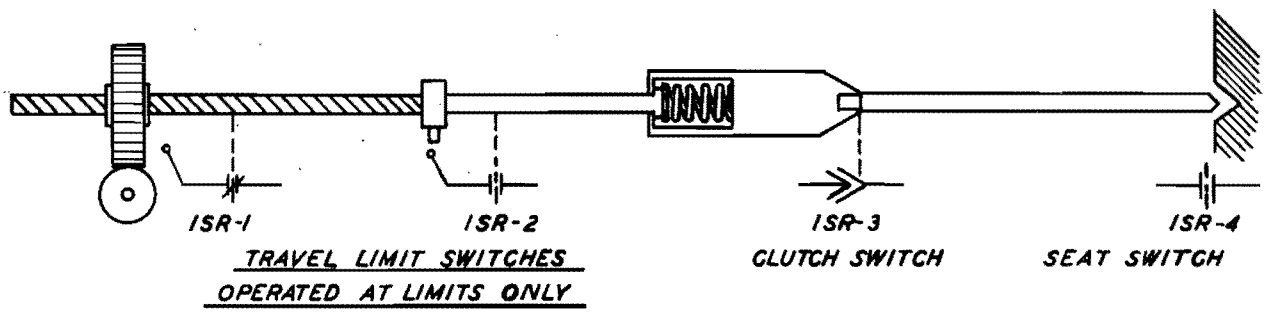

FIG. 5.2.E
SHIM ROD LIMIT SWITCHES

the incoming flow of demineralized water (partial make-up for the process cooling water). The clutch switch operates between the shim rod itself (which is grounded) and the magnet pole faces, which are insulated from ground; this circuit uses 12 volts alternating current.

The regulating rods are equipped with six limit switches (see Fig. 5.2.F). Of these, the two at the extreme positions serve to limit the travel of the regulating rod itself, while the intervening four enter into shim rod control. The regulating rod motion is held in both directions against shock absorbers. The servo motor torque is reduced by the action of the end limit switches to a value which keeps a light load on the shock absorber in the limited direction while leaving the system free to give full instantaneous torque in the opposite direction.

Instantaneous velocity of regulating rods is measured by tachometers mounted on the motor shafts. The Weston Model 724, type A, is used. The instrument has a sensitivity of 50 volts per 1000 rpm and an upper limit of 2000 rpm.

5.2.3 Auxiliary Facilities Instruments. In describing the general scope of the control problem in Section 5.1.1, reference was made to certain auxiliary facilities which are of some concern to the operator and therefore need a place in the control picture. It is, of course, possible that any conceivable detail of associated equipment, however remote, might under some circumstance be of concern to the operator. (This is one reason for having a telephone near the operator.) It seems reasonable to confine attention here to the three vital facilities: process water, cooling air, and control power. Since the instrumentation of these facilities is more or less fully discussed elsewhere (Chaps. 7, 8, and 10), only brief comment on the immediate relevance to control is needed here.

The process water which cools the reactor is perhaps the most important auxiliary facility. Undue changes in temperature or flow of this water can result in just as serious damage to the reactor as undue changes in neutron level. The radiation hazard to personnel is not so great, however, and, because of this and for other reasons, the water instrumentation works with considerably thinner safety margin than is designed into the radiation instrumentation. In particular, the principle of backing up every instrument with an alternative instrument is less thoroughly applied. Water level in the

DWG. #10547
NOT CLASSIFIED

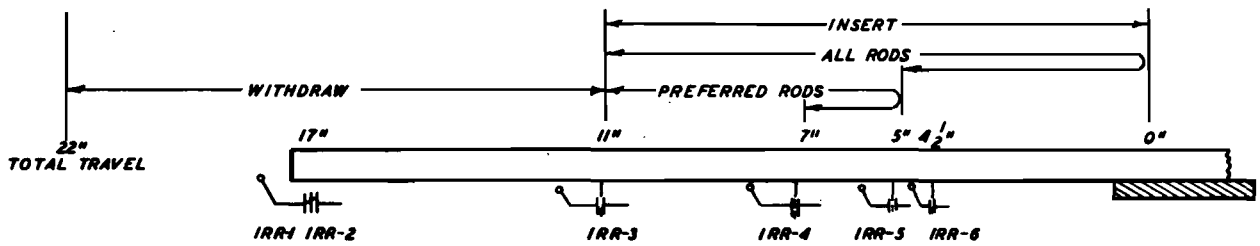

FIG. 5.2.F

REGULATING ROD LIMIT SWITCHES

main tank, or "working reservoir," is guarded with automatic safety actions (see Section 5.5.1, especially Table 5.5.A). The same is true for water flow although this depends on a single flow meter. The water system is provided with sundry alarms and recorders, which need not be detailed here. Most of these will engage the attention of personnel stationed in the process-water control and instrument center and will receive only marginal attention in the reactor control room.

So far as cooling air is concerned, the operator is warned by alarms on pressure and flow of air and also on radioactivity in the air stack. Air flow failure causes a mild automatic safety action (slow setback; see Table 5.5.A).

In order that reactor operation may be as free as possible from the effects of transient disturbances or outages on the purchased-power lines, electrical power for the control system is obtained from a special supply, labeled "Energy Conversion and Storage" in Fig. 5.1.A. This supply consists of two alternators operated from storage batteries. In normal operation one alternator would supply "instrument bus voltage" and the other alternator would supply "relay bus voltage."

The instrument bus furnishes power to those instruments most sensitive to disturbance while the relay bus (also called the "control bus") furnishes power to the less sensitive components, such as relays and motors, which not only are less sensitive to disturbance but are themselves actual sources of disturbance. If one of the alternator supplies breaks down or otherwise becomes unavailable, the relay bus would be switched to purchased power. To permit operation with the "rougher" purchased power, the relay circuits include a 2-sec timer and a number of time delay relays so that reactor shutdown does not ensue unless the relay bus voltage is off for 2 sec or longer.

Reaction of the operator to loss of control power is discussed briefly in Section 5.6.4. Annunciator signals from the control power center may be used to bring to the reactor control room information on such items as battery charger failure and frequency monitoring, but the main link between this center and the operator, both for conveying information to and action from the operator, will be by patrol operation on something like a once-per-hour basis.

5.3 ROD MOTION CONTROLS

5.3.1 Safety Rod Clutches. Safety rod motion is obtained, in general, by the combined action of gravity and water flow. There is also the buoyant force, but it is expected that the downward acceleration will never be less than 1g. The safety action is therefore accomplished by releasing the shim-safety rods from their holders by de-energizing the magnets in the magnetic clutches. This is a continuous process; the magnet current is decreased, not interrupted.

The magnet has been described in Section 2.4.2 of this report, but the control of the magnet current must now be explained. There are eight shim-safety rods and therefore eight magnets, which must be subject to a number of different possible causes of safety signal (these are enumerated in Section 5.5.1). The necessary interconnecting circuitry is centered about a signal line called the "sigma bus" because it carries the summation (more accurately, the net effect) of the various causative signals. The various instrument signals are fed to this bus by special "sigma amplifiers." Figure 5.3.A shows the circuit of a sigma amplifier, together with a typical PCP ionization chamber and preamplifier. The sigma bus is seen to be connected to the cathode of a triode, whose grid accepts the signal from the preamplifier. Increase of ionization current causes the preamplifier grid, and also the sigma amplifier triode grid, to go positive. Then the sigma bus is also driven positive. Assuming this action has occurred in only one of the five sigma amplifiers, the cathodes in the other four amplifiers are also carried positive, and the tubes tend to cut off. One of these tubes can "take over" from the first only if its grid is driven more positive than the first grid. Thus the sigma bus may be said to go along with the "highest bidder" of the various grid potentials. It has therefore been suggested that the sigma bus might be more appropriately named "auction bus." This predominance of auction effect over summation effect is important, for otherwise unwanted safety "scrams" (dropping of rods) would be initiated by cumulation of small effects.

The 16 magnet amplifiers (two for each magnet) are all connected in parallel to the sigma bus. If all 16 amplifiers and all eight magnets were identical in adjustment and operation, all safety rods might be expected to drop strictly simultaneously as the sigma bus potential rises past some critical value. What will actually happen, of course, is that one or several

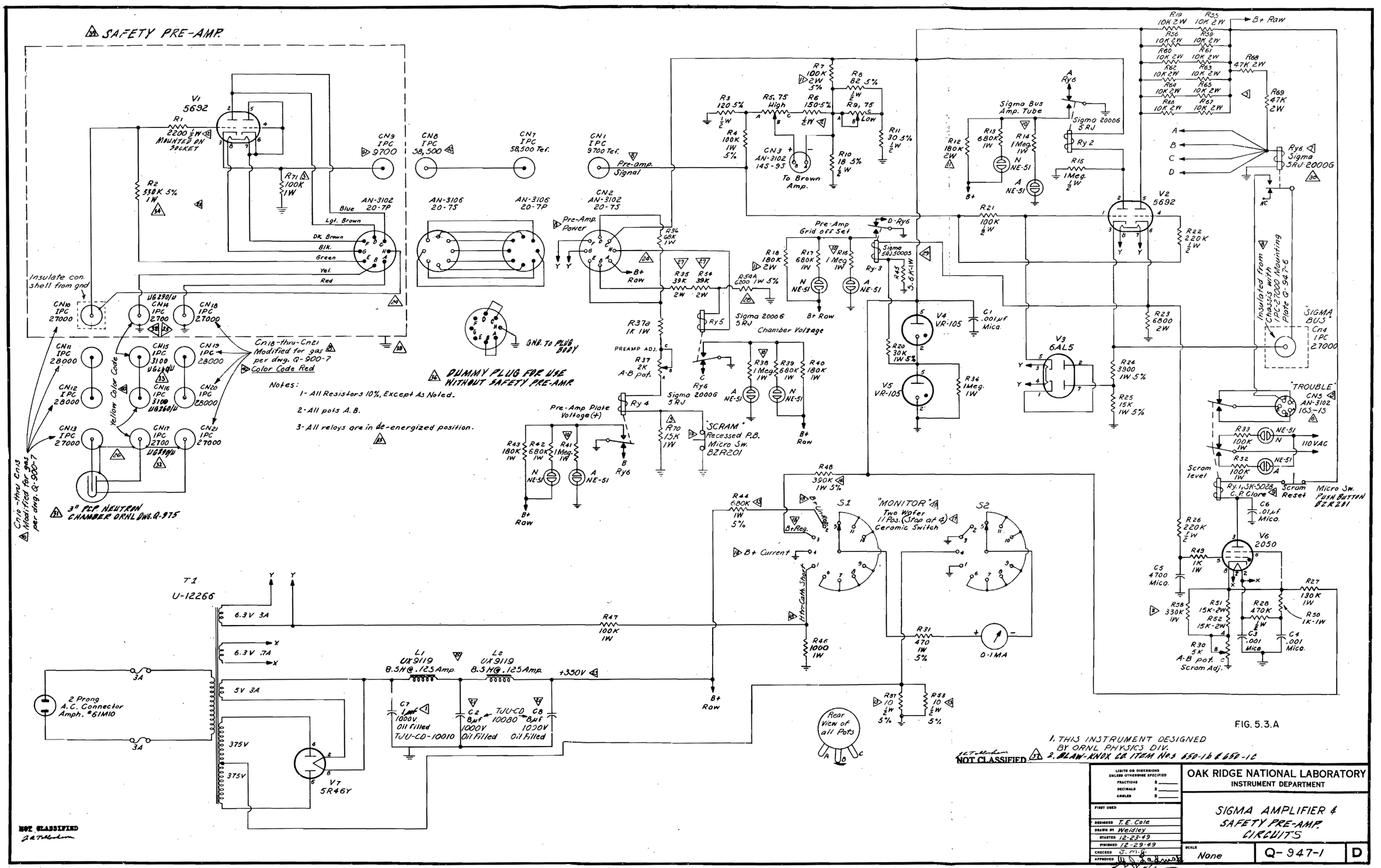
SAFETY PRE-AMP.
V1 5692
R1 2200 ½W MOUNTED ON SOCKET
R2 330K 5% 1W
R71 100K 1W
CN9 IPC 9700
AN-3102 20-7P
Blue
Lgt. Brown
DK. Brown
Blk.
Green
Yel.
Red
Insulate con. shell from gnd
CN10 IPC 27000
UG290/U
CN14 IPC 2700
CN18 IPC 27000
CN11 IPC 28000
CN15 IPC 3100 UG260/U
CN19 IPC 28000
CN12 IPC 28000
CN16 IPC 3100 UG260/U
CN20 IPC 28000
CN13 IPC 27000
CN17 IPC 2700 UG290/U
CN21 IPC 27000
Yellow Color Code
CN18 -thru- CN21 Modified for gas per dwg. Q-900-7
Color Code Red
CN19 -thru CN13 Modified for gas per dwg. Q-900-7
3" PCP NEUTRON CHAMBER ORNL DWG. Q-975
CN8 IPC 58,500
CN7 IPC 58,500 Ref.
AN-3106 20-7S
AN-3106 20-7P
CN1 IPC 9700 Ref.
Pre-Amp. Signal
CN2 AN-3102 20-7S
Pre-Amp. Power
R34 68K 1W
B+ Raw
GND. TO PLUG BODY
DUMMY PLUG FOR USE WITHOUT SAFETY PRE-AMP.
Notes:
1- All Resistors 10%, Except As Noted.
2- All pots A.B.
3- All relays are in de-energized position.
R3 120 5%
R4 100K 1W 5%
R5, 75 High
R6 150 5%
R7 100K 2W 5%
R8 82 5%
R9, 75 Low
R11 30 5%
R10 18 5%
CN3 AN-3102 145-95
To Brown Amp.
R35 39K 2W
R54 39K 2W
R54A 6200 1W 5%
Ry 5
Sigma 20006 5RJ
Chamber Voltage
R37a 1K 1W
PREAMP ADJ.
R37 2K A-B pot.
Ry 4
Ry6 Sigma 20006 5RJ
R38 1Meg 1W
R39 680K 1W
R40 180K 1W
Pre-Amp Plate Voltage (+)
R43 180K 1W
R42 680K 1W
R41 1Meg 1W
R70 15K 1W
"SCRAM" Recessed P.B. Micro Sw. BZR201
R48 390K 1W 5%
R44 680K 1W 5%
B+ Current
S1
"MONITOR" Two Wafer 11 Pos. (Stop at 4) Ceramic Switch
S2
Rear View of all Pots
R46 1000 1W
R47 100K 1W
R31 470 1W 5%
0-1 MA
R51 10 ½W 5%
R53 10 ½W 5%
T-1 U-12266
6.3V 3A
6.3V .7A
5V 3A
375V
375V
3A
3A
2 Prong A.C. Connector Amph. #61M10
V7 5R46Y
L1 UX9119 8.5H@.125Amp.
L2 UX9119 8.5H@.125Amp.
+350V
C7 1µf 1000V Oil Filled TJU-CD-10010
C2 8µf 1000V Oil Filled
TJU-CD 10080
C8 8µf 1000V Oil Filled
Pre-Amp Grid off Sel
R18 180K 2W
R17 680K 1W
R16 1 Meg 1W
Sigma 58,50005
Ry-3
R45 5.6K-1W
Ry6
Sigma Bus Amp. Tube
Sigma 20006 5RJ
Ry 2
R12 180K 2W
R13 680K 1W
R14 1Meg 1W
R15 1Meg ½W
R21 100K ½W
V2 5692
R22 220K ½W
V4 VR-105
C1 .001µf Mica
V5 VR-105
R20 30K 1W 5%
R34 1Meg 1W
V3 6AL5
R23 6800 2W
R24 3900 1W 5%
R25 15K 1W 5%
R19 10K 2W
R55 10K 2W
R56 10K 2W
R59 10K 2W
R60 10K 2W
R61 10K 2W
R62 10K 2W
R63 10K 2W
R64 10K 2W
R65 10K 2W
R66 10K 2W
R67 10K 2W
B+ Raw
R68 47K 2W
R69 47K 2W
Ry6 Sigma 3RJ 20006
Insulated from Chassis with IPC 27000 Mounting Plate Q-947-6
SIGMA BUS
CN4 IPC 27000
"TROUBLE"
CN5 AN-3102 165-13
R33 100K 1W
NE-51
110VAC
R32 100K 1W
Scram level
Ry 1, SK-5028 C.P. Clare
Scram Reset
Micro Sw. PUSH BUTTON BZR201
C6 .01µf Mica
R26 220K ½W
V6 2050
R49 1K 1W
C5 4700 Mica
R58 330K 1W
R31 15K-2W
R52 15K-2W
R28 470K ½W
R27 130K 1W
R30 1K-1W
C3 .001 Mica
C4 .001 Mica
R30 5K A-B pot. Scram Adj.
NOT CLASSIFIED
1. THIS INSTRUMENT DESIGNED BY ORNL PHYSICS DIV.
2. BLAW-KNOX CO. ITEM No. 650-1b & 650-1c
OAK RIDGE NATIONAL LABORATORY
INSTRUMENT DEPARTMENT
SIGMA AMPLIFIER & SAFETY PRE-AMP. CIRCUITS
DESIGNED T.E. Cole
DRAWN BY Weidley
STARTED 12-22-49
FINISHED 12-29-49
CHECKED J.M.G.
APPROVED
SCALE None
Q-947-1
D
NOT CLASSIFIED

FIG. 5.3.A

of the rods will drop before the others, and the number that drop will depend on subsequent time-dependence of the reactivity. Probably the usual scram will consist of the dropping of only one rod.

The circuit diagram of a magnet amplifier is shown in Fig. 5.3.B. The magnet current is drawn from a separate rectifier, fed from a separate power line. This provision for interruption of magnet power without affecting amplifier power makes possible the two kinds of scrams: fast scram by amplifier action, and slow scram by interruption of magnet power. The fast scram channels are reserved for those safety signals which call for action in minimum time; the slow scram is for less urgent signals.

The two amplifiers feeding a given magnet are connected (connector labeled "comp.") so as to share more or less equally the magnet current. If one of the amplifiers should fail, the other would keep the total current near normal, and closing the "normal-exchange" switch gives further margin for operation with one amplifier. A further safety feature incorporated in the design is that a short to ground of the sigma bus will shut off magnet current by increasing the current through the second half of the double triode V5.

5.3.2 Motor Drive of Shim Rods. The motor drives for the shim rods have been described in Section 2.4.5. Here it is necessary only to recapitulate those features directly relevant to control of rod motions.

The shim-rod motors are three-phase 220-volt 1/6-hp squirrel-cage motors, of 1800 rpm rating. Start, stop, and reverse are the only control actions called for. Reversal is accomplished by phase interchange. This simple control picture is, however, slightly complicated by two considerations: the desire to have a finer speed control than is obtained by simple on-off switching, and concern as to the possible safety implications of transition from three-phase to single-phase operation by loss (open circuit) of one power wire.

A highly satisfactory means of having fine control of motor speed was found in the simple device of inserting a single resistor for each phase in the supply to all the shim-rod motors. The large initial current required for high acceleration is cut down by the resistor, giving a low acceleration start. Thus manual on-off switching can give a close, fine-scale adjustment of rod position. This use of "low" speed is discussed in Section 5.5.2. The resistor is chosen with such power rating (350 watts) that it will safely

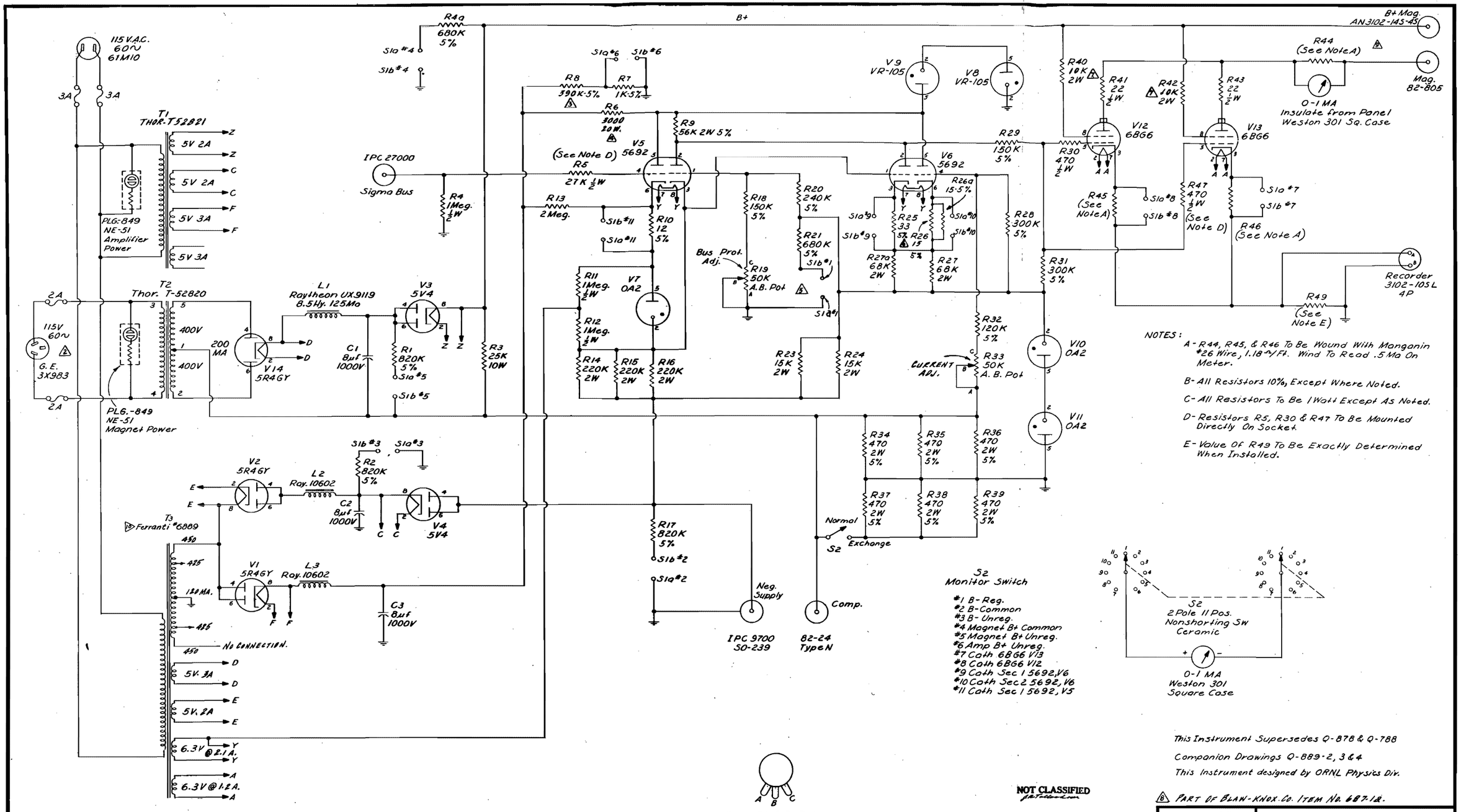
115 V.A.C. 60~ 61M10
3A
3A
T1 THOR-T52821
5V 2A
5V 2A
5V 3A
5V 3A
PL6-849 NE-51 Amplifier Power
2A
115V 60~
G.E. 3X983
2A
T2 Thor. T-52820
400V
400V
PL6-849 NE-51 Magnet Power
200 MA
V14 5R4GY
L1 Raytheon UX9119 8.5Hy. 125Ma
C1 8µf 1000V
V3 5V4
R1 820K 5% S1a #5
S1b #5
R3 25K 10W
R4a 680K 5%
S1a #4
S1b #4
IPC 27000
Sigma Bus
R4 1Meg. ½W
B+
S1a #6
S1b #6
R8 390K-5%
R7 1K-5%
R6 3000 20W.
R9 56K 2W 5%
V5 5692
(See Note D)
R5 27K ½W
R13 2Meg.
S1b #11
S1a #11
R10 12 5%
R11 1Meg. ½W
V7 OA2
R12 1Meg. ½W
R14 220K 2W
R15 220K 2W
R16 220K 2W
R18 150K 5%
R20 240K 5%
R21 680K 5%
S1b #1
Bus Prot. Adj.
R19 50K A.B. Pot
S1a #1
R23 15K 2W
R24 15K 2W
V9 VR-105
V8 VR-105
R29 150K 5%
V6 5692
R26a 15-5%
S1a #9
S1b #9
R25 33 5%
R26 13 5%
S1a #10
S1b #10
R27a 68K 2W
R27 68K 2W
R28 300K 5%
R31 300K 5%
R32 120K 5%
R33 50K A.B. Pot
CURRENT ADJ.
V10 OA2
V11 OA2
R34 470 2W 5%
R35 470 2W 5%
R36 470 2W 5%
R37 470 2W 5%
R38 470 2W 5%
R39 470 2W 5%
R40 10K 2W
R41 22 ½W
R42 10K 2W
R43 22 ½W
V12 6BG6
V13 6BG6
R30 470 ½W
R45 (See Note A)
R47 470 ½W (See Note D)
R46 (See Note A)
S1a #8
S1b #8
S1a #7
S1b #7
B+ Mag. AN3102-145-45
R44 (See Note A)
Mag. 82-805
0-1 MA Insulate from Panel Weston 301 Sq. Case
Recorder 3102-105L 4P
R49 (See Note E)
S1b #3
S1a #3
R2 820K 5%
V2 5R4GY
L2 Ray. 10602
C2 8µf 1000V
V4 5V4
T3 Ferranti #6889
450
425
120 MA.
425
450
No CONNECTION.
V1 5R4GY
L3 Ray. 10602
C3 8µf 1000V
5V. 3A
5V. 2A
6.3V @ 2.1 A.
6.3V @ 1.2 A.
R17 820K 5%
S1b #2
S1a #2
Neg. Supply
IPC 9700 SO-239
Normal
Exchange
S2
Comp.
B2-24 Type N
S2 Monitor Switch
#1 B-Reg.
#2 B-Common
#3 B-Unreg.
#4 Magnet B+ Common
#5 Magnet B+ Unreg.
#6 Amp B+ Unreg.
#7 Cath 6BG6 V13
#8 Cath 6BG6 V12
#9 Cath Sec 1 5692, V6
#10 Cath Sec 2 5692, V6
#11 Cath Sec 1 5692, V5
S2 2 Pole 11 Pos. Nonshorting Sw Ceramic
0-1 MA Weston 301 Square Case
A B C
Rear Of A.B. Pots
NOTES:
A - R44, R45, & R46 To Be Wound With Manganin #26 Wire, 1.18 Ω/Ft. Wind To Read .5 Ma On Meter.
B - All Resistors 10%, Except Where Noted.
C - All Resistors To Be 1 Watt Except As Noted.
D - Resistors R5, R30 & R47 To Be Mounted Directly On Socket.
E - Value Of R49 To Be Exactly Determined When Installed.
This Instrument Supersedes Q-878 & Q-788
Companion Drawings Q-889-2, 3 & 4
This Instrument designed by ORNL Physics Div.
PART OF BLAW-KNOX CO. ITEM No. 687-12.
NOT CLASSIFIED
OAK RIDGE NATIONAL LABORATORY
INSTRUMENT DEPARTMENT
MAGNET AMPLIFIER CIRCUIT
DESIGNED Cole
DRAWN BY Weldley
STARTED 10-4-50
FINISHED 10-5-50
SCALE NONE
Q-889-1
D

FIG. 5.3.B

carry the load when all eight motors are turned on. However, its resistance is such (of the order of 40 ohms) that it will normally permit the operation of only one motor at a time.

An open circuit in one of the three wires feeding the motors, causing single-phase operation with loss of ability to change direction of rotation, is a hazard that might be serious. For instance, if withdrawal were in progress and an overriding signal for reverse came through, it would be ineffective and withdrawal would continue. In any event, the safety circuits should protect the reactor. This loss-of-phase difficulty, in fact, represents a typical instance of a minor calculated risk. Acceptance of a few such risks permits savings in cost and complexity of equipment, savings which may reasonably be regarded as returns on the extensive investment in safety systems.

5.3.3 Motor Drive of Regulating Rods. The regulating rods are driven by servo-controlled d-c motors. The servo mechanism is a velocity servo giving a motor shaft speed $\dot{\theta}$ proportional to input voltage V_i. Figure 5.3.C shows how the input signal V_i is formed as the difference between a positive voltage measuring ionization current and a negative reference voltage. The positive voltage is the product of the ion-chamber current, proportional to neutron flux, and the resistance in the motor-operated rheostat (MOR). The servo functions so that a positive increment in V_i causes the regulating rod to be inserted. Thus, for any given setting of the MOR, an increase in neutron flux causes an increase in ionization current, and, hence, an insertion of the regulating rod or, conversely, a decrease in the neutron flux, results in rod withdrawal.

The particular function of the MOR is to manage reactor control over the considerable range between N_F (full operating flux) and N_L (about 1% of N_F). Suppose, for example, the reactor is rising with a 20-sec period. Then the current through the MOR would be rising as $e^{\lambda t}$, with $\lambda = 0.05\ \text{sec}^{-1}$. Now, if the motor of the MOR is turning at such speed and in such direction that its resistance is decreasing as $e^{-\lambda t}$, with the same value of λ, the positive part of V_i remains constant, and the regulating rod does not move. The servo might then be said to be holding the reactor on a 20-sec period. The desired action of the MOR is obtained by using a constant-speed motor and an exponential resistance winding. The winding is not continuous but consists of 250 steps,

DWG. #10545
NOT CLASSIFIED

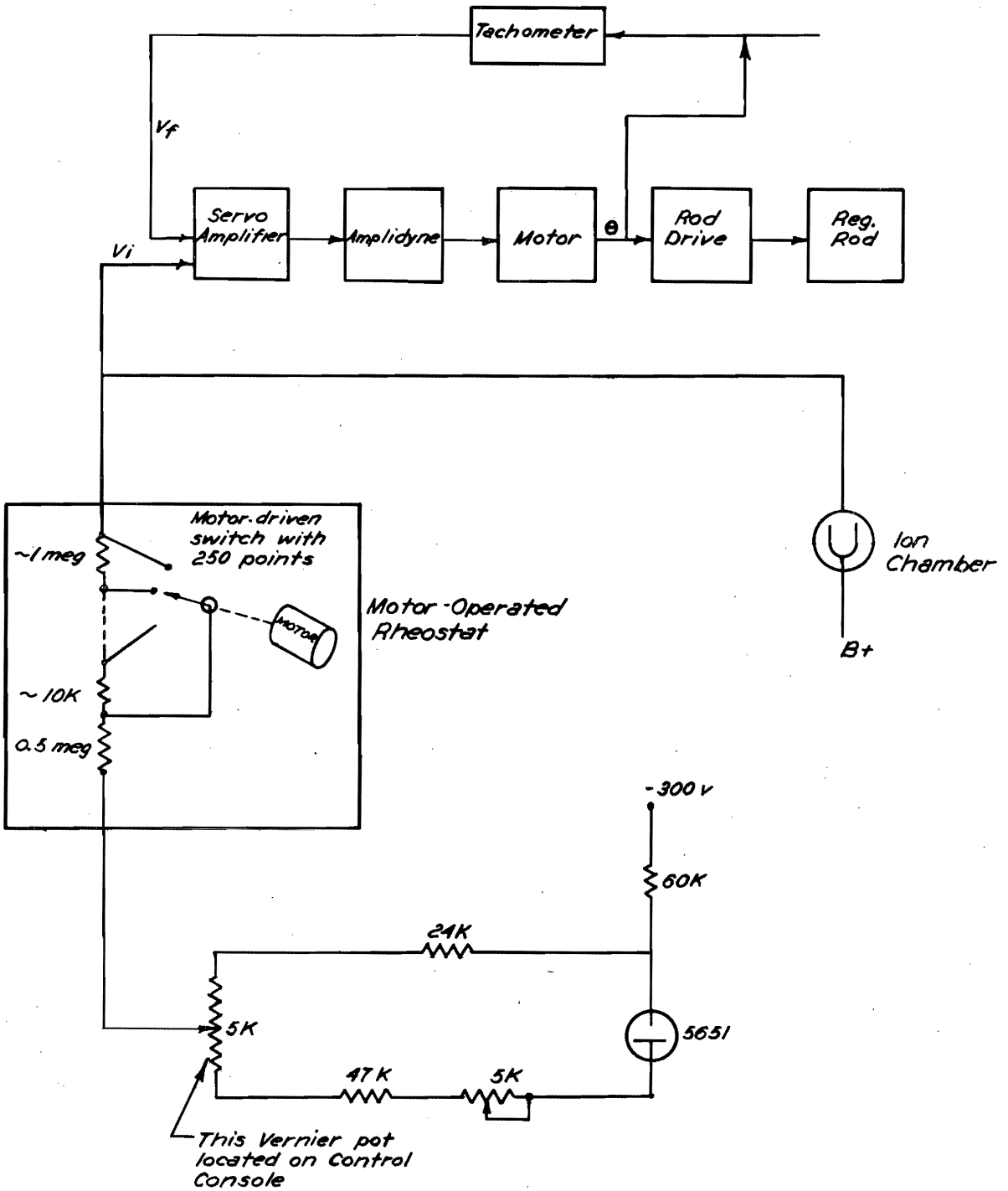

FIG. 5.3.C.

SERVO INPUT SIGNAL

giving a range from minimum resistance of 0.5 megohm to maximum value (after 330° rotation) of 50 megohms. The exponential effect is achieved by making each step proportional to the total resistance at that step. This means a first step of about 10,000 ohms and a final step of about 1 megohm, as indicated in Fig. 5.3.C.

For raising the reactor from N_L to N_F, a 20-sec period is chosen as a safe, fairly rapid possibility. In going down from N_F (i.e., in "setback") such a fast period cannot be managed by the regulating rod because of the latent (delayed neutron) reactivity. Fast setback is still useful as a fast way of lowering reactor level short of a scram, but a slower, 90-sec, period is also provided for slow setback. This means two different speeds for the MOR. To avoid mechanical gear changing, two motors with suitable gear reduction ratios are coupled to the rheostat through a differential. The actual time for the two-decade change is 90 sec for the fast and 7 min for the slow setback.

It is important that the rheostat should not turn in one step from the 50-megohm value to the 0.5-megohm value. Limit switches, backed by mechanical stops, prevent this. Because of the stops, a friction clutch is inserted in the rheostat shaft.

A selsyn reports the position of the MOR shaft to the control console on a scale which is logarithmic so as to match the exponential winding. The setting of the MOR can be changed in the upward direction by the fast motor drive, and in the downward direction by either the fast or slow. A vernier interpolation between the steps of the MOR may also be made from the control console with the 5K potentiometer shown in Fig. 5.3.C.

The d-c motor used to drive the regulating rod is a special General Electric model 5BBY79AB7, 1 hp, with permanent magnetic field. Armature current is derived from a 1500-watt amplidyne, model 5AM78AB78. The drive motor of the amplidyne is a three-phase 440-volt 3.6-amp motor. The rod motor is driven by the amplidyne with armature voltage proportional to the difference in currents flowing in the amplidyne fields. It is therefore the function of the servo amplifier to establish the current difference as proportional to V_i. The circuit of the servo amplifier is shown in Fig. 5.3.D. The amplidyne fields are in the plate circuits of the two pairs of 6BG6 output tubes, operating push-pull. Of each pair of tubes one may be designated "regular" and the other "helper." The two regular tubes have their cathodes tied together.

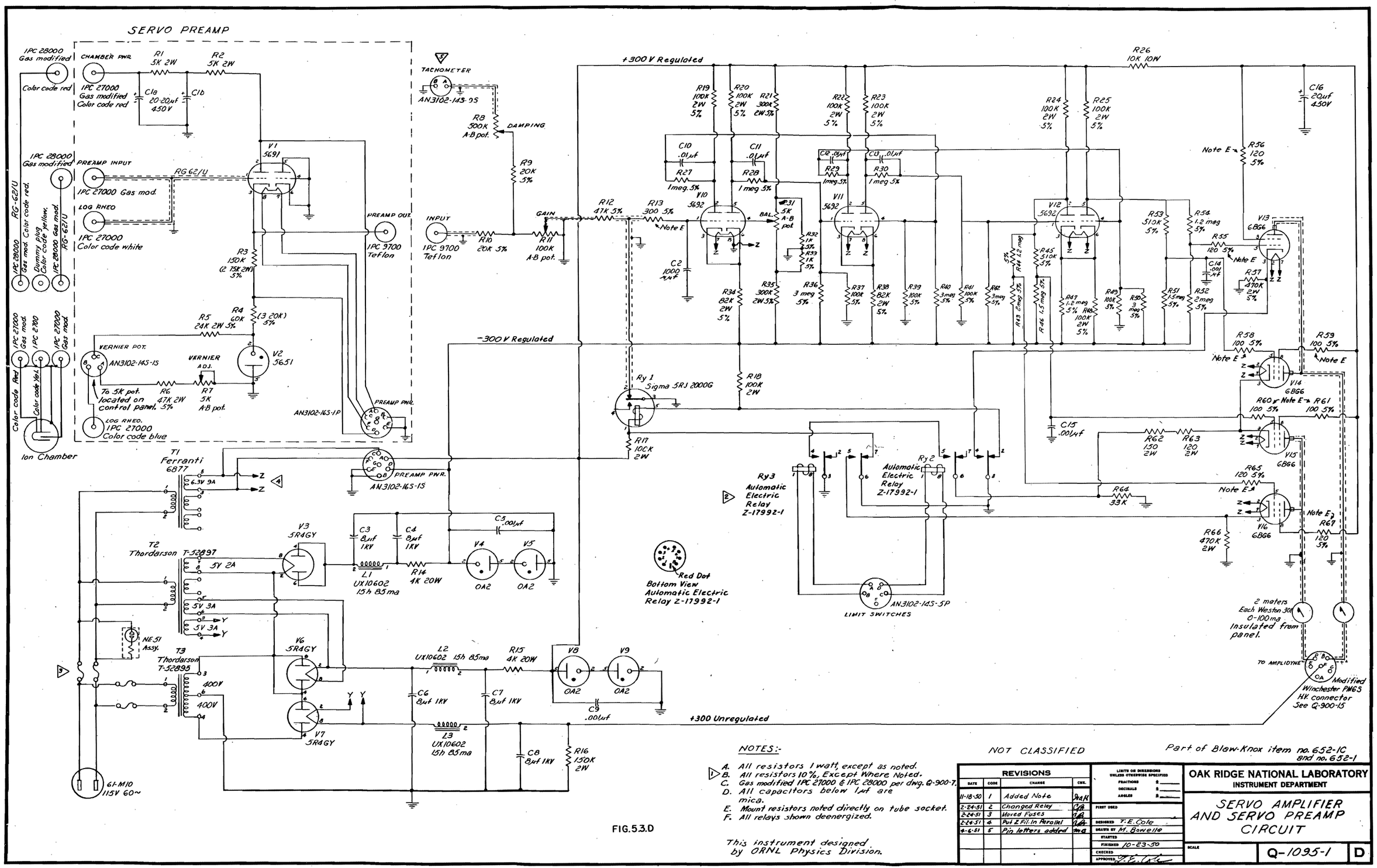
SERVO PREAMP
IPC 28000 Gas modified
CHAMBER PWR.
R1 5K 2W
R2 5K 2W
IPC 27000 Gas modified Color code red
C1a 20-20µf 450V
C1b
Color code red
IPC 28000 Gas modified
PREAMP INPUT
RG 62/U
IPC 27000 Gas mod.
LOG RHEO
IPC 27000 Color code white
V1 5691
PREAMP OUT.
IPC 9700 Teflon
R3 150K (2 75K 2W) 5%
R4 60K (3 20K) 5%
R5 24K 2W 5%
VERNIER POT.
AN3102-14S-1S
VERNIER ADJ.
V2 5651
To 5K pot. located on control panel.
R6 47K 2W 5%
R7 5K A-B pot.
LOG RHEO.
IPC 27000 Color code blue
AN3102-16S-1P
PREAMP PWR.
Ion Chamber
TACHOMETER
AN3102-14S-9S
R8 500K A-B pot.
DAMPING
R9 20K 5%
INPUT
IPC 9700 Teflon
R10 20K 5%
GAIN
R11 100K A-B pot.
+300 V Regulated
R12 47K 5%
R13 300 5%
Note E
BAL.
R31 5K A-B pot
R32 1K 5%
R33 1K 5%
C2 1000 µµf
R34 82K 2W 5%
R35 300K 2W 5%
R36 3 meg 5%
R37 100K 5%
R38 82K 2W 5%
R39 100K 5%
R40 3meg 5%
R41 100K 5%
R42 3meg 5%
R43 2meg 5%
R44 1.2 meg 5%
R45 510K 5%
R46 1.5 meg 5%
R47 1.2 meg 5% R48 100K 2W 5%
R49 100K 5%
R50 3 meg 5%
R51 1.5 meg 5%
R52 2 meg 5%
R53 510K 5%
R54 1.2 meg 5%
R55 120 5%
Note E
R56 120 5%
R57 470K 2W 5%
R58 100 5%
R59 100 5%
R60 Note E R61 100 5%
R62 150 2W
R63 120 2W
R64 33K
R65 120 5%
R66 470K 2W
R67 120 5%
R18 100K 2W
Ry 1 Sigma 5RS 2000G
R17 100K 2W
-300 V Regulated
R26 10K 10W
C16 20µf 450V
C15 .001µf
Ry 2 Automatic Electric Relay Z-17992-1
Ry 3 Automatic Electric Relay Z-17992-1
AN3102-14S-5P
LIMIT SWITCHES
Red Dot
Bottom View Automatic Electric Relay Z-17992-1
2 meters Each Weston 301 0-100 ma Insulated from panel.
TO AMPLIDYNE
Modified Winchester PW63 H.V. connector See Q-900-15
T1 Ferranti 6877
6.3V 9A
T2 Thordarson T-52897
5V 2A
5V 3A
T3 Thordarson T-52895
400V
NE51 Assy.
V3 5R4GY
V6 5R4GY
V7 5R4GY
C3 8µf 1KV
C4 8µf 1KV
C5 .001µf
L1 UX10602 15h 85ma
R14 4K 20W
V4 OA2
V5 OA2
L2 UX10602 15h 85ma
R15 4K 20W
V8 OA2
V9 OA2
C6 8µf 1KV
C7 8µf 1KV
C9 .001µf
L3 UX10602 15h 85ma
C8 8µf 1KV
R16 150K 2W
+300 Unregulated
61-M10 115V 60~
RG-62/U
IPC 28000 Gas mod. Color code red.
Dummy plug Color code yellow.
IPC 28000 Gas mod.
IPC 27000 Gas mod.
IPC 2700
Color code Red
Color code Yel.
NOTES:-
A. All resistors 1 watt, except as noted.
B. All resistors 10%, Except Where Noted.
C. Gas modified IPC 27000 & IPC 28000 per dwg. Q-900-7.
D. All capacitors below 1µf are mica.
E. Mount resistors noted directly on tube socket.
F. All relays shown deenergized.
This instrument designed by ORNL Physics Division.
NOT CLASSIFIED
Part of Blaw-Knox item no. 652-1C and no. 652-1
REVISIONS
DATE CODE CHANGE CHK.
11-18-50 1 Added Note
2-24-51 2 Changed Relay
2-24-51 3 Moved Fuses
2-24-51 4 Put Z Fil. In Parallel
4-6-51 5 Pin letters added
LIMITS OR DIMENSIONS UNLESS OTHERWISE SPECIFIED
FRACTIONS ±
DECIMALS ±
ANGLES ±
FIRST USED
DESIGNED T.E. Cole
DRAWN BY M. Bowelle
STARTED
FINISHED 10-23-50
CHECKED
APPROVED
OAK RIDGE NATIONAL LABORATORY
INSTRUMENT DEPARTMENT
SERVO AMPLIFIER AND SERVO PREAMP CIRCUIT
SCALE
Q-1095-1
D

FIG. 5.3.D

An important feature of this output circuit is the limit-switch action. These switches operate at extremes of regulating-rod travel of 12 in. in the uniform-sensitivity region at the middle of the reactor. The action of the limit-switch circuit, mentioned in Section 5.2.2, is to keep a light load on the shock absorbers in the limited direction while leaving the possibility of full torque in the opposite direction.

In attempting to trace out this action on Fig. 5.3.D, it is necessary to keep in mind that relays 2 and 3 are shown with their coils de-energized, corresponding to both end limit switches being actuated (open). If this is realized, four situations established by the limit switches can be seen: (1) normal operation with both limit switches closed and relays 2 and 3 energized, (2 and 3) two limited conditions with one or the other, but not both, relays energized, and (4) stand-by with both relays de-energized. The stand-by condition is achieved by manual switching, simultaneously opening both limit circuits. For normal operation the regular tubes have normal bias, and the helper tubes can also conduct on very large positive signal. (This particular action of the helper tubes does not affect linearity because it occurs only at such high signal that the amplidyne is already saturated.) In the other extreme of stand-by, both the regular and helper tubes are cut off, and, in addition, the amplifier input is grounded via relay 1. The two limited conditions call for cut-off of the regular tubes but leave one of the helper tubes capable of conducting on large positive grid signal, thus permitting rod motion in the unlimited direction.

Two complete servo channels are provided. The operator chooses the channel to be activated by a manual selector switch. Amplidyne motor power is cut off on the inactive channel, and during this stand-by condition a spring-action brake guards the inactive regulating rod against accidental insertion. When the channel is activated (amplidyne motor on), the brake is released by magnetic action.

The development work on the servo is summarized in ORNL-2. Performance tests therein reported, as well as experience on the MTR mock-up, show that the servo system operates within its design specifications (see Section 2.4.5).

5.3.4 Control System During Maintenance Shutdown. When the reactor is shut down for maintenance servicing, the top plug, carrying the drives and holders of the control rods but not the rods themselves, will be put in dry

dock (cf. Section 2.3.3). Instead of leaving all the instruments and controls completely disconnected, it seemed reasonable to provide connections to the top plug while it is in dry dock so as to permit some checking and servicing of instruments and controls. The general scheme for doing this is as follows:

When the top plug is in place on the reactor, the electrical connections (power connections for the rod drive motors, and signal connections for rod position and motion indicators) are brought to the plug on supporting arms called "semaphores." For removal of the plug to dry dock the cables are disconnected from the plug and the semaphores are dropped to a vertical position, bringing the free ends of the cables down to the sides of the cubicles on which the semaphore arms are mounted. Here they may be connected to cables in conduits running to another connector-board near the dry dock. From this board short connector cables serve the plug in dry dock. To minimize the cost of wiring, not all of the control rod drives can be tested simultaneously. Selection of the drives to be tested is made by selection of inter-connections at the cubicles.

Of the various instrument signals tied into the control system during operation, a certain number (e.g., water flow) must be disconnected during dry-dock testing, since otherwise rod-holder motion would be vetoed by lack of proper signal. This is done by pulling certain test blocks, thus isolating the control actions of the inactive instruments.

To ensure safe return from the dry-dock regime to the operating regime, interlocks on the semaphore arms and on the test blocks are provided. In addition, there is a loop circuit through the connecting cables which tells the operator (by annunciator) whether all the cables are connected for the operating regime. Thus operation is permitted only after the control cables are in place on the top plug, and after all the instrument signals have had their control actions restored.

5.4 CONTROL CONSOLE

The control console, located in the center of the reactor control room (see Section 5.7.1), is made up of five unit panels laid out on a circular arc of 51 in. radius and extending some 240°. At the center of this arc, the operator will be seated in a movable chair, giving him easy access to the information and control elements spread out on the panels. At his left hand is a telephone by which he can communicate with other control and instrument centers, such as the one in the Process Water Building. By looking over the top of the console, which is 40 in. from the floor, he can see the instrument panels, particularly panels D to H, standing in an arc directly in front of him.

On the outside of the console, each of its five units has vertical-hinged doors to give free access to the interior (see Fig. 5.4.A). Each panel is either hinged or otherwise removable so as to give access from the top.

Figure 5.4.A also shows the various indicating and control devices mounted on the panel. These items will be briefly mentioned here. Full significance of some of the terms thus introduced will become clear in the later sections devoted to the workings of the control system.

The panels will be discussed as faced by the operator, from his left to his right. On his extreme left is panel N, carrying eight identical units, one for each of the eight possible shim rod positions. Each unit contains two principal elements, a selsyn receiver dial and a switch. The selsyn dial is calibrated in inches from 0 to 30 with clockwise rotation indicating withdrawal. Associated with the dial are four amber lights which come on, respectively, when the magnetic clutch is not holding its rod, when the upper limit switch is actuated, when the lower switch is actuated, and when the seat switch is actuated. That is, in normal operation, all four lights would be off. The switch has six positions, giving different controls over rod motion, to be detailed in a later section. On either side of the switch are amber lights, the left indicating that a rod is selected for withdrawal, the right that it is preferred for insertion. Also on the left is a red light indicating that withdrawal is in progress, and on the right a similar green light for insertion. Finally, a name plate identifies the shim rod by number.

DWG #10549
NOT CLASSIFIED

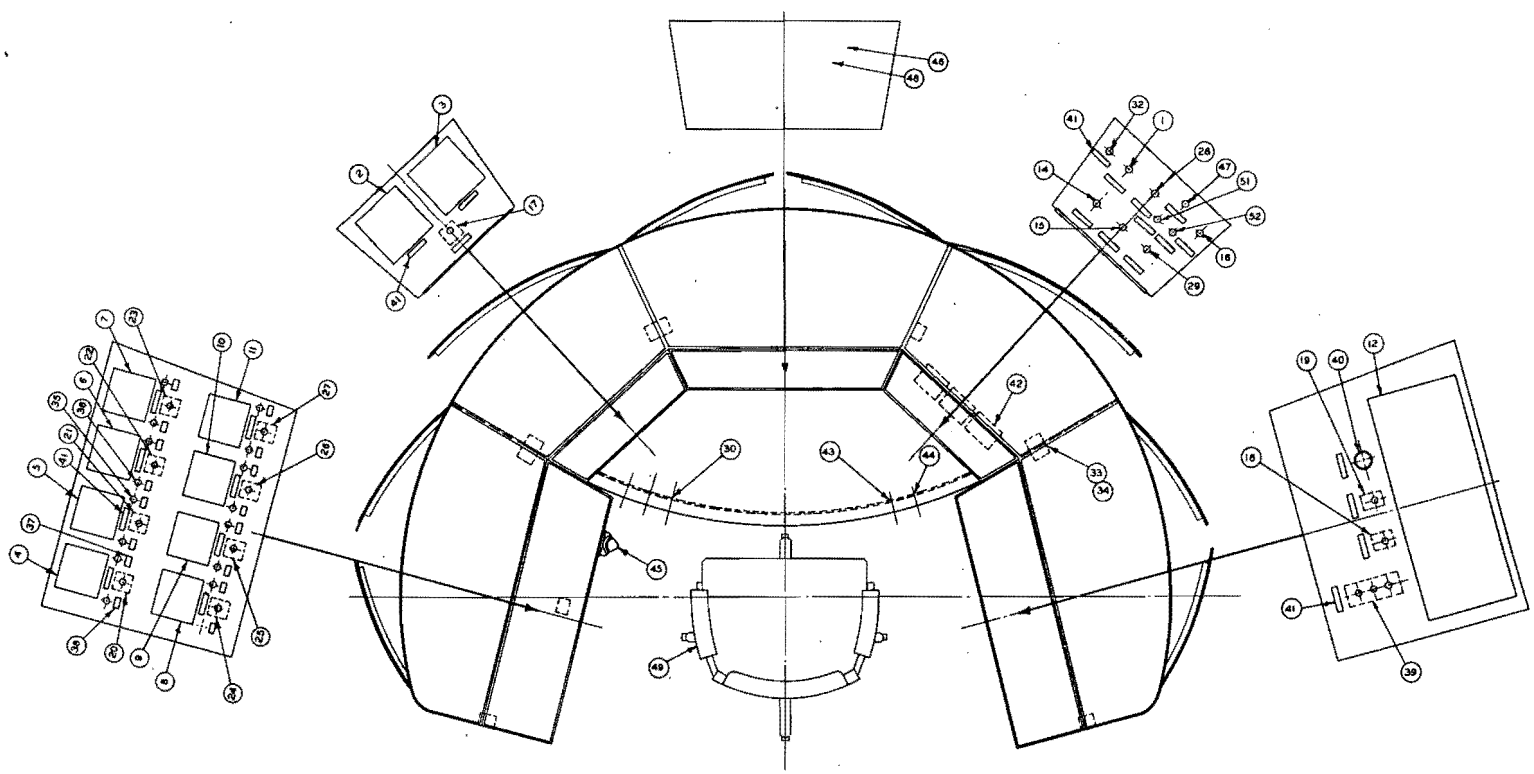

FIG 5.4 A
CONTROL CONSOLE LAYOUT

OAK RIDGE NATIONAL LABORATORY

CONTROL CONSOLE INSTRUMENT SCHEDULE		
ITEM	INSTRUMENT	SERVICE
1	REACTOR PERIOD	INDICATOR
2	SELSYN REC'R.	REG ROD #1 POS.
3	-DO-	REG. ROD #2 POS.
4	-DO-	#1 SHIM ROD POS.
5	-DO-	#2 SHIM ROD POS.
6	-DO-	#3 SHIM ROD POS.
7	-DO-	#4 SHIM ROD POS.
8	-DO-	#5 SHIM ROD POS.
9	-DO-	#6 SHIM ROD POS.
10	-DO-	#7 SHIM ROD POS.
11	-DO-	#8 SHIM ROD POS.
12	PROCEDURE PANEL	INDICATION
13		
14	S-1 SWITCH	SHIM ROD REVERSE BY-PASS
15	S2A SWITCH	SHIM RODS INSERT & WITHDRAW
16	S3 SWITCH	SHIM RODS SELECTOR
17	S4 SWITCH	REG. ROD SELECTOR
18	S5 SWITCH	SHIM RODS RAISE CLUTCH
19	S7 SWITCH	REACTOR LEVEL SET POINT
20	S21 SWITCH	#1 SHIM ROD CONTROL
21	S22 SWITCH	#2 SHIM ROD CONTROL
22	S23 SWITCH	#3 SHIM ROD CONTROL
23	S24 SWITCH	#4 SHIM ROD CONTROL
24	S25 SWITCH	#5 SHIM ROD CONTROL
25	S26 SWITCH	#6 SHIM ROD CONTROL
26	S27 SWITCH	#7 SHIM ROD CONTROL
27	S28 SWITCH	#8 SHIM ROD CONTROL
28	SX SWITCH	SHIM RODS MANUAL SCRAM
29	S28 SWITCH	SHIM RODS INTER-HIGH SPEED
30	SPST SWITCH	CONSOLE CEILING LIGHTS
31		
32	4POT SWITCH	PERIOD CHANNEL SELECTOR
33	WIRE TERMINAL BLOCKS	CONDUCTORS
34	WIRE FANNING STRIPS	CONDUCTORS
35	LIGHTS 12V "AMBER"	#1 TO #8 SHIM RODS PREFERRED
36	LIGHTS 12 V "AMBER"	#1 TO #8 SHIM RODS SELECTED
37	LIGHTS 12 V "GREEN"	#1 TO #8 SHIM RODS INSERT
38	LIGHTS 12 V "RED"	#1 TO #8 SHIM RODS WITHDRAW
39	S6 PUSHBUTTON	"OFF"-"START"-"RUN" OPERATION
40	VERNIER	SET POINT
41	NAME PLATES	IDENTIFICATION
42	TRANSFORMERS	INDICATING LIGHTS
43	SPST SWITCH	ANNUNCIATOR RESET BUTTON
44	SPST SWITCH	ANNUNCIATOR ACKNOWLEDGE
45	PHONE	COMMUNICATION
46	GALVAN. PANEL	PART OF GALVANOMETER
47	S2 PUSHBUTTON	SHIM RODS SCRAM RESET
48	GALVANOMETER	INDICATES LEVEL & COUNTING RATE
49	CHAIR	CONSOLE CONTR. OPERATOR
50		
51	LIGHT 12 V "RED"	"SLOW"-"SCRAM" INDICATOR
52	LIGHT 12 V "RED"	"SLOW"-"SCRAM" INDICATOR

Next is panel P, carrying the selsyn receivers for the regulating rods and also a regulating-rod selector switch. These selsyn dials are also calibrated in inches with clockwise pointer rotation indicating withdrawal. The 22 in. of possible rod motion is spread out for extra sensitivity over one and a quarter pointer revolutions so that the first few inches and the last few overlap. Amber lights mounted under the scale come on to indicate actuation of the regulating-rod limit switches.

Panel Q, at the center of the console, is devoted to two of the most important instruments, the flux-level galvanometer and the counting-rate galvanometer. These instrument signals are given in a pair of glass scales at the top of the panel, the upper one for flux level and the lower serving either for counting rate or for level deviation. The flux-level scale shows the signal coming from the compensated ion chamber. To give full range to this signal, two galvanometers, one of medium and one of high sensitivity, are used, each with three different decade values of Ayrton shunt. The total spread in these six ranges is thus 10^5. This choice of range is made on a flux-level range switch mounted in the lower right-hand corner of the panel.

The lower glass scale carries two sets of scale marks, an upper set constituting four decades of a logarithmic scale for counting rate and a lower set of linear marks from -250 to +250 for the level deviation readings. The galvanometer serving this scale can be switched by a "select circuit" switch next to the flux-level switch to "counting" (in which case its signal comes from the fission chamber) or to one of three (low, medium, high) sensitivities for the flux-level signal. This is the "deviation" measurement, which is useful for fine manual control when the level is high, and the flux-level galvanometer itself has therefore been cut back to low sensitivity.

Panel Q also carries a number of knobs for adjustment of zero, calibration, and adjustment of balance voltage for the galvanometers. There are, moreover, two additional items which deserve particular mention. One is the set of three (out, stop, and in) push button controls in the lower left corner for movement of the fission chamber. The other is the pair of alarm lights and reset buttons at the upper right-hand corner which work from phototube alarm circuits when any of the galvanometers go off scale.

To the right of panel Q is panel R with two (horizontal) rows of elements. From left to right on the upper row are a double throw switch for

selection between the two available compensated chamber period channels, the period indicating meter, the manual scram switch, the shim-rod withdrawal selector switch, and the scram reset push button. The selector switch is an eight-position switch for selection of any one of the shim rods to be withdrawn. On the lower row are three more switches relating to shim rod control. On the left is the reverse switch labeled "withdraw," "neutral," and "insert." On the right is the intermittent- and high-speed switch labeled "intermittent," "neutral," and "high."

On the extreme right of the operator is panel S. This is devoted largely to the procedure panel, which extends across the top. The procedure panel is an assembly of lights (green with one exception) with labels by means of which the overall status of the control system is reflected. Since a detailed discussion of the procedure panel will be included in Section 5.5.2, it need not be further described here. Underneath the procedure panel there are, from left to right, the vernier potentiometer for the reference voltage on the servo-amplifier input; the reactor level set-point switch, which controls the motor-operated rheostat; the switch controlling raising of a shim rod holder when there is no rod on it (e.g., during maintenance in dry dock), and, in its other position, for starting an amplidyne to cock a regulating rod; and three push buttons (off, start, run) for overall control, together with a cylinder lock requiring a key for starting.

5.5 CONTROL SYSTEM AND OPERATOR

In preceding sections a rather detailed picture has been given of the information-gathering and action-producing elements of the control system. It remains to describe the "brains" of the setup — that is, those elements that describe *which* actions should be produced in face of the given information. At the center of the picture there is, of course, the operator. In fact, the aim of this section may be said to be the description of how the operator's initiative fits into the control system, i.e., how this initiative is subject to a few outright automatic restraints and is guided by many precautionary and regulating automatic devices. An overall discussion of how the reactor is run appears in Section 5.6.

5.5.1 Automatic Rod Insertion. Operator initiative is overridden (or, one might say "ignored") by three categories of rod-inserting action: (1) scram, the dropping of safety rods; (2) setback, lowering of the servo set-point by the motor-operated rheostat; and (3) reverse, which is a simultaneous continuous insertion of all eight shim rods. It will be recalled that scram is of two types: fast, by electronic action of the ion chamber through the magnet amplifier, and slow, by electromechanical relay action cutting off magnet power. Somewhat similarly, setback can be either fast or slow, depending on the speed of the motor operating the rheostat.

It must be emphasized that the fast scram is in a class by itself, being the ultimate "safety" protecting the reactor. It is always operative and can never be vetoed by the operator. It is fast enough so that it will protect the reactor, by neutron level signal alone, against a 1/30-sec period, which is a reasonable estimate of the fastest period into which the reactor could be thrown in a start-up accident. In addition to level signals, the fast scram is at all times responsive to period signals.

Circumstances calling for the various automatic insertions are listed in Table 5.5.A. This tabulation is to be considered somewhat tentative, particularly in regard to numerical values of limits. The last item, manual, refers to the operator. Setback and reverse, caused manually or otherwise, continue only so long as the causative condition endures. When the manual-automatic switch is on "manual" (servos inoperative), setback is of course

meaningless, so under these conditions reverse is caused by those same signals which under automatic operation cause setbacks. This is not shown in Table 5.5.A but needs to be kept in mind.

The large number and variety of rod-inserting causes give rise to some concern as to the effects of trouble with the instrumentation itself. This is particularly significant with respect to scrams, which constitute the most serious interruptions of operation. With this in mind, the various instrument channels (with the exception of the safety ion chambers and the period meters) are each equipped with a test block which may be pulled without scramming the reactor if that instrument is behaving so as to jeopardize continued operation of the reactor. This admits the dangerous possibility of most of the instruments being out of operation at any time. Against this unfavorable situation there are two precautions: first, the fast scram circuits cannot be so disconnected; and second, the annunciators tell the operator that the blocks are out.

Each annunciator channel can give audible warning by means of the horn signal and visible warning by means of its own pair of lights, one red and one white. Both lights are dimly lit during normal operation of the instrument channel. Trouble (pulling of test block, danger signal, instrument failure) causes both lights to turn bright and the horn to sound. The operator can silence the horn by pressing a button, which also causes the white light to go out. The red light burns until the trouble is cleared, when it goes out and the white light comes back on. The operator acknowledges this signal by again pressing the button, causing the lights to return to normal dim operation.

5.5.2 Operator Initiative and the Procedure Panel. Description of the control console in Section 5.4 included mention of a special panel called the "procedure panel." This panel is shown in Fig. 5.5.A,* which also includes (at the bottom of the diagram) some information from other panels. The procedure panel can perhaps best be described as an "illuminated block diagram"; that is, it is a block diagram of the procedure of getting various control rod motors to run, together with lights to indicate the status of the procedure at any time. The panel is arranged so that, from top to bottom, lights come on successively as the necessary conditions for running the motor are satisfied; conversely, starting from the bottom, lights are out up to a point which indicates the last satisfied condition. The limits of the procedure panel

*For easier reference, Fig. 5.5.A is placed at the end of Section 5.6.

TABLE 5.5.A

Causes of Automatic Rod Insertion

	FAST SCRAM	SLOW SCRAM	FAST SETBACK	SLOW SETBACK	REVERSE
Neutron level (from safety ion chambers) = $1.5N_F$	X				
Neutron level = $1.2N_F$					X
Neutron level = $1.1N_F$				X	
Neutron level > $.3N_L$ (start)					X
1-sec period	X				
5-sec period					X
N^{16} activity = $1.5N_F$		X			
N^{16} activity = $1.2N_F$			X		
N^{16} activity = $1.1N_F$				X	
Neutron level (boron thermocouples) = $1.5N_F$		X			
Neutron level (boron thermocouples) = $1.2N_F$			X		
Neutron level (boron thermocouples) = $1.1N_F$				X	
Reactor power (water flow and temperature) = $1.5N_F$		X			
Reactor power (water flow and temperature) = $1.2N_F$			X		
Reactor power (water flow and temperature) = $1.1N_F$				X	
Water temperature rise > 105% of normal				X	
Main water tank level = 50,000 gal		X			
Main water tank level = 100,000 gal				X	
Water flow < 80% of normal		X			
Water flow < 85% of normal				X	
Water flow < 5% of normal		X			
Monitor tube water flow < 80% of normal differential		X			
Air flow failure				X	
Instantaneous loss of instrument bus voltage		X			
30-sec loss of purchased power		X			
2-sec loss of relay bus voltage		X			
Manual		X	X	X	X

itself, indicated by the heavy dotted line in Fig. 5.5.A, do not include all the relevant information. As far as shim rods are concerned, the other items (which are represented by switch markings or lights on the other panels of the control console) are included at the bottom of the drawing. As far as regulating rods are concerned, the story on the procedure panel ends with the motor-operated rheostat. Other information about the servos and regulating rods is presented to the operator on panels P and S below the procedure panel. Since the procedure panel is concerned only with getting motors to run, information is shown elsewhere as to whether given motors are running, how far they have run, and the ultimate effects on reactor level and reactor period.

In Fig. 5.5.A an attempt is made to display the actual appearance of the procedure panel, as far as position and color of lights and placing and labeling of blocks are concerned. Circles indicate principal end objectives; square blocks refer to manual operations or switches; and rectangular blocks represent automatically imposed conditions. Ganging of some switches is shown by dotted lines between square blocks. For the convenience of anyone who might wish to compare this diagram with the elementary circuit diagrams (not included in this report) reference numbers for switches, relays, and instrument contacts are included. In attempting such a comparison, one must keep in mind two facts: first, the procedure diagram is incomplete; for example, it shows only one servo channel and thus sheds no light on the interaction of the two servo channels; second, there is no point-by-point correspondence of the elementary diagram and the procedure diagram, since they are drawn to serve quite different purposes.

The procedure panel is divided vertically into three main regions: the left-hand section pertaining mainly to withdrawal of shim rods; the middle section pertaining to regulating rod motions; and the right-hand section pertaining to insertion of shim rods. Suppose one starts at the top left-hand corner. The light labeled "dry dock" (see Section 5.3.4) will be on when the reactor plug is in dry dock, and otherwise off. If the semaphore arms are up and cables are plugged in for normal operation and if, in addition, the dry-dock test blocks are back in place, the other green light comes on. (The dry-dock test blocks in the relay cabinets must not be confused with the operation test blocks on the control panels.) For either of these two conditions (dry dock or operation) the line running down to "raise and scram"

indicates that a selected shim rod motor can be run in the raise, or withdrawal, direction. (The terms "withdraw" and "insert" are used to refer to motions of the control rods; "raise" and "lower" refer only to empty rod holders.) Throwing of this switch (S-5) to raise a rod holder also causes a scram, ensuring that the rod holder is empty and thus guarding against inadvertent dangerous withdrawal. The other position of this switch permits starting of an amplidyne (provided it has been selected on the manual-automatic switch) subject again to automatic scram. Without the scram condition, it is safe to start the amplidyne when its regulating rod is fully withdrawn and the corresponding limit switch is actuated.

Following down from the "raise and scram" position of S-5 is seen to lead to the individual withdrawal circle, provided S-21 is on "raise" and provided the rod seat interlock (second precaution to ensure that rod is not being raised) is actuating relay R-51. The notation S-21 is used to represent any one of the eight individual shim rod switches, S-21 to S-28. Similar notations apply to the insert interlock MI-1 and the limit switch relay R-21. These conditions on withdrawal simply imply that one is not at the same time trying to run the motors in the opposite direction, and that the rod is not already withdrawn as far as it can go.

Returning to the top of Fig. 5.5.A, if the semaphore and test block light is on, the operator may proceed to use his key on the cylinder lock, releasing the start and run buttons. Assuming start-up from a low level, as with a cold, clean reactor, he would push the start button. The next condition concerns the motor-operated rheostats. The condition, enforced by limit switches, requires that one rheostat be at the top of its range and the other at the bottom. (Since the operator is in the sequence of getting shim-rod motors to run and since these rheostats concern the regulating rods, the reason for this condition may not be obvious. The point is that now is the time to get this situation in order, not later when the reactor is at a high level and juggling of the control points would be awkward or disastrous.) One then proceeds via the "manual" side of S-4, or via "automatic," provided the selected servo channel has its regulating rod cocked (fully withdrawn). Next comes period supervision, requiring that the period be 7 sec or longer. If the level is below $10^{-5}N_F$, one would proceed toward "intermittent," with the requirement that the counting rate meter be alive (off zero). The timer light then starts

blinking on for ½ sec and off for 4½ sec, corresponding to rod motion. Next comes a period control of 30 sec or more, though this can be by-passed by the spring-return switch S-1.

The trip relay, R-16, must be set by switches S-2A and S-2B being in neutral. It will then seal itself in around S-2B, subject to instrument contacts on the galvanometer (galvanometer on scale with correct shunt set) and limit switches on the fission chamber positioning drive (chamber in one of three standard positions). (The conditions which trip R-16 are not shown in Fig. 5.5.A.) Switch S-21 must be on normal, the rod clutch must be engaged, there must be no reverse (which via relay R-20A overrides withdrawal), and, with insert interlock and limit switch permitting, one arrives at group withdrawal.

If after passing the 7-sec period condition the level had been greater than $10^{-5}N_F$, use of high speed would have been permitted, subject to the same constraints as for intermittent speed. Moreover, low speed (continuous withdrawal of any selected individual rod) is permitted as shown.

This summarizes the "start" regime, one of the two main withdrawal regimes. The other is "run," which is permitted by the sag relay R-4 when the neutron level is above $10^{-3}N_F$. It is also subject to a precaution on the fission chamber, which must be in the outermost of its three positions. In "run" use of low speed is permitted at once by manual selection, or by automatic if on the selected servo channel the regulating rod is inserted less than 11 in. (This milder condition, compared to the one in "start," is acceptable because at levels above "sag" the danger from a short period is very much reduced.) In addition to low speed, intermittent and high speeds can be obtained by means of the spring-return by-pass switch.

Since a principal feature of the run regime is the servo control, attention will now be turned to the way in which the servo control point is changed by the motor-operated rheostat. As far as raising the control point is concerned, this involves establishing a sub-regime called "run auxiliary," governed by relay R-3. This can be reached either on manual, or on automatic with the regulating rod concerned uncocked (partially inserted, and therefore indicating that the servo has functioned properly). Other conditions are that the period be greater than 30 sec and that the level be approximately $10^{-2}N_F$.

Run auxiliary "seals in," subject to trip only by the sag relay. The rheostat limit switches are shown with red lights, because they come on to indicate a condition *preventing* motor operation; all the other lights come on to indicate conditions of *permission*. The control point is raised by running the high-speed motor. (Motors of two speeds are provided to permit fast and slow setbacks.) There is a one-way block in the raise-lower switching. The fast lowering can always override slow lowering or fast raising. Lowering of the control point in the servo channel selected on automatic can be done manually with S-7, and is done automatically by sag and setback relays.

Interest now reverts to the shim rods and the insertion procedure indicated on the right-hand part of the procedure panel. At any time the individual empty rod holder, selected on S-21, may be lowered. In fact, if switches S-21 to S-28 are on any position other than "off" or "raise," each rod holder will be automatically lowered whenever its clutch is released. Thus, in case of a scram, as soon as a rod is dropped its holder starts in after it. When the rod holder is not empty, the seat switch acts through R-51 as a preliminary limit switch, backed up by the mechanical limit switch on the rod holder acting through R-31. Individual rods can be inserted by the "jog" position of S-21. If S-21 is on "preferred," the rod(s) so selected can be inserted by manual operation of S-2A. The reader will note that only one selected rod can be withdrawn in low, but that any or all may be inserted via jog or low. This is, of course, reasonable from the standpoint of safety. Concerning insertion, there are two significant differences between jog and low: first, jog is a nonreturn switch position, while low is spring-return; second, switch S-2A has for both "withdraw" and "insert" the special low acceleration action due to the resistor in series with the shim rod motors, and thus permits fine adjustment of rod position. This particular use of low is called "inching." The series resistor limits the use of low to one rod at a time.

Preferred shim rods are also inserted automatically by regulating-rod limit switches. If the regulating rod is withdrawn less than 7 in. (R9), preferred rods are inserted, and, if the withdrawal is less than 5 in. (R10), all rods are inserted. This simultaneous insertion of all rods is called "reverse." It may at all times be initiated manually on S-1 or by a level of 20% above N_F. Reverse may also be caused by certain period or level signals. If the run auxiliary relay, R-3, is not picked up, a level greater than $3N_L$

will cause reverse, as will also a period of less than 5 sec. (The block labeled "start" should, more strictly, be labeled "not run auxiliary.") Under manual operation at levels above $3N_L$ reverse is caused by fast or slow set-back signals or by a short period.

Before leaving this section it may be well to add a few words on the relations between the two servo channels, since only the active channel shows on the procedure panel. The relay circuits for the motor-operated rheostats provide that when S-4 is on one servo channel the rheostat on the other channel is raised to its limit. Conversely, the active channel will have its rheostat run to the bottom when the level falls below "sag." This combination of actions would normally leave the rheostats satisfying the condition imposed on "start." Switching from one servo to another should not be done without first cocking the regulating rod that is being left since otherwise the procedure sequence does not permit return to this servo except with the automatic scram of switch S-5. (The rod could be cocked by going out on the plug and cranking it up by hand.) Normal procedure would be to insert a shim rod so that the servo, trying to hold to the control point, would cock the regulating rod. Then switching to the other servo would cause automatic raising of the first rheostat, thus leaving the first channel in optimum stand-by readiness, with its rod cocked and control point at the top.

5.6 REACTOR OPERATION

In order to review and integrate the detailed information of preceding sections, an attempt will be made here to recount briefly the operating procedure in a few typical situations. These will include start-up, shutdown of both the normal and scram varieties, manipulation of level near N_F, and operation in face of difficulty.

5.6.1 Start-up Operation. In the starting of a cold reactor the operator is most concerned about a reliable neutron signal. He would therefore give attention to seeing that the fission chamber is in its most sensitive, innermost position, and that it is giving a readable signal on the counting-rate meter. Assuming this to be so and that the auxiliary process instrumentation shows normal, the operator could go on as discussed on the procedure panel to the use of intermittent withdrawal. This is subject to his initial permission, but the switch S-2B is nonreturn. The intermittent motion gives the operator a good idea of the reactivity of the reactor by the rate of rise observed during the off period. As the level passes $10^{-5}N_F$, he can use high speed. Meanwhile, he will probably have moved the fission chamber to its center position. He cannot, however, use intermittent or high speed while the fission chamber is being moved. He will also now be picking up neutron signals from the ion chambers. When the level reaches sag, the fission chamber should be in its outermost position, and, if the operator forgets, the sag relay will see that it is. In addition to the time required to reach criticality and get into a period, something like 10 or 15 min is required to bring the level up to get into "run." This will depend on how hard the operator crowds the period controls. The start regime is manual, though S-4 may be either on manual or on automatic; in general it would seem reasonable to have the servo available for possible corrective action at N_L.

In "run" the normal procedure would be to let the servo level off the reactor at its control point of N_L and then to raise the control point. With the logarithmic rheostat holding the reactor to a period of about 20 sec, it would take about 90 sec (the running time of the fast rheostat motor) to negotiate the factor of 100 from N_L to N_F.

Start-up from the higher levels typical of a recently operating reactor will be easier because the operation is free of the acute danger of getting

into a fast period at low levels. Otherwise, the procedure would not be greatly different unless the operator was especially hurried to keep ahead of xenon poisoning or for some other reason. Problems of this sort are considered in Section 5.6.4.

5.6.2 Shutdown. For a normal intentional shutdown the operator has the choice of a variety of procedures. For example, he could set all shim rod switches (S-21 through 28) on "jog" and leave them there. This would run all the shim rods completely in. If the manual-automatic switch is on automatic, the operative servo will be left with its regulating rod completely withdrawn and its rheostat completely lowered. Since this procedure leaves all the shim rods at the bottom of their travel, it is suitable for a relatively permanent (e.g., maintenance) shutdown but would not be advisable if the plan was to raise the level back up in a short time. In such a case, lowering of the control point, followed by careful insertion of preferred rods, would be a better plan.

As a matter of fact, discussion of shutdown procedures is largely academic because intentional shutdowns offer excellent opportunity for testing the various scram circuits and will probably be used exclusively for this purpose.

In case of unintentional automatic shutdown actions (setback, reverse, scram), the operator's reaction will, of course, depend on circumstances. Accordingly, suitable operator reaction to automatic shutdown action is discussed in Section 5.6.4.

5.6.3 Manipulation of Operating Level. There are a number of cases in which the operator will need to deviate from the simple process of letting the servo hold the reactor to a fixed control point. An example is the case in which shading of the neutron-flux distribution in the reactor by modifying the positions of the various control rods is required. This will presumably be a common requirement of the experimental work being done.

The problem confronting the operator is that of shifting the spatial distribution of neutron flux, as observed with the boron thermopiles and ion chambers (or perhaps by special instruments associated with the experiment concerned), with minimum effect on the overall reactor level observed on the galvanometer scale. Since the operator is much more rigidly constrained by

automatic controls in withdrawal than in insertion, he must be careful that this asymmetry does not embarrass him. Thus, he may select (on S-3) only one shim rod for low-speed withdrawal, whereas he is free to insert as many as he puts on "jog" (on S-21). Shading would best be done with one rod selected for withdrawal and one rod preferred for insertion. Assuming the servo to be in control, the two shim rods could be carefully moved in their respective directions by manual switching (on S-2A) without getting the regulating rod to call for shim rod motion. Alternatively, a less "fussy" procedure would be to withdraw the selected rod manually (on S-2A) and let the regulating-rod limit switches initiate insertion of one or more preferred rods.

5.6.4 Operation in Face of Difficulty. There is no clear line to be drawn between normal operation and operation under difficulty. The purpose here is to comment on a few of the situations in which the operator will feel more than his average need for attention to instrument signals and control actions. The examples chosen for discussion are change-over of servos, loss or interruption of power, automatic shutdown action, and accumulation of poison after unintentional loss of level.

When it is necessary or desirable to change from one servo-regulating rod channel to the other, the operator must, of course, change switch S-4 from one rod through manual to the other rod. In general, however, it would not be wise for him simply to do this whenever necessary without attention to related matters. For example, if it is possible to do so, the regulating rod on the channel being left should be cocked before S-4 is changed, since otherwise it would have to be cocked by manual twisting of the drive before the operator could return to this channel. The motor-operated rheostats are so interconnected that whenever one channel is selected on S-4, the motor on the other rheostat runs to its top. Thus, a switch directly from one channel to another cannot cause a dangerous withdrawal or an embarrassing insertion of regulating rod; the rod is already completely withdrawn and the control point is at N_F. However, suppose the operator is using a servo channel and leaves it to go to manual on S-4, having first cocked the rod. Suppose the control point is left well below N_F, say at 0.1 N_F. Now, if on manual operation the reactor is brought above this level, say all the way to N_F, it would be possible to throw S-4 back to the same servo channel, in which case the regulating rod would be thrown in and the reactor put into a negative period. This seems to be the worst "accident" that might be caused by poor operation with the servo interchange circuits.

As far as loss of power is concerned, the operator may be left figuratively as well as literally in the dark. This would be true particularly if the instrument bus and the control bus should go dead simultaneously. Since all the instrument lights and all the relay-indicating lights would be out, the operator would have no way of knowing whether the scram (automatic on loss of magnet amplifier power) was effective. He would know that the power was off, and if he had a reasonable faith in the law of gravity, he would probably remain at his post until power was restored. If only the instrument bus were lost, all the instrument lights would go out, but the clutch and seat lights would be operative and so would indicate the effectiveness of the scram. Conversely, if the control bus alone went out, instrument signals would remain available to show the effects of the scram.

Whenever the reactor is subject to automatic shutdown action, the operator's concern will be divided between the questions of what the causative trouble was and what the chances are of returning the reactor to normal operation. The circuits are, of course, designed so that the operator cannot interfere with the shutdown actions as long as the causative conditions remain. Hence the operator's first reaction to anything less drastic than a scram would be to do whatever is possible to clear the responsible condition. The proper corrective action in case of a reverse (caused by excess period or signal level) is clearly to decrease the period or the level, but, since this is already being done at a maximum rate by the reverse itself, the operator can afford to think ahead to the problem of holding the reactor (avoiding a negative period) as soon as the reverse ends. In the event of slow setback the situation is much the same, except (see Table 5.5.A) that there are several possible causes not having to do with reactivity, which must therefore be corrected otherwise than by the setback itself. Fast setback gives the operator a more serious problem, for the chances are pretty good that the regulating rod would insert fully, causing a reverse, and that the combined effect would be to put the reactor into a substantial negative period. It is to recoup the loss of reactivity in such circumstances that the moment the shutdown stopped the operator would use the by-pass (switch S-1) to get the high-speed withdrawal.

When the reactor is scrammed, the chances of getting back into normal operation are dependent upon the time history of previous operation as well as upon the obvious need of remedying the causative trouble. This is because of

the rapid accumulation of xenon poison after shutdown. In the original reactor design it did not seem practicable to provide the large excess reactivity that would be needed to override xenon in any event. The length of complete shutdown that can be tolerated after prolonged operation at N_F is of the order of a half-hour. This depends on charge depletion and probably other factors which affect reactivity. In any case, either for a complete shutdown or for a partial dropping of level after any appreciable operation near N_F, the operator will want to get the level back up as soon as he safely can. Here again if the level has not dropped below sag, he would make use of the by-pass switch to avail himself of shim rod withdrawal at high speed.

5.7 GENERAL SUMMARY

In order to hold this chapter down to suitable length it has been necessary to leave out all but a bare minimum of explanatory discussion. The reader may therefore feel confused or unsatisfied in regard to the reasons for adopting certain features and ignoring others. It is hoped that this state of mind will be at least partially relieved by the summary to be given here in two parts: first, a recapitulation of some of the basic principles which guided, or emerged from, the control development; second, an attempt to assay the load of responsibility still resting on the operator.

5.7.1 Basic Principles. Perhaps the most fundamental principle is the sharp distinction between insertion and withdrawal of shim rods. Thus *either* operator or automatic signal can insert any number of rods at any time, whereas withdrawal is always subject to *both* operator and automatic permission. Withdrawal is limited, moreover, to what is needed or safe under given circumstances. At high levels (in "run") only one rod at a time is available, since at these levels it is hard to see a need for moving more than one at a time. At the low levels characteristic of a "cold" start, only intermittent withdrawal is permitted. Here the reliability of information is relatively poor, coming entirely from one instrument. It is therefore important to be able to keep watch on the subsequent effect of each short interval of withdrawal, thus gauging the growing reactivity. As higher levels are reached, the instrumentation furnishes more varied and more reliable signals so that the use of high withdrawal speed is less hazardous. Under the special conditions of restart, presenting a serious need for high speed, it is made as conveniently available as can safely be done.

DWG. #10548
NOT CLASSIFIED

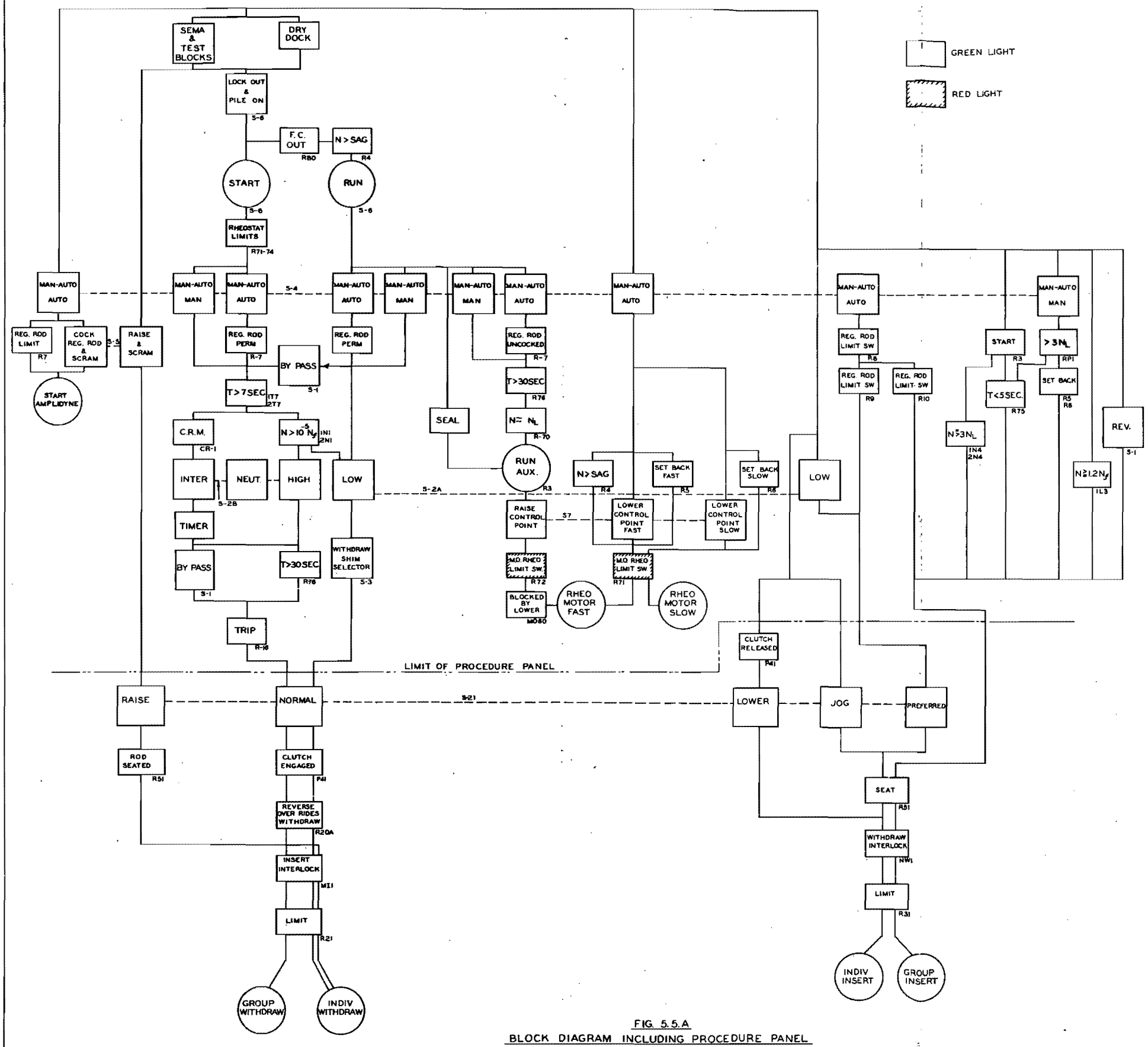

FIG. 5.5.A
BLOCK DIAGRAM INCLUDING PROCEDURE PANEL

The distinction between insertion and withdrawal is, of course, one aspect of the general philosophy concerning safety. Another aspect is the aim of having mild corrective measures come first, backed up thoroughly by ultimate action which is as foolproof as possible. All control equipment is designed to fail safe. There is continuous monitoring of the safety circuits in that currents are controlled only by hard vacuum tubes which, upon failure, cease conducting and thereby actuate annunciator or scram circuits. It is important to realize that not all apparent instances of instrument duplication overlap entirely. For example, the shading of neutron flux might cause signals from the ion chambers to be quite inaccurate measures of average reactor level. In such a case the additional information yielded by measurement of N^{16} activity is of real value.

It may be helpful to summarize the precautions applied in the period range and in the power range. Since most restarts will occur in the period range, high-speed withdrawal is necessary. Operation is manual and is under the supervision of the period meters as follows:

1. A 30-sec period trips "latched" withdrawal. Subsequent withdrawal requires constant operator attention.
2. A 7-sec period prevents any further withdrawal.
3. A 5-sec period inserts all shim rods.
4. A 1-sec period causes scram.

The top of the period range is guarded by the servo which levels the rise at $10^{-2}N_F$ or if the servo is turned off and the operator fails to level, all rods are inserted by the log N meter at about $3 \times 10^{-2}N_F$.

Short periods in the power range are both less probable and relatively harmless because of the proximity of the level safety setting and because of the corrective capacity of the servo. Therefore, of the period controls only the 1-sec-period scram is retained. In the region of full power, inadequate cooling of the reactor ranks equally with excessive power level and the two situations are treated in the same fashion in order of severity as follows:

1. Alarm.
2. Automatic continuous reduction of power level through servo control as long as the unsatisfactory coolant or power level situation exists or until the power level is reduced to 1% of full power.

3. Automatic rapid reduction of power level as above except that the reactor may be left substantially subcritical if the situation persists.

4. Scram on extreme unsatisfactory condition.

Loss of cooling water is guarded by:

1. A flow meter in the main water line to the reactor.
2. Water level monitoring of the overhead supply tank.
3. Monitoring of main water valve positions.

Rise in power is guarded by:

1. Level safeties.
2. Water power instrument ($\Delta T \times$ flow).
3. Boron thermopiles.
4. N^{16} activity instruments.

Whereas in the lower ranges the principal concern is that of short periods, at full power a slow drift upward of the power level can be dangerous to the reactor. Since the safety circuits are subject to variations in water flow, magnet air gap conditions, shading of the ionization chambers, and other variables, the level at which scram occurs must necessarily be set high enough to ensure uninterrupted operation. For this reason the protection afforded by the water power instrument ($\Delta T \times$ flow), the boron thermopiles, and the N^{16} monitor become important in guarding against small slow rises in power.

A word may be added, finally, about the philosophy of providing for automatic operation with the servo. In its early version the reactor now known as the MTR was a homogeneous reactor, and the servo system was designed to cope with the change in reactivity induced by bubbles. Since it is possible to run the MTR manually, the servo, though simplified, must now be regarded as something of a luxury. Presumably, manual operation at its best would not yield the smoothness which the servo can achieve. Just how much utilitarian worth (particularly for the experiments that are being done in the reactor) this extra smoothness will contribute remains for experience to show. There is also some extra safety in servo-controlled operation since the servo is considerably faster than human reaction.

5.7.2 Responsibility of Operator. The operator should realize that a prolonged intensive effort went into design of the control system. It is, however, most unlikely that this effort could possibly have provided for every conceivable operational situation. Nevertheless, the operator would do well, when he feels unduly constrained or frustrated by the control system, to try to keep in mind *all* the implications of his intended action. It is probable that, as operating experience accumulates, it will become evident that some changes in the control system could profitably be made. Until such experience is accumulated, it would seem reasonable to ask the operator to learn to live with the system as designed.

The operator must also realize that at all times the reactor is in his hands, despite all the automatic operating and safety devices. This means that he must remain alert and attentive. He must have foresight to prevent emergencies from arising and presence of mind to deal with those emergencies which, in spite of everyone's efforts, inevitably will arise. Although the exact nature of his responsibility will not be fully clear until the system is constructed and installed, the following list of specific suggestions will at least show the kind of "mental notes" which must guide the operator:

1. At low levels be sure the counting-rate meter is alive. It is the only source of information at such levels, and unless its pointer gives evidence of responding to signal it would be foolhardy to attempt reactor operation.

2. After every scram be sure to turn switch S-2B (intermittent, neutral, high) to neutral. Otherwise there may be nothing to prevent the shim rod holders, lowered automatically after rods are dropped, from picking up rods and starting (possibly even high speed) withdrawal.

3. For smooth change of reactor level under servo control, keep the shim rods in step with the motor-operated rheostat. In particular, try to avoid letting the regulating rod get within 5 in. of full insertion, since at this point it automatically calls for reverse.

4. Avoid leaving any shim rods fully inserted. Any such rod is incapable of contributing to the effectiveness of a scram. To have full benefit of prompt scram protection, all rods should be in position to contribute some effect.

5. Never permit the bolts holding down the top plug of the reactor to be loosened unless the reactor is first scrammed. A serious accident could occur if the plug were lifted by the crane or by water pressure while the rods are still held.

It may be that field modifications of the installed reactor will change the relevance of some of these remarks, but, in any case, the operator will need to know his responsibility and to live up to it.

5.8 CONTROL AND INSTRUMENT CENTERS*

From an early date in the conception of the MTR, a centralized control room was planned for the control and instrumentation of the reactor and its major cooling processes. This arrangement is desirable since the materials of construction permit the operation of the reactor only as long as proper coordination of the heat removal processes is maintained. However, this plan for centralization was changed by recent determinations that the time element, gained by control of the major reactor-cooling process from the reactor control center, would not facilitate the operation of the reactor. With the admission of this premise into the basis of design for the reactor control center, the requirements for simplifications of control problems have resulted in other locations for the controls of the heat removal processes.

In the separation of the major systems of control and instrumentation for the reactor and the reactor heat removal processes, two major control and instrument centers are provided. These major control centers are located in the Reactor Building and in the Process Water Building. The reactor is controlled from the former, while the latter center, which is primarily for the control and instrumentation of process-water flow through the reactor, includes the instrumentation of the locally controlled reactor cooling-air system. A number of the supporting process systems are like the cooling-air system in that they have locally controlled equipment but have some instrumentation extended to one or both of the major control centers.

5.8.1 Reactor Control and Instrument Center. The reactor control and instrument center is composed of an instrument room and a control room, respectively, on the second and third floors of the lean-to section on the west side of the Reactor Building. The control room, directly above the instrument room, is at the level of the reactor top with access thereto by a connecting walkway. A stairway connecting these rooms facilitates the maintenance of associated control and instrumentation devices. The partition walls of the reactor control room are formed of sectional metal construction,

*ANL contribution.

providing an area approximately 22 by 47 ft which may readily be varied in length as required. Windows or glass sections, located only in the east wall of the control room, permit observation of control operations without entering the room and observation of activity on top and near the reactor from within the control room.

The services provided within the control and instrument rooms are peculiar to the use of these rooms. For consistency of instrument performance, these rooms are air-conditioned for control of temperature and humidity. All lighting in the control room is by incandescent lamps, including a number of luminaries for general room illumination. Panel instrument illumination is provided by internal instrument lights and flush-mounted ceiling spotlights. Illumination in the instrument room is provided by fluorescent and incandescent lamps.

The control room layout includes an instrument panel to accommodate the initial requirements for indicators, recorders, and annunciators with a number of spare and partially utilized panel sections for future requirements. This panel board, facing in the direction of the reactor, is composed of eleven 4-ft-wide by 9-ft-high sections and extends the full length of the room with a rear access door at each end. Six panel sections, three at each end of the board, lie in a straight line. These two end panel groups are connected by the central panel sections which are arranged on a radius of approximaxely 7½ ft to allow for the control console.

The console in the control room mounts all devices for effecting manual control of the reactor, control indicating devices, and some indicating instruments. Other reactor indicating instruments and recorders are located on the central panel sections immediately in front of the console, as indicated in Fig. 5.8.A.

The instrument-room layout is provided with rows of instrument racks and boards to accommodate electronic components of automatic control and indicating devices, interlocking relay control groups, and power supply circuits for all reactor control and instrumentation devices. The instrument racks and relay boards extending lengthwise in this room are arranged to facilitate connections between the equipment mounted thereon and the instruments and controls in the room above. Electrical conductors pass to and from the racks and boards by way of floor and ceiling cutouts. The ceiling cutouts provide

NOT CLASSIFIED
DWG # 10785

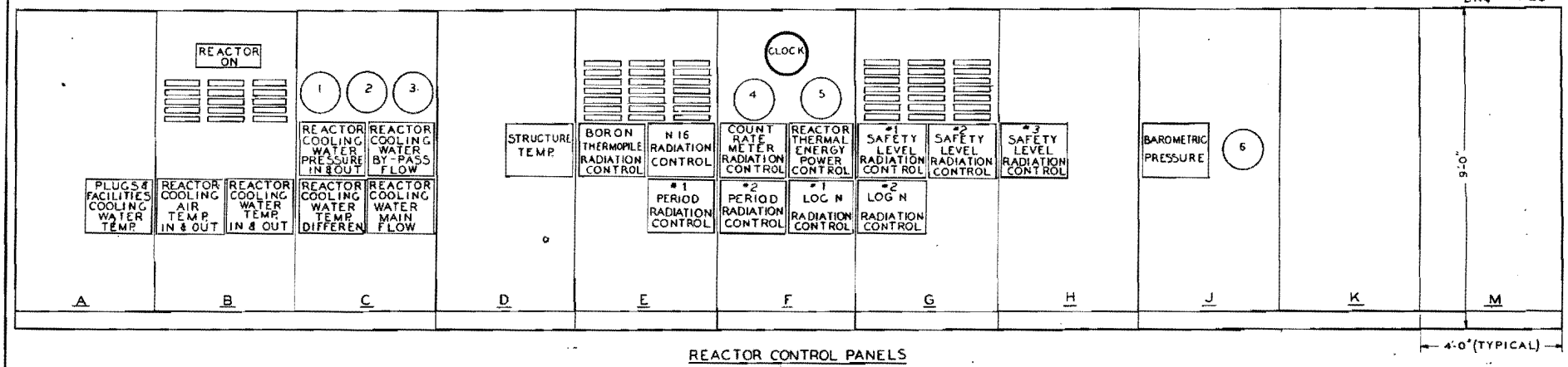

REACTOR CONTROL PANELS

DEVELOPED VIEW
SCALE ¾" = 1'0"

FUNCTIONS OF PRINCIPAL INSTRUMENTS

RECORDERS – AS INDICATED

INDICATORS

1. WORKING RESERVOIR LEVEL
2. INSTRUMENT AIR PRESSURE
3. REACTOR DISCHARGE AIR PRESSURE ALARM
4. NO. 1 SERVO ERROR
5. NO. 2 SERVO ERROR
6. DEMINERALIZED WATER BACK-UP RADIATION ALARM

LEGEND

RECORDER
INDICATOR
ANNUNCIATOR

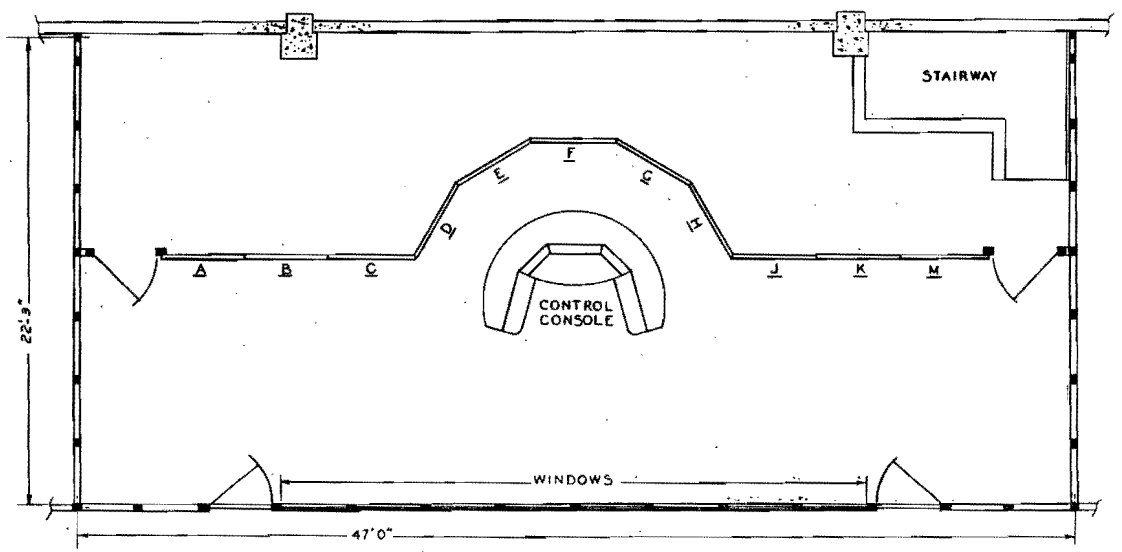

CONTROL ROOM

PLAN VIEW
SCALE ⅜" = 1'0"

TOLERANCES	ARGONNE NATIONAL LABORATORY	REACTOR CONTROL ROOM & INSTRUMENT PANEL — LAYOUT
	This drawing is the property of the Argonne National Laboratory	FIG. 5.8.A

for the most direct connections with the control room above. The floor cutouts provide for the entrance of the cableways or conduit groups from the reactor and the reactor control and instrument power source.

5.8.2 Process-water Control and Instrument Center. The process-water control and instrument center is located near the west end of the south wall of the Process Water Building. This location is in the vicinity of the electrical unit load center. The control center is composed of an operator's desk facing a semihexagonal instrument panel which mounts the devices for effecting control of process-water flow through the reactor and the instrumentation of the principal and supporting reactor heat removal processes.

The instrument panel is composed of seven 4-ft-wide by 9-ft-high adjacent sections arranged in three straight lines. Two of these lines, one extending north and the other extending west, are each composed of three sections. The other section of panel connects with each of these lines at an angle of 45°.

The control devices on the instrument panel are for effecting the position of valves to control the main and by-pass process-water flows to the reactor, to permit the recycling of process water from the seal tank to the reactor, and to permit the flow of water from the demineralized-water storage tank to the reactor.

In general, the indicating and recording instruments on the panel are associated with the principal processes, i.e., the process-water and cooling-air systems of the reactor. Some of these instruments and a number of the annunciators are associated with the supporting processes and the effluent control systems.

The development diagram of the instrument panel, Fig. 5.8.B, identifies briefly the more important control and instrument locations.

5.9 GLOSSARY OF TERMS AND SYMBOLS

N_F - full normal operating power level of the reactor.

N_L - lowest power level at which servo can control reactor; about 1% of N_F.

NOT CLASSIFIED
Dwg. #10786

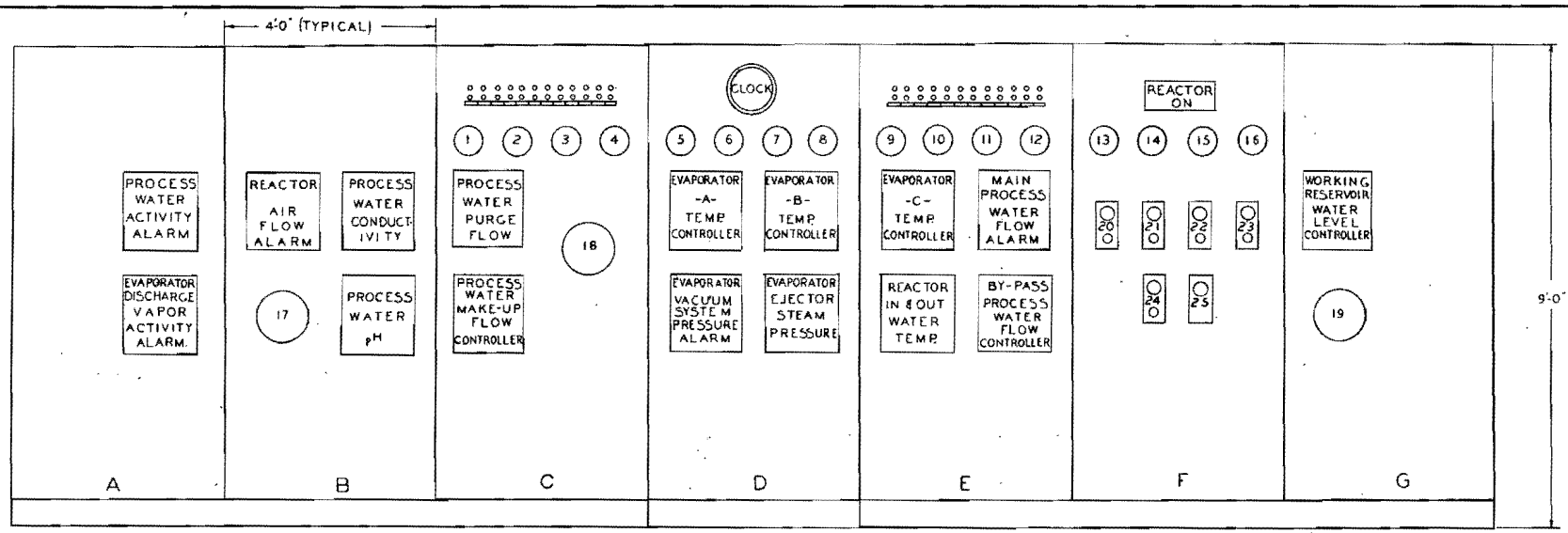

FUNCTIONS OF PRINCIPAL INSTRUMENTS

RECORDERS - AS INDICATED.

INDICATORS

1. INSTRUMENT AIR PRESSURE
2. STEAM SUPPLY PRESSURE
3. EVAPORATOR COOLING WATER PRESSURE
4. COOLING TOWER WATER TO EVAPORATOR 5 - FLOW
5. EVAPORATOR -A- OPERATING PRESSURE
6. " " PROCESS WATER FLOW
7. EVAPORATOR -B- OPERATING PRESSURE
8. " " PROCESS WATER FLOW
9. EVAPORATOR -C- OPERATING PRESSURE
10. PROCESS WATER FLOW
11. BY-PASS STRAINER DIFFERENTIAL PRESSURE
12. MAIN " " "
13. WORKING RESERVOIR LEVEL (CHECK)
14. PROCESS WATER SUMP TANK LEVEL
15. " " SEAL " "
16. DEMINERALIZED WATER TANK LEVEL
17. " " BACK-UP-ACTIVITY
18. EJECTOR & EVAPORATOR TEMPERATURES
19. WORKING RESERVOIR LEVEL

CONTROL AND/OR POSITION INDICATORS — WATER TO REACTOR

20. PROCESS WATER - MAIN FLOW CONTROL VALVE
21. " - BY PASS FLOW SHUT OFF VALVE
22. " " - EMERGENCY RECYCLE VALVE
23. DEMINERALIZED WATER - EMERGENCY SUPPLY VALVE
24. PROCESS WATER - MAIN FLOW SHUT OFF VALVE
25. " " - BY-PASS FLOW CONTROL VALVE

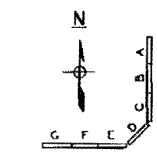

PLAN
INSTRUMENT PANELS

LEGEND

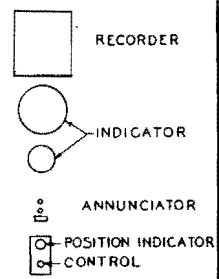

TOLERANCES	ARGONNE NATIONAL LABORATORY	PART	PROCESS WATER BLDG.
FRACTIONAL TOL. ± 1/64	This drawing is the property of the Argonne National Laboratory	ASSEMBLY	CONTROL & INSTRUMENT PANEL LAYOUT
DECIMAL TOL. ± .005			
ANGLE ± 1/2°			
ALL DIMENSIONS IN THIS DRAWING ARE IN INCHES			
UNLESS OTHERWISE NOTED			
DRAWN F.F. 1-3-51		SHEET	FIG. 5.8.B
NOTED LEVSE			

Sag - power level at which sag relay returns controls from "run" to "start" when level sags below $10^{-3} N_F$.

Start - operation regime at levels below $10^{-2} N_F$.

Run - operation regime at levels above $10^{-2} N_F$.

Run auxiliary - subregime, under run, permitting raising of servo control point on motor-operated rheostat.

Shim rod - designation of shim-safety rods in their function of providing coarse control of reactor level.

Safety rod - designation of shim-safety rods in their function of safety shutdown (for dropping of rods, see "Scram").

Regulating rod - the servo-controlled rod provided for fine control of reactor level.

Setback - lowering of control point on motor-operated rheostat; "fast setback" takes the control point from N_F to N_L in 90 sec, "slow setback" in 7 min.

Reverse - continuous insertion of all shim rods.

Scram - dropping of one or more safety rods; "fast scram" is entirely by electronic action (hard tubes); "slow scram" involves electromechanical relays.

High - high-speed continuous withdrawal of all shim rods.

Intermittent - intermittent speed of withdrawal; all shim rods run for ½ sec, off for 4½ sec.

Low - low-speed continuous insertion or withdrawal of a selected single shim rod.

Jog - insertion of individual shim rods; one switch for each rod.

Inching - on-off manual use of "low" for fine adjustment of shim rod position; made possible by resistor in series with shim rod motors.

Cocked rod - fully withdrawn regulating rod cocked for safety (i.e., insertion) action.

Insert - to move in downward direction a shim-safety rod holder holding a rod.

Withdraw - to move in upward direction a shim-safety rod holder holding a rod.

Lower - to move in downward direction a shim-safety rod holder not holding a rod (i.e., empty). (*Note:* "Lower" is also used to mean change of servo control point by running motor-operated rheostat.)

Raise - to move in upward direction a shim-safety rod holder not holding a rod (i.e., empty). (*Note:* "Raise" is also used to mean change of servo control point by running motor-operated rheostat.)

Manual - operating regime which is manual in the sense that the servo is not operative and the status of the regulating rod does not affect shim rods.

Automatic - operating regime in which servo may be operative and shim rods may be affected by regulating-rod limit switches.

Sigma - sigma amplifiers feed safety signals to the sigma bus, which thus combines these signals and feeds them to the magnet amplifiers, all in parallel.

5.10 REFERENCE REPORTS

(1) Newson, H. W., *The Control Problem in Piles Capable of Very Short Periods,* MonP-271, April 21, 1947.

(2) Weinberg, A. M., *Physics Division Quarterly Report, Period Ending February, 1948,* CNL-35, March 26, 1948.

(3) Nordheim, L. W., *Physics Division Quarterly Report for Period Ending May, 1947,* Part VII-i, MonP-314, June 21, 1947.

(4) Mead, L. W., *Development of an Ionization Chamber Suitable for a High Flux Pile,* MonP-316, August 25, 1947.

(5) Weinberg, A. M., *Physics Division Quarterly Report, Period Ending February, 1948,* Part VII-e, CNL-35, March 26, 1948.

(6) Straus, H. A., *An Electrically Driven Servo for the High Flux Pile,* ORNL-2, December 17, 1948.

(7) Huffman, J. R., *et al., Feasibility Report on Clinton High Flux Pile,* MonT-433, December 1, 1947.

(8) Jordan, W. H., *et al., An Instrument for Measuring the Logarithm of Neutron Level and Period of Pile,* ORNL-110, November 23, 1948.

(9) Lansing, N. F., *Analytical Prediction of Ion Chamber Response to Step Discontinuity in MTR Power,* ORNL CF-50-2-32, February 8, 1950.

(10) Jenks, G. H., *et al., Calorimetric Calibration of a Graphite-walled, Cavity-type Ionization Chamber,* ORNL-923, January 23, 1951.

5.11 REFERENCE DRAWINGS

DWG. NO.	TITLE
	(ORNL Drawings)
Q-541-A, C, D, E, H, K, L, U, U_2, U_3, V, W, X, Y, Z	Al Amplifier
Q-751-A through E_2	Logarithmic Count Rate Meter
Q-889-1 through 6	Magnet Amplifier
Q-915-1 through 5	Log *N* Amplifier
Q-947-1 through 8	Sigma Amplifier
Q-975-1B through 6B	Neutron Chamber
Q-900-7	I.P.C. Connector Modifications for use with Gas Chambers
Q-995-1 through 4	Power Supply Compensated Ion Chamber
Q-1092-1	Fission Chamber
Q-1093-1,2,3	Period Amplifier
Q-1095-1 through 6	Servo Amplifier
Q-1045-1 through 6	Compensated Ion Chamber
	(Blaw-Knox Construction Company Drawings)
BKC-3150-803-11	Architectural - Control Room Details
BKC-3150-603-31	Reactor Control Board - Layout and Instrument Schedule
BKC-3150-605-1	Process Water Building - Control Board Layout and Instrument Schedule

Chapter 6*

CANAL AND CANAL HANDLING FACILITIES

The canal contains the equipment for the handling of assemblies discharged from the reactor and provides space for the storage of spent operating assemblies, irradiated materials, and internal parts of the reactor. Water over these materials protects the operating personnel against the hazards of radiation.

6.1 CANAL

6.1.1 General Description. The general layout of the canal is shown by Fig. 6.1.A. The main section of the canal is 8 ft wide and extends eastward from the east face of the reactor. The canal section that lies partially beneath the reactor west wall is 6 ft wide. Connecting the above two sections is a 7-ft-wide section through the sub-pile room. The 7-ft width of this section provides ample space for the canal unloading mechanism and storage of the neutron curtain.

The parapet around the canal is 10 in. thick at the bottom and projects outward at the top to a width of 13 in. This projection provides ample toe space and also gives the operator better stability when working over the parapet. The top of the parapet is 3 ft above floor level.

The bottom of the rabbit canal is 6 ft below the basement floor level while that of the main canal is 16 ft below the basement floor level. The water level in the canal is maintained 2 ft above the basement floor level, thus providing depths of water in the rabbit canal and main canal of 8 ft and 18 ft, respectively.

The depth of water in the canal is sufficient to adequately shield against the fission product gammas from the stored reactor fuel assemblies. The original calculations indicated that a water depth of 17 ft would be adequate in the spent fuel storage section of the canal. However, recent experiments conducted at ORNL gave results showing higher fission gamma energies and lower attenuations for a thick layer of water than those used for the previous

*ANL contribution.

[redacted]

DWG # 10749

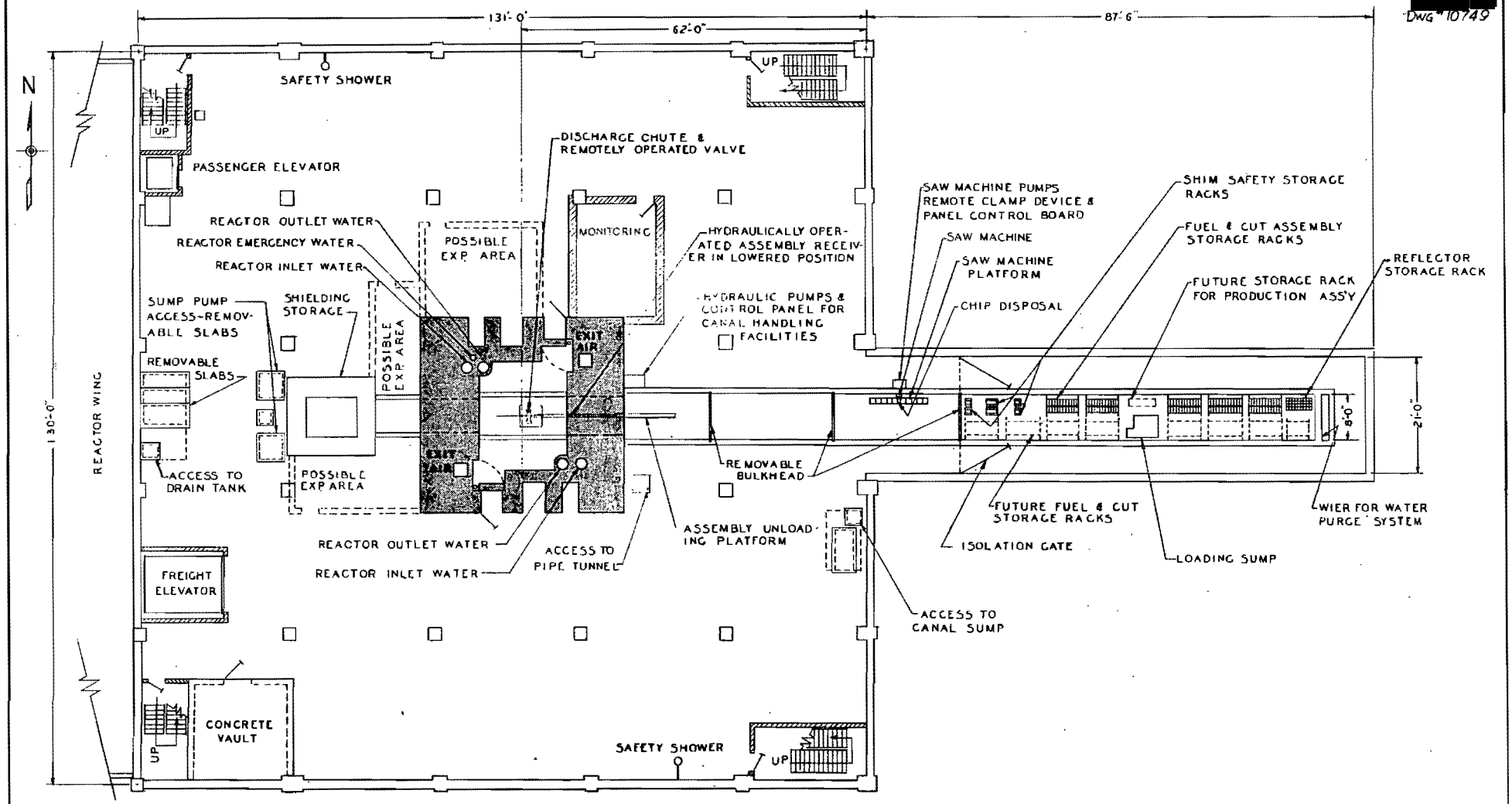

TOLERANCES: FRACTIONAL TOL. ± 1/64; DECIMAL TOL. ± .005; ANGLE ± 1/2°; 32 MICROINCHES OR THEIR EQUIVALENT FROM 32 TO 250 MICROINCHES; UNLESS OTHERWISE NOTED	DRAWN: E.F. 7/15/54; SUBMITTED: REPRESENTATIVE ROTTER & LEVSE	ARGONNE NATIONAL LABORATORY — This drawing is the property of the Argonne National Laboratory	SYM. / DRAWN / DATE / BY; PART: REACTOR BUILDING; ASSEMBLY: BASEMENT PLAN; SHEET / OF; DWG. NO.: FIG. 6.1.A; ITEM NO.

calculations. The main canal water depth of 18 ft limits the radiation levels to 0.01 r per 8 hr at the surface of the water in the reactor basement and to 0.1 r per 8 hr in the storage area.

The attenuation calculations for the design of the canal were based on the following factors:

1. Assume there are no 3-Mev gammas after a 15-day decay period.

2. Assume that for short decay periods (less than 76 hr) 20 percent of the total fission product gamma energy is from 3-Mev gammas.

3. The self-absorption relaxation length for 3-Mev gammas is 15 cm.

4. The build-up factor is equal to $e^{0.17b}$ (b = shield thickness in relaxation lengths).

5. The absorption coefficient of concrete at 3 Mev is 0.05 cm^{-1}.

Outside the Reactor Building the canal has a 6-ft-wide working space on each side and at the end. To provide this working space there is a 13-ft-8-in.-high and 21-ft-wide tunnel over the canal. The tunnel extends 87 ft 6 in. beyond the Reactor Building east wall. The canal and tunnel are about 25 ft longer than had been planned originally. This provides additional storage space for spent assemblies in case the chemical process plants are not completed until several months after the MTR is in operation.

The ceiling of the canal tunnel is constructed of reinforced concrete and is slightly below ground level. The section of roof below the road is reinforced to accommodate heavy trucks and the motor crane used to lift the spent fuel assembly coffins. The unloading hatch is located in an offset widened portion of the road and is at a point where traffic has the least effect upon the unloading operation. The portion of canal roof designed to withstand heavy loads is separated from the remainder of the roof by curbing which extends 50 ft along each side of the road. This prevents vehicles from traveling on the lightly constructed portion of the canal roof.

The canal walls are made of reinforced concrete. The canal floor is designed to withstand a load of 1 ton per square foot; the unloading sump can withstand a load of 2 tons per square foot.

The canal walls are covered with 4-in.-thick, 8- by 16-in. white glazed structural tile while the bottom is lined with 4 in. of white concrete. This construction satisfies the requirements that there be good visibility in the canal, and that cracks from which radioactive water could leak out of the canal be kept to a minimum. Other methods of construction, which were considered as satisfying either of these requirements, are listed below with reasons for their rejection:

1. Incorporation of a waterproof membrane in the canal walls to prevent outward leakage of water was discarded since gamma radiations from the spent fuel assemblies in the storage area might cause deterioration and eliminate failure of the membrane.

2. Painting of canal walls to enhance visibility was rejected since peeling and blistering would occur.

3. Covering the canal walls with a thin layer of white cement to aid visibility was rejected because of the likelihood of spalling.

4. The use of concrete wall surfaces was discarded because of their susceptibility to the accumulation of radioactive contamination.

The canal storage area is separated from the remainder of the canal by a bulkhead and gates. The underwater section consists of several removable bulkheads extending from the canal floor to the water level. The section above the water is isolated by gates that swing from the walls and meet at the center of the canal. At the end of the canal the purge water discharges over a weir into the canal sump. Provisions are made for two additional removable bulkheads which permit division of the canal into three sections.

6.1.2 Canal Purge System. A flow of 100 gpm is maintained through the canal to avoid an excessive build-up of radioactivity and turbidity. A solenoid valve, which automatically closes in case of power failure, is installed in the well waterline at the inlet to the rabbit canal. This provision obviates the possibility of flooding the canal sump when an electrical outage causes the canal sump pumps to fail.

Water from the canal overflows a weir, constructed the full width of the canal in the storage section, and flows through a discharge pipe to the canal sump. The purge water from the canal sump is pumped to the acid-treating unit for use as cooling tower make-up water, to the leaching pond, or to the retention basin, depending on the activity level. A radiation alarm is provided

in the sump, and manually operated valving for directing the flow is provided in the pump discharge header. A liquid-level controller governs the operation of the sump pumps.

6.1.3 Canal Flushing. Provisions are made for the future installation of two removable watertight bulkheads. These permit isolation of any section, except the rabbit canal, for cleaning and maintenance. Each section, except the rabbit canal, is provided with a drain and a waterline connection. The drains are interconnected in such a way that any section can be isolated and flushed. There are three adjustable overflow standpipes in the sub-pile room and rabbit canal sections. A continuous overflow to the reactor building process sump is maintained through these in order to prevent scum formation.

6.1.4 Heating and Ventilation of Canal Tunnel. The canal tunnel is heated and ventilated by air from a duct system that extends along one side of the tunnel ceiling. The air comes from the reactor building ventilation system. Since the air picks up negligible radioactivity in the tunnel, it is exhausted to the basement, where it mixes with the basement air before passing up to the reactor building first floor. There are six changes of air per hour in the tunnel. This number is required to prevent condensation due to variation of temperature in the canal tunnel.

6.1.5 Canal Lighting. Since the handling of assemblies in the canal is a manual operation carried on under 10 to 18 ft of water, it is necessary that good underwater lighting be provided. This lighting is supplied primarily by lights suspended from portable fixtures attached to the side walls of the canal. In addition to general overhead lighting supplied in the tunnel, special floodlights are provided in the loading platform area, canal storage area, sawing area, and loading sump.

6.1.6 Canal Crane. A manually operated crane with a 2-ton electric hoist is provided for the handling of heavy materials in the main canal. The highest hook position is 9 ft 9 in. from the floor. This provides a clearance of better than 6 ft between the hook and the top of the parapet. The hook cannot approach within 33 in. of one wall or 43 in. of the other wall of the canal tunnel. The maximum lift of the hoist is 25 ft 9 in.

6.2 UNLOADING MECHANISM

6.2.1 General Description. The function of the unloading mechanism is to receive the spent assemblies or control rods which have been lowered through the discharge chute of the reactor, rotate them from a vertical to a horizontal position, and eject them onto a receiving table at the bottom of the canal outside the sub-pile room shield. The assemblies are then removed from the receiving table and stored in racks at the far end of the canal. The complete mechanism includes the discharge tube, gate valve and safety devices, receiver, hydraulic seal, eject piston indicator, panel board, control valves, electrical interlocks, communication system, and assembly receiving table. The design is shown in Fig. 6.2.A.

The receiver is hydraulically operated and is a closed type, i.e., a seal and inward flow of water prevent any leakage of water from the reactor into the canal. It consists of a piston that operates in an assembly receiver cylinder. The piston performs the dual function of a receptacle for the several types of assemblies discharged from the reactor and of a means for ejecting the assembly onto the receiving table. The cylinder is open at the top and is supported near the closed bottom end by a trunnion shaft which is secured to the cylinder. The trunnion shaft bearings are carried in split bearing housings, the lower parts of which are cast integrally with the support base. The support base is bolted to a plate anchored in the canal concrete floor.

One end of the tipping cylinder pivots in a clevis which is cast as a part of the support base. The piston in the cylinder is fastened to a bell crank which is secured to one end of the receiver cylinder trunnion shaft. Orifices in the exhaust connections for the control valves govern the piston speed. The restriction of fluid flow by the orifices cushions the rise and fall of the receiver cylinder.

The hydraulic seal is fastened to the lower end of the discharge tube. It contains two hollow cylinders, of which one is stationary and one is movable. The stationary cylinder is the guide for the concentric movable cylinder. When the assembly receiver cylinder is in the vertical position, closing of the hydraulic seal joins the discharge tube and the receiver cylinder into a continuous passage. The closed gate valve in the discharge tube is

NOT CLASSIFIED

DWG. #10746

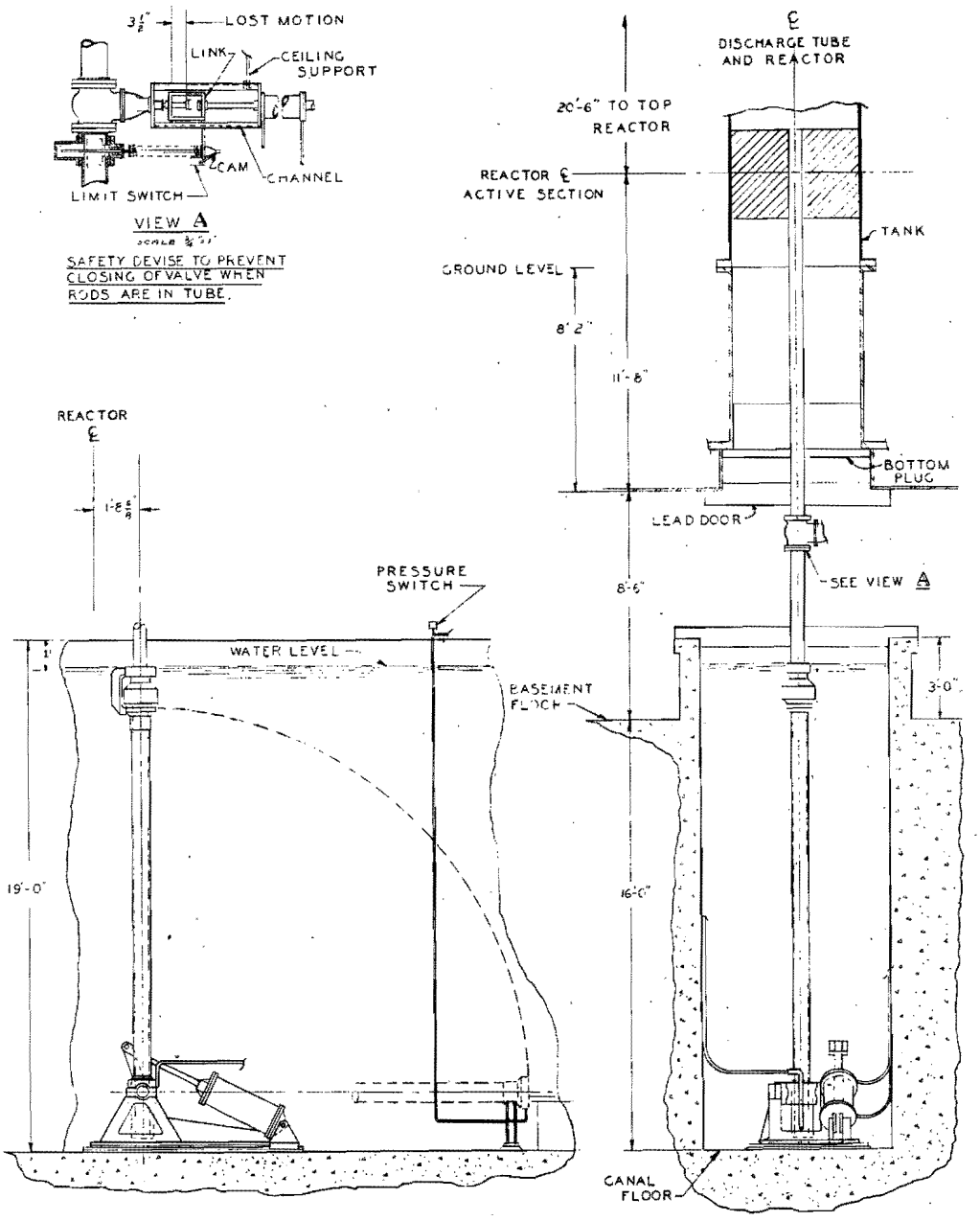

FIG. 6.2.A
UNLOADING MECHANISM

then the upper end of a sealed cylinder. This permits the eject piston to be raised or lowered by the operation of a four-way solenoid-operated valve. The valve piston closes all ports when in the neutral position and thus permits the eject piston to be locked in any position. A special Niagara water meter indicates the position of the piston in the receiver cylinder.

A purging line is attached to the upper end of the hydraulic-seal stationary cylinder. Water for this line is supplied at a pressure slightly greater than the head pressure in the reactor tank. This ensures a steady flow of water up the discharge tube once the remotely operated gate valve is open.

A mechanically operated open type receiver[1] was also considered but was discarded in favor of the hydraulically operated closed type.

6.2.2 Operation Sequence. The first step in the operation of the hydraulic unloading mechanism is to raise the receiver cylinder to its vertical position. In this position the remotely operated hydraulic seal at the lower end of the discharge tube may be closed; this joins the cylinder and the discharge tube into a single long fluid passage. Prior to opening the gate valve in the discharge tube, the piston may be raised or lowered to any desired position, depending on the type assembly to be received. This is accomplished by introducing demineralized water above or below the piston. The purge system is started before the gate valve is opened, and it is interlocked with the opening of the gate valve in order to ensure a flow of water up the discharge tube when the valve is open. After the gate valve is opened, the assembly being discharged is lowered into the receptacle in the piston, and the assembly handling rod is withdrawn. The gate valve is then closed, the purge stopped, the seal opened, the cylinder rotated to the horizontal position, and the assembly is ejected onto the receiving table. Finally, the assembly is picked up with long tongs or hooks and transferred manually to canal storage.

6.2.3 Control System. The operation of the reactor unloading mechanism is electrohydraulically controlled. The power that operates the mechanism is hydraulic. The flows in the hydraulic system are governed by solenoid-operated valves. The valve solenoids are operated by push-button switches in the various electrical control circuits. These circuits are interlocked by pressure switches, limit switches, and relays to ensure proper sequence of

operation. In order to keep electrical components out of the canal water, the various position switches are remotely mounted and are actuated by suitable hydraulic or mechanical linkages. Indicator lights and telephones are provided for the operators at the top of the reactor and at the control panel. The control panel is located at the canal, adjacent to the reactor, thus permitting observation of the ejection of assemblies onto the unloading platform. Diagrams of the control system and control board are shown in Fig. 6.2.B.

A pair of push buttons is provided at the control board for each of the following operations:

1. Elevating or lowering receiver cylinder.

2. Opening or closing of the seal at the discharge chute and receiver junction.

3. "Raising" or "lowering" of the eject piston in the receiver cylinder.

4. Purging of the discharge chute.

5. Opening or closing of the discharge-chute gate valve.

The position of the eject piston in the receiver cylinder is indicated by a dial mounted on the control board. Indicator lights on the control board provide information about the other operations.

Suitable interlocks provide the following limitations on the operation of the equipment:

1. The push buttons to elevate or lower the receiver cylinder are inoperable if the seal is closed.

2. The seal can be closed only when the receiver is vertical.

3. The seal cannot be opened unless the gate valve is closed; this prevents reactor water from entering the canal.

4. "Raising" or "lowering" of the eject piston is permitted only when the receiver is vertical or horizontal; because of the characteristics of the unloading mechanism, "lowering" of the eject piston cannot be accomplished when the receiver is horizontal.

5. The purge can be turned on only when the receiver is vertical and the seal is shut.

NOT CLASSIFIED

Dwg. # 10747

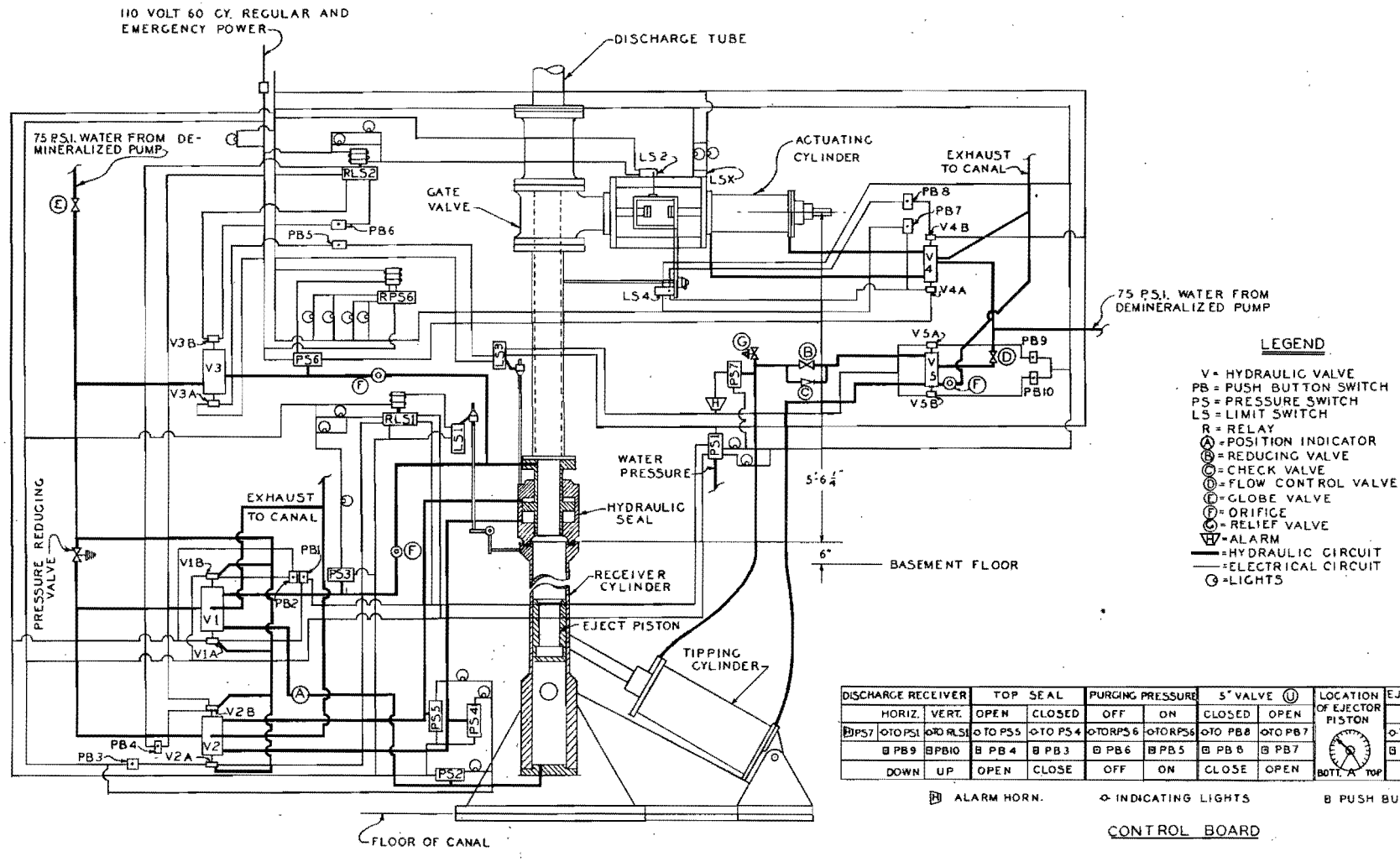

DISCHARGE RECEIVER		TOP SEAL		PURGING PRESSURE		5" VALVE (U)		LOCATION OF EJECTOR PISTON	EJECTOR PISTON	
HORIZ.	VERT.	OPEN	CLOSED	OFF	ON	CLOSED	OPEN		UP	DOWN
(H) PS7	○ TO PS1	○ TO RLS1	○ TO PS5	○ TO PS4	○ TO RPS6	○ TO PB8	○ TO PB7	BOTT. A TOP	○ TO PS2	○ TO PS3
⊡ PB9	⊡ PB10	⊡ PB4	⊡ PB3	⊡ PB6	⊡ PB5	⊡ PB8	⊡ PB7		⊡ PB1	⊡ PB2
DOWN	UP	OPEN	CLOSE	OFF	ON	CLOSE	OPEN		UP	DOWN

(H) ALARM HORN. ○ INDICATING LIGHTS ⊡ PUSH BUTTONS

CONTROL BOARD

TOLERANCES			
FRACTIONAL TOL. ± 1/32	APPROVED		
DECIMAL TOL. ± .005	PROJ. ENGR.		
ANGLE ± 1/2°	CHIEF ENGR.		
ALL WORKS TO BE FREE FROM FOR SUCH SHAP AS IS INDICATED ABOVE UNLESS OTHERWISE NOTED	CHIEF DRAFTSMAN		
	DRAWN	P.T.	12-12-58
	DRAWN BY	HUTTER	DRAFTSMAN LEYSE

ARGONNE NATIONAL LABORATORY

This drawing is the property of the Argonne National Laboratory

SCALE — SHEET — NO. REQD. —

SYM. | DRAWN | DATE | BY

UNLOADING MECHANISM

CONTROL SYSTEM

SHEET — OF — DRWG. NO. FIG. 6.2.B ITEM NO. —

6. The gate valve can be open only when the purge is on.

7. A safety device prevents closing of the gate valve while any obstruction is within it.

6.3 CANAL STORAGE

The various types of assemblies discharged from the reactor are stored in racks bolted to the floor at the end of the canal. The racks are designed to facilitate easy insertion and removal by providing unrestricted sidewise accessibility. The short assemblies are stored vertically or inclined at a slight angle to the vertical, while the long rods are stored parallel to the canal floor or at an incline to the horizontal. The canal purge is utilized to cool the assemblies.

6.3.1 Beryllium Assemblies. The storage of the beryllium reflector assemblies presents no problem except that they must remain adequately shielded. An aluminum rack provides for the storage of 36 of the assemblies.

6.3.2 Standard Fuel Assemblies. The fuel assemblies are stored at a slight angle to the vertical.[4,9] An "A" frame, fabricated from stainless steel, provides for the storage of 28 fuel assemblies. The sides and back of the pocket for the assembly are lined with a 1/32-in. cadmium sheet. The front is open toward the side wall or center of the canal for easy accessibility. Four holes in the bottom of the pocket permit water to flow into the assembly to keep it cool by thermal siphoning. Five racks, providing storage for 140 fuel assemblies, are installed in one side of the canal. Expansion anchors are installed in the other side of the canal for future installation of fuel assembly racks. This additional storage may be required if the chemical process plant is not completed for several months after the MTR is in operation.

6.3.3 Shim-safety Rods. The length of the shim-safety rod prohibits vertical handling unless shielding is provided in addition to that given by the canal water. To ensure thermal siphoning and adequate shielding, the rods are stored at a 15° angle to the horizontal.[2] They remain in this position until sufficient decay time has elapsed to permit the rods to be sawed into shorter lengths for transfer to decay storage or to chemical processing. The rods are stored with the bottom section at the lowest elevation. The canal purge dissipates the heat generated by the assemblies.

The racks for the storage of shim-safety rods are confined to groups of 16, four in a row and four tiers high. One rack is installed, while the future installation of racks in the other side of the canal is provided for by expansion anchors for the racks in the floor of the canal.

The rack consists of three sections, each of which is bolted to the canal floor and so located that the rod rests in all three. The end sections are *U* shaped to contain the rod and to permit easy insertion and withdrawal. The lower end section is closed at the bottom to stop the rod. The middle section supports the uranium section of the shim-safety rod. It is constructed in an angular shape and is lined with 1/32-in.-thick sheet cadmium to absorb neutrons.

6.3.4 Regulating Rods. Four regulating rods are stored parallel to the floor in *U*-shaped openings constructed at the bottom of the shim-safety storage rack. These openings are placed on the inside and outside of two adjacent shim-safety rods; this permits easy insertion and withdrawal of the rods.

6.4 ASSEMBLY DISPOSAL

6.4.1 Sawing Machine. The function of the sawing machine is to prepare the fissionable assemblies for transfer to the chemical processing plants. The conceptional design of the hydraulically operated sawing equipment is shown in Fig. 6.4.A. There is a sawing table with the necessary hydraulically operated locating devices and jigs for positioning and clamping of assemblies. The saw and its frame are clamped in a hydraulically operated reciprocating head which slides in a guide. The operating cylinder, control valves, and guide are attached to a long tube that fulcrums from a support bracket secured to the inside wall of the canal parapet. A hydraulic feed cylinder attached to the guide and a piston pushing against the canal wall and the guide provide the means to force the saw through an assembly. The saw, after sawing through an assembly, is returned to its starting position by a spring.

An electrically operated rotary sawing machine[1] was also considered but was discarded in favor of the hydraulically operated reciprocating type.

6.4.2 Chip Collector. A chip collector under the saw collects the heavy saw particles. The chips from this container will eventually be transferred out of the canal to a permanent disposal location. The diffusion of the

NOT CLASSIFIED

DWG. #10748

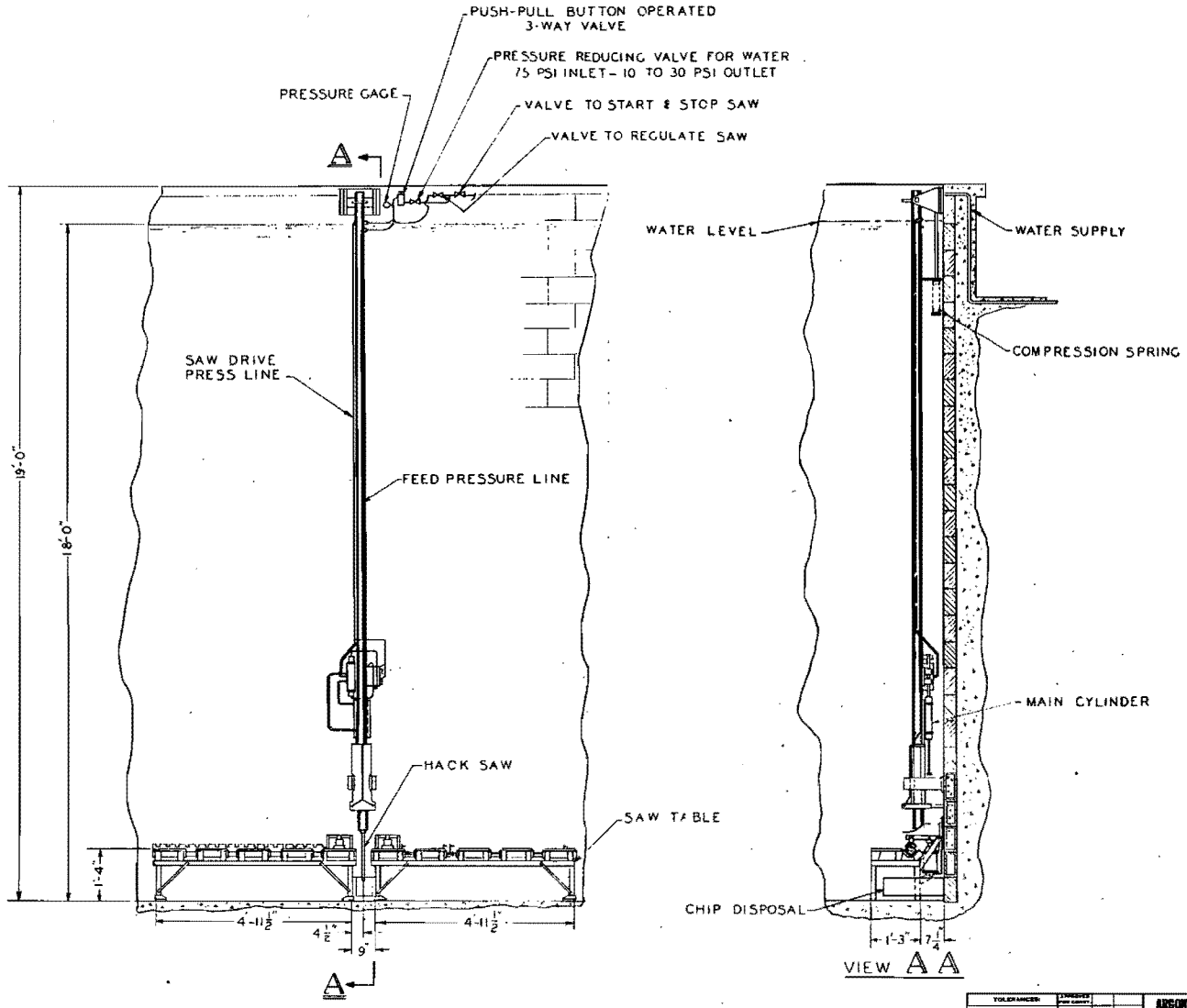

TOLERANCES: FRACTIONAL TOL. ± 1/64, DECIMAL TOL. ± .005, ANGLE ± 1/2°, ALL SURFACES TO HAVE 125 RMS OR BETTER FINISH UNLESS OTHERWISE NOTED	DRAWN PT 11-10-50	ARGONNE NATIONAL LABORATORY	SAWING MACHINE
	REPRESENTATIVE BITTERMAN/LEVSE	This drawing is the property of the Argonne National Laboratory	FIG. 6.4.A

light sawed particles in the canal water offers no problem in shielding. However, difficulties may arise in the accumulation of these light particles over a long period.

6.4.3 Transfer to Decay Storage. It is assumed that after a decay period of 21 days the fissionable material assemblies have decayed sufficiently for transfer from the canal to the chemical plants. This operation calls for the lowering of a carrier through an opening above the canal ceiling into a loading well in the canal floor. The various assemblies ready for transfer are loaded manually into the carrier in a vertical position. After four assemblies have been placed in the carrier or coffin, the cover is put in position and the carrier is lifted by a 20-ton motor crane onto a truck. No provision is made for water circulation in the carrier, since it is believed that thermal siphoning will be sufficient to cool the assemblies. A universal sized carrier for all assemblies appears practical as the sawed length of fissionable assemblies is the same.

6.4.4 Transfer Coffin. The thicknesses of lead walls required for a transfer coffin containing four irradiated fuel assemblies are computed to be 10.5 in. for the sides and 10 in. for the top and bottom.[10] The exposure from assemblies that have remained in the canal 15 days is then 0.04 r per 8 hr at the surface of the coffin.

The inside dimensions of the coffin are 12 in. square and 30 in. high. The inside is divided into four sections by steel plates covered with 0.002 in. of cadmium. The outside dimensions of the coffin, including the cover, are 32 in. square and 50 in. high. The corners of the coffin are rounded to the required shield thickness in order to reduce its weight.

6.5 REFERENCE REPORTS

(1) Nicoll, D., and Leyse, C. F., *Design Report No. 24, Canal and Canal Handling Facilities,* ANL-ABS-11.

(2) Leyse, C. F., *Cooling of Thorium Shim-Safety Rods in Canal,* ANL-ABS-10, November 16, 1949.

(3) Lennox, D. H., *Shielding of Fuel Assemblies in Canal,* ANL-EKF-4, August 12, 1949.

(4) Lennox, D. H., *Convection Cooling of Fuel Assemblies in the Canal,* ANL-EKF-5, September 20, 1949.

(5) Persiani, P. J., *Shielding of the Removable Beryllium Assemblies in Active Lattice,* ANL-EKF-10, October 14, 1949.

(6) Lennox, D. H., *Air Cooling of Fuel Assemblies,* ANL-EKF-15, November 23, 1949.

(7) Lennox, D. H., *Canal Water Heat Balance,* ANL-EKF-16, January 4, 1950.

(8) Lennox, D. H., *Decay Activity and Heat Generation Produced from Thorium Production Rods,* ANL-EKF-17, November 29, 1949.

(9) Lennox, D. H., *Danger of Fuel Assembly Cladding Failure with Natural Convection Cooling,* ANL-EKF-18, January 5, 1950.

(10) Lennox, D. H., *Fuel Assembly Coffin,* ANL-EKF-38, February 9, 1950.

6.6 REFERENCE DRAWINGS

(Blaw-Knox Construction Company Drawings)

DWG. NO.	TITLE
3150-570-1	General Arrangement of Submerged Saw for Storage Canal
3150-570-2	Main Frame and Drive Mechanism of Saw
3150-570-3	Submerged Design — Saw Guide and Frame
3150-571-1	General Arrangement of Reactor Discharge Mechanism
3150-571-2	Discharge Receiver Assembly
3150-571-3	Seal and 5-in. Valve
3150-572-1	Fuel and Cut Assembly Rack
3150-573-1	Removable Reflector Storage Rack
3150-574-1	Shim-safety Storage Rack
3150-579-1	General Arrangement of Main Canal
3150-903-44	Control Wiring for Discharge Mechanism

Chapter 7*

PROCESS-WATER SYSTEM

7.1 INTRODUCTION

The process-water system is the primary cooling system of the Materials Testing Reactor. The system provides a flow of water through the active lattice and other parts of the reactor that require water cooling. This chapter discusses the design and some of the problems encountered in the design of the process-water system. Although the active lattice and beryllium reflector form an integral part of the complete system, they are discussed only in a very general way in regard to some of the design problems. Detailed discussions of these two parts of the reactor are given in previous chapters.

During 1947 a design of the process-water system was conceived and developed for construction of the MTR at Oak Ridge National Laboratory. In the middle of 1949 the U. S. Navy Proving Ground in the Snake River Plains of Idaho was chosen as the Reactor Testing Station. With these fundamental data available, the design was redeveloped to suit the Idaho locality.

7.2 THE SYSTEM IN GENERAL

7.2.1 General Description of the System. Figure 7.2.A, schematic diagram of the MTR process-water system, presents an overall picture of all the vessels, pumps, pipe lines, and auxiliary equipment involved in the MTR process-water system.

Water at 100°F is pumped up to the working reservoir from the 60,000-gal sump tank by means of two 10,000-gpm 225-ft-head horizontal centrifugal pumps. A third pump is available in the event that either of the operating pumps fails or is shut down for maintenance. The water from the 150,000-gal working reservoir flows, under a normal head of 170 ft, directly to the reactor tank through a 30-in. stainless steel pipe outside the Reactor Building and a 36-in. stainless steel pipe beneath the Reactor Building. A flow instrument, strainer, and electric motor-operated flow control valve are located between the working reservoir and the reactor. These three items are blocked off in

* ANL contribution.

NOT CLASSIFIED
DWG. #10758

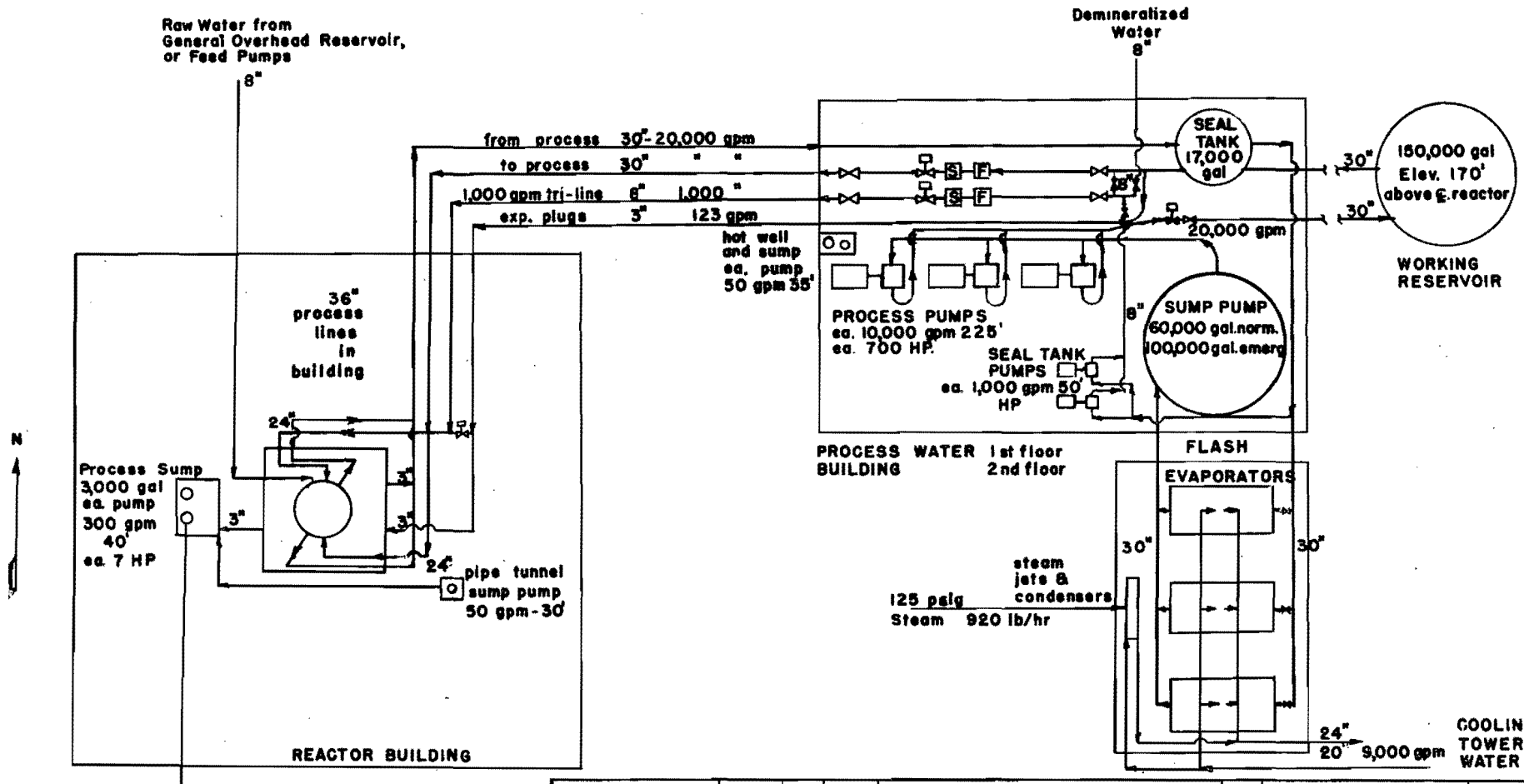

TOLERANCES:	APPROVED FOR CONST.			ARGONNE NATIONAL LABORATORY	SYM.	CHANGE	DATE	BY
FRACTIONAL TOL. ± 1/64	CHIEF ENG			This drawing [redacted] is the property of the Argonne National Laboratory, [redacted]	PART	SCHEMATIC DIAGRAM OF		
DECIMAL TOL ± .005	CHIEF DRAFTSMAN				ASSEMBLY	MTR PROCESS WATER SYSTEM		
ANGLE ± 1°	CHECKED							
ALL SURFACES TO HAVE AVERAGE 125 MICRO INCH OR AS RECEIVED FINISH. UNLESS OTHERWISE NOTED	DRAWN	12-21-58	J.W.M.	SCALE NONE / MATL. / NO. REQD.	SHEET OF	DRWG. NO. FIGURE 7.2.A		ITEM NO.
	GROUP	REPRESENTATIVE						

a pit by gate valves so that the water may be drained from them and they may be inspected or repaired. The 36-in. process-water line is split into two 24-in. stainless steel lines below the basement floor. These lines go up through diagonally opposite corners of the reactor biological shield and connect to the top section of the reactor tank. The water descends through the reactor tank sections, the active lattice, and beryllium reflector, and emerges from the bottom of the reactor tank through two 24-in. lines. The two exit lines are joined to a 36-in. line at the same location as that where the inlet line diverges from a 36-in. line into two 24-in. lines. The exit 36-in. line carries the water to the 17,000-gal seal tank in the process-water building.

The head losses between the working reservoir and the exit of the reactor tank are due almost entirely to the velocity head and friction losses across the active and beryllium sections, with relatively small losses contributed by the conveying pipe line. There are block valves and a flow control valve in the inlet line to the reactor, but there are no obstructions in the pipe line from the reactor to the seal tank.

There is an 8-in. line connected to the 30-in. inlet line at a point upstream from the valve pits and to the 36-in. line near the reactor. This 8-in. line provides a flow parallel to the main flow stream and contains two block valves, a flow instrument, a strainer, and a control valve. It can carry 1000 gpm and is used in the event that the main water line valve is closed off, thereby assuring a continuous water supply to the reactor at all times, particularly at shutdown. This same line, which allows 1000 gpm of process water to by-pass the main stream, can also be used to carry 1000 gpm of fresh demineralized water during periods of reactor flushing, or 1000 gpm of seal-tank water for recirculation through the seal tank and the reactor only.

The pipe tunnel beneath the Reactor Building is about 55 ft below the centerline of the active section and lies on bed rock. At the low point in the pipe tunnel there is a single 50-gpm sump pump which pumps out any water that leaks into the tunnel. This water is pumped to the 3000-gal process water sump, which is also located beneath the Reactor Building. The two 36-in. lines in the pipe tunnel lie one above the other; the inlet line is on top.

Water in the seal tank is drawn into the flash evaporators by means of the partial vacuum existing there. The water, in being flashed at a pressure that yields 100°F effluent, falls from the flash evaporators into the sump tank below. From the sump tank the water is once more pumped up to the working reservoir to complete the process-water cooling cycle. The reactor heat, liberated in the flash evaporators, is carried away by the cooling-tower water circulated through the condenser tubes in the evaporators.

7.2.2 Stand-by and Emergency Features. Certain provisions are made to ensure satisfactory operation of the process-water system under emergency conditions. The primary requirement in emergencies is that there always be some water flow through the reactor.

In addition to the water available in the working reservoir, raw water from the general overhead reservoir is available for cooling the reactor by a direct 8-in. line to the reactor tank. In the event both overhead tanks are destroyed, water can be pumped directly to the reactor from the two 500,000-gal ground-level reservoirs by means of two 850-gpm electric motor—driven or a 1000-gpm gasoline engine—driven centrifugal pump. If the motor-driven pumps in the demineralized-water line can be used, the reactor can be supplied through the two 24-in. inlet process-water lines with water from the 100,000-gal demineralized water storage tank. Within 30 sec of commercial electrical power failure, a Diesel electric generator set will provide electric power to strategic pumps and equipment. The reactor can be initially cooled under these circumstances by the reserve water in the working reservoir and then by 1000 gpm of process water recirculated by one of the seal-tank pumps, of which one is electric motor driven and one is gasoline engine driven.

The loops in the 24-in. water lines in the reactor structure help keep the active lattice under water at all times. This assures natural convection water cooling during an emergency shutdown and thereby prevents melting of the fuel assemblies. Should local water boiling occur, the localized steam pressure could conceivably force the water out of the active section and cause melting. However, sufficient pressurized water sources are available to practically ensure some water flow through the active lattice. A 2-in. line between the top of the reactor tank and the water loop is provided to prevent siphoning of the water from the active lattice if the process-water pipe line should be severed. In the event of any major emergency due to electrical outage, steam failure, etc., the reactor power will be nulled, and shutdown cooling will be the only requirement.

7.2.3 Instrumentation and Flow Balance. In order to maintain a continually balanced water flow through the process-water system, a scheme has been established in which water is pumped from the sump tank to the working reservoir. The valve that determines the amount of water lifted is governed by the level of water in the working reservoir. The water flow rate from the working reservoir to the reactor at a given control-valve setting and a constant head is uniform. The water flows from the reactor to the seal tank and then through the flash evaporators into the sump tank. Any overflow from the seal tank also goes to the sump tank. Any shortage of water in the seal tank is automatically compensated for by a decreased flow to the flash evaporators because the flash evaporators are fed water at a rate that is determined by the level of water in the seal tank and the pressure in the flash evaporators. In this manner the water flow through the whole system is kept in equilibrium. Normally the sump tank contains 60,000 gal of water. However, to accommodate undue surges and accumulations of water during emergencies such as electrical outages, the capacity of the sump tank is 100,000 gal.

Instrumentation on the flash evaporators provides the maximum possible vacuum. The flow of water to the flash evaporators is adjusted by means of valves in the inlet lines. The temperature of the water leaving the flash evaporators determines, by means of a thermal control, the quantity of cooling water passing through the condensing tubes.

The following instrumentation is related to the working reservoir: A temperature-indicating controller limits the lowest water temperature in the working reservoir by allowing steam to flow into a heating coil at the base of the reservoir. The floating roof of the working reservoir is arranged so that at water levels exceeding normal a mechanical switch shuts off the main process-water lift pumps. Within the normal operating range, the level in the working reservoir is maintained by means of an instrument which governs the opening of the main valve controlling the water flow up into the working reservoir. At lower water levels in the working reservoir the reactor is abruptly shut down and the main water valve is closed in 30 sec. The water flowing to the reactor passes through a pit in which there are two block gate valves which are pneumatically operated. The purpose of these block valves is to isolate the pit so that the portion of pipe between the block valves can be drained and inspected. Between the block valves, going downstream, there are, respectively, a flow recorder, a motor-operated control valve, and a strainer. Adjacent to the pit are taps for instruments which make continuous

recordings of the water resistivity and pH. Upstream of the first block valve is a 3-in. tap for water used in cooling the experimental plugs; the full head due to the height of water in the working reservoir is always available at this tap. The only valves that control the flow in this line are at the experimental plugs. An 8-in. by-pass line before the main motorized valve allows a flow of about 1000 gpm of water to the reactor when the main valve is shut. This line joins another 8-in. line from the demineralized water supply and an 8-in. line from the seal-tank pumps. Each of these three lines has an on-off remotely controlled pneumatic valve. Immediately after shutdown, process water goes through the 8-in. line directly to the reactor. Shortly thereafter demineralized water is used to purge the reactor—seal tank system, and, finally, seal-tank pumps recirculate the fresh water in this system. This 8-in. line enters the reactor-cooling water line at the point where the two 24-in. lines branch from the main 36-in. water inlet line. It also passes through the valve pit with the main water line and has two block gate valves. Going downstream there are, respectively, a flow meter, an 8-in. pneumatic flow-control valve, and a strainer.

The temperature and pressure of the water entering and leaving the reactor are recorded. The signal of the temperature difference between entering and leaving reactor water and that of the water flow are multiplied in a power recorder. The power of the reactor is also obtained from instruments measuring the gamma intensity of the water leaving the reactor and the neutron flux. Instruments are provided to record the temperature rise of the water in going through each fuel assembly, to record the radiation intensity of the water emerging from each fuel assembly, and to indicate the amount of flow through each assembly.

A flow recorder is provided on the water lines from each experimental plug, and, unless the flow through the plugs is satisfactory, the reactor cannot be started. A water meter is provided in the line supplying demineralized water to the rabbits and experimental plugs so that an inventory may be kept on the amount of water introduced into the process-water system in this manner.

The water leaving the reactor enters the seal tank in the Process Water Building. In the seal-tank entrance there is a radiation recorder for detecting fission breaks. The seal tank is provided with a demineralized-water inlet line and meter for supplying and metering make-up water. It also is provided with a temperature recorder and a level-indicating alarm. All pumps

in the process-water system are provided with pressure gauges. The flow to the flash evaporators from the seal tank is controlled by a valve and is indicated by an instrument in the outlet line from the flash evaporators. The flash evaporators are operated at full vacuum potential. Instruments are provided to indicate the vacuum on each evaporator and to control the amount of cooling water going to each evaporator condenser. The pressure of the steam going to the vacuum system is recorded and controlled. Temperatures in various points of the inter and after condenser vacuum-cooling system are indicated. The vapors discharged from the vacuum system are monitored by a radiation instrument which detects radiations and gives an alarm if large amounts of activity are discharged from the Process Water Building into the atmosphere. The sump tank is provided with a level-indicating-control-alarm and a temperature recorder. A flow recorder is provided for the purge from the sump tank.

7.2.4 Water-cooled Experimental Plugs and Rabbits. In the reactor there are seven water-cooled experimental plugs which require a total of about 125 gpm of cooling water. Water to cool these plugs is tapped from the main process-water line upstream of the valve pit. This assures that pressure sufficient to force the water through the plugs is always available, even during shutdown periods. The water leaving the experimental plugs flows into the process-water exit line from the reactor. In case it is not advisable to return the plug-cooling water to the process-water system, the water can be purged directly to the process-water sump. Demineralized water, which is one of the service facilities provided at beam holes, may also be used for plug cooling. During electrical outages these experimental plugs must have cooling water, and since demineralized-water pressure will fail at this time, a by-pass valve is provided from the process-water system to the demineralized-water system so as to maintain cooling of the plugs.

Entering the bottom of the reactor are four hydraulic rabbits used for experimental purposes. About 5 gpm of demineralized water is provided for each of these rabbits.

7.2.5 Process Water Building. The 20,000-gpm flow of MTR process water passes through the Process Water Building before entering and after leaving the reactor. This building contains the equipment for controlling the water flow, the pumps for lifting the water to the working reservoir, the shutdown

and emergency cooling-water pumps, and the flash evaporators for cooling and degassing the process water. Figures 7.2.B and 7.2.C show Process Water Building floor plans and building sections, respectively.

The seal tank receiving the water from the reactor section and the sump tank receiving the process water from the flash evaporators are enclosed in this building for shielding and instrument maintenance reasons. The equipment is located on seven main levels so as to obtain building compactness and to achieve proper hydrostatic balance between the seal-tank level, suction lift to the flash evaporators, and barometric discharge to the sump tank.

The 30-in. water line from the Reactor Building enters the Process Water Building through the control valve pit and then discharges into the 17,000-gal seal tank. From this tank the process water flows successively through the flash evaporators, sump tank, process-water pumps, and working reservoir, and then to the reactor through a control valve in the Process Water Building.

All piping and pumps are shielded with about 1 ft of concrete, and the valve control handles are extended through the shielding. All instrumentation and controls for maintaining proper process-water temperatures and flows are centralized in the Process Water Building instrument room. Overhead cranes and removable floor slabs provide accessibility to shielded pipes, valves, pumps, etc. Each pump cubicle is shielded from it neighboring cubicle so that repairs can be made during reactor operation.

7.3 MAJOR COMPONENTS OF THE SYSTEM

7.3.1 Sump Tank. The sump tank has a capacity of 100,000 gal. The primary functions of the sump tank are to receive the process water from the flash evaporators and to supply it to the process-water pumps. The tank normally contains a 3-min holdup of about 60,000 gal. This holdup is necessary for satisfactory operation of the process-water pumps. The additional 40,000 gal capacity of the tank provides for the accumulation of water in the event of failure of the process-water pumps. The sump tank also receives process water via an overflow from the seal tank.

7.3.2 Process Pumps. Three 10,000-gpm 225-ft-head horizontal single-stage double-suction centrifugal pumps, each driven by a 700-hp motor, are

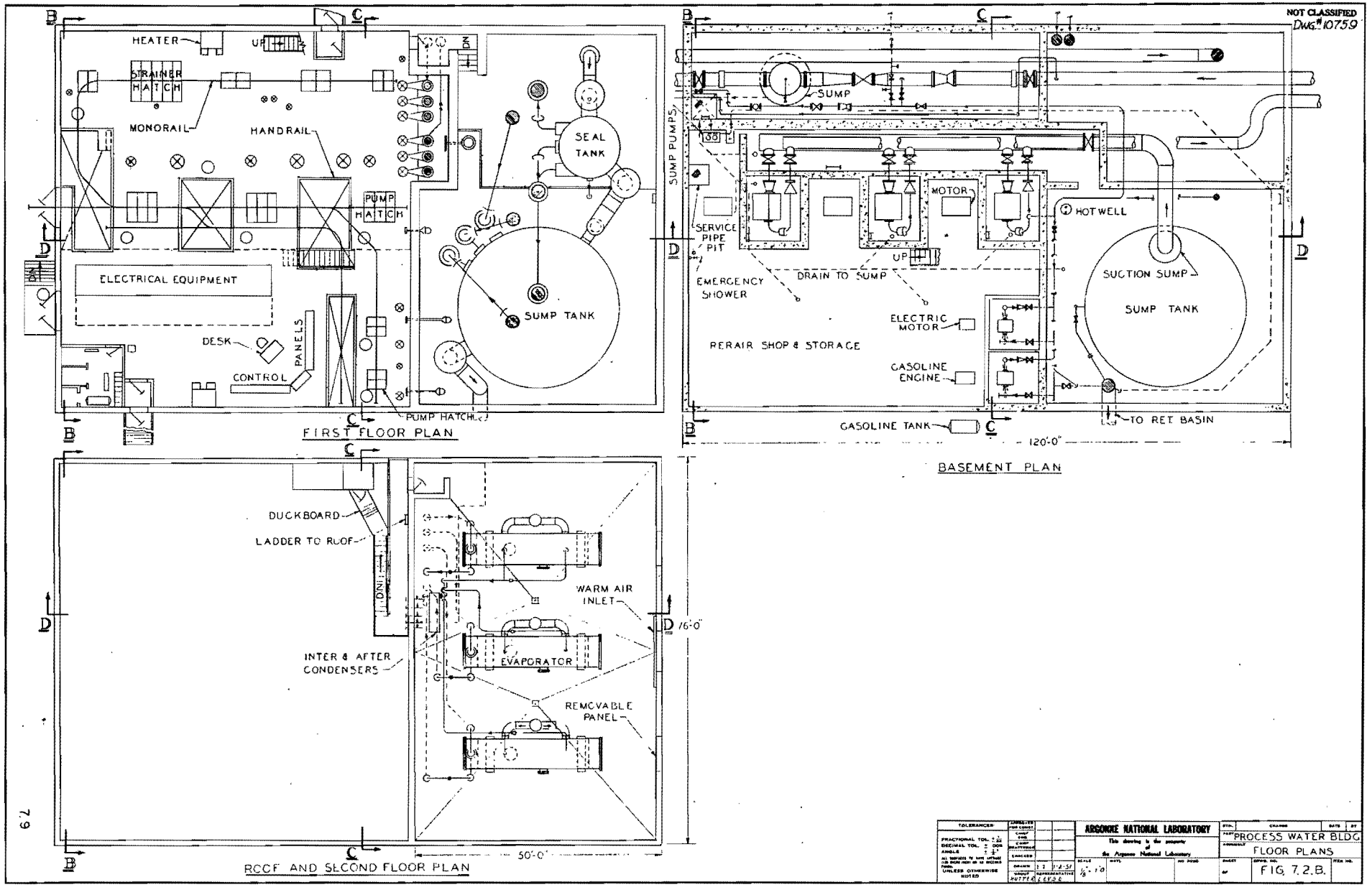
NOT CLASSIFIED
DWG. # 10759
HEATER
UP
STRAINER HATCH
MONORAIL
HANDRAIL
SEAL TANK
PUMP HATCH
ELECTRICAL EQUIPMENT
DESK
PANELS
CONTROL
SUMP TANK
PUMP HATCH
FIRST FLOOR PLAN
SUMP
SUMP PUMPS
MOTOR
HOTWELL
SERVICE PIPE PIT
EMERGENCY SHOWER
DRAIN TO SUMP
UP
SUCTION SUMP
SUMP TANK
ELECTRIC MOTOR
REPAIR SHOP & STORAGE
GASOLINE ENGINE
GASOLINE TANK
TO RET BASIN
120'-0"
BASEMENT PLAN
DUCKBOARD
LADDER TO ROOF
WARM AIR INLET
INTER & AFTER CONDENSERS
EVAPORATOR
REMOVABLE PANEL
76'-0"
50'-0"
ROOF AND SECOND FLOOR PLAN
ARGONNE NATIONAL LABORATORY
PROCESS WATER BLDG.
FLOOR PLANS
FIG. 7.2.B.

NOT CLASSIFIED
Dwg. #10760

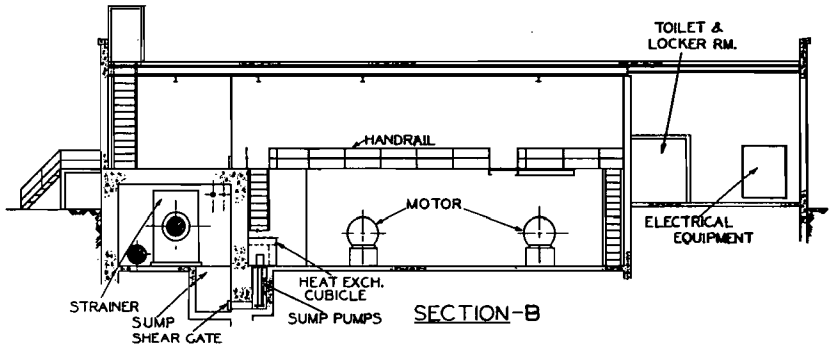

SECTION-B

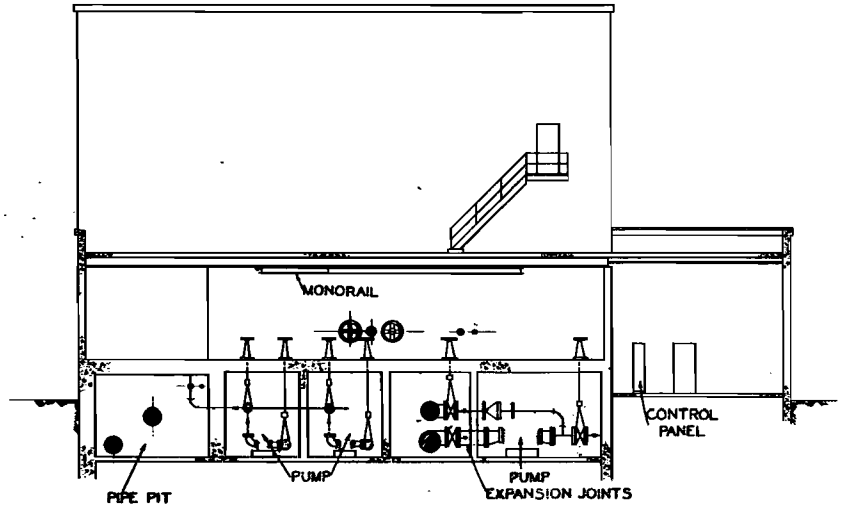

SECTION-C

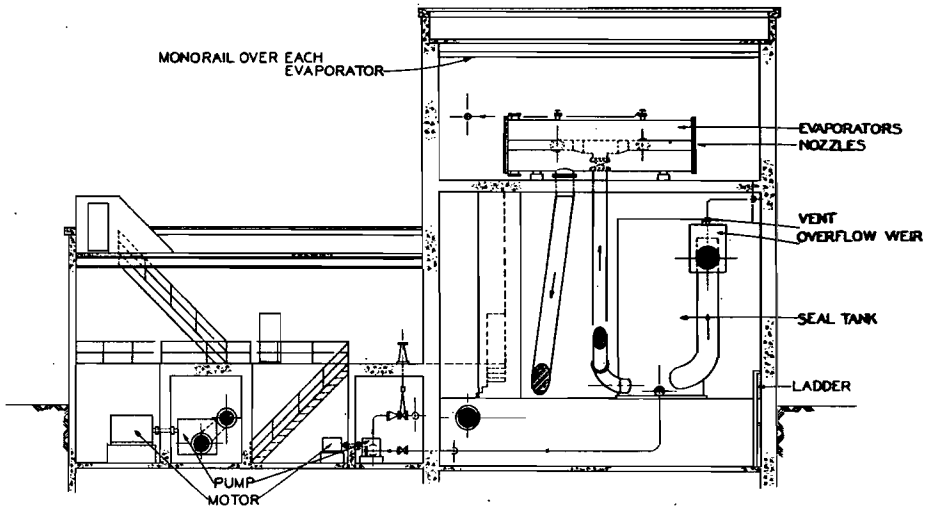

SECTION-D

TOLERANCES	DRAWN	C.C.	12-27-50	ARGONNE NATIONAL LABORATORY
FRACTIONAL TOL. ± 1/16	CHECKED			This drawing is the property of the Argonne National Laboratory
DECIMAL TOL. ± .005				
ANGLE ± 1/2°				
ALL DIMENSIONS IN THIS DRAWING ARE MADE FROM AN AS BUILT BASIS. UNLESS OTHERWISE NOTED				
	SCALE 1/8" = 1'-0"			

STD. | CHANGE | DATE | BY

PART OR ASSEMBLY: PROCESS WATER BUILDING
SECTIONS

SHEET | OF | DWG. NO. FIGURE 22-C | DWG. NO.

7.10

provided for lifting the process water up to the working reservoir. The process pumps are constructed of cast iron since it has been found relatively satisfactory in use with demineralized water, and since the area of the pumps that is exposed to the water is quite small compared to the whole water system. The use of two pumps to supply the 20,000 gpm required, with one stand-by pump, affords the least amount of moving equipment yet offers reserve in case of breakdown. Each pump is in a cubicle surrounded by 1 ft of concrete. This provides personnel radiation protection and permits isolation and repair. To prevent leakage of radioactive water from around the shafts, demineralized water under pressure can be added at the shaft seal. However, allowing the active water to leak into drainage to the retention basin is not serious.

7.3.3 Working Reservoir. The purpose of the working reservoir is to supply water at a constant head to the reactor active lattice. In the event of electrical or mechanical failure of the water-pumping system, the reserve of an overhead water supply is most advantageous. If local boiling would not occur in the active lattice and/or if a continual full water flow were not required, the pumps could deliver water directly to the reactor as is done at Hanford.

The height of the working reservoir is based on the allowable internal pressure for which the aluminum reactor tank is designed. Thus the working reservoir is 170 ft above a horizontal centerline through the active lattice. This elevation permits an increase of the process-water flow rate to the highest value attainable with the present reactor tank and fuel elements.

The size of the working reservoir is based on a full process-water flow of 20,000 gpm for 7.5 min. The 150,000-gal capacity of the reservoir can provide this flow. There are several reasons that such a large reserve capacity is desired. It is conceivable that an emergency condition may not be recognized or acted upon for several minutes. Also, during an electrical outage the flow does not cease for half a minute and it takes another half-minute to close the main water valve. In either of these situations an appreciable quantity of reserve water may be lost. In addition, the reactor must be cooled after it is shut down, and by allowing a 1000-gpm flow to the reactor for this purpose, about half the reserve can be lost in an hour.

Protection of personnel against radiation during reactor operation is provided by a fence around the base of the working reservoir. Since approach

to the reservoir is limited in this manner, and because of the height of the reservoir, shielding of the tank is not necessary. Immediately after reactor shutdown, radiation from the tank and pipes has been calculated[4,5] to be above tolerance (up to 0.8 r per 8 hr); however, they can be approached for short periods for maintenance of instruments, etc.

7.3.4 Valve Pit. The valve pit, at which all water flowing to the reactor is controlled, was appropriately designed as a part of the Process Water Building. In the pit there are two block gate valves which permit isolation of the strainers, a flow meter, and a motorized control valve, all of which are in the water line from the working reservoir to the reactor. This provides for maintenance of these items. Ahead of the upstream block valve there is an 8-in.-diameter pipe take-off which ties into an 8-in. demineralized-water line and an 8-in. seal-pump circulatory-water line. Each of these three feed lines has an open-closed motor-driven valve. When the 20,000-gpm flow is cut off by closing the main water-control valve, as after reactor shutdown, a 1000-gpm flow automatically by-passes the main water-control valve and flows to the reactor. The 8-in. line to the reactor also has two block gate valves, a strainer, flow meter, and motorized control valve in the valve pit. In case of emergency both the main water-control valve and the control valve in the 8-in. line to the reactor can be operated manually.

7.3.5 Seal Tank and Pumps. The purpose of the 17,000-gal seal tank is to maintain a definite water level in the reactor tank by means of the outlet weir during shutdown periods, and also to serve as a water supply source for the flash evaporator intakes. During normal shutdown periods cooling is provided by fresh demineralized water, circulated at 1000 gpm through the seal tank and reactor tank. During electrical outages a gasoline engine—driven 1000-gpm seal-tank pump can be utilized.

7.3.6 Flash Evaporators. Flash evaporators are used for cooling the MTR process water because they have been found to be the most efficient and economical of all types of equipment examined. These stainless steel flash evaporators, each 25 ft long and 8 ft in diameter, containing about 5000 ¾-in. cooling tubes, handle the 20,000-gpm flow and the 30,000-kw heat load of the MTR. The 110°F process water from the reactor is sprayed into the flash evaporators where the absolute pressure is 1.9 in. Hg, which is the saturation pressure of 100°F steam. Part of the process water evaporates, thereby cooling the bulk of the water, which falls into the sump tank below. The

evaporated water is condensed outside the water-cooled tubes and then rejoins the main process-water flow. Thus the process water is not only cooled 10°F, but it is degassed by the low pressure in the flash evaporators. During start-up the air is removed from the water at a rate of 175 lb/hr, and the hydrogen and oxygen formed in the active lattice during reactor operation are removed at a rate of 40 lb/hr. The water vapor pressure load under these conditions is 425 lb/hr or about two-thirds of the total vapor pressure load. At 1.9 in. Hg about 3.2 lb of 125 psig steam per pound of gas removed is required.

It is desirable to remove any gases in the water before returning it to the reactor since otherwise excessive gas evolution will occur in the active lattice where the water is heated and where hydrogen and oxygen are formed by water decomposition due to irradiation.

Analysis of gas solubility data for the MTR process water and existing operating piles show the following:

1. If nitrogen from the air is not removed from reactor-cooling water, it will be oxidized to nitrates under irradiation and increase the reactor-water acidity and, therefore, the corrosive aggressiveness on reactor structural materials in contact with water.
2. The process-water cycle should be closed with floating heads on storage tanks to prevent air absorption in water. If this is not done, the vacuum degassing system will have to be 35% larger.
3. With no re-absorption of air, the hydrogen and oxygen evolved from the water as a result of decomposition will almost saturate water at 212°F; hence the water must be de-aerated before returning to the reactor.

Instead of degassing the whole process-water stream, degassing of only a by-pass stream may be adequate. However, owing to the present state of knowledge, a conservative design demands degassing of all the process water. Also, it appears that if the process water could be completely demineralized by the recently developed mixed-bed resin deionization methods, the amount of induced activity and the amount of hydrogen and oxygen gas produced in the active lattice would be considerably reduced.

Other methods considered for cooling the process water are given below, each with the principal reason for rejection.

1. Outdoor spray cooling: This involved dispersion of radioactivity to the atmosphere and the pick-up of dirt particles therefrom.
2. Refrigeration: This was too expensive.
3. Heat exchangers: These were satisfactory for heat removal, but expensive auxiliary degassing equipment would be necessary for removing gases from the water.

7.3.7 Piping. The 30-in.-diameter pipe was selected primarily on the basis of a maximum allowable pressure drop of 25 psi from the working reservoir to the reactor tank. In the Reactor Building the main water line diameter is 36 in. to allow for future expansion without any major excavations or structural changes. The two 24-in. diameter water lines entering and leaving the reactor tank are primarily to distribute the water flow evenly. Since the greatest security against pipe rupture is desired in the line from the working reservoir to the reactor tank, all valves, the flow meter, and the strainer are made of stainless steel; in other locations cast iron is used. In the reactor structure the 24-in. process-water pipe is hung from the structural steel by suspension hangers and is free of any concrete contacts. However, it is surrounded by a spiral welded-steel pipe, and there is Zerolite fiber packing in the annulus between the two pipes. The exit part of the pipe is supported on the bottom stainless steel section of the reactor tank. Stainless steel—clad pipe, 20% or at least 1/16 in. thick, is used because it is more economical than solid stainless steel. The process-water pipe outside the reactor building lies in the ground, whereas in the Reactor Building it is suspended from spring-loaded hangers in the concrete tunnel.

The only possible cause of water hammer in the process-water system would be an instantaneous closing of the 24-in. main process-water-control valve. If this valve closed in less than 0.2 sec, the maximum possible increase in pressure would be 385 psi; if the closing time were 16 sec, the maximum pressure would be 4 psi. However, since the valve is designed to close in 30 sec, the possibility of water hammer is eliminated. Failure of the pumps lifting water to the working reservoir will not cause water hammer because the reverse momentum of the water is quite low.

Pipe with ¼-in.-thick walls is adequate to prevent collapse under vacuum or bursting due to the internal working pressures. Temperature stresses are not appreciable.

7.4 BASES FOR DESIGN

7.4.1 Flow Quantity and Heat Transfer. An over-all picture of the heat transfer and flow characteristics of the MTR is given in this section. The details of heat removal and water flow in the active lattice are discussed thoroughly in Section 2.7.1.

The quantity of water required for cooling the MTR is determined by the amount of heat liberated in both the active lattice and the beryllium reflector. Because of the high neutron flux the amount of heat liberated per unit volume is very large. Clean surfaces and high water velocities are therefore necessary in order to obtain high heat transfer fluxes. Also, high water velocities through the active lattice are required to carry away any bubbles of steam or air that may be formed. The water velocity provided through the active lattice is 30 ft/sec.

It became apparent during early investigations with the MTR mock-up that as much as a third of the total water flow was passing through the beryllium reflector. Previous to obtaining these data it had been believed that 15,000 gpm of process water would be sufficient for cooling the reactor. However, because of the large amount of water passing through the beryllium, the process-water system is designed for a total flow of 20,000 gpm. This flow is based on 30,000-kw operation of the reactor. However, it is expected that the same flow will be sufficient for operation at higher power levels.

The temperature of the process water increases about 20°F in passing through a fuel assembly, but the temperature rise of the 20,000 gpm total water flow is only about 11°F. This is because of the relatively large amount of water flowing through the beryllium.

Experiments conducted with a single fuel assembly showed that a 40-psi pressure drop is sufficient to produce a 30-ft/sec water velocity through an assembly. During the design of the MTR water system, it became apparent that, if higher water velocities were desired, a higher head of water would be needed in the working reservoir. Since the aluminum tank around the active section is designed for a pressure of only 74 psig, and since this is the pressure produced when the water is at its highest level (170 ft above the center of the active lattice) in the working reservoir, the greatest theoretical water velocity obtainable through the fuel assemblies is 42 ft/sec. This possible

40% increase in flow velocity could increase the heat transfer film coefficient only 31%. These two percentages are based on the assumption that the pressure drop and film coefficient are respectively proportional to the 1.8 and 0.8 powers of the water velocity. Thus the design of the reactor tank limits the heat transfer film coefficient attainable.

The amount of water flowing through the active lattice also depends on the fact that the pressure existing in the active section corresponds to a particular boiling point, and the temperature of the water film adjacent to the fuel plates must not closely approach this boiling temperature. Localized hot spots in the active lattice determine how high the temperature of the water film will be. Operation of the reactor will determine the highest possible working temperatures of the process water in the active lattice.

7.4.2 Degasification. In the MTR it is necessary to maintain a high heat transfer from the fuel elements to the passing water. In order to do this, bubble formation due to dissolved gases in the water must be prevented in the active section. If the amounts of dissolved gases in the process water are kept below their saturation values at the active-section operating pressures and temperatures, no gas evolution will occur. The following discussion describes briefly the degasification of the MTR process water and gives pertinent data connected therewith.

The water in the process-water system has essentially no contact with air since the tanks of the system are provided with floating heads. The dissolved gases in the process water during reactor operation are thus composed of the H_2 and O_2 produced by water decomposition in the active lattice, the air in the air-saturated demineralized make-up water, and water vapor. However, when the reactor is started, either initially or after a complete purge of the process-water system, the system contains air-saturated fresh demineralized water and functions primarily as a system in contact with air. Although the demineralized water in contact with air in the demineralized water storage tank will not come to saturation equilibrium, in order to have a conservative design it is assumed that it does. Thus the gas load anticipated during reactor start-up has the following composition: 4 to 8% H_2 and O_2 that are produced in the active section; 35% N_2 and O_2 from the air-saturated water; 57 to 61% water vapor. During continued reactor operation the contribution due to the N_2 and O_2 from air-saturated water is greatly reduced since only 50 gpm of demineralized water is added as make-up.

The rates of formation of H_2 and O_2 in the active section are related to the quantity of radiated energy that the water absorbs; an approximation is that one H_2 molecule is formed for every 100 ev absorbed, but this may vary severalfold depending on the purity of the water. The energy absorbed in the process water of the MTR at 30,000-kw operation is 28,500 kw, or 1.8×10^{25} ev/sec.[24] The rates of formation of H_2 and O_2 are then, respectively, 6.4 and 3.2 liters/sec at NTP.

The following two tabulations summarize the operating conditions in the active lattice, and the solubility of gases at these conditions. The gas solubilities are calculated for the surface temperature of most of the transfer areas of the fuel rods.

Active Lattice Operating Conditions

Temperature of entering water	95°F
Temperature of leaving water	115°F
Temperature of hot metal surface points	240°F
Temperature of most metal surface points	212°F
Absolute pressure	1.5 atm. absolute
Process-water flow	20,000 gpm
Reactor power	30,000 kw
H_2O_2 concentration	0.005 molar

Gas Solubilities at Active Lattice Operating Conditions: 212°F, 1.5 atm.

Nitrogen	5.0 cc/liter
Oxygen	3.0 cc/liter
Hydrogen	5.5 cc/liter
	13.5 cc/liter

The gas solubilites of the water under the conditions that exist in the demineralizer tank and upon entering the process-water system are as follows:

Gas Solubilities of Demineralized Water: 95°F, 1 atm.

Nitrogen	9.4 cc/liter
Oxygen	4.8 cc/liter
Carbon dioxide	0.2 cc/liter
	14.4 cc/liter

The amounts of the gases remaining in the process water when it leaves the flash evaporator after having been degassed are given in the following tabulation. These values are calculated and indicate the approximate amounts expected during operation.

Dissolved Gases in Degasified Water: 95°F, 1.8 in. Hg

Nitrogen	0.10 cc/liter
Oxygen	0.05 cc/liter
Hydrogen	0.10 cc/liter
	0.25 cc/liter

In the following table are summarized the quantities of the various gases and the total quantity of gases that the vacuum steam jet must remove. It is necessary to remove the water vapor because it is carried along with the other gases.

Vacuum Steam Jet Load

Gases formed due to water decomposition	
Hydrogen	5 lb/hr
Oxygen	35 lb/hr
Gases from air-saturated water	
Nitrogen	110 lb/hr
Oxygen	65 lb/hr
Water vapor	425 lb/hr
	640 lb/hr

The above table is based on start-up conditions. During continued operation the gas load from air-saturated water will be negligible.

7.4.3 Water Quality and Materials of Construction. In selecting the quality of water used for cooling the Materials Testing Reactor, the guiding principle was to minimize the amount of total dissolved solids in the water so as to maintain high heat transfer coefficients at the fuel assemblies. Any deposition of material from the water onto the hot surfaces of the fuel assemblies could reduce the heat transfer coefficients to undesirable values.

Any constituents in the water that would act as catalysts in the corrosion of aluminum, beryllium, or stainless steel parts of the process-water system would also be undesirable. For this reason it is necessary to minimize the amounts of lead, nickel, copper, and chlorides in the water. An additional advantage of a low mineral content in the water is that the amount of radioactivity induced in the water is appreciably reduced, thus reducing shielding requirements of the system.

In the original heat transfer experiments it became apparent that the water system should be constructed of stainless steel in order to minimize corrosion and maintain a low mineral content in the water. Columbium-stabilized type 347 stainless steel was selected so as to facilitate welding. At a later point in the heat-transfer experimentation program, it was found feasible to construct the MTR process-water system of cast iron. However, because of the limited experimental program and the resulting uncertainties in the use of cast iron piping, the process-water piping is of stainless steel while cast iron pump casings are used so as to minimize cost.

In comparing the MTR process-water system with water systems of other reactors, it is found that the Materials Testing Reactor is the first recycling natural-water—cooled reactor. The reactors at Hanford utilize coagulated and filtered Columbia River water on a once-through basis, and thus the amount of induced activity in this water is small. The heavy water pile at Argonne and the higher-flux heavy water pile at Chalk River, Canada, have their heavy water recirculated in a tank surrounding the fuel assemblies. The volume of natural water in the MTR system is many times the volume of water in either the Chalk River or Argonne heavy water systems. It is interesting to note that both heavy water reactors were operated for several years without any water treatment, and in the course of this time, the amount of iron and aluminum hydroxides increased. The *p*H values of the water decreased to as low as 4, and the amount of induced radioactivity in the water increased to values that necessitated removal of the dissolved radioactive solubles. At Argonne ammonium hydroxide made from heavy hydrogen was added to the water to raise the *p*H and thus reduce its corrosive effects on the aluminum parts. However, this developed into a vicious cycle in that owing to ionizing radiations the ammonium hydroxide appeared to decompose to nitric acid, once more reducing the *p*H of the water in the system. The addition of more ammonium hydroxide was required with a consequent build-up of total dissolved solids. The

problem was solved at Chalk River by redistilling the D_2O and then demineralizing the recirculating heavy water. This removed the accumulating dissolved minerals and helped increase the *p*H of the water to nearly 7, and at the same time eliminated any catalytic ions that might have caused corrosion in the heavy water system. Provisions have been made in the MTR system to add fresh demineralized water and to purge the same quantity of water from the system so as to maintain a high-quality circulating process water. It is expected that, when the MTR is in operation, the purge can be put through a demineralization system and used as make-up. With the recent development of mixed-bed deionizers, the water in the system can be brought to a resistivity of practically pure water, which is apparent from the following tabulation:

NaCl (ppm)	RESISTIVITY (ohms)
1.00	185,000
0:10	1,850,000
0.01	18,500,000
0.00 (pure water)	20,500,000

Ever since the Hanford reactors have been operated, sodium dichromate and sodium silicate have been added to the single-pass water system to minimize corrosion, and at one time it was believed that additions of similar reagents should be made to the MTR water system. A few years ago the sodium silicate addition to the Hanford water was removed, and no increased corrosion or scaling rate was found to occur. Although the additions of sodium dichromate have never been stopped, it is believed that they could be without increasing corrosion or scaling.

The heat transfer experiments conducted at Oak Ridge differed from the MTR system in that the water used at Oak Ridge was cycled in an open system whereby oxygen and nitrogen of the air were readily dissolved. It is expected that any gases in the MTR process water will be practically completely removed by the flash evaporation process, and therefore the corrosion rates may be even less than those determined by the experiments conducted at ORNL.

7.4.4 Induced Activity. Elements and sources which contribute to the water activity can be listed under the following categories:

1. Isotopes of oxygen in pure water itself.
2. Solutes in the water such as mineral impurities or dissolved gases.
3. Radioactive and nonradioactive elements corroded from structures in the reactor into the water.
4. Radioactive elements knocked into the water by recoil upon the instant of neutron capture.

Radioactive isotopes formed from oxygen produce an enormous amount of activity but lose their controlling influence in about 1 min because of their short half-lives. These isotopes are the primary source of induced radioactivity in the MTR process water. The dissolved impurities in the water form the main secondary source of water activity. During the first minute the radiation products of oxygen dominate radiation; Al^{28} (144 sec, 1.8 Mev) and Mg^{27} (692 sec, 1.02 Mev) are the principal activities for the next 5 to 10 min. Thereafter, Na^{24} (14.8 hr, 1.4 and 2.8 Mev) is the dominating radioactive isotope for the 15-min MTR water cycle.

The cooling water system of the MTR reactor is a closed recirculating system with a small percentage of purge and make-up water in order to control the intensity of long-lived induced activity and the accumulation of corrosion products.

When a recirculation system is employed, regardless of the method used for purge and make-up, the number of radioactive atoms (N) at equilibrium when production equals decay is given by[25]

$$N = \frac{nv\sigma N_v (1 - e^{-\lambda t_i})}{\bar{\lambda}(1 - Fa)}$$

where

nv = neutron flux, neutrons/cm^2-sec

σ = absorption cross-section, cm^2

N_v = concentration of target element, atoms/cc

t_i = time of irradiation (time to pass through active section), sec

$$F = \frac{\text{process flow rate}}{\text{process plus purge flow rate}}$$

$$a = e^{-\lambda t_c}$$

t_c = cycle time, sec

λ = transformation constant, sec^{-1}

The recoils from the aluminum in the active section can be calculated by[8]

$$P_r = \frac{(nv)\sigma N_v(R)AD}{4G(1 - a)} \quad \text{dis/sec-cc}$$

where

R = recoil range, cm

A = area of exposed aluminum, cm^2

D = density of aluminum, g/cc

G = cycle flow rate, g/sec

The constants used in the activity calculation for the MTR reactor are:

Flow rate	20,000 gpm
Purge rate	50 gpm
System holdup	350,000 gal (now 320,000 gal)
Cycle time	17.4 min
Irradiation time	0.08 sec
Slow flux	2×10^{14} neutrons/cm^2-sec
Fast flux	1×10^{14} neutrons/cm^2-sec
Exposed aluminum	10^6 sq cm

The desired composition of the MTR process water, which is the composition that is used in the activity calculation, is:

Fe	0.05 ppm	Cl	0.25 ppm
Al	0.05 ppm	Ca	0.5 ppm
CO_2	2.0 ppm	Mg	0.5 ppm
Na	2.0 ppm	A	0.6 ppm
SiO_2	1.0 ppm		

The results of the activity calculations are summarized in Table 7.4.A. The activities of the constituents in the process water and the total activity for water containing 2 and 8 ppm of Na are given as functions of decay time.

7.4.5 Shielding. The shielding calculations for the MTR process water system were based on the induced activities given in the previous section. In the calculations involving the process water piping it was assumed that the source was an infinitely long cylindrical source with self-absorption. The results of the calculations are given in Fig. 7.4.A, which shows the thickness of concrete shielding as a function of time. Separate curves are given for water containing 2 ppm of Na and 8 ppm of Na.

The following discussion gives a brief summary of the shielding of the process-water system. The intensity of radiation from the process water leaving the MTR active lattice requires 5 ft of concrete shielding within the Reactor Building. Within the reactor this shielding is provided by the biological shield; outside the reactor the pipe tunnel underneath the basement floor has sufficient concrete cover to meet the requirements. From outside the Reactor Building to the Process Water Building, 5 ft of earth covering bring the inlet and outlet process water pipes below the local frost line; this depth is sufficient to protect personnel from radiations above tolerance. In the Process Water Building the 12- to 18-in. concrete walls are adequate to reduce radiations from the pipes, valves, etc., to less than 50 mr/hr. No special shielding is required on the working reservoir owing to its height above the ground. A fence about the working reservoir base provides adequate protection by limiting the approach of personnel so that maximum daily tolerances are not exceeded.

7.4.6 Cooling After Shutdown. After an operating reactor is shut down, the total heat liberated due to the absorption of gamma and beta radiation

TABLE 7.4.A

Activity of MTR Process Water

REACTION	CONCEN-TRATION (ppm)	HALF-LIFE	CROSS-SECTION	RECOIL TYPE	RANGE (cm)	ACTIVITY (dis/cc-sec)				
						0 sec DECAY	50 sec DECAY	100 sec DECAY	500 sec DECAY	1000 sec DECAY
$O^{16}(n,p)N^{16}$		7.4s	0.04 mb			4.3×10^5	3,843	35		
$O^{18}(n,\gamma)O^{19}$		29.4s	0.44 mb			5,620	1,730	530		
$Al^{27}(n,\gamma)Al^{28}$		2.3m	0.21 b	Slow	10^{-6}	3,040	2,355	1,840	332	32
$Al^{27}(n,p)Mg^{27}$		10.2m	2.8 mb	Fast	10^{-4}	1,320	1,320	1,320	850	488
$Al^{27}(n,\gamma)Al^{28}$		2.3m	0.4 mb	Fast	10^{-4}	576	452	352	64	6
$Na^{23}(n,\gamma)Na^{24}$	2	14.8h	0.5 b			406	406	406	406	406
$Al^{27}(n,\alpha)Na^{24}$		14.8h	0.6 b	Fast	10^{-4}	163	163	163	163	163
$Mn^{55}(n,\gamma)Mn^{56}$		2.6h	13 b	Slow	10^{-5}	145	145	145	145	145
Total (2 ppm Na)						4.3×10^5	10,414	4,791	1,960	1,241
(8 ppm Na)						4.3×10^5	13,552	6,688	3,100	2,500

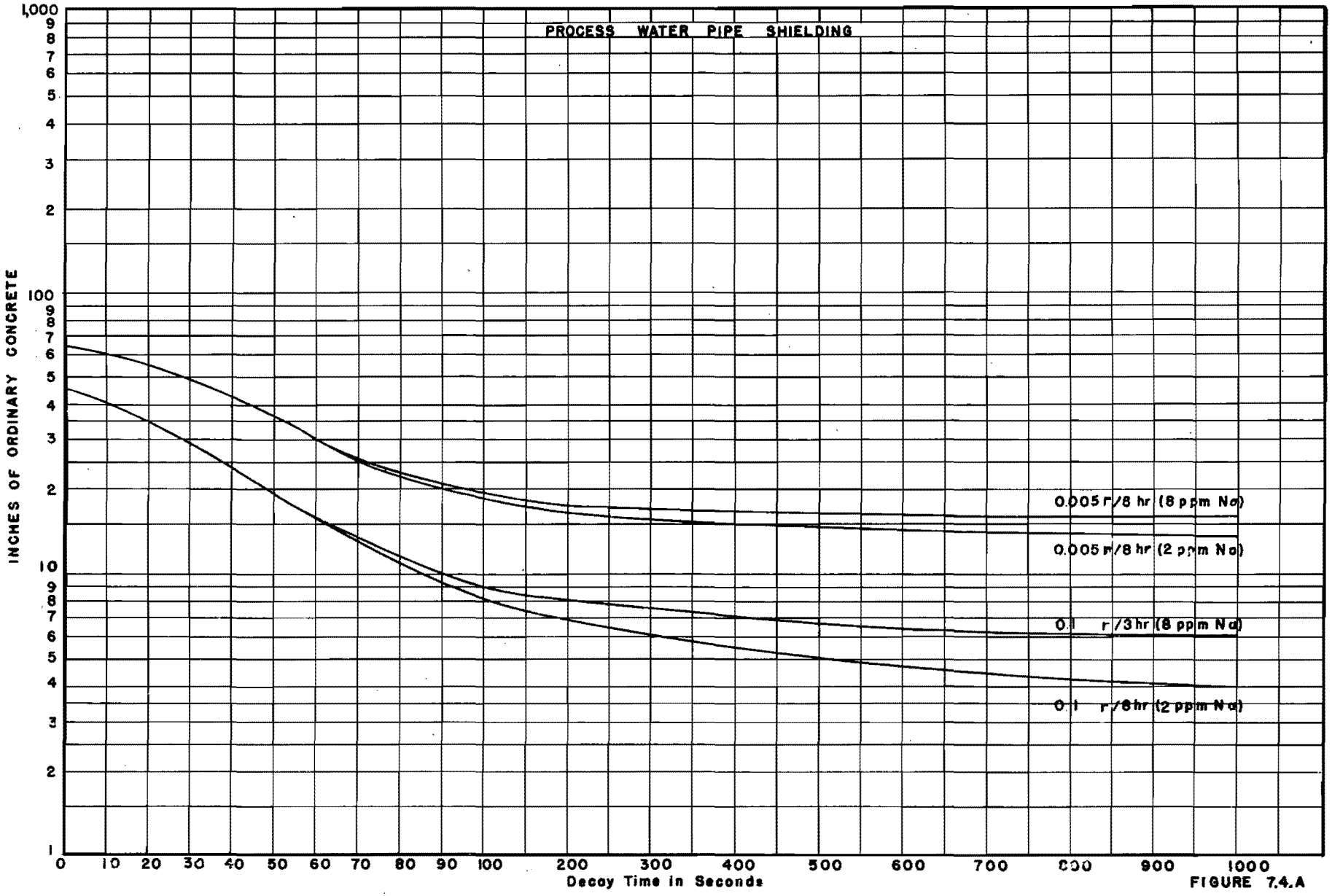

FIGURE 7.4.A

NOT CLASSIFIED

Dwg #10757

from the fission products is given by the empirical equation[23]

$$P = 187BFA[t^{-0.2} - (t + T)^{-0.2}] \qquad \text{Mev/sec}$$

where

B = reactor operating level before shutdown, kw

F = conversion factor, fissions/sec-kw

A = Reduction factor; a reasonable value is 0.08, which is an extrapolation to $t = 0$ from experimental measurements of energy after shutdown;[12] also, since at shutdown 14.7 Mev/fission of beta and gamma heat is released compared to 187 Mev/fission during operation, the ratio of the two heat values is 0.08 (i.e., 14.7/187).

t = time after shutdown, sec

T = time of pile operation, sec

From the above it is found that at the instant of shutdown the reactor heat falls from 30,000 to 2400 kw, of which 400 kw is in the beryllium reflector. The reactor active lattice heat development at shutdown falls from full power of 28,800 to 2000 kw or about a 1/15 reduction. Hence, although the water flow through the active lattice at shutdown can be reduced about 1/15, the water flow through the beryllium reflector can be reduced only 1/3 since its heat generation falls only from 1200 to 400 kw. Depending on the amount of excess water flow through the beryllium at full power, the total flow can be reduced from 1/3 to 1/15 at shutdown. At any time t after shutdown, the flow required will vary as $t^{-0.2}$. Calculations involving the varying film heat transfer coefficient and varying flow show that with a 220°F film temperature and 90°F entering water, 270 gpm must pass through the active lattice at the instant of shutdown. This gives a 50°F water temperature rise. The ratio of flow in the active lattice to that in the beryllium is estimated as 3:1. The following table gives the minimum process water flow required at various times after shutdown (Table 7.4.B).

TABLE 7.4.B

Minimum Process-water Flow After Shutdown

TIME AFTER SHUTDOWN (hr)	MINIMUM FLOW (gpm)
0	360
1	267
5	190
10	168
50	126

The shutdown cooling-water flow can be initially supplied by the reserve water in the working reservoir and, when the change-over can conveniently be made, by a 1000-gpm pump circulating water through a circuit including only the reactor and seal tank as major components. There are two 1000-gpm pumps supplied; one is electric motor driven while the other is gasoline engine driven.

It is of interest to show that the water in the closed seal-tank and reactor-tank circulating system will not reach a prohibitive temperature too quickly as a result of accumulation of shutdown heat. This heat is given by the equation

$$q = \int_0^t 30{,}000 \times 0.08 \left[t^{-0.2} - (t + T)^{-0.2}\right] dt \quad \text{kw-sec}$$

where 30,000 kw is the operating power level of the MTR.

The water temperatures given in the following table are based on this equation, a pile operating period of 15 days, and a 24,000-gal content of the circulating system.

TABLE 7.4.C

Process-water Temperature After Shutdown

TIME AFTER SHUTDOWN (hr)	q (Btu x 10^{-6})	WATER TEMPERATURE (°F)
10	7.5	110
20	12.0	130
30	15.5	150
40	18.5	164
50	21.5	174

Water from the demineralized-water storage tank can be added to the reactor-seal tank system at any time in order to cool this cycling water.

7.5 REFERENCE REPORTS

(1) Pettitt, E. N., *MTR Cooling Water Activity*, ANL-HLV-3, June 29, 1949.

(2) Krisberg, N. L., *Shielding of Water Pipes - MTR*, ANL-EKF-2, July 11, 1949.

(3) Lennox, D. H., *Retention Basin*, ANL-EKF-11, November 8, 1949.

(4) Krisberg, N. L., *Shielding Requirements of Reservoir and Associated Pipes*, ANL-EKF-23, December 1, 1949.

(5) Krisberg, N. L., *Shielding Calculations for the Working Reservoir Associated Pipes*, ANL-EKF-24, December 7, 1949.

(6) Lennox, D. H., *Shielding for the Retention Basin*, ANL-EKF-26, December 22, 1949.

(7) Lennox, D. H., *Retention Basin*, ANL-EKF-41, February 27, 1950.

(8) Lennox, D. H., *Process Water Activity*, ANL-EKF-44, March 8, 1950.

(9) Lennox, D. H., *Process Water Pipe Shielding*, ANL-EKF-46, March 30, 1950.

(10) Persiani, P. J., *Activity of the Process Water Effluent*, ANP-EKF-56, July 13, 1950.

(11) Wigner, E. P., *Cooling Water Radioactivity*, CP-499, March 1, 1943.

(12) Cannon, *et al.*, *Direct Calorimetric Study of Fission Product Decay in Active Slugs*, CC-2176, November 9, 1944.

(13) *Project Handbook - Chapter V*, CL-697, Metallurgical Laboratory, May, 1945.

(14) Monet, M., *Calculations of Pile Coolant Activities*, ORNL CF-49-7-240, December, 1946.

(15) Huffman, J. R., *Cooling After Shutdown*, ORNL CF-48-6-155, June 7, 1948.

(16) Lane, J. A., *Cooling After Shutdown, Supplement*, ORNL CF-48-10-263, October 22, 1948.

(17) Smith, N. M., *Shielding Subpile Room - Water Activity*, ORNL CF-49-1-238, January 18, 1949.

(18) Noderer, L. C., *Shielding Water Inlet Pipes*, ORNL CF-49-6-200, June 10, 1949.

(19) Lane, J. A., *Cooling Requirements at Reduced Power Level*, ORNL CF-50-4-17, April 3, 1950.

(20) Lane, J. A., *Cooling Requirements at Reduced Power Level*, ORNL CF-50-9-92, September 19, 1950.

(21) Farmer, W. S., *Activities in Process Water*, ORNL CF-47-4-115, April 7, 1947.

(22) Way, K., and Wigner, E. P., *The Rate of Decay of Fission Products*, ORNL MonP-303, May 19, 1947.

(23) Way, K., *Pile Technology Lecture No. 16*, M-3690.

(24) Etherington, H., *Water Cooled Pile for Naval Application*, ORNL-133, Septemper 1, 1948.

(25) Sivetz, M., "Radioactivity Induced in Water," *Atomics*, Vol. 6, No. 5, p. 4 (Sept. - Oct., 1950).

7.6 REFERENCE DRAWINGS

(Blaw-Knox Construction Company Drawings)

DWG. NO.	TITLE
3150-5-4	Process Water Pump House - Layout - Elevations
3150-5-5	Process Water Cooling Building - Plans
3150-5-6	Process Water Cooling Building - Plans and Sections
3150-5-7	Process Water Cooling Building - Layout and Sections
3150-19-1	Reservoir and Water Pump House - Layout
3150-92-6	Process Water System
3150-304-1	Working Reservoir
3150-702-2	Process Water Piping
3150-703-11	Piping - Internal Plan and Elevation - Process Water at Reactor
3150-703-12	Piping - External Plan and Elevation - Process Water at Reactor
3150-802-65	Valve Pits - Process Piping Plan - Sections and Details
3150-803-39	Process Water Pipe Tunnel - Support Details and Piping

Chapter 8*

REACTOR COOLING-AIR AND CONTAMINATED-AIR SYSTEMS

The reactor cooling-air system and the contaminated-air system are grouped together because the air from both is exhausted to the atmosphere through the main stack. However, they serve entirely different purposes. The reactor cooling-air system provides a flow of air through the reactor for cooling the graphite reflector; it is a secondary reactor-cooling system. The contaminated-air system removes radioactive gases from the hoods and caves of the laboratories.

8.1 REACTOR COOLING-AIR SYSTEM

8.1.1 Introduction. Immediately surrounding the reactor tank is the graphite reflector. This reflector is composed of a removable bed of 1-in.-diameter graphite balls adjacent to the tank and a section of graphite blocks between the balls and the thermal shield. Heating due to the absorption of gamma radiation makes it necessary to cool the graphite reflector. Because of relatively low heat generation, air cooling is satisfactory. The cooling and design of the graphite reflector are discussed in other sections. This section will deal with the flow path and processing of the air going through the reactor cooling-air system.

A schematic diagram of the reactor cooling-air system is shown by Fig. 8.1.A. The description of the system will in general follow the air flow path, starting with the inlet air filters at the reactor faces and ending with the stack.

8.1.2 Air Flow Data. The reactor is designed for normal operation at a power level of 30,000 kw. The design air flow of 2000 lb/min and pressure drop of 55 in. of water through the reactor cooling-air system are based on maximum temperatures of 570°F in the graphite pebble bed and 500°F in the permanent graphite at 45,000-kw operation of the reactor. The 2000-lb/min

* ANL contribution.

NOT CLASSIFIED

DWG. #10755

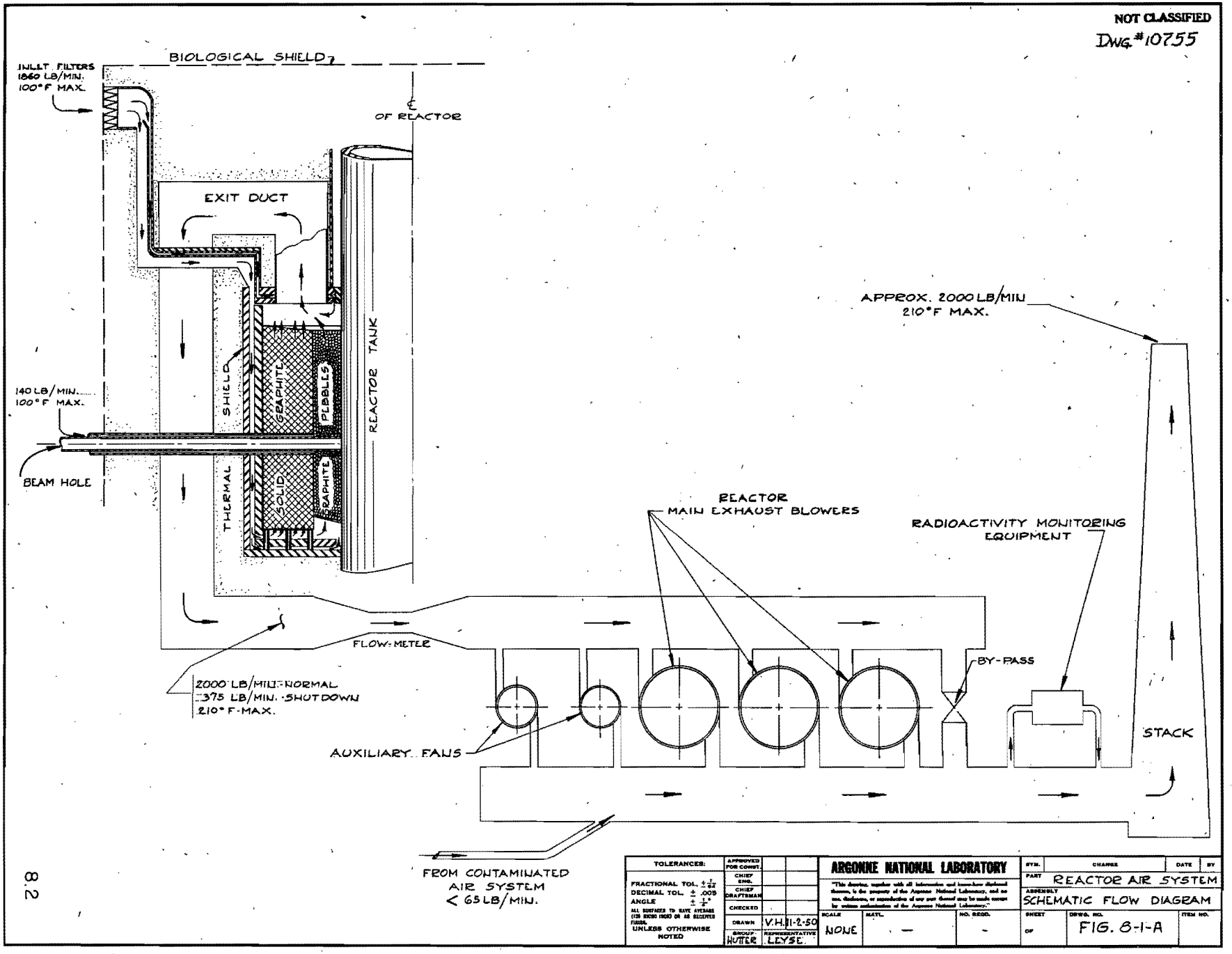

TOLERANCES:	APPROVED FOR CONST.		ARGONNE NATIONAL LABORATORY	SYM.	CHANGE	DATE	BY
FRACTIONAL TOL. ± 1/64	CHIEF ENG.		"This drawing, together with all information and know-how disclosed thereon, is the property of the Argonne National Laboratory, and no use, disclosure, or reproduction of any part thereof may be made except by written authorization of the Argonne National Laboratory."	PART	REACTOR AIR SYSTEM		
DECIMAL TOL. ± .005	CHIEF DRAFTSMAN			ASSEMBLY	SCHEMATIC FLOW DIAGRAM		
ANGLE ± 1/2°	CHECKED						
ALL SURFACES TO HAVE AVERAGE (125 RMS) FINISH OR AS SPECIFIED FINISH. UNLESS OTHERWISE NOTED	DRAWN	V.H. 11-2-50	SCALE NONE	MATL. —	NO. REQD. -	SHEET OF	DWG. NO. FIG. 8-1-A	ITEM NO.
	GROUP HUTTER	REPRESENTATIVE L.E.YST.					

design flow consists of the following quantities:

Air flow through graphite	1610 lb/min
Air to cool top thermal shield	250 lb/min
Allowed for leakage inward through experimental holes, etc.	140 lb/min
Total	2000 lb/min

Subsequent calculations gave the air requirements as 1526 lb/min to cool the graphite and experimental facilities, and 174 lb/min to cool the top thermal shield, for a total air flow of 1700 lb/min. Also, critical experiments conducted at ORNL indicated that the heat generation in the reflector would be somewhat less than that used for the above calculations and the air requirements would therefore be less. However, the design figures were maintained at 2000 lb/min flow and 55 in. of water pressure drop since it may be desirable and possible to operate the reactor at a power level as high as 60,000 kw at some time in the future.

The approximate pressure drops through the reactor air system for a flow of 2000 lb/min are summarized in Table 8.1.A.

TABLE 8.1.A

Approximate Pressure Drops in Reactor Air System

PART OF SYSTEM	PRESSURE DROP (in. H_2O)
Inlet filters and ducts	1.6
Thermal shield	0.4
Graphite reflector	29
Exit ducts and stack	5.4
Total	36.4

The total pressure drop of 36.4 in. of water given above is considerably lower than the 55 in. of water design value. Two factors enter to account for the difference. First, the reactor cooling-air system is designed without any filters on the exit air stream. If it should become necessary to add

filters in the future, additional head will be required. Based on the filter system used on the X-10 pile at ORNL, the additional head allowed for exit filters is about 8 in. of water. Second, to assure that the air system will be adequate for operation at a power level of 60,000 kw, the design head has been further increased to 55 in. of water.

The above discussion has been concerned with the air flow through the reactor air system during operation of the reactor. It is also necessary to maintain a flow of air through the reactor after it has been shut down. This flow serves to remove heat from the graphite reflector generated by the absorption of gammas from fission product decay and from induced activity, and also to prevent the escape of radioactive dust into the Reactor Building during removal of experimental hole plugs. To provide adequate cooling of the reactor after shutdown, a flow of about 135 lb/min is required. The flow necessary to ensure that radioactive dust does not escape into the Reactor Building is based on an air velocity of 150 ft/min directed inward along the annulus between a plug and liner. The air flowing into this annulus flows through holes at the inward ends of the liners and joins the reactor-cooling air flowing upward through the graphite pebbles. A satisfactory design of the experimental hole liners and plugs is obtained when the flow through the reactor is about 400 lb/min; therefore, this is the design flow through the reactor during shutdown. This is also the flow desired through the reactor in the event of an emergency shutdown of the reactor. The pressure drop through the graphite for a flow of 400 lb/min is about 0.5 in. of water, and the design pressure drop through the entire system is about 2 in. of water.

Once the reactor has been placed in operation there will always be active particles within the air passages. To prevent these active particles from entering the Reactor Building, a basic requirement of the reactor air system is that there always be a flow of air in the proper direction. Upon failure of the main exhaust blowers and the auxiliary fans, this flow will be induced by whatever stack draft is available.

After the reactor has been in operation long enough so that the reactor, reactor air system, and stack are hot, there is a stack draft of about 0.5 in. of water available. This is based on air temperatures of 200°F in the stack and 90°F atmospheric. It is estimated that this draft would produce a flow of 2000 to 3000 cfm through the reactor in the event of failure of all blowers

and fans. This flow is sufficient to meet shutdown cooling requirements. However, because of the possibility of a complete power failure within a short time after reactor start-up, in which case there would be essentially no stack draft, and because of the problem of radioactive dust escaping into the Reactor Building, the reactor cooling-air system does not rely on stack draft to produce the necessary shutdown air flow. This flow is provided by either of the auxiliary fans. Only as a last resort, i.e., in the event of complete failure of the blowers and fans, is the available stack draft utilized.

ADDITIONAL DATA

Air temperatures	
Inlet to reactor	75 - 100°F
Outlet from reactor	185 - 210°F
Site elevation	4930 ft
Barometric pressure	12.25 psi

8.1.3 Inlet Air Filters. Air used for cooling a reactor will emerge radioactive. The activity is due partially to gaseous atoms naturally occurring in air, such as argon, and partially to dust in the air. Not much can be done to reduce the activity from the first, but the latter can be reduced considerably by suitable filtering.

In the first considerations of the radioactivity problem of the MTR cooling-air system, a filter design similar to that used for the pile at ORNL was included in the exhaust side of the system. Further consideration of the problem along with economy measures prompted omission of the filters in the exhaust side of the reactor cooling-air system.

The only filters included in the reactor air system are the glass wool filters at the inlets to the system. A brief description of the processing the air encounters before entering the reactor is now given.

Normal atmospheric air enters the Reactor Building ventilation system through coarse-fiber-glass or wire-mesh prefilters. The air then goes through an electrostatic filter of 90% discoloration efficiency before passing into the Reactor Building. The Reactor Building is pressurized to about ½ in. of water so that leakage in through windows, doors, etc. will be kept to a

minimum. The air entering the reactor is taken directly from the Reactor Building and is filtered at the inlets by glass wool filters. There is an additional small amount of air (about 2%) which enters the air system via experimental holes without passing through the glass wool filters.

The elimination of the exhaust side filters, from the technical standpoint, is justified principally by a comparison of the MTR cooling-air system with that of the NRX pile at Chalk River, Ontario. The NRX pile has been operated satisfactorily since about September, 1946, without exhaust air filters. The air systems of the two reactors are similar in the following respects:

1. The major portion of air entering the reactor has been filtered to some degree.
2. The air does not make direct contact with the fuel elements, and thus fission products from ruptured fuel elements will not enter the air stream.
3. The air flows in direct contact with the graphite reflector.
4. The air flows indirect contact with the thermal shield; however, the NRX shield is cast iron while the MTR shield is low-carbon steel.
5. The air is susceptible to pollution from accidents occurring in the experimental facilities.
6. The exhaust air is not filtered.
7. The levels at which the effluent air is ejected into the atmosphere are 200 ft for the NRX pile and 250 ft for the MTR.

Rather extensive investigations have been conducted at the NRX with the finding that it is not necessary to add exhaust filters to the NRX air system. Based on this finding, the above general similarities, a more detailed comparison of the NRX pile and the MTR, and economics, the exhaust filters were omitted from the MTR air system. Should it be necessary to add exhaust filters at some later date, there is sufficient space for them adjacent to the Blower and Fan House.

The inlet filters are mounted in the inlets in the reactor faces. The filters are Airmat Type PL-24 units made by American Air Filter Company. Six units are mounted in a 2- by 12-ft opening in each pile face, giving a total of twenty-four 2- by 2-ft units. The face velocity of the air entering the

filters is about 350 ft/min. The pressure drop through the clean filters is approximately 0.1 in. of water.

8.1.4 System Within Reactor Structure. The system of duct work within the reactor is shown by Fig. 8.1.B, and the schematic flow of air within the reactor is shown by Fig. 8.1.A. In the design of the system within the reactor it was necessary to meet the following requirements:

1. The air must enter the pile structure at a level higher than 8 ft above the centerline of the active lattice, and the exit ducts must loop upward to a level at least that high in order for it to be possible, in so far as the air system is concerned, to flood the interior of the thermal shield with water.
2. All ducts must be arranged within the shield so that radiation outward, both in straight-line paths and in "shine" through the ducts, will not be sufficient to bring radiation at any point outside the shield above permissible levels.
3. The air must enter the thermal shield around the outer edge of its top and pass downward, cooling the inner and outer walls and possibly the top and bottom of the thermal shield before passing into a plenum chamber under the graphite. The air then must flow upward through the graphite to a plenum chamber above the graphite and out through exit ducts.
4. Exit air ducts must be shielded from the outside by the equivalent of 1 ft of ordinary concrete.
5. Arrangement of the air ducts within the reactor structure must not interfere with any experimental facilities.

The design shown in Figs. 8.1.A and 8.1.B essentially meets all the above requirements.

The inlet system consists of four sets of filters, plenum chambers, ducts and manifolds, one set in each wall of the reactor structure. The air enters each set through louvers located near the top of each pile face. Back of each set of louvers are six 2-ft-square filters and a 2- by 2- by 12-ft plenum chamber. Each plenum chamber is joined to the top edge of the thermal shield by five or six 8-in.-square ducts and a manifold which is continuous around the top of the thermal shield. A separate channel with a damper is provided in each of the 8-in. ducts whereby a small amount of air is by-passed for cooling the top thermal shield. There is a total of 22 8-in. ducts. Each duct has one 90° elbow and connects to the plenum chamber and the thermal shield manifold

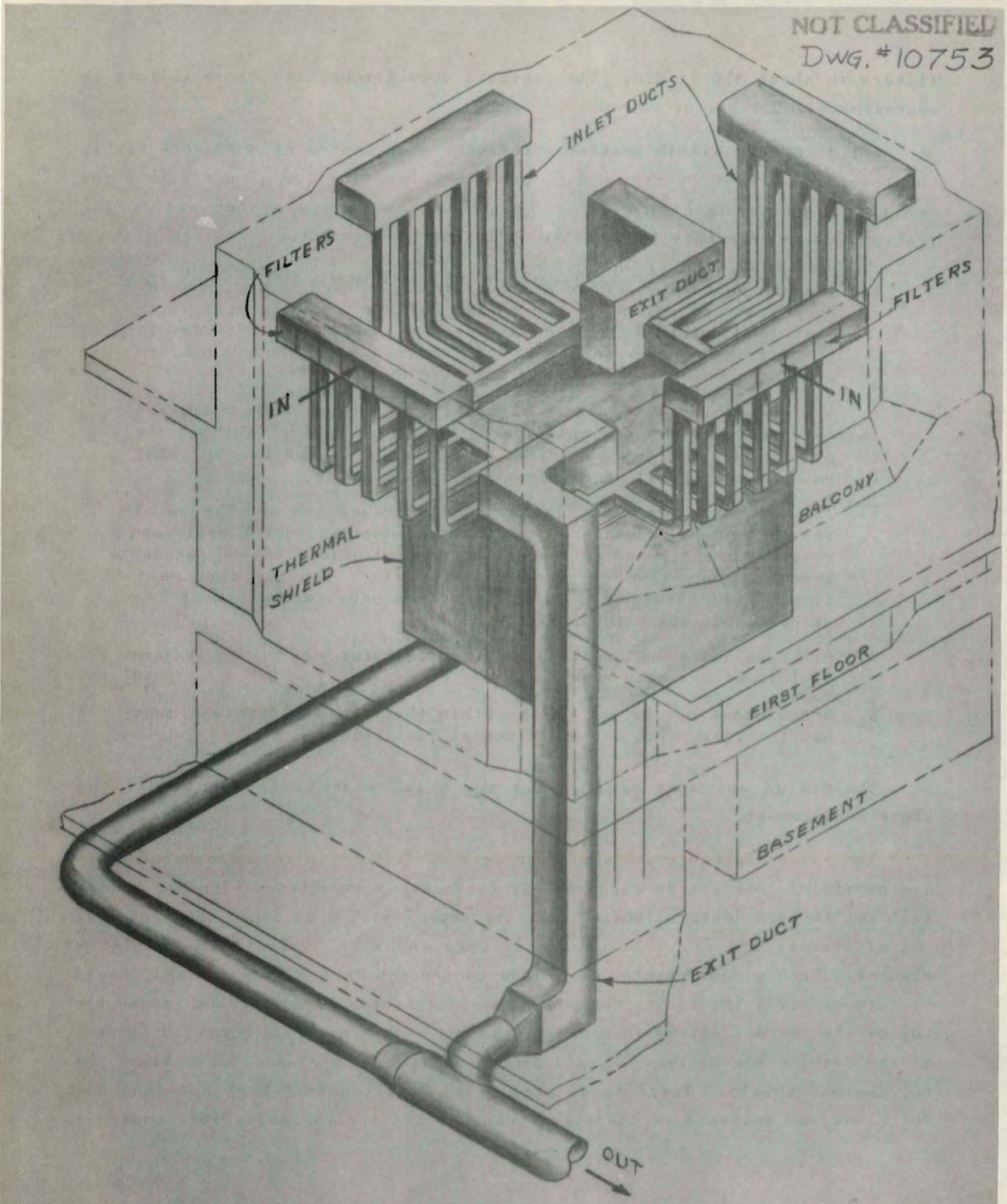

F.T. 11-8-50
LEYSE

MTR AIR SYSTEM
INSIDE REACTOR STRUCTURE

FIGURE 8.1.B

at 90° to the principal direction of flow. Thus there are effectively three 90° turns in the inlet air system. The walls of the ducts are lined with 1-in. steel plate to reduce gamma-ray leakage through the ducts.

The path followed by the air within the reactor proper is shown in Fig. 8.1.A. The main air stream flows down between the walls of the thermal shield, and some then passes directly into a plenum chamber beneath the graphite while a portion flows between the top and bottom plates of the bottom thermal shield before passing into the plenum chamber. The air from the chamber passes up through the graphite pebbles and cooling holes in the permanent graphite and is joined by air entering from the experimental facilities. The air enters a plenum chamber above the graphite where it is joined by the air by-passed to cool the top thermal shield. The air then enters the exit air ducts.

The exit air duct system within the reactor consists of two 30-in.-square ducts connected to the thermal shield at diagonally opposite corners of the top plate and turned downward through the biological shield to carry the air out below the basement floor. There are three 90° bends in each of these ducts, as shown in Fig. 8.1.B.

8.1.5 Exit Ducts. The 30-in.-square ducts leading down through the reactor connect to a single 48-in.-diameter steel duct beneath the basement floor. This duct connects to a plenum chamber outside the Reactor Building. An underground duct of 48-in.-diameter precast concrete pipe leads from this plenum chamber to a plenum chamber beneath the Blower and Fan House. The concrete duct is a minimum of 2 ft below grade so that the earth cover provides adequate shielding against radiation.

8.1.6 Blowers, Fans, and Auxiliaries. The blowers and fans of the reactor air system are housed in the Blower and Fan House, which is described in a later section; the reactor-air-system equipment contained in it is described here.

The blowers and fans for the reactor air system take their air from an inlet plenum chamber beneath the building and exhaust it to another, also beneath the building.

Blowers. There are three half-capacity blowers in parallel, one of which serves as a spare, for cooling during normal operation of the reactor. Each

blower is capable of delivering 1000 lb/min of 210°F air against a head of 55 in. of water, and is driven by a 250-hp motor.

The blowers are of the positive displacement type, this type being selected because of its adaptability to wide ranges of flow rates and pressure heads. This is important since, while it is desired to have a flow rate of 2000 lb/min, the pressure drop through the system initially will be considerably below the design value of 55 in. of water. Also, since the cooling requirements may be below design calculations, it is desirable for the units to operate economically at reduced flows and heads. The positive displacement type of blower offers the most economical operation at the reduced requirements.

The blowers are electric-motor driven and receive power from the normal commercial electrical supply only. Extra pulleys are provided with the blowers to provide for the slower speeds at reduced requirements. These pulleys will adequately cover the range from 700 to 1000 lb/min.

Auxiliary Fans. Besides the blowers there are two 400-lb/min fans for emergency and normal shutdown operation, each fan being in parallel with the three main blowers. One of the fans is driven by an electric motor and the other by a gasoline engine. The motor-driven fan receives its power from the normal commercial electrical supply and from the site emergency power supply and will be used during normal shutdown periods. The gasoline-driven fan will be used for emergency shutdowns when both electrical supplies have failed.

Valves. There are butterfly valves at both inlets and outlets of all blowers and fans. The valves on the inlet sides are manually operated while the valves on the exhaust sides are air operated. The valves on the exhaust sides can seal airtight to permit removal of a blower or fan without outward leakage of radioactive air. The valves on the inlet sides do not have to be absolutely airtight since any leakage here will be directed into the reactor air system.

Since the blowers are of the positive displacement type, it is necessary to have both the inlet and outlet valves open when the blowers are operating. To ensure this, limit switches are provided on both inlet and outlet valves. These switches require both valves to be open before the blowers can be started.

Also, because of the use of positive displacement blowers, it was necessary to provide a by-pass around all the blowers and fans so that the stack draft will be available to provide a flow of air through the reactor air system. The by-pass is provided by a valve between the plenum chamber ahead of the fans and blowers and the exit duct leading to the stack. This valve will be operated manually.

8.1.7 Instrumentation and Control. In the description of the instrumentation and control the flow path of the air will again be followed, starting with the inlets to the system.

There are four differential pressure indicators to determine the pressure drop across the glass wool inlet filters. They are mounted locally on the pile faces. Each indicator determines the pressure drop across the filters on one side of the pile.

In the exit duct near the reactor is a pressure indicator to determine the pressure in the air system at that point. The indicator is remotely mounted in the Reactor Control Room and is equipped with an alarm to notify the operator when the pressure has risen above a certain predetermined value.

Mounted in the concrete pipe line leading to the Blower and Fan House is a venturi tube for determining the flow rate through the system. The flow rate is indicated on a panel in the Blower and Fan House. Since the Blower and Fan House is an unattended station which will have periodic inspections only, the information for operation of the reactor air system is transmitted to the Process Water Building and the Reactor Control Room. The Process Water Building serves as the center for operational information on the reactor air system. The flow rate is therefore recorded at the control panel in the Process Water Building, and there are low flow rate alarms at both this panel and the panel in the Reactor Control Room. Besides the above, the venturi information is transmitted to the reactor control system to automatically shut the reactor down on failure of the air system.

In the exit air duct near the Blower and Fan House is a pressure indicator to measure the pressure in the system at this point. The information is indicated on a panel in the Blower and Fan House.

The valves on the inlet sides to the blowers and fans are manually operated. All of them will normally be open, being closed only if necessary to repair or remove a blower or fan.

The main exhaust blowers are started manually within the Blower and Fan House. To promote safe operation of the reactor air system, both of the auxiliary fans start automatically on failure on the main blowers, and one may then be shut down manually. However, in the event of failure of the one left running, the other will automatically start again. The bearings on the main blowers and their motors are provided with thermocouples to indicate bearing temperatures and give an alarm at the panel in the Blower and Fan House. The high bearing temperature is also indicated on a master alarm at the Process Water Building panel.

A pressure indicator is provided in the duct on the exhaust side of the blowers and fans. The pressure is indicated at the panel in the Blower and Fan House and is for operational information.

There are radiation-measuring instruments in the main duct leading to the stack. These instruments are located toward the stack from the point where the line from the contaminated-air system enters this duct. Thus the instruments measure the total activities of the gases going up the stack. In general, the contributions from the contaminated-air system will be small or nil, and the measurements are essentially those of the reactor air system. The total activity of the gases to the stack is determined by an ion chamber, while that part due to active dust particles is determined by a particulate-activity meter. The information from both is transmitted to recorders in the radiation-instrument area of the Blower and Fan House. Alarms to indicate excessive activity going up the stack are provided at the Blower and Fan House, Process Water Building, and the Reactor Control Room panels.

8.1.8 Shielding. The shielding requirements of the reactor air system are based on an air flow of 30,000 cfm through the reactor at 60,000-kw operation. These assumptions give shielding thicknesses which should be adequate for all reactor operating conditions. To correspond to the 60,000-kw operating level, an average flux of 4×10^{12} neutrons/cm^2-sec throughout the volume within the thermal shield was assumed. The volume of air subject to activation by this flux is approximately 850 cu ft.

An examination of the elements normally occurring in air shows that it is necessary to consider only the active atoms N^{16}, O^{19}, and A^{41}, which result from neutron capture by N^{15}, O^{18}, and A^{40}, respectively.

In Table 8.1.B are summarized the unit source intensities due to the active atoms, along with other pertinent information.

TABLE 8.1.B

Activity of Reactor-cooling Air

ORIGINAL ATOM	ABUNDANCE IN REACTOR AIR AT 150°F (atoms x 10^{-23}/ft^3)	ACTIVATION CROSS SECTION (cm^2)	ACTIVATION RATE (atoms/sec-ft^3)	ACTIVE ATOM	UNIT SOURCE STRENGTH (Mev/sec-ft^3)	γ ENERGY (Mev)
N^{15}	0.032	0.02×10^{-27}	2.56×10^5	N^{16}	3.12×10^5	6.5
O^{18}	0.0045	0.2×10^{-27}	3.5×10^5	O^{19}	7.8×10^5	1.6
A^{40}	0.049	0.62×10^{-24}	7.2×10^9	A^{41}	4×10^6	1.37

Using the source intensities given in Table 8.1.B the shielding requirements were determined with the use of standard shielding formulas. These are summarized in Table 8.1.C. The shielding thicknesses which are mentioned in other sections generally exceed the values given in Table 8.1.C.

TABLE 8.1.C

Shielding Requirements for the Reactor Air System

ITEM	TOLERANCE (r/8 hr)	SHIELDING THICKNESS	
		CONCRETE (in.)	STEEL (in.)
Ducts in reactor building			
2.5-ft square	0.005	11	
4-ft diameter	0.005	13.5	
Ducts outside			
4-ft diameter	0.05	6.5	
Main blower cells			
Outside walls (north and south)	0.005	4	1
Outside walls (east and west)	0.005	8	
Intercell walls	0.05	*	
Floor above inlet plenum chamber	0.05	3	
Floor above outlet duct to stack	0.05	3	
Roof above cells	0.1	*	
Auxiliary fan cells			
Floor above inlet plenum chamber	0.05	2	
Floor above exit duct	0.05	2	
All other walls		*	*

*Structural requirements only must be met.

8.2 CONTAMINATED-AIR SYSTEM

8.2.1 Introduction. The contaminated-air system removes radioactive gases and acid vapors from the hoods and caves of the laboratories. This is supplemental to the normal hood-ventilation system which removes air that is relatively free from acid vapors and radioactivity. The off-gas openings of the contaminated-air system provide a relatively high-velocity stream to remove the active gases and acid vapors. Figure 8.2.A shows a schematic flow diagram of the contaminated-air system. In general the description of the system will follow the flow diagram.

8.2.2 Air Flow Data. The system is based on the removal of a minimum of 50 cfm of gases from each hood, with a maximum of 10 hoods in use at any time. The system is sized for 500 cfm up to and including the scrubber. This is adequate to provide for a considerable increase over the present number of 15 hoods, since it is expected that normally only about 15% of the total off-gas openings would be in use at any one time. The capacity of the system after the scrubber is 1000 cfm; this is to provide for the future disposal of additional small volumes of radioactive gases. The pressure drop through the system is approximately 25 in. of water.

8.2.3 System from Hoods to Scrubber. The off-gas openings in the hood are 2 in. in diameter and are provided with quick-opening caps. The lines leaving the hoods are of 2 in. diameter. They connect to a 6-in. header leading to the scrubber. All the ducts ahead of the scrubber are of acid-resistant material. No shielding is provided for the ducts since the activity contained within them will generally be small unless an appreciable build-up occurs owing to deposits in the ducts. If the latter occurs, remedial steps will be necessary.

8.2.4 Scrubber. The purpose of the scrubber is to remove the acid vapors from the gases. It is not important that radioactivity be removed since the gases are ejected to the atmosphere through the main stack.

The scrubber has a packed column of Raschig rings. The removal of the acid vapors from the gases flowing up through the column is accomplished by the flow of a caustic solution down through the rings. The contaminated-air inlet line to the scrubber extends down to below the minimum operating level in the reservoir to prevent a back flow of vapors or radioactive gases to the hoods in the event of failure of the exhaust fans in the system.

NOT CLASSIFIED

Dwg. #10756

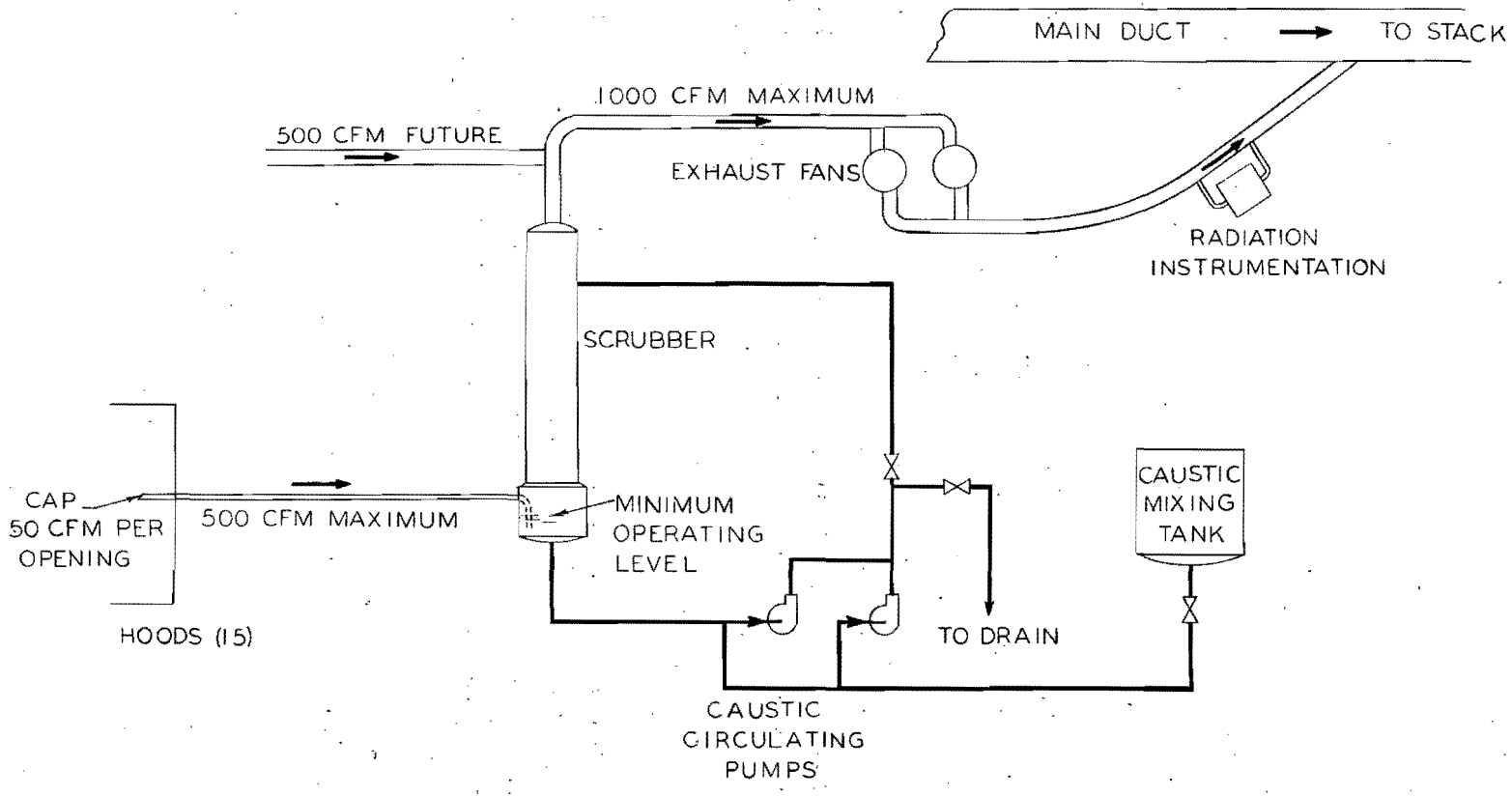

TOLERANCES:	APPROVED FOR CONST.		ARGONNE NATIONAL LABORATORY	SYM.	CHANGE	DATE	BY
FRACTIONAL TOL. ± 1/64 DECIMAL TOL. ± .005 ANGLE ± 1/2°	CHIEF ENG.		"This drawing, together with all information and know-how disclosed thereon, is the property of the Argonne National Laboratory, and no use, disclosure, or reproduction of any part thereof may be made except by written authorization of the Argonne National Laboratory."	PART	CONTAMINATED AIR SYSTEM		
ALL SURFACES TO HAVE AVERAGE (125 MICRO INCH) OR AS RECEIVED FINISH. UNLESS OTHERWISE NOTED	CHIEF DRAFTSMAN			ASSEMBLY	SCHEMATIC FLOW DIAGRAM		
	CHECKED		SCALE / MATL. / NO. REQD.	SHEET / OF	DRWG. NO. FIG. 8.2.A		ITEM NO.
	DRAWN	FT 11-3-50					
	GROUP HUTTER	REPRESENTATIVE LEVSE					

The caustic-circulating system for the scrubber has two pumps, one of which serves as a spare. The caustic solution for the scrubber is supplied from a caustic mixing tank where the solution is prepared as required to replace the depleted caustic solution in the scrubber. To provide for periodic sampling of the caustic solution a tap is provided at the bottom of the reservoir.

Since the amount of radioactivity which the scrubber may contain at any one time is very indefinite, the scrubber is not provided with shielding. Again, if necessary, this can be readily provided at a later date.

8.2.5 Exit Duct from Scrubber. The exit duct from the scrubber is an 8-in.-diameter carbon-steel pipe with suitable protective covering. The duct leads underground from the Reactor Building-wing basement to the Blower and Fan House, where it connects to the exhaust fans. The earth cover provides adequate shielding against radioactivity.

8.2.6 Exhaust Fans and Auxiliaries. *Exhaust Fans.* There are two full-capacity fans in parallel to provide the flow of gases through the contaminated-air system. One of these fans serves as a spare. Each fan is capable of delivering about 1000 cfm of air against a head of approximately 25 in. of water. The fans are of a standard centrifugal type and are motor driven. Motors of both fans are connected to both the normal commercial electrical supply and the site emergency power supply.

Valves. Butterfly valves are provided at both the inlet and outlet to each fan. The inlet valves are manually operated while the exhaust valves are air operated. The exhaust valves can be sealed airtight to permit repair or removal of the fan without leakage of radioactive air into the Blower and Fan House. It is not necessary to have the inlet valves seal airtight since any leakage is into the system.

8.2.7 Instrumentation and Control. The order of the following description will follow the flow diagram shown in Fig. 8.2.A, starting at the off-gas openings in the hoods.

There is a locally mounted pressure indicator in the off-gas line near each hood. This will inform the experimenter that there is or is not sufficient static head for him to use the off-gas opening.

At the scrubber, instrumentation is included to provide the following operational information:

1. Static pressure head at inlet of air line to the scrubber.
2. Pressure drop in the air passage through the scrubber.
3. Level of the caustic solution in the reservoir.
4. Temperature of the solution in the reservoir, which is desired during the neutralization of the depleted caustic with sulfuric acid.

Pressure indicators are provided at the caustic-circulating pumps. These indicators are locally mounted.

A pressure indicator is provided near the inlets to the exhaust fans. The indicator is mounted on the panel in the Blower and Fan House.

Radiation-measuring instruments are located in the duct leading from the exhaust fans. There is an ion chamber to determine the total activity of the gases from the scrubber and a particulate-activity meter to determine the radiation due to active particles in the gases. The information from both instruments is recorded. The recorders are located in the area of the Blower and Fan House that is designated solely for radiation instrumentation.

8.2.8 Shielding. It was difficult to estimate what the activity of the gases going through the contaminated-air system would be under actual operating conditions. The maximum radiation intensities of experiments conducted in the laboratory hoods and caves will be 1 and 10 curies, respectively. To arrive at some shielding requirements it was assumed that the activity is emitted at a rate of 0.01 curie per minute and that the gamma energy is 2 Mev.

The shielding requirements arrived at using standard shielding formulas and the above assumptions are summarized in Table 8.2.A.

Based on the shielding requirements listed in Table 8.2.A it was decided to provide no shielding of the contaminated-air system except the cells for the exhaust fans. The 8-in. pipe from the scrubber to the Blower and Fan House is shielded by an adequate earth cover, and the calculated radiation from the lines preceding the scrubber is small enough to make shielding of them initially unnecessary.

TABLE 8.2.A

Shielding Requirements for the Contaminated-air System

ITEM	TOLERANCE (r/8 hr)	SHIELDING	
		MATERIAL	THICKNESS (in.)
2-in. pipe	0.3 (at pipe)	Steel	1/16
6-in. pipe	0.3 (at pipe)	Steel	1/4
8-in. pipe outside	0.05	Earth	3
Fan cells			
Outside walls	0.005	Concrete	2.5
	0.005	Steel	1
Motor room wall, east-north	0.005	Concrete	2.5
	0.005	Concrete	6
Intercell wall	0.05	Concrete	*
Roof	0.1	Concrete	*

*Structural requirements only must be met.

8.3 BLOWER AND FAN HOUSE

8.3.1 Introduction. The Blower and Fan House contains the blowers and fans for the reactor-cooling- and contaminated-air systems along with their associated equipment. The equipment, function, and some phases of operation have already been discussed in Sections 8.1 and 8.2. The present section describes the general layout of the building equipment.

The general layout of the building is shown in Fig. 8.3.A. The building is a single-story structure and is located several hundred feet east-southeast of the Reactor Building.

8.3.2 Air Ducts and Plenum Chamber. The underground duct of the reactor cooling-air system enters the building at the north end of the west wall. This duct connects to a plenum chamber beneath the reactor air system blower

NOT CLASSIFIED

Dwg. # 10754

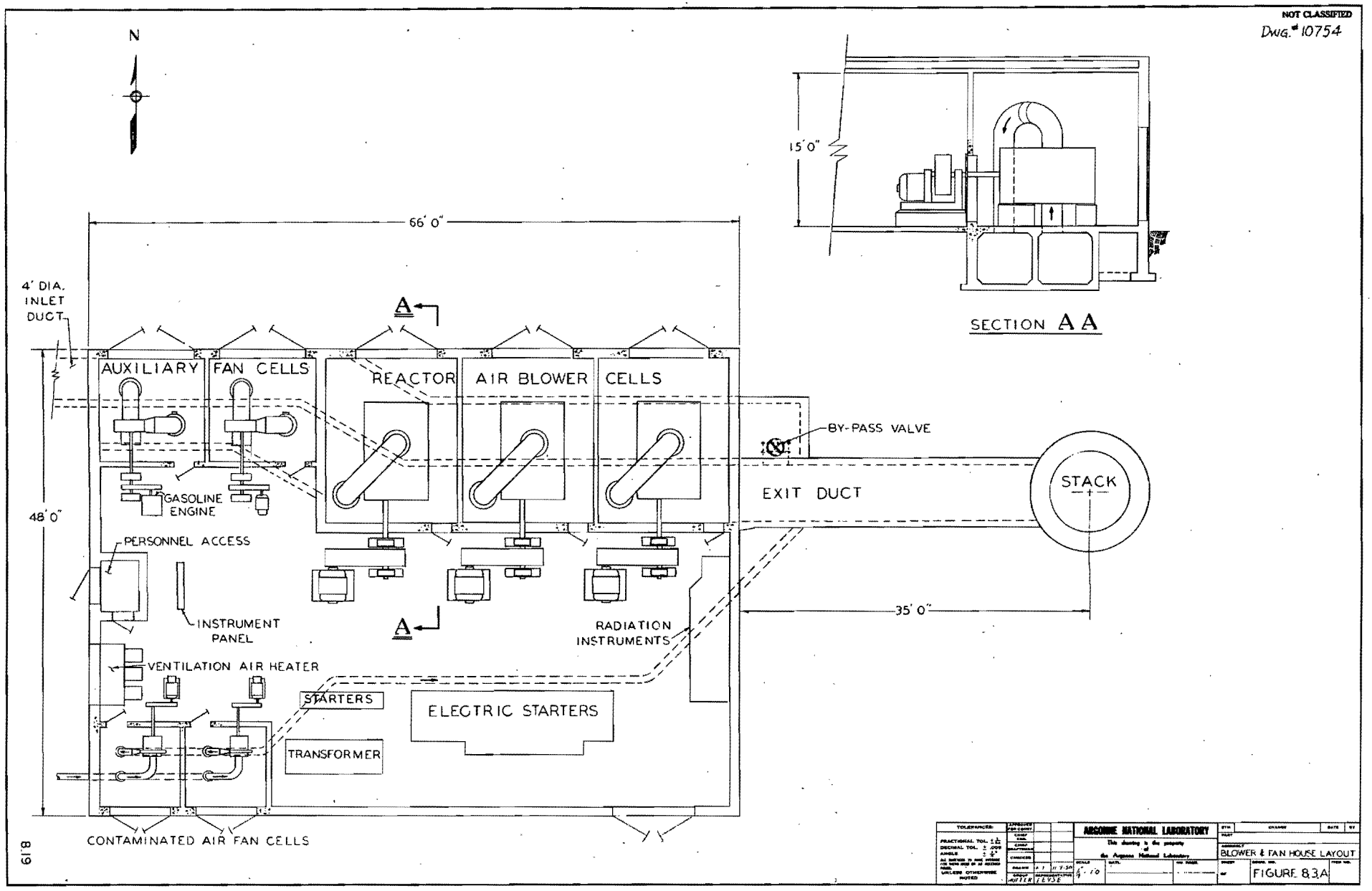

and fan cells. The plenum chamber extends slightly beyond the full length of and building. Starting at the west wall of the building, the exhaust plenum chamber also lies beneath the blower and fan cells and roughly parallels the inlet plenum chamber. The main exit duct to the stack is essentially an extension of the exhaust plenum chamber. The top of the duct is approximately at grade level. The plenum chambers and duct just described are constructed of poured concrete. Manways to the plenum chambers are provided. The by-pass valve linking the inlet plenum chamber to the exit duct is located at the east end of the inlet plenum chamber.

The duct of the contaminated-air system enters the building below grade at the south end of the east wall. This duct leads to the exhaust fans, and an exhaust duct leads from the fans, beneath the building floor, to connect with the main exit duct near the east wall of the building.

8.3.3 Blower and Fan Cells. The blower and fan cells for the reactor cooling-air system are located along the north wall of the building while those for the contaminated-air system are at the southwest corner. The inlets and exhausts to all blowers and fans are through the floors of the cells. The walls of all cells are of poured concrete construction. Poured concrete is used instead of masonry because it provides a more uniform and dense shield. The walls of all cells which form a part of the building external wall and the external walls of the reactor main blower cells are 1 ft thick. The remaining cell walls are 6 in. thick. These thicknesses are more than adequate for shielding requirements.

Each cell has a door which opens to the interior of the building. These doors are for convenience during periodic inspections and minor servicing. In an outside wall of each cell is a large double door. These doors provide access to the cells for installing, replacing, or making major repairs of the equipment. All doors are of steel and provide adequate shielding.

There is a plugged drain opening in each cell. The drains are provided for use during washdowns of any contaminated equipment within the cells. These drains, along with the one in the main exit duct, drain to a sump beneath the building floor. The waste is pumped from the sump to the retention basin.

8.3.4 Miscellaneous. Besides the blowers, fans, and associated equipment, the Blower and Fan House contains the recording instruments for the

radiation measurements of the activity of both reactor and contaminated-air systems. The recorders are situated in an area at the east wall of the building where they are convenient to the exit ducts from both air systems.

8.4 STACK

8.4.1 Introduction. The air from the reactor and contaminated-air systems contains more radioactivity than can be safely discharged to the atmosphere at ground level in an inhabited area. Thus it is necessary to eject this active air through a stack of considerable height. This results in the diffusion of the activity over a large area, thereby greatly reducing the hazard presented by the active gases.

8.4.2 Activity of Stack Gases. The activity in the stack gases due to air from the contaminated-air system will generally be negligible compared to that due to the air from the reactor. Thus the design of the stack is based principally on the radioactivity of the reactor-cooling air.

The activity of the reactor-cooling air is due to radioactive particles and gases. For obvious reasons, the activity due to particles does not lend itself to calculation. Therefore the activity of the stack gases is considered to be that due solely to the 110-min half-life A^{41} (argon) formed in the reactor.

The rate of activation of the argon in the reactor-cooling air is given by

$$\text{Activation rate} = \Phi N \sigma_a V$$

where

Φ = average flux over volume V, neutrons/cm^2-sec

N = number of A^{40} atoms per ft^3

σ_a = activation cross-section of A^{40} = 0.62×10^{-24} cm^2

V = volume of region, ft^3

The activation rates for the various regions are summarized in Table 8.4.A. The term "air in graphite" refers to the air spaces naturally occurring in graphite.

TABLE 8.4.A

Production of A^{41} in the MTR

REGION	VOLUME (ft^3)	FLUX, Φ (neutrons/cm^2-sec)	ACTIVATION RATE (atoms/sec)
Graphite ball zone			
Voids	130	6.75×10^{12}	3.1×10^{12}
Air in graphite	52	6.75×10^{12}	1.24×10^{12}
Permanent graphite zone			
Cooling holes	8.6	2.1×10^{12}	0.06×10^{12}
Beam hole annuli	2	1.4×10^{12}	0.01×10^{12}
Air in graphite	275	1.4×10^{12}	1.36×10^{12}
Plenum chambers			
Top	201	1.75×10^{11}	0.12×10^{12}
Bottom	175	3.5×10^{11}	0.22×10^{12}
Total			6.11×10^{12}

The 6.11×10^{12} atoms/sec activation gives a total activity of about 1500 curies/day for 30,000-kw operation with a thermal flux of 2.5×10^{14} neutrons/cm^2-sec at the center of the reactor. This amounts to a concentration of about 2.5×10^{-3} microcurie/cc at the stack exit. This is 2500 times the tolerance value of 10^{-6} microcurie/cc for A^{41} in the atmosphere.

8.4.3 Stack Height. The stack height depends on the amount of dilution necessary to reduce the concentration of the radioactivity to below tolerance before it reaches ground level. This involves consideration of the meteorological conditions encountered at the MTR site. The stack is located near the southeast corner of the MTR site. Since the winds at the site are predominantly southwest or northeast, the exhaust gases from the stack generally pass over the relatively uninhabited southeast corner of the site. Thus, from the standpoint of wind direction the stack is well situated.

Calculations of stack height necessary were made using O. G. Sutton's diffusion equation and also various other geometrical interpretations. Using the results from these calculations and experimental information from published literature, the stack height for the MTR was established at 250 ft. This

height is believed adequate to ensure that exposure to the radioactive stack gases will not exceed tolerance anywhere on the site. Also, it is believed sufficient to prevent a dangerous increase of background activity due to the deposit of active particles on or off the site.

In order to give some indication of the activity at ground level due to the stack gases, the results of several calculations using Sutton's equation are included. Sutton's equation yields a relation which says that the distance from the stack at which the maximum activity at ground level occurs is independent of wind velocity. For a 250-ft-high stack this distance is about 3600 ft; this is well outside the MTR site which lies within a distance of about 1600 ft from the stack. The maximum concentrations at ground level for the 250-ft stack are calculated to be 1.56×10^{-12}, 0.31×10^{-12}, and 0.156×10^{-12} curie/cc for wind velocities of 1, 5, and 10 mph, respectively. Also based on Sutton's equation, the wind velocity necessary to reduce the argon activity to tolerance (10^{-12} curie/cc) at ground level on the site is about 0.15 mph. A meteorology report[21] on the Reactor Testing Station Area states that winds of 0 to 3 mph occur 15 to 20% of the time. Thus, based on Sutton's equations, the activity at ground level should very seldom, if ever, exceed tolerance.

8.4.4 Stack Diameter. The exit diameter of the stack is 5 ft. This is based on the exhaust volume of the gases and the desired exit velocity.

The volume of air exhausted from the stack at present is about 41,000 cfm, of which a minor portion comes from the contaminated-air system. The diameter of the stack is based on a maximum flow of 80,000 cfm so as to provide for future additional requirements. It was desired to have the exit velocity as high as practical so as to minimize "downwash," a term referring to gases drawn downward in the vortices formed in the lee of a stack. With regard to stack noise and friction losses, a maximum exit velocity of 4,000 fpm can easily be tolerated. The exit velocity for the present flow is then about 2000 fpm. This velocity is sufficient to prevent "downwash" from conveying the highly active stack gases to the turbulent air around the buildings, a phenomenon which would give intolerable concentrations of radioactivity near ground level. The stack diameter of 5 ft provides the 2000-fpm exit velocity.

8.4.5 General Construction. The stack is constructed of reinforced concrete. There is a ladder extending the entire height of the stack. Lightning arresters are provided at the top of the stack. Aircraft obstruction warning lights are not provided.

8.5 REFERENCE REPORTS

(1) Gall, W. R., *MTR Report of Internal Air System*, ORNL CF-49-11-208, November 21, 1949.

(2) Gall, W. R., *MTR Internal Air System Design Report - Addendum*, ORNL CF-50-2-61, February 13, 1950.

(3) Leyse, C. F., *Argon Activity from the Materials Testing Reactor*, ANL-EKF-19, November 17, 1949.

(4) Lane, J. A., *Argon Activity in Reactor Cooling Air*, ORNL CF-49-11-180, November 17, 1949.

(5) Lane, J. A., *Air Cooling System*, ORNL CF-49-11-219, November 23, 1949.

(6) Leyse, C. F., *Maximum Temperature Rises in Graphite During Reduced Air Flow*, ANL-EKF-28, January 6, 1950.

(7) Leyse, C. F., *Cooling Requirements of Graphite After Shutdown*, ANL-EKF-29, January 6, 1950.

(8) Leyse, C. F., *MTR Shutdown Air Requirements*, ANL-EKF-30, January 10, 1950.

(9) Leyse, C. F., *Preliminary Investigations of Stack Height*, ANL-EKF-31, January 17, 1950.

(10) Leyse, C. F., *Shielding of the External Reactor Air System*, ANL-EKF-32, January 26, 1950.

(11) Leyse, C. F., *Shielding of the Contaminated Air System*, ANL-EKF-35, February 7, 1950.

(12) Lane, J. A., *MTR Shutdown Cooling Requirements*, ORNL CF-49-12-84, December 16, 1949.

(13) Leyse, C. F., *Reactor Air System Pressure Drops*, ANL-EKF-36, February 8, 1950.

(14) Leyse, C. F., *Pressure Drop Through the Contaminated Air System*, ANL-EKF-37, February 9, 1950.

(15) Leyse, C. F., *Design Report No. 32, MTR External Air System*, ANL-EKF-40, February 14, 1950.

(16) Leyse, C. F., *Stack Design for the MTR*, ANL-EKF-45, March 30, 1950.

(17) Leyse, C. F., *Omission of MTR Cooling Air System Discharge Filters*, ANL-EKF-47, March 31, 1950.

(18) Briggs, R. B., *Cooling of the Graphite Reflector for the MTR*, ORNL CF-50-3-102, March 20, 1950.

(19) Leyse, C. F., *Determination of Stack Dimensions*, ANL-EKF-49, April 6, 1950.

(20) Leyse, C. F., *Addendum No. 1, Design Report No. 32, MTR External Air System*, ANL-EKF-52, April 25, 1950.

(21) U. S. Weather Bureau, Meteorology of the Reactor Test Site, Arco, Idaho, September 16, 1949.

8.6 REFERENCE DRAWINGS

(Blaw-Knox Construction Company Drawings)

DWG. NO.	TITLE
3150-92-10	Flow Diagram - Reactor Air System
3150-92-13	Flow Diagram - Air Exhaust System
3150-10-1	Fan House and Stack - Layout

Chapter 9 *

SITE AND BUILDINGS

9.1 SITE PLAN

An artist's sketch of the MTR site is shown in Fig. 9.1.A. The Materials Testing Reactor site plan is shown in Fig. 9.1.B. The layout shown by these figures is based on consideration of the following major factors:

1. The building or facility function and its relation to the reactor and other facilities.

2. Accessibility to and from the site and facilities from the viewpoint not only of function but also of security.

3. Contamination and pollution as they affect other facilities.
   a. Wind direction.
   b. Deep water direction.
   c. Subterranean drainage.
   d. Surface drainage.

4. Power, railroad, and highway connections.

5. Topography of the MTR plot.
   a. Flat terrain for the quarter-mile beam.
   b. Natural drainage for the retention basin.
   c. Overburden.

6. Security.
   a. Fire fighting.
   b. Patrolling.

7. Future expansion of initial facilities.

8. Future buildings and facilities.

9. Most feasible and shortest piping, air ducts, wiring, fencing, roads, and walks.

The general layout of the site is centered around the Reactor Building in an area where the terrain is reasonably level. The level terrain is necessary

*ANL contribution.

Dwg. 10768

[redacted]

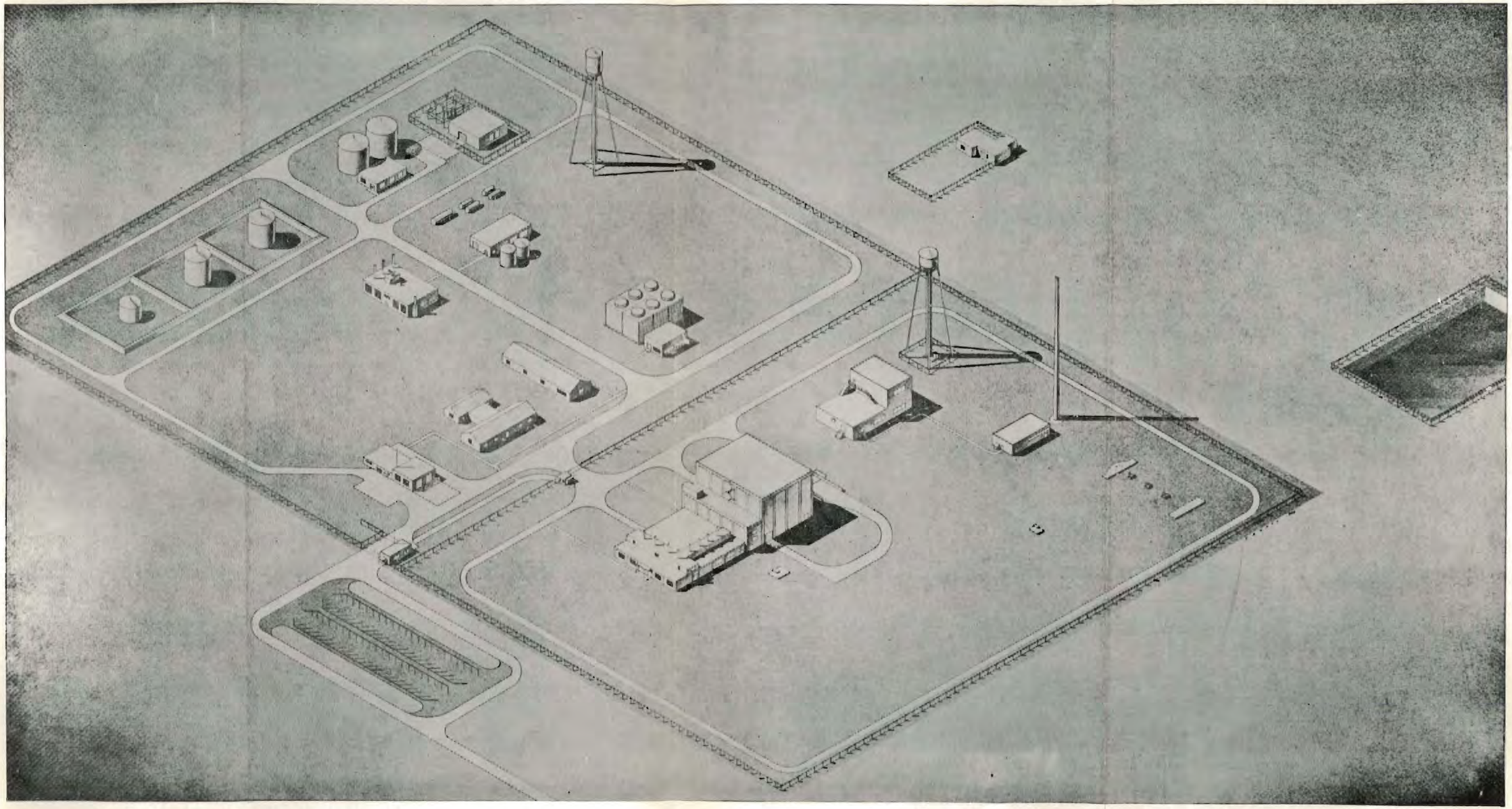

FIG. 9.1.A

M.T.R. SITE - ARTIST'S SKETCH

NOT CLASSIFIED
Dwg # 10741

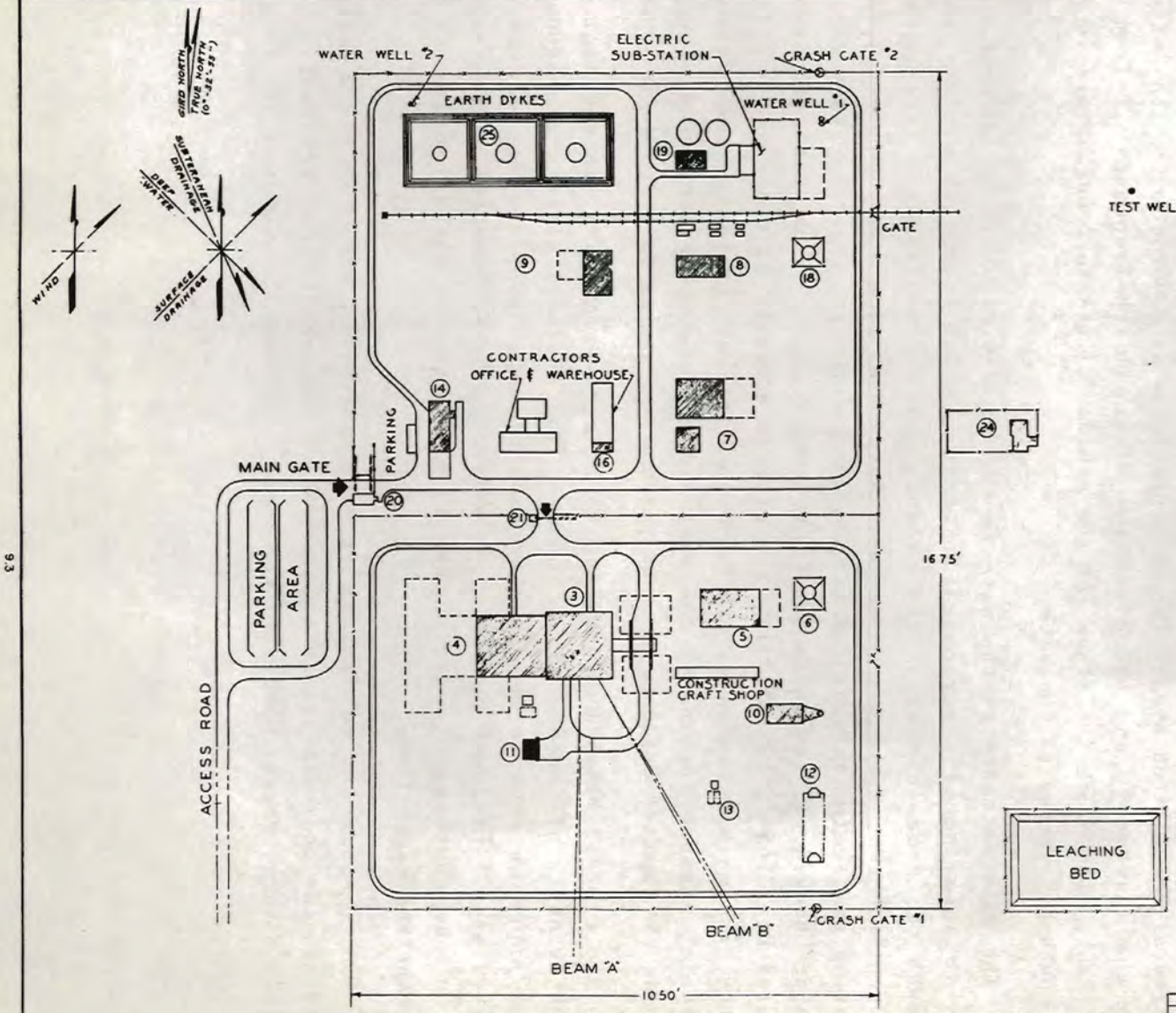

LIST OF AREAS

NO.	DESCRIPTION
1.	YARD (OUTSIDE FENCE)
2.	YARD (INSIDE FENCE)
3.	REACTOR BUILDING
4.	REACTOR BUILDING WING
5.	PROCCESS WATER BLDG.
6.	WORKING RESERVOIR
7.	COOLING TOWER & PUMP HOUSE
8.	DEMINERALIZER BLDG.
9.	STEAM PLANT
10.	FAN HOUSE & STACK
11.	PLUG STORAGE
12.	RETENTION BASIN
13.	EFFLUENT CONTROL
14.	SERVICES BLDG.
15.	
16.	CANTEEN
17.	
18.	EMERGENCY O.H. WATER TANK
19.	RESERVOIR & WATER PUMP HOUSE
20.	CONTROL HOUSE-LIMITED AREA
21.	CONTROL HOUSE EXCLUSION AREA
22.	
23.	
24.	SANITARY SEWAGE TREATMENT PLANT
25.	OIL STORAGE

-·-·-·- UNDERGROUND
------ FUTURE

TOLERANCES	ARGONNE NATIONAL LABORATORY		
FRACTIONAL TOL. ± 1/32	This drawing is the property of the Argonne National Laboratory		SITE PLAN
DECIMAL TOL. ± .005			
ANGLE ± 1/2°			
ALL DIMENSIONS TO BE CHECKED ON THE JOB			
UNLESS OTHERWISE NOTED	SCALE 1"=100'	DATE F.T. 11-13-56	FIG. 9.1.B

since beam experiments may be conducted at distances up to one-quarter of a mile from the reactor. The location has a minimum of 40 ft of overburden above the underlying rock strata, thus eliminating costly and time-consuming rock blasting for the extensive foundations of this building.

The site area is divided into two general areas. A "limited" or "clean" area containing most of the nonradioactive operations and service functions is separated by a fence from an "exclusion" or "hot" area containing the reactor and its closely related radioactive auxiliaries. The exclusion area is approximately the south half of the plot. Since the subterranean and deep water flows are to the southeast, this location decreases the possibility that escaping radioactive water may flow toward the wells located in the north portion of the limited area. The most prominent wind direction at the site is from the southwest, and the direction of secondary frequency is from the northeast. Therefore the stack for the exhaust of reactor-cooling air is near the southeast corner of the site.

The main entrance to the site is at the west side of the limited area. This location permits personnel to travel to and from work without going through the area into which the exhaust reactor-cooling air is generally swept. With the main entrance on the limited area side, the number of persons entering the exclusion area can be kept at a minimum. The laboratory facilities are housed in the Reactor Building wing adjacent to the west side of the Reactor Building. This presents the closest approach of these two buildings to the site main entrance gate. Personnel for both buildings enter through a single entrance located on the west side of the laboratory wing, thereby keeping the Reactor Building free of persons not having specific duties there.

The Process Water Building and working reservoir are located east and slightly north of the Reactor Building. This location effects a reasonably close approach both to the reactor and the water supplies located in the limited area. Effluent control, the retention basin, and the effluent pond are in the southeast corner of the site because of the direction of the undersurface water flows.

The arrangement of facilities in the limited area has the Services Building near the main site entrance and the canteen located centrally. The various water-storage, pump, and treatment buildings lie north of the Process

Water Building and are arranged approximately in the sequence of flow starting from the wells near the north fence and going south to the various points of usage.

In accordance with AEC security regulations all facilities are located a minimum of 150 ft inside the perimeter fence. The perimeter fence is made of 8-ft-high chain-link fencing topped with three strands of barbed wire angling outward. The limited and exclusion areas are separated by similar fencing. A truck trap is provided at the main entrance to allow thorough guard inspection of vehicles entering or leaving the site. Limited- and exclusion-area control houses are provided at the entrances to each area. These serve as guard stations for badge exchange and personnel screening. A patrol road encircles each subarea and is located within approximately 25 ft of the site perimeter fence. A stationary lighting system provides continuous lighting during hours of darkness. Pendant luminaries with refractory lenses designed so as to direct most of the light in the direction needed are used. A portion of this lighting circuit is on the emergency power system.

Largely for purposes of fire protection all buildings have a minimum of 50 ft separation from adjacent buildings.

A parking lot for vehicles not used on the site is provided outside the west perimeter fence near the main entrance.

Sufficient space remains for future additions to the Reactor Building wing , Process Water Building, Cooling Tower, Water Treatment Building, and Boiler House. Also, space is provided for future facilities such as an administration building, reactor service building, cafeteria, and hot laboratory.

The plot plan originally conceived for the Idaho area, was considerably larger than the one shown in Fig. 9.1.A. The north-south dimension was slightly longer and the east-west dimension was approximately 900 ft longer. When economy forced a cut-back of the facilities planned for the reactor, the site was decreased in size. The sewage-treatment plant remains in its original location, which is now outside the perimeter fence. As this plant is a potential source of odors, it is isolated as much as is practical.

9.2 REACTOR BUILDING

An artist's sketch of the Reactor Building and wing is shown in Fig. 9.2.A. This figure shows the architectural treatment of the two adjoining buildings.

Dwg. 10769 [redacted]

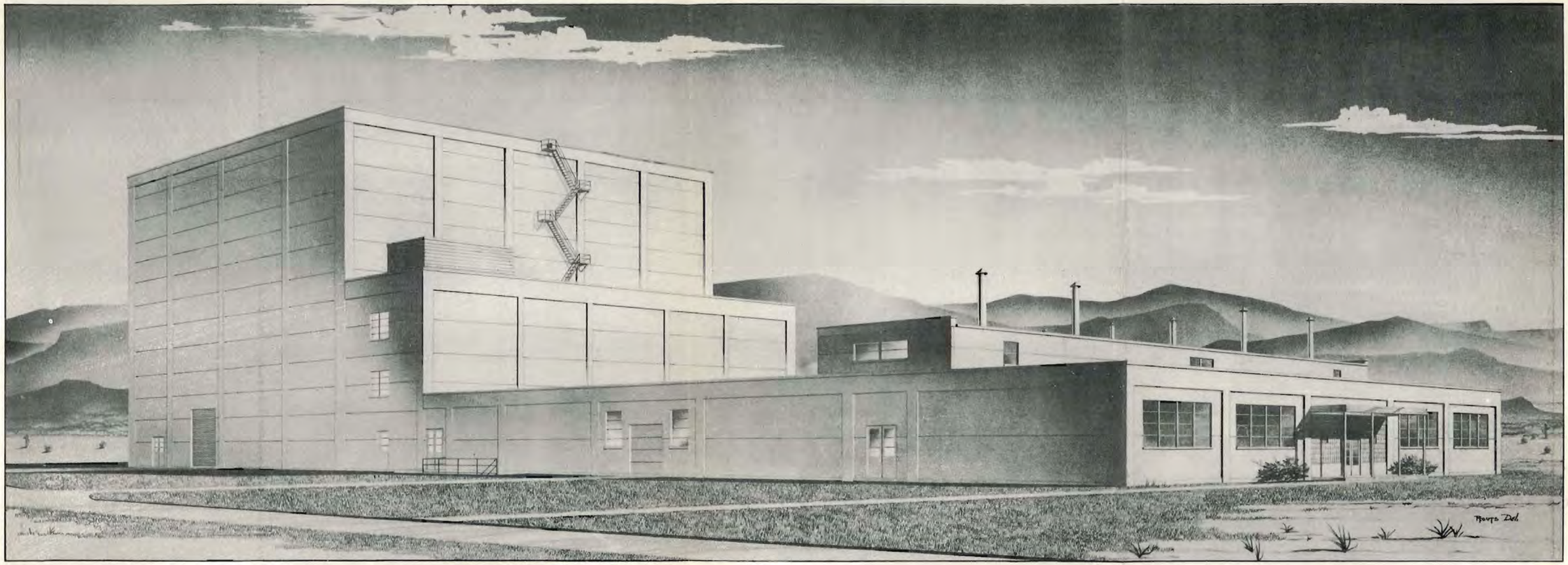

FIG. 9.2.A

REACTOR BLDG. AND WING
ARTIST'S SKETCH

The wing is in the foreground, and on its west side is the main entrance to the two buildings.

9.2.1 General Building Details. The height of the main portion of the building is based on the requirements of the main building crane. The main hoist of the crane has a capacity of 30 tons. The 30-ton hook is 30 ft above the reactor top when at its highest position. The upper limit of travel is governed entirely by the height necessary to permit hoisting the top plug over the railing around the reactor top. The crane capacity is such that it can handle the 22-ton coffins for dummy plugs and also heavier coffins for probable experimental plugs. A 5-ton auxiliary hoist is available on the main crane, since this load capacity is sufficient for the major portion of crane work. Since the auxiliary hoist has a higher lifting speed, jobs under 5 tons can be dispatched in less time than if the relatively slow 30-ton hoist were the only one available. Each hoist on the main crane has sufficient cable to provide a 75-ft lift, which length is sufficient for operations involving the placing of objects into or taking them out of the canal located below basement floor level. The crane span of 100 ft gives coverage between the control room balconies and the east outside wall. The bridge can travel along the full north-south building dimension. This wide working latitude of the crane permits servicing of the entire operating area of the first floor.

The ventilation requirements of the building are consistent with standard practice. Six air changes per hour prevail in all areas except the reactor room, the instrument room, and control room. The six air changes exist in such areas as the sub-pile room, the vault, and the canal tunnel. As the reactor room is 75 ft high, only two air changes per hour are provided in this area.

The entire Reactor Building is pressurized to a minimum of 1/8 in. water. This promotes air leakage out of rather than into the building and thereby tends to prevent outside dust particles from contaminating the filtered building air. This is important since the reactor draws its cooling air supply from within the building.

The instrument and the control rooms are air-conditioned and humidity controlled. The actual quantity of air used in these two rooms is governed by the heat load involved. Seventy-five percent of the air is recirculated.

These two rooms have a slightly higher static pressure than the remainder of the building.

9.2.2 First Floor. The building, the layout of which is illustrated in Figs. 9.2.B, C, and D, is planned around the first floor area. Figure 9.2.B shows the first floor plan. Survey work among the scientific personnel interested in conducting experiments on a high-flux reactor such as the MTR revealed that some experiments required apparatus reaching out 25 ft from a reactor face. History of experimental work indicates that this distance has grown rather steadily in the past few years. Assuming that the high flux available in the MTR would speed up this trend of elongated apparatus, an additional 15 ft is available. An 8-ft traffic aisle remains when experiments require all of the 40 ft allowed. To provide this space for experimental apparatus the first floor is approximately 130 ft square.

The first floor area is kept as free as possible of permanent equipment so that few areas are restricted from experimental apparatus. The instrument and the control rooms are on the second and third floor levels, primarily to avoid first floor congestion.

The features of the first floor and the reasons for their existence are as follows:

Stairways. Stairways in the northeast and southeast corners are for traffic between the first floor and basement; stairways in the northwest and southwest corners are for traffic between all floor levels. This number of stairways is necessary not only for convenience, but also for safety considerations. The stairways are encased to provide fire wall protection. A one-way escape door is located on the first floor level of each stairwell. The southwest stairwell contains the main entrance door into the Reactor Building. A similar setup is provided in the northwest stairwell; however, this door should be normally locked so that only one screening point is necessary for personnel entering the Reactor Building.

Truck doors. Two truck doors are provided, one in the south wall west of the north-south building centerline and one in the north wall east of the same centerline. These two are necessary for ease of vehicle movement, particularly in the event that the quarter-mile beam experiment is installed. The doors are made sufficiently large to allow a highway-size tractor-trailer unit

NOT CLASSIFIED
Dwg # 10742

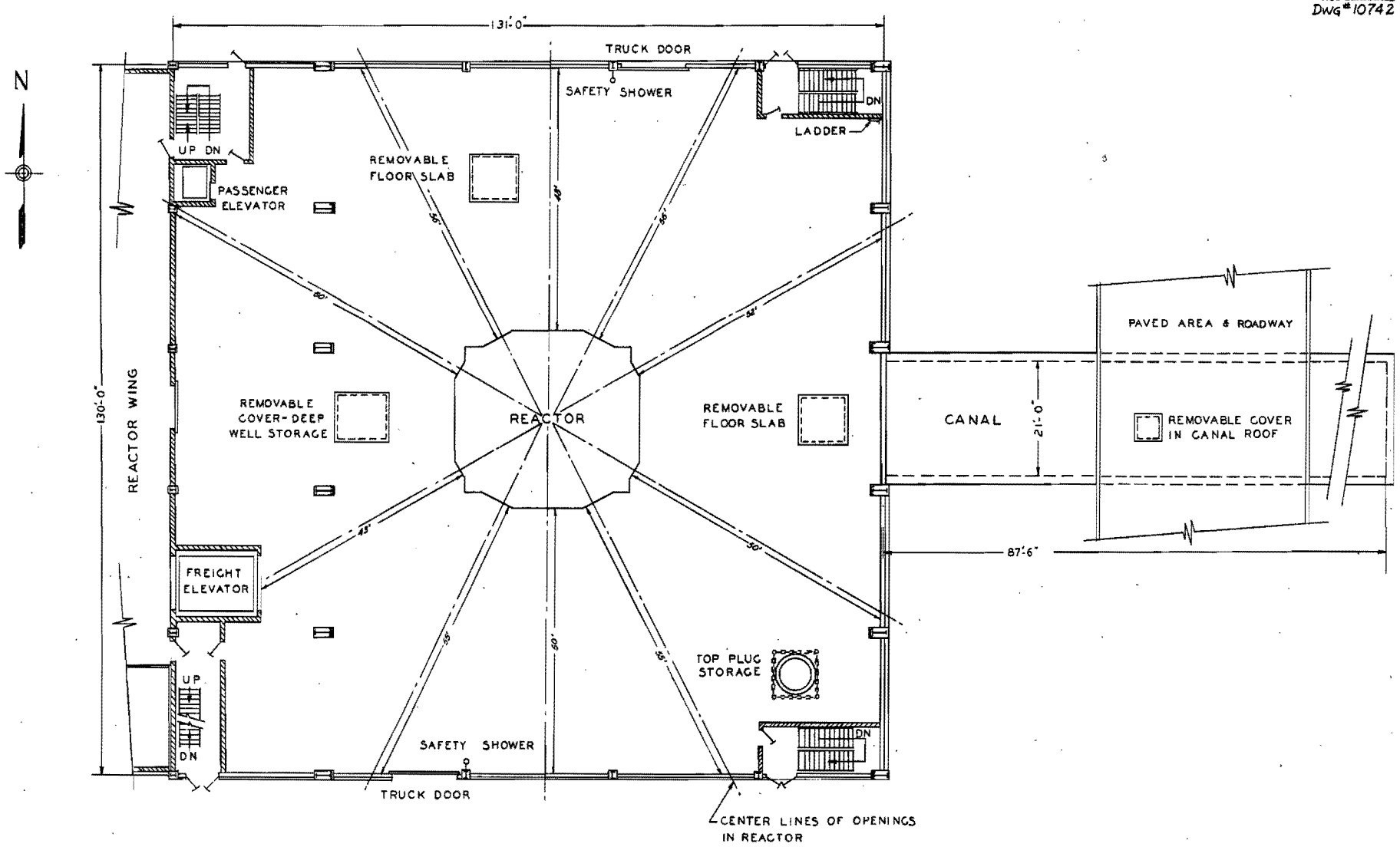

TOLERANCES: FRACTIONAL TOL. ± 1/32; DECIMAL TOL. ± .005; ANGLE ± 1/2°; ALL DIMENSIONS IN THIS DRAWING ARE IN INCHES UNLESS OTHERWISE NOTED	APPROVED (PROJ. ENGR.) / CHIEF ENGR. / CHIEF DRAFTSMAN / CHECKED / DRAWN FT 11-16-56 / GROUP REPRESENTATIVE HUTTER & LEVSE	ARGONNE NATIONAL LABORATORY — This drawing is the property of the Argonne National Laboratory	SYM. / CHANGE / DATE / BY; PLANT REACTOR BLDG.; DESCRIPTION FIRST FLOOR PLAN; SCALE 1/8" = 1'; DATE; NO. REQD.; SHEET; DWG. NO. FIG. 9.2. B; ITEM NO.

NOT CLASSIFIED

Dwg.# 10743

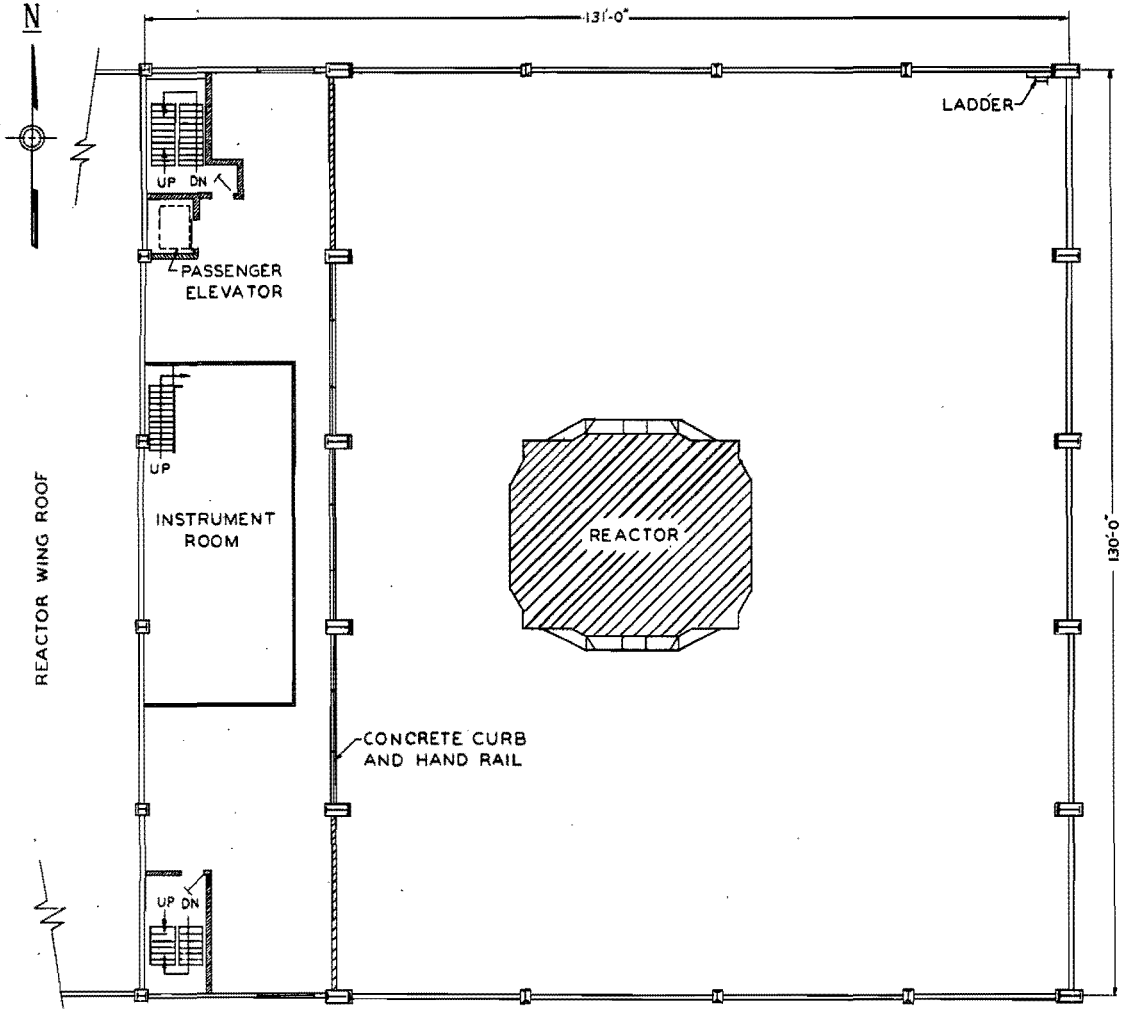

SECOND FLOOR PLAN

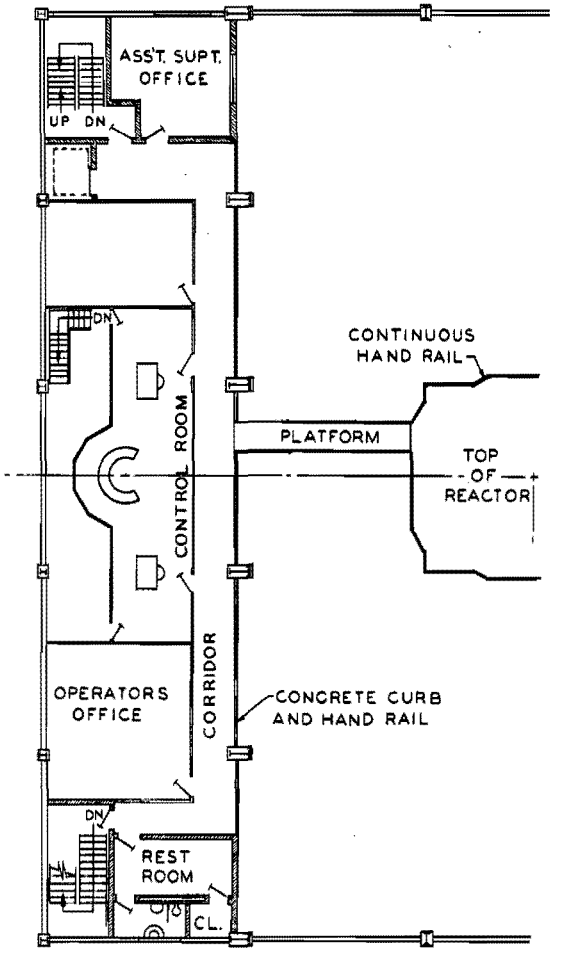

PARTIAL THIRD FLOOR PLAN

TOLERANCES		ARGONNE NATIONAL LABORATORY	REACTOR BUILDING
		This drawing is the property of the Argonne National Laboratory	SECOND & THIRD FLOORS
			FIG. 9, 2, C

[redacted]

DWG # 10749

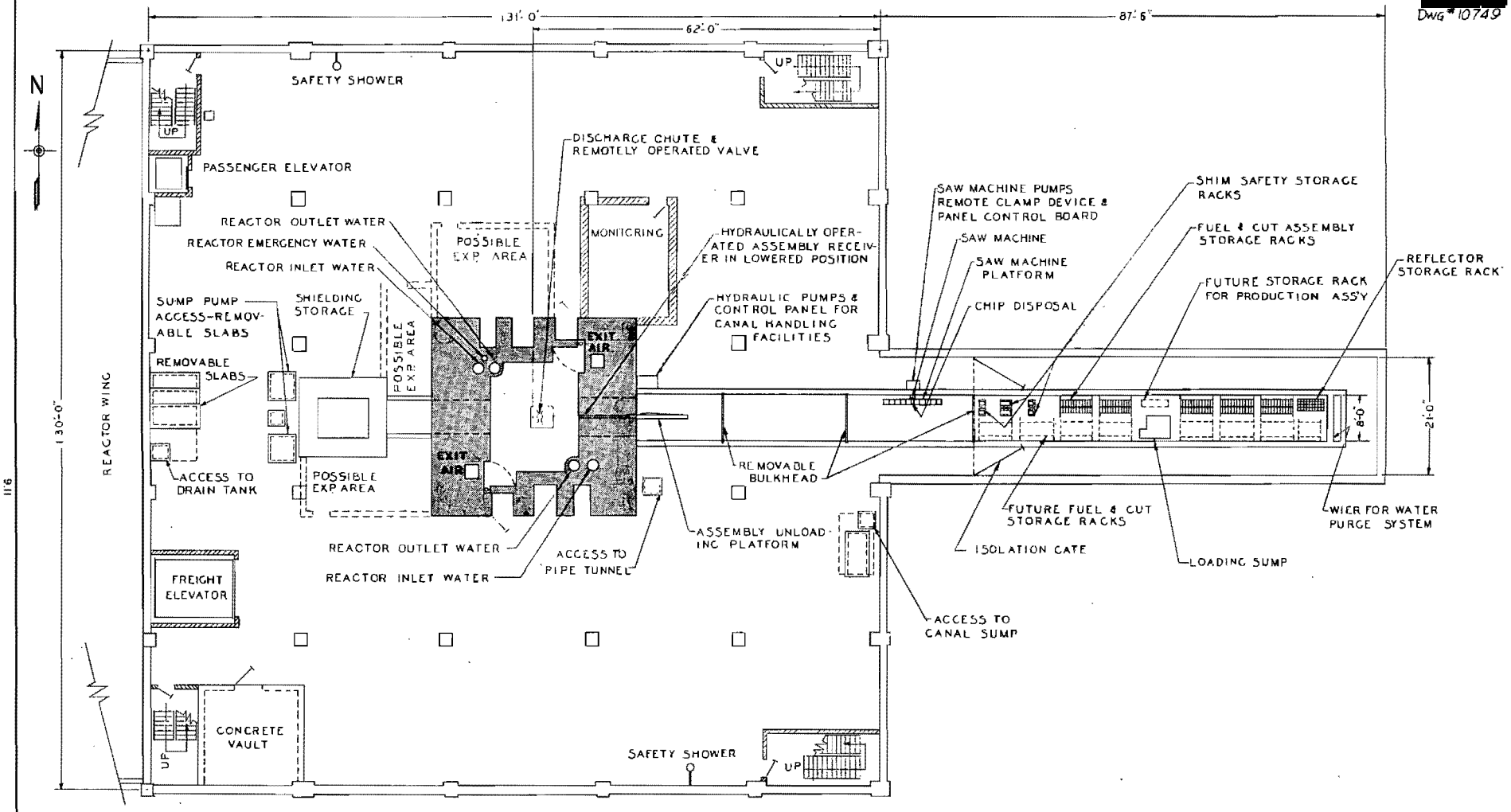

TOLERANCES: FRACTIONAL TOL. ± 1/16 DECIMAL TOL. ± .005 ANGLE ± 1/2° ALL DIMENSIONS IN THIS DRAWING FOR FINISH GRIND AT 1/8 MAXIMUM FINISH. UNLESS OTHERWISE NOTED	ARGONNE NATIONAL LABORATORY The drawing is the property of the Argonne National Laboratory	TITLE REACTOR BUILDING	
	SCALE 1/8" = 1'	ASSEMBLY BASEMENT PLAN	
	DRAWN F.T. 7-15-54	SHEET 6	FIG. 9.2.D

to be brought into the building. To cut down the amount of dirt carried into the building, cold drains are available directly inside the truck doors to allow for hose cleaning of vehicle wheels.

Elevators. For convenience of operators and visitors, a passenger elevator operates between the basement and control room levels with outlets on all floors. A 10-ton hydraulically operated freight elevator operates between the first floor and basement, and has an intermediate stop at the Reactor Building wing basement level. This freight elevator provides for the normal movement of supplies and equipment between floors. The elevator has a 10- by 14-ft platform; it is capable of handling a 7000-lb-capacity electric fork-lift truck with a fully loaded skid on the forks.

Removable floor slabs. The first floor has two 8- by 8-ft removable floor slabs, one located directly over the canal, and the other over a clear area of the basement. The first permits heavy coffins to be placed into or taken from the canal, while the second allows heavily shielded apparatus to be placed onto or taken from the basement floor.

Top plug storage. To accommodate storage of the top plug during the reactor loading and unloading operations, a 6-ft-diameter hole is located near the southeast corner of the building. The hole is placed so that adequate working space is available on all sides of the plug. The weight of the top plug is carried on the first floor slab by the plug cover flange. In this position the magnet end of the plug is at a convenient working height above the basement floor.

First floor thickness. As protection for personnel working in the basement when "hot" experiments are being conducted on the first floor and to protect personnel on the first floor when the reverse situation is true, the floor is 3 ft thick in a zone of approximately 25 ft around the reactor. The thickness is an arbitrary one which gives good shielding and yet is within practical construction limits. The 25-ft distance is the most likely zone for "hot" work.

Floor loading. The first floor loading is the result of studies of probable loads resulting from lead shielding walls and plug coffins. The floor designed for these concentrated loads allows 900 lb per square foot of uniform load. Concentrated loads in excess of 4000 lb per square foot can be

sustained.

First floor services. The most frequently used services are steam, compressed air, filtered water, and 110-volt single-phase and 220-volt three-phase current. Outlets for these services are provided at numerous spots on the reactor faces and at two locations on each of the north, east, and south walls of the building. Sufficient space is available at these outlet locations for future additions.

Facility holes. Since it is impractical to install all services which are desired by the experimenter, the so-called "facility holes" are placed in the first floor at likely points of use. By means of these holes, special services can be added by running leads from the source of supply along the basement ceiling and through the hole nearest the user. This will prevent cluttering the first floor and the reactor faces with future piping.

9.2.3 Second and Third Floors. The layout of the second and third floors is shown in Fig. 9.2.C, as mentioned in the discussion of the first floor; the instrument and control rooms are on the second and third floor levels. These two rooms operate much as a unit with the instrument room having the amplifiers and relays and the control room having the indicating and recording instruments for reactor operation. The control room is at the higher level so that conduits and raceways do not come from an overhead position.

The third floor level is at the same elevation as the reactor top. This gives a level 4-ft walkway between these two areas. This walkway provides the main access path to the mechanisms located on the reactor top.

The second and third floor levels extend completely across the building even though the two primary rooms require somewhat less than half the total area available. A rest room, toilet, chart storage room, stairwells, elevator shaft, reactor operator's office, and probable office space for reactor operating or technical personnel occupy the remainder of the space.

Standard metal partitioning is used for the wall construction around the instrument and control rooms, adding flexibility to the design. These rooms can be made larger or smaller or additional rooms can be added without upsetting reactor operations. The wall construction used is completely salvable.

The instrument room is restricted to all but instrument maintenance and repair personnel. For the convenience of these technicians, a special stairway between the instrument and control rooms is provided.

Other features of these floor levels are the following:

Balconies. There are corridors on the reactor side of this section of the building. A railing along the reactor side of these corridors allows them to be used as observation balconies.

Toilet and rest room. This facility is located on the third floor for the convenience of the reactor operators.

Reactor operator's office. This office is for the reactor shift supervisors and the operators themselves. It is placed adjacent to the control room for their convenience.

Assistant Superintendent's office. The Assistant Superintendent is defined on the tentative organization chart as being the man directly in charge of reactor operations. For this reason his office is on the third floor at the end nearest the passenger elevator. The office has a window overlooking the reactor and the first floor.

Additional floor area. The remaining area on these floors is not subdivided. The operating contractor can subdivide to suit his organizational setup.

9.2.4 Basement. The Reactor Building basement has the same outside dimensions as the first floor. The floor elevation corresponds to that of the sub-pile room. The general layout is shown in Fig. 9.2.D.

The sub-pile room is directly below the reactor and is a shielded room allowing access to several experimental facilities and reactor components. The experimental facilities include two VG holes which originate at the top of the reactor and terminate in the sub-pile room, the two standard hydraulic rabbit tubes which extend up alongside the active lattice, possible hydraulic rabbit tubes to be inserted into the shim or control rod locations, and possible VT holes extending from the top of the reactor through the shim rod locations. In addition to serving these facilities, the sub-pile room permits access to the canal and to several reactor components for maintenance, repair,

or replacement. These include items such as the reactor bottom plug, neutron curtain, and unloading machine. Heavy lead shielding doors are available on each of the two sub-pile room entrances to provide protection for personnel outside the room during reactor unloading operations. Service connections for compressed air, demineralized water, warm drain, electricity, telephone, and hot exhaust are located in this room for the benefit of those conducting experiments.

The remaining facilities of the basement and their functions are as follows:

Canal. This is designed for the handling and storage of radioactive materials in general and spent fuel elements in particular. The canal and its facilities are discussed fully in Chap. 6.

Storage vault. This vault is designed in accordance with security regulations. Walls and ceiling are of 1-ft-thick reinforced concrete. The entrance door is a Merchandise Vault Door, Class D. The vault is primarily a storage place for nonactive fissionable material.

Monitoring room. This shielded room contains the instruments and other equipment used in the continual monitoring of reactor cooling-water temperature and flow and to detect fission breaks in the fuel elements. In addition, instrumentation for the log N measurements is located in this room.

Sumps. Three sumps are located below the basement floor; each one is set at an elevation that provides gravity flow toward it. The canal sump is provided as the pumping point for the canal cooling-water overflow and for the water resulting from draining the canal or sections of the canal. The process-water sump collects water which might possibly, but not probably, pick up some radioactive contamination. The sump is both a retention and a monitoring station. The effluent sump contains a collecting tank where water that has a higher degree of radioactive contamination can be collected and held if necessary.

Piping and conduits. Process piping and duct work are installed in tunnels under the basement floor. This is necessary not only to properly shield them but also to keep them from occupying basement space. The bulk of the electrical conduits, excluding reactor control and instrument circuits, are

also placed under the floor since there appears to be little need for maintenance or repairs on such lines. Service piping and reactor conduits are suspended from ceiling hangers, for it is anticipated that changes and repairs on these lines will be necessary from time to time. Groupings of service outlets are set along the outside basement wall in a fashion similar to those on the first floor.

Experimental area. Much of the remaining open space in the basement is available for various "hot" experiments. Experiments involving the circulation of liquids into an active zone of the reactor are to have their auxiliary apparatus located in the basement. Piping from beam-hole experiments to their auxiliary apparatus is taken through the facility holes. This keeps the major portion of "dirty" work in the basement area.

9.3 REACTOR BUILDING WING

9.3.1 General Building Details. The architectural treatment is consistent with that used for the Reactor Building. While these two buildings appear to be one, they are separate facilities. They have no structural dependence on each other in order to avoid transmission of vibrations from one building to the other.

The wing building is a single-story structure whose internal layout is determined primarily by the laboratories and their auxiliary facilities. This laboratory building has a flexibility such that offices can be readily converted to laboratories or the reverse. A modular plan is the means of achieving this flexibility.

The windows are provided to utilize daylight and to eliminate blank wall space. Owing to the dust problem and the severity of the winters, these windows are sealed-in, double-glazed sash.

The ventilation system represents considerable planning in accordance with general principles set down for radioactive work in laboratories. In general, six air changes per hour are supplied. The air flow pattern is such that the flow within the building is from "subnormal" to "normal" to "above normal" areas. This procedure is based on proved project experience and requires that 100% fresh air be brought into the single "subnormal" area, the

counting room. The air exhausted from this room is used for any remaining areas. "Normal" facilities, such as offices and shops, exhaust their air into the corridors for reuse in the laboratories. The "above normal" facilities, the laboratories, completely exhaust their air supply to the atmosphere. To make certain that no laboratory air enters the corridor, the fresh air supply to the room is set below the exhaust fan capacity. With this provision the excess is taken into the room from the corridors through louvers in the doors. These elaborations on normal building ventilation are made in order to avoid spread of contamination in the event of spills involving radioactive materials.

Basement ventilation is set at one air change per hour and is based on the entire basement volume. The total air supply is provided through one register. As the need arises for subdivision of the basement area into rooms, ventilation ducts can be connected to this outlet.

9.3.2 First Floor. The plan of the first floor of the Reactor Building wing is such that the facilities having a permanent operating function as their initial function could have fixed partitions. Those not falling into this classification follow a modular plan with partitions of a type readily removed or set in place.

The facilities in the former class are the machine shop, staff shop, instrument shop, glass shop, stores, shipping and receiving rooms, counting room, and men's and women's toilets and change rooms. In the latter classification are the offices and laboratories. Although the laboratories are in no sense temporary, some are smaller than desired because of the necessity of providing temporary office space in this building. The first floor layout is illustrated in Fig. 9.3.A.

Machine shop. The prime purpose of this shop is to provide maintenance and repair facilities for reactor components. It is located as shown in the figure chiefly in order to be convenient to the Reactor Building. The floor is capable of taking a uniform load of 250 lb/sq ft, which permits fabrication of or repairs to light-to-moderately heavy coffins. Layouts of several possibilities of machine tools are available which prove the feasibility of placing a variety of light- and medium-capacity machines. Specifying the size, number, and brand of this equipment is left to the operating contractor. As opinions vary widely on the relative merits of machine tools, it appears that the shop superintendent should choose those in which he has most confidence.

NOT CLASSIFIED
DWG# 10744

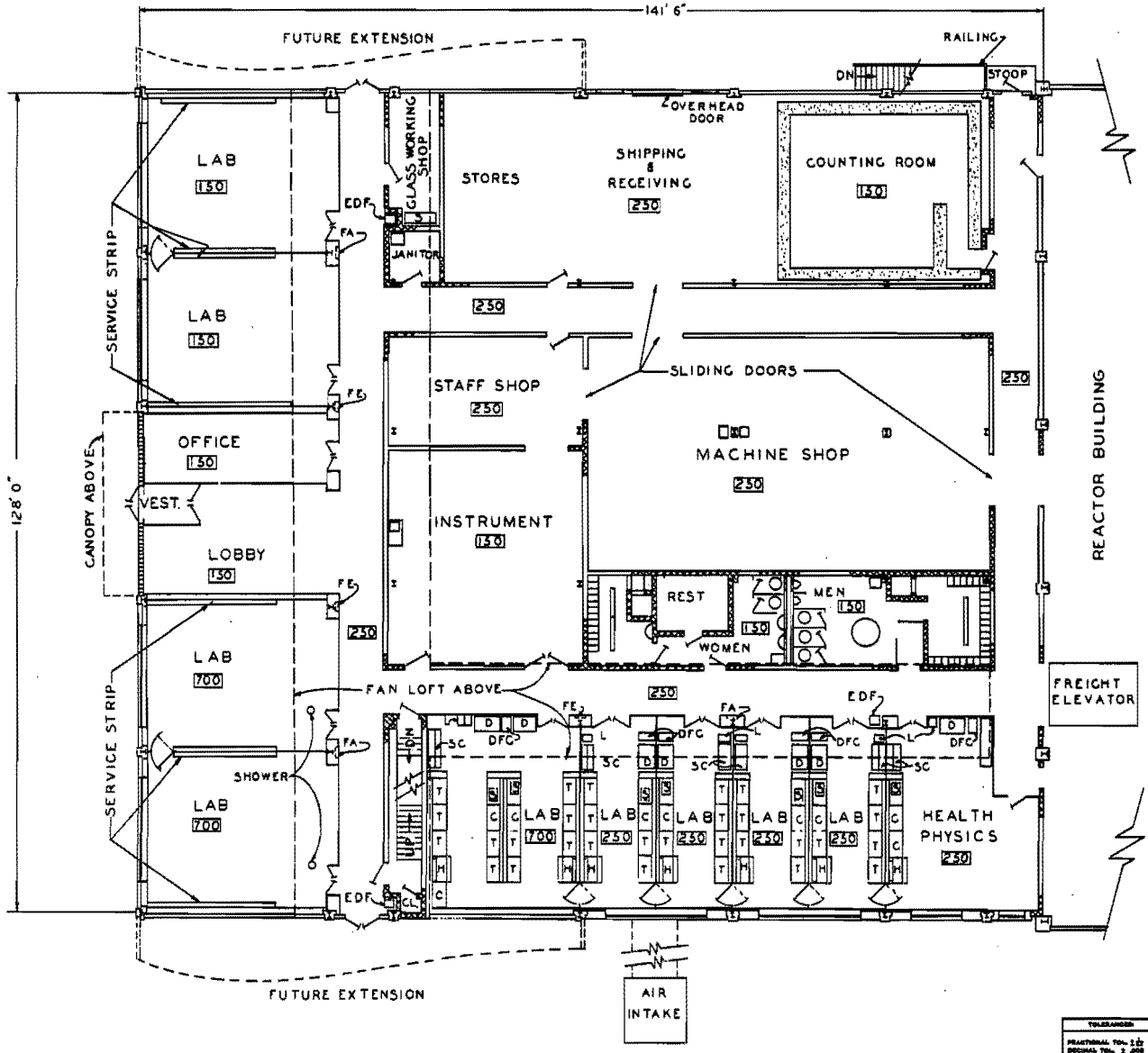

SYMBOLS FOR FURNISHINGS AND EQUIPMENT

UNDERBENCH CABINET	C
DESK	D
DIAL LOCK FILE	DFC
HOOD	H
LOCKER	L
SINK	S
SUPPLY CABINET	SC
TABLE	T
FIRE EXTINGUISHER	FE
FIRST AID CABINET	FA
ELEC. DRINKING FOUNTIAN FIRE HOSE ABOVE	EDF

NOTE:

▭ INDICATES LIVE LOAD ~ LBS. PER SQ. FT.

TOLERANCES: FRACTIONAL TOL. ± 1/32; DECIMAL TOL. ± .005; ANGLE ± 2°; ALL DIMENSIONS IN THE DRAWING MUST BE IN INCHES UNLESS OTHERWISE NOTED

ARGONNE NATIONAL LABORATORY

This drawing is the property of the Argonne National Laboratory

DRAWN JY 11-24-50

BUTTER LEVSB

REACTOR BLDG. WING

FIRST FLOOR

FIG. 9, 3, A

Staff shop. This shop is adjacent to the machine shop, convenient to the supply point, and centrally located to the possible users. It is provided to serve the experimenter who wishes to do some of his own machine work. It also contains the light power tools necessary for instrument shop work.

Instrument shop. This shop is primarily for maintenance and repair of the electronic instruments used for reactor operations. The shop size is such that it also permits some maintenance of electronic instruments used for experiments. Construction of new instruments is beyond the intent or facilities of this shop. As with the other shops, equipment and its layout are placed within the operating contractor's jurisdiction.

Glass shop. This small shop is intended to be a service function for the experimenter. The room itself is relatively small but should be adequate for the initial testing program.

Counting room. This room is next to the corridor separating the reactor and the wing buildings. This represents a somewhat central location to facilities in both buildings. Its location is along an outside wall, rather than in the center of the building, in order to aid in eliminating the transmittal of machine vibrations into the room. Although present philosophy states that the counting instruments rather than the room proper should be shielded, 2-ft-thick concrete walls and ceiling are provided. The reasons for adhering to the older practice are (1) the unknown factors connected with the stray radiations from a high-intensity reactor located approximately 60 ft away and (2) the increase of cosmic radiations due to the relatively high altitude of the site. Beta and gamma counting are done here, but alpha counting is done in the laboratories. The foundations for this room are separate from the remainder of the building, which is an additional precaution in the elimination of transmitted machine vibrations. Services into this room are low-pressure air, hot and cold water, and 110-volt regulated current. The room is air-conditioned and the humidity is controlled to 40% R.H. ± 10%. The air supplied is 100% fresh air. Air exhausted from this room is reused as a portion of the ventilating supply in the remainder of the building.

Stores, shipping, and receiving rooms. Although these are labeled as somewhat separate areas, they represent a single integrated unit. The only barriers necessary are a counter or possibly a wire mesh partition. The functions of these facilities are defined adequately by the title.

Laboratories. All remaining facilities are designed for use as laboratories. To achieve a flexibility for enlarging or subdividing laboratories, a modular plan is used. The module selected is 12 ft wide and 28 ft deep. The width is one which has had some degree of general acceptance in laboratory design. The depth provides 20 ft for bench space for test work, and 8 ft for desk, storage cabinets, and locker. The first 8 ft in from the corridor wall is for this office-storage function. If any laboratory experiment should involve considerable amounts of alpha work, this 8-ft space can be readily partitioned off from the remainder of the laboratory. This would form somewhat of an air lock to prevent spread of air-borne contamination. The remaining 20 ft of laboratory is used for work bench service. A 4-ft sub-module is used for determining the sizes of equipment such as benches and cabinets and for setting the locations of service outlets such as gas, water, air, and electricity.

Metal partitioning is used because of the following characteristics:

1. Ease of installation or removal without dust problem.
2. Factory baked-on finish, easily cleaned or decontaminated.
3. Nonporous surface giving minimum absorption of radioactivity.
4. Absence of large cracks for accumulation of dusts; the fine cracks between panels are sealed with a putty or a plastic tape.

The ceilings are perforated metal pans with insulation placed in the pans. These are effective, both as sound deadeners and heat insulators. Lighting is by means of fluorescent strip lights set flush with the ceiling.

The floor covering is vinyl sheet flooring. This is used because of its resistance to most reagents and many of the common organic solvents. Also, this material requires less maintenance than other available floor coverings.

The services or utilities available in the laboratories are steam, low-pressure air, gas, hot and cold soft water, 110-volt single-phase and 220-volt three-phase power, demineralized water, and telephone. All but the last two have connection outlets at 8-ft intervals along a bench. Demineralized water and telephones are provided on the basis of one outlet per laboratory, regardless of whether the laboratory is a 12- or 24-ft-wide room. All services are brought into the room from the supply headers located in the basement. Floor slots for these pipes are centered on the 12-ft module separation lines.

Ventilating-air supply is through anemostats. Exhaust is to the atmosphere through fans, of which one is provided for each module. These exhaust fans have a capacity higher than the supply inlets to the room. By this means, air is constantly entering the room from the corridors through louvers in the doors. The exhaust fans have a capacity to provide a minimum of 100 cfm of air through the working openings of two 4-ft hoods. When the hoods are not in use, the same quantity of air is drawn into a dampered by-pass in the hood duct work.

An opening leading to the contaminated-air system is provided in each hood. These off-gas openings are for use with dry-box work and experiments which may give off radioactive or acidic vapors. Each off-gas opening provides an exhaust flow of about 50 cfm.

Four laboratory modules intended for normal laboratory work permit floor loadings of 150 lb/sq ft. The four modules that permit 250 lb/sq ft floor loadings are forwork involving moderate activity requiring light lead shields. The six modules that permit floor loadings of 700 lb/sq ft can take one cave per double module. Such a cave could have a 4- by 6-ft working area and be shielded by 30- to 36-in. concrete walls 6 to 7 ft high. A cave of this type could handle up to 10 curies of activity.

Owing to lack of office space on the site, laboratory furnishings for most of the laboratories along the west wall are not provided. This space will be used for offices until such time as an administration building is constructed.

9.3.3 Basement. The building has a full basement which gives adequate space for ventilating and air-conditioning equipment for areas 3 and 4, electrical switch gear for these same areas, the battery room for emergency use by the reactor operating instruments, and the scrubbing system for the contaminated air from laboratory hoods. This is illustrated in Fig. 9.3.B. The massive foundation work for the counting room forms a fireproof record room. Of the total basement area, all space is fairly well occupied except the first bay starting at the west wall and extending the full north-south dimension of the building. This can be used for placing future equipment or for subdividing into storage rooms such as a parts storage room for the instrument shop.

NOT CLASSIFIED
Dwg. #10745

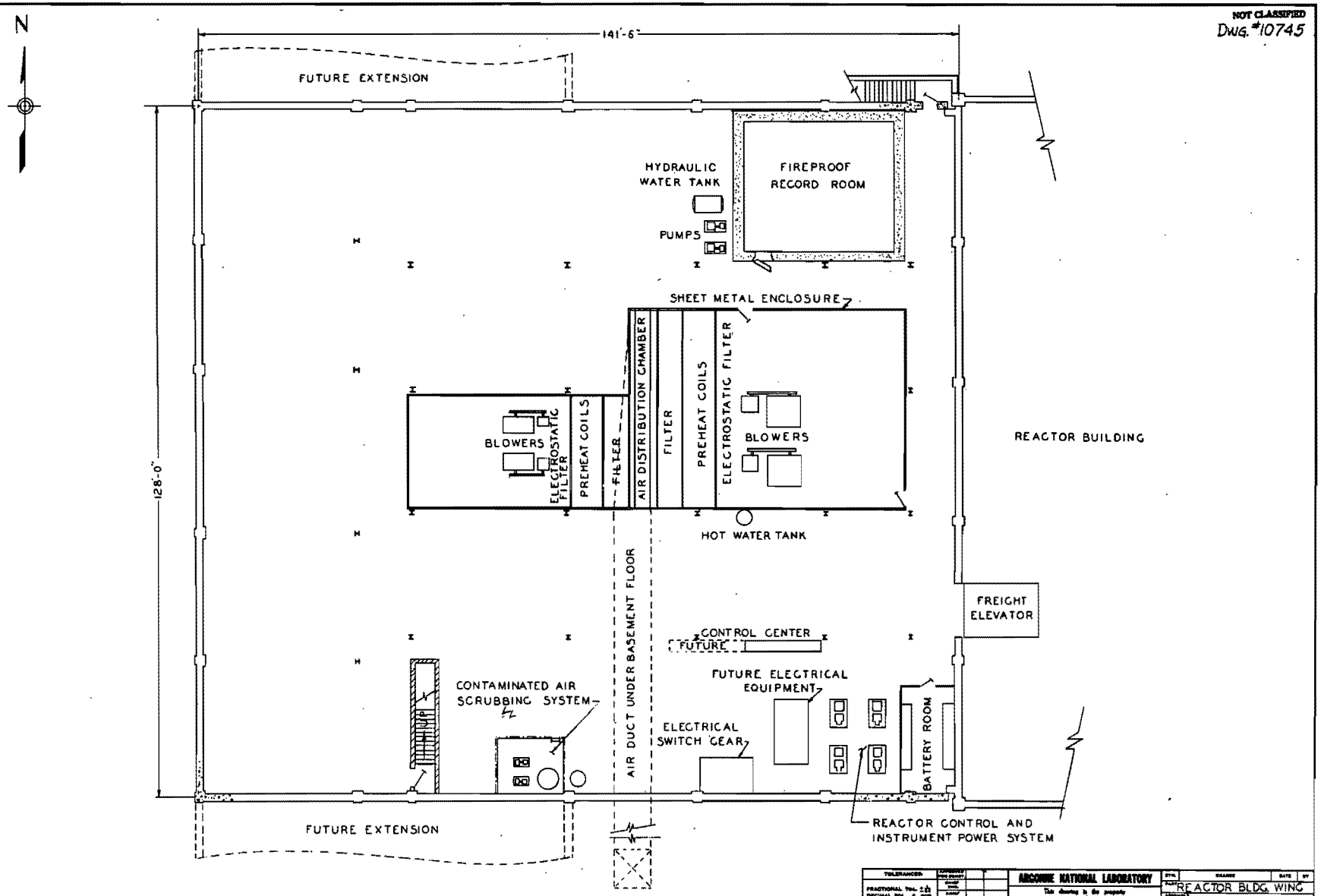

TOLERANCES: FRACTIONAL TOL. ± 1/8; DECIMAL TOL. ± .005; ANGLES ± 1°; ALL DIMENSIONS IN THIS DRAWING ARE MADE USED IN 20 DIGITS UNLESS OTHERWISE NOTED	ARGONNE NATIONAL LABORATORY — This drawing is the property of the Argonne National Laboratory	SYM. / TITLE / DATE / BY	
		PLANT: REACTOR BLDG. WING	
		DESCRIPTION: BASEMENT	
		SCALE: 1/8" = 1'	FIG. 9.3.B

9.3.4 Future Additions. This building is so designed that 70-ft-wide wings can be added both north and south of the present structure. The points of future extension are shown in Figs. 9.3.A and B. The original building layout included extensions of 72 ft both north and south to give a T-shaped building. Budgetary limitations brought about a cut-back of twenty-four 12- by 28-ft laboratory modules, and thus eliminated facilities such as a library, drafting room, and technical staff offices. These are necessary functions for a long-period operation of the reactor, and for this reason will probably be added shortly after reactor operation begins.

9.4 SERVICE BUILDINGS AND AREAS

9.4.1 Service Building, Area 14. This single-story 42- by 102-ft building combines four separate service functions into one structure:

1. First aid. This section has a two-bed infirmary, waiting room, first aid room which can be used for physical examinations, toilet rooms, and assorted closets for storage of medical and janitorial supplies.

2. Guards' section. This portion is subdivided into two rooms. One room has locker, shower, and toilet facilities for a total of 50 guards with a maximum of 20 per shift. The second room is the guards' ready room.

3. Communications. This section is also a two-room portion of the building. One room houses the dial telephone exchange equipment; the other has the radio apparatus required by Security.

4. Fire house. This section has garage space for one pumper truck, the firemen's office, and sleeping quarters for firemen on 24-hr shift basis.

9.4.2 Limited-area Control House, Area 20. This 22- by 42-ft single-story building is located at the main entrance gate and is the screening point for all personnel and vehicles entering or leaving the site. Guard stations are provided along the central portion of both the north and south walls. These two stations can take two lines of persons checking in or out. In addition, the north guard station has a door leading into the truck trap located directly outside the building, which constitutes the screening point

for vehicles. Both the east and west ends of the building are small lobby sections which can accommodate the back-up of employees during heavy periods of personnel movement. All badge exchange is handled in this building.

9.4.3 Exclusion-area Control House, Area 21. This is a single-story 12- by 12-ft building which acts as a second screening point for persons entering the exclusion area. The building is subdivided north and south into two portions, one the guard station and the other a corridor section through which personnel pass on their way to or from the exclusion area.

9.4.4 Canteen, Area 16. The canteen is a portion of one of the temporary metal buildings erected for the construction firm. Cafeteria style service is provided. The food is prepared at AEC Central Facilities. Seating capacity is relatively small so that three or four seatings may be required to serve all those purchasing their lunch.

9.4.5 Plug Storage, Area 11. Plug storage is located south of the Reactor Building on the main truck road leading out of the building. This is an earth-filled structure with a concrete charging face on the east side. Steel liners used for the holes are held level by means of the concrete charging face and a supporting wall located 13 ft into the earth-filled section. Fourteen holes, ranging in size from 19 by 15 in. to 5½ in. inside diameter, are located at a convenient height above the roadway for charging plugs into the holes. A minimum of 8 ft of earth shielding is used on top, sides, and ends of all these 20-ft-long tubes.

9.4.6 Reactor Service Building. This building is not a part of the initial construction. However, planning has progressed to a point where the building layout and facilities have been fairly well established. The building has four prime functions: (1) plug storage, (2) machine shop, (3) warehouse, and (4) operations testing. The four facilities require approximately the same square footage of floor area, 6000 sq ft each, so that a 160-ft-square building is used. The overall building height is 30 ft with 22 ft clearance under the roof trusses.

Plug-storage equipment consists of a concrete block 75 ft long by 10 ft high by 21 ft deep. One of the 10- by 75-ft faces is the charging face for placing the plugs into coffins or into storage. A 20-ton 75-ft-span crane operates over this area. The crane can handle the plugs and coffins or the

storage of shielded pots on top of the plug-storage block. The remainder of the room area in front of the storage block is required for vehicle movement, for storage of vehicles and coffins, and for the erection of cave structures for dismantling "hot" plugs.

The machine shop is adjacent to the plug storage room so that the plug-handling crane can be utilized by the shop. The shop provides for machine tool work, lead burning, welding, and sheet metal and pipe work. All these functions are designed specifically for exclusion-area work.

The warehouse section is a two-floor area. The lower floor is designed for storage of heavy materials such as lead bricks or steel shielding plates. The space, in general, is to store items needed for exclusion-area work. Some office space is also available on this floor. The upper floor is designed for lighter storage and/or offices.

The operations testing area is designed for the setup of mock-up or functional test apparatus. A 10- by 50- by 10-ft-deep pit is located in one corner to allow for vertical apparatus height approaching 40 ft. Service outlets are provided in the pit and along the outer walls for the benefit of the experimenter.

There will be a definite need for such a building on the site. Although it has not been constructed as a part of the initial program, it should be actively considered within the first year of operation.

9.4.7 Other Buildings and Areas. The remaining buildings and areas as defined by the Site Plan (Fig. 9.1.B) are directly or indirectly associated with other major sections of the handbook and are discussed therein.

9.5 REFERENCE REPORTS

(1) Guzik, R. F., and Link, L. E., *Reactor Building,* MTR Design Report No. 26, October 10, 1949.

(2) Guzik, R. F., and Link, L. E., *Addendum to Reactor Building Report,* MTR Design Report No. 26A, November 11, 1949.

(3) Guzik, R. F., and Link, L. E., *Reactor Building Wing,* MTR Design Report No. 27, October 12, 1949.

(4) Guzik, R. F., and Link, L. E., *Addendum to Reactor Building Wing Report,* MTR Design Report No. 27A, November 25, 1949.

(5) Guzik, R. F., and Link, L. E., *Site Plan,* MTR Design Report No. 36, May 3, 1950.

(6) Sullivan, T. E., *Subpile Room,* MTR Design Report No. 46, ANL-ABS-19, April 19, 1950.

9.6 REFERENCE DRAWINGS

(Blaw Knox Construction Company Drawings)

DWG. NO.	TITLE
3150-3-1, Rev. 4	Reactor Building - Basement Plan
3150-3-2, Rev. 3	Reactor Building - First Floor Plan
3150-3-3, Rev. 3	Reactor Building - Second and Third Floor Plans
3150-3-5, Rev. 3	Reactor Building - Longitudinal Section
3150-3-6, Rev. 3	Reactor Building - Transverse Section
3150-3-7, Rev. 2	Reactor Building - Facilities Below Basement
3150-4-1	Reactor Building Wing - Basement Plan
3150-4-2	Reactor Building Wing - First Floor
3150-4-2, Rev. 1	Reactor Building Wing - First Floor
3150-4-3	Reactor Building Wing - Elevations and Section
3150-11-1	Reactor Service Building
3150-14-1, Rev. 1	Safety and Security Building
3150-20-1, Rev. 1	Control House - Limited Area
3150-21-1, Rev. 1	Control House - Exclusion Area
3150-91-5, Rev. 1	Plot Plan Study
3150-91-5, Rev. 9	Plot Plan
3150-502-3, Rev. 2	Mechanical Design - Subpile Room

Chapter 10*

SUPPORTING FACILITIES AND AUXILARIES

10.1. STEAM PLANT

The steam plant is a 66- by 110-ft building located approximately in the center of the northern half of the MTR site. This building contains the following equipment:

(1) Steam-generating facilities to supply process and heating steam requirements

(2) Diesel-electric generator to supply emergency power requirements

(3) Air compressors, two to supply plant air during normal operation and one to supply instrument air during emergencies

The steam-generating facilities consist of three package-type steam-generator units with fire-tube boilers and their associated equipment. Each unit has a maximum capacity of 16,500 lb/hr at a design pressure of 150 psig. Two of the units are adequate to supply the maximum process and heating steam requirements, while the third unit serves as a stand-by. The units are oil-fired but can readily be converted to be oil-gas-fired at any time. The operation of the units is fully automatic.

In the event of commercial power failure the Diesel-electric generator, which is rated at 750 kva, can supply power to processes requiring electricity for emergency operation. Each of the two plant air compressors can supply 300 scfm of air at 150 psig. Only one of these is in operation normally, the second serving as a spare. The third compressor can supply 60 scfm of air at 125 psig to instruments during commercial power outages.

10.2 ELECTRICAL SYSTEMS

10.2.1 Introduction. The electrical systems incident to the operation of the MTR have been designed for high reliability in accord with requirements peculiar to operation of the project and local conditions. As the principal means for precluding interruption or failure of these electrical systems, dual

*ANL contribution.

feeder arrangements are used as a basis of design wherever practical. The systems providing power within the MTR site for all uses are discussed with regard to sources of electrical power, distribution systems, load power factor, and electrical grounding.

10.2.2 Sources of Electrical Power. Since the requirements of processes and facilities of the MTR project vary as to the permissible duration of interruptions in electrical power, it has been necessary to provide other sources of electrical power in addition to the normal power from the public utilities. These other sources of electrical power have been made locally available within the site for continuous and emergency use.

The normal electrical power is provided to the MTR site substation through the RTS (Reactor Testing Station) Central Facilities Control Station over a high-line operating at 132 kv. This high-line comprises part of the ultimate RTS distribution system which initially provides only a single power feeder to the MTR and other sites. When the present plan for distribution of power at 132 kv within the RTS area is complete, this feeder will be extended through the area and back to the Central Facilities Control Station to provide a loop transmission system. The loop system will, in effect, provide two feeders to each of the sites so that power transmission to any site may be over either one or both sections of the loop associated with the site.

The MTR substation is located within the MTR site on the north building line near the east corner. This location complies with the requirement that there be a minimum distance of 1000 ft between any electrical system operating at voltages as high as 150 kv and the precise electronic equipment located in the Reactor Building. The location is also desirable with regard to future site considerations and minimizes the problems of interference associated with the entrance and exit of the high-line feeder circuit.

The principal high-voltage equipment at the site substation includes two high-line transformers and one high-line breaker. Each of the transformers, having a self-cooled rating of 3750 kva and forced air cooling to permit a maximum capacity of 4687 kva, is equipped with automatic tap changing equipment which operates under load to permit some control over voltage variations caused by load factors and other conditions. The primaries of these transformers are connected to the high-line circuit with the high-line breaker between them so that opening of this breaker may permit power to be received

by either of the transformers over the associated section of the loop (when completed). The secondary of each transformer delivers power through a breaker to one of the 2400-volt bus sections in the substation control house. These bus sections of the 2400-volt dual feeder system are associated with a tie breaker to permit independent operation of each section or unitary operation of the entire system.

Although an operator at the substation control house may have control over all 2400-volt circuits, the incoming bus circuits and the bus tie circuit may also be controlled by the RTS area power dispatcher. Control over a number of motor-driven disconnects has been made available to the area dispatcher so that control of high-voltage equipment and the distribution at the site substation may be accomplished with only a single high-line breaker.

The sources of locally available electrical power for continuous use are power-accumulator systems which provide uninterrupted power to a number of important loads. The basic components of each system are a storage battery and a conversion device. During normal operation the normal power system furnishes power through the conversion device to maintain the battery "floating" at full capacity and supply the average power required by the load. Since the arrangement of the battery and conversion device permits the load to be supplied from either one or both simultaneously, there is no interruption to the load when an interruption occurs in the principal power system.

A number of relatively small power-accumulator systems are included as parts of the equipment to which they provide power. Equipment having these systems includes the automatic dial and conference telephone system, the security and fire-alarm system, radio installations, and engine-starting systems.

Other power-accumulator systems, each supplying power to a number of different loads, are strategically located in the substation control house, the steam plant, and the basement of the Reactor Building wing. The first two of these systems are primarily to provide continuous power for control of electrical circuits and emergency lighting. The third system primarily serves the power system for control and instrumentation of the reactor.

The power system for operation of reactor controls and instrumentation is provided to ensure these loads continuous a-c power free of interruptions exceeding 2 cycles duration with voltage dips during this time not greater

than 30%. In addition to the conversion devices and battery of the power accumulator, the principal operating components of this system include two independent inversion devices. For reasons of precedence in reliability, M-G (motor-generator) sets are used for both conversion and inversion. Each of the M-G inversion sets operates continuously from the power accumulator to provide a-c power to its respective bus with very close regulation of the voltage and frequency. One of the M-G conversion sets is a spare while the other one operates continuously to maintain a balance of power through the reactor power system. The busses of the two independent inversion systems provide the control and instrument power. These busses are associated by circuit breakers so that the control load may be operated directly from normal or emergency power and the instrument load may be carried by either one or both of the inverters.

Locally available power for emergency use only is provided by a Diesel-electric stand-by unit located in the steam plant. This unit has a capacity of 750 kva for the provision of power during emergency to a limited number of processes and facilities of the project which must operate during shutdown of the reactor. The operation of this emergency unit and part of the associated electrical systems is entirely automatic so that power may be provided to most of the emergency loads with the least possible delay when normal power is interrupted. A very fast starting system for the Diesel engine is arranged with a "fail safe" control circuit associated with the 2400-volt bus sections of the substation. The control circuit initiates starting any time that both busses are de-energized. Since the sizing of this emergency unit has been determined primarily on the basis of the automatically connected emergency loads, other loads that may be connected during emergency have been identified for dispatch control. Some of these other loads which require large amounts of power are provided with control circuits to the stand-by control panel. These circuits are controlled by the dispatcher to permit the connection of the loads only at times when the generator has sufficient reserve capacity to maintain voltage regulation.

10.2.3 Distribution Systems. The systems for the distribution of all electrical services for the operation of processes and facilities are installed underground throughout the MTR site as indicated by Fig. 10.2.A. With the exception of the perimeter lighting circuits, the electrical conductors for the transmission of power, control, instrument signals, and communications pass from one part of the site to another through underground concrete-encased fiber ductsat a depth below the frost line.

NOT CLASSIFIED

Dwg. # 10761

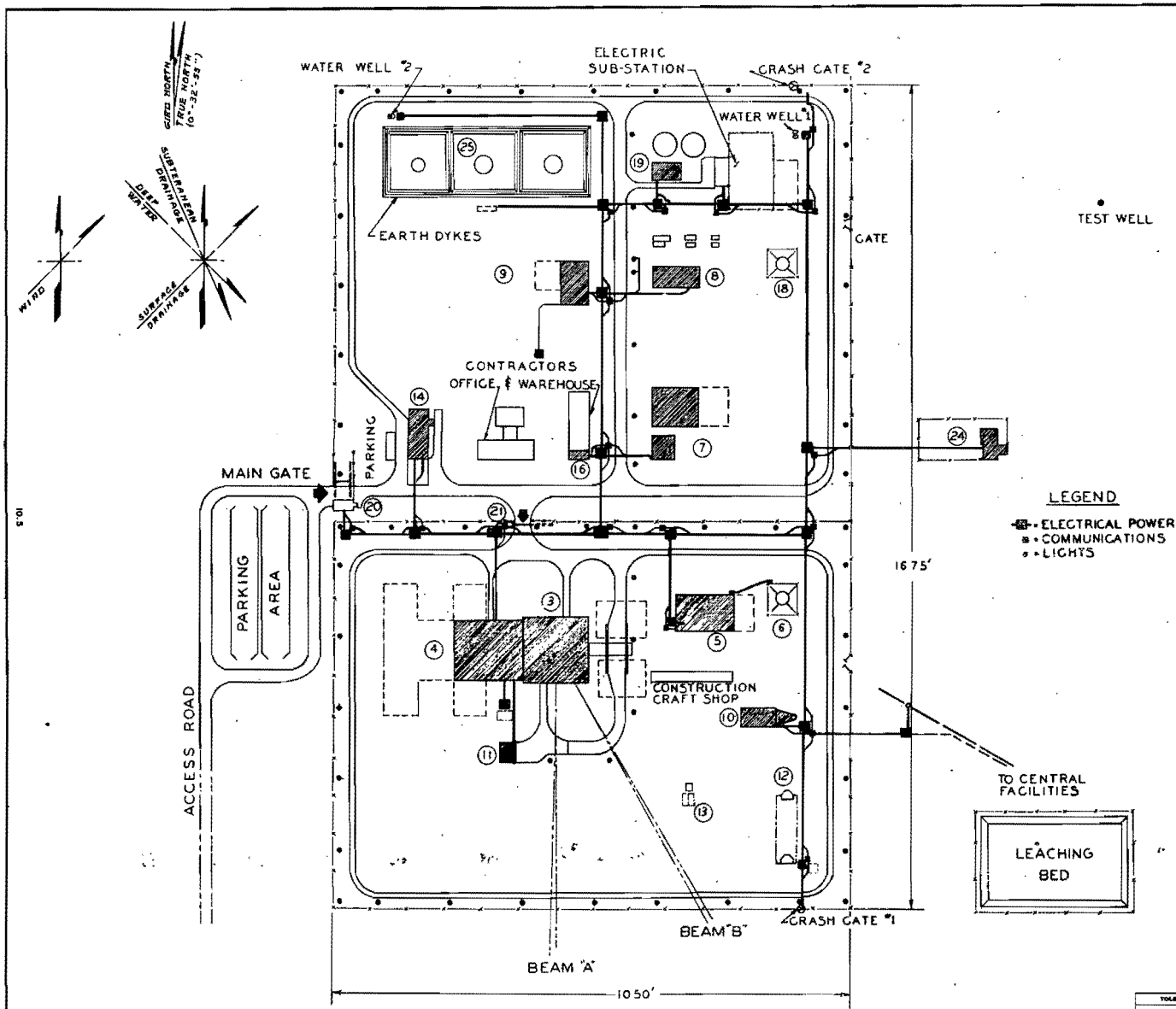

LIST OF AREAS

NO.	DESCRIPTION
1.	YARD (OUTSIDE FENCE)
2.	YARD (INSIDE FENCE)
3.	REACTOR BUILDING
4.	REACTOR BUILDING WING
5.	PROCCESS WATER BLDG.
6.	WORKING RESERVOIR
7.	COOLING TOWER & PUMP HOUSE
8.	DEMINERALIZER BLDG.
9.	STEAM PLANT
10.	FAN HOUSE & STACK
11.	PLUG STORAGE
12.	RETENTION BASIN
13.	EFFLUENT CONTROL
14.	SERVICES BLDG.
15.	
16.	CANTEEN
17.	
18.	EMERGENCY O.H. WATER TANK
19.	RESERVOIR & WATER PUMP HOUSE
20.	CONTROL HOUSE-LIMITED AREA
21.	CONTROL HOUSE EXCLUSION AREA
22.	
23.	
24.	SANITARY SEWAGE TREATMENT PLANT
25.	OIL STORAGE

——·——·— UNDERGROUND

– – – – – – FUTURE

TOLERANCES	ARGONNE NATIONAL LABORATORY	ELECTRICAL UNDERGROUND DISTRIBUTION & SITE LIGHTING	
FRACTIONAL TOL. ± 1/64 DECIMAL TOL. ± .005 ANGLE ± 1/2°	This drawing is the property of the Argonne National Laboratory		
ALL DIMENSIONS IN INCHES EXCEPT ANGLES IN DEGREES UNLESS OTHERWISE NOTED	DRAWN C.T. 12-13-56	1"=100'	FIG. 10.2.A
	NOTICE 12978		

10.5

The perimeter lighting is part of the area lighting system for the site which includes the interior roadway lighting. These parts of the area lighting system are similar series circuits operated in two groups, each from its own constant-current transformer. One circuit provides power to every second light along the site boundary fence and roadway, while the other circuit includes all other area lights. Since there are no overhead service installations within the site, the feeders from the transformers to each of the lighting circuits pass through underground ducts. Each of the series lighting circuits passes underground from light to light, except around the perimeter where overhead service is carried by the poles that support the lights.

The underground system of fiber ducts is arranged in two groups in the concrete encasement. A large group is provided for power and control cables, with a small group provided for communication and instrument signals. As required for installation of the cables, manholes located between sections of the ducts are provided with a large section for power and a small section for communications. Each section of the combination manhole is accessible from above through a top cover plate.

The transmission of normal electric power is by a dual feeder system, wherein a feeder is extended from each of the two 2400-volt substation bus sections to each of a number of site load centers. In addition to breaker protection at each end of the feeders, there is a breaker between the feeders at each load center to prevent circulatory power transmission. Thus each load center has in effect a two-section bus. Wherever economy of design and division of processes or facilities has permitted, dual power feed is carried onto the load so that faulting of one part of the distribution system affects only part of a given load.

The emergency power generated by the stand-by unit in the steam plant is transmitted by single feeders operating at 2400 or 440 volts. These feeders pass through the underground ducts to the automatic switches of the different emergency load centers. The automatic switches operate in interlocked sequence to transfer their associated loads from normal power circuits to the emergency feeders only when there is an interruption of normal power and when emergency power is available. The transfer switching arrangement precludes any necessity for synchronizing since the load is removed from one power circuit before connecting to the other. With the return of normal power, these switches must be returned to the normal position by manual control before the emergency stand-by unit can be shut down.

10.2.4 Load Power Factor. Electrical power consumption in the project is principally by electric motors. Since the resultant overall load is predominantly inductive, power factor correction has been studied with regard to the effects on voltage regulation and penalty costs for excessive amounts of reactive power. In the absence of power contract data and other information pertinent to design for a good operating power factor or low reactive power demand, the use of synchronous motors was abandoned in favor of other means of correction.

Arrangements have been made for power factor correction at some time in the future if required. This is simply the provision of available space for the addition of capacitor banks to the operating circuits of the large motors and to the main substation bus. The "bus correcting" capacitor bank at the substation will in effect correct for the reactive power demand of the numerous small motors in use throughout the site.

10.2.5 Electrical Grounding. Adequate protection to personnel and equipment has been provided by extensive grounding systems, including approved methods of grounding throughout the site to prevent electrical hazards. Additional provisions have been made for establishing a constant radio-frequency ground reference for electronic instrumentation within the Reactor Building and Reactor Building wing.

The electrical-hazard grounding arrangements are provided for all electrical services, static discharge, and high potential surges due to lightning. A general grounding system provides appropriate grounding of electrical equipment and metallic structural members of buildings, fences, etc., to underground cables extending to the casings of the water wells as zero ground reference. Additional grounding means for surge absorption of static or lightning are provided in the form of underground grids. These grids, composed of buried mats or driven arrays of grounding rods cabled directly to the zero ground reference, are located in the immediate vicinities of the electrical substation and elevated structures such as the stack, water towers, and certain buildings equipped with lightning rods.

The radio-frequency grounding arrangements for precise electronic instrumentation to be used within the Reactor Building and Reactor Building wing are designed to maintain instrument background interference at a very low level by restricting the generation, transmission, and radiation of extraneous

voltages within or near these buildings. The generation of these unwanted voltages, which is inherent to some degree in many types of electrical equipment, may be amplified by varying potential gradients in partially grounded structural members. These electrical resistance variations between closely adjacent metallic members in the structure of the buildings and within the buildings have been eliminated by isolating or bonding these members. Radiation of disturbances into the buildings is reduced by a Faraday cage effect obtained by grounding the electroweld reinforcing grids of the precast concrete walls and roof panels to the structural steel.

Even though the electrical equipment associated with dust collections, commutation, and the opening or closing of simple circuits includes design to prevent the transmission or radiation of extraneous voltages, it is anticipated that additional filtering and shielding will be designed when complete installation test data are available.

10.3 WATER

10.3.1 Introduction. The various kinds of water used at the MTR site are classified according to their treatment and use. Demineralized water is used in the MTR process-water system and for experimental purposes. A blended, partially softened well water is in general use throughout the MTR site. The softened water minimizes scaling in hot-water systems and facilitates washing. The water used in the cooling-tower water system is well water which is acid neutralized in order to minimize scaling and corrosion. All these treatments are made in the water-treatment building. Raw water is used in the canal. A flow sheet of the entire water-distribution system is shown in Fig. 10.3.A.

10.3.2 Water Requirements. The water-flow requirements of the several different kinds of water used on the MTR site are summarized below. Breakdowns of the uses of each kind of water are given where they are appropriate. The designs of the water-treatment facilities are based on the total flow requirements given in this summary.

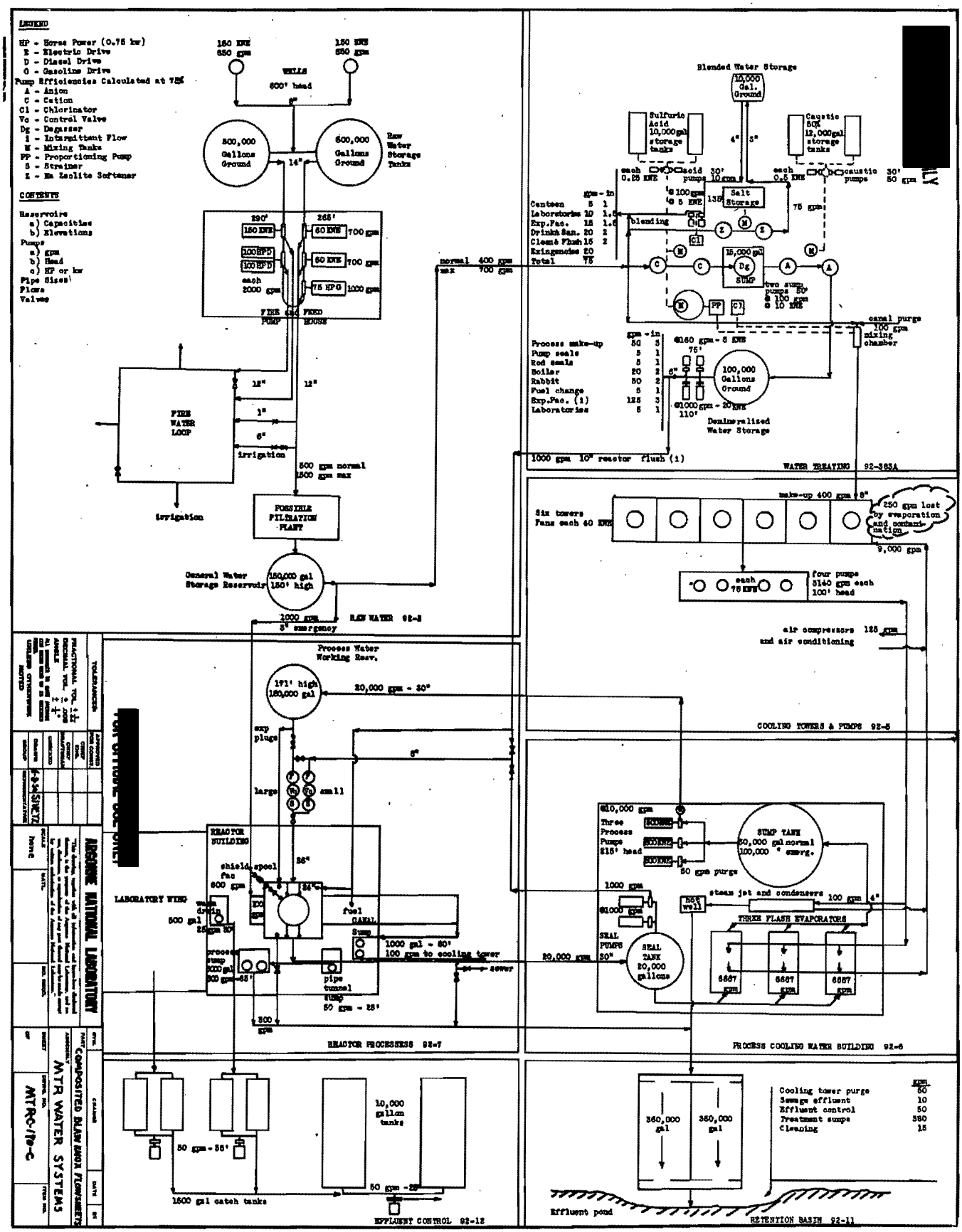

FIGURE 10.3.A

M.T.R. WATER SYSTEMS

TABLE 10.3.A

Total Water Requirements

Demineralized water	
Process water make-up	50 gpm
Boiler	20
Rod and pump seals	10
Rabbits	30
Laboratory	5
Experimental purposes and contingencies	35
Total	150 gpm
Softened water	
Canteen	5 gpm
Laboratories	10
Experimental facilities	15
Drinking and sanitary	20
Cleaning and flushing	15
Contingencies	10
Total	75 gpm
Cooling-tower water	
Evaporation	250 gpm
Purge	50
Contingencies	100
Total	400
Raw water	
Canal purge	100 gpm

10.3.3 Water Analysis. The raw water analysis is given in Table 10.3.B. The analysis was made by the U. S. Department of the Interior. The sample was obtained from the MTR test well.

TABLE 10.3.B

Raw-water Analysis

Analysis by the United States Department of the Interior, Geological Survey, Water Resources Branch

Analytical Statement

SW NE ¼ Sec. 14 T3N R29E

(Parts per million)

LOCATION: Butte Co., Arco, Idaho

SOURCE: Well (test)

AEC MTR WELL

DEPTH: 588 ft

DIAM: 8 in. ID

WATER LEVEL: 453.9 ft below TC

YIELD: 80 G.M. pump

OWNER: AEC, Idaho Falls

CHEMIST: W. M. Webster

LAB. NO.: 3896

COLLECTOR: RWK

DATE OF COLLECTION: November 30, 1949

USE: Observation

TEMPERATURE: 55 degrees

COLOR: Clear pH: 7.2

SUSPENDED MATTER:

HARDNESS AS $CaCO_3$

N.C.: 31 TOTAL: 208

IGNITION LOSS: 27

DISSOLVED SOLIDS: 240

SPECIFIC CONDUCTANCE AT 25°C (MICROMHOS): 398

T/A FT: 0.32

*TOTAL FE: 0.15

MN: 0.0

SiO_2	19
*FE(SOL)	0.06
CA:	52
MG:	19
NA:	2.7
K:	2.2
CO_3:	0
HCO_3:	216
SO_4:	20
CL:	12
F:	0.2
NO_3	4.1
B:	0.1
SUM:	238

Lab. No. 3896

rCa	2.595	
rMg	1.562	
rNa	0.117	4.371
rK	0.056	-4.330
	4.330	0.041
rCO_3		8.701
$rHCO_3$	3.540	
rSO_4	0.416	
rCl	0.338	+0.5% error
rF	0.011	
rNO_3	0.066	3% Na
	4.371	

HYPOTHETICAL COMPOUNDS

Raw Water		Hardness $CaCO_3$	(TDS)	Alkalinity $CaCO_3$
$Ca(HCO_3)_2$	2.6 epm	130 ppm	130	130
$Mg(HCO_3)_2$	1.0	50	42	50
$MgSO_4$	0.4	20	24	
$MgCl_2$	0.2	10	9	
NaCl	0.1		6	
KNO_3	0.1		10	
	4.4	210	221	
		SiO_2	19	
			240	

DATE COMPLETED: 12-13-49

CHECKED BY: E. L. Singleton

PROJECT: AEC MTR well

TRANSMITTED: 12-14-49

REMARKS:

Demineralized Water. The desired demineralized-water analysis is given in Table 10.3.C. The design of the demineralization system is based on obtaining water that satisfies this analysis.

TABLE 10.3.C

Demineralized-water Analysis

CONSTITUENT	MAXIMUM
TDS	3 ppm
Fe	0.05
Al	0.05
Ca	0.5
Mg	0.5
Na	2
CO_2	2
SiO_2	1.
Cl	0.25
SO_4	0.50
Cu, Pb, Ni, Co, B	None
Process water pH	5.5 to 6.5
Specific resistance at 18°C	300,000 to 500,000 ohms

Soft Water. The soft water has the same analysis as the raw water except that all the Ca and Mg are replaced by sodium. This completely softened water is blended with raw water to give the blended partially softened water of 50 ppm hardness that is used throughout the MTR site.

10.3.4 Demineralization System. *Cation Exchangers, Acid Tanks, and Pumps.* Sufficient cation capacity must be available to continually process 150 gpm of well water. Two cation exchanger units are provided for this purpose; each is 5½ ft in diameter and 9 ft high. Each has about 2 ft of height available for Anthrafilt base, about 3 ft of head room for resin expansion during backwash, and 4.5 ft of resin. The units are regenerated about every 12 hr. A 60-day supply of 98% sulfuric acid for cation resin regeneration is stored out of doors in two 10,000-gal steel storage tanks. The acid is pumped from these storage tanks to a dilution or mixing tank in the water-treatment building where it is prepared for cation regenerative use.

Degasser and Sump. In order to remove the CO_2 from the decationized water the water is sprayed down over wooden slats in a wooden tank and falls into a lined sump below. The water is pumped from the sump through the deanionizers.

Anion Exchangers, Caustic Tanks, and Pumps. Sufficient anion capacity must be available to process the 150 gpm of decationized and degassed well water. Two deanionizers of about the same physical size as the decationizers are provided. However, only about half the depth of resin is required. A 60-day supply of 50% NaOH liquid caustic for anion resin regeneration is stored out of doors in two 12,000-gal steel storage tanks; its temperature is thermostatically controlled and it is heated by steam. The caustic is pumped from these tanks to a dilution or mixing tank where it is prepared for anion regenerative use. The units are regenerated at about 24-hr intervals.

Demineralized-water-Storage Tank and Pumps. After demineralization the water is stored at ground level in a 100,000-gal storage tank. All linings in the demineralized-water system are of stainless steel or inert organic base so as to contribute no minerals to the water. This consequently helps to reduce scale formation on the reactor fuel assemblies in the process-water system. Either of two 75-psig 160-gpm centrifugal pumps continually supplies demineralized water for general use while the other pump serves as a spare. A 75-psig 1000-gpm centrifugal pump supplies reactor flush water during shutdown while a second identical pump serves as a spare.

10.3.5 Softeners. Sufficient zeolite resin capacity must be available to continually process 75 gpm of softened, blended water. Two zeolite beds about 2.5 ft in diameter and with a 3-ft resin depth are provided for this purpose. These units are regenerated automatically every 12 hr. A 60-day supply of salt (16 tons) is maintained in a brine pit leached with water. Pumps deliver the saturated brine to the dilution-regeneration tank.

The softened water is blended with raw water to yield a blended water of about 50 ppm hardness. It is stored in a 10,000-gal lined steel ground tank so that about a 3-hr supply is available. It is chlorinated before being sent to its points of use. Two pumps are available to keep the blended water line under continual pressure; one of these pumps serves as a spare.

10.3.6 Acid-neutralization System for Cooling-tower Make-up Water. Well water is partly neutralized and mixed with dilute sulfuric acid before being sent to the cooling towers, where scaling is controlled in accordance with *p*H records and Langelier saturation indexes. Chlorine is added occasionally to eliminate growth of algae. The chlorine is stored in cylinders in a separate room inside the building. The 98% acid is measured manually into a 50-gal tank and is propeller-mixed and diluted in a 2500-gal tank. The diluted acid is fed into the make-up water line by means of a flow-controlled proportioning pump; this pump delivers the dilute acid and well water in the proper proportions.

10.3.7 Design and Operating Data Summary. The pertinent design and operating data for the softening, decationizing, and deanionizing units are summarized in Table 10.3.D.

TABLE 10.3.D

Water System Design and Operating Data

	SOFTENING	DECATIONIZING	DEANIONIZING
Resin capacity (grains/cu ft)	20,000	10,000	7,000
Resin bed height (ft)	3	5	2.5
Resin bed area (sq ft per bed)	5	20	20
Resin bed diameter (ft)	2.5	5	5
Number of resin beds	2	2	2
Design resin bed volume (cu ft per bed)	15	100	50
Calculated resin bed volume (cu ft per bed)	13.3	92.8	49.4
Resin bed design safety factor (%)	12.8	7.8	1.4
Flow rate (gpm/sq ft)	6	5	5
Throughput/unit for two units (gpm)	30	100	100
Hardness, cations + anions (ppm)	210	219	41
Time between regenerations (hr)	12	12	24
Amount of water treated (gpd)	86,400	288,000	288,000
Regenerant used	NaCl	93% H_2SO_4	50% NaOH
Regenerant capacity (lb/cu ft)	10	2.5	7
Amount of regenerant storage	16 tons	6,000 gal*	4,160 gal*

*This figure includes 2500 gal of H_2SO_4 needed for neutralizing the make-up water to the cooling tower.

10.3.8 Instrumentation, Laboratory, and Housing. All demineralization, softening, and water-neutralization processes are carried out in the water-treatment building, and all related storage tanks are just outside. A water-analysis laboratory, as well as a water supervisor's office, washroom, lockers, and lavatory are provided.

Instruments are furnished to record the production flow of (1) make-up water to the cooling towers, and (2) blended and demineralized water to the storage tanks.

Level indicators and alarms are provided on the blended-water and demineralized-water tanks. The acid tank has a level indicator, but the caustic tank does not. Normal flow through the cation and anion exchangers, backwash flow, and rinse flow are indicated, and the total flow is recorded. As quality checks on FMA (Free Mineral Acidity) break-through, the *p*H values of the water leaving the cation units are recorded. A final check is provided by recording the *p*H of the water passing to the demineralized-water storage tank. Resistivity of the treated water is also recorded. Sodium and silica break-through require manual periodic tests.

10.4 EFFLUENT CONTROL

10.4.1 Introduction. The purpose of the effluent control system is to collect, hold, and dispose of both process and nonprocess radioactive fluid wastes. The radioactive fluid wastes expected from the MTR site are generally classified and disposed of as follows:

1. The 50-gpm purge from the process-water system is sent direct to the retention basin for a holdup period of about 90 hr. This holdup time reduces the activity, which is due primarily to Na^{24}, from 1200 dis/ml/sec to about 20 dis/ml/sec. The discharge from the retention basin flows to the effluent pond, where it percolates into the earth.
2. Mildly active experimental and laboratory fluid wastes are drained to underground holdup tanks. When the tanks are full, the activity and decay trends of the contents are evaluated. According to the activity, the contents are then sent to the effluent pond, retention basin, or the underground permanent storage tanks.
3. "Hot" fluid wastes are collected locally in shielded containers. The contents are either sent to the underground permanent-storage tanks or to the Chemical Processing Plant for disposal.

10.4.2 Retention Basin. *General Description.* The retention basin is a tank for holding flowing radioactive water for a period of time that is long enough to allow the radioactivities of the short-lived water components to decay to tolerable values. The entering water must not mix with the leaving water, and, ideally, there should be no mixing at any intermediate points. The time necessary for decay of Na^{24} radioactivity and the given effluent flow are the main factors determining the size of the basin. Effluent waters from the Process Water Building and the Reactor Building process sump mix in the line going to the retention basin. The 1200 dis/ml/sec activity based on 50 gpm of solution containing 5 ppm of Na^{23} plus a recoil equivalent of 1 ppm requires a 266,000-gal basin to provide the 88-hr holdup necessary for decay to a tolerance value of 18.5 dis/ml/sec. In order to have storage space available for intermittent flushes, future expansion, and also for the 320,000 gal of process water in case it becomes overly contaminated, there are two 360,000-gal basins provided. Thus, one of these is large enough to store the entire contents of the process-water system. During normal operation, one basin is in service while the other is available for the emergency discharge of radioactive process water. If the reactor power level is doubled, the load on the retention basin will not appreciably increase and the two 360,000-gal basins will easily accommodate the effluent flow.

Shielding. The roof over the basin is concrete with several feet of earth covering. This reduces radiation directly over it to less than a tolerance value of 50 mr/hr.

Effluent Flows. The water flows that the retention basin is required to accommodate are summarized in Table 10.4.A. The normal operating flows are those listed under "Continuous Flows," while the "Intermittent Flows," constitute the flows encountered during periodic reactor operations and during emergencies.

Size and Structure. The retention basin has a capacity of 720,000 gal and is made up of two 360,000-gal sections, each about 125 by 20 by 20 ft deep, placed side by side. An inlet trough with adjustable sluice gates distributes the water entering the basin. Outlet weirs measure the discharge into the exit trough. Each of the two sections of the basin can be drained separately and thoroughly, and may be entered for inspection and cleaning. The underground feature of the basin obviates any algae growths.

TABLE 10.4.A

Water Flows to Retention Basin

	CONTINUOUS FLOWS (gpm)	INTERMITTENT FLOWS	
		RATE (gpm)	DURATION (hr)
Effluent control			
Catch tanks*		50	0.5
Reactor Building process sump			
Experimental plugs		90	
Control rod seal	2		
Monitoring tubes	5		
Normal sump overflow in water-cooling building			
Process purge	50		
Steam jet condensate	2		
Reactor Building canal sump			
Canal flow*		100	
Canal flush		400	6
Emergency overflow from sump tank in water-cooling building			
Fuel assembly change		200	10
Emergency overflow	2	20,000	0.25

*Normally little or no activity expected here.

Ventilation. The operating level of water in the retention basin is fixed at roof level by the overflow weir. Thus there is essentially no air over the water. This design eliminates the accumulation of radioactive argon, and/or an explosive mixture of hydrogen and oxygen. The basin effluent inlet must be ventilated to remove any A^{41} activity. This is done by means of wind-induced turret vanes on 20-ft-high stacks.

Instrumentation. The activity of incoming and outgoing effluents is monitored continuously. The activity is measured by a gamma-radiation recorder a few feet above water level at the entrance and exit of the basin. The exit water flow is measured at the discharge weir and recorded.

Emergency. In the event of a fission break or high radioactive contamination in the cycling 320,000-gal process-water system, the entire contents of the system can be emptied into the retention basin for decay and holdup until disposal action can be taken. The 130,000-gal contents of the canal can be handled similarly if so desired.

10.4.3 Effluent Pond. Since there are no rivers available for water disposal near the MTR site, it is necessary to dispose of the water from the retention basin by allowing it to percolate through the ground, sand, and gravel until it reaches the water table below. A percolation rate of 0.3 cu ft per square foot per day was determined by laboratory tests of ground cores obtained at the MTR site. This figure is exceedingly low and a field test was later made in which the percolation rate was found to be 100 cu ft per square foot per day. Since the higher figure was so different from the smaller one, it was decided from the experimental data that a rate of 1 cu ft per square foot per day would be realistic and conservative for design purposes. Based on this percolation rate and a continuous discharge flow of 179 gpm, an effluent pond 130 by 240 ft, giving an area of approximately 30,000 sq ft, is provided. The sides of the effluent pond basin are sloped at about a 45° angle. This basin is deepest at the water inlet and from there the bottom slopes upward in all directions. The highest point of the basin floor is 4 ft above the water inlets. The water inlets are at the low point of the basin in order to eliminate freezing at the inlets. The basin is enclosed by a fence to prevent animals or unauthorized persons from entering the area. Although little activity is expected to accumulate in the pond, the barriers are furnished as a safety precaution.

10.4.4 Nonprocess Active Effluents. In addition to process wastes, the effluent control system must handle nonprocess liquid wastes originating from experimental work or accidental spills in the Reactor Building and laboratory wing. Large quantities of very "hot" wastes are not anticipated, and therefore provisions are only made for the handling of moderate quantities of "warm" wastes.

Since the bulk of the wastes was increased and the methods of subsequent waste treatment were made more difficult by neutralization of acid wastes in the past, the wastes at the MTR site are not neutralized. Thus the storage tanks and handling systems are such that they can withstand acidities of *p*H 2.

The type of wastes expected and the planned disposal of them are discussed briefly in this paragraph. The "hot" wastes from the reactor area will be transferred to the Chemical Processing Plant for disposal. Radioactive material from experimental equipment will be collected in shielded pots and, according to whether it is "hot" or "warm," will be sent to the Chemical Processing Plant or to the permanent-storage tank farm. Alpha particle wastes and slightly active wastes and solvents will be collected in stainless steel drums and, depending on the activity, will be sent either to the Chemical Processing Plant, permanent-storage tank farm, or the underground holdup tanks. It is expected that the largest volumes of wastes will come from accidental spills and laboratory sinks, and that only about 5% of these will be radioactive. The description of the system as given in the following paragraphs refers particularly to this large volume of wastes from spills and laboratory sinks.

The wastes are accumulated in four 1000-gal underground holdup tanks located near the Reactor Building and laboratory wing. Two of these tanks receive effluent from the basement and main floor drains of the Reactor Building via a Reactor Building sump tank and pump; the other two tanks receive radioactive effluent from the sinks in the laboratories. While the contents of one tank of each pair are being monitored, the companion tank is filling. The nonradioactive effluents caught in these tanks are sent direct to the effluent pond. The highly radioactive wastes are pumped to the permanent-storage tank farm. The tank farm, based on a one-year capacity, initially consists of two 10,000-gal underground storage tanks.

Each holdup tank is constructed on a concrete pad that drains to a dry well so that monitoring for leaks is possible. Each pair of tanks is supplied with one self-priming 50-gpm pump located above it so that leakage from the pump drains back to the tanks. The pump and tank piping is such that (1) the tank can be stirred by recirculation, (2) a sample can be taken, or (3) the contents can be delivered to the retention basin, the effluent pond, or the 10,000-gal permanent-storage tanks. The tanks in each pair have overflow lines to each other. Each tank is provided with a level gauge and a high-level alarm.

The water table at the MTR site is about 600 ft below the surface. It is estimated that it takes 150 years for water to percolate through the lava beds under the Snake River Plains back to the Snake River. If this is true, the activity of wastes that leak from the effluent system and reach the Snake River will be greatly reduced.

10.5 COOLING TOWERS

10.5.1 General Description. A water-cooling tower indirectly dissipates most of the reactor heat load to the atmosphere. The 30,000 kw, or 1,700,000 Btu/min, developed in the reactor active section passes directly to the process water and raises its temperature from 100 to 110°F. The process water yields this acquired heat to the cooling-tower water circulating through the condenser tubes of the flash evaporators. The 200 gpm of flashed process-water vapors is condensed and returned to the process-water stream. The cooling-tower water passes through the cooling towers, collects in the cooling-tower basin, and is again pumped through the flash-evaporator condensers to complete its cycle. Water is provided to the basin to make up for the quantity lost by evaporation and drift and to dilute the concentrating water solids so as to prevent scaling. Provision is made to add chlorine solution intermittently to the circulating cooling-tower water to inhibit algae growth. Dilute acid solution is mixed with the make-up water so as to stabilize the water by neutralizing part of the well-water alkalinity. Up to 100 gpm of the cooling-tower make-up water comes from the canal purge. Strict control of the Langelier saturation index is kept on the circulating cooling-tower water to minimize corrosion, scaling, and delignification of the wood. Particular design consideration was given to operation of the cooling towers during icing weather and under heavy dusting conditions.

10.5.2 Heat Load. If the air leaving the tower is saturated with water vapor at 95°F and the air entering is saturated with water vapor at 72°F, then 66,500 lb of dry air per minute is needed to handle the heat load as follows:

TEMPERATURE (°F)	*H* (Btu per lb dry air)	DRY AIR (lb/min)	WATER (lb/min)	OPERATING CONDITIONS	
				(cfm)	(cu ft/lb)
95	60.7	66,500	2,420	1,000,000	14.8
72	35.1	66,500	1,120	920,000	13.8
23	25.6		1,300		

Following is a summary of the heat data:

Latent, 1,300 lb of water	1,300,000 Btu/min
Sensible, 1,300 lb of water	15,000
Sensible, 66,500 lb dry air	382,000
Total	1,697,000 Btu/min

10.5.3 Operation and Description of Cooling Towers and Basins. The cooling-tower operations are based on a 7°F wet-bulb approach to the highest summer wet-bulb temperature (65°F). A medium-height tower of 28 ft requires, according to accepted practice, about 600 sq ft of ground area per 1000 gpm of throughput. Thus, five 30- by 40-ft (ground area) towers provide the 6000 sq ft needed. Dust conditions require especially deep basins for collecting mud and silt, while severe winter conditions require ice defrosting by means of reversible fan gear drives. For a pressure drop of ½ in. of water across the fans and a fan efficiency of 60%, the entire fan air load is 115 hp. The fans have waterproof and dustproof motor drives for outdoor operations. Each cell has an independently drainable basin section which is 4 ft deep and holds about 175,000 gal. Make-up is estimated as 0.1% of the circulated flow times the cooling range, or 210 gpm. The drift losses should be about 0.1 to 0.2% of the circulating flow and thus are estimated as 10 to 20 gpm. The make-up requirements are then about 250 gpm during the summer, plus a 50-gpm basin purge. Normal purge is accomplished by means of an adjustable overflow weir. With a 300-gpm make-up, and assuming 250 gpm is vaporized, a sixfold increase in concentration of dissolved solids in the cooling-tower water will occur.

A brief summary of an analysis of the raw water from the wells is given in the following table:

MTR Raw Well Water

CATIONS	AMOUNT (epm)	ANIONS	AMOUNT (epm)	HARDNESS AS $CaCO_3$ (ppm)	ALKALINITY AS $CaCO_3$ (ppm)	TDS (ppm)
Ca	2.6	HCO_3	3.6	205	172	239 (19 ppm SiO_2)
Mg	1.6	SO_4	0.4			
Na	0.1	Cl	0.3			
K	0.1	NO_3	0.1			
	4.4		4.4			

Partly neutralizing with sulfuric acid or 3.0 epm of SO_4 gives the following analysis for the cooling-tower make-up water:

Acid-neutralized Well Water for Cooling Tower

CATIONS	AMOUNT (epm)	ANIONS	AMOUNT (epm)	HARDNESS AS $CaCO_3$ (ppm)	ALKALINITY AS $CaCO_3$ (ppm)	TDS (ppm)
Ca	2.6	HCO_3	0.6	205	0	219 (19 ppm SiO_2)
Mg	1.6	SO_4	3.4			
Na	0.1	Cl	0.3			
K	0.1	NO_3	0.1			
	4.4		4.4			

The 2.6 epm of $CaSO_4$ gives a concentration of about 170 ppm. A sixfold increase would increase this to about 1000 ppm of $CaSO_4$, which is still far below its solubility of about 1700 ppm at 0 °C. $MgSO_4$ is very water soluble and thus it offers no problem with regard to crystallizing out of solution. A sixfold increase in concentration would also give about 1400 ppm of TDS.

10.5.4 Pumping Station. The pump house is some distance from the cooling towers so as to facilitate air circulation and minimize the amount of water spraying the pumping station. Acidulation and chlorination control of the cooling-tower make-up water are performed in a mixing chamber in the water-treatment building. Four vertical flooded turbine type pumps, each of 3300 gpm at about a 100-ft head, are used. Three pumps are in continual operation, while one is held as a spare or alternate. It is recommended that the pump-house and cooling-tower-area equipment be inspected hourly, but that no one be stationed there permanently. The inlet ventilating air is filtered and the building is pressurized so as to prevent the infiltration of dust and thereby protect electrical and other equipment.

10.5.5 Instrumentation. At the pump house each of the four cooling-water pump motors is provided with an ammeter. A voltmeter is provided across the power supply feeder to these motors. A two-point *p*H recorder in the water-treatment building helps the operator guide the acid-neutralization dosage by recording the *p*H of the entering acidulated make-up water and the circulatory

water streams. Each pump has a pressure gauge. The adjustable weir overflow is calibrated so that the purge flow is indicated visually. At the water-treatment building, the cooling-tower circulatory flow and inlet and outlet water temperatures are recorded. A low water level in the basin is indicated by an alarm in the water-treatment building; a dry-wet bulb two-point outdoor recorder is also located here. When the water level in the basin is adequate, the make-up from the general water reservoir is shut off but the make-up from the canal continues.

10.5.6 Emergency Operation. In the event of power failure, the cooling-tower system is shut down completely, and the flow of make-up water is automatically stopped. Make-up water is also shut off automatically if the general water reservoir content is low.

10.5.7 Design Data. Following is a summary of the design data:

Heat load	1,700,000 Btu/min or 30,000 kw
Maximum wet-bulb temperature	65°F
Approach temperature	7°F
Altitude	5,000 ft above sea level, 25 in. Hg, 28 ft water
Water flow	9,000 gpm, 100 ft water, 120 hp each pump
High temperature	95°F
Basin temperature	72°F
Air flow	66,500 lb/min, ½ in. water, 110 hp total
Dust	Moderate-to-strong "dust devils"
Winds	Moderate-to-strong, SW and NE prevailing 2:1

ARCO TEMPERATURES (°F)[6]

1948	Jan	Feb	Mar	Apr	May	June	July	Aug	Sept	Oct	Nov	Dec	Annual
Average max.	28	34	43	57	66	73	84	83	73	60	45	31	56
Average	14	20	31	43	51	56	66	64	55	44	32	19	41
Average min.	10	16	24	31	39	45	52	49	40	31	23	13	31

POCATELLO RELATIVE HUMIDITY (%)[6]

1948	Jan	Feb	Mar	Apr	May	June	July	Aug	Sept	Oct	Nov	Dec	Annual
8 A.M.	80	79	73	69	67	60	55	54	59	68	73	79	68
Noon	71	67	56	45	38	31	27	29	32	47	60	70	48
8 P.M.	73	67	54	42	37	30	24	25	30	45	60	72	47

ABSOLUTE HUMIDITY (grains water/lb dry air)

8.5	10	13	20	20	20	26	27	20	22	23	20

10.6 PROCESS RADIATION INSTRUMENTATION AND AREA MONITORING

10.6.1 Process Radiation Instrumentation. In detecting the radioactivity of the air and water systems some commercially available instruments are applicable. For those installations in which such instruments prove inadequate, modifications of currently used instruments or entirely new designs are required.

The methods used in detecting radiation give only relative values. Radiochemical analyses are to be used when accurate quantitative determinations are necessary.

Cooling-air and Contaminated-air Systems. In the reactor cooling-air system the instrumentation is set up primarily to measure the argon activity and the particulate activity of the air before it is discharged into the atmosphere. The monitoring system extracts air from the main air duct, passes it first through a particulate monitoring device, then through a gas-monitoring chamber, and finally discharges it back into the main air stream.

To detect the particulate activity, a modification of the continuous room-monitoring system used at Brookhaven National Laboratory is used. The instrument consists of a strip of filter paper moving across a series of openings through which air is pumped. The paper, after collecting the dust, passes in front of a mica end-window Geiger counter, where the counts are transmitted

through a scaler into a recording system. The major alterations of the Brookhaven design are (1) elimination of the alpha scintillation counter, (2) addition of an air inlet tube that leads directly to the filter paper strip from the main air duct, and (3) the encasement of the unit in an air-tight container.

The air, after passing the dust-monitoring device, is passed through a C.W.S. filter and then into the annular type ionization chamber. The purpose of the second filter is to further ensure dust-free air. The annular type chamber consists of two concentric cylinders and utilizes maximum geometry by allowing the radioactive air or gas to pass through the innermost cylinder while the outer chamber is filled with argon gas at a pressure of 20 atm.

Normally, radioactive gases and particles will be vented through the off-gas system and discharged to the stack. To detect and measure this activity, a similar arrangement as described above for the reactor air system is used.

Process-water System. In the water system the annular type ionization chamber is used. By-pass valves and conduits allow the radioactive water or gas to pass through the chamber. Activities are measured by this method at the seal tank, liquid vent seal, and in the demineralized-water system.

The measurement of the water activity at the seal tank tends to serve a dual purpose. First, it records the total water activity for the process-water system at approximately 60 sec flow time from the active lattice; secondly, the reading is used as a check on the background activity for the scanning unit which is to detect a fuel plate rupture.

The liquid vent seal evicts gases such as argon, oxygen, neon, and fluorine, which are present or formed in the process water. These gases are radioactive and a measurement of the radiation is required before venting to the atmosphere to serve as a check on the release of activity.

Ionization chambers are placed on the demineralized-water system to detect a possible back-up of radioactive water from the reactor. The back-up of radioactive water may occur through the leakage of valves or the failure of check valves.

Calibration tests performed on the annular type ionization chamber, using radioactive Na^{24} in an aqueous solution, yielded a sensitivity of 1.55×10^2 curies/cc-amp and 1.12×10^2 curies/cc-amp for gas pressures of 29.9 atm and

20.75 atm, respectively. Similar tests for the (activated) Co^{60} aqueous solution yielded a sensitivity of 2.22×10^2 curies/cc-amp at a gas pressure of 20.1 atm. Since Na^{24} will be the main radioactive constituent of the exit process water, the sensitivity of the actual installation should be essentially that indicated above.

Canal. The water in the canal may become contaminated with minute radioactive particles from the fuel and beryllium assemblies that are handled and stored in the canal, and possibly from fission products in the event of a fuel assembly rupture. When this water is not contaminated it is pumped to the cooling-tower make-up water. If the water becomes contaminated it is directed to either the sewer or the retention basin, depending on the amount of activity. These measurements are also made with the annular type ionization chamber.

Retention Basin. The radiation emitted by the radioactive water in the retention basin is measured by placing G.E. air-wall type chambers above the inlet and outlet troughs.

10.6.2 Area Monitoring. Area monitoring will be required wherever the radiation might exceed levels considered to be safe for personnel. In general, monitoring will be required in the following areas: (1) Reactor Building wing, (2) Reactor Building, (3) Process Water Building and (4) Fan House. A variety of types of instruments for area monitoring can be classified according to their respective functions as follows:

CLASSIFICATION	FUNCTION	RADIATION	INSTRUMENT
a	Health physics, personnel monitoring	Gamma Beta Alpha	Hand and foot counters
b	Survey (portable)	Gamma Gamma	Zeus Zeus with probe, Cutie Pie
c	Area monitoring (stationary)	Gamma Alpha Beta or gamma	Beckman MX3A or equivalent Air monitoring - air particle
d	Monitoring of experiments	Fast neutron Slow neutron Alpha and beta	Cheng and Eng Neut Zeuto

In Table 10.6.A are listed the numbers of each type of instrument to be used in each of the four general areas requiring monitoring. It will be noted that the greatest number of instruments is required for the Reactor Building and wing.

TABLE 10.6.A

Area Radiation Monitoring Instruments

TYPE	USE	NUMBER REQUIRED				
		REACTOR BLDG.	WING BLDG.	PROCESS WATER	FAN HOUSE	TOTAL
Hand and foot	Health physics		2			2
Zeus	Survey	5	10	2	2	19
Zeus with probe	Survey	4	2			6
Cheng and Eng	Experimental	4				4
Air particle	Air monitoring	4			1	5
Slow neutron Monitron neut	Experimental	6				6
Gamma Detector for stationary installation	Area monitoring	7		2	2	11
Alpha	Experimental	4				4
						57

The only instruments to which definite locations in the various buildings can be assigned are the area-monitoring instruments, classification "c" above. The locations selected for these instruments have been arbitrarily chosen, and actual survey when the reactor is in operation may result in these locations being changed.

10.7 REFERENCE REPORTS

(1) Lennox, D. H., *Retention Basin*, ANL-EKF-11, November 8, 1949.

(2) Lennox, D. H., *Shielding for the Retention Basin*, ANL-EKF-26, December 22, 1949.

(3) Persiani, P. J., *Activity of H_2O as Discharged from Retention Basin*, ANL-EKF-33, February 2, 1950.

(4) Lennox, D. H., *Retention Basin*, ANL-EKF-41, February 27, 1950.

(5) Persiani, P. J., *Activity of the Process Water Effluent*, ANL-EKF-56, July 13, 1950.

(6) Smith, Hinchman, and Grylls, Inc., *Survey Report - Fort Peck, Montana; Pocatello, Idaho Sites*, March 26, 1949.

10.8 REFERENCE DRAWINGS

(Blaw-Knox Construction Company Drawings)

DWG. NO.	TITLE
3150-9-1	Layout of Boiler House
3150-9-2	Boiler House - Sections
3150-9-3	Mezzanine Plan and Sections
3150-902-1	Electrical, Underground Distribution System
3150-902-5	Electrical, 2300 Volt - One Line
3150-902-20	Electrical, Road and Fence Lighting
3150-92-2	Flow Diagram, Filtered Water System
3150-92-3	Flow Diagram, Water Treating System
3150-92-3A	Flow Diagram, Water System Demineralizer and Water System
3150-12-3	Retention Basin, Plan and Section
3150-13-3	Effluent, Control, Plan and Sections
3150-92-11	Water Retention System - Flow Diagram
3150-92-12	Effluent Control - Flow Diagram
3150-7-1	Cooling Tower and Pump House - Pump House Layout
3150-7-2	Cooling Tower and Pump House - Cooling Tower Layout
3150-92-5	Flow Diagram - Cooling Tower

Appendix 1

CRITICALITY STUDIES ON ENRICHED URANIUM—HEAVY WATER SYSTEMS[1]

A1.1 EXPERIMENTAL ARRANGEMENT

The design and construction of the apparatus for these experiments were carried out by members of the Technical Division (of Clinton Laboratories). The reactor was a vertical welded stainless steel cylindrical tank 140 cm in diameter and built to be filled to a depth of 144 cm with heavy water. The top of the tank was covered by a perforated stainless steel tube sheet which was bolted and gasketed on the rim of the tank proper (Fig. A1.A). "Fuel tubes" containing U^{235} could be lowered through the tube sheet into the heavy water, and thus a lattice could be built up by adding fuel tubes until the assembly became critical. The perforations in the tube sheet and the amount of U^{235} in the fuel tubes were arranged so that if contiguous holes were filled, the mean concentration of U^{235} in the region of the lattice so built up in the heavy water moderator was 10.35 g/liter. Specifically, the holes were in a square lattice of 8.4 cm spacing, and the fuel tubes, containing 45.45 g of U^{235} in the form of a heavy water solution of uranium oxyfluoride (UO_2F_2), were filled to a depth of 61.79 cm. Because neutrons have such a large mean free path for diffusion in heavy water, the lattice arrangement can be treated as a homogeneous distribution of U^{235} without large error provided the foreign material in the fuel tubes is considered as well. By omitting alternate holes, it would be possible to obtain a lattice spacing of 16.8 cm or a mean concentration of 2.58 g/liter using the same fuel tubes and tube sheet, and, by using the square lattice at 45° to the foregoing, the mean concentration of 5.17 g/liter could be easily achieved.

Five vertical control and safety rods penetrated the active lattice region through the tube sheet. Each was composed of a sleeve of cadmium in an otherwise empty aluminum thimble which ran down through the heavy water to the bottom of the active region of the lattice. The thimbles and rods could be moved individually as desired. The cadmium rods were supported by electromagnets hung from piano wires, which in turn passed over pulleys on the ceiling to counterweighted controls in a control room. Electrical safety circuits

Drawing # 4305

[redacted]

FIG. A1.A

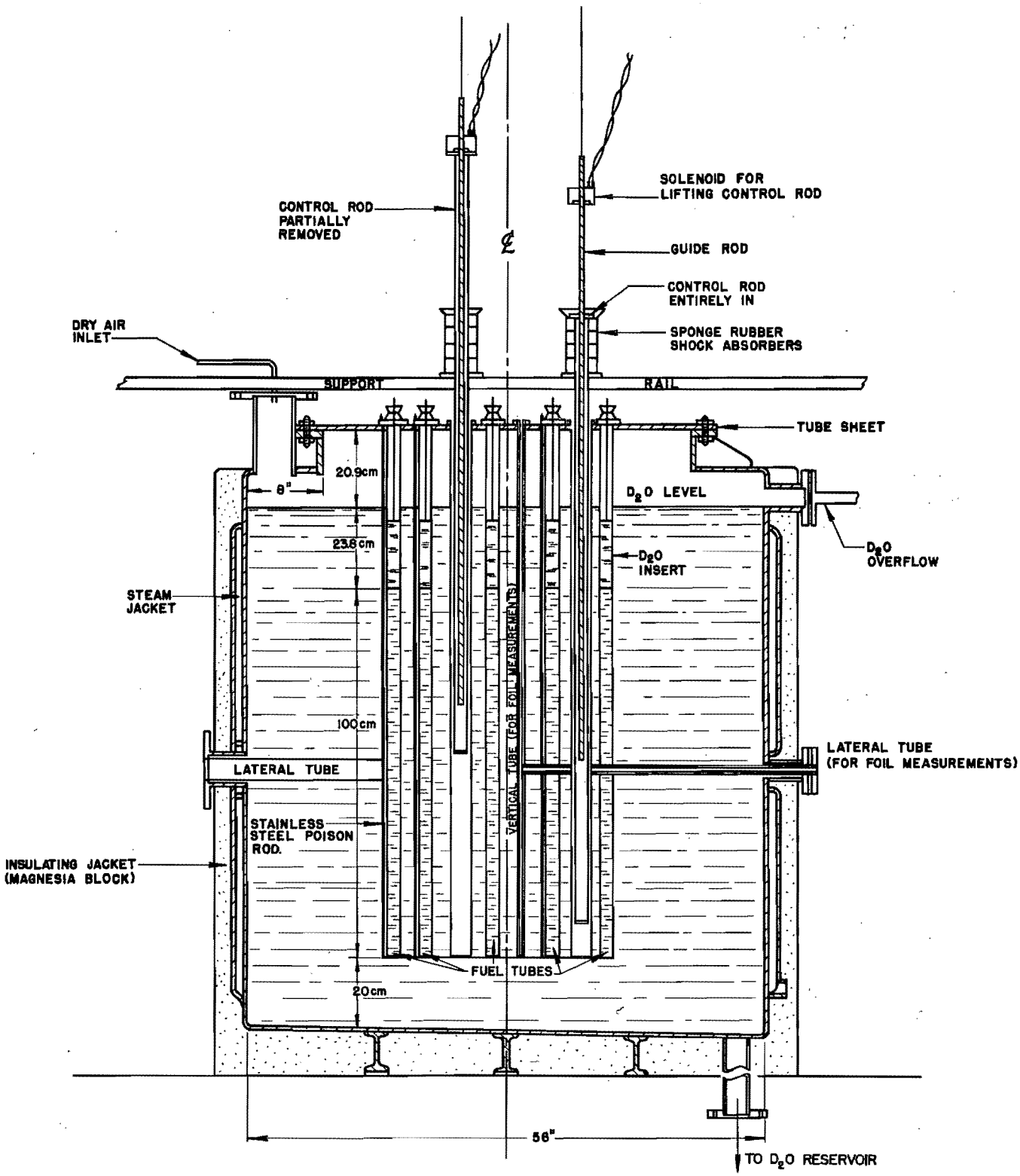

[redacted]

were so arranged that if either of two Monitrons* near the reactor were to trip, the electromagnets would become deactivated and the cadmium rods would drop into their thimbles upon shock absorbers.

A typical tube sheet lattice arrangement is given in Fig. A1.B. A blacked-in spot on the position of a tube sheet hole means that the hole contained a fuel tube with a full complement of U^{235}, viz., 45.45 g for solution depth of 61.8 cm or 73.57 g for a depth of 100 cm. Fractional fuel tubes were also made up in order to permit close bracketing of the critical mass in an assembly. One phase of the experimentation called for the calibration of the control rod position against known amounts of poison distributed in the lattice.

Besides the reactor tank, an elaborate stainless steel system was provided for handling the heavy water. The entire experimental arrangement occupied a two-level concrete cell enclosure so that the heavy water could be raised from a reservoir tank on the lower level into the reactor tank on the upper level by means of dried compressed air. The heavy water could be dropped quickly, if necessary, to stop a chain reaction. Side holes in the reactor tank made possible the insertion of foils to be activated by the neutron flux for flux distribution measurements on a horizontal line through the reactor, and vertical flux measurements were conveniently made in an empty fuel tube hole. Typical horizontal and vertical flux distributions are given in Figs. A1.C and D.

During changes in the lattice arrangement, boron trifluoride counters and Geiger counters with registering circuits and audible signals kept operators informed on reactor activity levels. The progress of the critical reactor was observed by means of an Esterline-Angus recorder driven by the Monitron.

A1.2 CRITICAL MASS EXPERIMENTS

The main purpose of these measurements was to ascertain the amounts of U^{235} required for criticality as a function of average concentration. The

* A Monitron is an ionization chamber and amplifier device which trips a relay when the ionizing radiation falling upon it exceeds a predetermined level.

Dr 5055

[redacted]

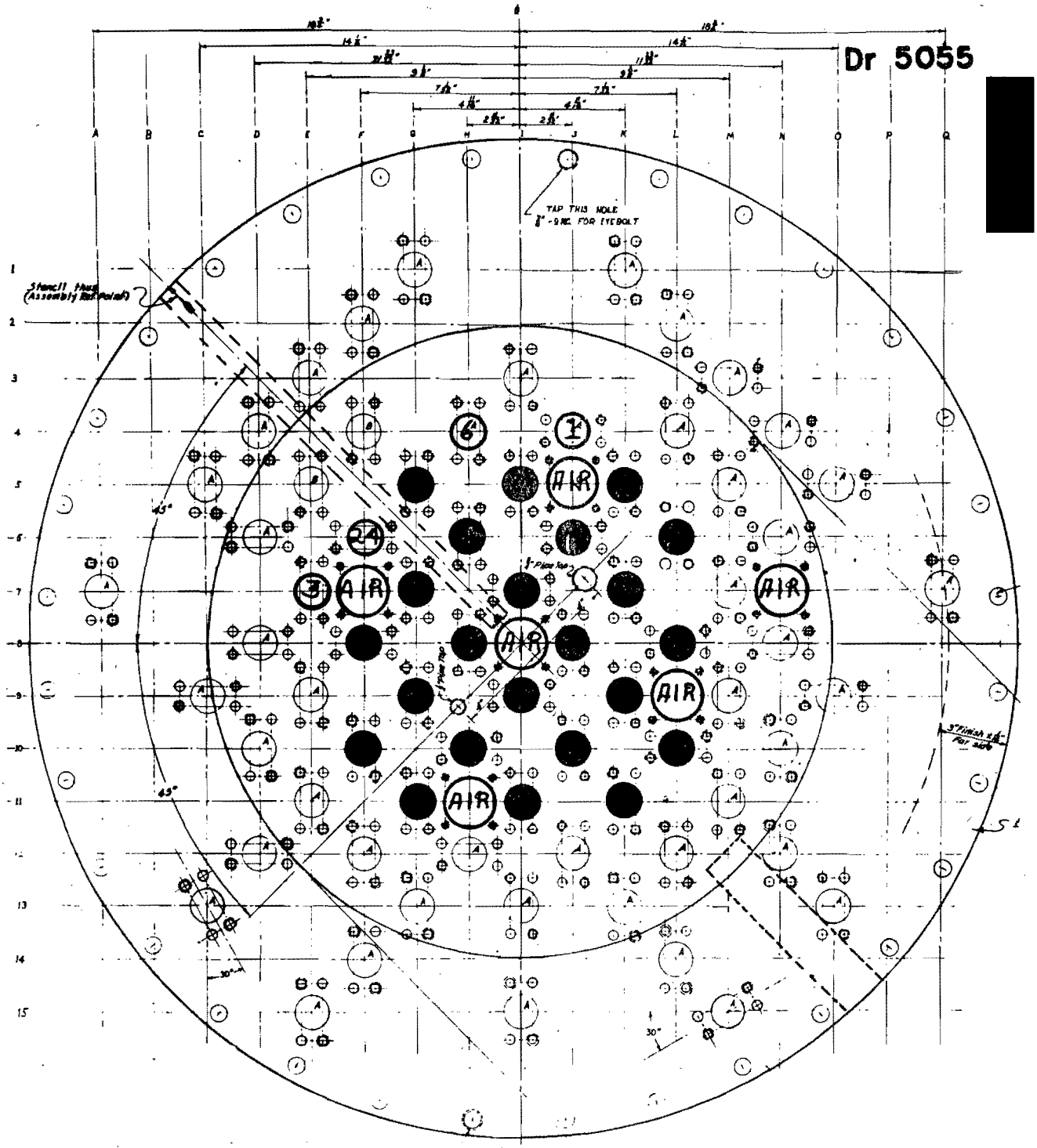

FIG. AI.B h= 61.8 cm.

Critical Mass: 1078 g.

[redacted]ET

CNL-P821

FIG. A1.C RADIAL NEUTRON DISTRIBUTION IN 2.58 ½ ASSEMBLY

Dr 5084

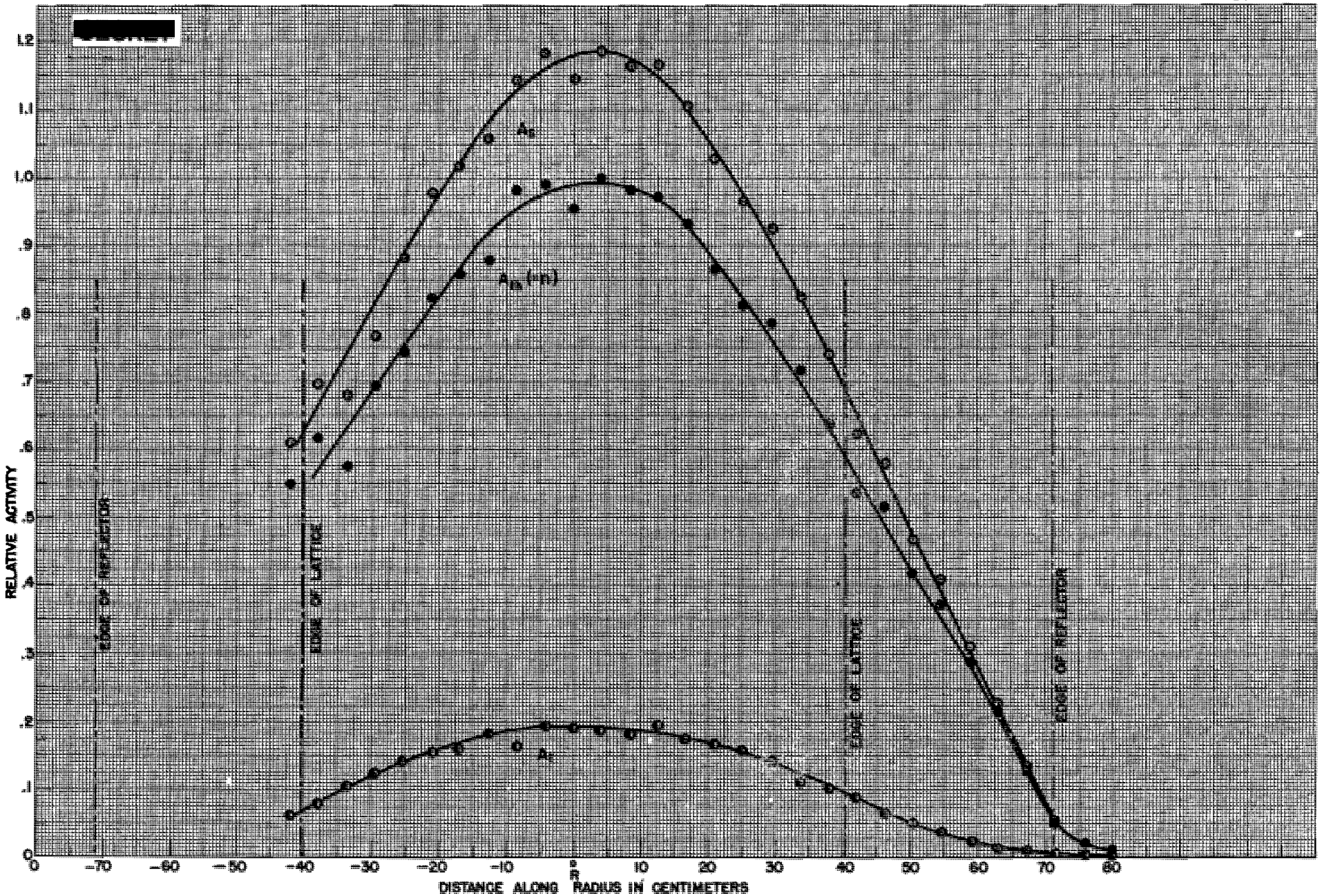

[redacted]

FIG. A1.D LONGITUDINAL NEUTRON DISTRIBUTION IN 2.98 g/l ASSEMBLY

[redacted]

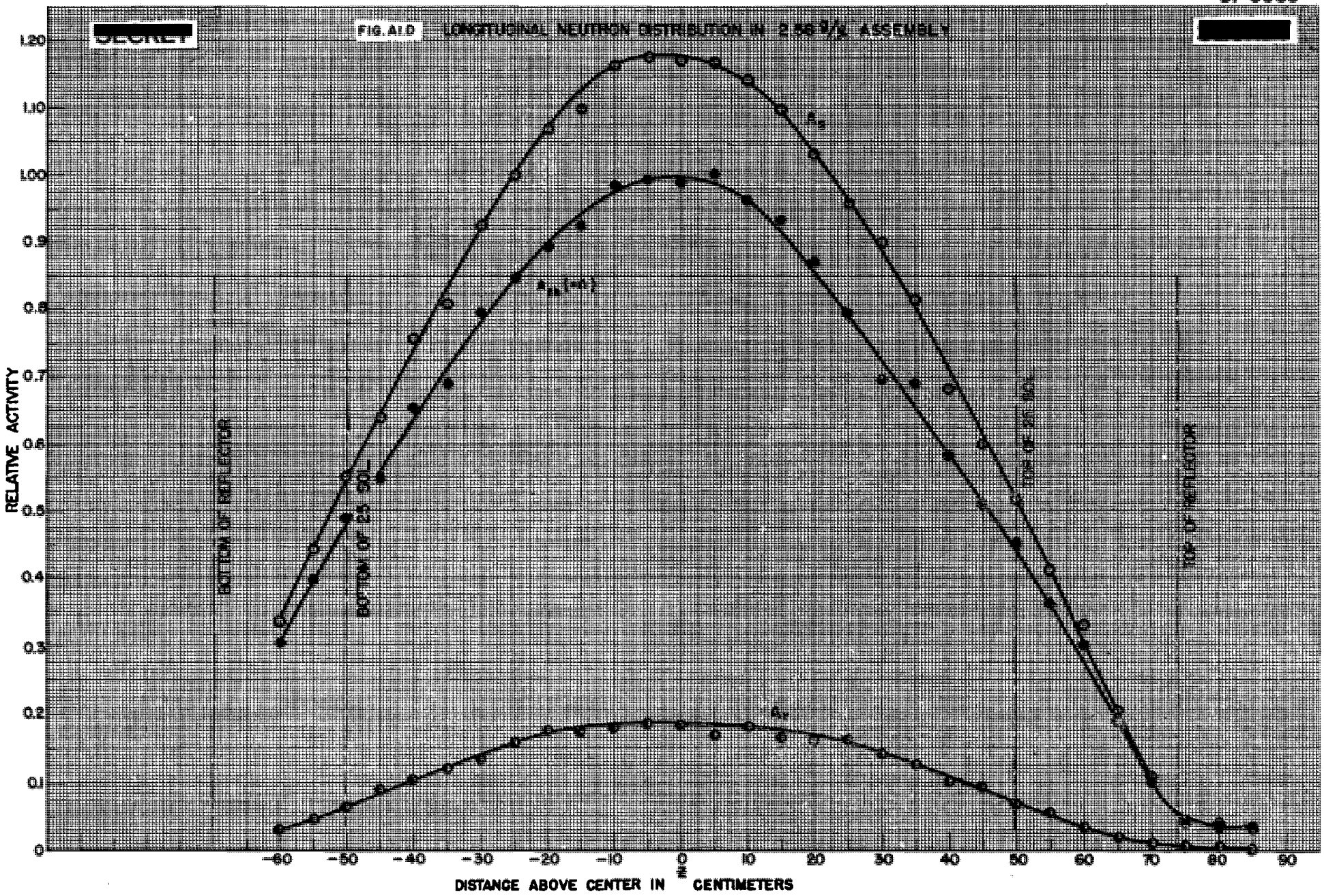

initial approach to criticality was made by adding successive fuel tubes to the heavy water tank, meanwhile following the neutron multiplication of a polonium-beryllium source quantitatively by plotting the reciprocal activity, as measured by several detectors, against fissionable mass present. When experience had been gained, it was sufficient to look for a certain amount of multiplication of the source as indicated on the Monitrons, and then to remove the source while the apparatus was in operation and retract the control rod a little more to get the critical condition. The amount of U^{235} was then adjusted so that the reactor was just critical when the cadmium was all out. Table A1.A gives a concise summary of the critical mass data as they were obtained. A general summary of the dimensions and constants of the experiments is given in Table A1.B.

TABLE A1.A

Amounts of U^{235} Required for Criticality in Various D_2O Systems

ITEM	MEAN CONCENTRATION (g/liter)	HEIGHT OF LATTICE, h (cm)	TEMPERATURE (°C)	D_2O REFLECTOR THICKNESS (cm)			MEAN LATTICE RADIUS, R (cm)	LATTICE VOLUME, V (liters)	CRITICAL MASS OF U^{235} (g)	LATTICE AS IN FIGURE
				BELOW	ABOVE	LATERAL				
1	1 control rod thimble at r = 0; 4 control rod thimbles at r = 18.8 cm; 1 control rod thimble at r = 30.3 cm; 1 2¼-in.-O.D. radial tube through reflector; 1 1¼-in.-O.D. radial tube to axis									
	10.35	61.8	20	20	62	47.9	23.1	104	1078	5a
2	1 control rod thimble at r = 0; 3 control rod thimbles at r = 18.8 cm; 1 thimble at r = 30.3 cm; 2 radial tubes as in Item 1									
	10.35	61.8	20	20	62	48.2	22.8	101	1046	5b
3	1 control rod thimble at r = 0; 2 control rod thimbles at r = 18.8 cm; 1 thimble at r = 30.3 cm; 2 radial tubes as in Item 1									
	10.35	61.8	20	20	62	48.6	22.4	97.5	1009	5c
4	2 control rod thimbles at r = 18.8 cm; 1 thimble at r = 30.3 cm; 2 radial tubes as in Item 1									
	10.35	61.8	20	20	62	49.2	21.8	92.7	959	5d
5	1 control rod thimble at r = 18.8 cm; 1 thimble at r = 30.3 cm; 2 radial tubes as in Item 1									
	10.35	61.8	20	20	62	49.6	21.4	89.3	924	6a
6	1 control rod thimble at r = 18.8 cm; 2 radial tubes as in Item 1									
	10.35	61.8	20	20	62	49.7	21.3	87.8	909	6b
7	1 control rod thimble at r = 18.8 cm									
	10.35	61.8	20	20	62	49.8	21.2	87.3	904	6c
8	No-hole extrapolation									
	10.35	61.8	20	20	62	50.2	20.8	84.0	869	
9	1 control rod thimble at r = 18.8 cm; no other holes of consequence									
	5.17	61.8	20.8	20	62	40.1	30.9	185	954.5	6d
10	No-hole extrapolation (estimated)									
	5.17	61.8	20.8	20	62	(40.6)	(30.4)	(180)	(930)	
11	2 control rod thimbles at r = 18.8 cm									
	2.58	100	22.7	20	24	29.0	42.0	552	1425	7a

TABLE A1.A (Cont'd)

ITEM	MEAN CONCENTRATION (g/liter)	HEIGHT OF LATTICE, h_e (cm)	TEMPERATURE (°C)	D_2O REFLECTOR THICKNESS (cm)			MEAN LATTICE RADIUS, R (cm)	LATTICE VOLUME, V (liters)	CRITICAL MASS OF U^{235} (g)	LATTICE AS IN FIGURE
				BELOW	ABOVE	LATERAL				
12	1 control rod thimble at r = 18.8 cm									
	2.58	100	22.7	20	24	29.8	41.2	532	1374	7b
13	No-hole extrapolation									
	2.58	100	22.7	20	24	30.6	40.4	512	1323	-
14	2 control rod thimbles at r = 18.8 cm; 1 control rod thimble at r = 30.3 cm									
	10.35	100	23.5	20	24	52.4	18.6	109	1126	7c
15	2 control rod thimbles at r = 18.8 cm									
	5.17	100	23.5	20	24	45.0	26.0	212	1098	7d
16	2 control rod thimbles at r = 18.8 cm; circle of iron at r = 51.9 cm									
	5.17	100	21.6	20	24	41.6	29.4	272	1404	8a
17	1 control rod thimble at r = 18.8 cm									
	2.86	61.8	21.2	20	62	20.7	50.3	491	1405	8b

TABLE A1.B

Collected Dimensions and Constants of the Experiments

U^{235}	Average isotopic concentration = 95.4% U^{235}
D_2O	Average isotopic concentration = 99.7% D
Mean concentration of U^{235}	(*a*) 2.58 g of U^{235} per liter (*b*) 5.17 g of U^{235} per liter (*c*) 10.35 g of U^{235} per liter
Constants of theory	$f = 0.963$; $L^2 = 90.42$ cm^2; $k = 2.09$
Fuel tubes	O.D. = 1.500 in.; 2S aluminum; wall thickness = 0.035 in.; bottom thickness = 1/8 in.; length below top of tube sheet = 4 ft 9¾ in.; thermal-neutron cross-section = 0.89 cm^2 per tube for solution depth of 61.8 cm
Control rod thimbles	2S aluminum; 2-3/8 in. O.D.; 1/8-in. wall; 1/8-in. bottom; thermal-neutron cross-section = 4.62 cm^2
Control rods	O.D. = 1¾ in.; type 304 stainless steel No. 16 BWG; length 6½ in. overall; 0.020-in. Cd sleeve cemented inside
$UO_2F_2 + D_2O$ solution	Height in fuel rods (*a*) 61.8 cm, (*b*) 100 cm; amount of fuel per tube (*a*) 45.45 g, (*b*) 73.57 g; thermal-neutron cross-section = 74.5 cm^2 per tube for 61.8 cm solution height
Reactor tank	142 cm I.D.; ¼-in. wall; type 304 stainless steel
Tube inserts	1.25-in. O.D.; wall thickness = 0.035 in.; 24ST aluminum; bottom thickness = 1/8 in.; overall length = 10 in.; about 9 in. filled with D_2O
Poison rods	Length below top of tube sheets = 4 ft 8¾ in.; type 304 stainless steel; diameters = 3/16 and 1/4 in.; thermal-neutron cross-section = 0.0273 cm^2 per gram, giving for 61.8 cm depth, 2.58 cm^2 and 4.58 cm^2 per rod for 3/16- and 1/4-in. rods, respectively, and 4.18 cm^2 and 7.41 cm^2 for 100 cm depth, respectively, for the rods
Square lattice spacing	2.59 g/liter: 16.86 cm 5.17 g/liter: 11.92 cm 10.35 g/liter: 8.43 cm
Iron rods simulating thorium	Armco iron; diameter 3.65 cm; length overall = 139.7 cm; spaced 14.8 cm, center to center on circle 51.9 cm in radius
Thorium insert in iron rod	Diameter 4.00 cm; length 7½ in; centrally located in iron rod

Total neutron absorption cross-section of materials in active volume of assembly

(1) For depth of 61.8 cm:

Vertical experimental tube (Al)	0.63 cm^2
Radial experimental tube (Al)	2.61 cm^2
Control rod thimble (Al)	4.62 cm^2
Fuel Tubes (Al), each	0.89 cm^2
Solution, per fuel tube	74.53 cm^2

TABLE A1.B (Cont'd)

Thorium insert in iron rod (cont'd) (2) For depth of 100 cm:

Vertical experimental tubes		1.02 cm^2
Vertical experimental tubes,	small	0.08 cm^2
	large	1.64 cm^2
Control rod thimble		7.48 cm^2
Fuel tubes, each		1.44 cm^2
Solution, per fuel tube		120.6 cm^2

A1.3 REFERENCE REPORT

(1) Snell, A. H., *Critical Studies on Enriched Uranium—Heavy Water Studies*, MonP-454, December 15, 1947.

Appendix 2

WORK ON CRITICAL EXPERIMENTS, JULY 1946 TO DECEMBER 1948

A2.1 CRITICAL EXPERIMENTS WITH Al + H_2O MODERATOR AND HEAVY WATER, LIGHT WATER, AND BERYLLIUM REFLECTORS[1]

The experiments with Al + H_2O as a moderator and heavy water, D_2O, as reflector were a direct continuation of those initially undertaken and described in Appendix 1 relevant to the "heterogeneous" reactor design, p. A2.1. While the decision for a beryllium reflector had been made, a sufficient quantity could not be available soon enough to justify the removal of the heavy water system. Consequently a broad experimental program on enriched small reactors was initiated to include reflectors of ordinary water, heavy water, pure beryllium, and beryllium plus a small percentage of ordinary water. The last case was in anticipation of cooling water in a beryllium reflector for the MTR.

The first group of experiments in the enriched reactor program, beginning in the summer of 1946, involved the heavy water reflector, and it is these which are now to be described.

A2.1.1 Experimental Facilities. Some extensive changes were made in the physical arrangement of the equipment described in Appendix 1 which increased safety, ease of operation, and control of the critical assembly. The general arrangement is sketched in Fig. A2.A. Not shown is an exit from the control room to the outside as an emergency exit and security gate.

With respect to instrumentation, new and faster Monitrons (ion chambers and associated circuits) were added so that three were in operation at all times and all were connected to the control rod safety system. The time constants of the safety circuits were about 0.2 to 0.5 sec. Esterline-Angus recorders installed in the control room were driven by two of the Monitrons so that visual monitoring of the pile was provided. In addition, the usual array of counters, gamma ray and neutron, were in use with mechanical recorders for counting rate purposes and loud speakers for continuous auditory monitoring.

DWG.NO.4423

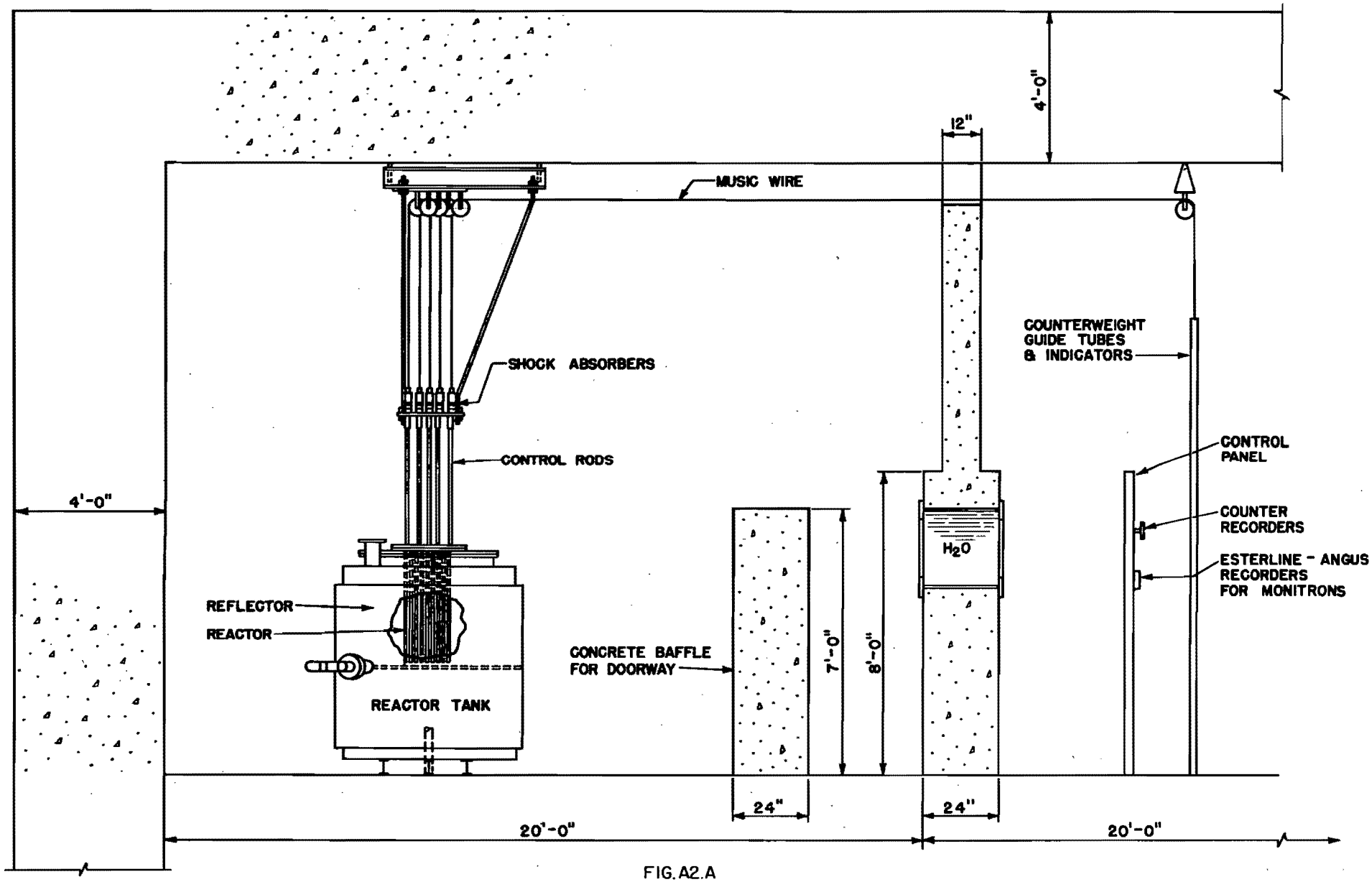

FIG. A2.A

SECTION THROUGH ASSEMBLY & CONTROL ROOMS

A2.1.2 Pile Geometry and Design. In the design of the high-flux reactor going on during 1946 and 1947 the core would contain a considerable quantity of aluminum in alloy with uranium or otherwise in structural form. It therefore became desirable to study, in the critical experiments, the effect of various volume ratios of aluminum to light water on the fluxes and critical masses. The new high-flux reactor design called for such a close spacing of fuel plates, that, to a very good approximation, the reactor core could be treated as a homogeneous mixture of uranium, aluminum, and water. Consequently, experiments were undertaken in which the concentration of U^{235} was held constant while the volume ratio of aluminum to water was varied for the reasons that (1) engineering design depended upon the allowable quantities of aluminum in the reactor, and (2) the dependence of critical mass, fast flux to slow flux ratio, and neutron "age" on the Al/H_2O ratio is of both theoretical and practical interest. The Al/H_2O ratios studied were 0.88, 0.76, 0.65, and 0.303.

The problem of constructing and assembling a reactor that was essentially homogeneous in reasonably small integral parts was solved by the use of square aluminum tubes, each of which contained about 20.3 g of U^{235} in the form of UO_2F_2 in light water solution. A square tube satisfies the requirement of close packing and approximation to homogeneity, and a reasonable size was available, namely 1 by 1 in. with 1/16-in. wall thickness.

The pertinent physical data for the D_2O reflector experiment were as follows:

Concentration of U^{235} = 35.6 g per liter of reactor volume
Height of active portion = 70 cm
Size of individual fuel tube = 2.54 by 2.54 by 90 cm
U^{235} Content of fuel tube = 20.3 g per tube
Al/H_2O volume ratios attainable = 0.88, 0.76, 0.65, 0.303

The actual pile geometry utilized was cylindrical with no reflection above and below the core but D_2O reflection on the cylindrical side. For this purpose a concentric inner tank was built into the D_2O tank described in Appendix 1, p. A1.1. The final arrangement is given in Fig. A2.B.

The procedure during assembly was as follows: (1) the reactor tank has a full complement of tubes at all times; (2) some tubes initially are fuel

DWG. NO. 4425

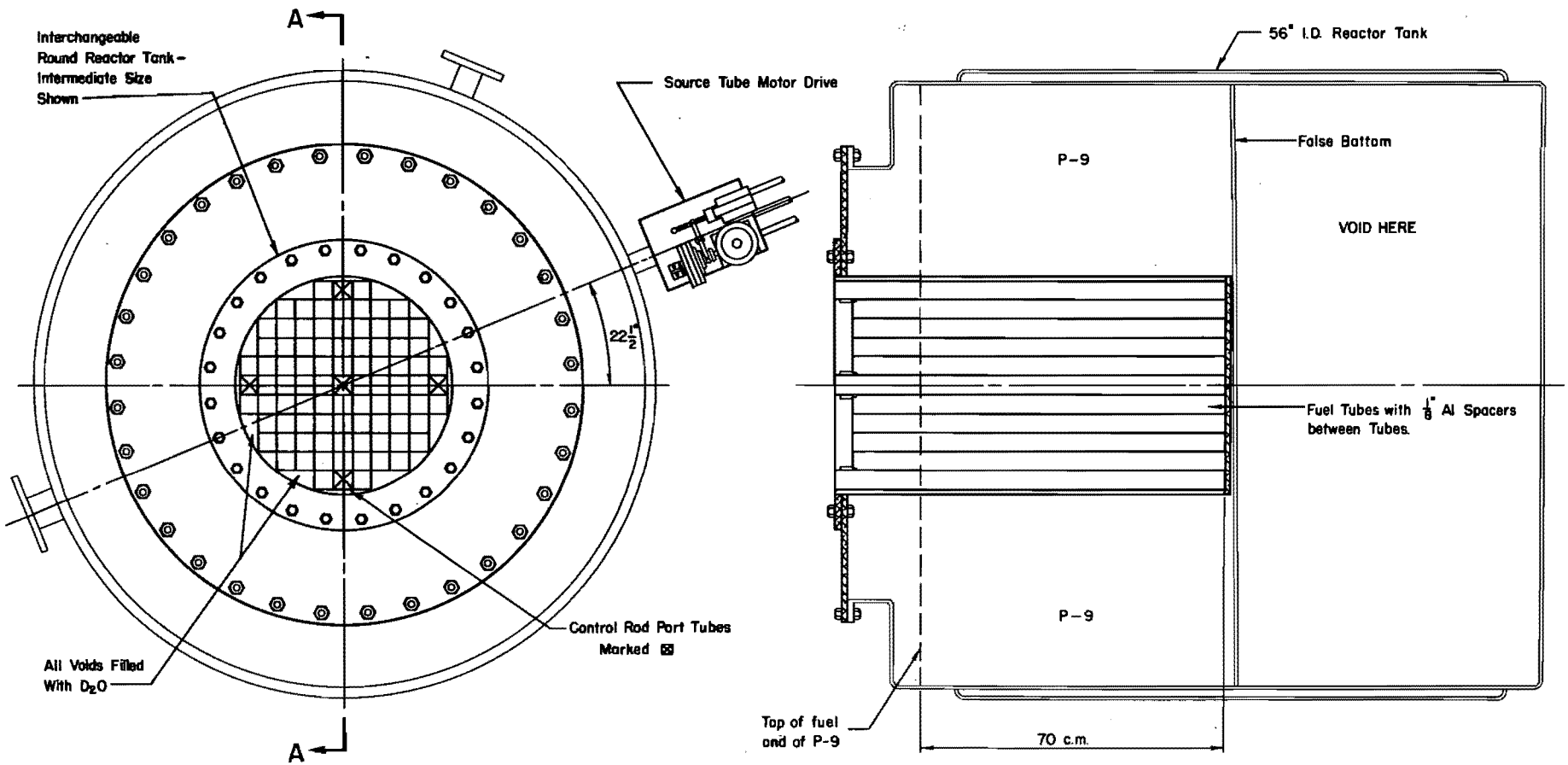

PLAN

SECTION A-A

FIG. A2.B

ASSEMBLY FOR D_2O REFLECTOR

tubes and the rest are D_2O; and (3) the gaps between the square tubes and the cylindrical tank are filled by D_2O introduced into the core tank for this purpose, i.e., to prevent a gap between core and reflector. However, the rather large percentage of aluminum in the reflector region near the core tank essentially required a three-region theoretical treatment of the experiment.

All the above statements relating to the D_2O experiment apply equally well to the arrangement and procedure used in the case of the H_2O reflector. The experiments in which H_2O was employed as reflector were carried out for two reasons: (1) the results would provide information regarding the effect of the water that would be present on top and bottom of the high-flux pile, and (2) the study of a pile in which both the moderator and the reflector are of the same substance is of considerable interest to theoreticians.

When beryllium was used for the reflector the experiment was somewhat "cleaner" with a square arrangement in that it was possible to do away with the irregular region between reactor and reflector. This will be evident from Fig. A2.C. It turned out that the beryllium-reflected pile became critical just four fuel tubes short of a nine-tube square, and the reactor was built out to completely fill this square geometry, the excess k being taken up by poison. Figure A2.D is a photograph looking down on the beryllium assembly.

A2.1.3 Results and Discussion. Experiments were performed with D_2O, beryllium, and H_2O reflectors to find (1) critical mass, (2) neutron distributions, and (3) values of control rods, cavities, etc., in terms of fuel. Various ratios of Al to H_2O were used. These experiments served as a check on the theoretical calculations of critical masses under the same conditions. The values for the critical mass found in both theory and experiment are compared in Table A2.A.

The situation in spatial neutron distribution is shown in Fig. A2.E, which contains both experimental and theoretical radial distributions. These distributions were measured at a height of 35 cm above the bottom of the pile.

It will be noted that in general the observed densities of both thermal and epithermal neutrons in the reflector are somewhat greater than expected from a two-group calculation. The rise in thermal-neutron density just outside the reactor is quite pronounced, the maximum experimental value being 40% higher than the minimum, whereas the rise for a two-group picture is 15%.

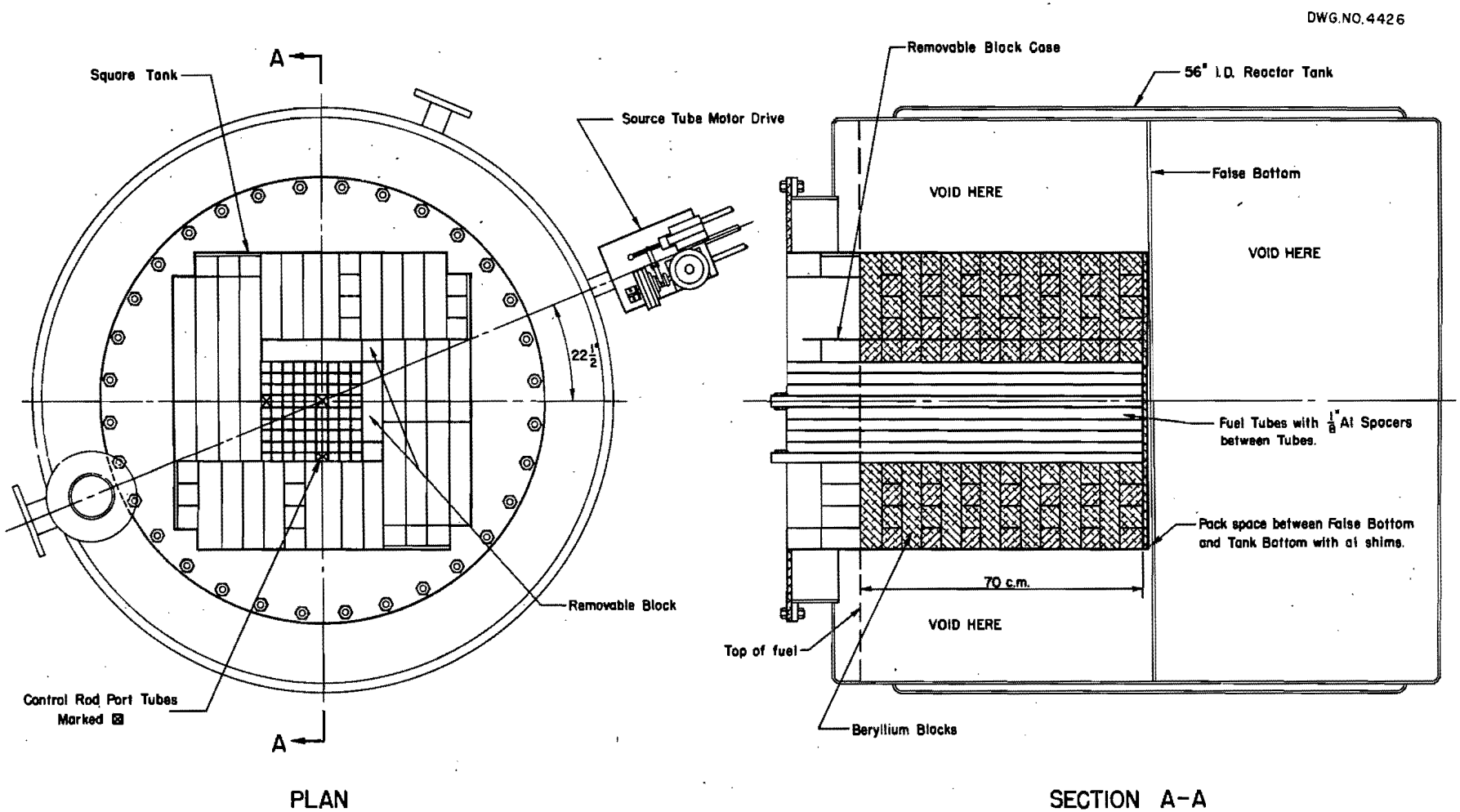

FIG.A2.C

ASSEMBLY FOR
BERYLLIUM REFLECTOR

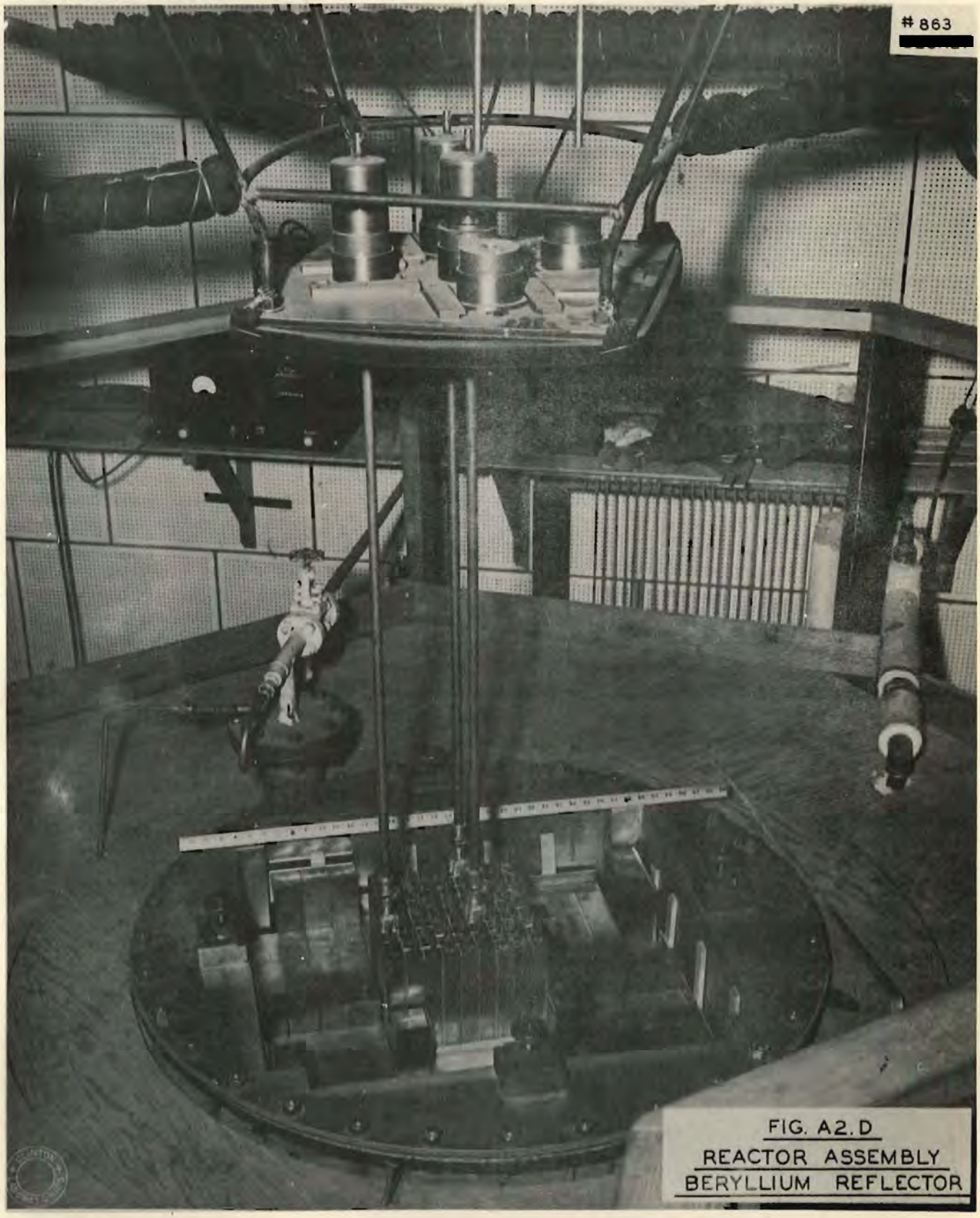

FIG. A2.D
REACTOR ASSEMBLY
BERYLLIUM REFLECTOR

FIG. A2.E

DWG. NO. 4428

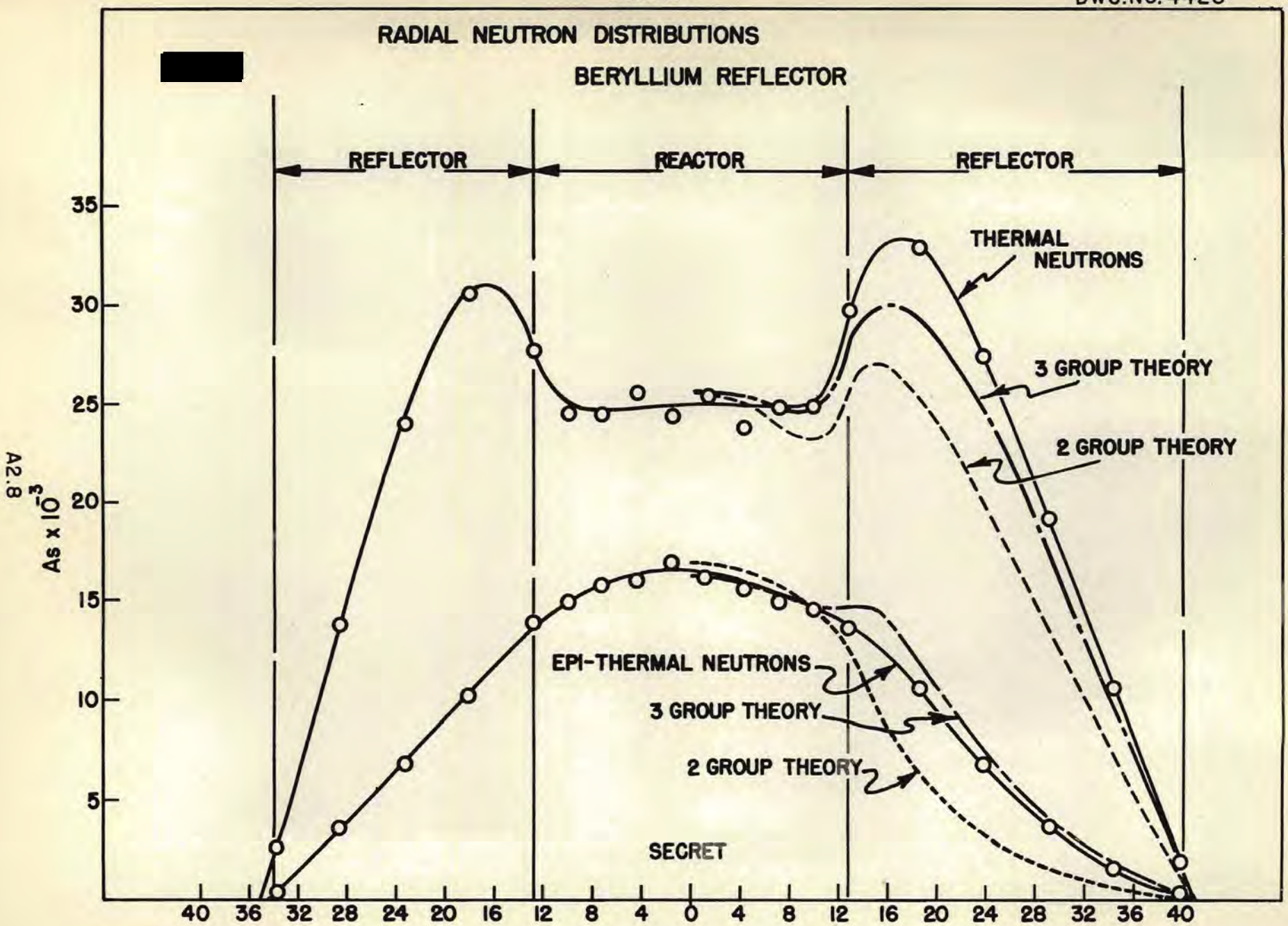

TABLE A2.A

Critical Masses in Kilograms of U^{235}

REFLECTOR	VOLUME RATIO Al/H_2O	OBSERVED		CALCULATED, 2-GROUP	
		GROSS	CORRECTED FOR EMPTY CONTROL ROD PORTS, ETC.	2-REGION	3-REGION
D_2O	0.88	2.48	2.40	2.10	2.64
D_2O	0.76	2.23	2.15		2.43
Be	0.76	1.54	1.42	1.54*	
H_2O	0.76	3.29	3.22		3.34
H_2O	0.66	2.82	2.72		3.04

*Where critical K = 0.988 x k of pile without poison.

One might be tempted to conclude that beryllium exhibits advantages as a reflector which were unsuspected, but it seems probable that the experiment merely emphasizes known shortcomings of a two-group theory. A three-group calculation is shown in Fig. A2.E. The source of the remaining discrepancy between theory and experiment was not yet clear. Age measurements in beryllium were in progress at Argonne.

Vertical neutron distributions were studied also; typical results will be found in Fig. A2.F. It will be recalled that no reflector was present at top or bottom of the experimental pile, and the solid lines are cosine curves fitted to points near the center by a least-squares method. The slight lateral shift of the data from center is apparently due to the presence of a portion of a control rod in the top of the pile. It is clear that the extrapolation distances for thermal and epithermal neutrons are the same, within the experimental limits.

A few rough measurements of the values of control rods were made. In the beryllium case, the rod near center was found equal to 160 g of U^{235} and a cavity (empty tube) approximately halfway from the center to the periphery was equal to 18 g. On this basis the center cavity equal 35 g.

FIG. A2.F

DWG. NO. 4431

[redacted]

VERTICAL DISTRIBUTION – Be EXPT.

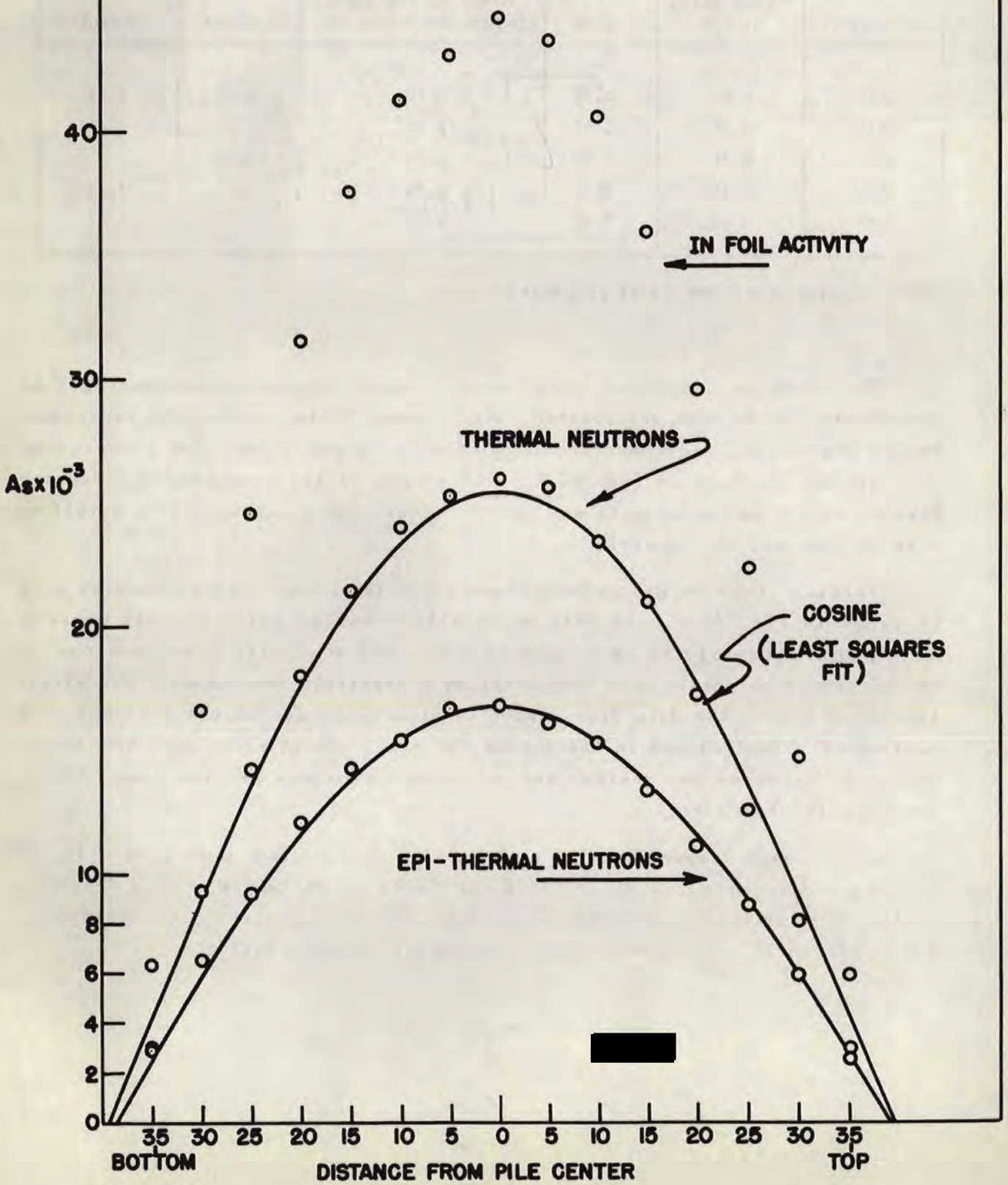

[redacted]

A2.2 FURTHER CRITICAL EXPERIMENTS ON ENRICHED REACTORS WITH Al + H_2O MODERATOR AND SOLID BERYLLIUM REFLECTOR[2]

With the termination of the experiments dealing with liquid reflectors and in preparation for a series of experiments on reactors having solid reflectors, it was decided that it would be worth while to make certain major changes in the experimental arrangement in the criticality cell in order to provide for greater flexibility and greater convenience in stacking solid reflectors. The entire liquid storage and piping system was removed from the cells, and in place of the tank assemblies which had been used for D_2O and H_2O reflectors, a low platform framework of steel was erected. A ½-in. plate of 2S aluminum was placed over the steel framework to serve as a floor on which to build critical assemblies. The center portion of the plate was cut out, and flanges were provided to hold a center plate of ½-in. aluminum, through which was drilled a rectangular array of holes accurately spaced to position the lower ends of the fuel tubes for Al/H_2O ratios equal to or greater than 0.65. Thus the bottom of the reactor was relatively clean, the core and a considerable portion of the reflector having only the ¼-in. perforated aluminum plate immediately under them.

A2.2.1 Experimental Facilities. Figure A2.G shows a core of square cross-section with the beryllium reflector assembled on the platform. The level of the fuel was at the same height as the top of the reflector in these assemblies, the remaining upper portion of the fuel tubes being empty up to the rubber stoppers.

Practically all the radiation detection and monitoring instruments were replaced by improved circuits of more recent design. In particular, it was found that the vibrating-reed Monitrons, two of which can be seen in Fig. A2.G, are a decided improvement over the older designs in stability, sensitivity, and response time.

The operation of the control rod system was improved by replacing the hand-operated control rod counterweights and clamps by small gear boxes (one for each control and safety rod), which were designed to limit the maximum rate of withdrawal of the rods. While the operation of the rods was still basically manual, the use of the gear boxes ensured a reasonably slow and constant rate of withdrawal of the rod and also facilitated changing the control rod position in small increments with accuracy.

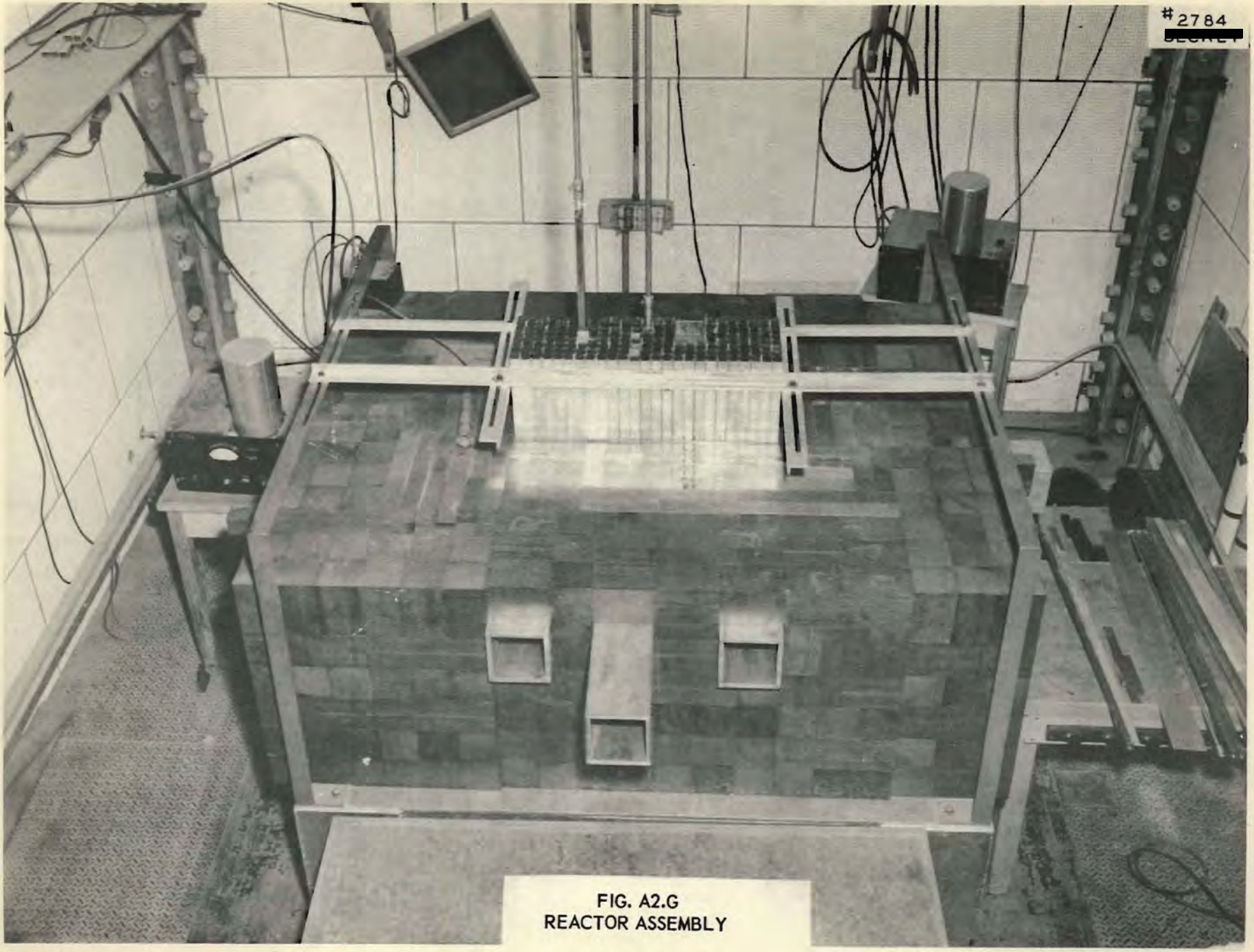

FIG. A2.G
REACTOR ASSEMBLY

A2.2.2 Experimental Results. *Bare Pile.* While waiting for the arrival of sufficient beryllium to continue the studies for the high-flux pile, it was decided to try to obtain a figure for the bare critical size as a check on the fundamental characteristics of this reactor. A bare assembly was built with cadmium sheets around the sides of the reactor to reduce the effect of nearby objects, and, although criticality was not finally reached, a multiplication of about 11.6 was obtained at a load of 5050 g. The extrapolation of the reciprocal counting rate versus mass curve (Fig. A2.H) indicates a critical mass of about 5.5 kg. After correcting for the presence of holes for control rods, it was estimated that the bare critical mass was 5.3 ± 0.1 kg. The Al/H_2O volume ratio in this case was 0.65, the height of the core was 66 cm, the maximum loading attained was 48 by 43 cm in area, approximating square geometry.

Beryllium-reflected Reactors. The description will be limited to a discussion of the experiments which have been done on relatively "clean" beryllium assemblies, i.e., assemblies which have simple, calculable geometries.

The first experiment in this series on beryllium-reflected reactors was that on the measurement of the critical mass of a square assembly having an Al/H_2O volume ratio in the core of 0.65. In this experiment the geometry of sources and BF_3 counters was apparently very good since the counting rate versus mass plots turned out to be approximately straight lines, showing no tendency to either turn downward or curve upward near the critical mass, as happens in many cases. Two Po-Be sources were used, one (10^7 neutrons per second) located directly beneath the lower surface of the reactor below the center of the core, and another (10^5 neutrons per second) suspended in an empty tube at the core reflector boundary at mid-height of the reactor. Two BF_3 proportional counters were used to observe the multiplication of the reactor during the build-up to criticality. These counters were located in such a manner that a large portion of the core lay between the sources and the counters, i.e., the counters must "look through" the multiplying medium to "see" the sources. One counter was placed on the top surface of the reflector in the immediate vicinity of the core (Fig. A2.G), the other was placed about 15 ft from the pile at an elevation about 4 ft higher than the top surface of the assembly.

It was found that the square assembly became critical just three fuel tubes short of an 8- by 8-tube array. In order to complete the square geometry,

[redacted]

DWG. NO. 4819

FIG. A2.H
APPROACH TO CRITICALITY
BARE PILE
AL/H_2O VOLUME RATIO 0.65

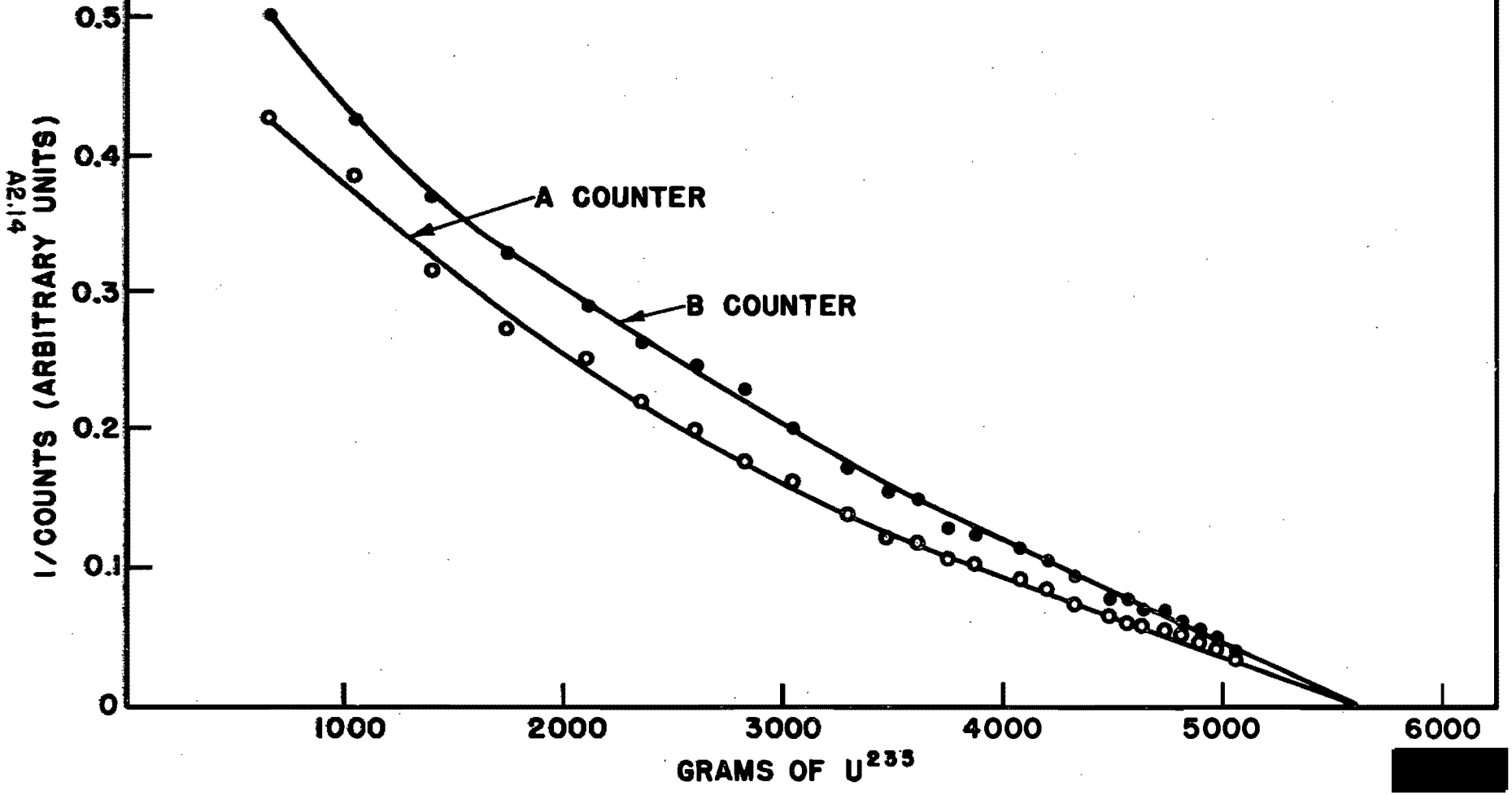

[redacted]

it was necessary to add a small amount of poison (about 60 cm^2) in the form of thirty-one 0.030-in.-diameter gold wires, uniformly distributed throughout the core. The resulting reactor then has a core 22.5 by 22.5 cm in cross-section and 66 cm in height and containing 1.21 kg of U^{235} at a fuel concentration of 38 g of uranium per liter of reactor volume. The Al/H_2O ratio in the core was 0.65. The core was reflected on all sides, the reflector consisting of more than 30 cm thickness of beryllium, but there was no reflector on the top or bottom. When corrections were made for the presence of control rod ports (air holes) and for distributed gold wires in the core, the minimum critical mass of a square reactor of this type turned out to be 1.07 kg.

The second clean beryllium-reflected pile to be built was a thin-slab assembly. It was desired to find the critical mass of a rectangular geometry having a length-to-width ratio of approximately 5. The width selected for the core of the pile was four fuel tubes, or 11 cm, and the assembly became critical at a length of 19 fuel tubes (51 cm) with 30 cm^2 of excess poison in the core. The mass of U^{235} in this case was 1.35 kg, and when corrections were made for excess poison and control rod ports, the minimum critical mass for this thin-slab geometry was 1.28 kg. The height of the reactor, reflector thickness, fuel concentration, and the Al/H_2O volume ratio in the core were the same in this case as for the square assembly.

The plot of the reciprocal counting rate versus fuel aboard, shown in Fig. A2.I, indicates the linearity of results that can be obtained with reasonably good source and counter geometry.

Spatial distributions of thermal and epithermal neutron flux were measured in both the square reactor and the thin-slab reactor. The measurements were made with indium foils, used alternately bare and cadmium covered. Figure A2.J shows the distributions of thermal and epithermal neutron flux along a perpendicular bisector of the side of the square reactor. Figure A2.K shows the same distributions along a diagonal of the square assembly. All these foil measurements were taken at mid-heights of the assemblies.

The ratio of the thermal-neutron flux at certain points in the pile to that at the center of the core is of interest; these data are presented in Table A2.B.

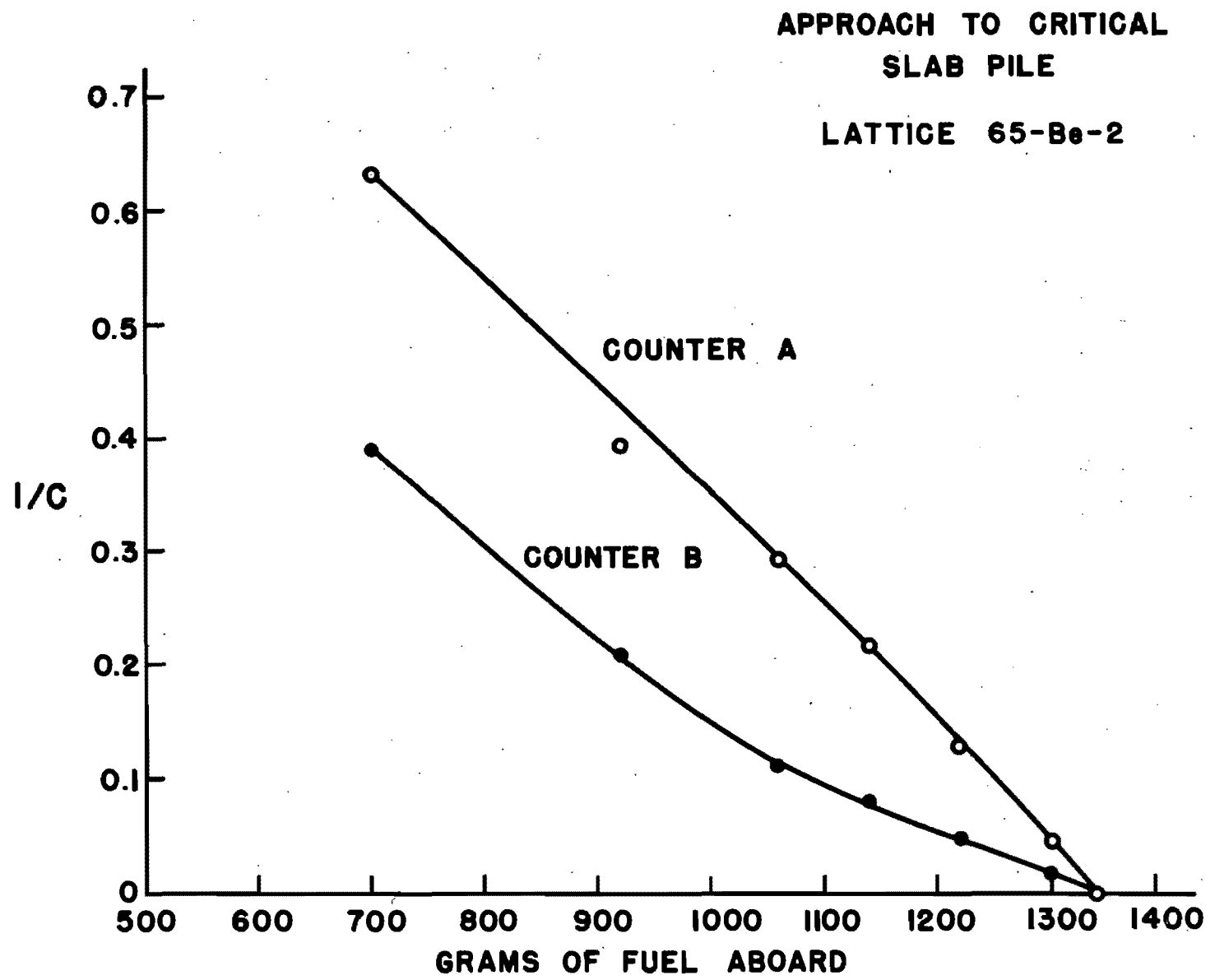
APPROACH TO CRITICAL
SLAB PILE
LATTICE 65-Be-2
COUNTER A
COUNTER B
I/C
0.7
0.6
0.5
0.4
0.3
0.2
0.1
0
500
600
700
800
900
1000
1100
1200
1300
1400
GRAMS OF FUEL ABOARD

FIG. A2.1

Dr 5196

[redacted]

SQUARE Be PILE

LATTICE 65-Be-1

LATERAL NEUTRON DISTRIBUTIONS

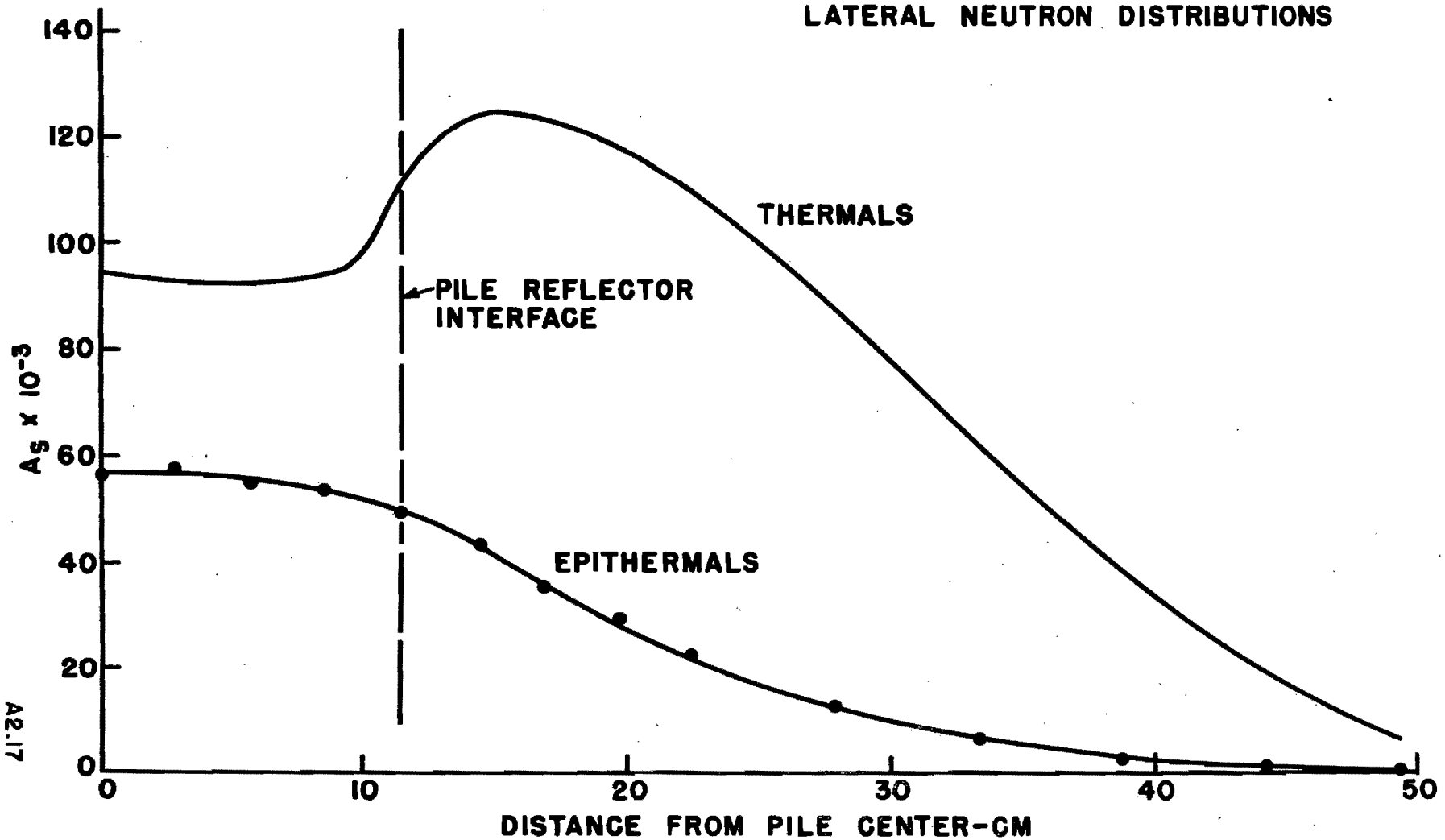

FIG. A2.J

A2.17

[redacted]
Dr 5199

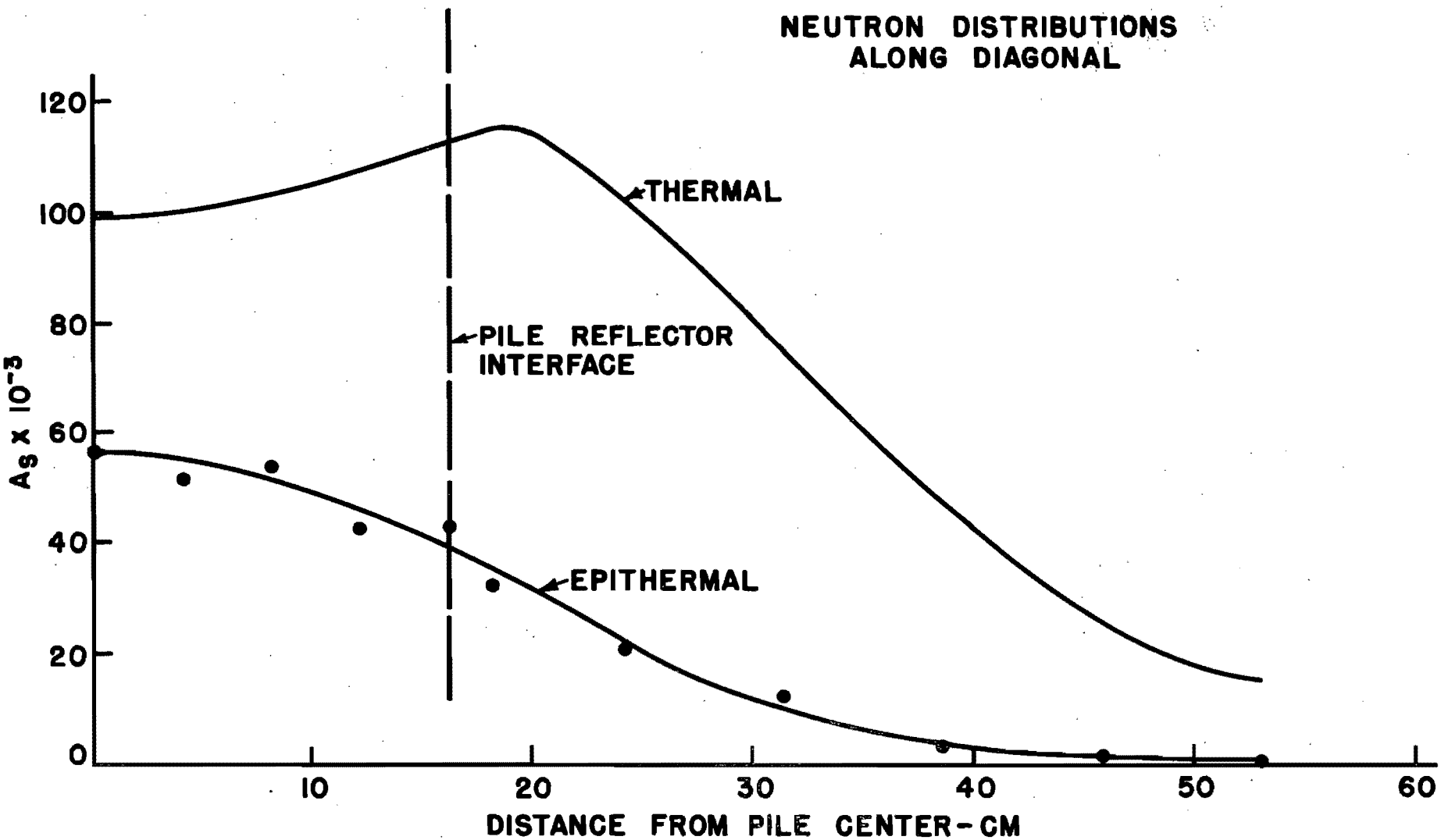

FIG. A2.K

TABLE A2.B

Relations Between Thermal Flux at Certain Locations in the Reactor and That at Center of Core

ASSEMBLY NO.	$\frac{\phi_{th}\ (\text{peak})}{\phi_{th}\ (\text{center})}$	$\frac{\phi_{th}\ (\text{edge})}{\phi_{th}\ (\text{center})}$	DISTANCE TO FALL TO CENTER VALUE (cm)	
			FROM CENTER OF CORE	FROM EDGE OF CORE
1 (lateral)	1.32	1.19	26.5	15
1 (diagonal)	1.16	1.13	25	9
2 (lateral)	1.42	1.24	22	16.5
2 (longitudinal)	0.90	0.85		

The ratio of the peak thermal flux to the thermal flux at the center is an indication of the maximum slow flux, for a given operating level, which the assembly will provide for experimental purposes. The ratio of a thermal flux at the edge of the core to that at the center is a measure of the maximum heat production per unit volume to be expected in the core. The extent to which the thermal flux holds up in the reflector is of interest in planning experiments which will make use of this flux.

A few preliminary experiments were carried out which yield an estimate of fast-neutron flux in these reactors. A threshold type fission chamber[3] was constructed using 145 mg of uranium from K-25 which was depleted in U^{235} content to approximately 1 part in 100,000.

The fission chamber was first placed in a graphite column containing an Sb-Be source at a position where the thermal-neutron flux and the Cd ratio were known from standard indium foil measurements. By exposing the chamber alternately bare and Cd covered, it was determined that 93% of the fissions in U^{235} were caused by neutrons of energy below the Cd cutoff at a position in the graphite column approximately 10 cm from the Sb-Be source where the Cd ratio was 3.7.

The chamber was then placed at the center of the active lattice of the thin-slab pile where the counting rate, when corrected for thermal fissions in U^{235}, indicated that the flux of neutrons having energies above the U^{238} threshold (>1 Mev) is 0.50 $(nv)_{th}$. This result is in reasonably good agreement with the calculated virgin flux in this core, 0.60 $(nv)_{th}$ (see MonP-272). The correction for thermal fissions in U^{235} in this case amounts to only 2% of the total counting rate.

A2.3 REFERENCE REPORTS

(1) Mann, M. M. and Martin, A. B., *Critical Experiments on a Small Reactor of Enriched U-235/Al-H_2O Moderator and D_2O, Beryllium, and H_2O Reflectors*, MonP-357, August 18, 1947.

(2) Mann, M. M. and Martin, A. B., *Further Critical Experiments on a Small Reactor of Enriched U-235/Al-H_2O Moderator and Beryllium Reflector*, ORNL-79, September 16, 1948.

(3) Jordan, W. H. and Bell, P. R., *Instructions for Use of Al Amplifier and Preamplifier*, MonP-323, July 29, 1947.

Appendix 3

CRITICAL EXPERIMENTS ON SIMULATED MTR STRUCTURE[1]

In particular, the third set of critical experiments was designed to study the following:

1. The critical mass (or, more directly, the excess of $\Delta k/k$) of slab reactors as a function of the length-to-width ratio of the core.
2. The effect of holes on the k of the reactor.
3. The heat load in the reflector arising from gamma-ray absorption.
4. Spatial distributions of thermal, indium resonance, and fast ($E > 1$ Mev) neutron flux in the core and in the reflector, particularly the distributions of thermal and indium resonance neutrons in the experimental holes.
5. The effectiveness of control rods of various materials and of various sizes in terms of $\Delta k/k$.

A3.1 THE EXCESS REACTIVITY OF U-Al-H_2O REACTORS, WITH Be REFLECTOR, AS A FUNCTION OF GEOMETRY AND REFLECTOR COMPOSITION

The starting point for these experiments was the small clean-slab reactor which is described in Appendix 2, p. A2.15. The core was 51 by 11 cm in cross-section and 66 cm high. It had a 30-cm beryllium reflector on each face except the top and bottom. The volume ratio of Al to H_2O was 0.65, and the fuel concentration in the core was 37.1 g of U^{235} per liter of core.

The size of the reactor was increased in a series of discrete steps, the final objective being a core of dimensions 71 by 22.5 by 66 cm, with a reflector on all sides (except top and bottom) consisting of 30 cm of beryllium, diluted with about 2% water (imitated by plexiglas). This final assembly approximated very closely the dimensions and composition of one of the probable configurations of the high-flux reactor.

The major steps in building up the small slab to final size were the following:

1. Increase in length of the slab from 51 to 71 cm and addition of a 30-cm graphite layer to one side (long side of the beryllium reflector).
2. Increase in thickness of the slab from 11 to 17 cm.
3. Increase in thickness of the slab from 17 to 22.5 cm.
4. Completion of a simulated high-flux reactor, putting 30 cm of graphite on each side of the beryllium reflector and introducing the seven large experimental holes in the reflector. The final assembly has been shown in Fig. A3.A.

As the size of the reactor was increased over that of the small clean slab, it was necessary to add uniformly distributed poison in the core to hold k-effective to a value close to unity. The poison used in these experiments was type 347 stainless steel in the form of strips 1/8 by 15/16 by 126 in. These were inserted in place of aluminum strips of the same dimensions which were used to attain the desired Al/H_2O volume ratio in the core. Although this substitution changed the Al/H_2O ratio to some extent, the magnitude of the change was small and the effect on the neutron age was also small.

Beginning with the 51- by 11- by 66-cm reactor, containing 1.35 kg of fuel, both poison and fuel were added in appropriate increments until a length of 71 cm was reached. At this stage the reactor contained 1.94 kg of fuel, and the excess 0.59 kg (over the clean critical mass of 1.35 kg) required 266 cm^2 of uniformly distributed poison to hold the excess reactivity to zero with all control rods removed. Table A3.A shows the excess reactivity, represented by poison content, for each of the assemblies studied. The excess $\Delta k/k$ is obtained by computing the k for each assembly from $k = \sigma_{25}/\sigma_{total}$ where $\sigma_{total} = \sigma_{25} + \sigma_{Al} + \sigma_{H_2O} + \sigma_{poison}$; then $\Delta k/k = (k_0 - k_i)/k_i$, where k_0 refers to the clean, unpoisoned core and k_i to the poisoned assembly.

When the reactivity is changed by a means which does not alter the total amount of fuel in the core or the concentration of fuel, it can easily be shown that the fractional change in k is given simply by $\Delta k/k = \Delta\Sigma/\Sigma$, where $\Delta\Sigma$ is the amount of uniform poison added or removed from the core and $\Sigma = N\sigma$ is the total cross-section of the reactor having the smaller amount of poison. For example, when graphite is added to one side of the beryllium reflector of assembly 3 (Table A3.A), 37 cm^2 of additional poison is required to offset the increased reactivity, and the effect of the graphite layer is given by

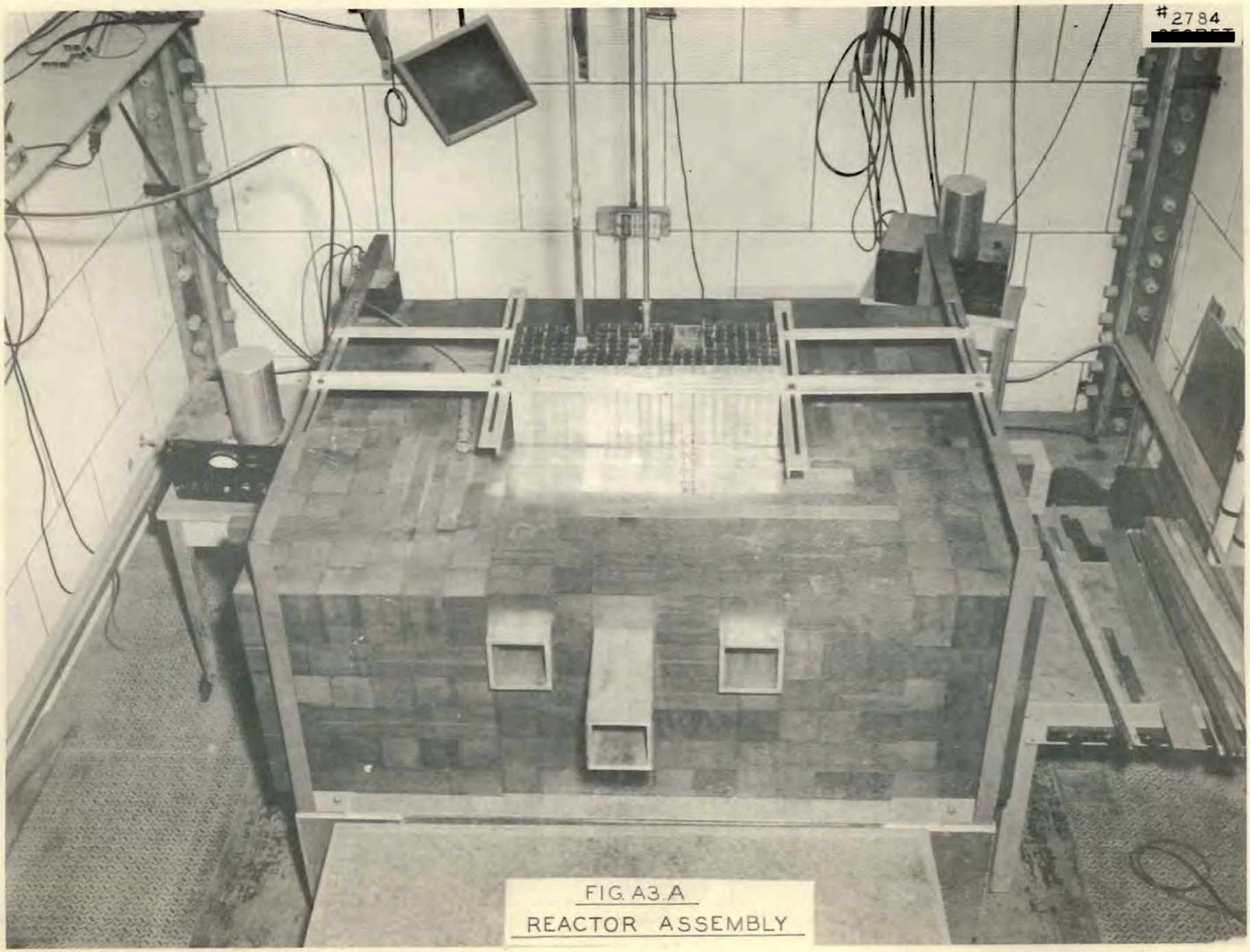

FIG. A3.A
REACTOR ASSEMBLY

$$37/4384 = \Delta\Sigma/\Sigma = \Delta k/k = 0.9\%$$

Table A3.A summarizes the pertinent criticality data for each of the beryllium-reflected reactors in this series. Column 3 indicates the amount of U^{235} required to fill the core having the dimensions shown in Column 2 at a fuel concentration of 37.1 g per liter of core. Column 4 shows the amount of uniformly distributed poison required to hold the excess k of the assembly to zero, i.e., to hold the reactor just at criticality with all control rods withdrawn. For each assembly, the $\Sigma_{pile} = \Sigma_{25} + \Sigma_{Al} + \Sigma_{H_2O}$ is given in Column 5, the experimental k is shown in Column 6, and in Column 7 is shown the excess $\Delta k/k$ which can be made available by the removal of distributed poison.

TABLE A3.A

Critical Mass and Poison Content (Excess k) of U-Al-H_2O Reactors with Be Reflector

(Al/H_2O volume ratio = 0.65; Be thickness = 30 cm; reactor bare top and bottom; k_0 = 1.6167 for clean core)

ASSEMBLY NO.	DIMENSIONS $L \times W \times H$	MASS (kg)	POISON (cm^2)	PILE (cm^2)	k	$\Delta k/k$ EXCESS (%)
1	22 x 22 x 66	1.21	66	2591*	1.5626	3.5
2	51 x 11 x 66	1.35	30	2882*	1.5849	2.0
3a	71 x 11 x 66	1.94	266	4118	1.5184	6.5
3b (30 cm graphite on one side)	71 x 11 x 66	1.94	303	4118	1.5057	7.4
4 (30 cm graphite on one side)	71 x 14 x 66	2.44	640	5179	1.4388	12.4
5 (30 cm graphite on one side)	71 x 17 x 66	2.94	1140	6240	1.3670	18.3
6 (30 cm graphite on one side; 2% water in Be)	71 x 22.5 x 66	3.95	1848	8384	1.3247	22.0
7 (30 cm graphite on all sides of Be; seven 6-in.holes in reflector; 2% water in Be)	71 x 22.5 x 66	3.95	1580	8384	1.3603	18.8

* These contain fractional fuel tubes.

A3.2 EFFECTS OF THE EXPERIMENTAL HOLES THROUGH THE REFLECTOR

The research facilities of the high-flux reactor as conceived in 1948 included seven large experimental holes, four of which began at the core reflector. The other three holes began 15 cm out in the beryllium and extended through the remainder of the reflector. In connection with these irregularities in the reflector a number of experiments were of interest: (1) the cost of the holes in terms of $\Delta k/k$, or in terms of additional fuel, (2) the effect on the reactivity of the core of filling any one or all of the holes with water, and (3) the effect of various absorbers, such as experimental apparatus, at various positions in the holes. Item 2 is of interest from the standpoint of safety since it is conceivable that an accident might occur in which the wall of the hole would collapse or otherwise fail, causing the hole to fill with water and thereby increasing the reactivity. Furthermore, it is likely that water cooling will be desired for experimental apparatus in one or more of the holes on certain occasions, and the data obtained here will indicate the maximum effect of water cooling on $\Delta k/k$.

The location of the holes in the critical experiments is shown in Fig. A3.A, and also in Fig. A3.B which is a sketch of the assembly 3b of Table A3.A. The so-called 6-in. hole is made up of a hollow aluminum tube of square cross-section, having ½-in. wall thickness and measuring 6 in. overall along the edge. The 8-in. hole is of similar construction and measures 8 in. along the outer edge.

The effects of the various holes were measured by the following procedure: A reactor which was just critical with a given amount of poison and with no holes in the reflector was used. A portion of the graphite and beryllium in the region of the hole to be studied was removed, a square aluminum shell was inserted at the proper place, and the reflector was restacked around it. In order to offset the leakage through the hole and bring the reactor back to the point of criticality, an amount of distributed poison must be removed from the core. The effect of the hole on the reactivity of the reactor is given by $\Delta k/k = \Delta\Sigma/\Sigma$. Before inserting a close-fitting paraffin block into the aluminum shell to simulate water filling, the core was poisoned excessively to offset the expected increase in reactivity. When the hole was filled with paraffin, the distributed poison was again adjusted until the reactor was just critical and the reactivity change due to the introduction of paraffin was determined as before.

[redacted]

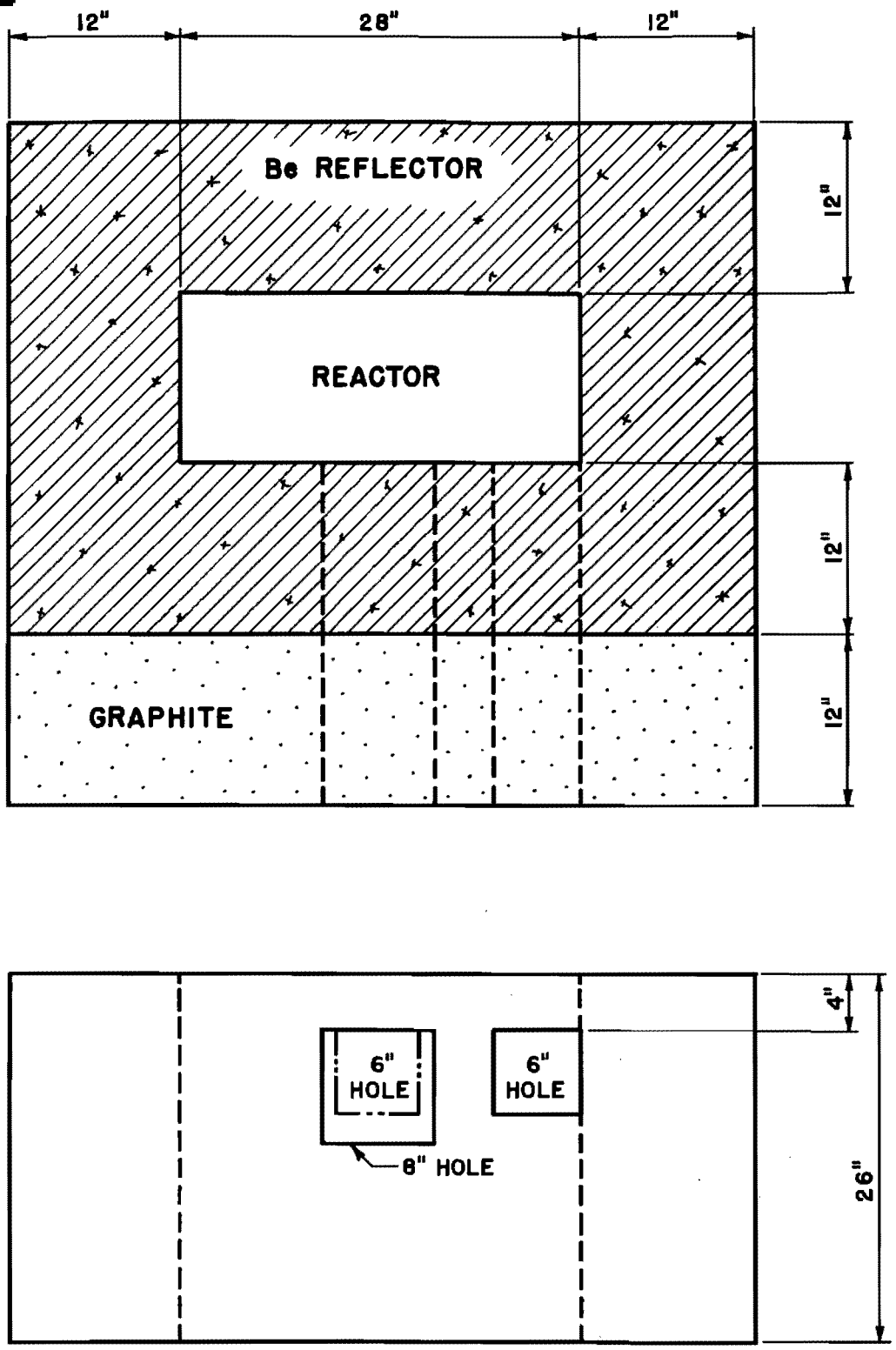

FIG. A3.B

CRITICAL ASSEMBLIES

LOCATION OF HOLES IN REFLECTOR

Table A3.B presents the results of the experiments just described for assemblies 3, 5, and 6 of Table A3.A. Measurements were taken for 6-in. holes at the edge positions and for both 6- and 8-in. holes at the center position. It was thought at one time that some interaction between the holes might take place, but measurements made on individual holes and on various combinations of two or more holes indicated that the effects were approximately additive.

TABLE A3.B

Effect of Experimental Holes in the High-flux Reactor Critical Assemblies

Assembly No.	3	5	6
Reactor dimensions (cm)	71 x 11 x 66	71 x 17 x 66	71 x 22.5 x 66
Critical mass (kg)	1.94	2.94	3.95
Pile (cm^2)	4,118	6,240	8,384
Poison (cm^2)	303	1,140	1,848
Total (cm^2)	4,421	7,380	10,232
Effect of the Holes in $\Delta k/k$ (%) Where k Is the k of the Reactor with Solid Reflector			
Holes extending to reactor-reflector interface			
6-in. hole on edge	1.17	0.75	0.49
6-in. hole in center	2.20		0.86
8-in. hole in center	4.80	2.84	1.71
Holes beginning 15 cm from reactor			
6-in. hole on edge	0.17	0.12	0.08
6-in. hole in center	0.34		0.13
8-in. hole in center	0.68	0.40	0.22
Holes extending to reactor, water filled			
6-in. hole on edge	0.90	0.65	0.42
6-in. hole in center			0.84
8-in. hole in center	3.88	2.45	1.53
Holes beginning 15 cm from reactor, water filled			
6-in. hole on edge		0.08	0.06
6-in. hole in center	0.24		0.06
8-in. hole in center	0.37	0.23	0.11

It is interesting to note that the effect of the holes decreases percentagewise as the thickness of the slab is increased. This was expected on theoretical grounds.

Table A3.C contains a summary of the total cost in $\Delta k/k$ for two alternate provisions for experimental holes. This table shows the change in $\Delta k/k$ that would be expected if the holes in these two cases should be filled with water. An estimate of the cost of the holes in terms of critical mass can be obtained by use of the empirical relation $\Delta M/M = 4.5\ \Delta k/k$. However, this relation leads to a reasonably accurate result only in the case of fuel ΔM added to the periphery of a cylindrical core. In the case of a rectangular geometry, the cost in critical mass (ΔM) corresponding to a given Δk will depend strongly on the statistical weight of the position at which the additional fuel is added, and the figure obtained from $4.5\ \Delta k/k$ is a reasonable approximation only for positions of average statistical weight.

TABLE A3.C

Summary of Total Effect of Experimental Holes

Assembly No.	3	5	6
Reactor dimensions (cm)	71 x 11 x 66	71 x 17 x 66	71 x 22.5 x 66
Mass (kg)	1.94	2.94	3.95
Cost in $\Delta k/k$ of two 8-in. holes plus five 6-in. holes (%)	9.33	5.73	3.56
Cost in $\Delta k/k$ of seven 6-in. holes (%)	6.39	4.23	2.62
Effect in $\Delta k/k$ of water filling two 8-in. holes and five 6-in. holes (%)	2.14	0.94	0.54
Effect in $\Delta k/k$ of water filling seven 6-in. holes (%)	1.41	0.66	0.34

The effect of possible absorbers (experimental apparatus) in the holes on the excess k of the pile was studied by taking the extreme case of a cubical Cd box (0.020 in. of Cd, 10 cm along an edge). The effect of this relatively large absorber on the k of the pile when it was placed at various positions in the holes is shown in Fig. A3.C. From these measurements it is estimated that the maximum excess k required to offset the effect of experimental apparatus in the holes is 1.5%.

[redacted] Dr 5643

FIG. A3.C

EFFECT OF ABSORBER

10 x 10 x 10 CM .020" CD BOX

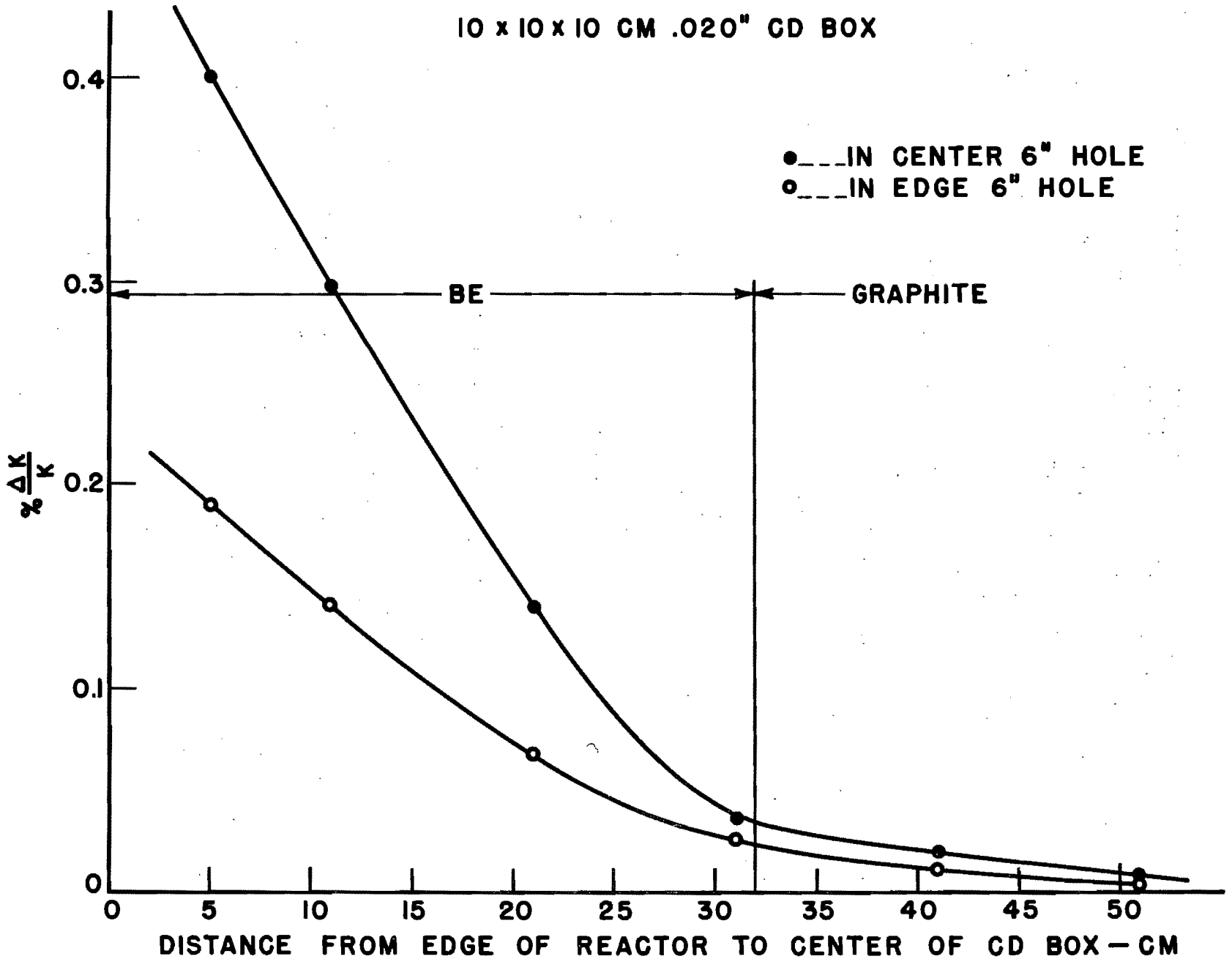

Finally the excess k of the 3.95-kg mock-up of the high-flux reactor was measured. The characteristics of this mock-up include: (1) a core of dimensions 71 by 22.5 by 66 cm, containing 3.95 kg of U^{235} in water solution at a concentration of 37.1 g uranium per liter of pile volume, (2) Al/H_2O volume ratio in the core = 0.65, (3) a reflector on all sides consisting of 30 cm of beryllium plus 30 cm of graphite, (4) no reflector top or bottom, (5) lucite distributed throughout the beryllium to simulate 2% in cooling water, and (6) seven 6-in. experimental holes through the reflector as prescribed in the design of the high-flux reactor. The excess k of this mock-up assembly is found to be 18.8%. When allowance is made for the top and bottom water reflectors of the high-flux machine, the total available excess k is increased to about 20% for this loading. Therefore it appears that a comfortable margin exists over the total k requirements, which are estimated (see Chapter 4) to be as follows:

Xenon	9.6%
Depletion	3.5%
Temperature coefficient	0.5%
Experimental apparatus in holes	1.5%
Total $\Delta k/k$ required	15.1%

A3.3 NEUTRON DISTRIBUTIONS

The spatial distributions of thermal and epithermal neutron flux in the 2.94-kg pile, the 3.95-kg pile, and in the various experimental holes of the mock-up assembly, as indicated in the listing below, were measured. These measurements were made with indium foils, used alternately bare and cadmium covered, as described previously. A calibration of foils in the standard (sigma) reactor indicated that the absolute flux (nv) is obtained from the measured saturated activities, A, shown in the attached figures by the following relations:

$$(nv)_{thermal} = 6.50A_{thermal}$$

? Indium resonance

$$(nv)_{epithermal} = 1.66A_{epithermal}$$

Several of the neutron distributions were measured as follows:

1. Figure A3.D: A lateral traverse across the 2.94-kg reactor (along the short axis of the slab, at mid-height).

2. Figure A3.E: A series of measurements along the centerline of the 6-in. hole which is located at the edge of the long side of the core: (a) with solid reflector in place, (b) with hole extending to the core-reflector interface, and (c) with the hole beginning 15 cm out from the edge of the core. These curves show the depressions in the "solid reflector" neutron distributions caused by the presence of a single 6-in. hole in the reflector.

3. Figures A3.F, G, H: These show the neutron distributions along the axes of the various experimental holes which were planned for the high-flux reactor. These measurements were made with all seven 6-in. holes (or equivalent) in the reflector.

4. Figure A3.I: The fast-neutron flux ($E > 1$ Mev) and the indium resonance flux, measured along a line midway between two of the large experimental holes that extend through the reflector.

The U^{238} fission chamber used to measure the flux of fast neutrons has been described in previous ORNL reports.[2,3]

The results of these experiments indicate that the $(nv)_{fast}$ near the center of the 3.95-kg assembly is 40% of the $(nv)_{thermal}$, in reasonably good agreement with the calculated value of $(nv)_{virgin}$ = 60% of $(nv)_{thermal}$ given in the report MonP-272.

A3.4 GAMMA HEAT PRODUCTION IN THE REFLECTOR

In the high-flux reactor the beryllium is water cooled and there is no concern regarding the possibility of excessive heating in this portion of the reflector. The graphite, however, is cooled only by air, and empirical information on the heat production in graphite was desired to substantiate theoretical calculations. In the reflector, heat production is primarily from absorption of gamma rays. Most of these come from the core of the reactor, but some arise from neutron capture in beryllium and in graphite.

The gamma-ray absorption measurements were made in the rectangular assembly having core dimensions 71 by 17 by 66 cm and loaded to 2.94 kg of fuel. Measurements were made in the core and in the reflector along a line

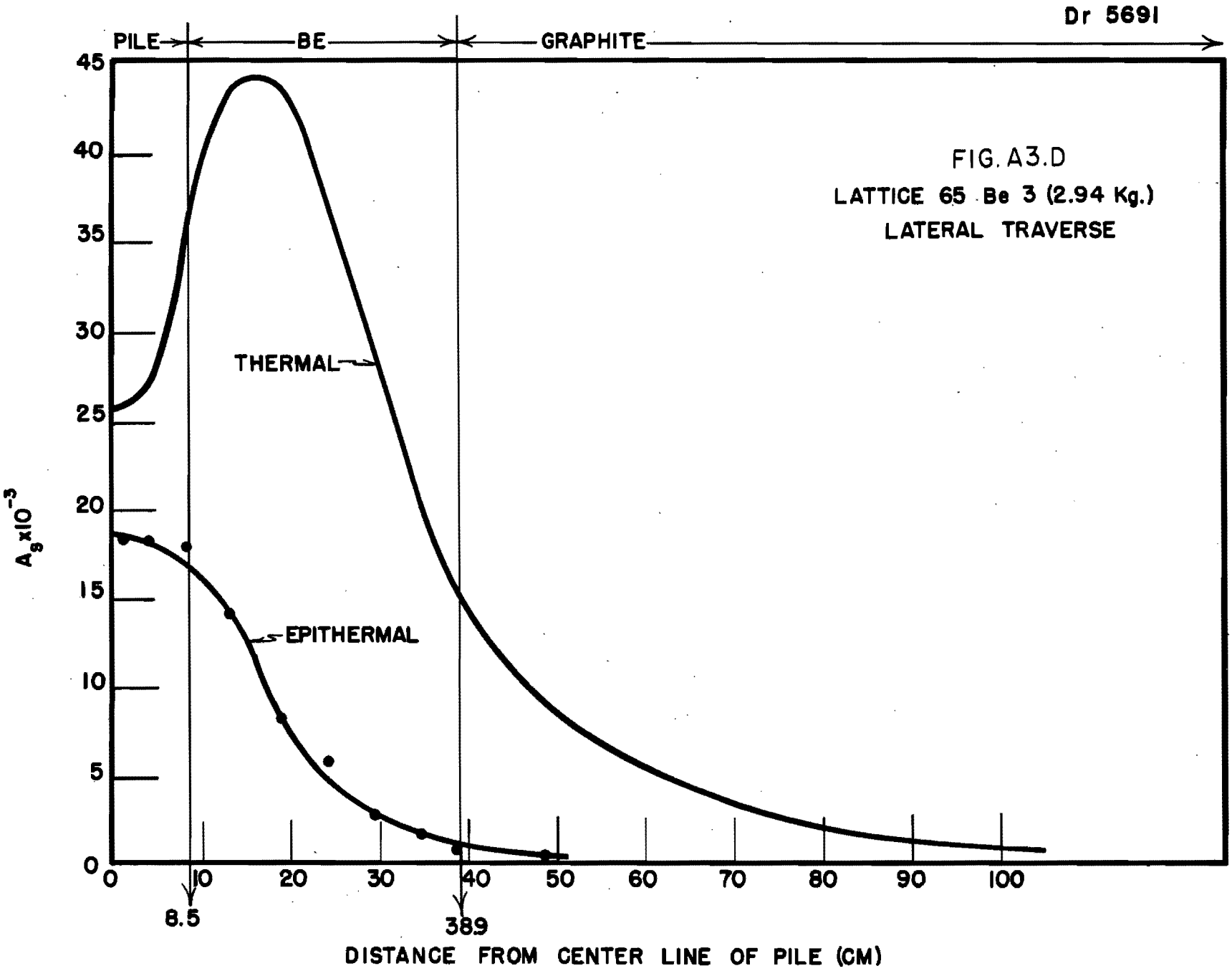

FIG. A3.D
LATTICE 65 Be 3 (2.94 Kg.)
LATERAL TRAVERSE

FIG. A3.E

4 KG SLAB PILE (71 x 22.5 x 66 CM)

2% H_2O IN BE

NEUTRON DISTRIBUTIONS ALONG AXIS OF 6" HOLE AT EDGE OF REACTOR

Dr 5640

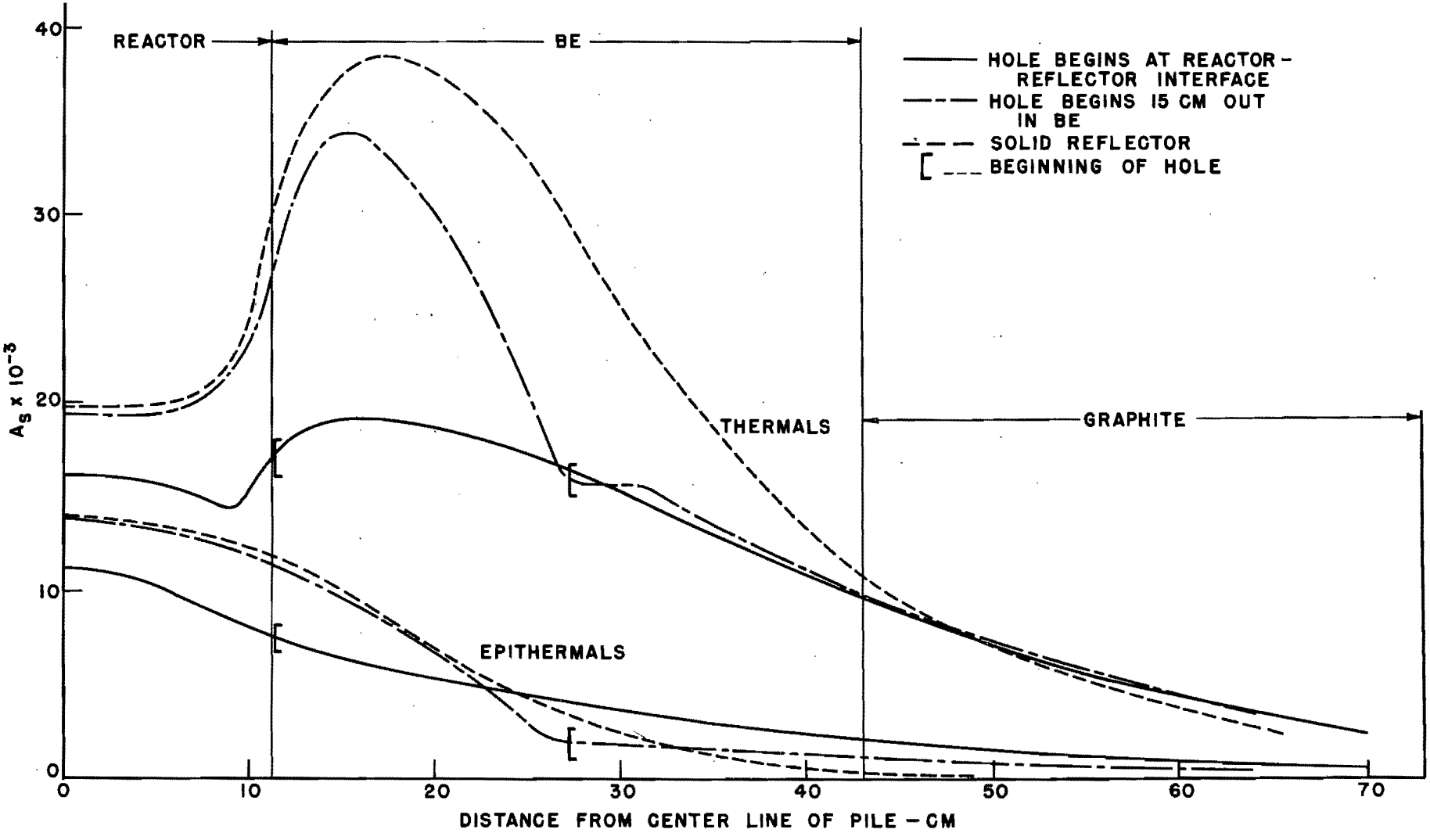

[redacted]

FIG. A3.F

4 Kg SLAB PILE (71 x 22.5 x 66 CM)

7 SIX INCH HOLES IN REFLECTOR

LATERAL NEUTRON DISTRIBUTIONS (ALONG AXIS OF CENTER HOLE)

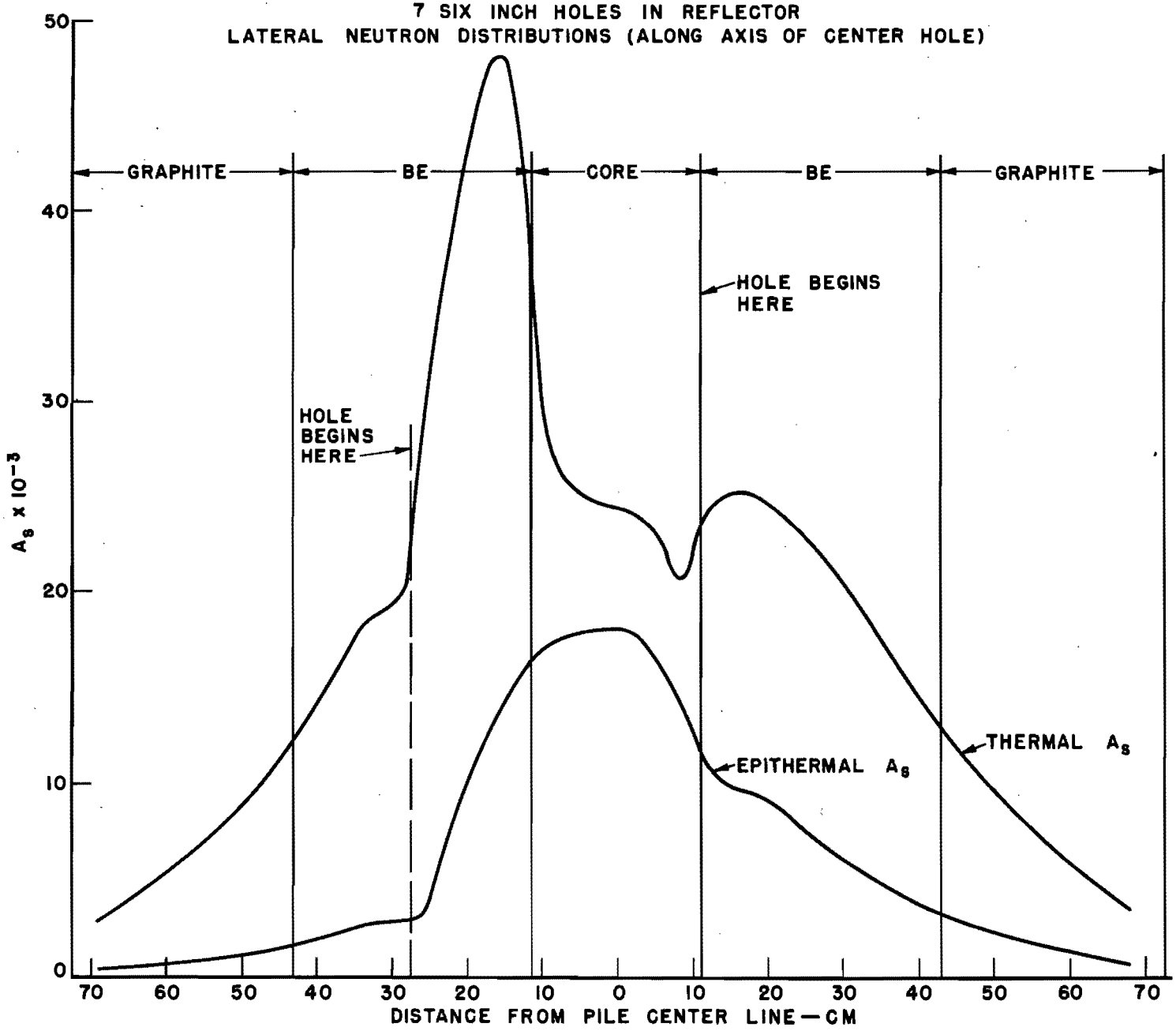

FIG. A3.G

4 KG SLAB PILE (71 X 22.5 x 66 CM)
7 SIX INCH HOLES IN REFLECTOR
LATERAL NEUTRON DISTRIBUTIONS (ALONG AXIS OF EDGE HOLE)

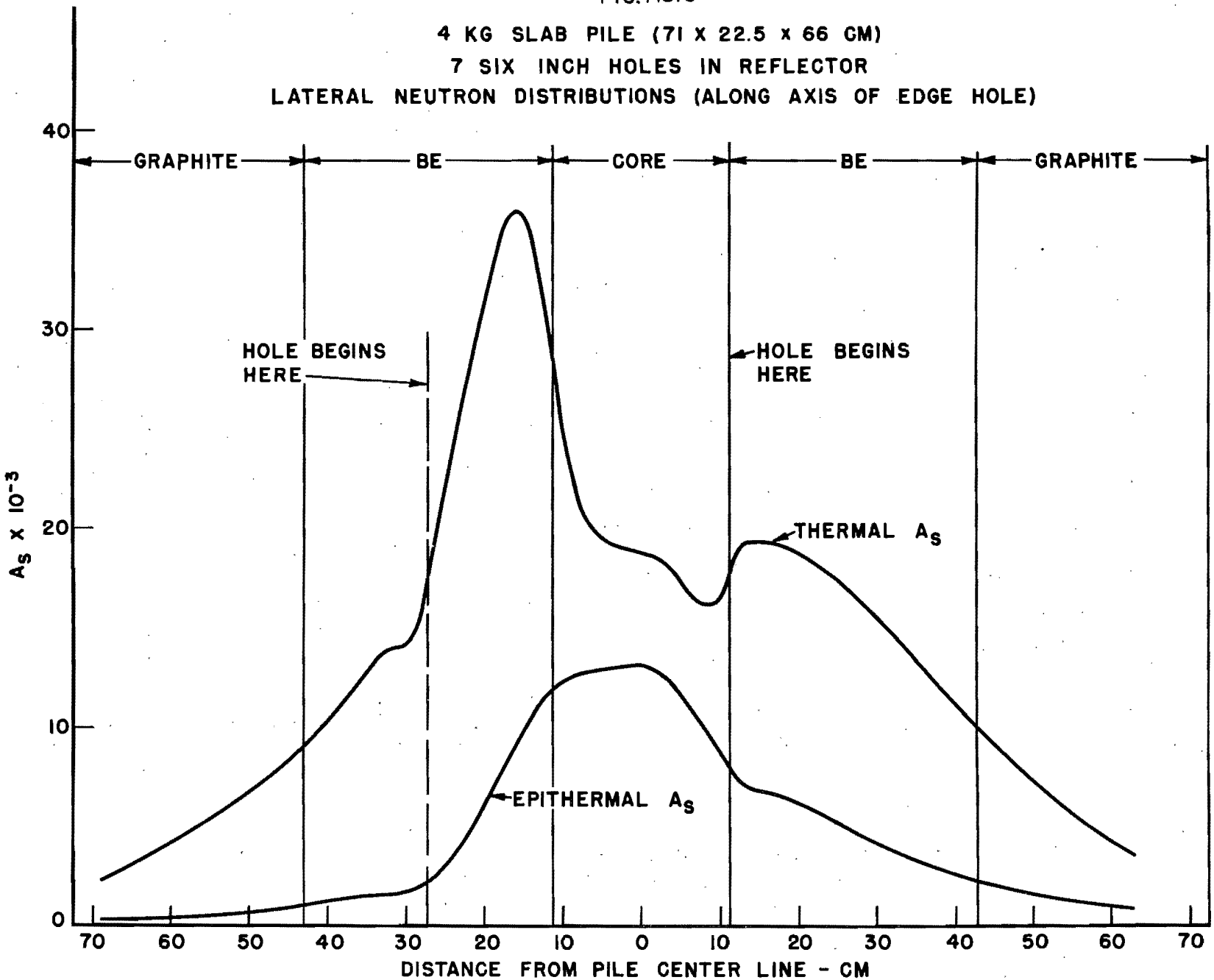

Dr 6081

FIG. A3.H

4 Kg SLAB PILE (71 x 22.5 x 66 CM)
7 SIX INCH HOLES IN REFLECTOR
LONGITUDINAL NEUTRON DISTRIBUTIONS (ALONG AXIS OF END HOLE)

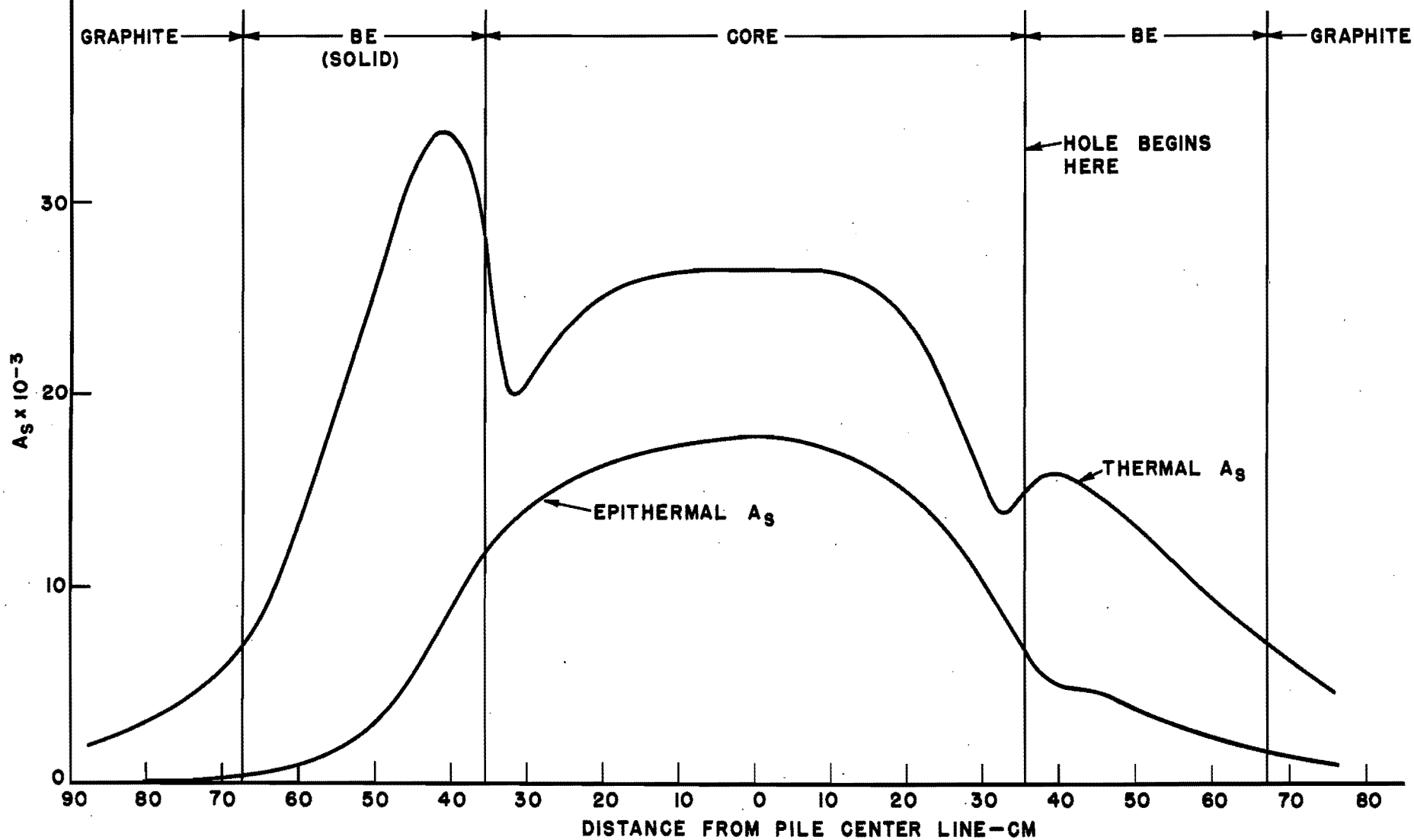

Dr 6087

FIG. A3.1

TRAVERSE TAKEN BETWEEN TWO DEEP HOLES AT MIDHEIGHT OF PILE

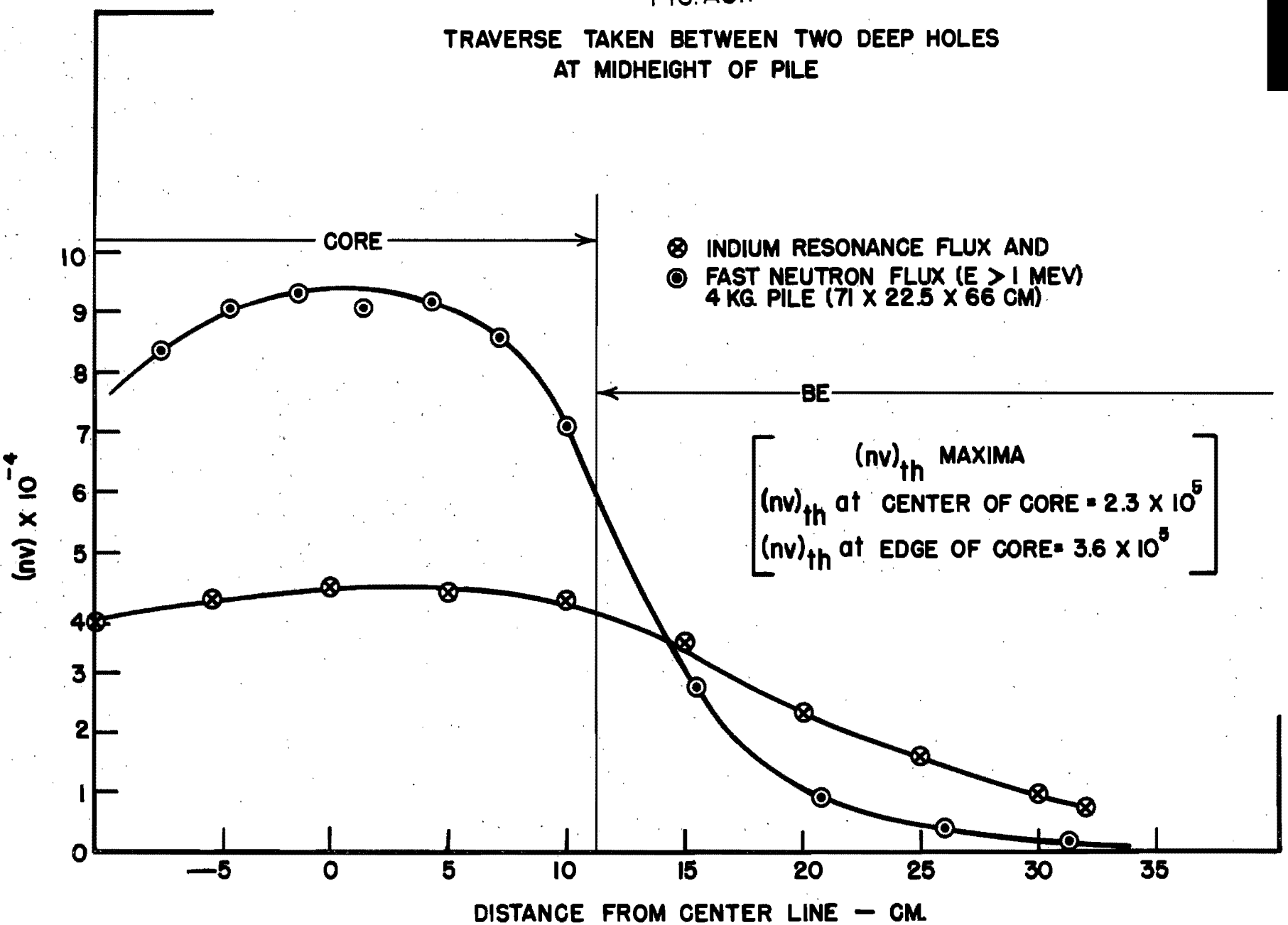

perpendicular to the long dimension of the reactor. Three graphite ion chambers having volumes of approximately 1, 10, and 200 cc were used to cover the range of gamma flux encountered in going from the interior of the core through the beryllium reflector and out to the edge of the graphite portion of the reflector. In order to minimize the possibility of measuring ionization due to unforeseen neutron reactions in the gas of the ion chamber, the measurements were taken with each of four filling gases: air, argon, CO_2, and helium.

The lower solid-line curve in Fig. A3.J represents the total heat production in the reflector calculated from theoretical considerations. This calculation was based on the neutron distribution for a thinner slab pile (70 by 11 by 60 cm) where the heat load in the reflector is somewhat heavier than in the case of the assembly in which our measurements were made (71 by 17 by 66 cm). The measured spatial thermal-neutron distribution in this assembly is shown as a dotted curve.

A3.5 CONTROL ROD EXPERIMENTS

A number of experiments were carried out to study the effectiveness of control rods of various sizes in the 4-kg mock-up of the high-flux reactor. The experiments are performed in the following way: the uniform poison in the "clean" core (before the control rod is inserted) is adjusted until the assembly is just critical. The control rod is inserted and the amount of uniformly distributed poison in the core is reduced until the assembly is just critical. When the experiment involves no change in the amount or concentration of fuel in the core, the percentage change in k, i.e., $\Delta k/k$, is given simply by $\Delta\Sigma/\Sigma$ where $\Delta\Sigma$ is the change in uniform poison and Σ is the total cross-section of the active portion of the core after the rod is inserted. In experiments which entail the removal of fuel *and* the insertion of a control rod, the k of the clean core, k_1, is calculated, the k of the active portion of the core after insertion of the rod, k_2, is calculated, and $\Delta k/k$ is then given directly by $(k_1 - k_2)/k_2$.

The Cd control rods tested in these experiments were essentially replicas of those designed for the high-flux reactor in so far as dimensions and composition are concerned. They were in the form of hollow cylinders of square, 3¼ by 3¼ in., cross-section and 26 in. long and were filled with water to duplicate the conditions that will be obtained in the case of the high-flux reactor.

[redacted]

Dr 5690

FIG. A3.J

GAMMA HEAT PRODUCTION IN REFLECTOR OF 3 KG PILE (71 x 17 x 66 CM)

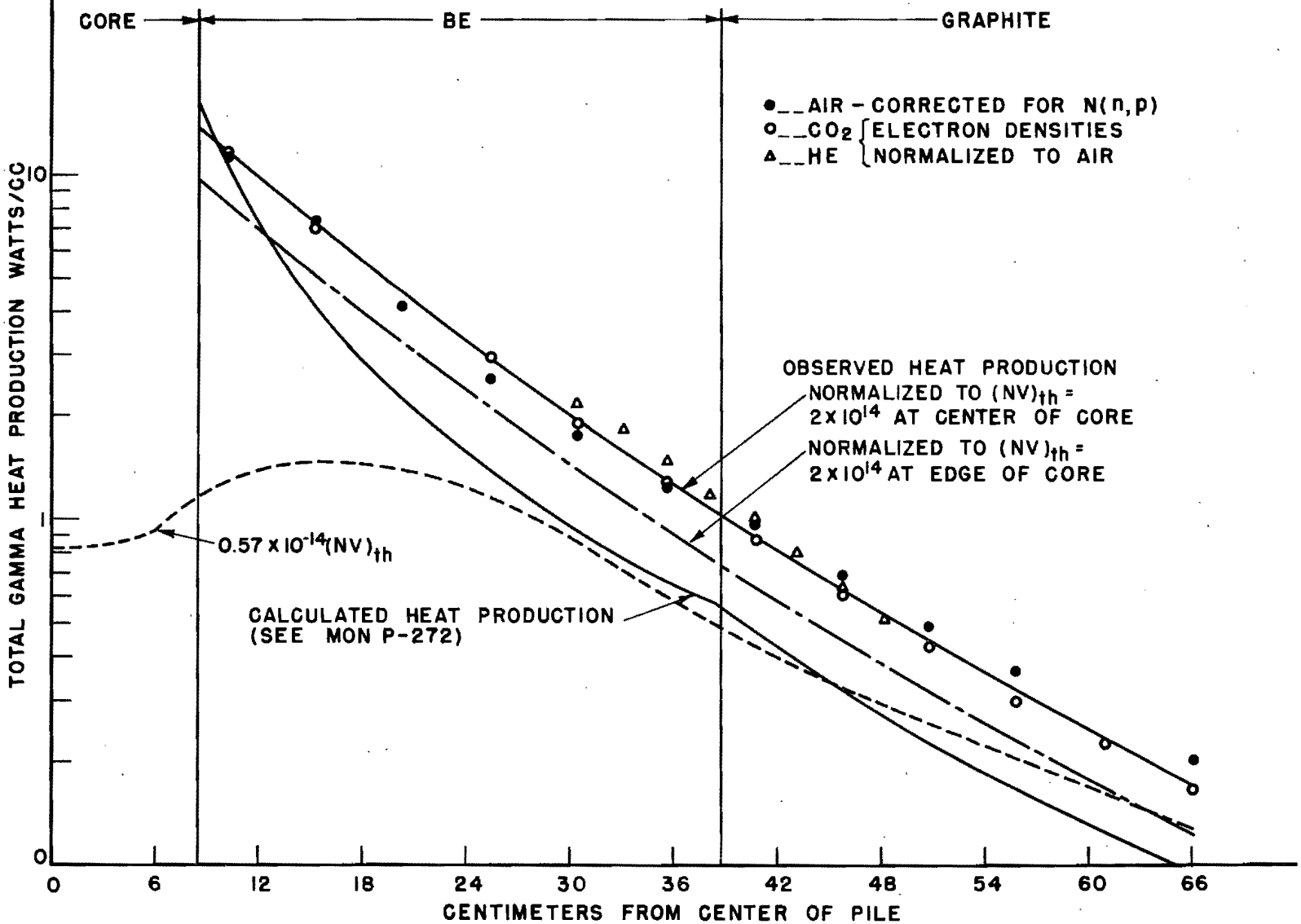

[redacted]

The thorium rods for the high-flux reactor are designed to be made up of several plates; they are stacked in a sandwich-like assembly, with spaces between plates for the passage of cooling water. Iron was used instead of thorium for reasons of availability and ease of fabrication, the amount of iron being adjusted to give the same total thermal cross-section as that provided by the thorium rods. The test rod then consisted of a rectangular sandwich of iron and lucite plates having the same dimensions as the Cd rods described above.

For use in the high-flux reactor it was planned for these rods to be attached at one end to fuel assemblies so that as a rod is withdrawn fuel is inserted in its place and vice versa. Therefore the measurement of interest was the effect of the rod versus fuel in the same position. The percentage changes in reactivity of the active portion of the core, when these rods were inserted in place of fuel, were as follows:

ROD	$\Delta k/k$ (%)
Cd	7.3
Cd	20.7
Th	4.2
Th	9.0

It was also observed that the reactivity change due to the removal of 180 g of fuel (nine tubes or a 3¼- by 3¼-in. section) from a central position amounted to about 3%.

A3.6 REFERENCE REPORTS

(1) Martin, A. B. and Mann, M. M., *Critical Experiments for the High Flux Reactor*, ORNL-167, October 22, 1948.

(2) *Quarterly Report of the Physics Division for March, April and May, 1948*, ORNL-51, July 15, 1948.

(3) Mann, M. M. and Martin, A. B., *Further Critical Experiments on a Small Reactor of Enriched U-235/Al-H_2O Moderator and Be Reflector*, ORNL-79, September 16, 1948.

Appendix 4

MOCK-UP

INTRODUCTION

In 1947 when the design of the MTR's predecessor, the High Flux Pile, was nearing completion it was recognized that many features of the reactor would require thorough testing before the design could be considered final. It appeared logical, economically and experimentally, to assemble a full-scale model with which many studies could be made rather than to construct separate equipment for each experiment. It was planned to fabricate major parts (e.g., top plug, aluminum tank, grids, castings) with the intention of using them later, if proved satisfactory, in the actual reactor. The reflector, an item of major importance for hydraulic testing, was to be fabricated of aluminum because beryllium production was still in the development stage.

Two general groups of experiments were made. Studies of a mechanical nature included assembly and alignment techniques, stress-strain investigation of major structural parts, performance of the safety and regulating rod systems, and the development of tools for refueling and remote disassembly of all parts.

Hydraulic studies were made to investigate the adequacy of cooling in the reflector, safety rods, and fuel pieces.

After completion of this "mechanical" program in September, 1949, it appeared that much could be learned by converting the Mock-Up into equipment for low-power nuclear experiments such as critical mass determination, neutron- and gamma-flux measurements, and operation of the control system. These studies occupied the period from February, 1950 to September, 1950.

A4.1 DESCRIPTION OF FACILITY

In an effort to keep the cost of the project at a minimum, the Mock-Up structure was designed for outdoor operation with the enclosed space limited to the control room. The structure, illustrated in Fig. A4.A, consists of four main steel columns to support the reactor tank and a 10-ton traveling crane. The working level at the top of the tank, 22 ft above grade level, is floored. A 12-ft deep "sub-pile room," 15 by 15 ft, is provided underneath the reactor tank.

[redacted]

DWG. 7911

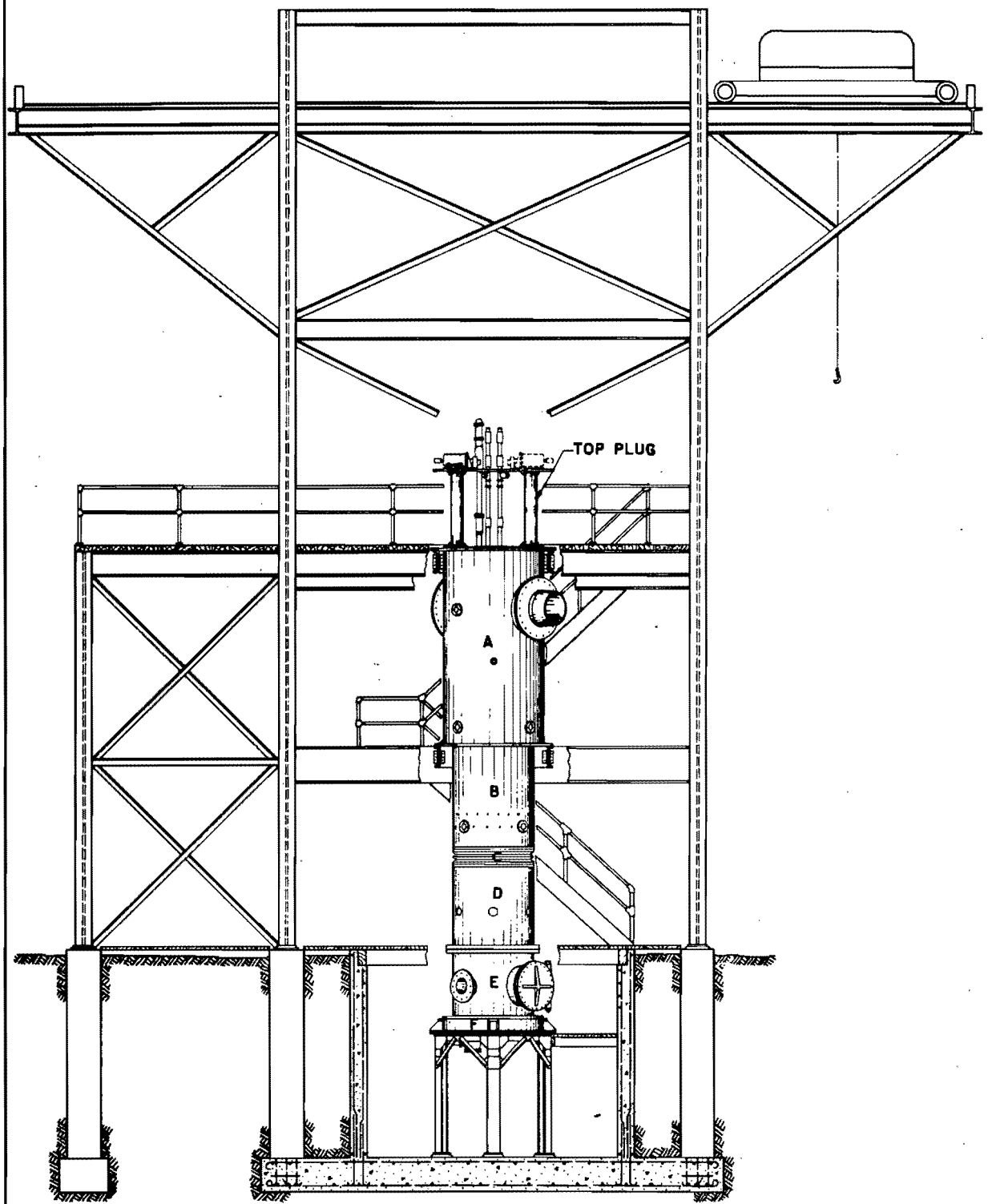

FIG. A4.A

DIAGRAM OF PILE TANK

The water-circulating system was greatly simplified as compared to the MTR. Its only purpose was to provide a maximum flow of 15,000 gpm, and it consisted of two 7500-gpm 100-psi-head pumps which fed the reactor tank through 20-in.-diameter pipe lines. The discharge from the base of the reactor flowed to a 6000-gal capacity surge tank and thence back to the pumps. Six small shell-and-tube heat exchangers were supplied to remove the energy input (about 350 kw) of the pumps. The entire circulating system with the exception of the aluminum section of the reactor tank was constructed of mild steel and coated with Amercoat, a plastic material for corrosion protection.

The reactor tank from top plug to bottom plug was identical to the actual reactor design[1] of that date except for the substitution of Amercoat-covered mild steel for stainless steel at tank sections A, B, E, and F. The top plug was equipped with two safety rods and one regulating-rod drive. All bearings, grids, etc. were supplied for the aluminum tank section. The reflector was made of aluminum, as already mentioned, and the "fuel" was fabricated as uranium-aluminum alloy.

A detailed description of all parts of the Mock-Up may be found in the *Mock-up Design Report*.[2] Information concerning the assembly and erection of the system is presented in *Procedure for Erection of the MTR Mock-Up*.[3]

After approximately six months of study on the dummy reactor, changes were made to allow operation as a nuclear machine intended to duplicate MTR conditions at very low power levels. A detailed account of the alterations made at that time appear in ORNL CF-50-5-140.[5] The alterations consisted essentially in providing the following necessities:

1. Fuel in the form of standard MTR assemblies.
2. A beryllium reflector built with small beryllium bricks to approximate MTR dimensions on two faces of the lattice with Class II reflector pieces ("L" pieces, Be in lattice) on the other two faces.
3. A graphite reflector consisting of 300,000 graphite pebbles and 50 tons of block graphite arranged in three quadrants of the reactor tank.
4. A 4-ft-thick shield of concrete block, unmortared, surrounding the graphite.
5. Instrumentation equivalent to two MTR safety channels and other necessary operating circuits.

These details are shown in Figs. A4.B and C.

[redacted]

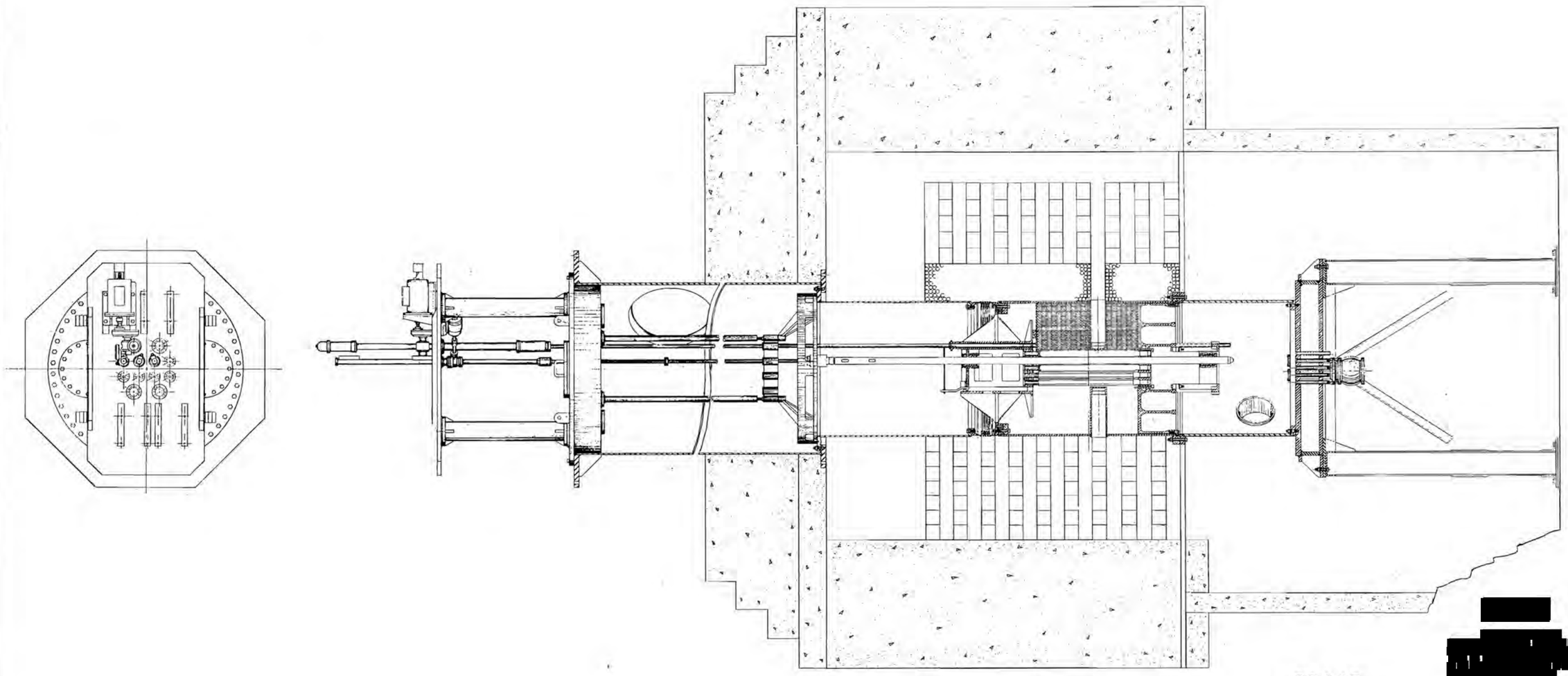

[redacted]

FIG. A.4.B

TOLERANCE UNLESS OTHERWISE SPECIFIED FRACTIONS ± DECIMALS ± ANGLES
BREAK ALL SHARP EDGES UNLESS OTHERWISE SPECIFIED
FINISH MARKS ASA STANDARD
DO NOT SCALE THIS DRAWING

APPD.	DATE	OAK RIDGE NATIONAL LABORATORY
		TECHNICAL DIV — P.O. BOX — OAK RIDGE, TENN.
		MTR MOCK-UP ASSEMBLY FOR LOW POWER EXPERIMENTS
		DRAWN BY / DATE / SCALE
		CHECKED BY / DATE / DRAWING NO. TD-1968 / REV.

REV. NO.	REVISION	APPD.	DATE

Dwg. No. 8916

[redacted]

FIG. A4.C

LAYOUT OF HOLES FOR FLUX MEASUREMENTS OUTSIDE OF REACTOR TANK

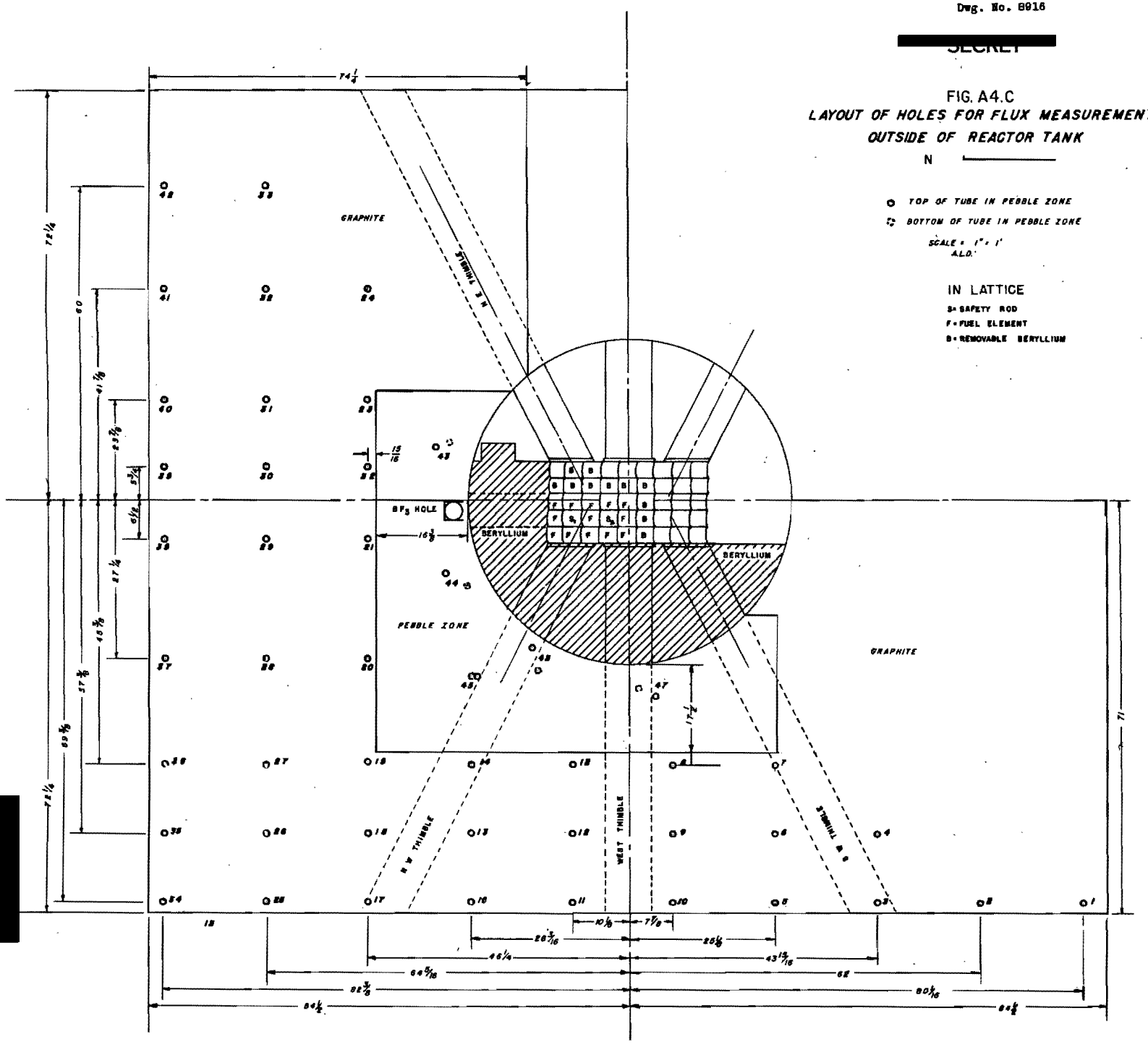

[redacted]

A4.2 MECHANICAL EXPERIMENTS

The mechanical and hydraulic investigations were begun in May, 1949 and consisted of the following:

1. Stress-strain measurements.
2. Mechanical test of the control system.
3. Development of remote-handling tools.
4. Hydraulic measurements in lattice and reflector.

A4.2.1 Stress-Strain Measurements. The complexity of tank structure D with respect to stress analysis made it desirable to obtain measurements at questionable points in the Mock-Up. The required information was obtained from Baldwin-Southwork strain gauges attached directly to the various components of the tank. The results of these measurements are reported in ORNL-472.[4]

The electric resistance wire elements were attached according to the following plan:

	NO. OF ELEMENTS
Tank section D, outside surface	14
Skirt plates	4
Upper assembly grid	2
Upper support casting	5
Lower support casting	5

Roughly half of the strain gauges were single elements which were employed at locations where the direction of the stress could be easily predicted. Where the direction was unknown, a triangular arrangement of three elements was used so that both the magnitude and the direction of the stress could be determined.

Measurements were made early in the experimental program and before the full pressure drop across the lattice was applied. However, the magnitude of the stresses calculated from the strain measurements were low enough in all cases to provide assurance that no component was in danger of being overstressed even at much higher pressure drops.

Maximum stresses for the components during operation at about 30 psi ΔP were:

LOCATION	STRESS (psi)
Tank section D, 6 in. below upper flange	1920 (tension)
Skirt plate, center	1850 (tension)
Upper assembly grid, center	950 (compression)
Upper support casting, center bottom	1300 (compression)
Lower support casting (side, center of grid opening)	2020 (compression)

The 356-T7A aluminum alloy with which the castings were made has a yield strength of 25,000 psi at 0.2% set. Tank section D was fabricated of 3SF aluminum with a tensile strength of 17,850 psi and a minimum yield strength of 6,000 psi.

A4.2.2 Control System. Except for the control system, which includes both shim-safety and regulating rods, the reactor has practically no moving parts. Because this system is roughly the brain and nervous system of the reactor and should operate for its lifetime, it was important that the control mechanics be tested very thoroughly.

For these reasons the Mock-Up was provided with two complete shim-safety rod channels and one regulating rod channel. The control room contained the operating console which served as the study model for the MTR desk and a relay panel, both equipped with the necessary electrical equipment for testing system performance.

Console. The console for the Mock-Up was little different from that planned for the MTR. A few switches were relocated and the functions of one or two were changed. The wings to the right and left of the operator were moved inward to bring them within easier reach. Except for these minor changes, the design was considered adequate and was approved for the MTR.

Shim-Safety Rods and Drive Mechanisms.[6,7] The shim-safety rods and drive mechanisms constituting the original Mock-Up controls were considerably different from the elements currently designed for the MTR. A brief history of the evolution of the present MTR shim-safety assemblies will be given for each part of the assembly.

(*a*) Shim-Safety Rods. Originally the rods consisted of five separate sections which were, from top to bottom: armature section, upper stainless steel section, cadmium (or thorium) section, fuel (or beryllium) section, and lower stainless steel section. These rods were expensive (about $3,000 each) to manufacture considering their estimated life (one month). In the course of testing the rods several possible refinements to the original design became apparent.

In the armature section the cadmium plating was not sufficient protection to prevent rusting of the 1010 steel. Nickel plating was substituted for better corrosion protection. The nickel plating, being magnetic, had the additional advantage of reducing the magnet-to-armature air gap, allowing a gain of about 25 lb in magnet holding force. The original sharp-edged corners of the armature made it difficult to position the upper assembly of grids over the rods, and as a result the corners were beveled to make this operation easier.

The upper section of the rod serves three purposes: (1) as bearing surface for the guide bearings, (2) as inlet port for cooling water, and (3) as a "spacer" to keep electromagnets outside the intense neutron-flux region. Being necessarily long, this stainless steel section was also heavy (about 50 lb). Mass at this point and in the absorber section below is undesirable because of the large force exerted on the comparatively weak uranium-aluminum section during deceleration of the rod. In fact, after repeated drops the aluminum was found to be deformed at its joints and the machine screws holding these joints were loosened. It was apparent that the upper sections of the rod should be made of lighter material, and an aluminum extrusion with a cadmium box insert was designed to replace the upper stainless steel and cadmium sections.

Although this weight reduction was desirable from the standpoint of damage to the fuel section and joint strength, it was considered necessary to keep the total weight of the rod above 100 lb for the situation requiring a scram with no water flow. Experiments showed that buoyancy and bearing-friction forces were great enough to keep a rod weighing less than 70 lb from falling if the 350-lb driving force due to water pressure were absent.[8] To eliminate this danger lead was added to the lower stainless steel section, and guide bearings were redesigned to minimize friction.

Velocity measurements on the original rods showed a peak speed of 16 ft/sec with full water flow (see Fig. A4.D). An acceleration of about 4g is indicated, and these data should hold for present MTR rods.

The Mock-Up was equipped with safety-rod shock absorbers with bellows-sealed plungers at the base to indicate the presence of the rod. The indicating function is unrelated to the primary purpose of the shock absorber, that of decelerating the falling rod, but is important from the standpoint of control. The plunger type indicator gave constant trouble by water leakage to the limit switches underneath and from galling. Hydraulic actuators were designed for the MTR but could not be tested in the Mock-Up because of limited time.

The operation of the dash pots as decelerators is illustrated by the curve of Fig. A4.E which shows a terminal rod velocity of 3 ft/sec. Maximum pressures were measured for various entrance velocities and found to be 200 psi for the 16-ft/sec velocity resulting from a 10-psi pressure drop across the reactor tank.

The bearings which serve to guide the upper and lower ends of the rods originally contained spring-loaded graphite pads as the bearing surfaces. The graphite scored easily and was found to offer a resistance of approximately 40 lb to the fall of the rods. Stainless steel rollers with graphite inserts have been designed to replace the graphite and have proved adequate during several months of usage.

(*b*) Electromagnets. The initial design of the electromagnets was based on the requirement that they operate under a water pressure of 50 psi, support 1000 lb load at 200 mamp current, and release this load in less than 30 msec (the minimum period of which the reactor is capable in a start-up accident). After test units had been constructed, it was found that the release times were about double those expected and that the watertight seals were inadequate.

The release time deficiency was traced to shorted turns in the coils. Subsequent coils were redesigned and manufactured by the Westinghouse Electric Corporation. In the course of the investigation, the coils were tested on core materials of Permandure and Hypersil alloys in addition to the 1010 steel chosen for the final design. With properly manufactured coils on the 1010 steel cores, release times of considerably less than 30 msec were measured.

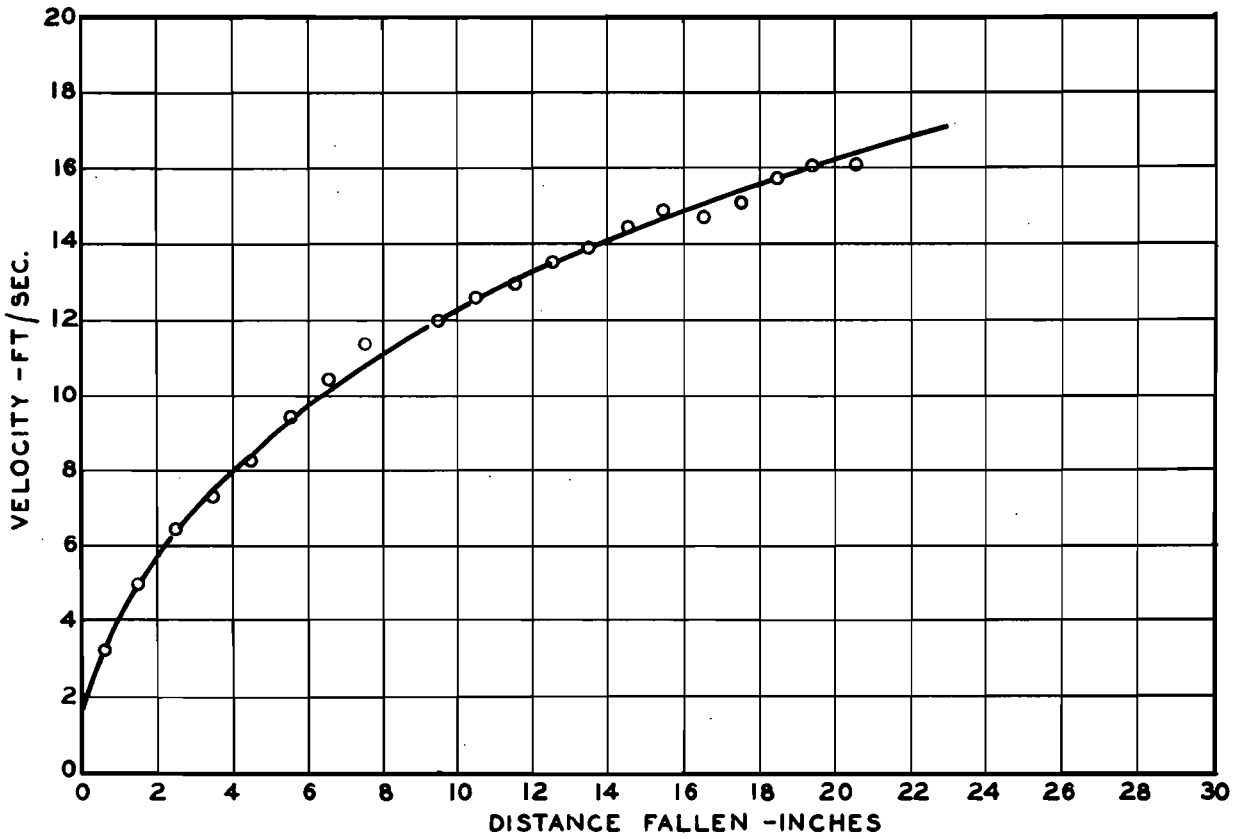

FIG. A.4.D
RATE OF FALL - SAFETY ROD
40 PSI ΔP

DWG. # 10805
NOT CLASSIFIED

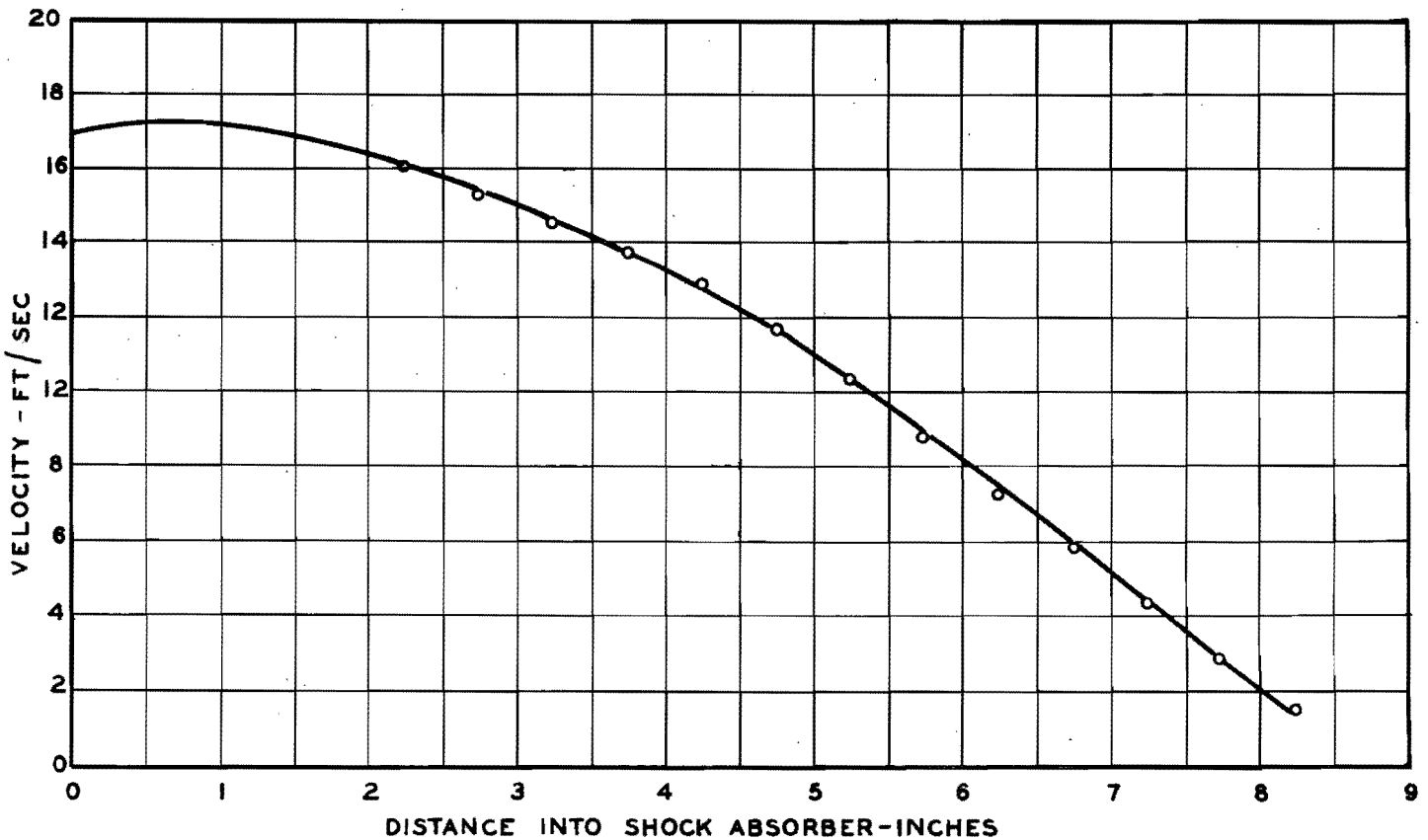

FIG. A.4.E
DECELERATION OF SAFETY ROD

DWG. #10804
NOT CLASSIFIED

In fact if one minimizes the ratio of holding force to force actually held by varying the current, the armature-to-pole-face air gap, or the load supported, the release time can be reduced to 2 or 3 msec. The net result of much experimentation with these factors was to specify a current of 100 mamp and an air gap of about 0.010 in. which can be adjusted to give a holding force of 600 lb. For the case of full water flow, the total load on the magnets is about 500 lb and a release time of about 10 msec can be expected. With no water flowing and only the dead weight of the rod (about 100 lb) supported, the release time is 30 to 40 msec. The holding-force curve for a typical magnet is presented in Fig. A4.F. In Fig. A4.G are the records of two release-time measurements.

The failure of the gasketed water seals on the pole pieces of the initial design led to a complete enclosure of the core with a stainless steel can. This change necessitated removal of a microswitch and a bellows-sealed actuator which were contained inside the old can for the purpose of indicating physical contact with the shim-safety rod. The indicator currently in use takes advantage of the fact that the rods are at ground potential electrically and the demineralized water has a high resistance. By insulating the magnets from the drive shafts and applying a 6-volt potential, the current which flows when the magnet face contacts the rods is sufficient to trip a relay which indicates contact and energizes the magnets.

The magnets installed at the Mock-Up were fastened to the drive shafts by six ½-in. bolts. Calculations indicated that the magnets would be considerably above tolerance radiation after long-time operation at MTR levels. To simplify the replacement of faulty magnets a quick-release mechanism has been adopted for MTR magnets.

The requirement for an insulating and shielding liquid with which magnets and drive shafts could be filled is that the liquid not suffer radiation damage (i.e., loss of insulating qualities or severe degassing), that it be heavier than water (so that leakage water will not accumulate above the magnets), and that it not attack the magnet construction materials. The liquid now used is the only insulator of many tested which adequately fills these requirements.

The flexible connections now incorporated in the shim-safety rod design were previously a section of the drive shafts, immediately above the magnets.

DWG. #10806
NOT CLASSIFIED

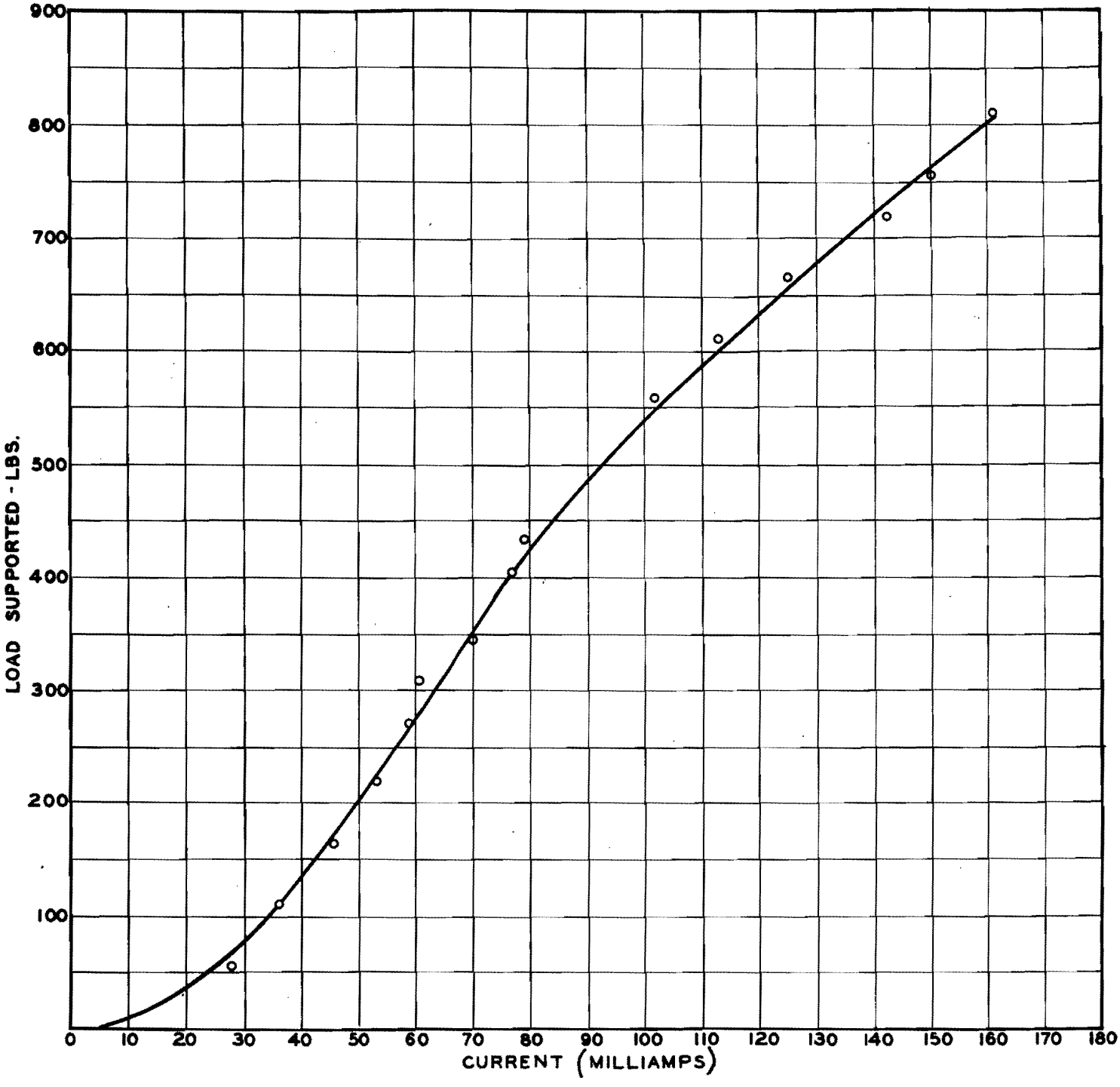

FIG. A. 4.F

WESTINGHOUSE BUILT MTR MAGNET #1
LOAD VS RELEASE CURRENT

0.002 MICA SHIM
0.008 STAINLESS STEEL SHIM

DWG. #10811
NOT CLASSIFIED

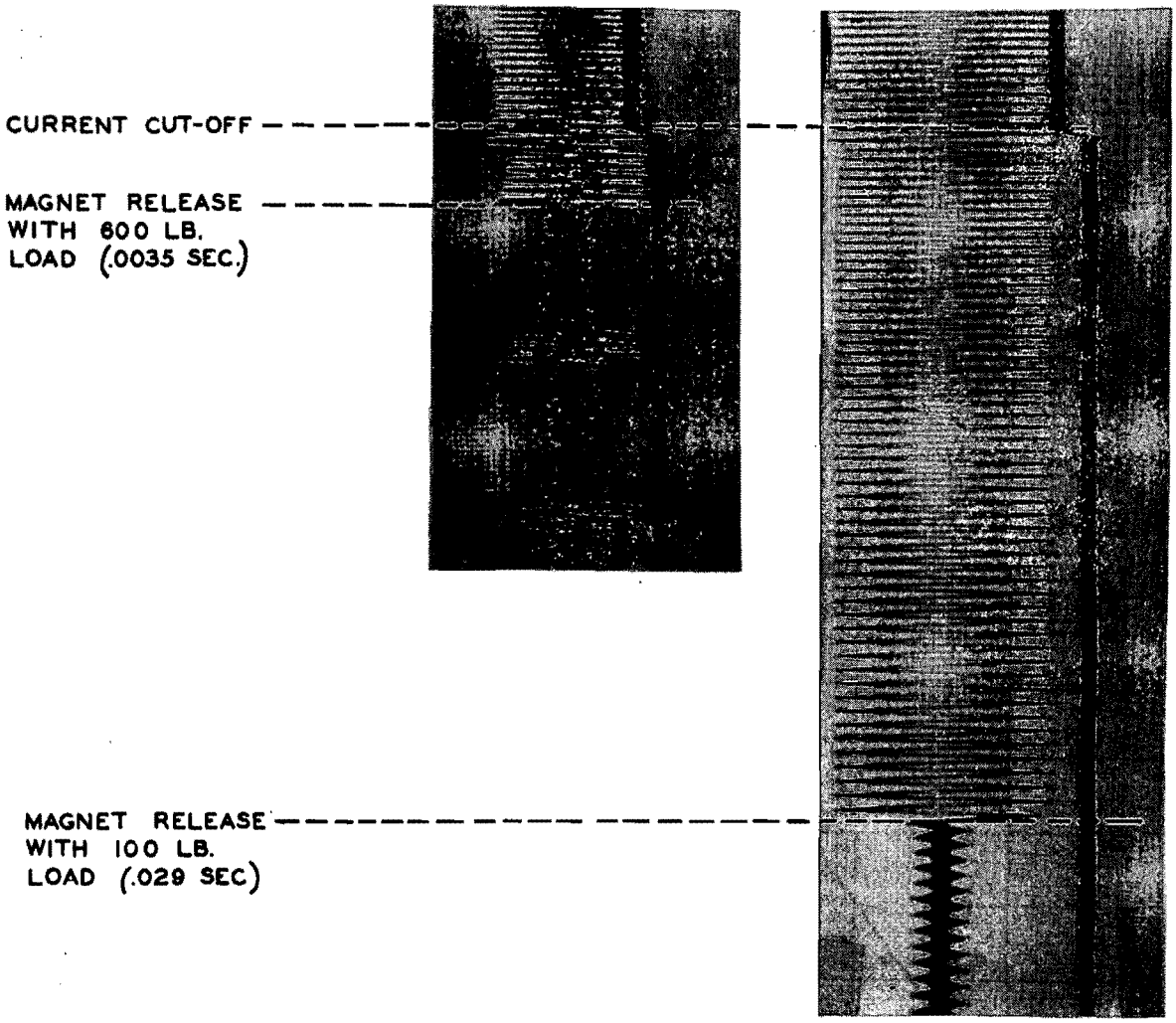

FIG. A.4.G

TYPICAL MAGNET RELEASE TESTS

(2000 cps Time Trace)

Their purpose is to correct misalignment and to allow approximately 3/8-in. overtravel of the drive motors after current cut-off. The original design allowed excessive movement of the magnets under full water flow and gave considerable difficulty through abrasion of the magnet leads. The simpler joint now at the top of the safety rod appears to be adequate.

(*c*) Drive Mechanisms. The worm gear—acme thread speed reduction units were studied with respect to measurement of backlash, overtravel, wear, actual speed reduction, and time of reversal. Total backlash from motor shaft to magnet drive shaft was less than 0.010 in. Overtravel was 0.10 in. upward and 0.17 in. downward. The actual speed of rod withdrawal was 5.0 in./min, and time of reversal was less than 0.1 sec. All measurements were made with shafts loaded to 600 lb. After approximately 400 hr of operation the total backlash had not increased, and it was assumed that no serious wear had resulted.

Regulating Rod and Drive Mechanism.[9] The MTR regulating-rod and drive mechanism assembly are very similar to the originals installed in the Mock-Up. The Mock-Up rod was thoroughly tested from standpoints of general operability, mechanical design, and reactor control.

Some difficulty was experienced with the sleeve guide bearing located in the upper and lower support castings. Because of grit particles the rod and bearings galled severely, necessitating removal and refinishing. The bearings were redesigned as spring-loaded stainless steel rollers which eliminated the galling trouble. However, during the low-power nuclear experiments with full water flow it was learned that the bearings permitted lateral movement of the rods, which affected neutron detection instruments as would a minor instability of the reactor. The low-power experiments were completed before stronger springs could be tested.

Another difficulty with the original design was the method of attaching the rod to its drive shaft. The coupling was designed as a screw joint to be actuated by a 20-ft-long bolt after removal of the upper shock absorber. Rotation of the rod during the coupling operation was prevented by a horizontal pin through the rod which mated with a slot in the upper bearing. Awkward features were eliminated by a redesign including a new upper shock absorber which need not be removed to accomplish attachment or detachment of the rod; a ball-and-socket joint replaced the threaded joint, and the necessity for a pin and slot were thus eliminated.

The lower shock absorber of the drive mechanism exhibited an annoying quirk of not returning to its rest position after compression. This trouble was corrected by insertion of a stronger spring and by attachment of a small check valve at the oil-fill port.

Before the regulating rod was used with its servo mechanism as a control device, experiments were devised to measure its response time. The test consisted in unbalancing the electronic system with an applied voltage (instead of an ion chamber signal) and measuring the time required for rebalancing. The response time for the maximum unbalance was found to be about 0.1 sec and is considered adequate for control of known MTR instabilities.

Full-scale test of the servo mechanism as an automatic control device was accomplished during the low-power nuclear experiments described in Section A4.5.7. The system performed satisfactorily for several months at power levels from 100 watts to 175 kilowatts.

A4.3 HYDRAULIC EXPERIMENTS

The high-power density (about 300 kw/liter) at which the MTR operates imposes rather stringent requirements for heat removal. Cooling-water velocities of 30 ft/sec and heat fluxes as high as 500,000 Btu/sq ft-hr are necessary for the realization of design performance.

The desire for more complete knowledge of the complex hydraulic characteristics of the MTR was an important reason for construction of the full-scale Mock-Up.

Early design calculations indicated that the following conditions could be expected in the reflector and fuel lattice:

LOCATION	VELOCITY (ft/sec)	PRESSURE DROP (psi)
(1) 1/8-in.-diameter holes in reflector pieces	10	6
(2) 0.118-in. slot between fuel elements	25	17
(3) Fuel elements with 0.118-in. gaps	30	42 (including end boxes)
(4) Shim-safety rods (Th-U)	30	42
(5) Across upper assembly grid		12
(6) Across lower assembly grid		13
(7) Across lower support casting		36

Water requirements for 42 psi pressure drop were:

ELEMENT	FLOW OF WATER (gpm)
23 fuel pieces (slab loading)	10,500
8 shim-safety rods	3,200
Reflector	1,000
Lattice interstices and Be in lattice	1,500
Total water requirement	16,200

The Mock-Up problem assignment was to determine whether the calculated pressure drops and flow rates actually existed.

The experimental work was divided into two groups: (1) flow in the reflector, and (2) flow inside the fuel lattice.

A4.3.1 Flow in Reflector Outside the Fuel Lattice. The reactor is designed in a manner such that the beryllium reflector occupies the space (15 by 30 in.) between the rectangular lattice area at the center and the wall of the 54-in.-diameter aluminum tank. At the time the Mock-Up was built the reflector consisted of approximately two hundred separate pieces, each roughly 3 by 3 by 40 in. high. In general, each separate piece was provided with several 1/8-in.-diameter cooling holes extending through the piece from top to bottom. A few pieces of odd sizes and shapes, such as those above and below the experimental thimbles, had larger or different cooling passages. The general aim in the design of the reflector cooling passages was to provide sufficient water to remove approximately 6,000 kw of heat produced by γ-ray and neutron energy from the fuel lattice.

The problem of measuring the various velocities and pressures was approached by selecting a typical quadrant of the reflector for detailed study. A few pieces were chosen in other quadrants as check points and others where special situations arose. Figures A4.H and I show these selections. One cooling channel in each reflector piece was provided with two static pressure taps and calibrated for flow versus pressure drop before installation.

After positioning a particular piece in the Mock-Up reflector, small stainless steel tubing leads from the pressure points were attached to Cannon

[redacted]

Drawing #7641

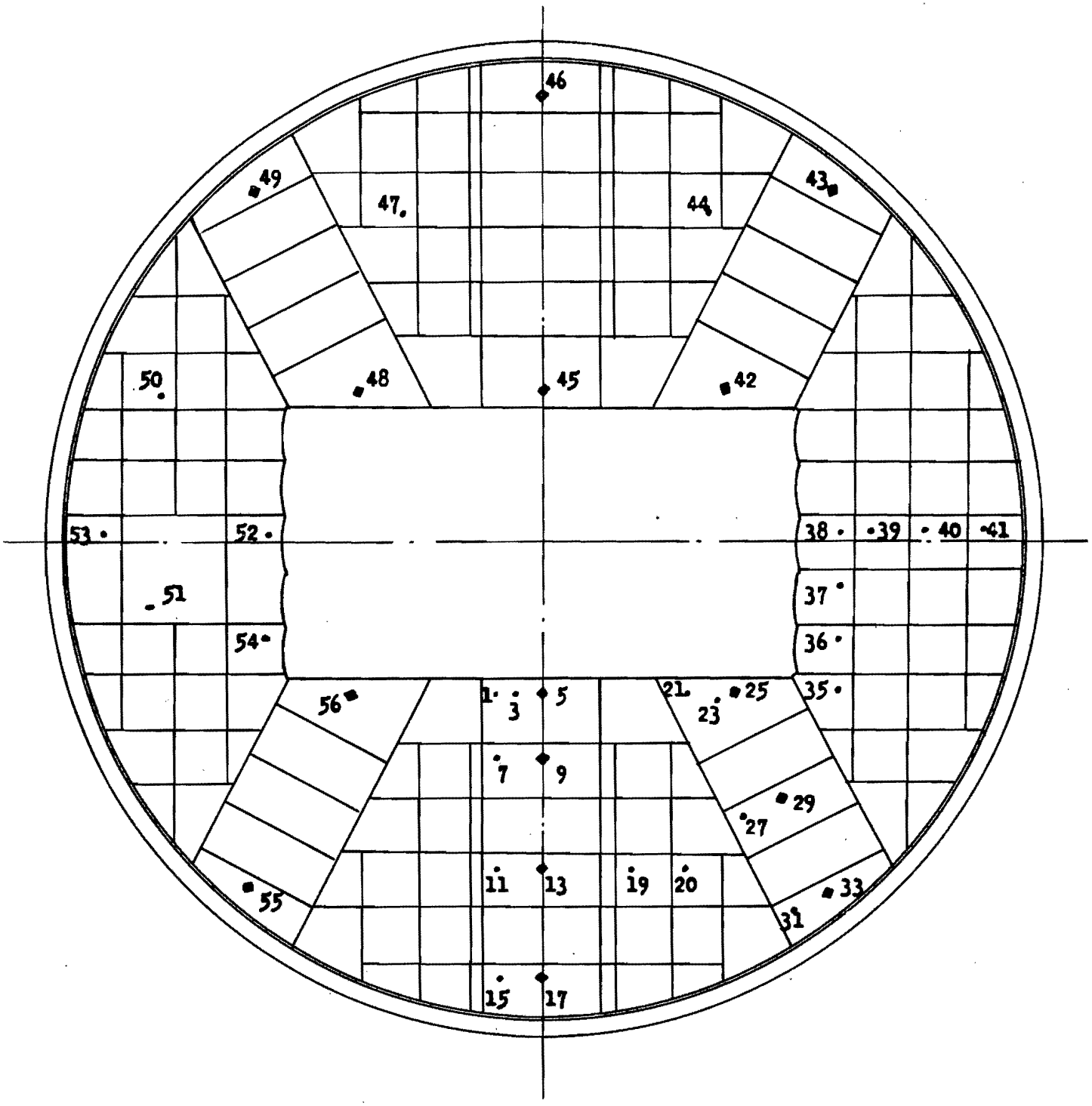

Fig. A 4. H

LOCATION OF PRESSURE TAPS ABOVE THIMBLES

(References: Dwg TD-500)

[redacted]

Drawing 7642

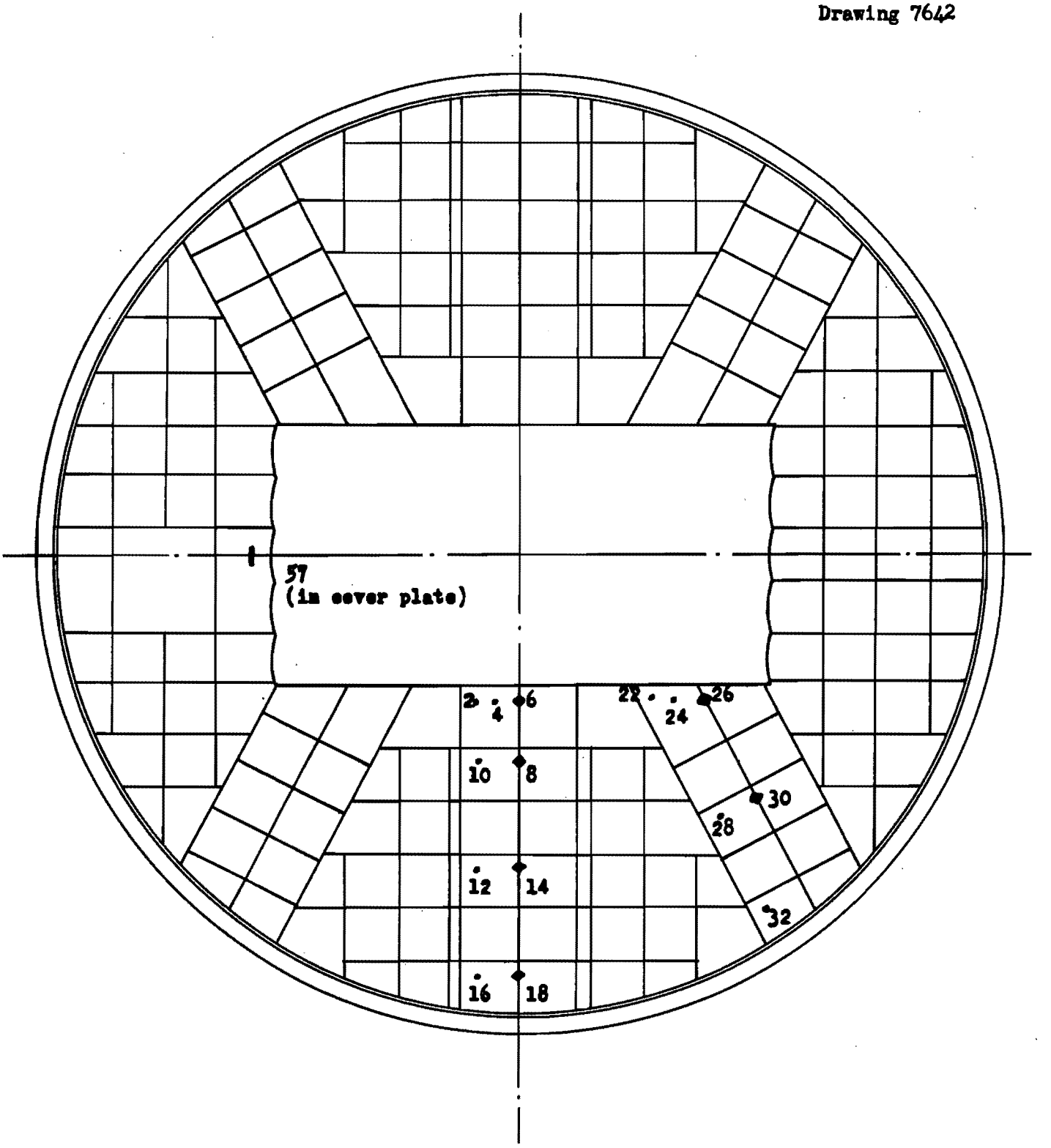

Fig. A 4. I
LOCATION OF PRESSURE TAPS BELOW THIMBLES

(Reference: Dwg TD-502)

[redacted]

type connectors in the reactor tank wall and then run directly to a manometer board in the control room. Approximately 120 lines were connected from inside the reactor tank to manifolds and thence to mercury and oil-filled Merriam manometers.

Nine experimental determinations of velocities were made in the 56 reflector pieces selected for study at pressure drops ranging from 17.5 to 33.7 psi. After two runs it was seen that flow in the reflector was considerably in excess of that anticipated. An unsuccessful attempt was made to reduce the flow by plugging weep holes in the lower support casting and filling some open area at the "A" piece end box sockets. Mean velocities in various types of channels for a typical test at 33.6 psi, after reducing the open area in the lower support casting, are shown in Table A4.A.

TABLE A4.A

Water Velocities in Various Reflector Channels

CHANNEL	VELOCITY (ft/sec)
"A" pieces (1/8-in. holes)	18.7
5/16-in. holes above thimbles	9.0
5/16-in. holes below thimbles	8.9
1/8-in. holes above thimbles	10.9
1/8-in. holes below thimbles	3.8
1/8-in. holes above ½-in. horizontal tubes	15.2

Using these velocities as a basis, the total flow rate through the reflector was computed as follows:

A section was taken above the thimbles and just below the top surface of the reflector. Counting the numbers of various types of holes and using measured dimensions, flow rates in gallons per minute for each foot per second measured velocity were derived. These are shown in Table A4.B.

TABLE A4.B

Flow Rates for Various Reflector Holes

TYPE OF CHANNEL	NO. OF HOLES	CROSS-SECTION (sq in.)	FLOW RATE (gpm) AT 1 ft/sec
1/8-in. holes above thimbles	320	0.0129	12.9
5/16-in. holes above thimbles	86	0.101	27.1
Full length 1/8-in. holes	744	0.0129	30.0
1/8-in. holes in "A" pieces	208	0.0129	8.4
1/8-in. holes above ½-in. horizontal tubes	44	0.0129	1.8
1/8-in. holes above 1-in. horizontal tubes	64	0.0129	2.6

Flow through gaps between reflector components was estimated as a function of gap thickness. Assuming that the velocities vary as the 2/3 power of the equivalent diameters, and that the equivalent diameter of a wide thin slot is approximately twice the thickness T,

$$V_2 = V_1\left(\frac{D_2}{D_1}\right)^{2/3} = V_1\left(\frac{2T_2}{D_1}\right)^{2/3}$$

The 0.127-in. hole designated as pressure tap 41 (Fig. A4.D) is suitable as a standard. Then

$$V_2 = V_1\left(\frac{2}{0.127}\right)^{2/3}(T_2)^{2/3} = 6.30\ V_1(T_2)^{2/3}$$

Values of flow rates in gallons per minute at 1 ft/sec measured velocity at pressure tap 41 are thus derived for the gaps between reflector pieces. These values are shown in Table A4.C.

TABLE A4.C

Flow Rates at Pressure Tap 41

CLEARANCE, T_2	NO. OF GAPS	$(T_2)^{2/3}$	CROSS-SECTION (sq in.)	FLOW RATE (gpm) AT 1 ft/sec
0.017	228	0.065	0.051	14.9
0.0435	6	0.122	0.130	1.9
0.060	20	0.153	0.180	10.9
0.080	12	0.185	0.240	10.5
0.1065	2	0.225	0.320	2.8
0.0625 (at tank wall)	1	0.158	10.6	33.0
Total				74.0

Components of the reflector flow rate are computed in Table A4.D, using the factors derived above and the measured velocities in Table A4.A.

TABLE A4.D

Flow Rates in Reflector

	FLOW RATE (gpm) AT 1 ft/sec	TOTAL FLOW (gpm)			
		TEST 6 ΔP 33.5 psi	TEST 7 ΔP 33.5 psi	TEST 8 ΔP 33.7 psi	TEST 9 ΔP 33.6 psi
Components of flow rate					
1/8-in. holes above thimbles	12.9	138	140	138	141
5/16-in. holes above thimbles	27.1	244	264	255	244
Full length 1/8-in. holes	30.0	362	362	362	372
1/8-in. holes in "A" pieces	8.4	154	152	152	149
1/8-in. holes above ½-in. horizontal tubes	1.8	25	28	30	27
1/8-in. holes above 1-in. horizontal tubes	2.6	33	34	30	30
Subtotal		956	980	967	963
Clearance channels	74.0	898	898	898	920
Total reflector flow		1854	1878	1865	1883

During these experiments measurements were also made of total flow and velocities through fuel elements (see Section A4.3.2, Lattice Measurements). A typical flow balance at 33.5 psi pressure drop was as follows:

Total flow, by calibrated orifice (gpm)	14,900
Component flow, by calibrated pressure taps (gpm)	
1. 19 fuel elements (27.5 ft/sec velocity)	8,300
2. Shim rods and substitutes	2,890
3. "Beryllium" lattice pieces	70
4. Lattice interstices	1,577
5. Open 1-in. rabbit tubes	220
Total flow, by components except reflector (gpm)	13,057
Flow through reflector, by difference (gpm)	1,843

This excellent agreement of two independent measures indicates accuracy better than the ±1% which more probably existed.

On the basis of these data and simultaneous lattice measurements (Section A4.3.2), which indicated that a pressure drop of approximately 40 psi would be required to realize a 30-ft/sec velocity through the fuel, reflector requirements at 40 psi were estimated as approximately 2000 gpm. This figure was roughly double the amount of water originally allowed for the reflector area. For this and for other perhaps more important reasons, a redesign of the reflector was undertaken.

A4.3.2 Flow and Pressure Drops Inside Fuel Lattice. Velocity measurements were taken inside fuel elements and shim-safety rods and in the interstices between fuel elements. Pressure drops were studied wherever significant reductions in static pressure were thought to occur. The points selected for measurement are shown in Fig. A4.J. An analysis of these data is presented in ORNL CF-50-6-102.[10]

Flow Through Fuel Elements. A group of six fuel elements was selected for calibration. Two static pressure taps were installed in each of these assemblies and used to measure pressure drop as a function of velocity through the fuel plates. Calibrations were obtained in a separate experiment before the fuel pieces were installed in the reactor lattice. Figure A4.K is a plot of the calibration of these assemblies. Also shown are data from a previous

[redacted]

Drawing # 9101

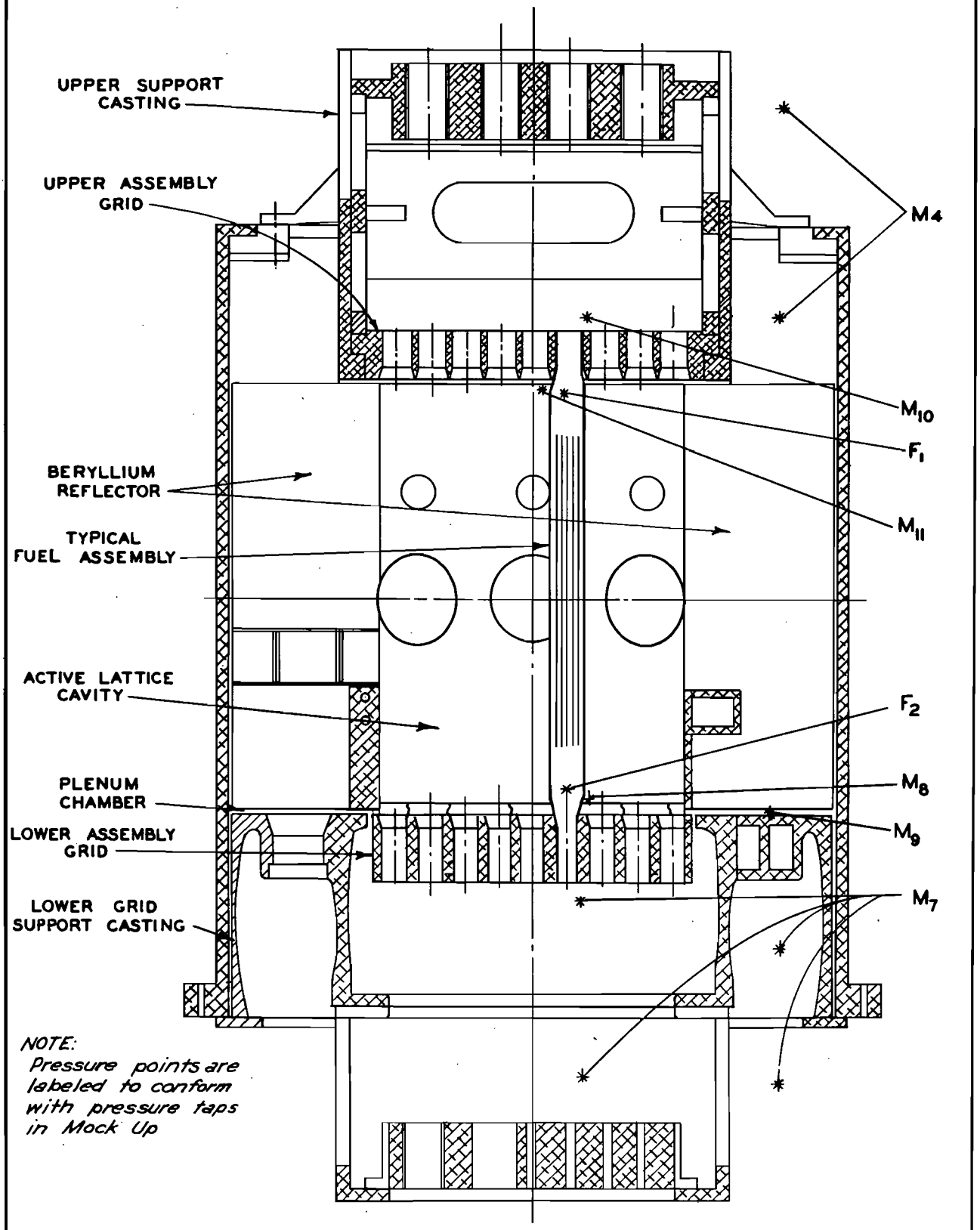

FIG. A4.J

CROSS SECTION OF MTR

[redacted]

DWG. #10810 [redacted]

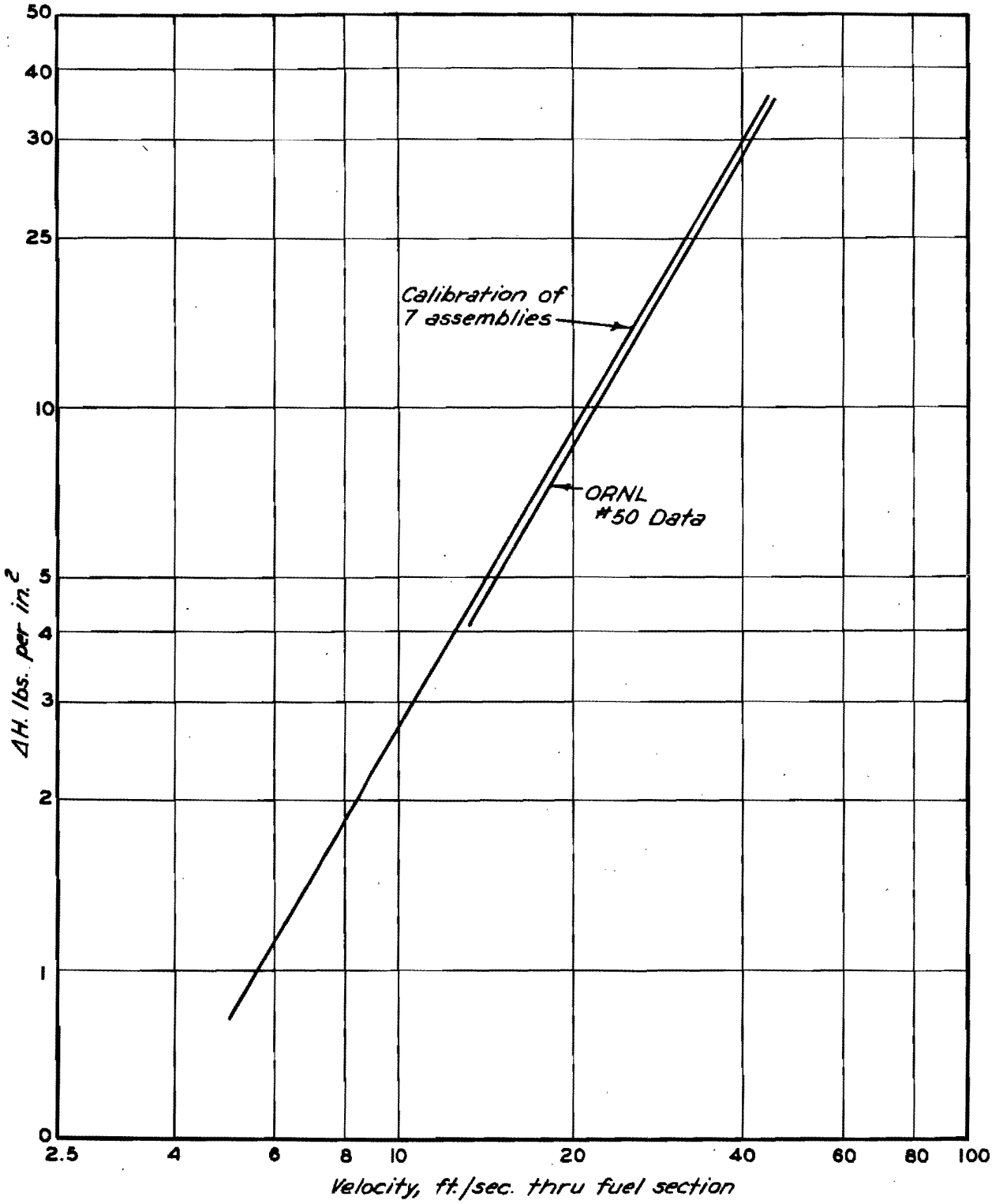

FIG. A.4.K

VELOCITY - PRESSURE DROP CURVE FOR FUEL ASSEMBLIES

calibration of a single assembly reported in ORNL-50. The pressure drops were measured over the length of the fuel plates and the agreement of the two independent calibrations is good.

The overall pressure drop, which includes losses in both upper and lower end boxes (reported in ORNL-50), indicated that the desired velocity of 30 ft/sec past the plates would be realized at a total pressure drop of 30 to 35 psi. This value was taken as the basis for design of the hydraulic system for the MTR. However, full-scale measurements in the Mock-Up indicated that an overall pressure drop of about 40 psi was required to attain the 30-ft/sec velocity.

This diagreement of 5 to 10 psi was the subject of an investigation which resulted in an explanation of the difference in the two cases. It was found that the upper end box of the fuel piece used in the experiments described in ORNL-50 had an inside diameter 1/8 in. longer than the end boxes of more recent design used in the Mock-Up. A calculation of the two cases confirmed a loss of about 4 psi for the smaller Mock-Up end boxes. An additional loss of 3 psi was measured across the upper support casting, through which the water must pass before it reaches the fuel. Thus the total design pressure drop for the reactor tank was increased to 40 psi, which may be broken down as follows:

RESISTANCE	PRESSURE DROP (psi)
Upper support and grid spacer castings	3
Upper end box	13
Fuel plates	18
Lower end box	6
Total pressure loss in tank section D	40

Flow Through Interstices Between Fuel Elements. In order for cooling water to flow between adjacent fuel elements, it must move past the upper assembly grid, down past the outer fuel plates, and discharge through the lower assembly grid. It was desired to maintain a velocity of 25 ft/sec in the spaces between fuel elements, but the Mock-Up measurements indicated

velocities of roughly 15 ft/sec. It was found that the pressure drop across the upper assembly grid was about 10 psi and across the lower assembly grid was 18 psi. Subsequently the open area in the lower grid was increased and its pressure drop reduced to 10 psi to give the correct velocity through the interstices.

Flow Through Safety Rods. The shim-safety rods also require a cooling velocity of 30 ft/sec through the fuel section. Measurements in a previous experiment[11] indicated a pressure drop of 40 psi for this velocity. Calibration of the Mock-Up rods agreed with this figure. The curve of velocity versus pressure drop is presented in Fig. A4.L.

On the basis of the Mock-Up measurements, the pressure drops and flow rates through tank section D are summarized in Table A4.E.

TABLE A4.E

Pressure Drops and Flow Rates Through Tank Section D

LOCATION	PRESSURE DROP (psi)	FLOW (gpm)	
		COMPONENTS PARALLEL	COMPONENTS NONPARALLEL
Upper support casting	3		17,670
Upper assembly grid	10		2,500
Fuel assemblies (23 required)	37	10,925	
Lattice beryllium pieces (14 required)	37	35	
Gaps in lattice	17	2,500	
Shim rods, cadmium (4 required)	40	1,725	
Shim rods, beryllium (4 required)	40	10	
Reflector (Mock-Up design)	9	2,000	
Lower support casting	31		2,000
Lower assembly grid	10		2,500
By-pass		475	
Total flow required (with 4 cadmium shim rods)		17,670	

DWG. #10809 [redacted]

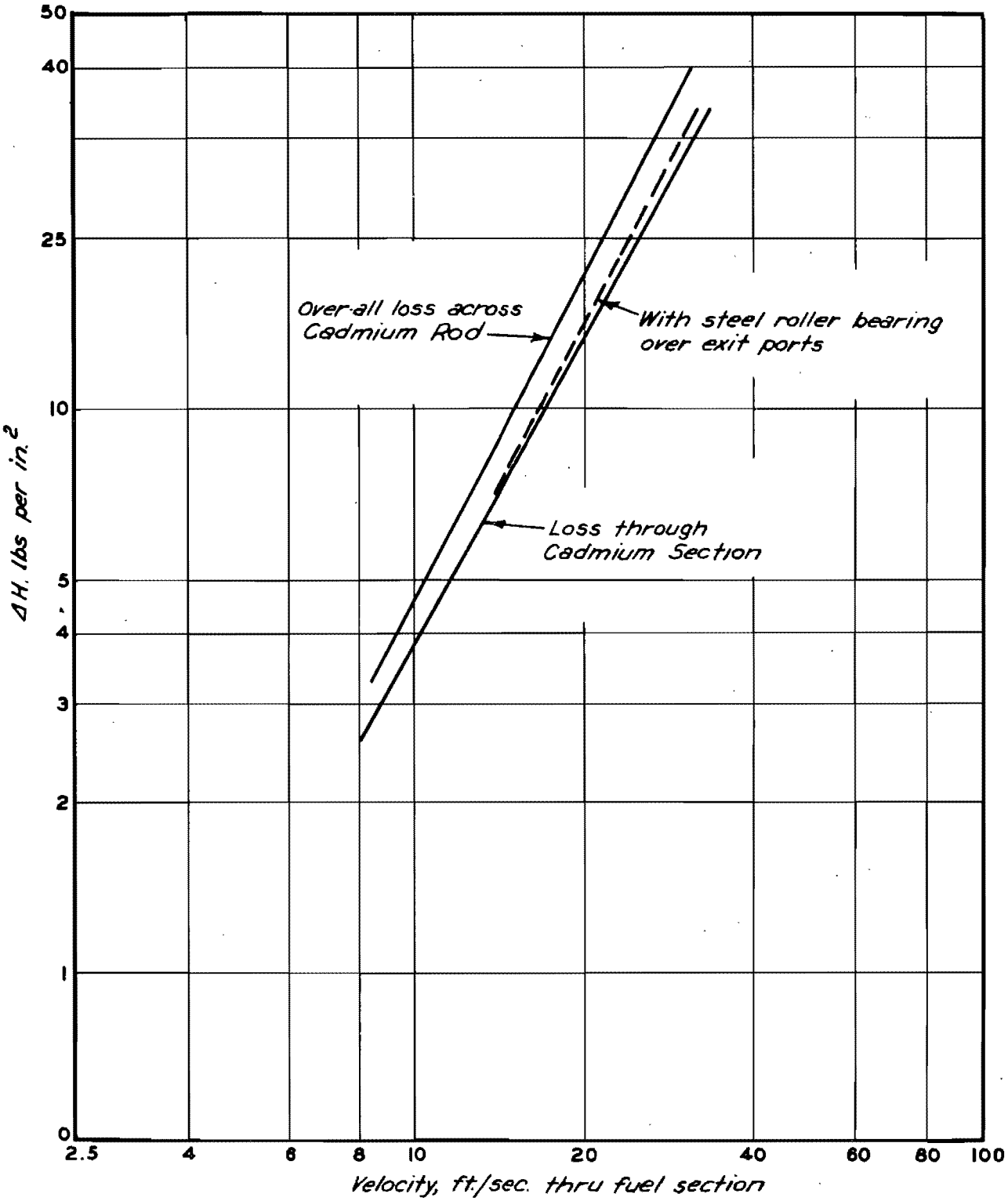

FIG. A.4.L

CALIBRATION OF CADMIUM SHIM SAFETY ROD

NEW TYPE - 0.060" FUEL PLATES

A4.4 HANDLING TOOLS

Normal and frequent operations such as fuel replacement and adjustment of reactor and reflector geometry for experiments require special tools and appurtenances for remote handling. It will be recalled, furthermore, that one of the basic design requirements of the MTR is that any part of the reactor proper be replaceable. Because many parts will be intensely radioactive after extended operation, remote handling is required. Working models for most of the operations noted have been tested in the Mock-Up; Figs. A4.M and N are shown as typical of this work.

The results of Mock-Up experience have been incorporated in the MTR handling tools mentioned in Section 2.9.

A4.5 NUCLEAR EXPERIMENTS

Problems associated with the nuclear characteristics of the operating reactor were studied for a period of seven months (starting in February, 1950) using the assembly illustrated in Figs. A4.B and C. As is often the case when a heavy program is undertaken with limited time available, it was impossible to refine the experiments as desired. However, from the MTR design standpoint little could have been gained by greater precision because MTR experimental conditions could not be exactly duplicated. The principal topics of study were the following:

1. Determination of critical mass for a slab type loading.
2. Calibration of regulating rod.
3. Measurements of temperature coefficient.
4. Measurements of reactivity changes caused by water flow, air bubbles, and open beam holes.
5. Performance of the control and safety systems.
6. Measurements of neutron and gamma fluxes inside and above the fuel, in the graphite reflector outside the tank, and in the thermal shield.

A4.5.1 Critical Mass Determination. Several extraordinary safety precautions were taken for the initial fuel loading. For instance, a standard safety rod was rebuilt with a beryllium section in place of the fuel section

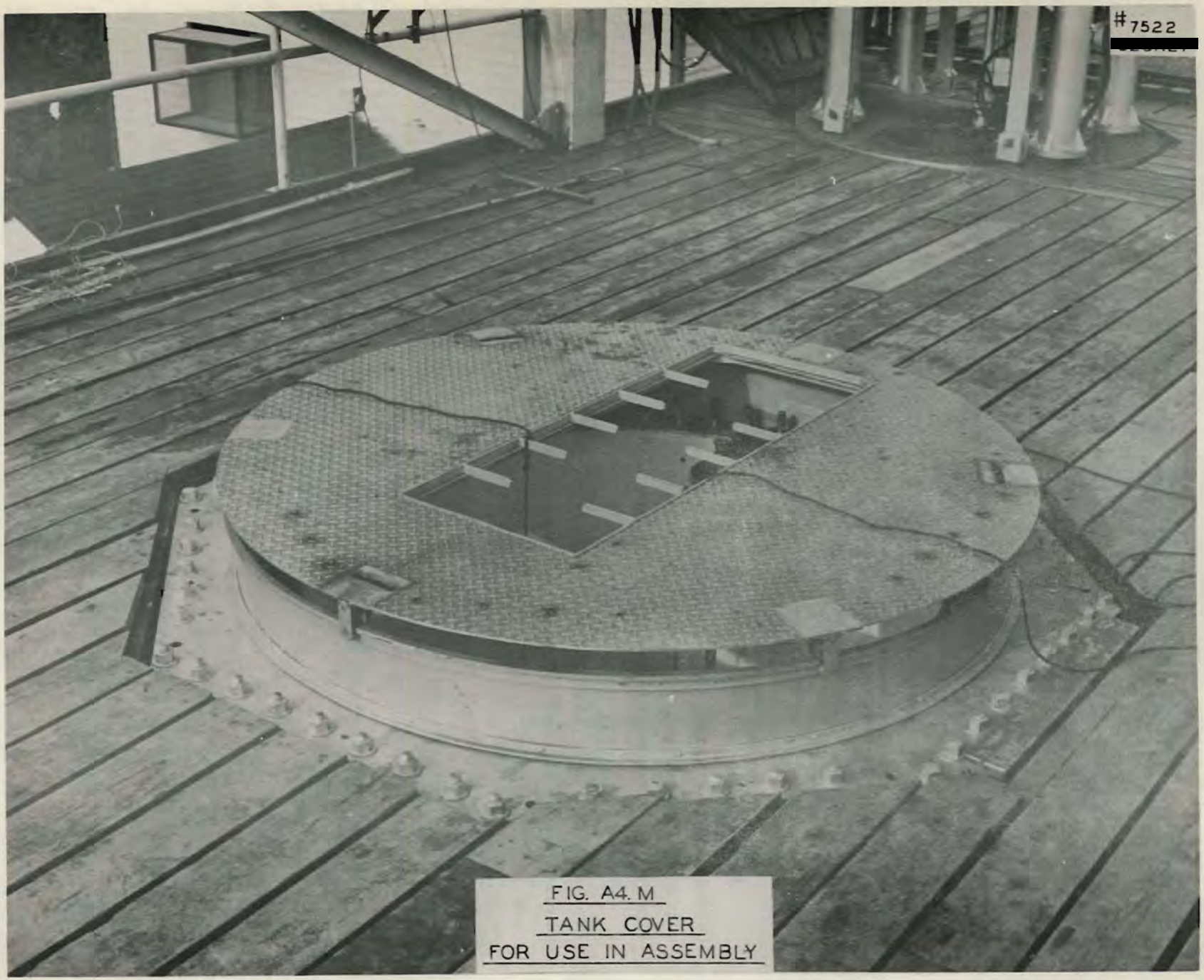

FIG. A4. M
TANK COVER
FOR USE IN ASSEMBLY

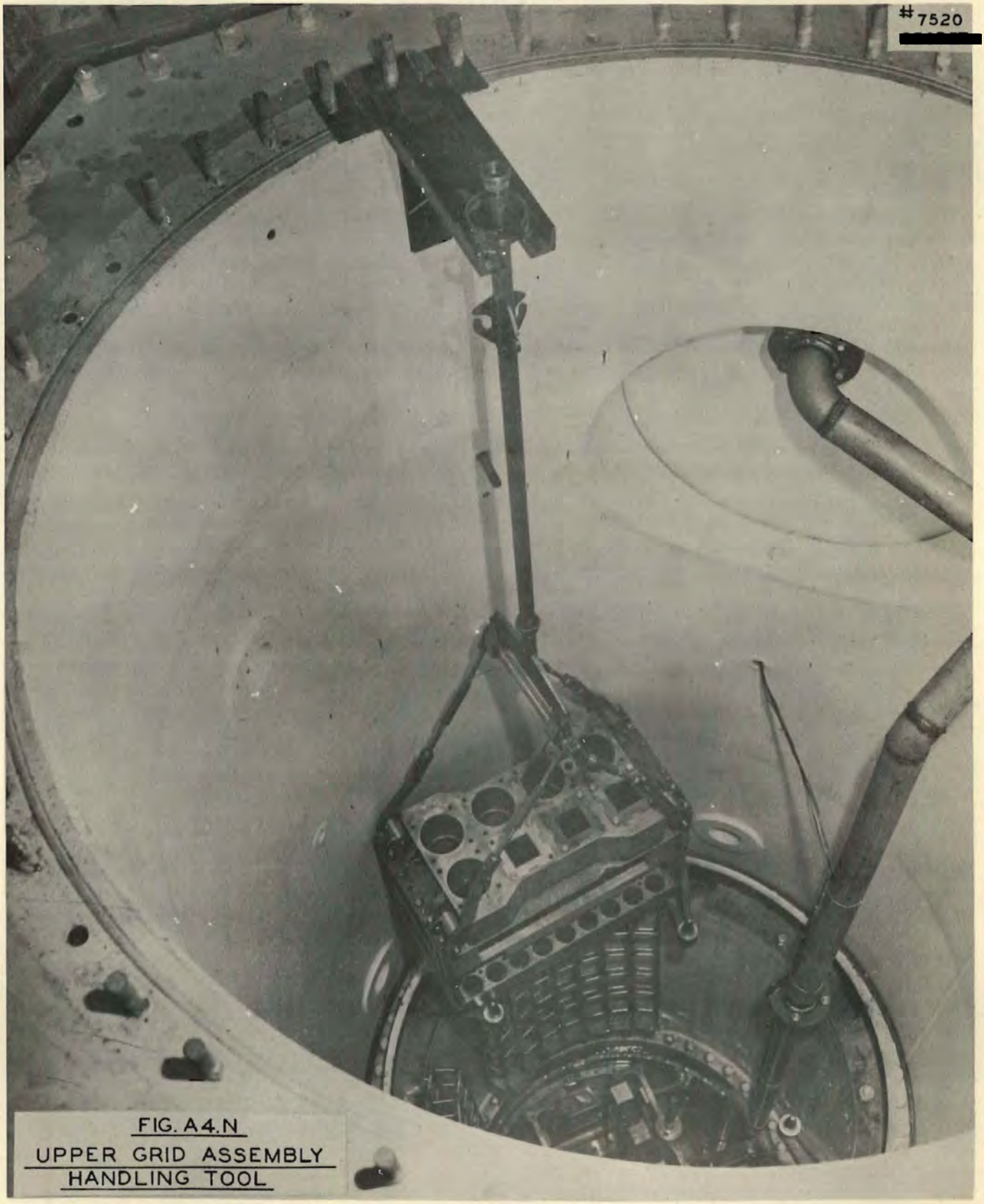

FIG. A4.N
UPPER GRID ASSEMBLY
HANDLING TOOL

for use as a "cocked" safety during loading. The cadmium section of this rod was kept suspended above the lattice by an electromagnet while each fuel piece was inserted.

Another precaution was the installation of separate neutron-level and period indicators at the loading platform which was 30 ft above the control room. Also, a boron fluoride neutron detector was used in addition to the slow fission chamber and three other neutron chambers. The relative locations of source, fuel, and detectors is shown in Fig. A4.O.

The critical mass determination was begun after recording backgrounds of all the neutron detectors with the addition of four fuel pieces containing a total of 560 g of U^{235}. The control rods were then withdrawn completely and the new counting rates were measured with pulse counters. The usual plot of reciprocal counting rate against mass of U^{235} was made upon addition of each additional fuel element (140 g of U^{235}). As the critical point was approached, smaller quantities of uranium in the form of partial fuel elements were added. Criticality was attained with approximately 2000 g of U^{235}.

A4.5.2 Regulating-rod Calibration. The regulating rod is a 1½-in.-diameter aluminum rod with a 20-in.-long cadmium tube inserted at its center; it is located in the permanent beryllium at the edge of the lattice. The total reactivity of the rod, expressed as $\Delta k/k$, is intended to be less than the delayed neutron fraction to prevent sudden complete removal from making the reactor "prompt-critical." For safety, therefore, it was necessary to be certain of the total reactivity change possible from the regulating rod. Furthermore, for control purposes it was desirable to determine a curve of sensitivity as a function of rod position.

The method of calibration was as follows: Beginning with the rod completely inserted and the reactor level (infinite period), the rod was withdrawn a short distance manually and the resultant period was measured as the slope of the logarithmic plot of neutron level. After complete withdrawal of the rod, similar points were obtained by stepwise insertion. The reactivity, $(\Delta k/k)_{eff}$, was obtained from the usual in-hour-relation.[12] Curves of sensitivity and total reactivity are presented in Figs. A4.P and Q.

Considering the accuracy of the determination (about ±5%), it is seen that the original rod was possibly worth as much as 0.7% in $(\Delta k/k)_{eff}$.

DWG. #10808 [redacted]

TANK FILLED WITH WATER

B - REMOVABLE BERYLLIUM
F - FUEL ELEMENT - 140 *gms.* U235
S - SAFETY ROD

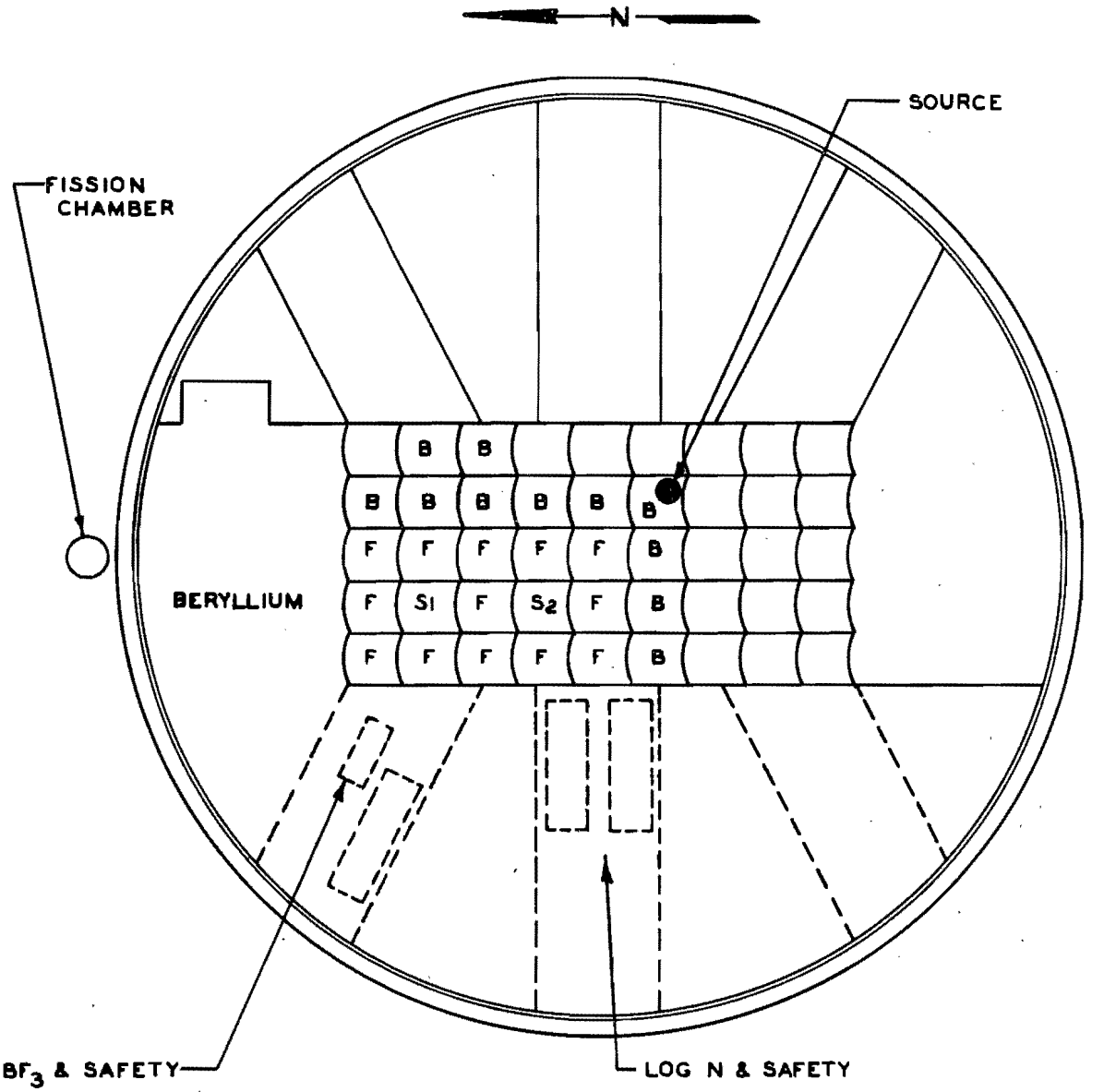

FIG. A.4.0

REACTOR TANK SHOWING ARRANGEMENT OF LATTICE AND BERYLLIUM REFLECTOR

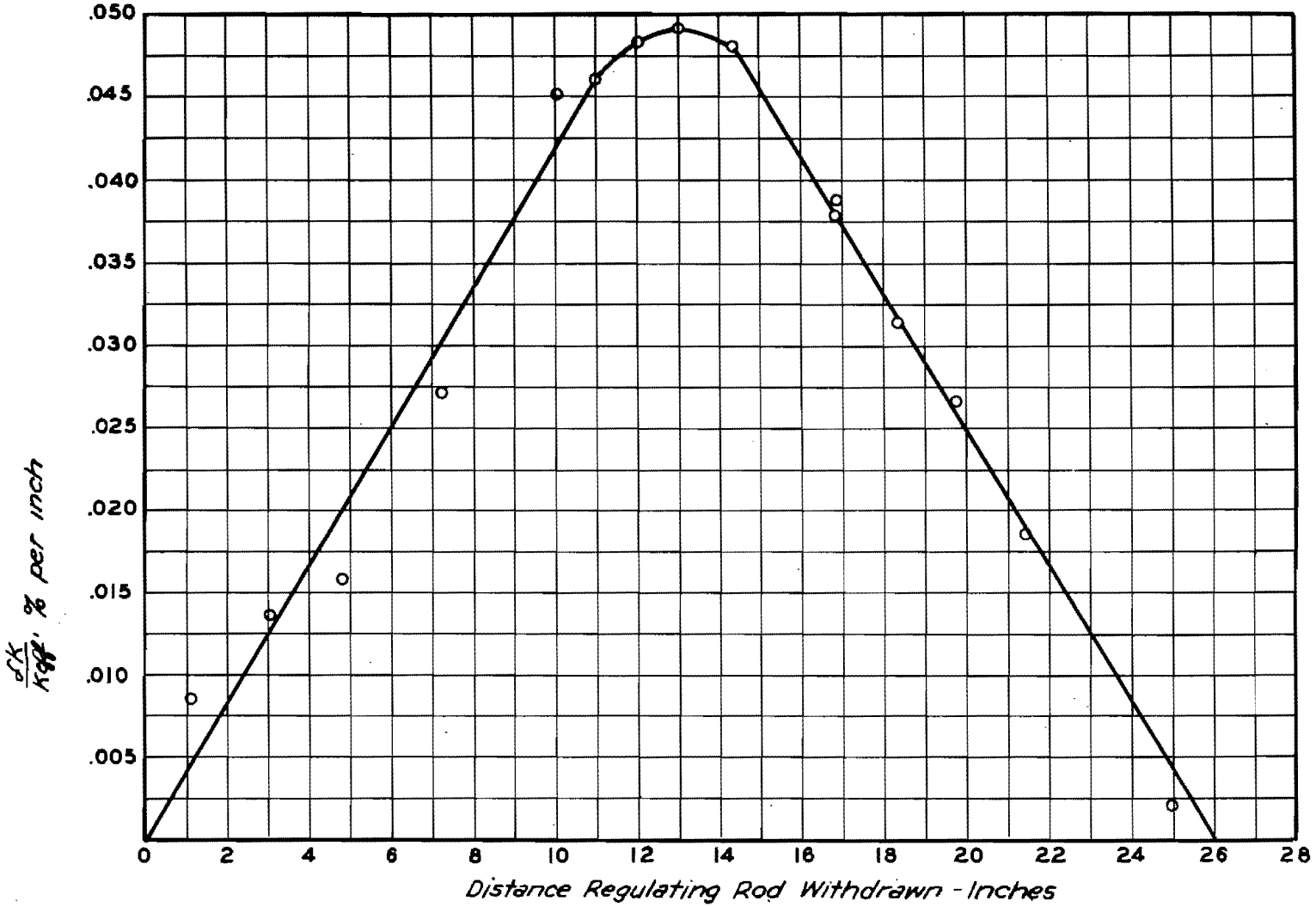

FIG. A.4.P

CALIBRATION OF REGULATING ROD

DWG. #10812

DWG. #10813

[redacted]

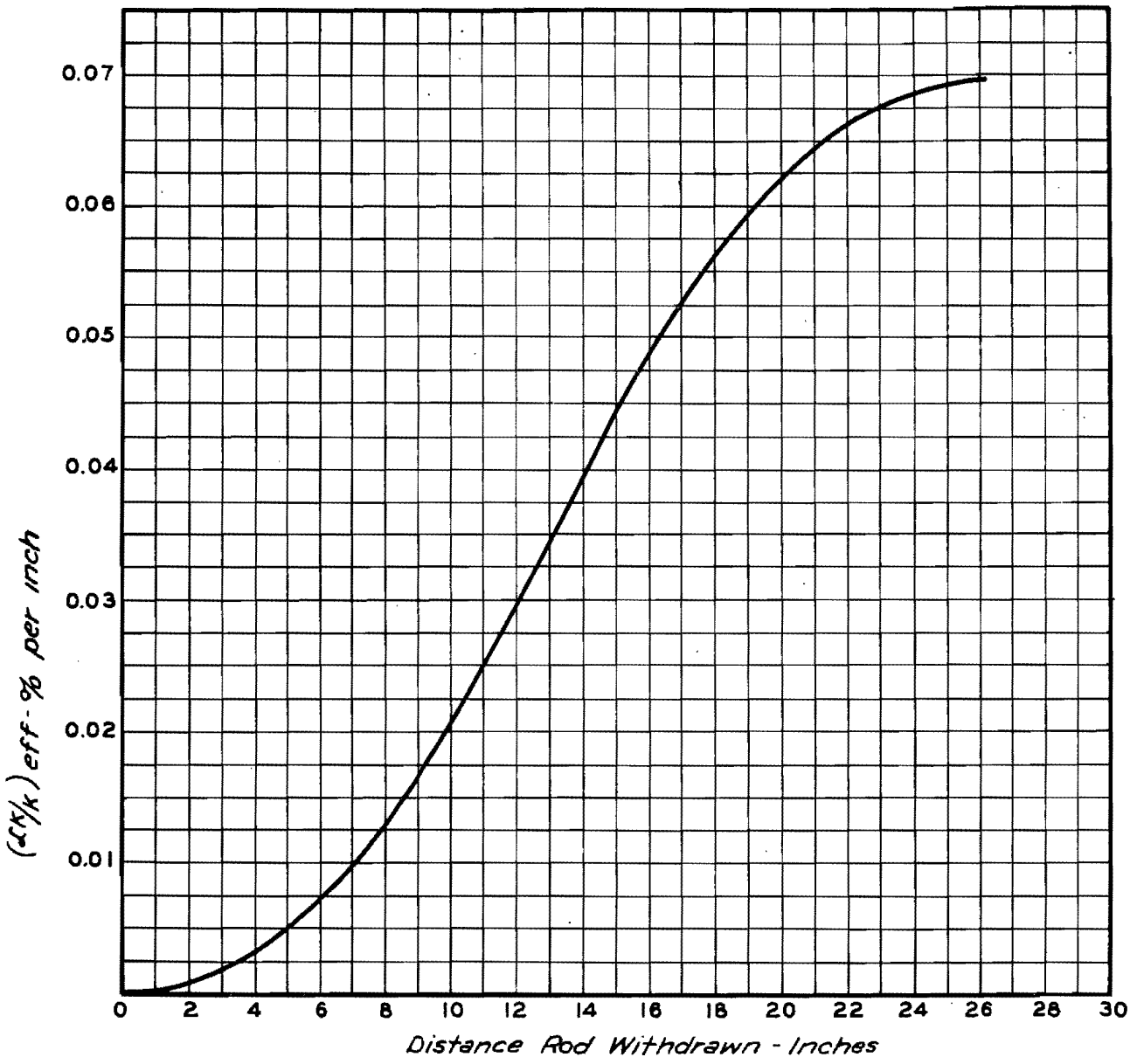

FIG. A.4.Q

SENSITIVITY OF REGULATING ROD

As a result, the total movement of the cadmium section of the rod was reduced by 4 in. with a resultant reduction in equivalent reactivity to about 0.65%. It is expected that the regulating rod in the MTR will contain less than 0.65% in $(\Delta k/k)_{eff}$ because the MTR core will be larger than that in the Mock-Up.

A4.5.3 Temperature Coefficient. The measurement of the Mock-Up temperature coefficient was made in the following way: The reactor was made critical at the ambient bulk water temperature (usually 20 to 25°C), and positions of the shim and regulating rods were carefully recorded. After the reactor was shut down, the water pumps were operated until the pump input energy (about 350 kw) had increased the temperature of the circulating water a sufficient amount (5 or 10°C). At the new temperature, the pumps were stopped and the reactor was again brought to some low power level with the shim rods set exactly at their previous locations, corrected for rod expansion at the increased temperature, and the new position of the regulating rod was recorded. From the rod calibration curve the change in reactivity for that particular temperature increment was read. This change in $(\Delta k/k)_{eff}$ was checked later by measuring the reactor period resulting from the same movement of the regulating rod.

Measurements made in this manner are listed in Table A4.F. The average of 0.013 is in fairly good agreement with the calculated value of 0.017% per degree centigrade for the Mock-Up core with a k of about 1.58.

TABLE A4.F

Experimental Values for Temperature Coefficient

TEMPERATURE (°C)	PERCENT $(\Delta k/k)_{eff}$ PER °C
36.1	-0.013
37	-0.012
43	-0.012
45	-0.012
46.5	-0.014
48	-0.012
53	-0.014
54	-0.013
	-0.013 (avg.)

A4.5.4 Effect of an Empty Experimental Beam Hole. The effect on reactivity of removing a beryllium plug from the 6-in.-diameter northwest experimental thimble (see Fig. A4.C) extending to the lattice face was determined by comparison with changes in the position of the regulating rod. For the Mock-Up core the effect was a 0.6% reduction in $(\Delta k/k)_{eff}$. Filling the empty hole with a paraffin plug resulted in a $(\Delta k/k)_{eff}$ increase of 0.3%. Although the effect of an empty hole measured here is considerably greater than that observed in the critical experiments, the difference in core size and asymmetry of reflector are probably responsible, and it is expected that the MTR will exhibit effects more similar to those of the critical experiments.

A4.5.5 Effect of Water Flow. It has been speculated that high-velocity water flow in the fuel assemblies might result in sufficient movement to be detectable as small fluctuations in reactivity, and an experiment was conducted to investigate this possibility. The upper fuel-positioning grid was removed so that fuel elements would be unconfined at their upper ends. A water velocity of 30 ft/sec was maintained through the cooling clearances. The ion chamber which normally fed the servo control mechanism was used as the detector of reactivity changes. Several measurements were made both with and without water flow, but no difference was detectable. It was therefore concluded that water flow had no significant effect on the stability of the reactor. Furthermore, since many small air bubbles were visible in the circulating water, it was concluded that, as expected, uniformly distributed air bubbles would not cause reactivity fluctuations.

A4.5.6 Performance of Control and Safety Circuits. The two instruments in which most interest has been evidenced are the period indicator and the servo mechanism.

The period meter is a direct indicator of rate of increase or decrease of reactor level. Its scale is calibrated in seconds so that the period, i.e., the time required for the power level to change by a factor of 2.7, can be read directly. This instrument proved extremely valuable in start-ups and was also useful for making changes in power level when the reactor was being controlled manually.

The servo mechanism performed exceptionally well. With this device any desired power level in the operating range could be maintained for hours with

only minor attention from the operator. The response of the circuit to large disturbances was measured as approximately 0.1 sec by applying an electrical pulse equivalent to a $(\Delta k/k)_{eff}$ step of about 0.6%. During operation, steps as high as 0.3% $(\Delta k/k)_{eff}$ were added in approximately 1 sec by injecting compressed air at the center of the fuel lattice. The servo mechanism easily followed these disturbances without losing control of the reactor.

Another feature of the MTR control arrangement is the safety circuits which protect against higher-than-normal power levels. Unsafe levels cause a reduction in current to the electromagnets and subsequent release of the control rods. The time required for release of the rods had been measured as approximately 15 msec before installation in the Mock-Up. During operation the time interval between the "scram" signal and shutdown of the reactor was observed to be approximately 30 msec.

Although a number of minor changes in the control instrumentation were deemed desirable before construction of the final MTR instruments, it can be said that their performance in the Mock-Up was very satisfactory.

A4.5.7 Measurement of Neutron Fluxes. The data presented below have been analyzed and compared with previous calculations.[13,14] Neutron flux distributions were measured by determining the saturated activity (A_s) induced in bare and cadmium-covered metal foils. The measurements can be divided into three series of experiments, based on the experimental conditions and the information sought in each series.

In the first group of experiments the northwest thimble was left open. Fluxes were measured in the fuel lattice, the northwest quadrant of the graphite reflector, and at other miscellaneous points in the structure.

In the second series the northwest thimble hole was closed, as described later, and additional foil exposures were made at many of the locations mentioned above. Neutron attenuations in the water above the lattice up to the elevation of the shim-rod electromagnets were measured also.

The third series included attenuation in concrete blocks and in paraffin stacked behind a portion of the steel thermal shield outside the graphite stack.

Gold foils (1 cm square, 0.005 in. thick) were used for exposures in the graphite. The foils were spaced 6 in. apart on 1/16-in.-thick aluminum strips

for exposures in the fuel lattice and in the 1-in.-diameter holes which extended vertically through the graphite reflector. Measurements of very low fluxes (e.g., in the water above the fuel) were made with large indium foils (25 cm square, 0.005 in. thick) which were held on lucite strips during exposure. Correction for the activity induced by resonance and fast neutrons was made by exposing foils covered with cadmium. The cadmium covers were 0.020 in. thick and were coated with lacquer to prevent contamination of the foils.

Mica-window Geiger tubes were used to count the 1-cm foils, and the glass tubes were used with the large indium foils. The small foils were placed on a flat aluminum plate beneath the mica-window tubes; the large foils were enclosed in a brass cylinder and slipped over the glass tubes. Only the side of the foil which had faced the reactor was counted, and this side was always placed nearest the counting tube.

The foils and counters were calibrated by irradiating foils in positions of known flux in a standard graphite pile.[16]

In almost all instances exposure time and start-up time were comparable; consequently a start-up correction has been applied to the foil data.[16] The power levels for the many foil activations varied from 10 watts to 2 kilowatts.

First Series. Experimental conditions for the first series were:

1. Lattice arrangements as shown in Fig. A4.C.
2. No thermal shield.
3. Experimental holes filled as follows:
   - (*a*) Southwest thimble — filled solidly with graphite from edge of the lattice to outer edge of graphite.
   - (*b*) Center west thimble — filled with an 18-in.-long by 6-in.-diameter cylinder of beryllium beginning 1 in. from the edge of the lattice; the differential chamber and one safety chamber occupied the otherwise empty space behind the beryllium plug.
   - (*c*) Northwest thimble — empty except for the U^{235} fission chamber and one safety chamber.
   - (*d*) Southeast and center east thimbles — filled with paraffin.
   - (*e*) Northeast thimble — filled with graphite backed by a concrete plug.

4. Regulating rod removed.

5. Shim rod No. 1 completely withdrawn, shim rod No. 2 withdrawn 80%.

6. Graphite reflector arranged as indicated in Fig. A4.C with 1-in.-diameter holes extending from top to bottom in the numbered positions.

7. Reactor tank filled with demineralized, deaerated water.

All measurements in this series were normalized by comparing gold foils activated in graphite hole 44 during each run.

Figures A4.R and S show the data for the mid-plane and top plane of the active lattice. Typical curves showing vertical distribution of neutron fluxes in several holes in the graphite reflector are presented in Figs. A4.T, U, and V. Table A4.G lists the thermal-neutron flux values at various mid-plane positions in the graphite reflector with the cadmium ratio at the points where it was measured.

TABLE A4.G

Neutron Flux in Mid-plane

First series: Northwest Thimble Open

HOLE NO.	nv (thermal)*	CADMIUM RATIO**
44	123 $\times 10^{-3}$	
45	81	19
46	107	
13	27	
19	16	100
15	13	44
16	5.0	140
34	0.3	230
38	1.83	
11***	0.92	
16	1.1	
34	0.24	
37	0.65	

*Normalized to nv (thermal) of 1.0 neutron/cm^2-sec at center of lattice.
**Corrected for absorption of resonance neutrons in cadmium.
***Outer surface of graphite behind hole.

FIG. A4.R

Thermal Neutron Flux in Midplane of Active Lattice

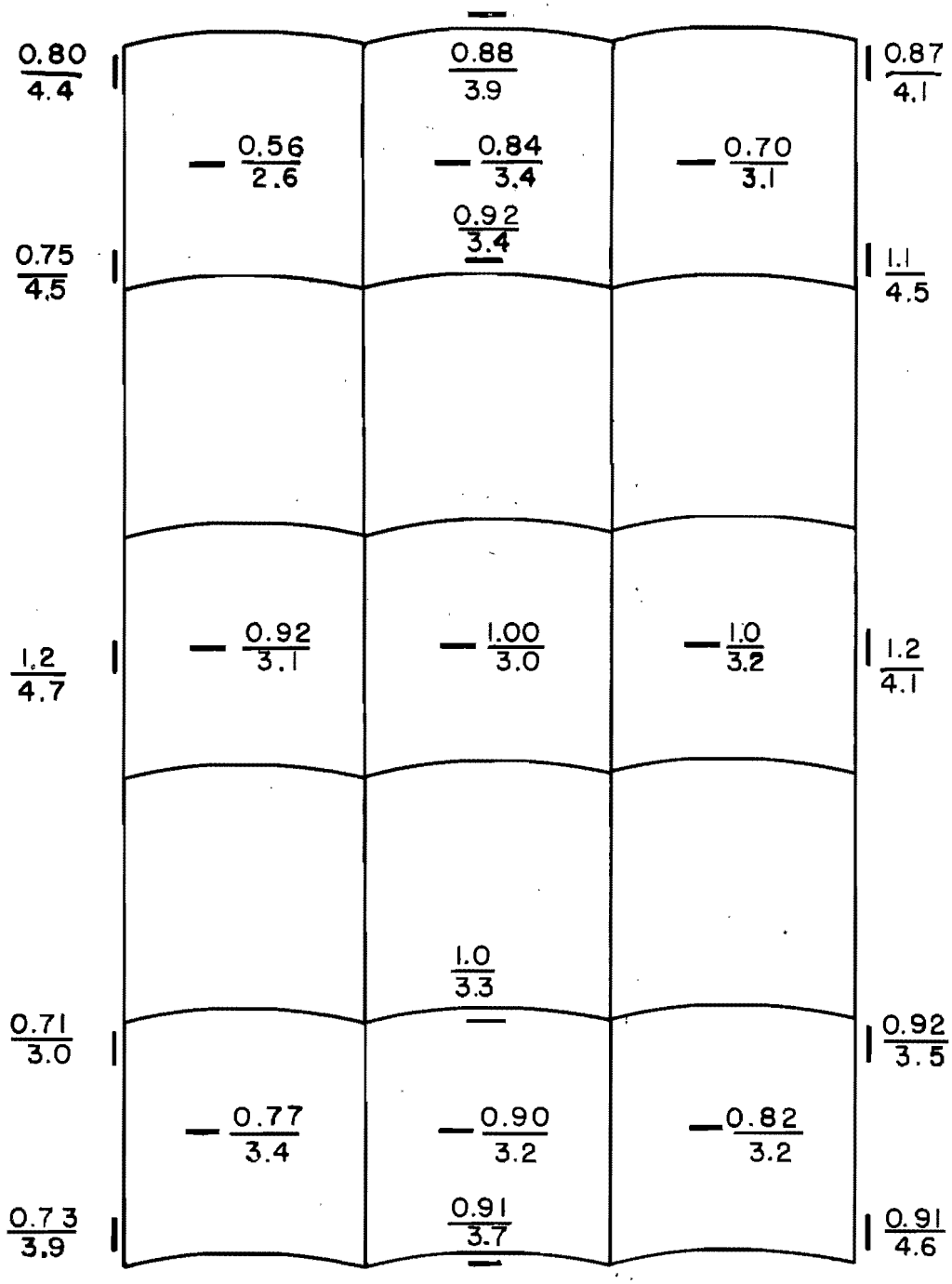

Numerator is NV_{th} Relative to NV_{th} at Center of Lattice

Denominator is Cadmium Ratio

Dwg. 9792

FIG. A4.S

Thermal Neutron Flux in Top Plane of Active Lattice

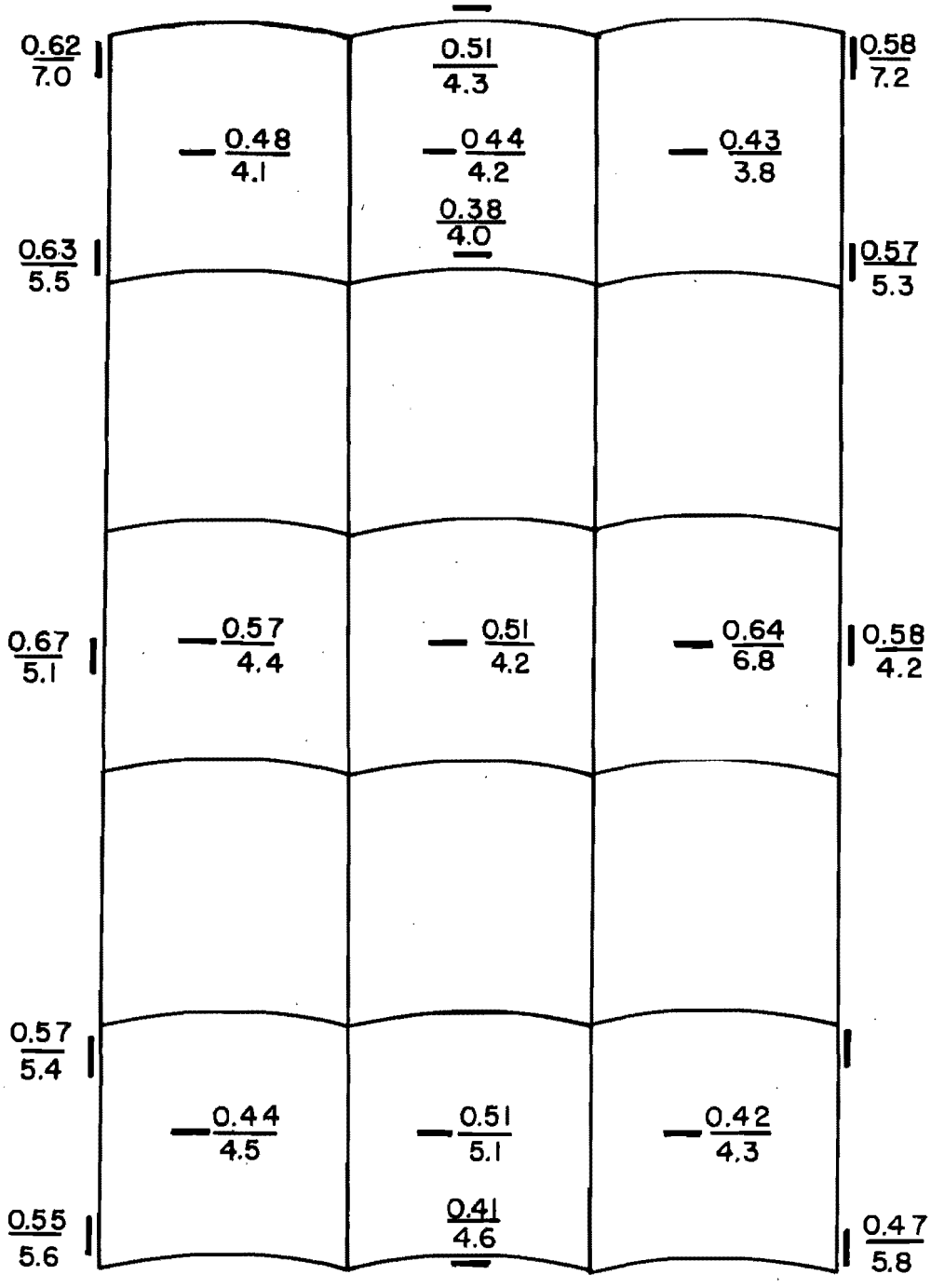

Numerator is NV_{th} Relative to NV_{th} at Center of Lattice

Denominator is Cadmium Ratio

DWG. # 10816 [redacted]

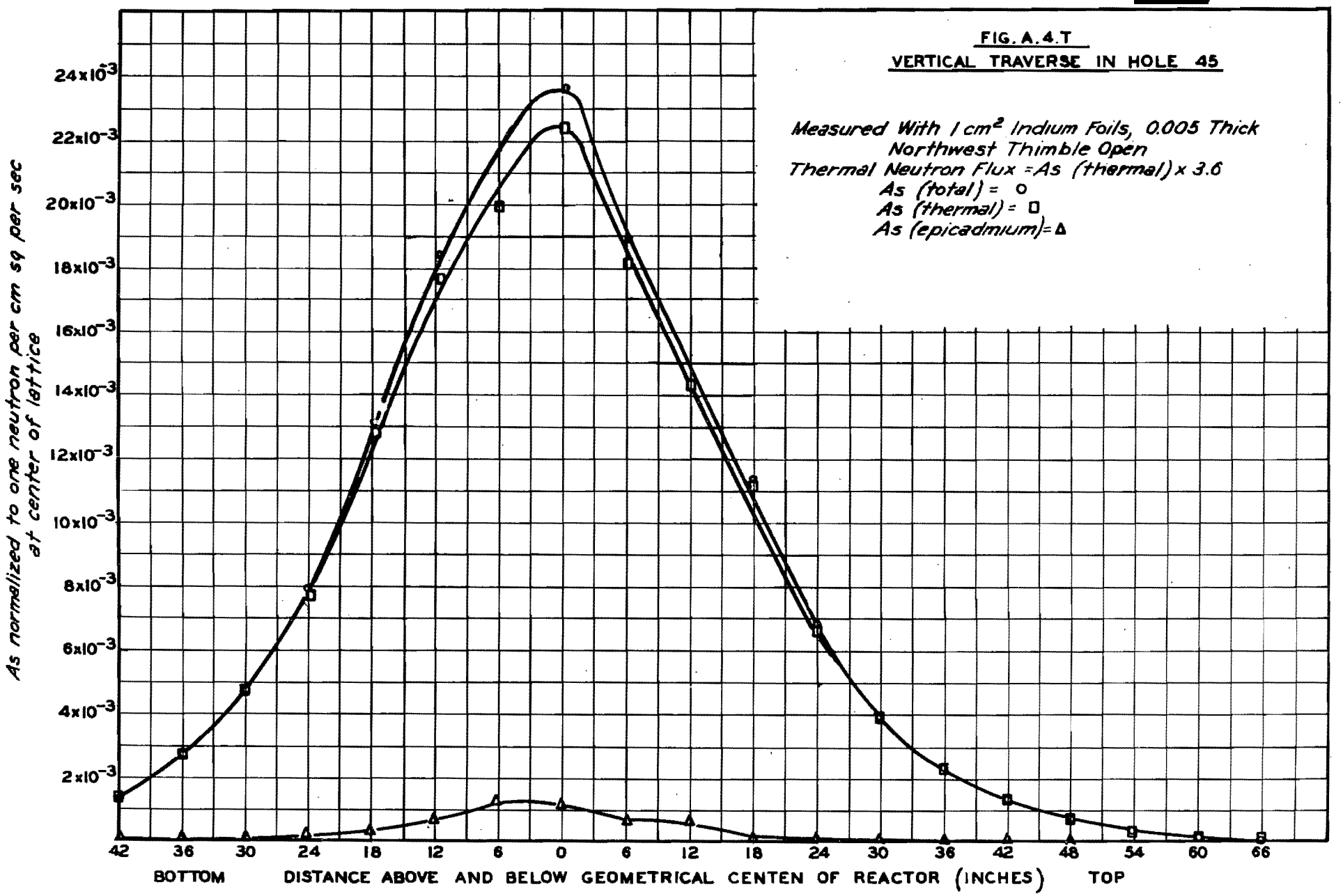

DWG. #10814
[redacted]T

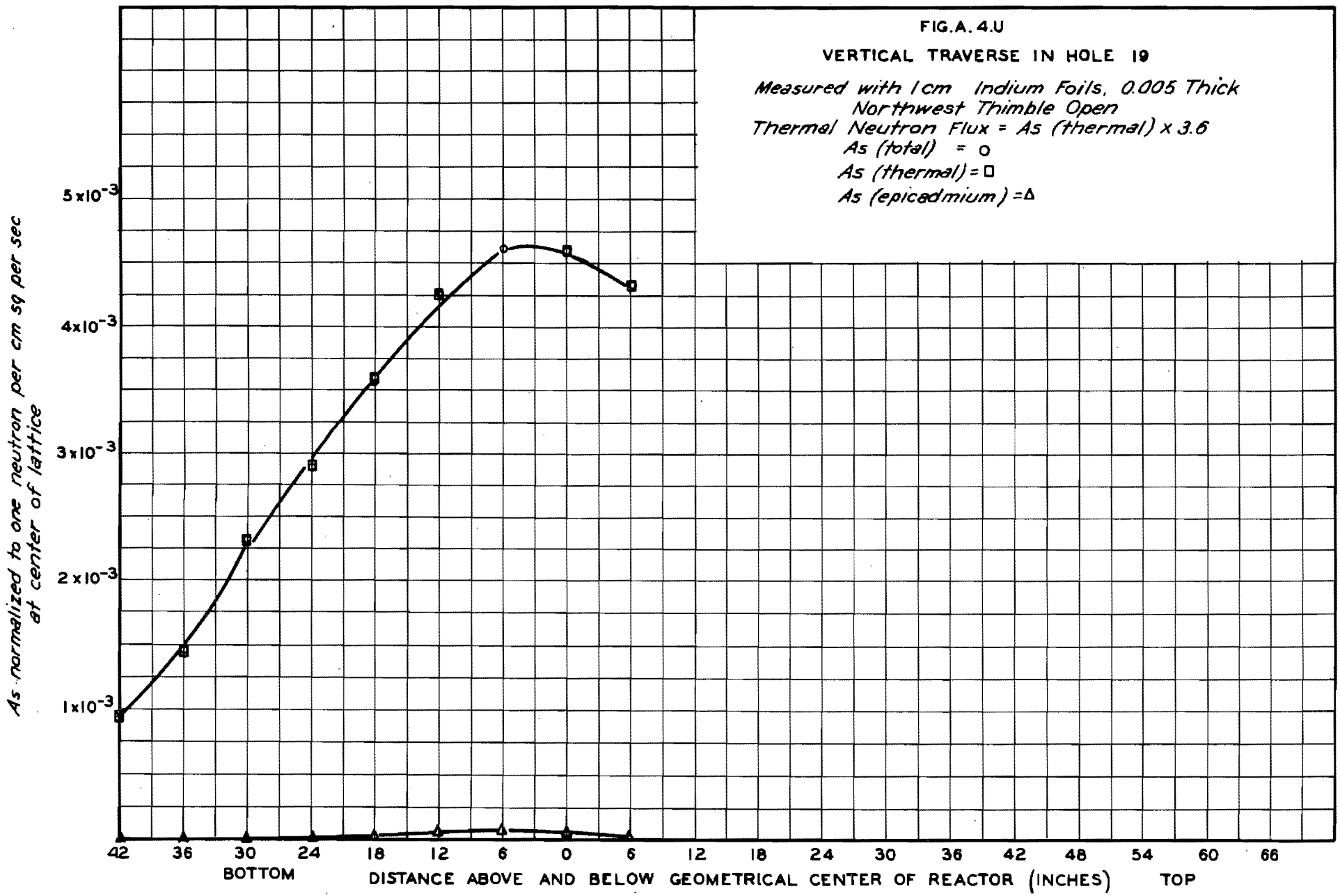

DWG. # 10815

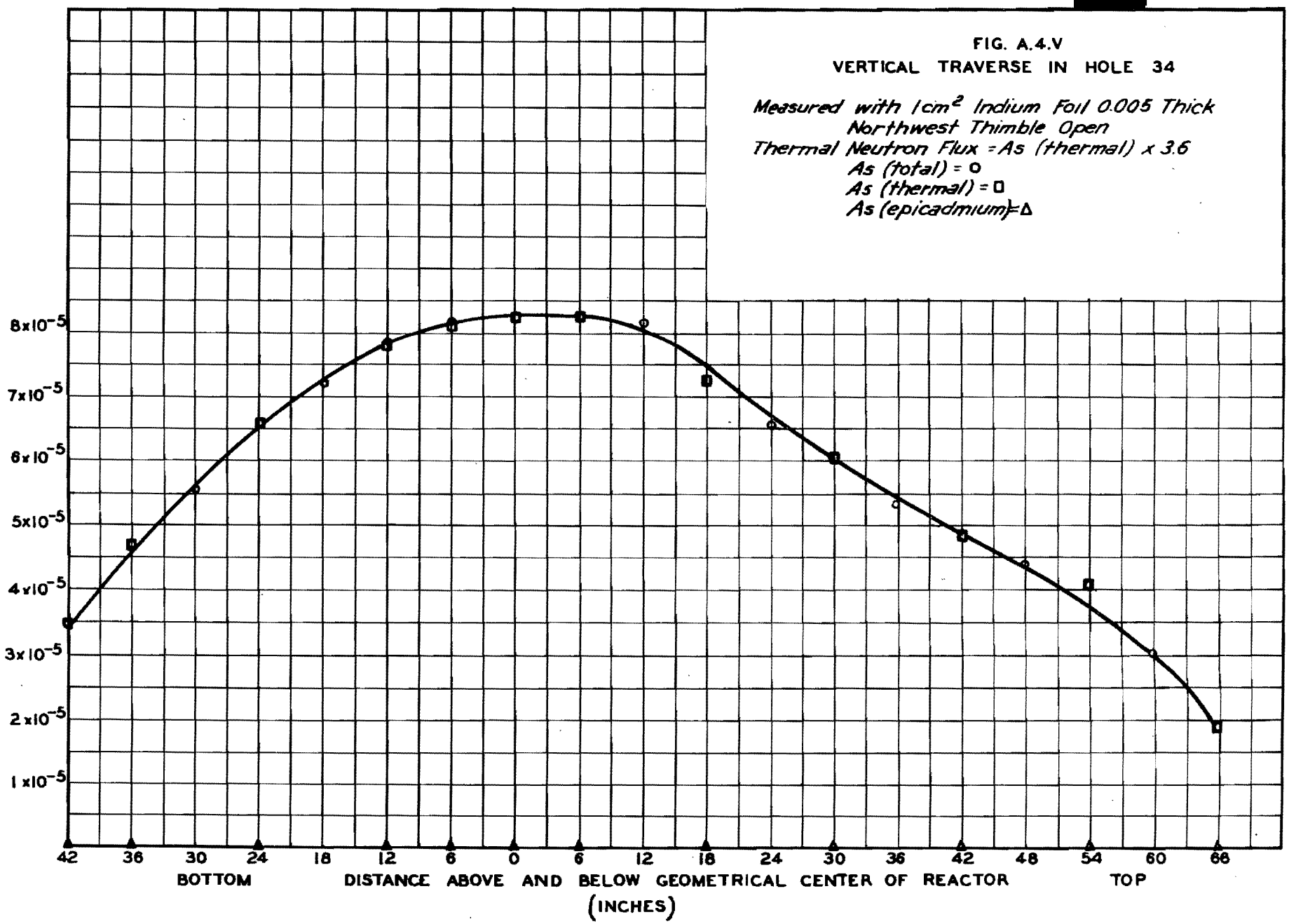
FIG. A.4.V
VERTICAL TRAVERSE IN HOLE 34
Measured with 1cm² Indium Foil 0.005 Thick
Northwest Thimble Open
Thermal Neutron Flux = As (thermal) x 3.6
As (total) = o
As (thermal) = □
As (epicadmium) = Δ
As normalized to one neutron per cm sq per sec at center of lattice
8x10⁻⁵
7x10⁻⁵
6x10⁻⁵
5x10⁻⁵
4x10⁻⁵
3x10⁻⁵
2x10⁻⁵
1x10⁻⁵
42 36 30 24 18 12 6 0 6 12 18 24 30 36 42 48 54 60 66
BOTTOM
DISTANCE ABOVE AND BELOW GEOMETRICAL CENTER OF REACTOR
TOP
(INCHES)

Second Series. The significant changes from the experimental conditions in the first series were:

1. The beryllium cylinder in the center west thimble was moved to the northwest thimble; the space behind the beryllium was filled with graphite.
2. The regulating rod was put into operation.
3. Both shim rods withdrawn to the same height (approximately 26 in.).
4. Center west thimble empty except for ion chamber.
5. Southwest thimbde empty except for ion chamber.
6. A partial thermal shield 4 ft by 4 ft by 4 in. thick was placed temporarily behind hole 17 at the edge of the graphite for the measurements reported in Table A4.I.

Table A4.H lists the flux at mid-plane in most of the holes in the northwest quadrant of the graphite reflector and the cadmium ratio in the positions where it was measured. Table A4.I shows the measurements taken on the top and bottom of the graphite reflector. Traverses on the west face of the graphite behind hole 17 with and without the partial steel thermal shield section in place are presented in Table A4.J.

Figure A4.W is a plot of the neutron flux along the vertical centerline of the active lattice, starting at the bottom of the lattice and continuing up to the shim rod electromagnets. The flux at the magnets is seen to be too low to give good counting statistics. To check this measurement the neutron attenuation curve from the X-10 reactor lid tank was normalized and plotted with the curve from the Mock-Up, considering the top of the Mock-Up lattice to be the source plate.

Third Series. This series includes two sets of measurements taken behind a 4-ft-square section of the steel thermal shield.

For the first measurements barytes concrete blocks were stacked behind the steel thermal shield and covered with a boron-tygon sheet and paraffin. Other experimental conditions were as described for the Second Series except that the center west thimble was filled with paraffin backed with graphite. Fluxes were measured in the concrete blocks using small indium foils (1 cm square) which gave activities too low for accurate counting.

DWG. # 10803
NOT CLASSIFIED

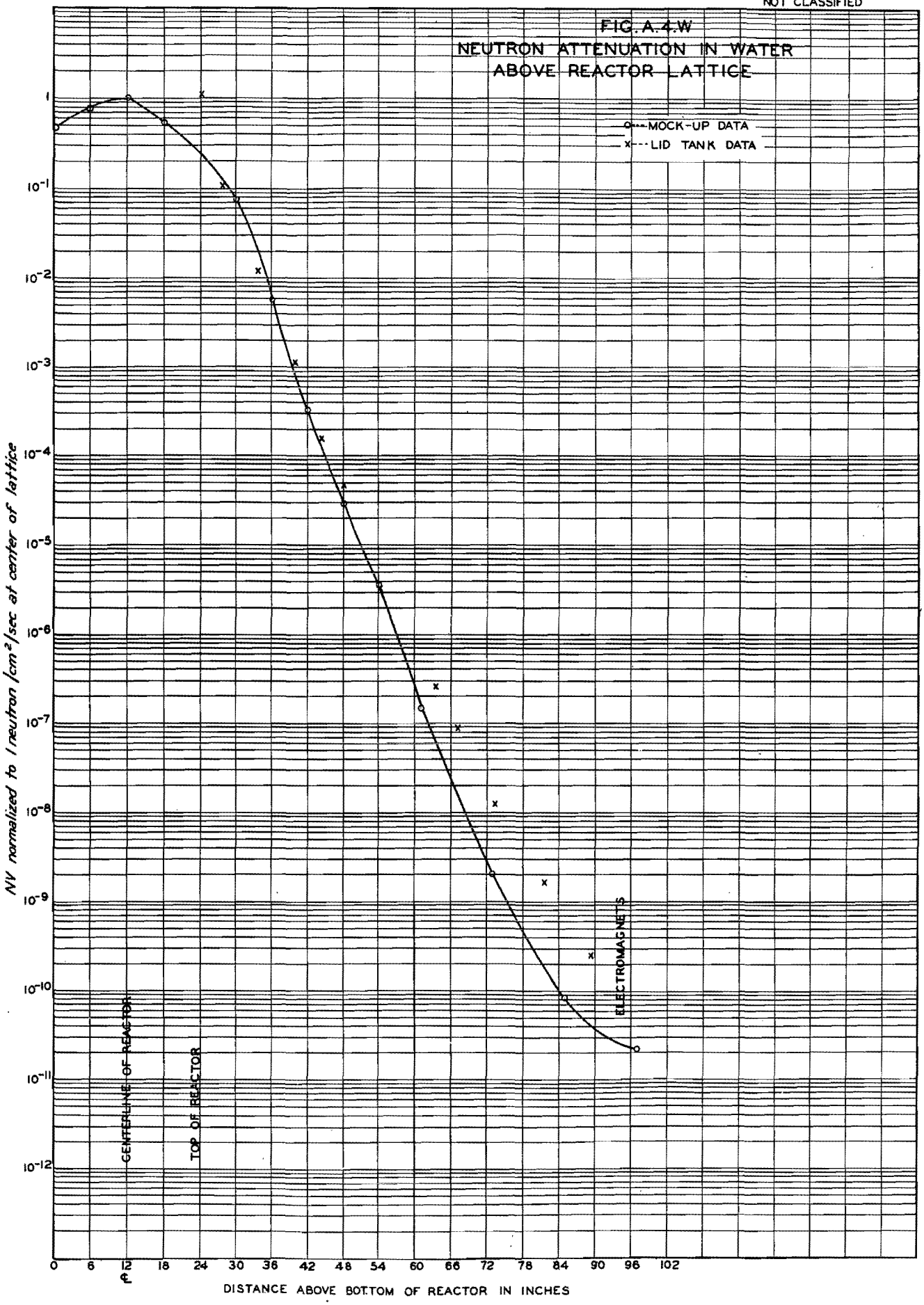

TABLE A4.H

Neutron Flux in Mid-plane

Second Series: Northwest Thimble Closed; Center Thimble Open

HOLE NO.	nv (thermal)*	CADMIUM RATIO**
44	126 x 10^{-3}	40
45	61	80
46	82	60
13	31	
19	12	600
20	28	160
21	54	
12	12	900
15	8.5	
18	4.9	1600
26	2.0	2100
27	4.4	2200
28	8.5	1300
29	12	
11	3.1	
16	2.0	800
17	1.2	1800
25	0.54	1600
34	0.18	1050
35	0.49	
36	0.87	
37	1.6	
38	2.0	1300
11***	1.1	
16***	0.55	
17***	0.36	
25***	0.22	
34***	0.19	
35***	0.29	
36***	0.46	
37***	0.65	
38***	0.85	

*Normalized to nv (thermal) of 0.1 neutron/cm^2-sec at center of lattice.

**Corrected for absorption of resonance neutrons in cadmium.

***Outer surface of graphite behind hole.

TABLE A4.I

Horizontal Traverse

DISTANCE FROM TANK WALL (in.)	nv (thermal)*
On Bottom Plane of Graphite on North-South Centerline of Reactor	
6	1.20×10^{-3}
18	0.56
24	0.45
30	0.32
On Bottom Plane of Graphite from Tank Wall Toward Hole No. 17	
6	0.47×10^{-3}
18	0.69
24	0.73
30	0.44
47	0.10
59	0.050
62	0.045
On Top Plane of Graphite from Tank Wall Toward Hole No. 17	
6	0.14×10^{-3}
18	0.22
24	0.21
30	0.24
47	0.071
59	0.049
62	0.047

*Normalized to 1 neutron/cm^2-sec at the center of the lattice.

TABLE A4.J

Traverses Behind Hole No. 17 on Surface of Graphite

POSITION	DISTANCE BETWEEN ADJACENT FOILS (in.)	nv (thermal)* NEGLECTING EPI-CADMIUM FLUX	
		WITHOUT STEEL	WITH 4-in. STEEL
Vertical			
Top	10	0.34×10^{-3}	0.35×10^{-3}
	12	0.32	0.38
Centerline	12	0.32	0.42
	10	0.30	0.33
Bottom		0.27	0.23
Horizontal			
North	10	0.19	0.14
	12	0.24	0.24
Centerline	12	0.32	0.41
	10	0.43	0.53
South		0.52	0.73

*Normalized to 1 neutron/cm^2-sec at the center of the lattice.

After this unsuccessful attempt to measure fluxes in the concrete, the barytes blocks were removed and the space behind the steel was filled with a block of paraffin, 4 ft by 4 ft by 20 in. thick (Fig. A4.X), containing horizontal and vertical slots for the exposure of large indium foils (25 sq cm). The paraffin cube was surrounded by sheets of boron-tygon plastic and had additional paraffin (left after the concrete experiment) on the north face and underneath.

Figure A4.Y is a centerline traverse perpendicular to the steel thermal shield through 18 in. of paraffin. It shows that leakage from the concrete biological shield behind the paraffin distorts the attenuation curve as far as the middle of the paraffin.

In Figs. A4.Z and AA horizontal and vertical traverses taken behind various thicknesses of paraffin show the centerline traverse to be relatively unaffected by leakage from the top and sides of the block, making Fig. A4.Y useful through the first half of the curve. Many of the cadmium-covered foils exposed in the paraffin showed essentially no activity above background and are not plotted.

A4.5.8 Heat Production in Graphite, Thermal Shield, and Concrete. One of the most important MTR design problems has been the determination of the cooling requirements of the graphite, thermal shield, and concrete portions of the reactor structure. It was felt therefore that measurements of the heat generation in these media in the Mock-Up were of particular importance because once the reactor has been constructed major changes in the structure will be impossible.

Measurements of this kind have been made for the beryllium reflector in the critical experiments.[18] For this purpose, small thimble-type ion chambers were used; this method also was employed in the present experiments.

The chambers used were of three sizes, 10, 50, and 95 cm^3. Figure A4.BB shows a typical design. A six-channel vacuum-tube electrometer circuit[19] was used with the chambers, making it possible to minimize the time required for the necessarily large number of measurements.

The chambers were calibrated by two independent methods: (1) against radium and cobalt sources (in air), and (2) against a sensitive liquid-nitrogen calorimeter by comparison of heat generated in a graphite block inserted in the ORNL graphite reactor with that calculated from ion chamber measurements in a similar block.[20]

DWG. #10820
NOT CLASSIFIED

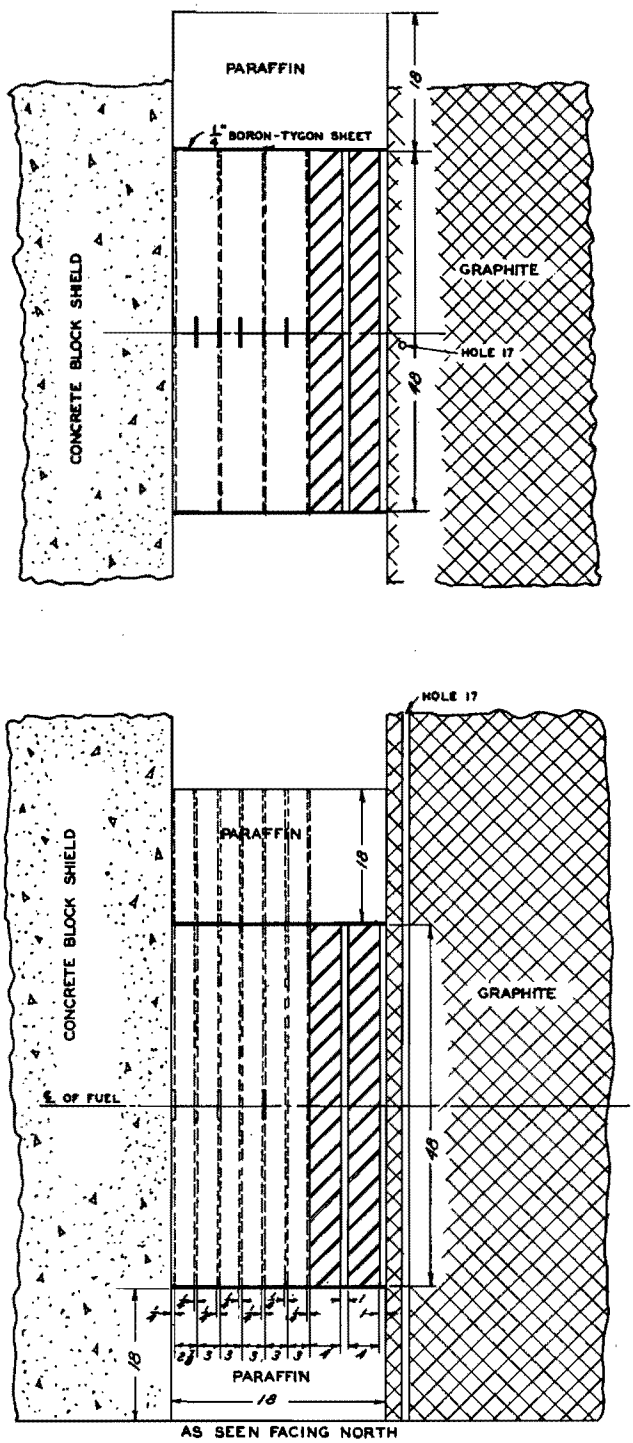

FIG. A.4.X
ARRANGEMENT OF PARAFFIN AND STEEL THERMAL SHIELD SHOWING FOIL EXPOSURE SLOTS

DWG 9788 [redacted]

FIG. A4.Y

NEUTRON ATTENUATION IN PARAFFIN BEHIND THE THERMAL SHIELD

Points are As vs Thickness of Paraffin behind 8 in. of steel
Foils are Indium, 25 cm sq, 0.005 in. thick
Reactor Power ~ 2 KW
NV(th) = As(th) X 0.13

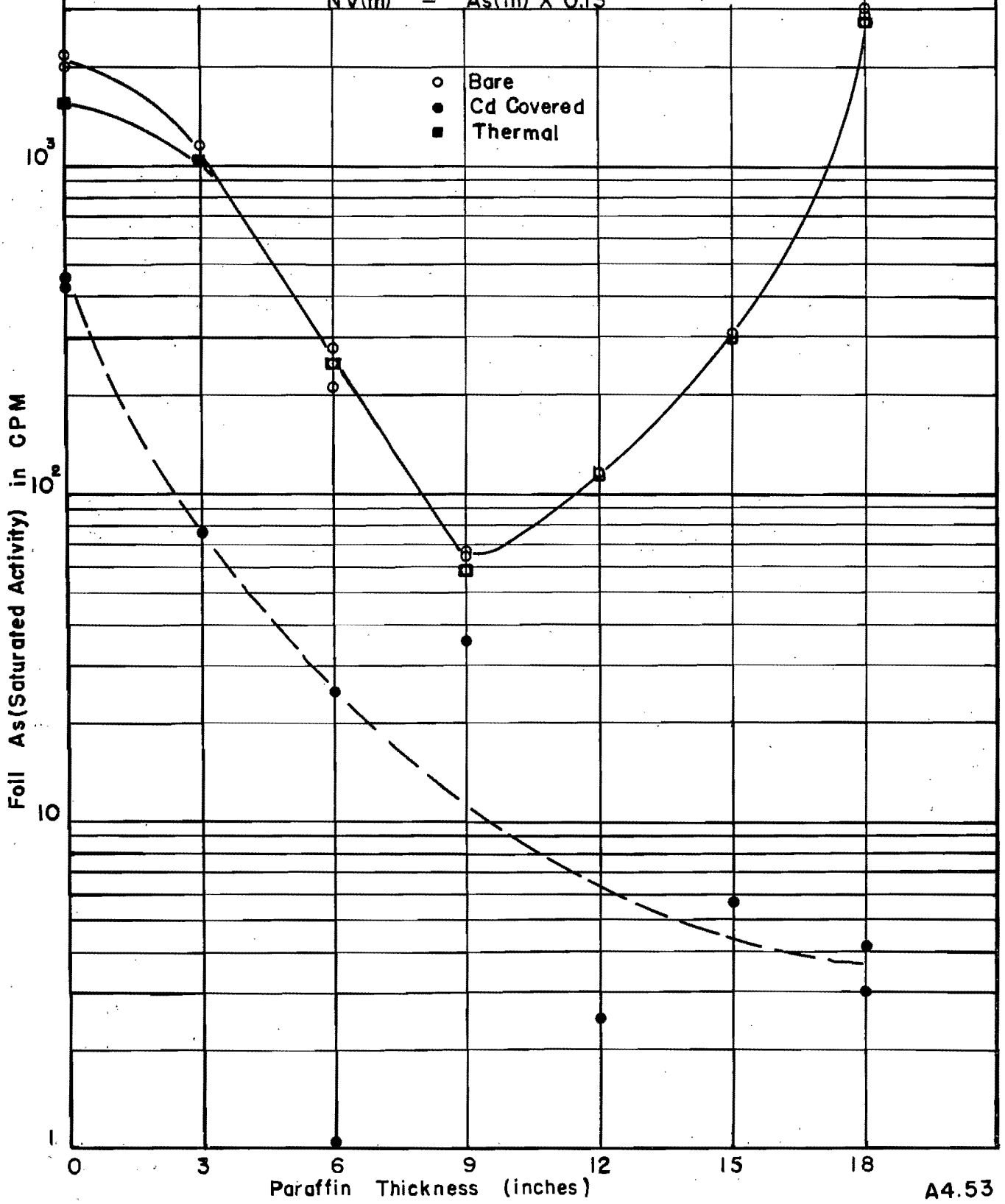

A4.53

FIG. A4.Z

HORIZONTAL TRAVERSE BETWEEN PARAFFIN AND STEEL

Points are saturated activity vs distance from the south end of a block of paraffin placed behind eight inches of steel.

Foils are Indium, 25 cm sq, 0.005 in. thick,

Reactor Power ~ 2 KW

NV(th) = As(th) X 0.13

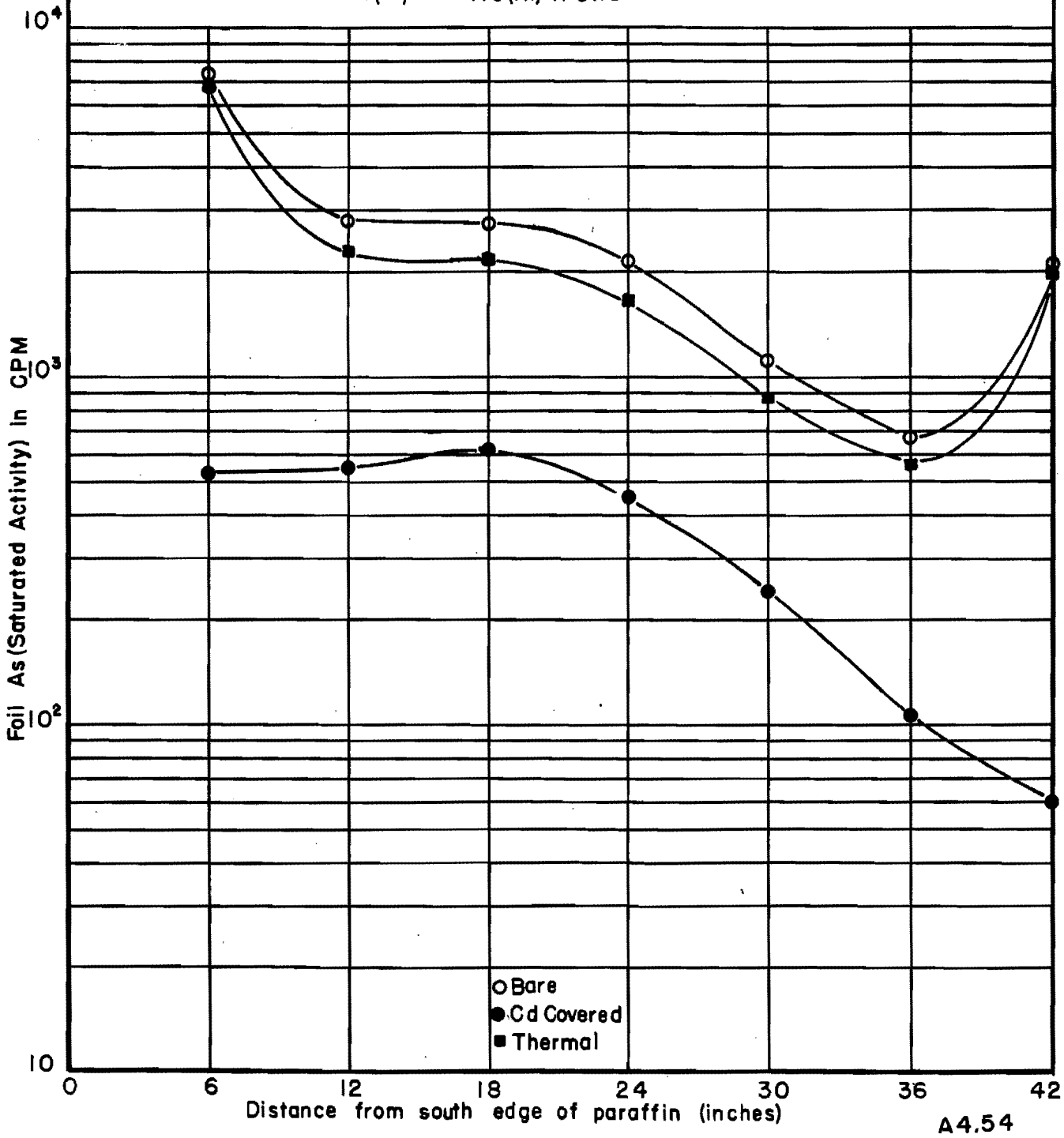

FIG. A4.AA

VERTICAL TRAVERSE BETWEEN PARAFFIN AND STEEL

Points are saturated activity vs distance below the top of a block of paraffin placed behind eight inches of steel.

Foils are Indium, 25 cm sq, 0.005 in. thick.

Reactor Power ~ 2 KW

NV(th) = As(th) X 0.13

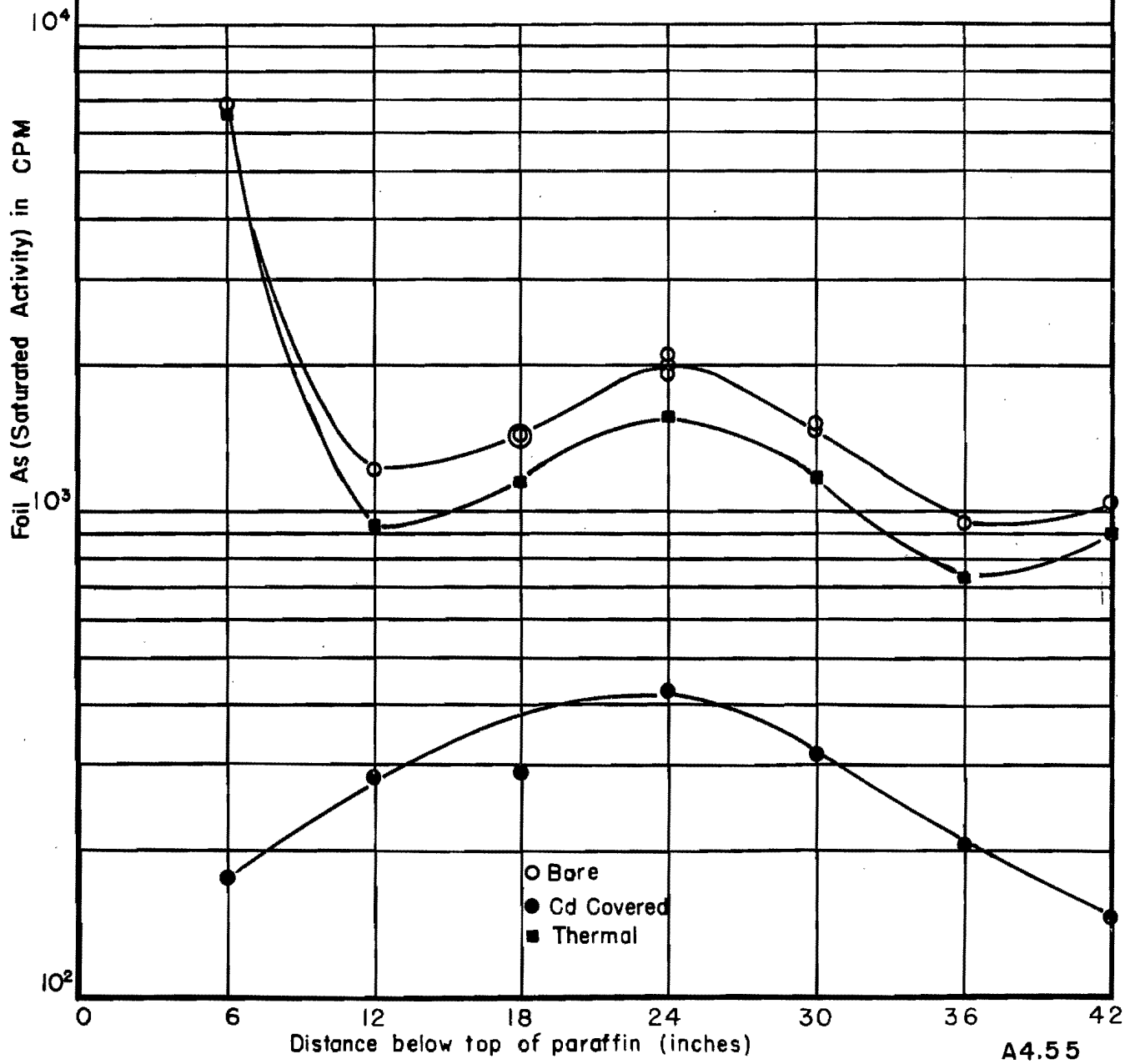

DWG. #10807
NOT CLASSIFIED

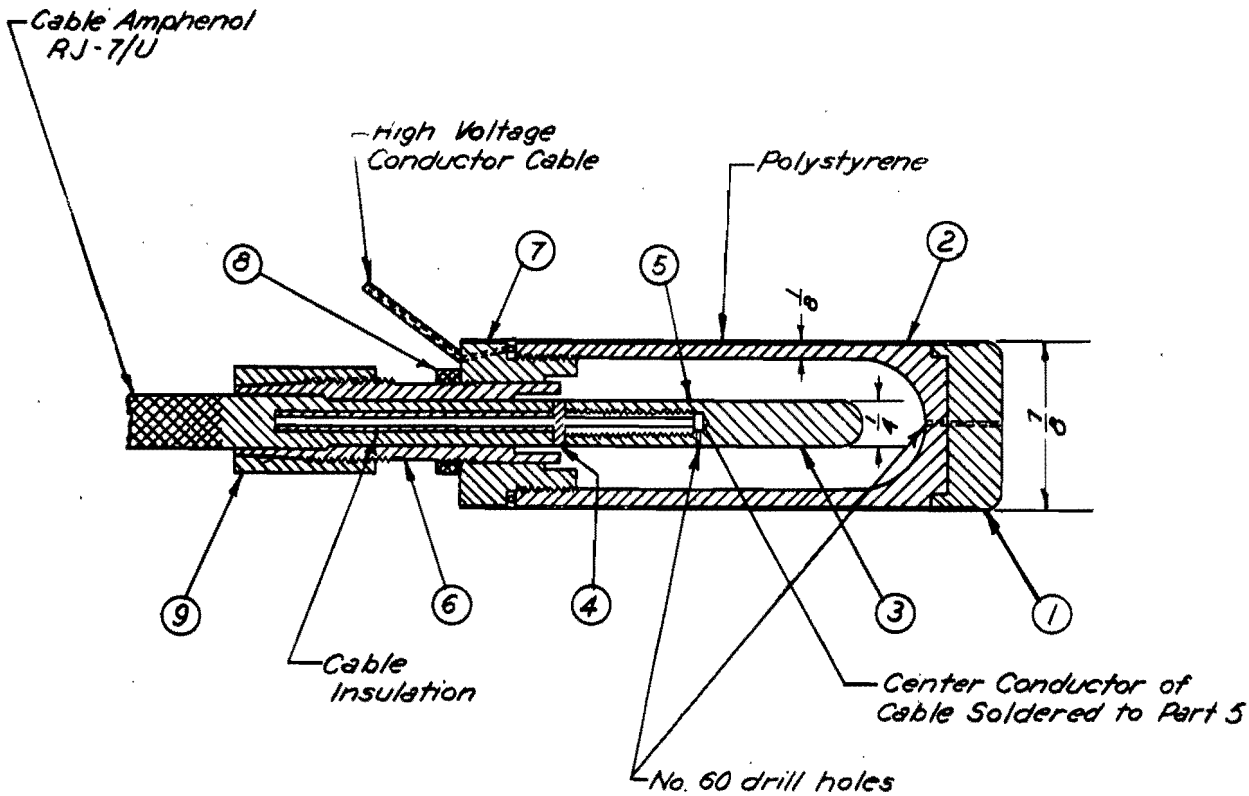

1. End Cover
2. Shell
3. Electrode
4. Connector
5. Sleeve
6. Cable Clamp
7. Chamber Cap
8. Nut
9. Nut

FIG. A.4.BB

$10cm^3$ GRAPHITE IONIZATION CHAMBER USED IN MTR MOCK-UP HEAT PRODUCTION MEASUREMENTS

Calibrations were made with air, CO_2, argon, and helium, but CO_2 was used for the measurements, making it unnecessary to correct for ionization by protons from the nitrogen (n,p) reaction. Constant flow of gas through the chambers was supplied through the coaxial cables and connectors.

The method of measurement consisted simply of insertion of ion chambers in the various holes provided in the graphite for this purpose (see Fig. A4.C) and observation of the ion current with the reactor operating at a constant power level. For the purpose of normalization, ion chambers in two holes (8 and 13) were checked carefully against neutron (foil) measurements in the core, and thereafter all measurements were referred to chambers in these holes.

In computation of the heat production, the ion chamber measurements have been referred to a neutron flux of 1 neutron/cm^2-sec at the center of the core.

Two major groups of measurements were made at various points in the graphite reflector. In the first experiments the arrangement of the experimental holes and tank thimbles was that of the first series of neutron-flux measurements. The second series of ion chamber measurements corresponds to the second series of neutron experiments. Tables A4.K and L and Figs. A4.CC, DD, EE, and FF contain the results. These data have been analyzed in ORNL CF-50-7-86.

Measurements were also made in sections of barytes concrete which were placed behind the simulated thermal shield. For this purpose a special chamber with a polystyrene wall of 0.010 in. thickness was constructed. This modification produced, in effect, an air-wall chamber, and it is believed therefore that the measurements in concrete are probably correct within about 25%. Typical results are shown in Fig. A4.GG.

A4.5.9 Attenuation of γ-Rays Inside Reactor Tank. The top plug of the MTR tank is designed so that it can be filled with lead to a maximum thickness of 10 in., although the exact thickness required for shielding at 60,000 kw was thought to be less than 10 in. An estimation of this thickness has been obtained from measurements of γ-ray attenuation in the Mock-Up tank with the active lattice operating at approximately 270 watts.

Attenuation measurements were made with sensitive watertight ion chambers along two vertical lines above the active lattice. Data are plotted in Fig. A4.HH and indicate a factor of e reduction in 29.5 cm. The discontinuity

DWG. 10818

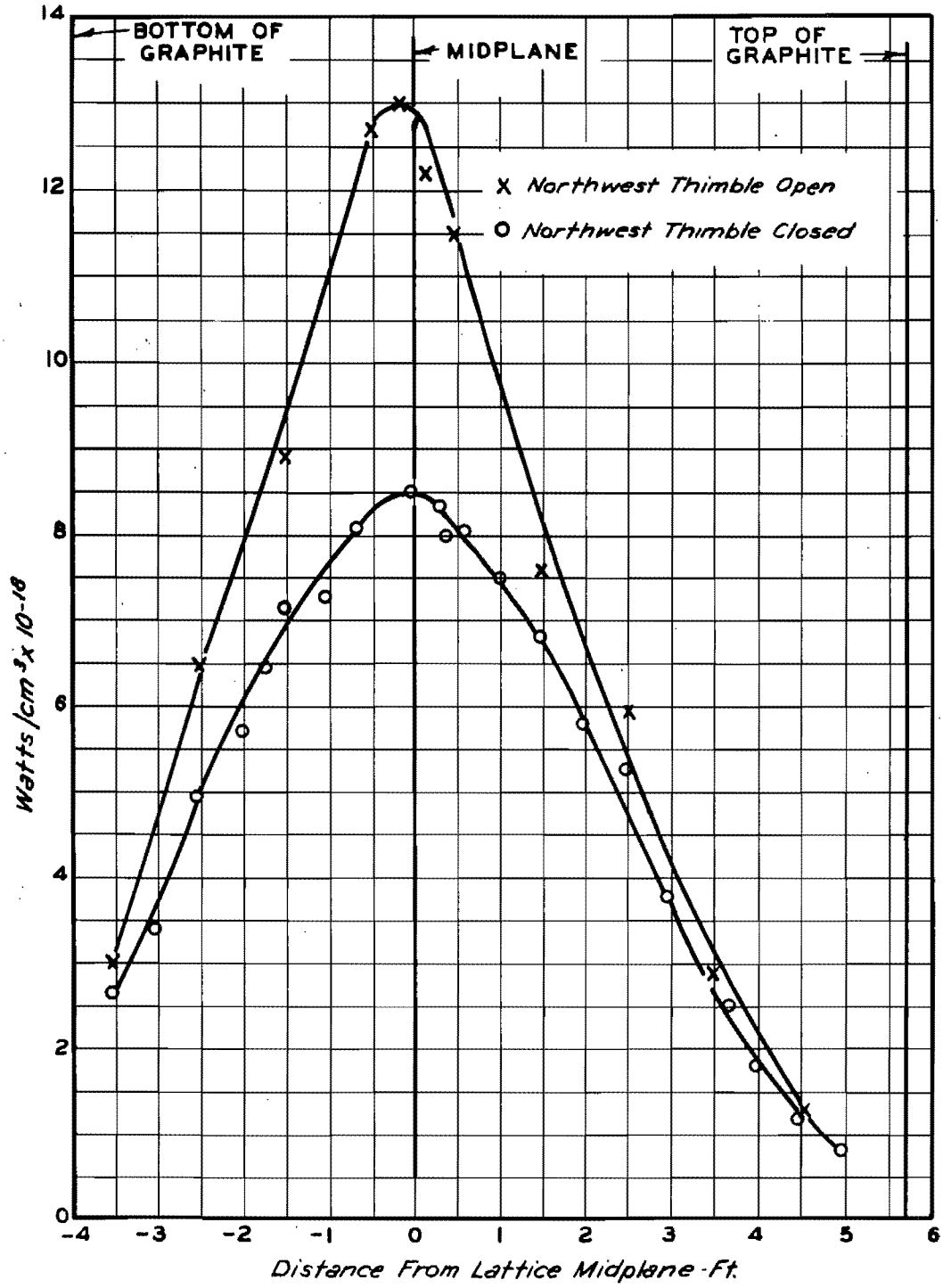

FIG. A.4.CC

HEAT PRODUCTION IN HOLE 19

Values Normalized To NV_{th} = 1.0n/cm² sec at Core Center

DWG. #10817
[redacted]

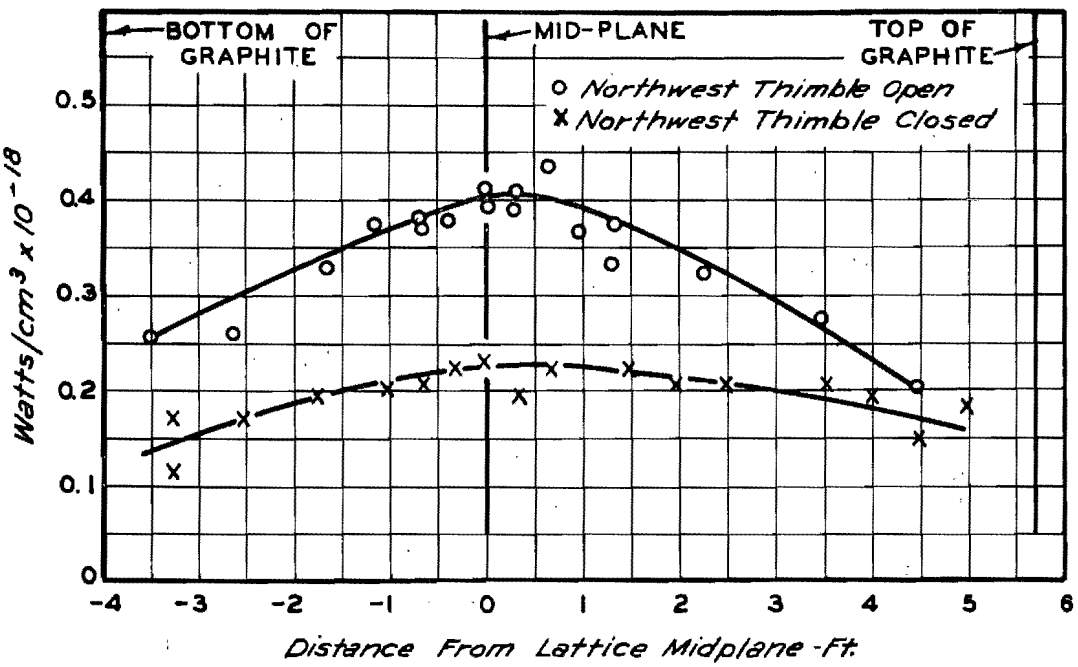

FIG. A.4.DD
HEAT PRODUCTION IN HOLE 34

Values Normalized To $NV_{th} = 1.0 n/cm^2$ sec At Core Center

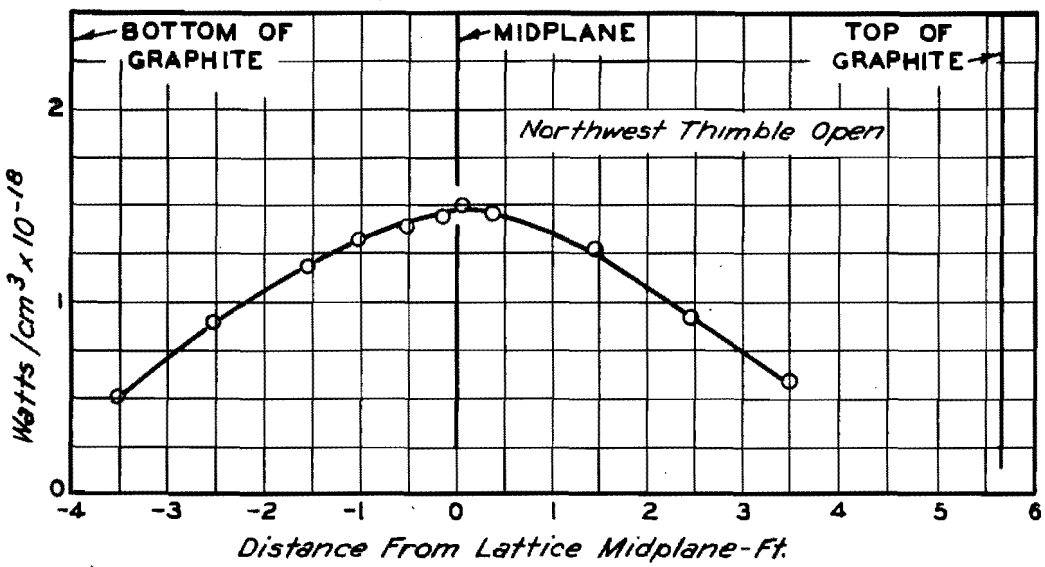

FIG. A.4.EE

HEAT PRODUCTION IN HOLE 26

Values Normalized To NV_{th} = 1.0 n cm²/sec At Core Center

DWG. # 10767
[redacted]

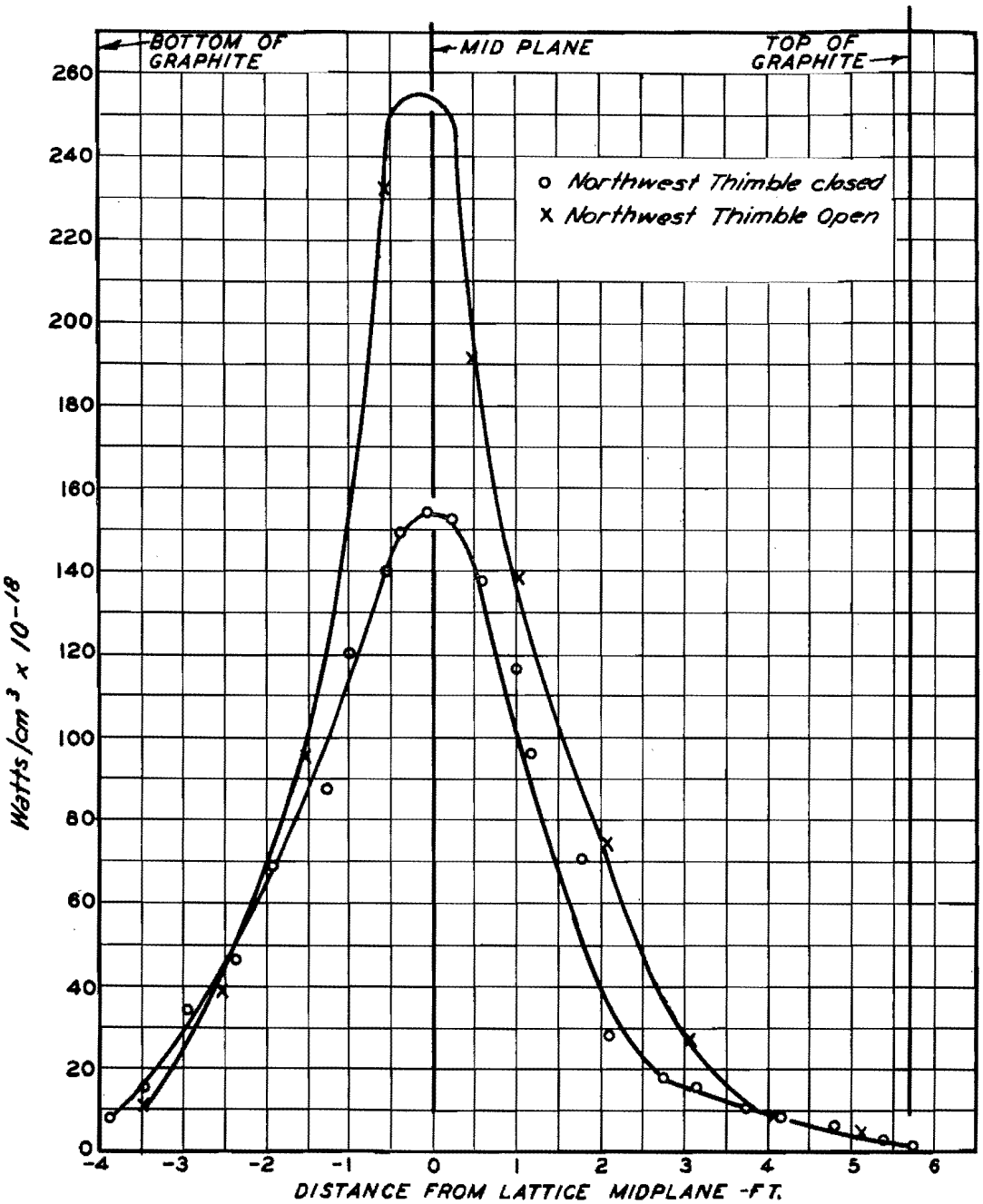

FIG. A.4.FF

HEAT PRODUCTION IN HOLE 45

Values Normalized to NV_{th} = 1.0 /cm² sec At Core Center

DWG 9787 [redacted]

FIG. A4.GG

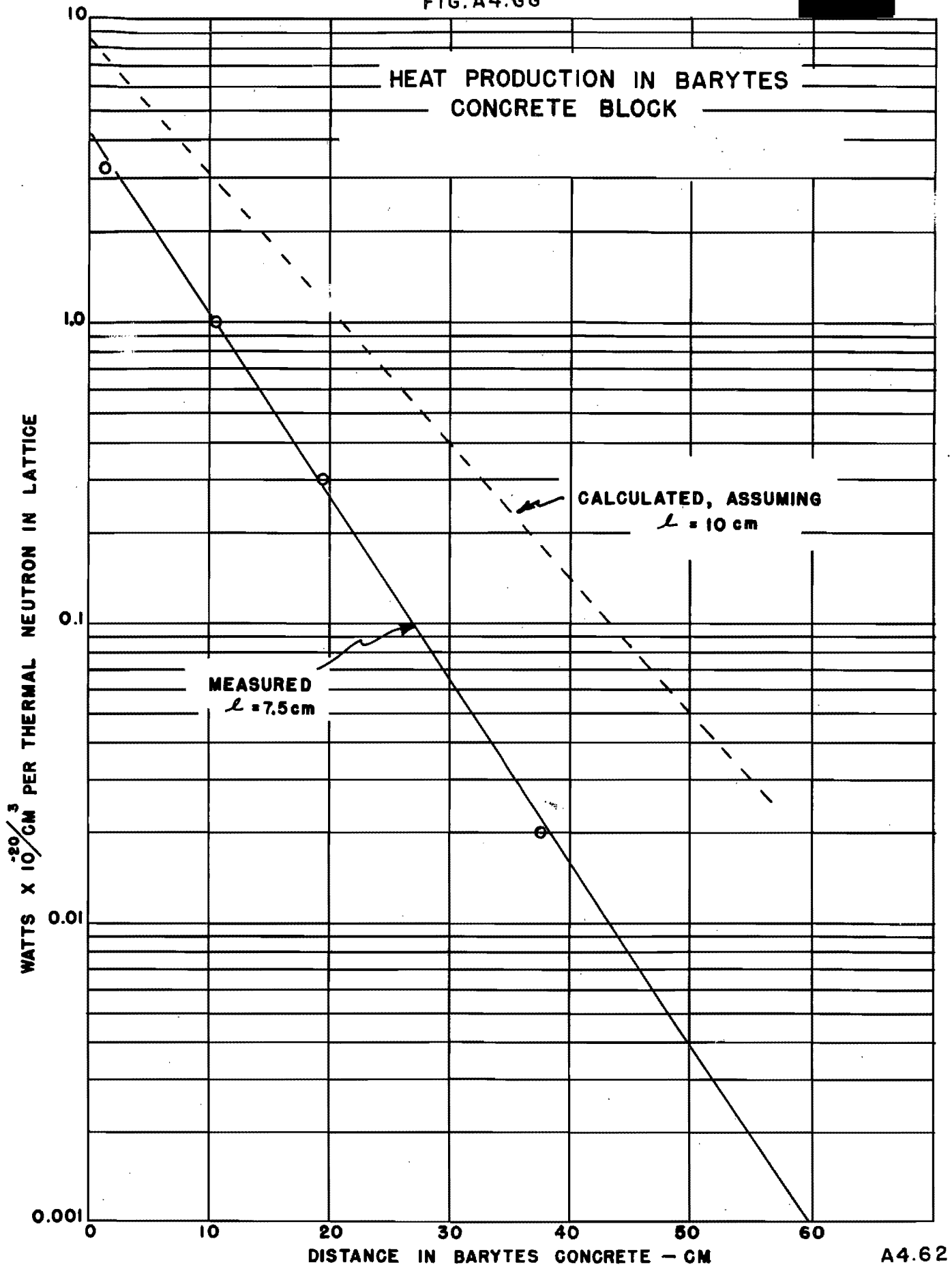

A4.62

[redacted] DWG. 9401

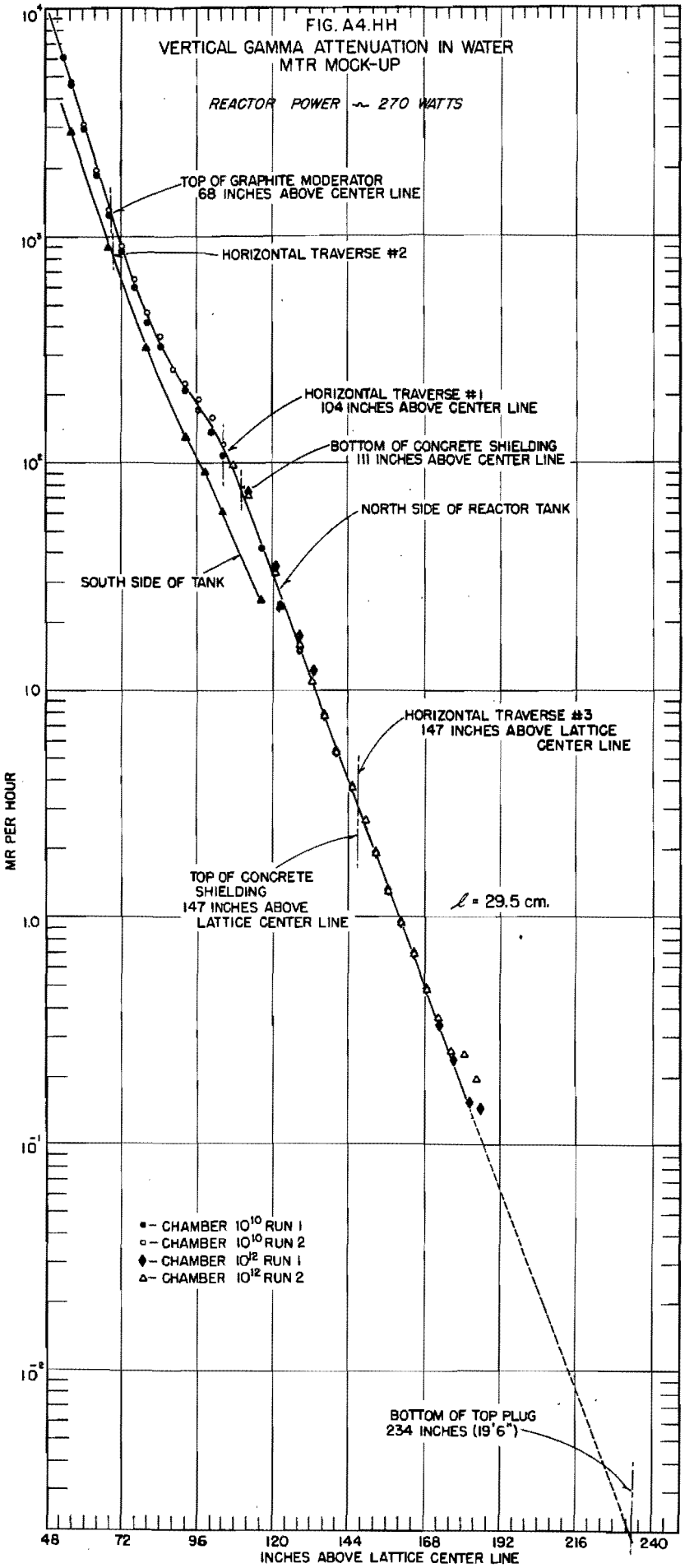

TABLE A4.K

Heat Production in Mid-plane, Graphite Reflector

HOLE NO.	HEAT PRODUCTION (watts/cm^3/unit neutron flux in core)	
	NORTHWEST THIMBLE CLOSED, CENTER THIMBLE OPEN	NORTHWEST THIMBLE OPEN, CENTER THIMBLE CLOSED
11	2.4×10^{-18}	2.8×10^{-18}
12	8.2	7.5
13		36.3
15	6.1*	
16	2.3*	3.8
17	1.9* (0.7)	4.2
18	2.95* (3.35)	6.0
19	(8.9)* (8.5)	11.6
20	32	29
21	74.5	70.5
22	68.0	71
25	0.85* (0.4)	0.75
26	1.07	1.3
27	2.3	
28	5.0	
29	7.55	
30		53
34	0.23	0.36
35	0.31	
36	0.52	
37	0.96	
38	1.1	
44	445	
45	155	185
46	380	

*Steel section, simulating thermal shield, behind graphite; parentheses indicate no steel behind graphite.

TABLE A4.L

Measured Heat Production in Top and Bottom Planes of Graphite Reflector

HOLE NO.	HEAT PRODUCTION (watts/cm^3/unit neutron flux in core)	
	TOP PLANE 6 in. BELOW TOP GRAPHITE	BOTTOM PLANE 6 in. ABOVE BOTTOM GRAPHITE
11	0.5×10^{-18}	0.6×10^{-18}
12	1.0	1.5
13		
15	0.7	1.5
16	0.5	1.0
17	0.4	0.4
18	1.2	1.0
19	0.8	3.0
20	6.0	7.0
21	1.4	8.65
22		
25	0.2	0.2
26	0.2	0.5
27	0.3	0.8
28	0.5	1.14
29	0.4	1.4
30		
34	0.2	0.3
35	0.3	0.3
36	0.3	0.3
37	0.2	0.3
38	0.2	0.3
44	1.9	15
45	2.0	10.5
46	1.6	9.5

of the curves, beginning at approximately 70 in. above the fuel, was studied further with three horizontal traverses, plotted in Fig. A4.II. Traverse No. 1 clearly indicated an additional γ-ray source on the north side of the tank. This source is explained by the construction of the graphite reflector and the concrete shield as shown in Fig. A4.JJ. The graphite and the air space above permit a high thermal flux to exist up to the 111-in. elevation. The capture of these neutrons by the steel tank sections provides the additional γ-ray source which disrupts the attenuation curves of Fig. A4.HH.

With these measurements it was possible to extrapolate the attenuation lines to the top plug (elevation 234 in.). Normalization of this point to 60,000 kw indicated approximately 500 mr/hr, requiring a 6-in. thickness of lead shot in the top plug for adequate protection.

Complete details of this work are reported in ORNL CF-50-8-85.[21]

[redacted]

DWG. 9402

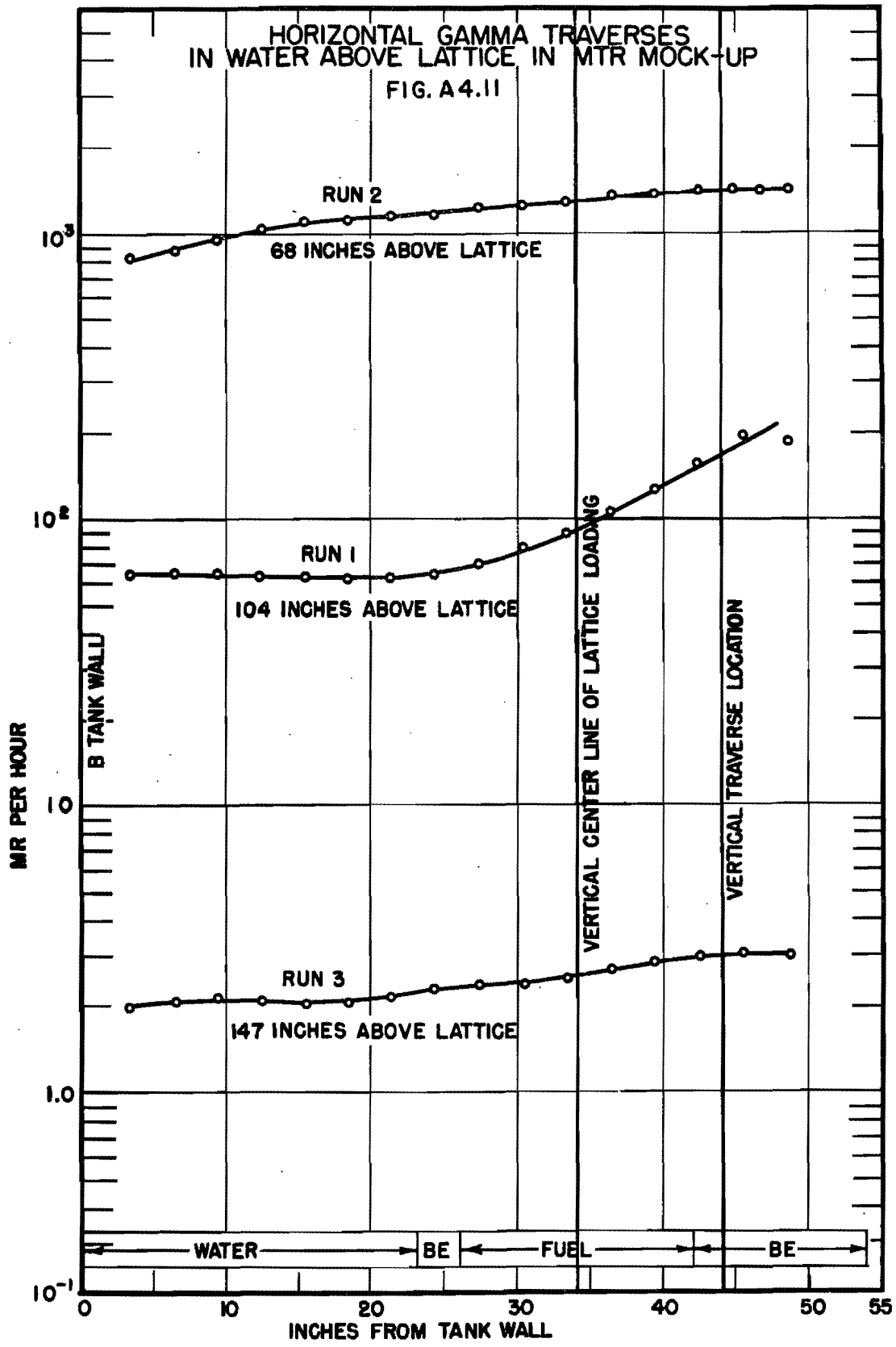

[redacted] DWG. 9404

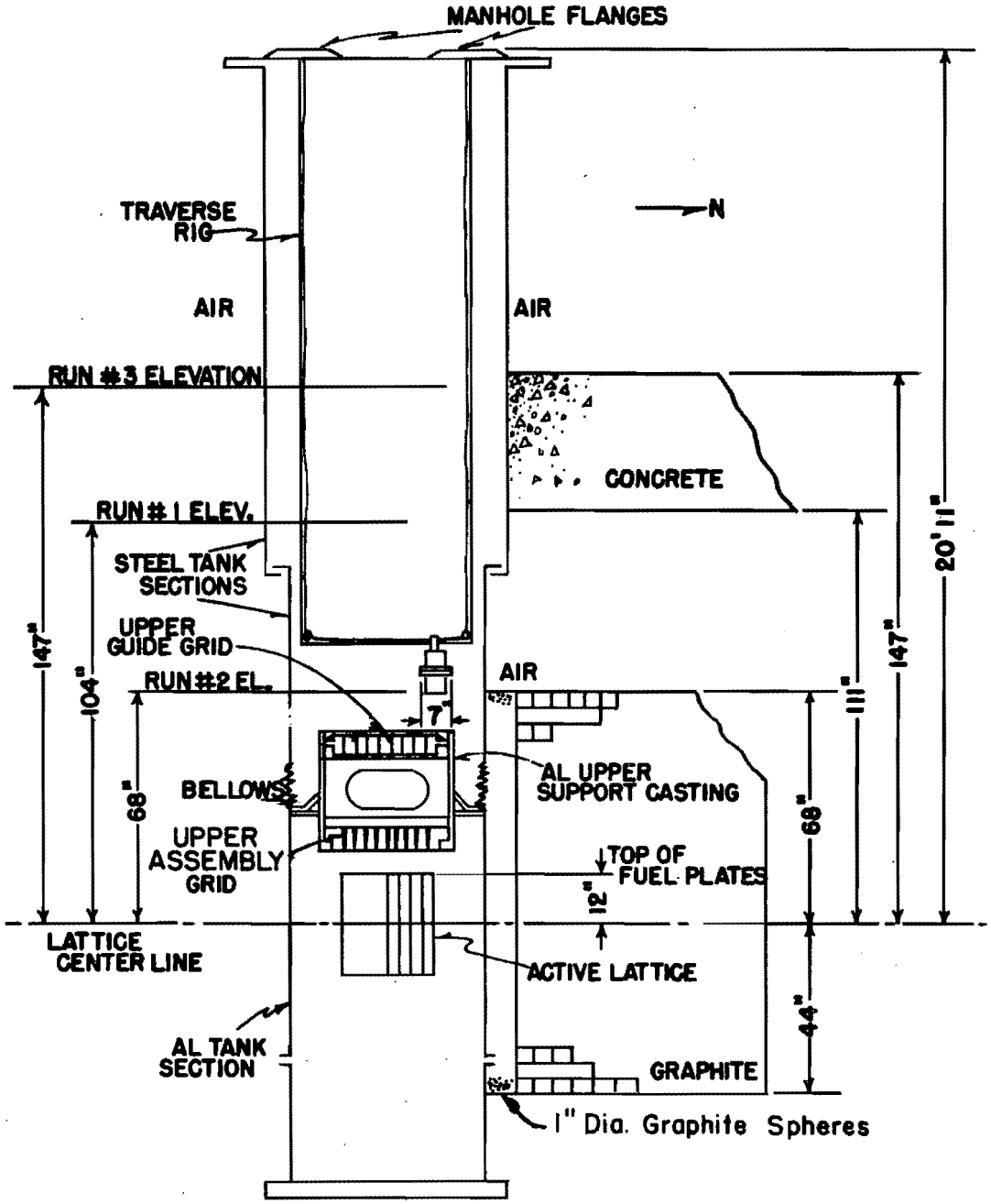

FIG. A4.JJ

CHAMBER ELEVATIONS FOR HORIZONTAL GAMMA TRAVERSES AND RELATIVE LOCATIONS OF GRAPHITE, AIR AND CONCRETE IN MTR MOCK-UP

A4.6 REFERENCE REPORTS

(1) Huffman, J. R., *et al.*, *Feasibility Report on Clinton High Flux Pile*, MonT-433, December 1, 1947.

(2) Gall, W. R., and Mallon, D. J., *Mock-Up Design Report*, ORNL CF-49-10-185, October 27, 1949.

(3) Beall, S. E., *Procedure for Erection of MTR Mock-Up*, ORNL-692, May 18, 1950.

(4) Savage,, H. C., *MTR Strain Measurements*, ORNL-472, November 20, 1949.

(5) Beall, S. E., *Interim Report of Neutron and Gamma Experiments in the MTR Mock-Up*, ORNL CF-50-5-140, May 11, 1950.

(6) Nicoll, D., *Design of Shim-Safety Rods*, ORNL CF-48-2-139, February 4, 1948.

(7) Nicoll, D., *Supplementary Report to Design of Shim-Safety Rods*, ORNL CF-49-1-65, December 31, 1948.

(8) Beall, S. E., *Shim-Safety Rod Data*, ORNL CF-49-8-188, August 17, 1949.

(9) Nicoll, D., *Design of Regulating Rods for High Flux Reactor*, ORNL CF-49-4-123, March 14, 1949.

(10) Kasper, S., *Water Flow in Materials Testing Reactor*, ORNL CF-50-6-102, June 15, 1950.

(11) Winters, C. E., *Technical Division, Section II, Report for Period Ending September 15, 1948*, ORNL CF-48-9-278, September 17, 1948.

(12) *Calibration of Control and Shutoff Rods in Gleep by Relaxation Time Measurements*, AERE-NR-130, December 5, 1947.

(13) Briggs, R. B., *A Comparison of Design Neutron Fluxes and Heat Production in the Graphite Reflector and Thermal Shield of the Materials Testing Reactor with Values Measured in the MTR Mock-Up*, ORNL CF-50-7-86, July 20, 1950.

(14) Lane, J. A., *Shielding Requirements, Top and Bottom Plugs*, ORNL CF-50-7-7, July 5, 1950.

(15) Arnette, T., and Jones, H., *Thermal Neutron Flux Distribution in a Standard Graphite Pile*, CP-2804, April 30, 1945.

(16) Weinberg, A. M., *Physics Division Quarterly Report for Period Ending February, 1948*, CNL-35, March 26, 1948.

(17) Kunstadter, J. W., "A Correction to Be Applied to the Activity of Neutron-Activity Cadmium Covered Indium Foils," *Phys. Rev.*, **78**, 484 (1950).

(18) Mann, M. M., and Martin, A. B., *Critical Experiments for High Flux Reactor*, ORNL-167, October 22, 1948.

(19) Glass, F. M., *Low Drift Electrometer*, ORNL-486, December 20, 1949.

(20) Jenks, G., Breazeale, W. M., and Hairston, J. J., *Calorimeteric Calibration of a Graphite-Walled, Cavity-Type Ionization Chamber*, ORNL-923, January 23, 1951.

(21) Clifford, C. E., and Mauney, T. H., *Gamma Attenuation Measurements Through Water in the MTR Mock-Up*, ORNL CF-50-8-85, November 3, 1950.

Appendix 5

BERYLLIUM

A5.1 CHEMICAL AND MECHANICAL TESTS

When it became evident in 1947 that the beryllium supply was to be adequate, immediate tests were started to determine its corrosion resistance and mechanical properties. The first beryllium* to become available was extruded material, and most of the initial corrosion testing was done on this. The corrosion-test procedures and preliminary results are fully described in ORNL-298.[1] This and later reports emphasize that the corrosion of beryllium in simulated cooling water can be controlled to a large extent by:

1. Controlling the amounts of impurities present in the metal through improved processing techniques. Corrosion-test data indicate that these impurities are a very important factor in determining the corrosion resistance of this metal.
2. Controlling the quality of the demineralized water used as a cooling medium. A water of high specific resistance is desired as well as one relatively free from such detrimental ions as chlorides, sulfates, copper, and iron.

In general, however, data presented in ORNL-298 and in ORNL-733[2] indicate that the corrosion resistance of either extruded or hot-pressed beryllium is such that no serious corrosion problems are to be expected. As a result of the data in ORNL-733, the decision was made to use hot-pressed beryllium for the MTR rather than extruded material because:

1. The hot-pressed method allowed the manufacture of large odd-shaped pieces and hence reduced the stacking problem in the MTR.
2. Hot-pressed beryllium appeared then to have a somewhat better corrosion resistance. It is now known that there is very little difference between the two in this respect.

*The following types of beryllium are mentioned in various reports:

1. Extruded beryllium.
2. Q.M.: Normal high-purity beryllium used to produce powder for hot pressing into required shapes.
3. Q.R.M.: Recast from previous pressings of Q.M.
4. Q.M.V.: High-purity beryllium cast by a vacuum method into billets which are then pulverized into powder for hot pressing. This method reduces the oxygen content and therefore reduces the beryllium oxide. All the MTR beryllium is Q.M.V. metal.

A final report on the corrosion tests on beryllium is now in composition and will be issued sometime after March, 1951 as an ORNL report.

The mechanical tests on beryllium involved both machining tests and calculation and experimental work on thermal stresses. An example of the machining tests is given in ORNL CF-50-4-110,[3] which is a report on deep-hole drilling in beryllium. As of Jan. 1, 1951 the machining of the MTR beryllium had been 95% completed by the Y-12 Beryllium Shop with no major difficulties encountered.

Some concern was felt that the temperature differentials in the beryllium would be sufficient to set up stresses large enough to crack the metal blocks. Calculations were made for blocks containing various sizes of cooling holes. The results for the 3- by 3-in. beryllium bars with 3/16-in. axial cooling holes (pieces labeled "A" in Fig. 2.2.A) are given in ORNL CF-50-6-9.[4] These calculations showed that for MTR operation at 30 megawatts the maximum thermal stresses occurring are 12,000 psi at the surface of the bar and 4700 psi at the surface of the axial hole, well within the tensile strength of beryllium.

To check these calculations, experiments[5] were performed in which thermal stresses were set up in beryllium bars using the same basis of calculation as above. It was found experimentally that the minimum stress at failure for the hot-pressed beryllium was 28,200 psi, well above the value obtained in MTR operation.

A5.2 MANUFACTURE AND SPECIFICATIONS OF MTR BERYLLIUM

Since a full report on the method of manufacture and chemical analysis of each piece of MTR beryllium is being prepared (Gregg, J. L., *Beryllium for the MTR*, to be issued as an ORNL report), only a brief summary and an example of the chemical analyses will be given here.

All the beryllium for the MTR is being made by hot pressing of the powder obtained from pulverizing vacuum-cast billets. The raw metal is refined and then is melted and cast in vacuum. The castings are cut on a lathe, rolled, and pulverized to produce particles that will pass through a 200-mesh screen. This fine powder is put into dies and placed in a vacuum furnace at approximately 1050°C and 100 psi pressure for 20 to 30 hr. When these pressings are removed from the furnace, they are cut into rough shapes and shipped to Y-12 for final machining.

The specifications set up for the rough sections of beryllium are given in detail in ORNL CF-50-3-114.[6] These include chemical, corrosion, and physical requirements and test procedures. Since the chemical specifications may be useful in future checking, they are given below.

> The chemical composition of the beryllium shall be such that the total danger summation (see Section A5.3) does not exceed 15 for all impurities or elements other than boron, and the boron content shall be below that which increases the total danger summation by 15. In addition, the chemical composition shall be within the following limits:

Free beryllium metal assay	98.0% min.
Total carbon reported as Be_2C	0.25% max.
Aluminum	1500 ppm max.
Cobalt	2 ppm max.
Copper	500 ppm max.
Iron	2000 ppm max.
Lithium	3 ppm max.
Magnesium	3000 ppm max.
Manganese	250 ppm max.
Nickel	200 ppm max.
Silicon	700 ppm max.
Silver	5 ppm max.
Zinc	150 ppm max.

An example of how well the metal is meeting these specifications is given in Table A5.A, which is an excerpt from the Beryllium Control Record for one pressing of the MTR metal from which were obtained five "A" pieces (see Fig. 2.4.A).

TABLE A5.A

SINTERED PRODUCT

DATE OF PRESSING	DIMENSIONS OF BLOCK (in.)	WEIGHT OF BLOCK (lb)	FURNACE	COMPACTING PRESSURE (psi)	SINTERING TEMPERATURE (°C)	SINTERING TIME (hr)	SINTERING ATMOSPHERE	SINTERING PRESSURE (μ Hg)	RADIOGRAPH NO.	DENSITY
7-14-50	41 x 21 x 3.6	211.6	Horizontal	125	1050	30%	Vacuum	100		1.855

ANALYSIS

	(percent)			(parts per million)															TDS Excl. B	TDS Incl. B
	Assay	BeO	Be_2C	Ag	Al	B	Ca	Cd	Co	Cr	Cu	Fe	Li	Mg	Mn	Ni	Si	Zn		
Brush	99.45	1.03	0.20	-1	700	0.4	-10	-0.2	-1	73	80	900	-0.3	50	88	85	380	-30	8.21	10.59
N.B.				~1	290	0.9	-20	ND	~1	180	27	980	-1	~15	100	~100	1500	~20	9.33	14.69

Remarks: Si over limit based on New Brunswick analysis.

AUTOCLAVE

PIECE NO.	WEIGHT (lb)	PRESSURE (psi)	TEMPERATURE (°C)	TIME (hr)	AUTOCLAVE NO.	PLACE	GRADING	COMMENTS	DISPOSITION
A-14	26.03	550 ± 30	250 ± 5	96	1	Cleveland	Excellent	No visible attack noticed	All pieces shipped on 7-31-50 to Oak Ridge on MTC No. 1346B BG/L No. AT-85193; total weight 155.98 lb
A-15	26.08	550 ± 30	250 ± 5	96	1	Cleveland	Excellent	Same	
A-16	25.86	550 ± 30	250 ± 5	96	1	Cleveland	Excellent	Same	
A-17	26.02	550 ± 30	250 ± 5	96	1	Cleveland	Excellent	Same	
A-18	25.90	550 ± 30	250 ± 5	96	1	Cleveland	Excellent	Same	
A-19	26.09	550 ± 30	250 ± 5	96	1	Cleveland	Excellent	Same	

A5.3 DANGER COEFFICIENT AND TOTAL DANGER SUM (TDS) AS APPLIED TO BERYLLIUM

The definition of danger coefficient is given in the Project Handbook (CL-697, Chap. IV, p. 17) as follows: "The danger coefficient of a substance is a measure of the ability of that substance to absorb thermal neutrons compared with the ability of some reference substance to absorb thermal neutrons, or

$$K_s(i) = \frac{S_i}{S_s} = \frac{N_0\sigma_i/A_i}{N_0\sigma_s/A_s} = \frac{\sigma_i \times A_s}{\sigma_s \times A_i} \qquad (1)$$

where

K_s = danger coefficient with respect to reference or standard substance (usually natural uranium).

S_i = effective area presented to neutrons by 1 g of impurity (cm^2/g).

S_s = effective area presented to neutrons by 1 g of reference substance (cm^2/g).

N_0 = number of atoms in one mole of any substance (6.03×10^{23} atoms/mole).

A_i = atomic weight of impurity (g/mole).

A_s = atomic weight of reference substance (g/mole).

σ_i = atomic cross-section of impurity for absorption of thermal neutrons (cm^2/atom).

σ_s = atomic cross-section of reference substance for absorption of thermal neutrons (cm^2/atom)."

The total danger sum (TDS) is defined as the value which is equal to the sum of the products of the concentration of each impurity in a substance and the danger coefficient for that impurity. It is used to determine whether the total number of thermal neutrons absorbed by the material exceeds the allowable absorption. For example, the MTR beryllium specifications call for a maximum TDS of 30, which means that the increase in absorption of thermal neutrons due to impurities in beryllium metal shall not be greater than 30%

of the absorption due to beryllium alone. Since the cross-section of beryllium is 0.01 barn, the allowable cross-section due to impurities cannot be greater than 0.003 barn, giving a total absorption cross-section of no greater than 0.013 barn.

The following example shows the calculation of danger coefficient and TDS for boron in beryllium.[7]

Using formula (1) above,

$$K_s(i) = \frac{\sigma_i \times A_s}{\sigma_s \times A_i}$$

For boron in beryllium,

$$K_{Be}(B) = \frac{705 \times 9.02}{0.01 \times 10.82} = 58,800$$

for the concentration of boron in beryllium expressed in percent, or 5.88 for concentration in parts per million.

If we assume 0.0002% boron in beryllium, then the TDS is 58,800 × 0.0002 = 11.76. Similarly expressed as 2 ppm, 5.88 × 2 = 11.76.

A.5.4 REFERENCE REPORTS

(1) English, J. L., *Interim Report on the Corrosion of Beryllium in Simulated Cooling Water for the Proposed Development Reactor*, ORNL-298, March 16, 1949.

(2) Olsen, A. R., *Initial Corrosion Tests on Brush Process QM and QRM Beryllium*, ORNL-733, July 14, 1950.

(3) Cunningham, J. E., *Deep Hole Drilling of Hot-pressed Beryllium Metal*, ORNL CF-50-4-110, April 20, 1950.

(4) Lane, J. A., *Thermal Stress in Beryllium Class II Pieces*, ORNL CF-50-6-9, June 2, 1950.

(5) Savage, H. C., *Thermal Stresses in Beryllium*, ORNL-571, February 9, 1950.

(6) Mann, M. M., *Specifications for Rough Sections of Beryllium for the MTR*, ORNL CF-50-3-114, March 22, 1950.

(7) Liss, B., *Danger Coefficients for Impurities in Several Substances*, NYO-108, March 6, 1950.

Appendix 6

FUEL ELEMENTS

A6.1 DEVELOPMENT

The active ingredient of the MTR, 93.5% enriched uranium, is introduced as an aluminum alloy, 14% by weight, rolled to sheet form and clad on the edges and faces with 2S aluminum. The finished core dimension is to be 0.020 by 23.75 by 2.55 in. and is to be centered with respect to edges, ends, and faces. Dimensional details are given in Table A6.A. Eighteen of these fuel plates are then furnace brazed to grooved aluminum side plates to form subassemblies. A cross-section of such an assembly is shown in Chap. 2, Fig. 2.2.A.

In preliminary work at Battelle Memorial Institute[1] and later at ORNL,[2] it was shown that uranium-aluminum alloys containing up to 30% uranium by weight could be cast and rolled without too much difficulty. Two methods of alloying were studied. The direct method consisted in melting a mixture of metallic uranium and metallic aluminum. In the reduction method, some compound of uranium — UF_4, U_3O_8, or UO_2 — was added to a bath of melted aluminum, together with a flux (cryolite), where it was reduced by excess aluminum. While the reduction method was used in fabrication of plates for the MTR critical experiment, the direct method was the one finally adopted[3] because it was fast and produced a smaller volume of contaminated wastes.

For cladding,[4] the alloy was at first enclosed in an aluminum "picture frame," another sheet of aluminum was wrapped over both frame and core, and the assembly was hot rolled for a total reduction of 50%. The resulting laminate usually developed large blisters at the trailing end of the sheet (when tested by annealing for 1 hr at 900°F). This was considered to be the result of a poor fit between core and frame; air entrapped in voids at the core-frame interface became compressed during rolling. Frames for these first rollings were made with hand tools and consequently were quite crude.

Later work at ORNL[5] showed that entrapment of air could be avoided if the core and frame were blanked out with a punch and die, assembled, and then

TABLE A6.A

Fuel Assembly Plates

Overall dimensions	
Length, internal plates (in.)	24-5/8 ± 1/64
Length, external plates (in.)	28-5/8 ± 1/64
Width, before curving (in.)	2.845 ± 0.001
Thickness (in.)	0.060 ± 0.001
Core dimensions	
Length (in.)	23¾ ± ¼
Width (in.)	2.55 ± 0.01
Thickness (in.)	0.021 ± 0.001
Composition	
Total uranium in U-Al alloy (%)	14.1 (approx.)
U^{235} enrichment (%)	93.2 (approx.)
U^{235} content per plate (g)	7.70 ± 1%
Quality	
Blister free	

hot rolled 50% prior to cladding. It was also shown[6] that there was a direct relationship between absolute humidity and blistering. During periods of high humidity, about 8×10^{-4} lb/ft^3 H_2O, very low yields of blister-free plates were obtained. In addition to the obvious cure of air-conditioning the working area, two solutions to this problem were found. Either vacuum annealing of the clad plates or heating them, while coated with a slurry of brazing flux, to 1100°F allowed the blister-forming gas (hydrogen[7]) to escape.

The fuel subassembly went through three shape changes before the present design was frozen. The first design conception was that of a spiral, about 3 in. in O.D. by about 30 in. long, made from a 0.060- by 27- by 30-in. plate. An annulus of 0.120 in. between turns provided space for cooling water. Since flow tests showed this type of assembly to be mechanically unstable, it was discarded. The second type consisted of a plate which was folded back and forth with annuli of 0.120 in. between folds. This design was discarded for two reasons: (1) The cladding became too thin on the outside of the 180° bends, and (2) there was mechanical instability during flow testing.

The third and final design consisted of narrow 3-in. curved plates brazed to aluminum side plates with cooling annuli between the active plates. A complete list of drawings concerned with the fuel assembly is given at the end of this appendix.

A6.2 CONSTRUCTION OF PLATES

A full report on the fabrication of the active plates and assemblies is being prepared,[8] but, since this type of element is still new to the reactor business, a brief summary of these operations is given here.

The flow sheet shown in Fig. A6.A shows that operations of melting, rolling, punching, cladding, hydrogen removal, shearing, machining, and forming take place in sequence. The ingots of 14.1% U-Al alloy are made in batches containing 800 g of uranium, each batch making two ingots. After being melted and thoroughly rinsed, the charge (usually aluminum, virgin uranium, recycled U-Al alloy, and reject clad plates) is cast into two graphite molds, forming ingots of about 4.5 by 8 by 1¼ in. usable size.

[redacted]

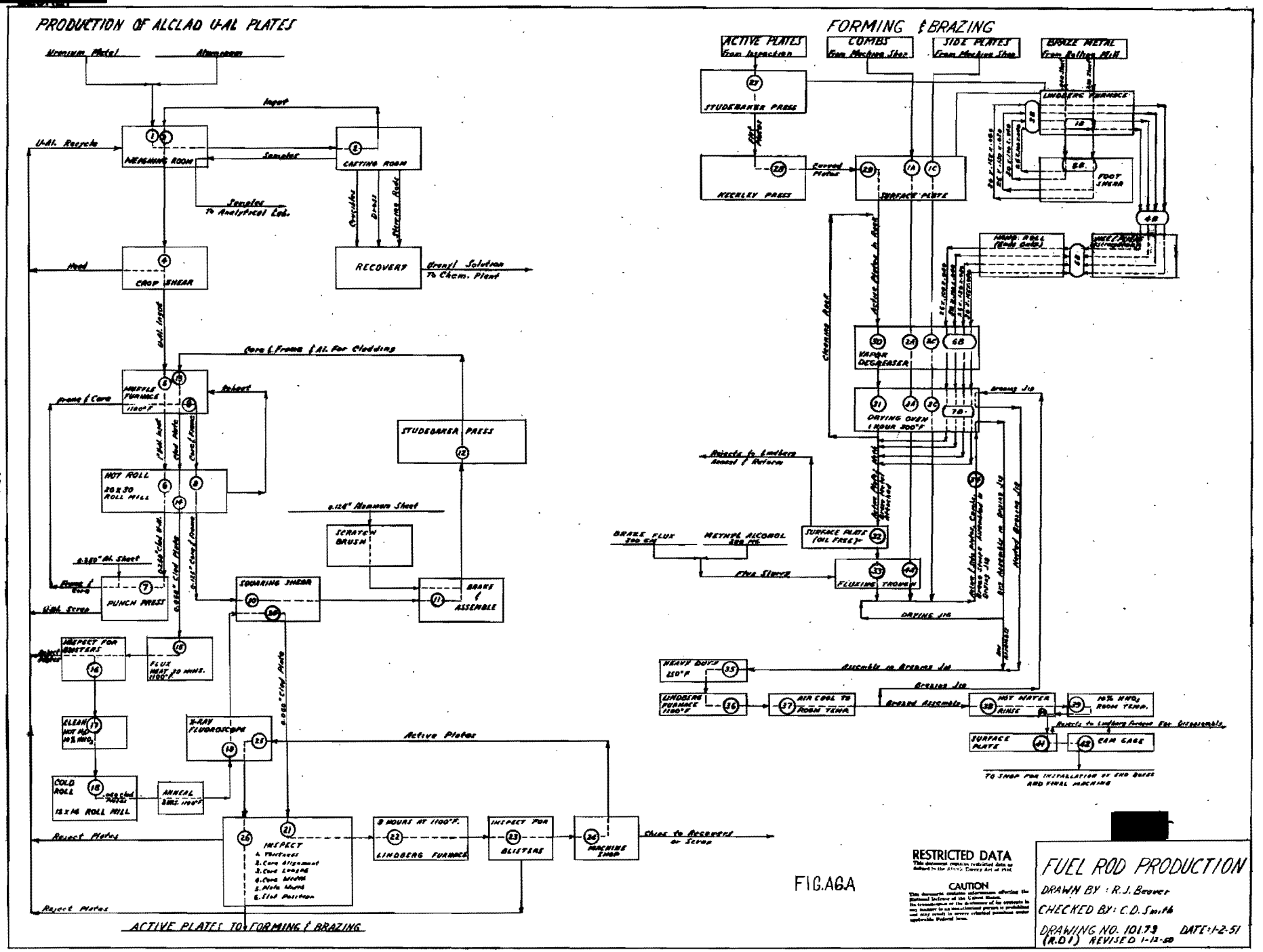

FIG.A6A

RESTRICTED DATA

This document contains restricted data as defined in the Atomic Energy Act of 1946.

CAUTION

This document contains information affecting the National Defense of the United States. Its transmission or the disclosure of its contents in any manner to an unauthorized person is prohibited and may result in severe criminal penalties under applicable Federal laws.

FUEL ROD PRODUCTION

DRAWN BY : R.J. Beaver

CHECKED BY: C.D. Smith

DRAWING NO. 101.73 (R.D.1) DATE: 1-2-51 REVISED 1-12-50

[redacted]

After preheating, the ingots are rolled to a thickness of 0.250 in. and width of 5 in. Using a double-acting punch and die, rectangular cores 2 by 2.35 in. with 1/8-in.-radius corners are blanked from the alloy slab. About thirty cores are produced per ingot. Using the same punch and die, two holes 4 by 8 in. are punched in 0.245-in. aluminum, forming two picture frames into which two cores are pressed. This assembly is preheated and rolled to 0.125 in. thickness and then cut to allow individual handling of each core. Each core and frame is then clad by insertion into 2S aluminum cover sheets 1/8 by 4 by 13 in. which are scratch-brushed and bent into a U shape with the scratched surface inside. The sandwich is then pressed flat and rolled.

In periods of high absolute humidity a considerable amount of hydrogen is absorbed by the U-Al alloy during melting and hot rolling. When this is present in sufficient quantities, it tends to collect at bond interfaces and around UAl_4 particles and cause blistering. To avoid this, it is necessary to coat each plate with an alcohol slurry of brazing flux and heat to 1100°F for ½ hr. The dissolution of the oxide layer on the surface apparently allows the hydrogen to escape.

After cold rolling, the exact location of the core in each plate is found by fluoroscopic examination, and the plate is then marked and sheared to rough plate dimensions. After being sheared, the plates are milled to finish dimensions and again checked by X ray so that any plates with exposed cores can be discarded. Finally, the milled plates are formed to a 5.5-in. radius in a 25-ton press.

Before further assembly, each plate is checked for longitudinal straightness and correctness of lateral curvature. This is, of course, exceedingly important because of the small clearance between the plates in the final assembly.

A6.3 FABRICATION OF THE FUEL ELEMENTS

As shown in the flow diagram (Fig. A6.A), fabrication of fuel elements is a complex series of operations involving machining, furnace brazing, and arc welding. A finished fuel subassembly has already been shown in Fig. 2.2.B; a summary of the construction details follows.

The grooved side plates are prepared by gang milling sheets of 2S aluminum of proper thickness. The inside ends of these side plates are milled to provide proper fit for the end boxes, which are plug brazed into position. Combs milled from Alcoa No. 12 braze-clad aluminum sheet are placed at each end of the fuel assembly to aid in alignment and reinforcement at the centerline.

Before final assembly, all parts except the fuel plates are carefully cleaned by processing, as follows: (1) vapor degreasing, (2) air drying for 1 hr at 300°F, (3) acid dipping (10% HNO_3), (4) water rinsing, and (5) air drying as above. The fuel plates are degreased only.

In final assembly braze strips (silicon-aluminum alloy) are fastened to the edges of the fuel plates by bending over the ends. The brazing strip is then fluxed, and the fuel plate is inserted between the side plates, which are held in a jig. After all plates are inserted and the combs are in place, the jig is closed to put the side plates into correct position. The whole assembly is then dried and charged into a box type electric furnace for preheating to 800°C. After being preheated, the assembly is placed in another furnace at 1100°C to accomplish final brazing.

After cooling, the assembly is carefully inspected for spacing, plate curvature, overall dimensions and properly brazed joints. If the assembly passes this inspection, the end adapters are inserted, aligned, and plug welded into place ready for final machining.

The final machining determines the position of the fuel assembly bodies relative to each other in the reactor core according to the bottom and top supporting grids. The sequence of operations is as follows:

1. Sides. The plug welds are milled flush.
2. Top. A shaped cutter is used to mill the assembly body ends to 5½-in.-radius flush with the surface of the top plate. This operation trims the side plates and removes excess plug material. About 2-in. from the end of the assembly body the cutter is raised gradually and continues along the assembly length, providing a curved side plate edge.
3. Bottom. The bottom is prepared similarly by a second shaped cutter.

4. Top adapter. The assembly is aligned in a special machining fixture, using the top and bottom plate centerline surfaces as references. The sequence is:

   a. Machining of cylindrical surface.

   b. Machining of slot to fit a retaining ring for the helical spring and beveled ring which will be fitted later.

   c. Machining of the inside to the required diameter.

   d. Cutting away of excess metal at end.

   e. Drilling of a 3/8-in. hole diametrically to provide a grip for the assembly handling tools.

5. Bottom adapter. Using the same fixture as a guide, the various bosses are milled to specification.

A6.5 REFERENCE DRAWINGS

DWG. NO.	TITLE
Casting Drawings	
TD-1543	Upper Adapter
TD-1542	Lower Adapter
Preassembly Machining Drawings	
TD-1166	Upper Adapter
TD-1165	Lower Adapter
Brazing Alignment Drawing	
TD-1167	
Final Machining Drawing	
TD-1472	
Fuel Assembly Drawings	
TD-966A	Side Plate
TD-1533	Comb
TD-1534	Standard Fuel Plate
TD-1535	Outside Fuel Plate
TD-256	Beveled Ring
TD-257	Retaining Ring
TD-251	Upper End Spring

Appendix 7

PROPERTIES OF SHIELDING MATERIALS

During the analysis of the MTR shield, the values shown in Table A7.A were employed for the pertinent material properties:

TABLE A7.A

	μ (cm^{-1})	L^2 (cm^2)	τ (cm^2)	ρ (g/cc)	λ_n* (cm)
Lead	0.45			11.1	
Iron	0.235	1.7		7.85	9
Water	0.025			1.0	
Barytes concrete	0.10		350	3.5	8.2

*Asymptotic relaxation length for fission neutrons.

Some other useful information has been compiled in the balance of this appendix. Two sets of curves entitled "Mass Absorption Coefficients" are included, both of which are taken from ORNL-421. Figures A7.A and B, comprising Supplement 1 to this report, give the macroscopic total cross-section divided by density. Figures A7.C and D, which form Supplement 2, present the macroscopic absorption cross-section divided by density. In the latter case, an averaged probability for energy absorption in Compton interaction has been added to the photoelectric and pair cross-sections.

Table A7.B, a convenient summary of some declassified nuclear data, is taken from "Thermal Neutron Cross Sections and Related Data" by H. R. Kroeger* and is used with permission.

Figure A7.E presents the energy dependence of the same linear absorption coefficients, based on the total cross-sections of some materials of particular interest.

Nucleonics, Vol. 5, No. 4, pp. 51-54, October, 1949.

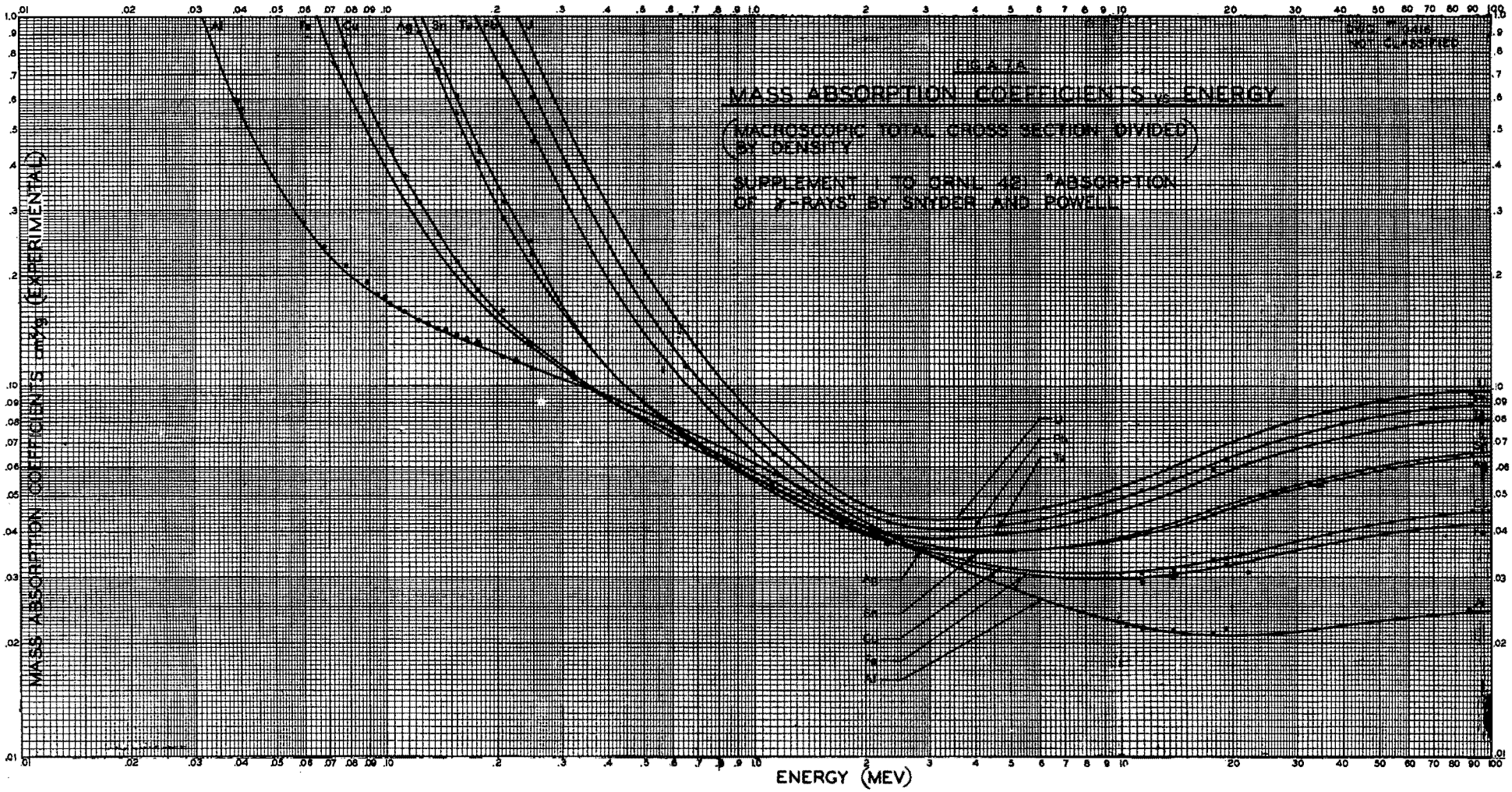
FIG. A 7.A
MASS ABSORPTION COEFFICIENTS vs ENERGY
(MACROSCOPIC TOTAL CROSS SECTION DIVIDED BY DENSITY)
SUPPLEMENT I TO ORNL 421 "ABSORPTION OF γ-RAYS" BY SNYDER AND POWELL
MASS ABSORPTION COEFFICIENTS cm²/g (EXPERIMENTAL)
ENERGY (MEV)
W
Pb
Cu
Ag
Sn
Ta
Fe
Al
Mg
Be
C
H
O
N

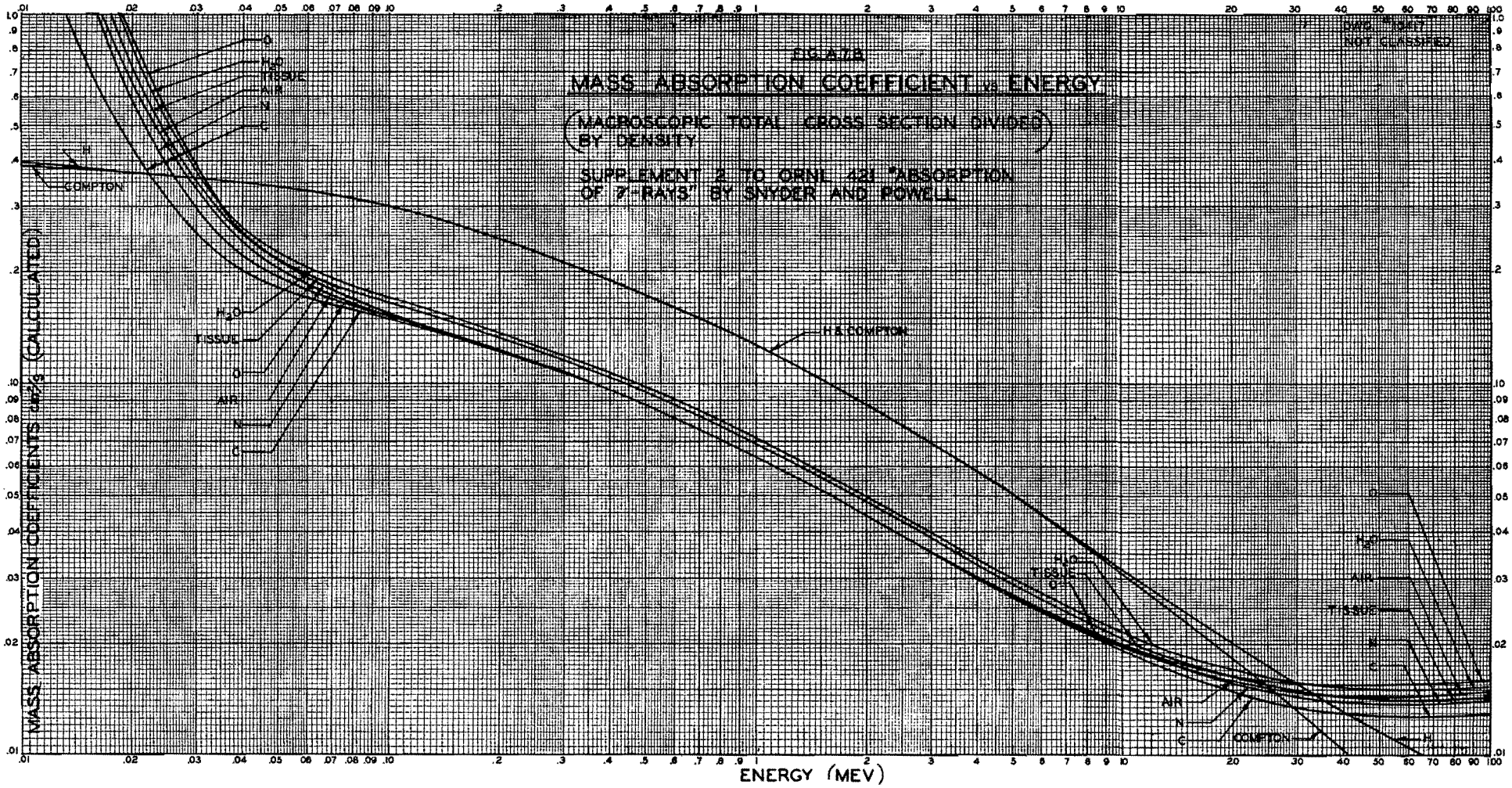
FIG. A7B
MASS ABSORPTION COEFFICIENT vs ENERGY
(MACROSCOPIC TOTAL CROSS SECTION DIVIDED BY DENSITY)
SUPPLEMENT 2 TO ORNL 421 "ABSORPTION OF γ-RAYS" BY SNYDER AND POWELL
MASS ABSORPTION COEFFICIENTS μ/ρ (CALCULATED)
ENERGY (MEV)
O
H_2O
TISSUE
AIR
N
C
H
COMPTON
H & COMPTON
UNCLASSIFIED

Dwg. 8118
Not Classified

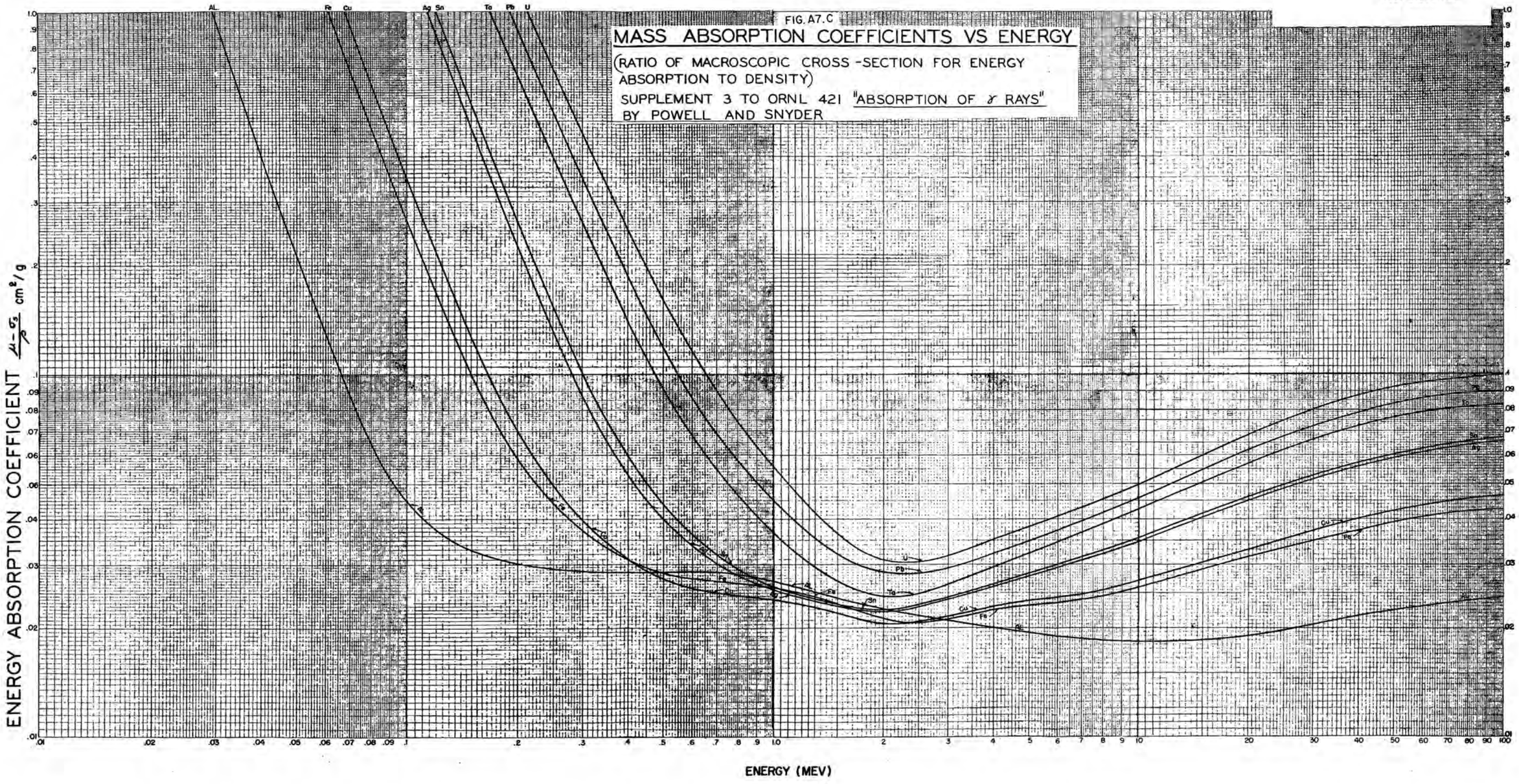

Dwg. 8117
Not Classified

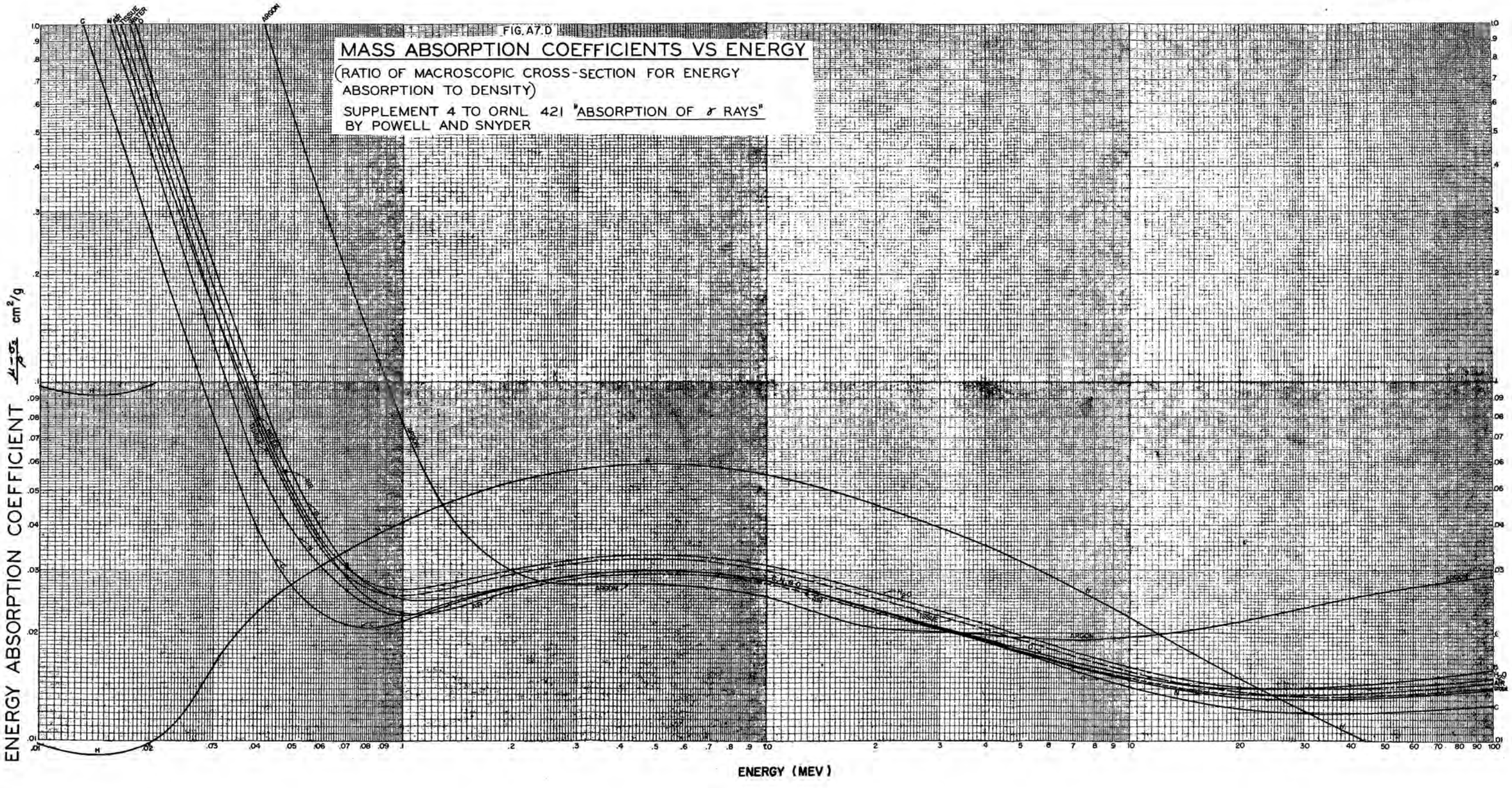

DWG. #10532
NOT CLASSIFIED

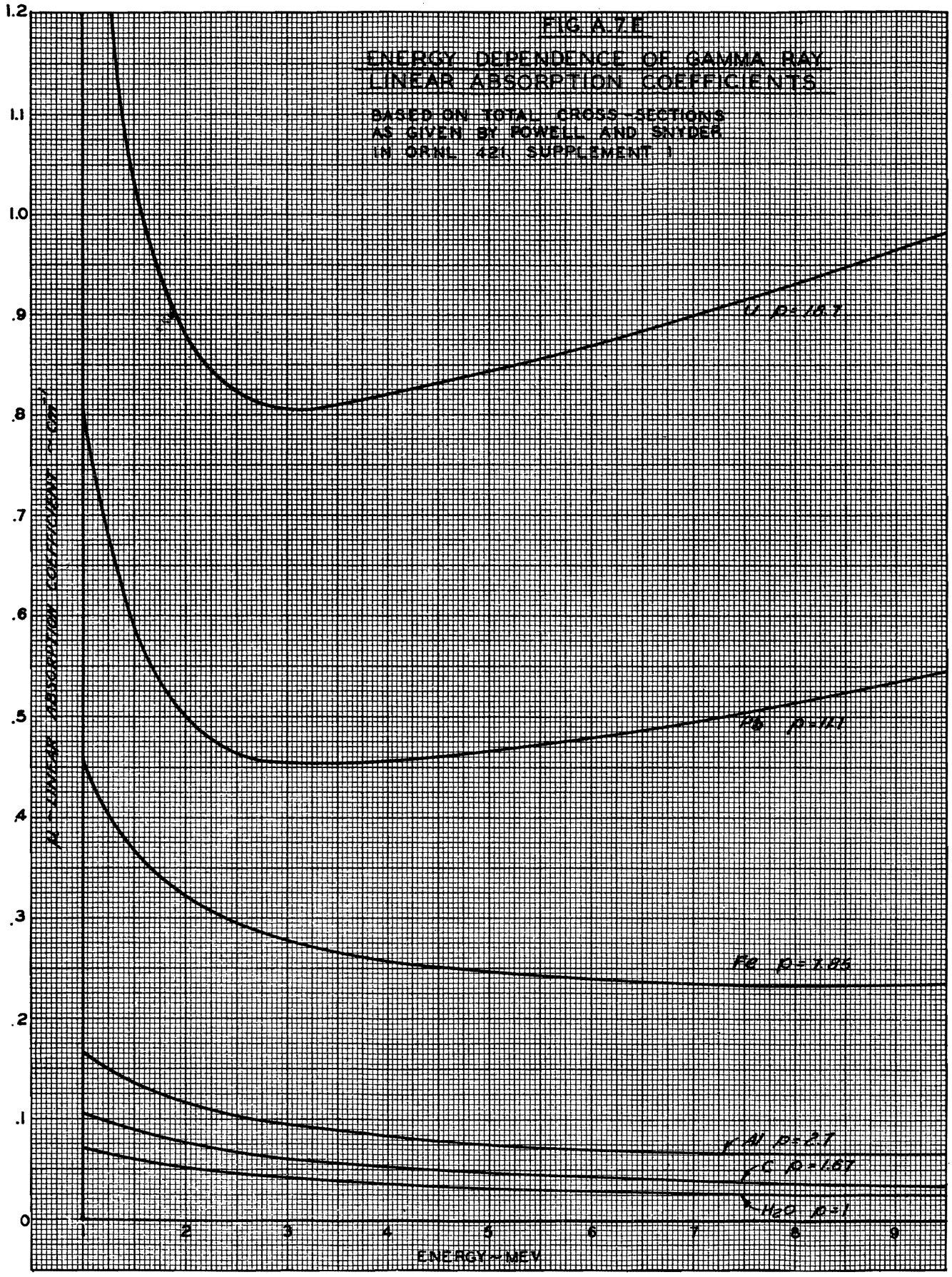

TABLE A7.B

Symbols which are undefined in the table are:

b = average cosine of the scattering angle relative to the initial direction; σ_T = total microscopic cross-section for collision; σ_S = microscopic cross-section for a scattering collision; σ_{TR} = microscopic cross-section for a transport collision; σ_A = microscopic cross-section for an absorption collision.

Cross-sections for hydrogen and deuterium are for H and D atoms in combination with O (H_2O and D_2O). The density given for $_{86}Rn^{222}$ is for liquid radon.

The atomic weights and densities are from "Handbook of Chemistry and Physics" (Chemical Rubber Publishing Co., Cleveland). The macroscopic cross sections, mean free paths, slowing-down powers, and moderating powers are based on thermal neutron cross-section data gathered from the following sources:

1. K. Way, G. Haines, *Thermal neutron cross sections for elements and isotopes*, CNL-33, 2/29/48.
2. E. Melkonian, L. J. Rainwater, W. W. Havens, *Neutron beam spectrometer studies of oxygen*, M-2554.
3. R. G. Nucholls, *The total scattering cross-sections of deuterium and oxygen for fast neutrons*, MDDC-37, 6/17/46.
4. K. Way, G. Haines, *Tables of neutron cross-sections*, MonP-405, 10/28/47 (supplement issued 4/20/48).
5. H. H. Goldsmith, H. W. Ibser, *Neutron cross-sections of the elements*, MUC-HHG-7, 12/5/45.

Atomic Number Z	Name	Chemical Atomic Weight A	Density (ρ) gm/cc, 20°C 760 mm Hg	Nuclei per cc ($\times 10^{-24}$) N	(1-b)	Avg. Log Energy Loss ξ	Thermal (0.025 ev) Neutron Cross-Sections (σ) in barns				Thermal (0.025 ev) Macroscopic Cross-Sections, $\Sigma = \sigma N$				Thermal (0.025 ev) Mean Free Path cm				Slowing Down Power $N\sigma_S\xi$	Moderating Ratio $(\sigma_S/\sigma_A) \times \xi$
							σ_T	σ_S	σ_{TR}	σ_A	Σ_T	Σ_S	Σ_{TR}	Σ_A	λ_T	λ_S	λ_{TR}	λ_A		
1	H	1.008	.00008	.00005	.3329	1.0	46	46	15	0.32										140
1	D	2.0147	.00017	.00005	.6662	.7261	5.3	5.3	3.5	0										
2	He	4.003	.00016	.000025	.8320	.4281	1.5	1.5	1.2	.008										80
3	Li	6.940	.534	.0463	.9031	.2643	66.5	1.5	1.4	65	3.1	.07	.07	3.0	.33	14	15	.33	.018	.006
4	Be	9.02	1.84	.1229	.9255	.2078	6.1	6.1	5.6	.0085	.75	.75	.69	.001	1.3	1.3	1.5	950	.156	150
5	B	10.82	2.535	.1411	.9379	.1756	719	3.8	3.6	715	100	.54	.51	100	.01	1.9	2.0	0.01	.094	.001
6	C	12.01	1.67	.0838	.9440	.1589	4.8	4.8	4.5	.0045	.40	.40	.38	.0004	2.5	2.5	2.6	2600	.064	170
7	N	14.008	.00116	.00005	.9520	.1373	11.7	10	9.5	1.7										.81
8	O	16.000	.00133	.00005	.9580	.1209	4.1	4.1	3.9	.001										500
9	F	19.00	.00158	.00005	.9646	1025	4	4	4	0.01										41
10	Ne	20.183	.00084	.000025	.9667	.0967	2.8													
11	Na	22.997	.9712	.0254	.9708	.0852	4.5	4	4	0.45	.11	.10	.10	.011	8.8	9.8	9.8	88	.009	.76
12	Mg	24.32	1.741	.0431	.9724	.0807	3.0	2.7	2.6	0.3	.13	.12	.11	.013	7.8	8.6	8.9	77	.009	.73
13	Al	26.97	2.699	.0603	.9751	.0730	1.6	1.4	1.4	0.22	.097	.084	.084	.013	10	12	12	77	.006	.47
14	Si	28.06	2.42	.0519	.9760	.0702	2.5	2.3	2.2	0.2	.13	.12	.11	.010	7.7	8.4	8.8	96	.008	.81
15	P	30.98	2.34	.0455	.9783	.0637	4.4	4.1	4.0	0.3	.20	.19	.18	.014	5.0	5.4	5.5	73	.012	.87
16	S	32.06	2.0	.0376	.9790	.0616	1.4	1	1	0.4	.053	.038	.038	.015	19	27	27	67	.002	.15
17	Cl	35.457	.00295	.00005	.9810	.0558	55	20	20	35										.032
18	A	39.944	.00166	.000025	.9832	.0497	3	2	2	1										.099
19	K	39.096	.87	.0134	.9828	.0507	4.0	1.5	1.5	2.5	.054	.020	.020	.034	19	50	50	30	.001	.030
20	Ca	40.08	1.54	.0231	.9832	.0495	4	3.5	3.4	0.5	.092	.081	.079	.012	11	12	13	86	.004	.35

TABLE A7.B (Cont'd)

Atomic Number Z	Name	Chemical Atomic Weight A	Density (ρ) gm/cc, 20°C 760 mm Hg	Nuclei per cc (x 10^{-24}) N	(1-b)	Avg. Log Energy Loss ξ	Thermal (0.025 ev) Neutron Cross Sections (σ) in barns				Thermal (0.025 ev) Macroscopic Cross Sections, $\Sigma = \sigma N$				Thermal (0.025 ev) Mean Free Path cm				Slowing Down Power $N\sigma_S\xi$	Moderating Ratio $(\sigma_S/\sigma_A)\times\xi$
							σ_T	σ_S	σ_{TR}	σ_A	Σ_T	Σ_S	Σ_{TR}	Σ_A	λ_T	λ_S	λ_{TR}	λ_A		
21	Sc	45.10	2.5	.0334	.9851	.0441				22				.74				1.4		
22	Ti	47.90	4.5	.0566	.9860	.0415	11	6	6	5	.62	.34	.34	.28	1.6	2.9	2.9	3.5	.014	.050
23	V	50.95	5.96	.0705	.9868	.0391	12	7	7	4.5	.85	.49	.49	.32	1.2	2.0	2.0	3.2	.019	.061
24	Cr	52.01	6.92	.0801	.9871	.0383	6.5	4	4	2.5	.52	.32	.32	.20	1.9	3.1	3.1	5.0	.012	.061
25	Mn	54.93	7.2	.0789	.9878	.0363	15.3	2.3	2.3	13	1.2	.18	.18	1.0	.83	5.5	5.5	.95	.007	.006
26	Fe	55.85	7.85	.0847	.9880	.0357	13.5	11	11	2.5	1.1	.93	.93	.21	.88	1.1	1.1	4.7	.033	.16
27	Co	58.94	8.71	.0890	.9886	.0338	41	5	5	36	3.7	.45	.45	3.2	.27	2.3	2.3	.31	.015	.005
28	Ni	58.69	8.9	.0913	.9885	.0340	22	17	17	4.5	2.0	1.6	1.6	.41	.50	.65	.65	2.4	.053	.13
29	Cu	63.57	8.89	.0842	.9894	.0314	10.2	7.2	7.1	3	.86	.61	.60	.25	1.2	1.7	1.7	4.0	.019	.075
30	Zn	65.38	7.19	.0662	.9897	.0305	4.5	3.6	3.6	0.9	.30	.24	.24	.060	3.4	4.2	4.2	17	.007	.12
31	Ga	69.72	5.9	.0510	.9904	.0287	18	16	16	2.2	.92	.82	.82	.11	1.1	1.2	1.2	8.9	.023	.21
32	Ge	72.60	5.46	.0453	.9907	.0275	9	6	6	2.8	.41	.27	.27	.13	2.5	3.7	3.7	7.9	.007	.059
33	As	74.91	5.73	.0461	.9910	.0267	8.8	4.5	4.5	4.3	.41	.21	.21	.20	2.5	4.8	4.8	5.1	.006	.028
34	Se	78.96	4.5	.0343	.9915	.0253	28	13	13	15	.96	.45	.45	.52	1.0	2.2	2.2	1.9	.011	.022
35	Br	79.916	3.12	.0235	.9916	.0250	11.5	5	5	6.5	.27	.12	.12	.15	3.7	8.5	8.5	6.5	.003	.019
36	Kr	83.7	.00348	.000025	.9920	.0239	27	27	27	0.05										13
37	Rb	85.48	1.532	.0108	.9921	.0234	12.6	12	12	0.6	.14	.13	.13	.006	7.4	7.7	7.7	150	.003	.47
38	Sr	87.63	2.6	.0179	.9923	.0228	11.3	9.5	9.4	1.8	.20	.17	.17	.032	5.0	5.9	5.9	31	.004	.12
39	Y	88.92	3.8	.0257	.9924	.0225	4.2	3	3	1.2	.11	.08	.08	.031	9.3	13	13	33	.002	.057
40	Zr	91.22	6.44	.0425	.9926	.0220	8.4	8	8	0.4	.36	.34	.34	.017	2.8	2.9	2.9	59	.007	.44
41	Cb	92.91	8.4	.0545	.9928	.0216	8.2	7	7	1.2	.45	.38	.38	.065	2.2	2.6	2.6	15	.008	.13
42	Mo	95.95	10.2	.0640	.9930	.0209	9.6	7	7	2.6	.61	.45	.45	.17	1.6	2.2	2.2	6.0	.009	.056
43	Tc	99			.9932	.0202														
44	Ru	101.7	12.2	.0723	.9934	.0197	9	6	6	3	.65	.43	.43	.22	1.5	2.3	2.3	4.6	.009	.039
45	Rh	102.91	12.5	.0732	.9935	.0195	155	6	6	149	11	.44	.44	11	.088	2.3	2.3	.092	.009	.001
46	Pd	106.7	12.16	.0686	.9937	.0188	10.5	4.5	4.5	6	.72	.31	.31	.41	1.4	3.2	3.2	2.4	.006	.014
47	Ag	107.880	10.5	.0586	.9938	.0186	66	6	6	60	3.9	.35	.35	3.5	.26	2.8	2.8	.28	.007	.002
48	Cd	112.41	8.65	.0463	.9940	.0178	2500	6	6	2500	120	.28	.28	120	.009	3.6	3.6	.009	.005	0
49	In	114.76	7.28	.0382	.9941	.0175	192	2	2	190	7.3	.08	.08	7.3	.14	13	13	.14	.001	0
50	Sn	118.7	7.3	.0370	.9943	.0169	4.6	4	4	0.6	.17	.15	.15	.022	5.9	6.8	6.8	46	.003	.11
51	Sb	121.76	6.691	.0331	.9945	.0165	9	4	4	5	.30	.13	.13	.17	3.4	7.6	7.6	6.0	.002	.013
52	Te	127.61	6.25	.0295	.9947	.0157	9	5	5	4	.27	.15	.15	.12	3.8	6.8	6.8	8.5	.002	.020
53	I	126.92	4.94	.0234	.9947	.0158	10	3	3	7	.23	.07	.07	.16	4.3	14	14	6.1	.001	.007
54	Xe	131.3	.00546	.000025	.9949	.0153	37													

TABLE A7.B (Cont'd)

Atomic Number Z	Name	Chemical Atomic Weight A	Density (ρ) gm/cc, 20°C 760 mm Hg	Nuclei per cc ($\times 10^{-24}$) N	(1-b)	Avg. Log Energy Loss ξ	Thermal (0.025 ev) Neutron Cross Sections (σ) in barns				Thermal (0.025 ev) Macroscopic Cross Sections, $\Sigma = \sigma N$				Thermal (0.025 ev) Mean Free Path cm				Slowing Down Power $N\sigma_S\xi$	Moderating Ratio $(\sigma_S/\sigma_A) \times \xi$
							σ_T	σ_S	σ_{TR}	σ_A	Σ_T	Σ_S	Σ_{TR}	Σ_A	λ_T	λ_S	λ_{TR}	λ_A		
55	Cs	132.91	1.873	.0085	.9949	.0151	50	24	24	26	.43	.20	.20	.22	2.4	4.9	4.9	4.5	.003	.014
56	Ba	137.36	3.78	.0166	.9951	.0146	9.3	8	8	1.3	.15	.13	.13	.022	6.5	7.5	7.5	46	.022	.090
57	La	138.92	6.15	.0267	.9952	.0145	28	20	20	8	.75	.53	.53	.21	1.3	1.9	1.9	4.7	.008	.036
58	Ce	140.13	6.9	.0297	.9952	.0143	29	23	23	6	.86	.68	.68	.18	1.2	1.5	1.5	5.6	.010	.055
59	Pr	140.92	6.475	0277	.9952	.0142	15	5	5	10	.42	.14	.14	.28	2.4	7.2	7.2	3.6	.002	.007
60	Nd	144.27	6.96	.0291	.9953	.0139	100				2.9				.34					
61	Pm	147			.9954	.0137				60										
62	Sm	150.43	7.7	.0308	.9955	.0134	8900			8900	270			270	.004			.004		
63	Eu	152.0	5.24	.0208	.9956	.0132	6000			6000	120			120	.008			.008		
64	Gd	156.9	7.94	.0305	.9957	.0128	40000			40000	1200			1200	.001			.001		
65	Tb	159.2	8.33	.0315	.9958	.0126				10				.32				3.2		
66	Dy	162.46	8.56	.0317	.9959	.0124	1200			1200	38			38	.026			.026		
67	Ho	164.94	8.76	.0320	.9959	.0122	65	5	5	60	2.1	.16	.16	1.9	.48	6.3	6.3	.52	.002	.001
68	Er	167.2	9.16	.0330	.9960	.0120	200				6.6				.15					
69	Tm	169.4	9.34	.0332	.9960	.0119	120	20	20	100	4.0	.66	.66	3.3	.25	1.5	1.5	.30	.008	.002
70	Yb	173.04	7.01	.0244	.9961	.0116	60				1.5				.69					
71	Lu	174.99	9.74	.0335	.9962	.0115	170	30	30	140	5.7	1.0	1.0	4.7	.18	1.0	1.0	.21	.012	.002
72	Hf	178.6	11.4	.0384	.9962	.0113	125	20	20	105	4.8	.77	.77	4.0	.21	1.3	1.3	.25	.009	.002
73	Ta	180.88	16.6	.0553	.9963	.0111	25	5	5	20	1.4	.28	.28	1.1	.73	3.6	3.6	.90	.003	.003
74	W	183.92	19.3	.0632	.9963	.0109	23	5	5	18	1.5	.32	.32	1.1	.69	3.2	3.2	.88	.003	.003
75	Re	186.31	20	.0647	.9964	.0108	98	13	13	85	6.3	.84	.84	5.5	.16	1.2	1.2	.18	.009	.002
76	Os	190.2	22.48	.0712	.9965	.0106	32	15	15	17	2.3	1.1	1.1	1.2	.44	.94	.94	.83	.011	.009
77	Ir	193.1	22.42	.0699	.9965	.0104	464	14	14	450	32	.98	.98	31	.031	1.0	1.0	.032	.010	0
78	Pt	195.23	21.37	.0659	.9966	.0103	18	10	10	8	1.2	.66	.66	.53	.84	1.5	1.5	1.9	.007	.013
79	Au	197.2	19.3	.0589	.9966	.0102	102	6.5	6.5	95	6.0	.38	.38	5.6	.17	2.6	2.6	.18	.004	.001
80	Hg	200.61	13.546	.0407	.9966	.0100	415	15	15	400	17	.61	.61	16	.059	1.6	1.6	.061	.006	0
81	Tl	204.39	11.86	.0349	.9967	.0098	12	9	9	3	.42	.31	.31	.11	2.4	3.2	3.2	9.5	.003	.029
82	Pb	207.21	11.347	.0330	.9968	.0097	8	8	8	0.2	.26	.26	.26	.007	3.8	3.8	3.8	150	.003	.39
83	Bi	209.00	9.8	.0282	.9968	.0096	6.5	6.5	6.5	0.015	.18	.18	.18	.0004	5.5	5.5	5.5	2400	.002	4.2
84	Po	210			.9968	.0096														
85	At	211			.9968	.0095														
86	Rn	222	4.4	.0119	.9970	.0091														

TABLE A7.B$_7$ (Cont'd)

Atomic Number Z	Name	Chemical Atomic Weight A	Density (ρ) gm/cc, 20°C 760 mm Hg	Nuclei per cc (x 10^{-24}) N	(1-b)	Avg. Log Energy Loss ξ	Thermal (0.025 ev) Neutron Cross Sections (σ) in barns				Thermal (0.025 ev) Macroscopic Cross Sections, $\Sigma = \sigma N$				Thermal (0.025 ev) Mean Free Path cm				Slowing Down Power $N\sigma_S\xi$	Moderating Ratio $(\sigma_S/\sigma_A) \times \xi$
							σ_T	σ_S	σ_{TR}	σ_A	Σ_T	Σ_S	Σ_{TR}	Σ_A	λ_T	λ_S	λ_{TR}	λ_A		
87	Fr	223			.9970	.0090														
88	Ra	226.05	5	.0133	.9970	.0089														
89	Ac	227			.9970	.0089														
90	Th	232.12	11.5	.0298	.9971	.0087														
91	Pa	230.9			.9971	.0087														
92	U	238.07	18.7	.0473	.9972	.0084														
93	Np	237			.9972	.0085														
94	Pu	239			.9972	.0084														
95	Am	241			.9972	.0083														
96	Cm	242			.9972	.0083														

Appendix 8

SHIELDING CALCULATION AIDS

The data in Figs. A8.A through F are included with the expectation that they may be of service in reading Section 4.6.3 as well as in connection with the solution of other problems. The nomenclature employed in the figures is presented in the following tabulation.

The shield is presumed to consist of one or more slabs of thickness t_1, t_2, t_3, ... The source elements are assumed to be isotropic emitters.

The following symbols are used:

ϕ_E = undirected energy flux (Mev/cm^2-sec)

E = energy of the primary γ rays (Mev)

B = build-up factor to correct for multiple scattering

Q_0 = source strength of a point source (γ rays/sec)

Q_L = source strength of a line source (γ rays/cm-sec)

Q_A = source strength of a plane source (γ rays/cm^2-sec)

Q_V = source strength of a volume source (γ rays/cm^3-sec)

μ_R; μ_s; μ_1, μ_2 = absorption coefficients of receptor; source; shield (cm^{-1})

$b_1 = \mu_1 t_1 + \mu_2 t_2 + \ldots$

$b_2 = b_1 + \mu_s Z$

$b_3 = b_1 + \mu_s h$

Z = effective self-absorption distance (cm)

C = radius of disk or cylindrical source (cm)

l, a, h, d = dimensions as indicated (cm)

$$F_0(b) = \int_b^\infty \frac{e^{-y}\,dy}{y}$$

$$F_1(b) = b \int_b^{\infty} \frac{e^{-y}}{y^2}$$ Note: $F_1(0) = 1$

$$F(\phi, b) = \int_0^{\phi} e^{-b} \sec \phi \, d\phi$$ Note: $F(\phi, 0) = \phi$ (in radians)

NOT CLASSIFIED Dwg. # 8182

SOURCE	ENERGY FLUX (mev/cm²/sec)	SPECIAL CONDITIONS
STRAIGHT LINE 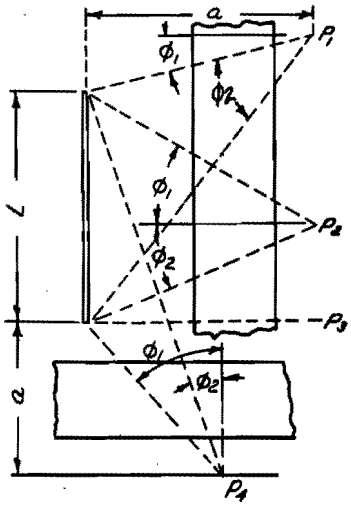	@P_1 $\phi_E = B\,\frac{Q_L E}{4\pi a}\left[\mathcal{F}(\phi_2,b_1)-\mathcal{F}(\phi_1,b_1)\right]$	
	@P_2 $\phi_E = B\,\frac{Q_L E}{4\pi a}\left[\mathcal{F}(\phi_2,b_1)+\mathcal{F}(\phi_1,b_1)\right]$	
	@P_2 $\phi_E = B\,\frac{Q_L E}{2\pi a}\,\mathcal{F}(\phi_1,b_1)$	$\phi_1=\phi_2$
	@P_2 $\phi_E = B\,\frac{Q_L E}{2\pi a}\,\mathcal{F}(\frac{\pi}{2},b_1)$	$L=\infty,\ \phi_1=\phi_2=\frac{\pi}{2}$
	@P_3 $\phi_E = B\,\frac{Q_L E}{4\pi a}\,\mathcal{F}(\phi_1,b_1)$	$\phi_2=0$
	@P_3 $\phi_E = B\,\frac{Q_L E}{4\pi a}\,\mathcal{F}(\frac{\pi}{2},b_1)$	$\phi_2=0,\ L=\infty$
	@P_4 $\phi_E = B\,\frac{Q_L E}{4\pi a}\left[\mathcal{F}(\phi_1,b_1)-\mathcal{F}(\phi_2,b_1)\right]$	
DISC SOURCE 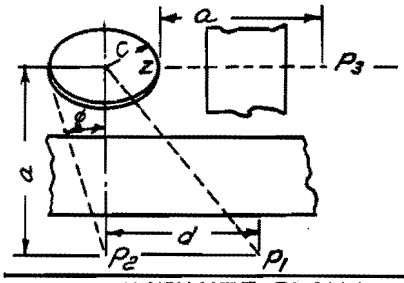	@P_1 $\phi_E = B\,\frac{Q_A E}{4}\left\{\ln_e\frac{c^2+a^2-d^2+\sqrt{(c^2+a^2-d^2)^2+4a^2d^2}}{2a^2}-\frac{2b_1}{a}\left[\sqrt{a^2+d^2+c^2}-\sqrt{a^2+d^2}\right]+\frac{1}{2}\left(\frac{cb_1}{a}\right)^2\right\}$	
	@P_2 $\phi_E = B\,\frac{Q_A E}{2}\left[F_0(b_1)-F_0(b_1\sec\phi)\right]$	
	@P_3 $\phi_E = B\,\frac{Q_A E c^2}{4(a+z)^2}\,e^{-b_2}$	
INFINITE PLANE 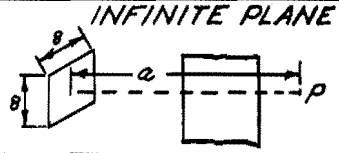	$\phi_E = B\,\frac{Q_A E}{2}\,F_0(b_1)$	
INFINITE SLAB 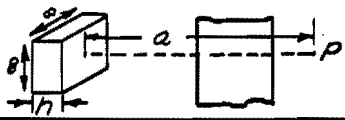	$\phi_E = B\,\frac{Q_V E}{2\mu_S}\left[F_1(b_1)-F_1(b_3)\right]$	
CYLINDRICAL SOURCE 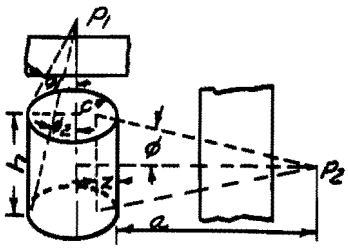	@P_1 $\phi_E = B\,\frac{Q_V E}{2\mu_S}\left[F_1(b_1)-F_1(b_3)+\frac{F_1(b_3\sec\phi_1)}{\sec\phi_1}-\frac{F_1(b_1\sec\phi_1)}{\sec\phi_1}\right]$	Upper Limit
	@P_1 $\phi_E = B\,\frac{Q_V E}{2\mu_S}\left[F_1(b_1)-F_1(b_3)+\frac{F_1(b_3\sec\phi_2)}{\sec\phi_2}-\frac{F_1(b_1\sec\phi_2)}{\sec\phi_2}\right]$	Lower Limit
	@P_2 $\phi_E = B\,\frac{Q_V E c^2}{2(a+z)}\,\mathcal{F}(\phi_1,b_2)$	P_2 opposite center
POINT SOURCE	$\phi_E = B\,\frac{Q_P E e^{-b}}{4\pi a^2}$	

FIGURE A8.A

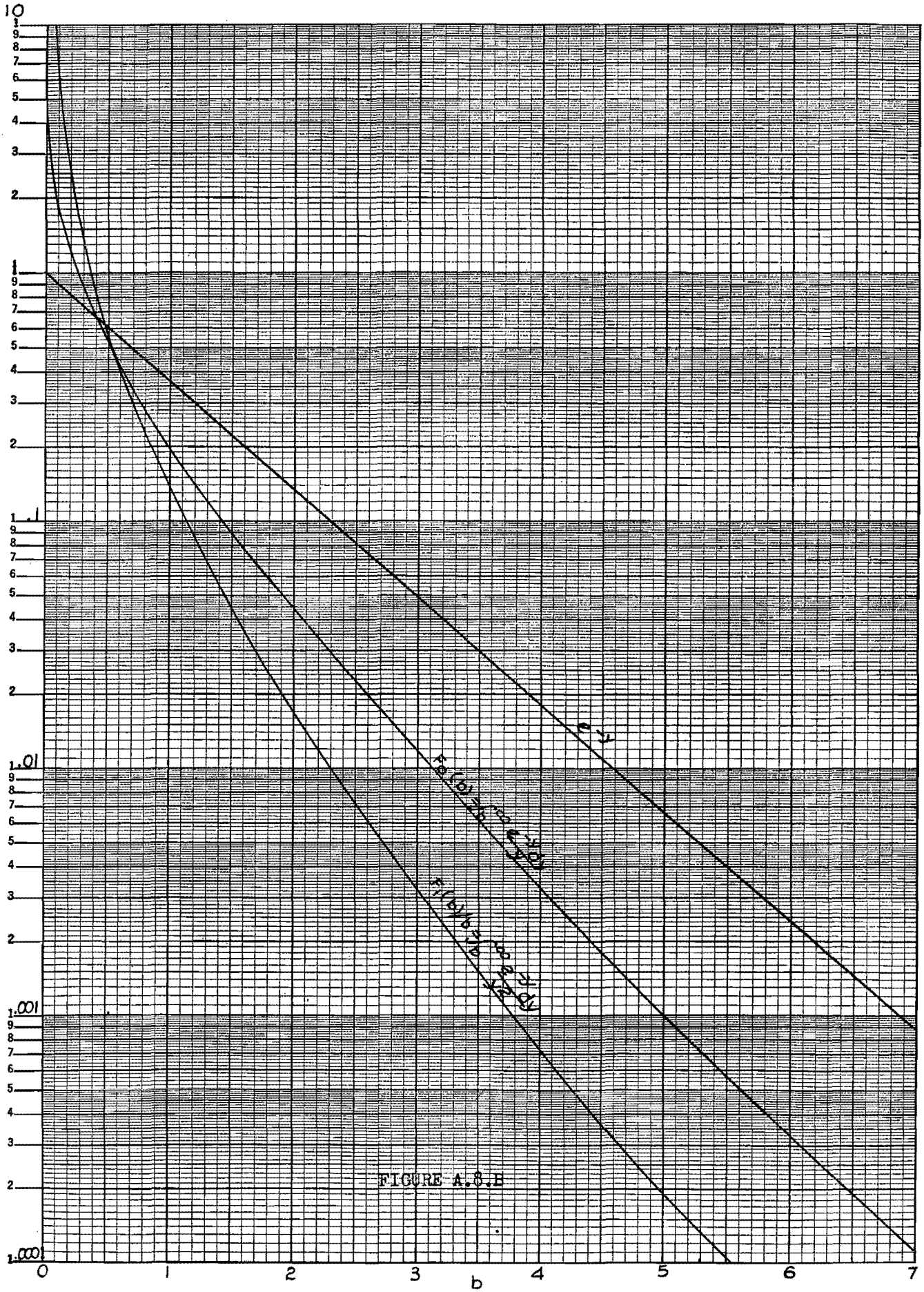

FIGURE A.8.B

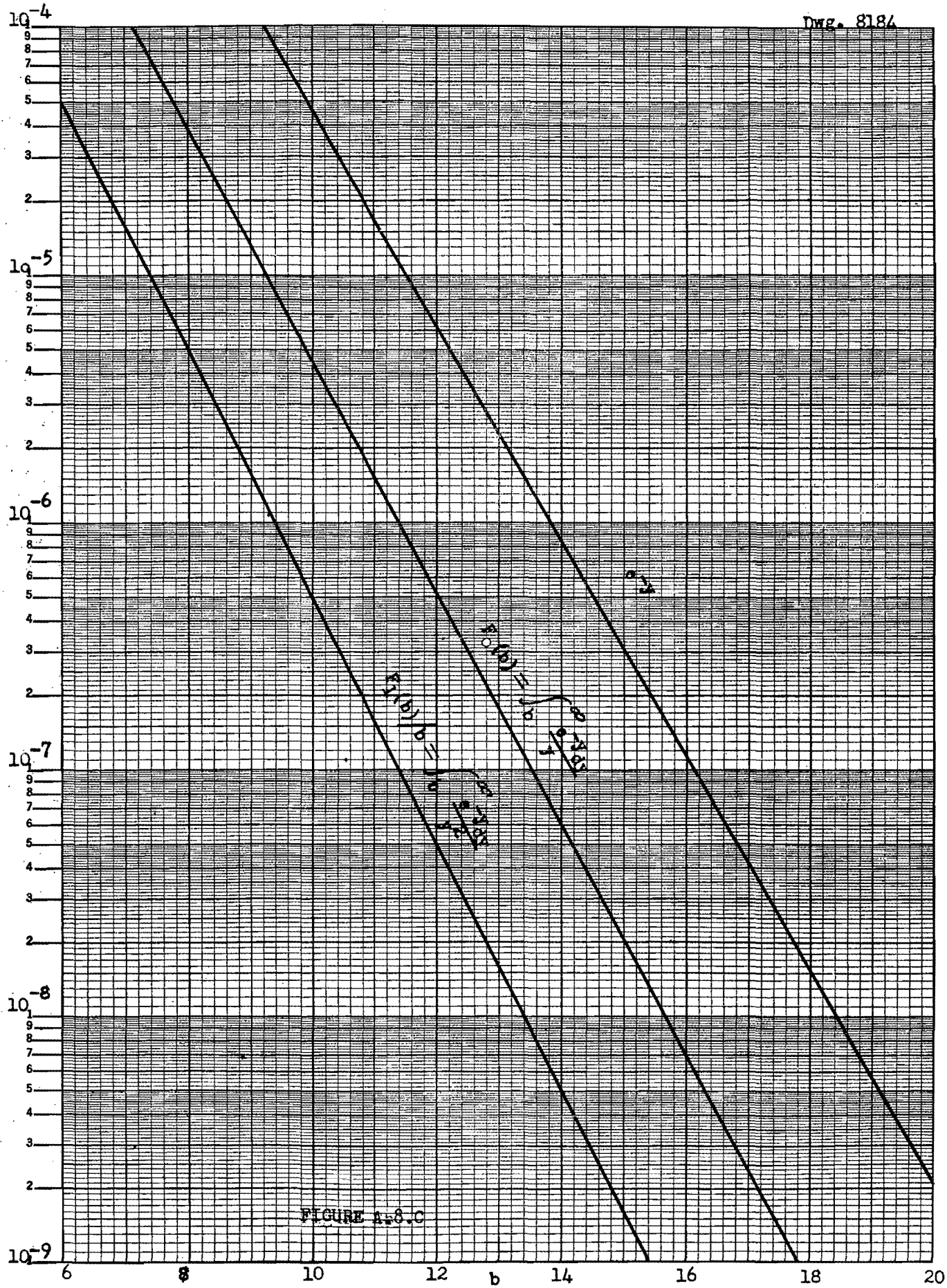
Dwg. 8184
10^{-4}
10^{-5}
10^{-6}
10^{-7}
10^{-8}
10^{-9}
6
8
10
12
14
16
18
20
b
F_c
$F_s(b) = \frac{a}{b}$
$F_r(b) = \frac{a}{b}$

FIGURE A.8.C

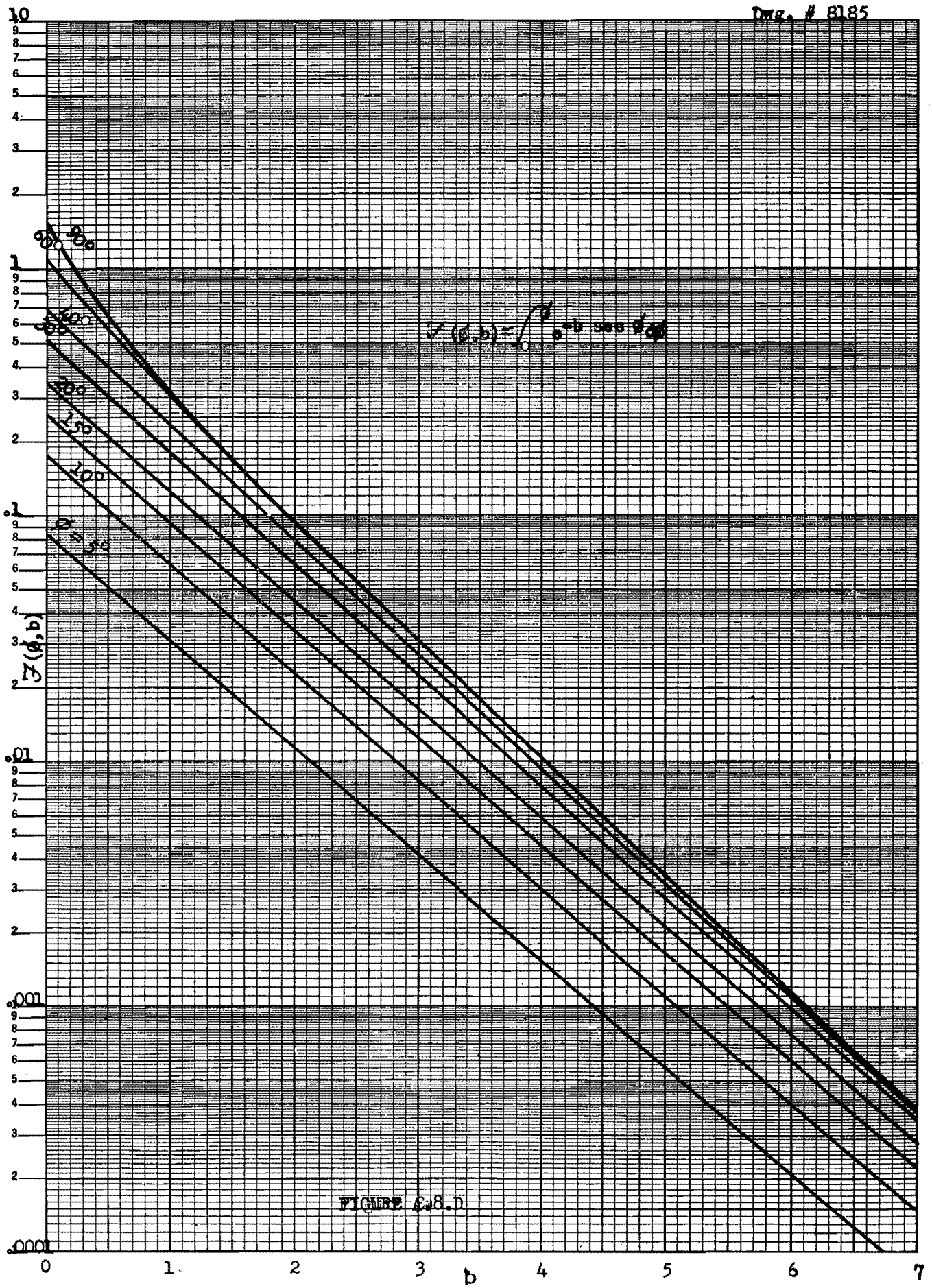
Dwg. # 8185
$\mathcal{F}(\phi,b) = \int_0^{\phi} e^{-b\cos\phi}\,d\phi$
$\mathcal{F}(\phi,b)$
b
0
1
2
3
4
5
6
7
10
1
.1
.01
.001
.0001

FIGURE A.8.D

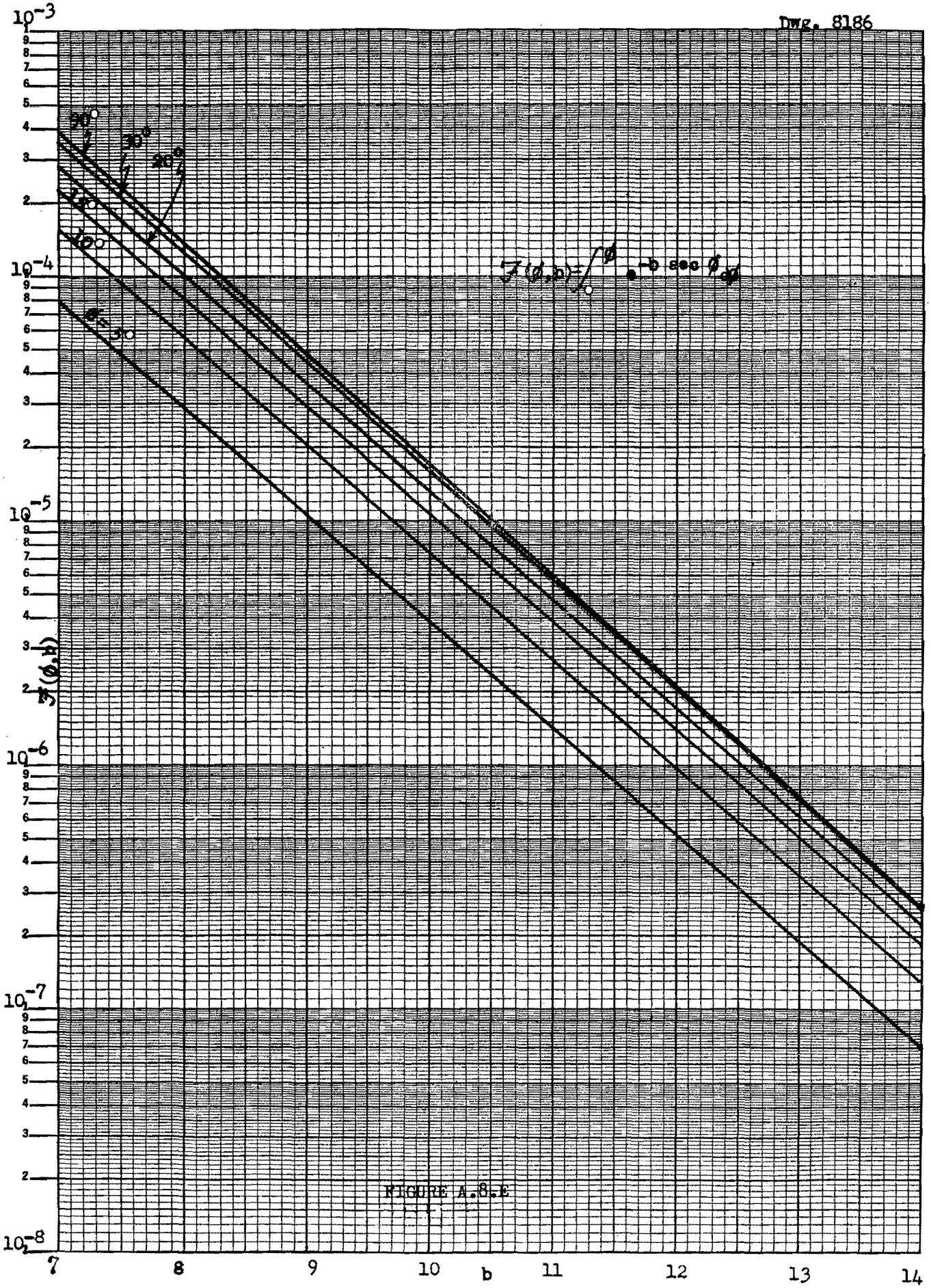
Dwg. 8186
$\mathcal{F}(\phi,b)=\int_0^{\phi} e^{-b\sec\phi}\,d\phi$
$\phi=90°$
$\phi=80°$
$\phi=70°$
$\phi=60°$
$\phi=50°$
$\phi=30°$
$\phi=20°$
$\mathcal{F}(\phi,b)$
10^{-3}
10^{-4}
10^{-5}
10^{-6}
10^{-7}
10^{-8}
7
8
9
10
11
12
13
14
b

FIGURE A.8.E

Dwg. # 8187

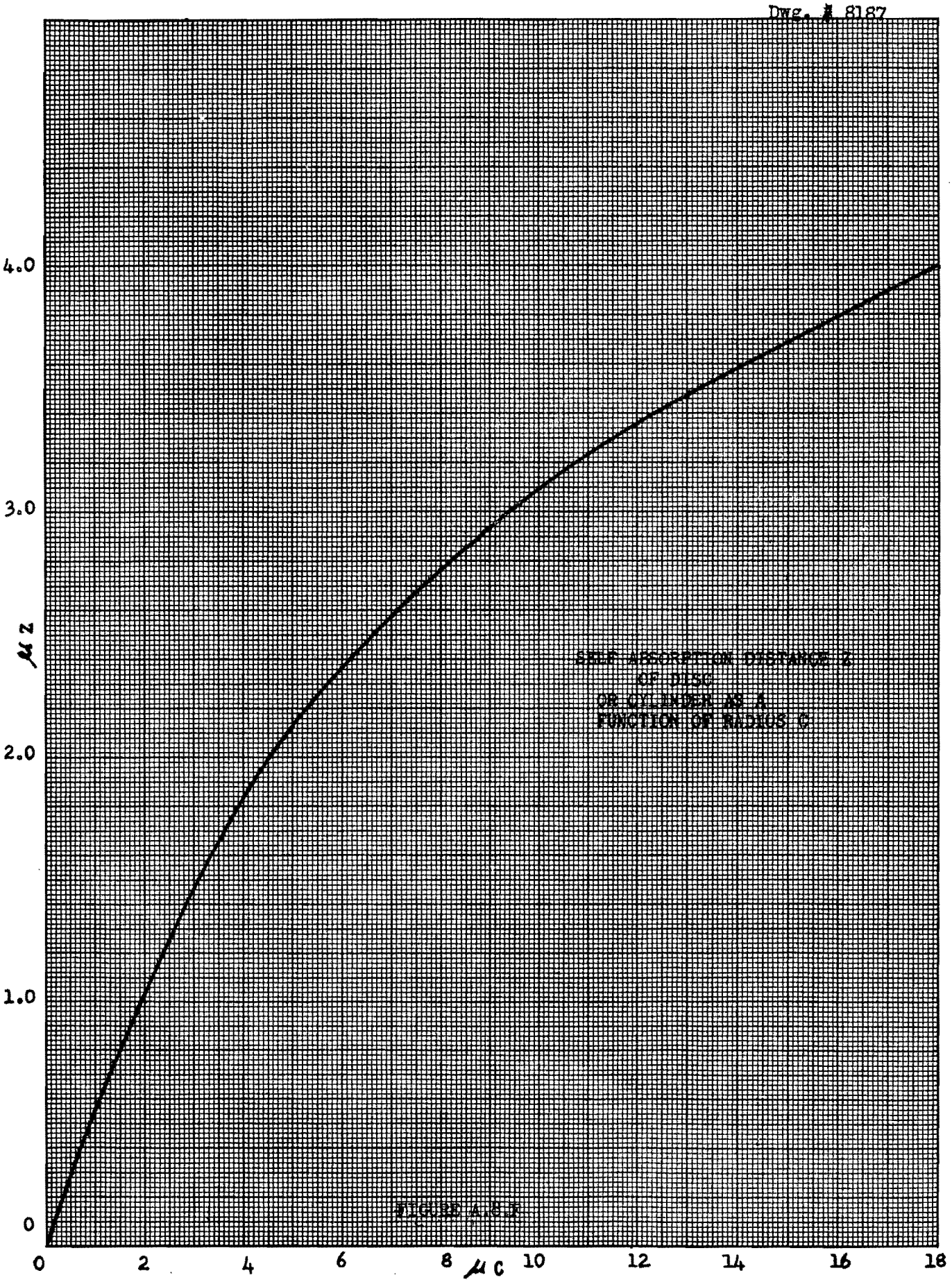

FIGURE A.8.8

Appendix 9*

PNEUMATIC RABBITS

A9.1 GENERAL DESCRIPTION OF PROPOSED RE-ENTRY SHUTTLE SYSTEM

The layout of the re-entry shuttle system is shown in Figs. A9.A and B. The equipment provides for the introduction of the shuttles into the system in the basement and provides a means of propelling them to the inner end of the rabbit tube. After a predetermined irradiation time in the reactor, they are expelled either to the laboratories or to an unloading station in the basement. The major components of the system are a loading terminal, a shock absorber, a transfer unit, a laboratory selector, and unloading terminals. An electric circuit provides timing and operation of the solenoid-operated valves that control the flow of air and motion of the shuttle through the system.

The loading terminal provides the means for insertion of the loaded shuttle into the system. Two "S" bends in the section within the reactor structure reduce the streaming of radiation outward through the tube. The shuttle is stopped at the active lattice by a pneumatic shock absorber. After irradiation the shuttle is propelled out of the reactor to the transfer unit, from which it is sent either to the unloading terminal in the basement or to the laboratory selector. If sent to the laboratory selector, it is then directed to the unloading terminal in any one of the four laboratories provided with this facility.

A9.2 PROPOSED EQUIPMENT AND FACILITIES FOR RE-ENTRY SHUTTLE SYSTEM

The following items are included in the design of the re-entry shuttle:

1. Rabbit tube HR-2.
2. Remotely operated solenoid valves to control direction of air flow in pressure and vacuum lines.
3. Electric air-controlled gate valve to permit passage of shuttle and to isolate the laboratory system from the reactor propelling pressure system.

*ANL contribution.

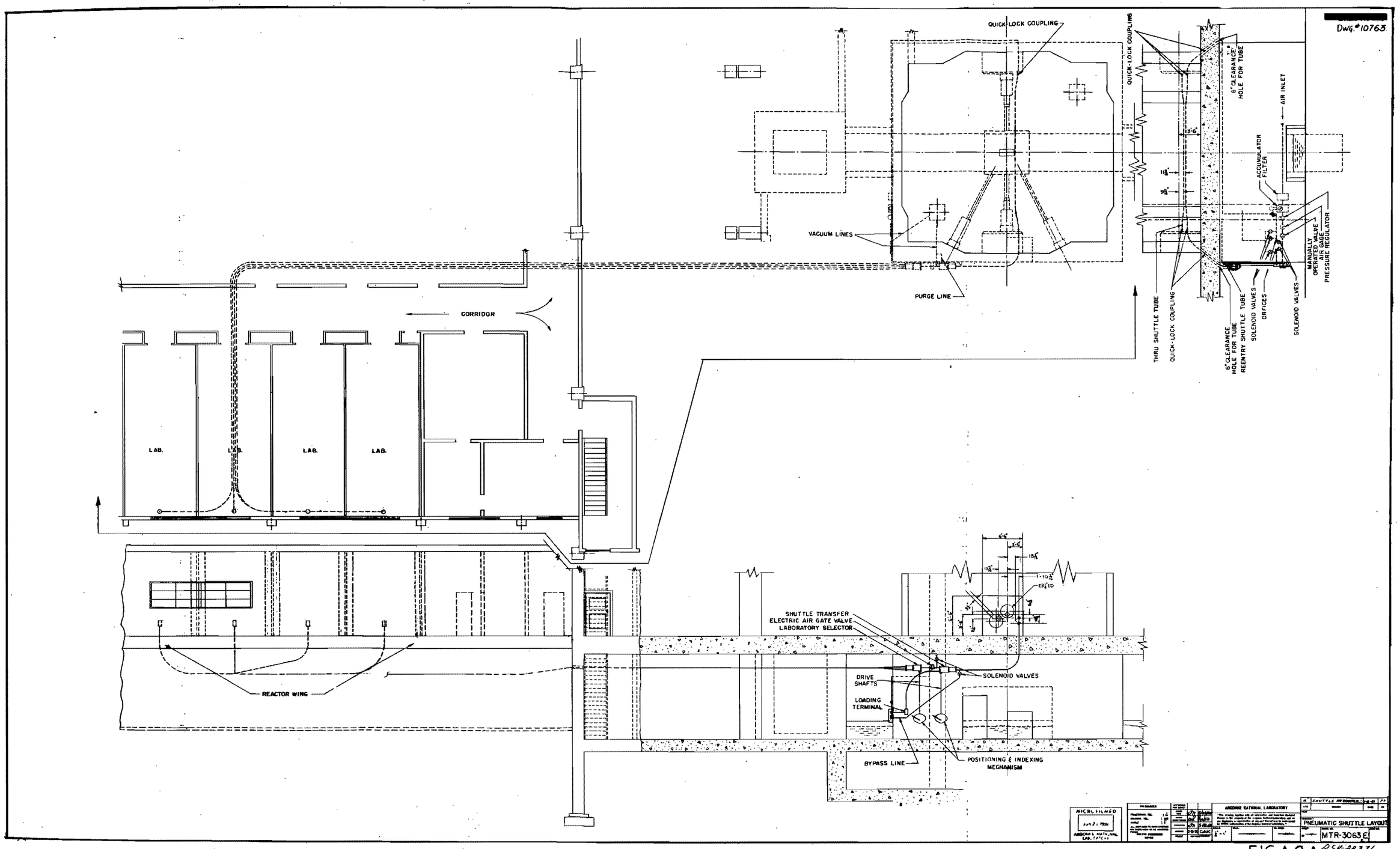
Dwg. # 10763
QUICK-LOCK COUPLING
QUICK-LOCK COUPLING
6" CLEARANCE HOLE FOR TUBE
AIR INLET
ACCUMULATOR FILTER
MANUALLY OPERATED VALVE
AIR GAGE
PRESSURE REGULATOR
VACUUM LINES
PURGE LINE
THRU SHUTTLE TUBE
QUICK-LOCK COUPLING
6" CLEARANCE HOLE FOR TUBE
REENTRY SHUTTLE TUBE
SOLENOID VALVES
ORFICES
SOLENOID VALVES
CORRIDOR
LAB.
LAB.
LAB.
LAB.
REACTOR WING
SHUTTLE TRANSFER
ELECTRIC AIR GATE VALVE
LABORATORY SELECTOR
DRIVE SHAFTS
LOADING TERMINAL
SOLENOID VALVES
BYPASS LINE
POSITIONING & INDEXING MECHANISM
MICROFILMED
ARGONNE NATIONAL LABORATORY
PNEUMATIC SHUTTLE LAYOUT
MTR-3063.E

FIG. A9.A

NOT CLASSIFIED
DWG #10759

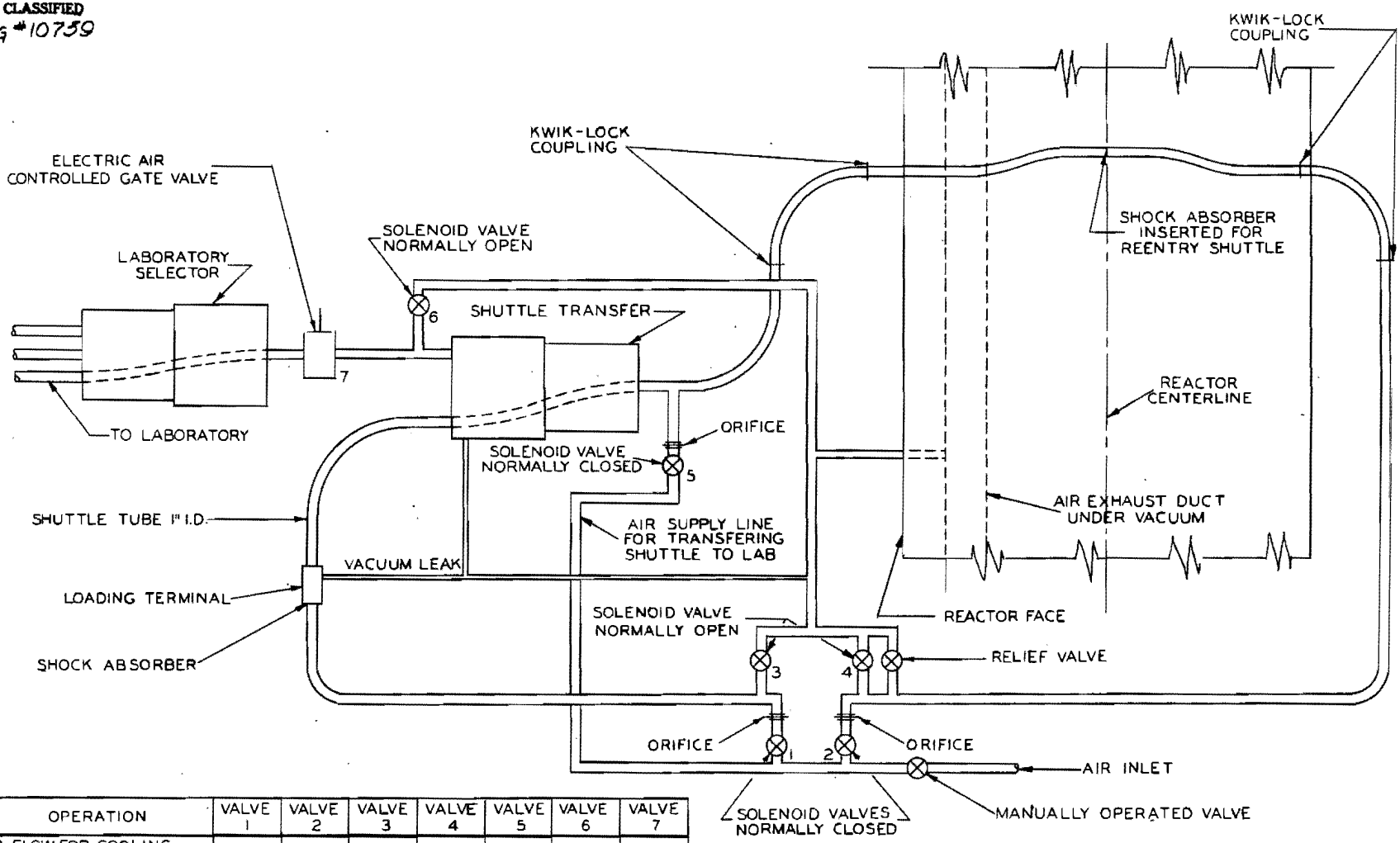

OPERATION	VALVE 1	VALVE 2	VALVE 3	VALVE 4	VALVE 5	VALVE 6	VALVE 7
AIR FLOW FOR COOLING SHOCK ABSORBER	CLOSED	CLOSED	CLOSED	OPEN	OPEN	CLOSED	CLOSED
INSERTING SHUTTLE IN TERMINAL	CLOSED	CLOSED	OPEN	OPEN	CLOSED	OPEN	CLOSED
DRIVE SHUTTLE TO CENTER OF REACTOR	OPEN	CLOSED	CLOSED	CLOSED	CLOSED	CLOSED	CLOSED
COOL SHUTTLE	OPEN	CLOSED	CLOSED	OPEN	CLOSED	CLOSED	CLOSED
RETURN SHUTTLE TO TERM	CLOSED	OPEN	OPEN	CLOSED	CLOSED	CLOSED	CLOSED
SEND SHUTTLE TO LAB	CLOSED	OPEN	OPEN	CLOSED	CLOSED	OPEN	OPEN
AFTER PASSING TRANSFER STATION	CLOSED	CLOSED	OPEN	CLOSED	OPEN	CLOSED	OPEN

[redacted]

MICROFILMED
JUN 20 1950
ARGONNE NATIONAL LABORATORY

TOLERANCES: FRACTIONAL TOL. ± 1/64; DECIMAL TOL. ± .005; ANGLE ± 1°; ALL SURFACES TO HAVE ROUGHNESS (125 RMS) OR BETTER UNLESS OTHERWISE NOTED

APPROVED FOR CONST.: CHIEF ENG. 2-7-50; CHIEF DRAFTSMAN 2-7-50; CHECKED 2-7-50; DRAWN 2-1-50 GAK; REPRESENTATIVE 2-7-50

ARGONNE NATIONAL LABORATORY

"This drawing, together with all information and know-how disclosed thereon, is the property of the Argonne National Laboratory, and no use, disclosure, or reproduction of any part thereof may be made except by written authorization of the Argonne National Laboratory."

SYM. | CHANGE | DATE | BY

PART: SCHEMATIC LAYOUT

ASSEMBLY: PNEUMATIC SHUTTLE SYSTEM

SCALE: — | MATL. — | NO. REQD. —

FIG. A.9.B

4. Loading terminal.

5. Shuttle transfer unit.

6. Laboratory selector.

7. Shock absorber to position re-entry shuttle.

8. Electric timing device.

9. Monitoring device to determine flux at center of shuttle tube.

The more important items in this list are discussed in the following paragraphs.

A9.2.1 Rabbit Tube. The proposed layout of the pneumatic shuttle system is shown in Fig. A9.A. The shuttle tube begins at an inlet air valve on the west wall of the reactor in the basement, continues around the south wall, passes up through the first floor of the Reactor Building, and enters the reactor face approximately 1 ft 10 in. east of the reactor north-south centerline at an elevation of approximately 98 ft 10 in. In the concrete shield it makes an offset bend and passes through the graphite and reactor tank approximately 1 ft 3 in. east of the reactor north-south centerline at an elevation of approximately 99 ft. Beyond the graphite, the tube again makes an offset bend to emerge from the north wall of the reactor in a location similar to its entry point in the south wall. From here it bends down through the floor and continues along the basement ceiling to the other inlet valve at the west wall. In the recesses in the north and south reactor faces at the first floor level, the curved sections of tubing are equipped with quick-lock couplings to facilitate their removal. The quick-lock couplings provide a ready means for disassembling the shuttle tube when it is desired to insert the shock absorber into the reactor or withdraw it into a coffin. The shuttle tube through the reactor tank and the thermal shield is constructed of aluminum. Beyond the reactor structure the section that is utilized by the shuttle is stainless steel, but the other sections are constructed of copper tubing.

A9.2.2 Electric Air-controlled Gate Valve. An electrically operated air-controlled gate valve, located between the shuttle transfer unit and the laboratory selector, separates the system into two sections and stops the flow of air into the laboratory while the shuttle is propelled into the reactor, irradiated, and expelled.

The laboratory section consists of the laboratory selector and the four tubes that terminate in separate laboratories. At each unloading terminal a

line to the contaminated-air system withdraws any air that is discharged from the shuttle tube during the delivery or unloading of a shuttle. This is a precaution to prevent escape of contaminated air into the laboratory building.

A9.2.3 Shuttle Transfer. The shuttle transfer design is illustrated in Fig. A9.C. The transfer unit consists of a housing that encloses the transfer tube, indexing gear, and guide disk. Four tie rods unite these parts into a single unit. Both the section of the tube connected to the laboratory selector and the section of tube leading from the loading station fasten to the gear end of the housing. At the other end a single tube leads to the reactor.

The shuttle transfer unit and the indexing mechanism, connected by means of an arrangement of bevel gears and shafting, provide for the indexing of the shuttle tube. One-third of a revolution of the indexing handle rotates the transfer unit through an angle of 180°.

A9.2.4 Laboratory Selector. No drawings have been prepared for the laboratory selector unit as its construction will be very similar to the shuttle transfer unit. It differs only in the arrangement and number of tubes required for servicing the laboratories. The selector can be located close to the transfer unit or it can be set up at some convenient location in the laboratory building.

A9.2.5 Shock Absorber. Experiments which require that the shuttle be delivered in a very short time, ½ sec or less, need a special shock absorber to stop the shuttle. A suitable design, illustrated in Fig. A9.D, has been engineered from the standpoint of high speed, adequate cooling, and ease of insertion and withdrawal. It consists of a series of alternate sections of bellows and straight tubes, approximately 12 ft long and fastened to the shock absorber body, to provide the means for insertion and location of the shock absorber in the shuttle tube. Three openings formed between the shock absorber and the inside diameter of the shuttle tube provide the space for the passage of cooling air when the shuttle rests against the shock absorber. They also form the small orifices that restrict the flow of air when the large orifice is closed during the slowing down of the shuttle. The large orifice is formed by the seat and the beveled surface of the valve. When the valve is open the larger portion of the air flows through the valve opening and then out the portholes to mix with the air flowing through the small orifices. The air continues to flow in the annulus formed between the body diameter and the

[redacted]
Dwg. # 10762

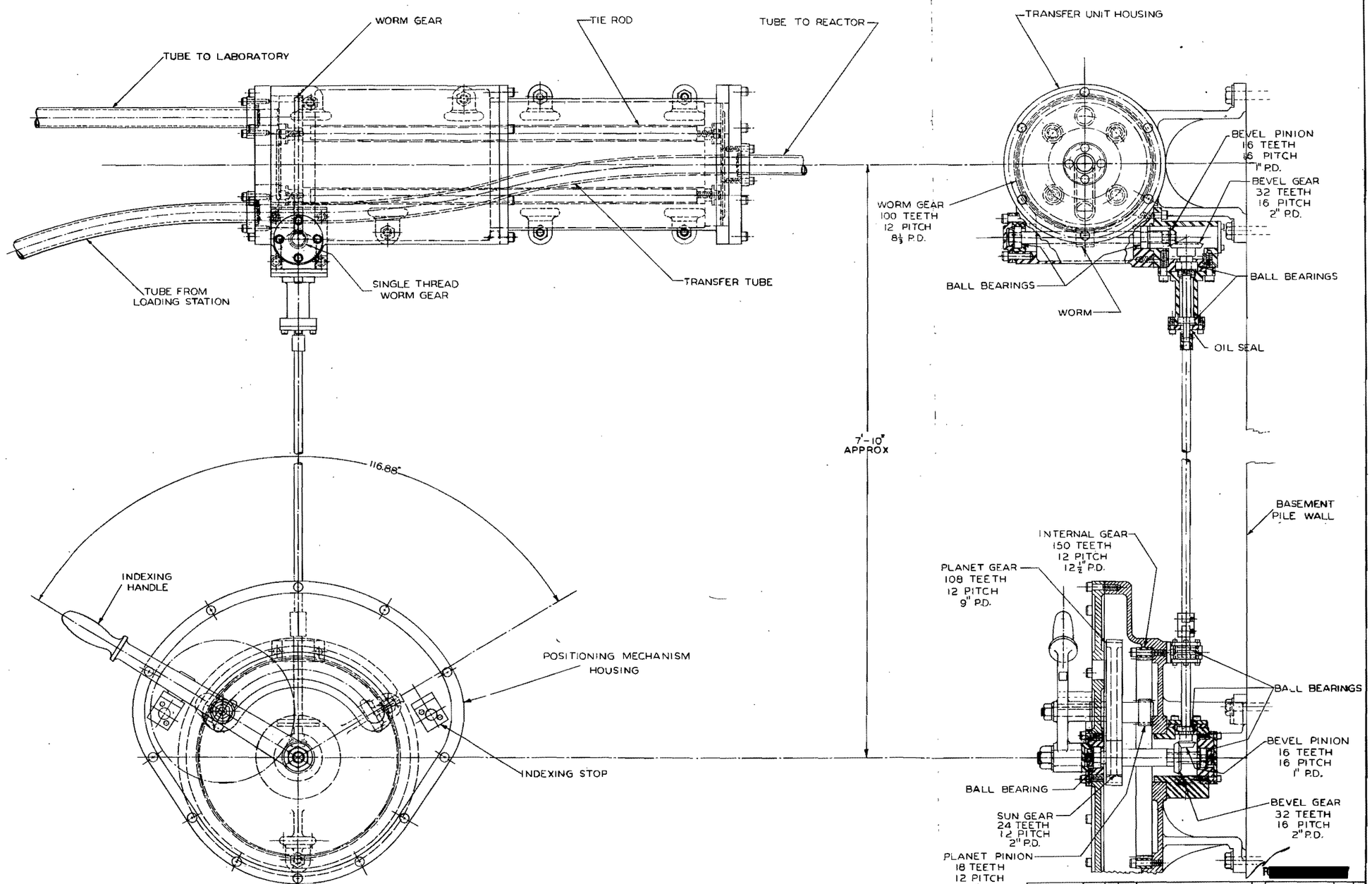

FIG. A.9.C

NOT CLASSIFIED

DWG # 10740

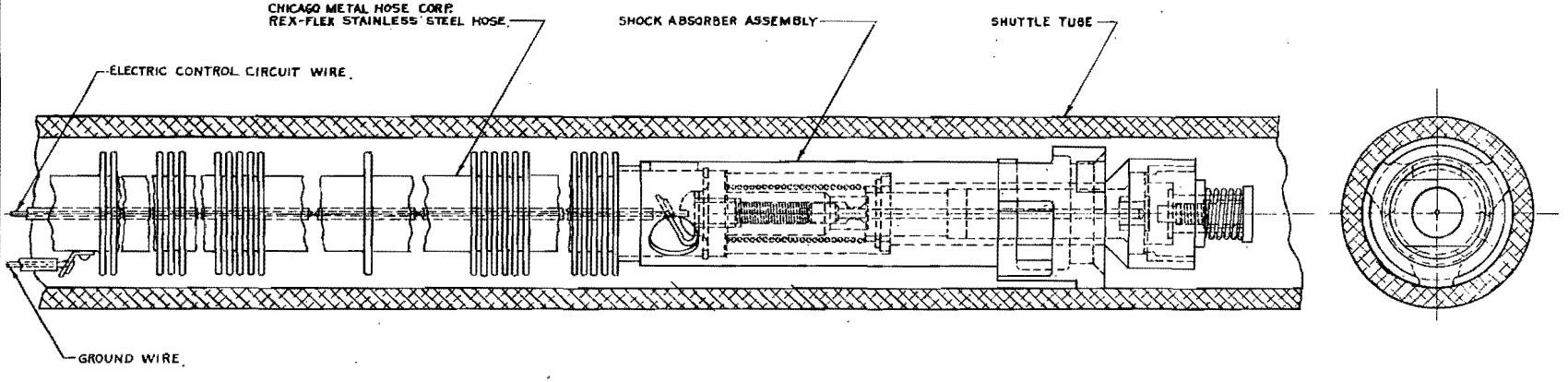

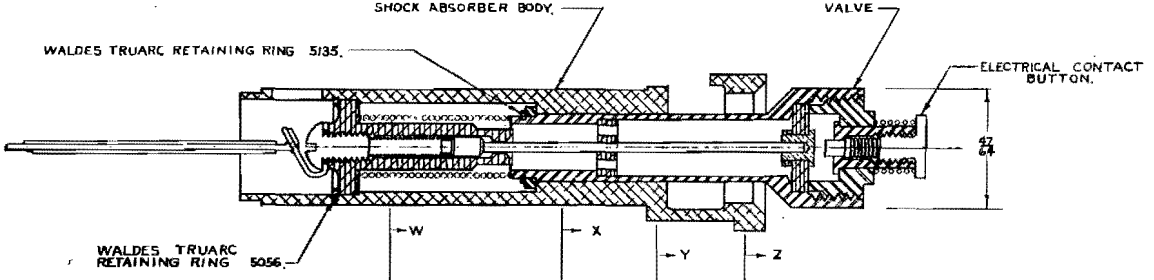

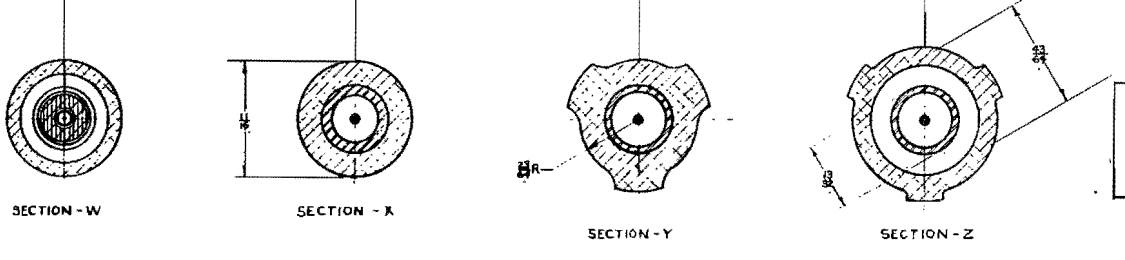

MICROFILMED
JUN 20 1950
ARGONNE NATIONAL LABORATORY

[redacted]

TOLERANCES:	APPROVED FOR CONST.			ARGONNE NATIONAL LABORATORY	SYM.	CHANGE	DATE	BY
FRACTIONAL TOL. ± 1/64	CHIEF ENG.		3-2-50	"This drawing, together with all information and know-how disclosed thereon, is the property of the Argonne National Laboratory, and no use, disclosure, or reproduction of any part thereof may be made except by written authorization of the Argonne National Laboratory."	PART	SINGLE CONTACT SHOCK ABSORBER.		
DECIMAL TOL. ± .005	CHIEF DRAFTSMAN		3-2-50		ASSEMBLY	PNEUMATIC SHUTTLES.		
ANGLE ± 1/4°	CHECKED		3-2-50					
ALL DIMENSIONS TO BE ACTUAL (TO BEING MADE OR AS SHOWN HERE) UNLESS OTHERWISE NOTED	DRAWN		3-2-50	SCALE 2:1	MATL.	NO. REQD.		
	GROUP	REPRESENTATIVE						

FIG. A.9.D

inside surface of the shuttle tube. Three holes located in the body in front of the bellows permit the air to divide into two streams, one flowing inside and the other outside the bellows. A spring enclosed in a sealed chamber in the shock absorber body holds the valve open until the pressure of the air in front of the shuttle overcomes the spring force. After the valve closes a greater pressure is required to force the air displaced by the shuttle through the small orifices. This increase in pressure acts as a retarding force to slow down and stop the shuttle. When the shuttle depresses a spring-backed button secured in the valve head, an electrical circuit for controlling the shuttle timing device is completed. The wires for the timing device enter through connections at the removable section of the shuttle tube. One wire is grounded to the flexible tubing and the other continues through the bellows and terminates at the electrical terminal mounted in an insulation bobbin that is pressed into the shock absorber body. The electrical circuit is completed by means of a spring, a plunger, and a rod that is secured in an insulation bushing mounted in the valve.

The parts that comprise the shock absorber should be made as light as possible in order to minimize the heat generated by gamma absorption. A continuous flow of air at the rate of 0.04 lb/sec is required to cool the shuttle and shock absorber.

A9.2.6 Delivery Stations and Delivery-station Shock Absorbers. Speed of delivery of the shuttle to the laboratory may be of prime importance; hence the delivery velocities may be high and adequate shock absorbing means must be provided at the delivery stations. For this purpose conventional pneumatic dash-pot delivery stations can be used, since heating due to nuclear reactions is not involved. In general these consist merely of a 3-ft blind length of tubing beyond the exit for the propelling air. Suitable doors are provided to remove the shuttles after delivery. The doors should not be opened until the delivery air has been shut off (by automatic timing of the delivery cycle), thereby placing the delivery stations under a slight vacuum.

A9.2.7 Pneumatic Driving System. The incoming air from the plant air compressor is cleaned, filtered, and dehumidified before it enters the accumulator tank. A relief valve controls the maximum pressure in the tank. A pressure regulator controls the pressure of the air prior to its entry into the pneumatic shuttle system through the solenoid-operated valves that govern

the direction of air flow. A secondary solenoid valve controls the flow of air after the shuttle transfer has been rotated and also when it is desired to transfer a shuttle to a laboratory. Solenoid valves at the extremities of the shuttle tube control the direction of the air after it has passed through the reactor and prior to its entering the reactor cooling-air exhaust duct. These two valves remain open except during a charging operation. A relief valve governs the maximum pressure allowed in the exhaust line during charging of a shuttle. A solenoid valve permits the escape of gas when the shuttle transfer tube has been rotated to the laboratory position.

A9.2.8 Vacuum System. Both ends of the shuttle tube are connected, through solenoid-operated valves, to a single pipe which terminates at the reactor cooling-air exhaust duct. Since the exhaust duct is under vacuum and the valves are normally open, one or both ends of the shuttle tube are always under a vacuum. This tends to clear the shuttle tube of dust particles and simplifies the periodic purge required to clear the lines. Vacuum leak lines, continually open to the exhaust line that leads to the reactor cooling-air exhaust duct, place the loading terminal and the shuttle transfer unit under a continuous negative pressure and provide against leakage of contaminated air into the Reactor Building.

Vacuum exhaust connections for the through shuttles are provided at the face of the reactor for the convenience of experimenters in setting up their equipment. These are part of the experimental services normally provided at all beam hole facilities.

A9.3 OPERATION OF RE-ENTRY SHUTTLE SYSTEM

Prior to delivery of a shuttle to the reactor, the pneumatic shuttle system is under a slight vacuum since the solenoid valves at the ends of the shuttle tube are open to the reactor cooling-air exhaust system. The sequence of operations that take place during the delivery of a shuttle can be better understood by reference to Fig. A9.B.

Shuttles prepared for delivery to the reactor are introduced into the system at the loading terminal. After the cover is secured, the operator presses a switch which automatically closes all valves in the vacuum lines and

opens the solenoid valve in the pressure line to admit the air that propels the shuttle. The incoming air, metered through an orifice, increases the pressure in the section of pipe between the shuttle and the orifice, and drives the shuttle against the shock absorber at the center of the reactor. The air in front of the shuttle is compressed since it is not permitted to escape. The pressure continues to build up and eventually overcomes the spring force that normally holds the shock absorber valve open. With closure of the valve the flow area at the body section is reduced to that of the three small openings formed between the shock absorber body and the inside of the shuttle tube. This decrease in orifice area increases the pressure required to discharge the air displaced by the shuttle. The volume of air displaced is a function of the pressure and the velocity of the shuttle. In an effort to reach a state of equilibrium, the pressure acts as a retarding force on the shuttle. The maximum pressure build-up in the low-pressure section of the line is limited by a relief valve. When the shuttle contacts the shock absorber, an electrical circuit is completed which simultaneously operates an electric timing device and opens the solenoid valve that permits the gas to escape into the reactor cooling-air exhaust system. The steady flow of air through the tube cools the shock absorber and shuttle.

If the shuttle is to be sent to the laboratory, the shuttle transfer tube is rotated to the laboratory position during the time interval in which the shuttle is irradiated. Rotation of the shuttle transfer tube automatically closes the solenoid valve that has been supplying the air to propel and cool the shuttle and, after a fraction of a second delay, opens the solenoid valve in the air-supply line that by-passes the shuttle transfer unit. This now provides the air necessary to cool the shuttle and the shock absorber.

At the end of a preset exposure time for the shuttle, the electric circuit in the timing device is broken. This automatically reverses the solenoid valves that control the direction of air flow, thereby expelling the shuttle. At the same time, the solenoid valve on the vacuum side of the transfer unit opens to permit the air in front of the shuttle to discharge into the reactor cooling-air exhaust system. After a delay period, to ensure that the shuttle is beyond the transfer unit, the valve in the vacuum line closes and the shuttle transfer by-pass air-supply valve opens to drive the shuttle to the unloading terminal in the laboratory. After a suitable time delay to ensure delivery of the shuttle and to purge the system, the valves in the vacuum line open automatically. The unloading terminal cover can then be opened and the shuttle removed. The air-supply valve can still be open to permit a flow of air to cool the shock absorber.

A9.3.1 Pressure Drop. When the shuttle is positioned at the center of the reactor by the shock absorber, an approximate pressure drop of 38 lb/sq in. is required to force 0.04 lb of air per second through the shuttle tube. This is equivalent to 31.8 cfm of air at 70°F and atmospheric pressure of 14.7 lb/sq in.

A9.3.2 Anticipated Operating Curves. The curves shown in Fig. A9.E are not to be construed as the actual representation of the air pressures in the tube and the velocities of the shuttle. They merely indicate a trend and are helpful in understanding some of the problems in designing the mechanism for propelling and slowing down the shuttle in the pneumatic system.

The propelling force starts at the pressure produced by the vacuum in the reactor cooling-air system. A constant supply of air into the chamber increases the pressure behind the shuttle and drives it to the center of the reactor. The maximum pressure is reached when the shuttle velocity and the speed of the incoming air in the tube are equal. Maximum acceleration also occurs at this point. A decrease in the propelling pressure occurs when the shuttle travels faster than the air velocity in the tube. This is due to the volume behind the shuttle increasing at a greater rate than the build-up in pressure.

During the driving of the shuttle, no air is permitted to escape through the exhaust valves. The travel of the shuttle compresses the volume in front of the shuttle and thereby increases the back-pressure. The difference between the propelling pressure and the back-pressure is the unbalanced pressure that decreases the acceleration. This continues until the two pressures are equalized, at which time the acceleration becomes zero and the velocity becomes a maximum. Further increase in back-pressure results in deceleration of the shuttle. When the pressure in front of the shuttle overcomes a spring force in the shock absorber, the valve closes.

After the valve closes, a greater pressure is required to force the air, displaced by the shuttle, through the small orifices between the shock absorber body and shuttle tube. This accounts for the sharp rise in the back-pressure curve, the increase in deceleration, and the decrease in shuttle velocity. It should be noted that the velocity is practically zero when the shuttle is approximately 8 in. from its stop. The shuttle continues to stall until the propelling and back-pressure are again equal, at which time the shuttle is

NOT CLASSIFIED
DWG #10738

PNEUMATIC SHUTTLE SYSTEM
SPACE VS. TIME
PRESSURE VS. TIME

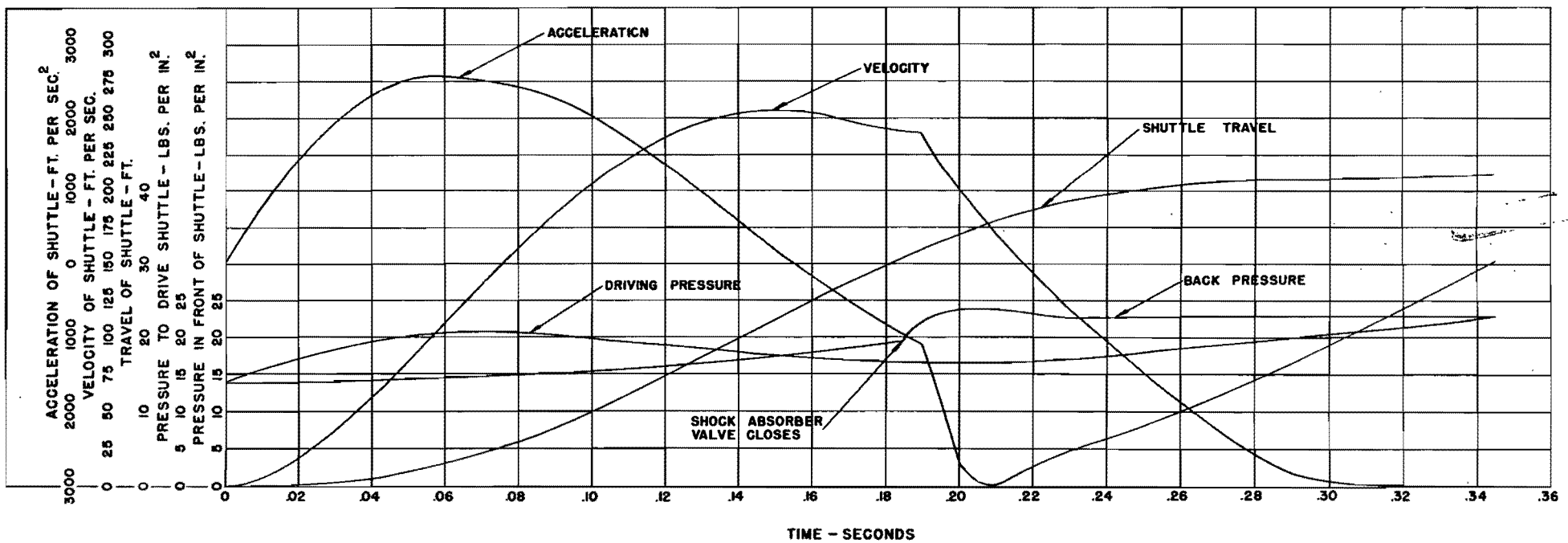

FIG. A.9 E
ANTICIPATED OPERATING CURVES

MTR-G-144

forced against the shock absorber valve head. The pressure in back of the shuttle then increases until the steady flow required to cool the shuttle and shock absorber is attained.

A9.3.3 Shuttle Material. Some of the characteristics of an ideal shuttle material are (1) low-activation cross-section, (2) low density, (3) high thermal conductivity, (4) stability to radiation, and (5) structural strength.

The first property is desirable to prevent the carrier's becoming active enough to require shielding during the unloading operation. Materials that satisfy this requirement are electrolytic iron, beryllium, zirconium, carbon, polystyrene, and bakelite.

Of the preceding materials, iron is attractive with respect to thermal conductivity, stability to radiation, and structural strength, but, because of its density, it has a high rate of gamma heat generation that introduces cooling difficulties. However, the cooling problem can be minimized by limiting the weight of the carrier to approximately 12 g. For a 3-in.-long shuttle, the maximum wall thickness would then be 0.01 in. An additional restriction on the use of iron is that in order to limit the induced activity to tolerable values it must not contain appreciable quantities of manganese.

The use of beryllium or zirconium would permit a larger wall thickness for a given weight carrier. The activity of these elements is controlled by the impurities aluminum and hafnium.

Some of the plastics are promising, but the inherent low thermal conductivity makes cooling of the sample difficult. Information on the effects of radiation on plastics is rather incomplete at this time. However, from experiments made with low neutron fluxes, it appears feasible to use bakelite and polystyrene as shuttle materials.

A9.3.4 Cooling of the Shuttle. The cooling required by the loaded carrier is a function of the total mass and the desired maximum temperature. Since it may become necessary to irradiate samples that have a low decomposition temperature, such as hydrocarbons, the cooling system should be capable of limiting the maximum sample temperature to approximately 300°F. In addition, the use of a plastic carrier would limit the temperature to a similar maximum. It is estimated that the upper limit on the mass of a loaded shuttle will be 25 g. To cool this shuttle and the shock absorber with air, a flow of 0.04 lb/sec is required. This value is based on a heat transfer area of 9.6 sq in. with a 3-in.-long carrier.

A9.3.5 Shielding. The exposure hazards in the shuttle system will be from activation of the propellant gas or the sample and carrier. Computations indicate that no permanent shielding will be required to satisfy health physics requirements, and temporary shielding will be adequate when needed to provide instrument background.

The air used as a propellant will contain active argon, nitrogen, and oxygen. To prevent the escape of active air it is necessary for the parts of the system that operate at a positive pressure to be leakproof.

A9.3.6 Use of Air vs. CO_2 for Propellant. Air is used as a medium to drive the pneumatic shuttle in and out of the reactor. It was selected because it is economical to use as a cooling medium for the sample and shock absorber. A comparison of CO_2 and air made on the basis of cost and radiation hazard indicates that air is preferable. The inherent disadvantage of air is the formation of 110-min argon. However, the exhaust lines in the proposed shuttle system will operate at a negative pressure so that the escape of active argon is not likely.

The exposure at the surface of a 1-in. shuttle tube containing active exhaust air is calculated to be 0.02 r per 8 hr. At short decay periods no decrease in exposure can be realized through the use of CO_2 because the significant fast flux at the shuttle tube gives appreciable $O^{16}(n,p)N^{16}$ activity.

A9.4 REFERENCE REPORTS

(1) Nicoll, D. and Lennox, D. H., *Pneumatic Shuttle,* Design Report No. 44, ANL-ABS-16, March 27, 1950.

(2) Scott, D., *Pneumatic Rabbits in the X-Pile,* ORNL CF-47-11-35, October 31, 1947.

(3) Scott, D., *Status of the Pneumatic Rabbit Design in the High Flux Pile,* ORNL CF-48-6-134, June 9, 1948.

A9.5 REFERENCE DRAWINGS

DWG. NO.	TITLE
BKC-3150-538-1 through 10	HR-1 and HR-2 - Rabbit Tubes
BKC-3150-540-1 through 5	HR-3 and HR-4 - Rabbit Tubes

Appendix 10

HYDRAULIC RABBITS

The hydraulic rabbit system for the MTR consists of two 1-in.-I.D. vertical tubes through the east end of the beryllium reflector (see Beryllium Layout, Figs. 2.4.A and B) and a 1.310-in.-I.D. tube through each of the regulating rod holes not in use.

The following description of the system is a tentative proposal for the design. The final design of the system may vary somewhat from this presentation, but the overall principles will be the same.

The proposed system is shown in Fig. A10.A. Shuttles from the laboratory, after being sealed, are lowered into the loading chute and pushed through valve C into the loading chamber. Valve C is then rotated into the insertion position and valve B is opened, permitting the rabbit shuttle to be driven to the top of the reflector where an orifice acts as a stop. (The shuttle can be stopped lower than this by insertion of appropriate dummies ahead of it.) When the irradiation is finished, the demineralized-water flow is decreased until the shuttle falls into the canal. This occurs when the demineralized-water flow into the reactor is so low that resistance of the shuttle to the flow is not sufficient to overcome gravity. With valve A closed, it is possible to discharge the shuttle into a bucket type coffin in the canal without letting any great volume of active water get into the canal. Since valve A is normally an open solenoid valve, it will not trap the shuttle in case of power failure but will allow it to fall into the canal.

Vertical holes in the upper support casting, in line with the rabbit tubes, permit the use of a long rod for pushing any shuttle which might stick above the canal.

The actual design of the shuttle is, of course, best done by the MTR operator or the experimenter. If a shuttle design similar to that of the hydraulic rabbit system of the X-10 reactor is used, the tubes should have a minimum radius of curvature of 48 in. The rabbit tube positions at the east end of the reflector will accommodate 1.190-in.-O.D. tubes, and the regulating rod holes will accommodate 1.500-in.-O.D. tubes. The inside diameters of these tubes have been set at 1.000 in. and 1.310 in., respectively.

DWG. # 10712

[redacted]

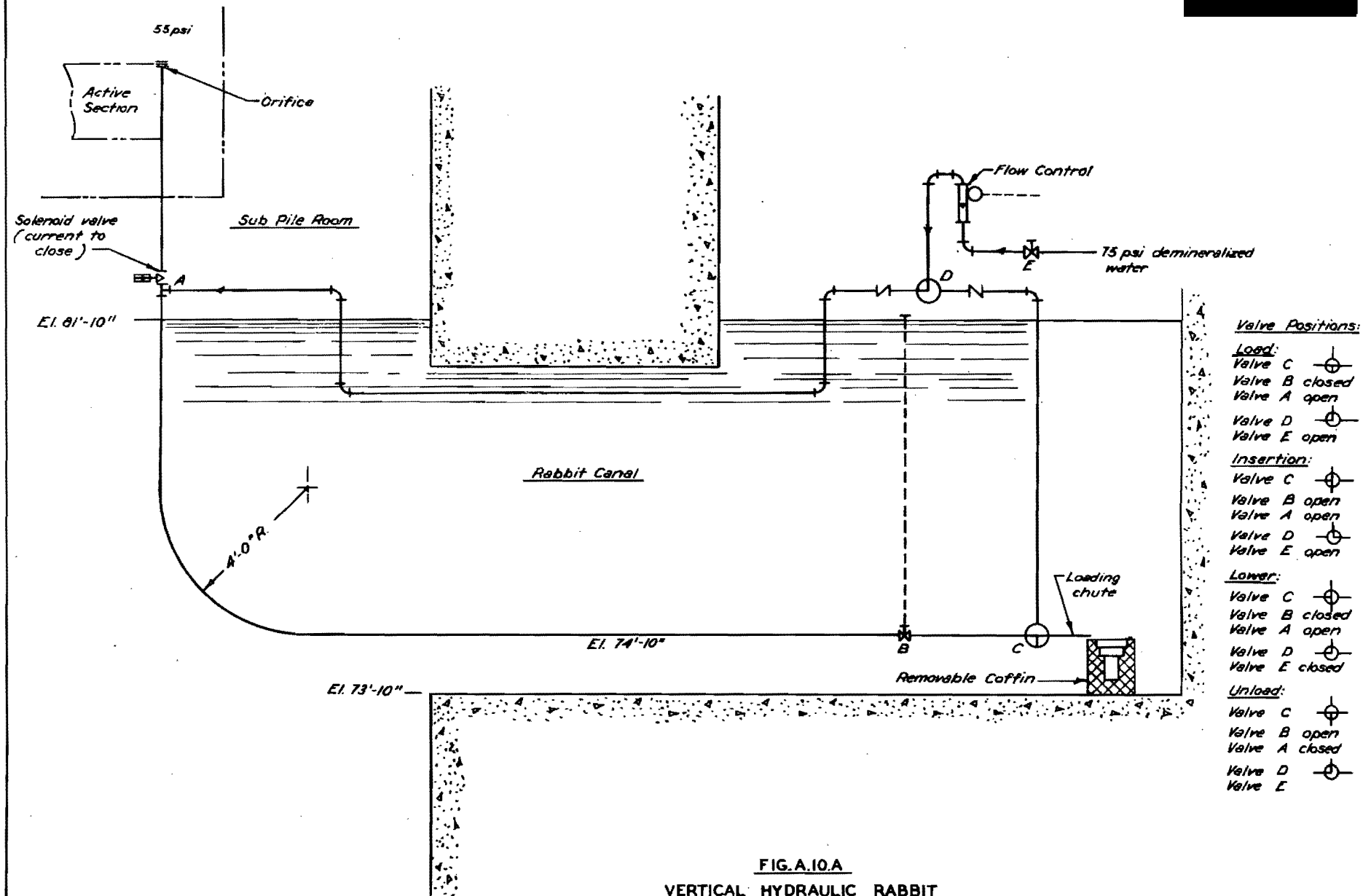

FIG. A.10.A

VERTICAL HYDRAULIC RABBIT

PIPING ARRANGEMENT

Demineralized water at 75 psi will be available at the rabbit canal, and approximately 5 gal of water per minute past the shuttle will be necessary for cooling. No shock absorbers are provided, but speed of insertion can be easily regulated by the demineralized-water flow.